CRANFIELD UNIVERSITY

PAULA ALEKSANDRA MISIEWICZ

THE EVALUATION OF THE SOIL PRESSURE DISTRIBUTION AND CARCASS STIFFNESS RESULTING FROM PNEUMATIC AGRICULTURAL TYRES

SCHOOL OF APPLIED SCIENCES
Natural Resources Department

PhD

CRANFIELD UNIVERSITY

SCHOOL OF APPLIED SCIENCES
Natural Resources Department

Doctor of Philosophy

2010

PAULA ALEKSANDRA MISIEWICZ

The evaluation of the soil pressure distribution and carcass stiffness resulting from pneumatic agricultural tyres

Supervisors:
Prof. Richard J. Godwin
Dr. Terence E. Richards

3 August 2010

This thesis is submitted in partial fulfilment of the requirements for the degree of Doctor of Philosophy.

ABSTRACT

Introducing loads onto the soil via pneumatic tyred equipment is the major cause of compaction of agricultural soils, which causes damage to the soil-water-air-plant system. The degree of soil compaction is largely influenced by the loads applied to the soil and resulting surface and subsurface pressure. Therefore, this study was conducted in order to determine an effective method to measure the pressure distribution under a selection of pneumatic agricultural tyres on a hard surface and in the soil profile. As a result of this, it has been possible to evaluate the influence of tyre inflation pressure, load, ply rating and tread pattern on the resulting pressure. Also, the carcass stiffness of the tyres studied was determined and alternative methods to predict the carcass stiffness were evaluated and an improved technique was developed.

The pressure distribution resulting from a range of tyres on a hard surface and in the soil profile was determined using a commercial pressure mapping system (Tekscan sensors mounted on a 70 mm steel plate). This has been possible after the capabilities of the system were improved by:

i. the use of a purpose built pneumatic calibration device,
ii. the design of a multi-point per-sensel calibration,
iii. the rejection of sensing elements that fail to meet calibration criteria (this with (i) and (ii) resulted in a reduction of Tekscan errors from +/- 20% to +/- 4%),
iv. the establishment of a procedure for normalising the recorded pressure by adjusting the recorded load output to equal the applied load.

The hard surface study using the Tekscan system was designed to determine the tyre carcass stiffness, defined an equivalent pressure resulting from tyre stiffness and calculated as the difference between the surface contact pressure and tyre inflation pressure. This enabled the evaluation of a range of alternative methods to estimate tyre carcass stiffness, namely:

i. The pressure difference method using ink to estimate the size of the contact patch and hence mean contact pressure,
ii. Tyre load - deflection method,
iii. Tyre manufacture specification data method (2 methods).

Both methods (i) and (ii) were found to give lower results, which were approximately equal to 30 – 50% of the tyre carcass stiffness obtained by Tekscan system. The methods based on tyre manufacture specification data were developed in this study and they gave a better estimation of the mean tyre carcass stiffness. The technique based on the tyre manufacture data, using the theoretical load that the tyre is able to sustain at zero inflation pressure, produced estimates that were within +/- 20% of the mean carcass stiffness determined from Tekscan. It is recommended that this method should be used in the absence of a pressure mapping system and the results of this should be added to the tyre manufacturer's specification data. The use of the Tekscan system also allowed the maximum carcass stiffness to be determined with typical values between 2.5 – 4 times greater than the mean carcass stiffness.

Both the hard surface and soil profile study, showed that changes in the tyre ply rating (from 8 to 16) of a Goodyear 11.50/80–15.3 implement tyre, whilst demonstrating a positive trend, did not have a significant effect on the mean and maximum surface contact pressure and on the sub-surface soil pressures resulting from these implement tyres and hence, did not significantly affect the carcass stiffness.

Tyre tread pattern of a Trelleborg 600/55-R26.5 rear combine tyre was found to have a significant effect, over that of an equivalent smooth tyre, on the contact area, mean and maximum contact pressure generated on a hard surface. Nevertheless, the tread pattern does not have a significant effect on the soil area of tyre influence and the mean soil pressure in the profile. The maximum soil pressure was found to be influenced by the tyre tread to a soil depth of 100 mm.

The pressure transfer in the soil was studied for the Trelleborg 600/55-R26.5 smooth tyre, where the area of tyre influence was found to increase in an approximately linear manner with soil depth and explains the hyperbolic relationship of a decrease in soil pressure with depth which was found in this and previous studies.

Finally, contrary to the assumptions used by some previous researchers, the tyre mean contact pressure on a hard surface should not be estimated using the contact area, as this gives a value lower than the inflation pressure and the mean pressure determined using Tekscan system. Using this concept of the area determination in the soil profile, the mean subsurface pressure was estimated to be with 0.5% of the mean soil pressure recorded using Tekscan.

ACKNOWLEDGEMENTS

I would like to thank:

Prof. Dick Godwin and Dr. Mike Hann who provided me with direction, great support and who both became friends. I thank Prof. Dick Godwin for guiding me through the project, technical support, brilliant ideas, being generous with his time and giving me all his help and support during the 'writing-up' period. I thank Dr. Mike Hann for continuous support, encouragement and friendship.

Dr. Terence Richards for enormous help with everyday problems, discussions, providing technical support and reading the thesis.

Dr. Kim Blackburn for showing me that nothing is simple and always giving his invaluable help, especially on Matlab data processing and instrumentation.

Roy Newland, who assisted me in conducting all experimental work, for his friendly technical assistance, patience and helpful advice in the soil bin tests.

Phil Trolley for his support and producing/repairing whatever got broken.

Pat Bellamy, Sandra Richardson, Simon Stranks, Roger Swatland and David White for their kindness and assistance.

My study would not have been possible without the financial support from the Douglas Bomford Trust, hence, all the support is gratefully acknowledged. I also would like to thank the Royal Academy of Engineering and Harper Adams University College for their support.

My great thanks go to all my friends for all their friendship and support.

I would also like to thank Ron Wells for all his encouragement.

A very special thanks goes out to Max for always being there and for continuous support and encouragement.

Finally, many thanks to my parents, Alicja and Franciszek, and my brother Kamil for their love and sincere encouragement through my entire life.

TABLE OF CONTENT

LIST OF FIGURES

LIST OF TABLES

NOMENCLATURE

a – contact area ratio

a_1, a_2, a_3, a_4 – empirical constants ($a_1 a_3 = 5.6$, $a_2 = 0.35$ and $a_2 + a_4 = 0.7$; parameters introduced by Painter, 1981)

A_0, A_2, A_4, A_5, A_6 – empirical constants ($A_0 = 61$, $A_5 = 16$, $A_6 = 448$ and $A_2 + A_4 = 0.7$, parameters introduced by Painter, 1981)

a', b' – are half the width of the minor and major axes of the super ellipse (mm)

b – contact area width (often considered as tyre width; mm)

c_1 – constant expressing the effect of the carcass stiffness of the tyre (parameter introduced by Karafiath and Nowatzki, 1978)

C – tyre cross section equivalent diameter of the tyre section (mm)

c_r – elastic constant of rubber

C_1 – parameter depending on tyre design (1.15 – conventional tyres, 1.5 – radial tyres; radial tyres have not been tested, parameter introduced by Komandi, 1976)

D – outside diameter of the tyre (mm)

d – soil depth (mm)

DOT – direction of travel

f – tyre deflection (mm)

$f_{\max}$ – maximum tyre deflection (mm)

K – Komandi's parameter (1976) equal to $15 \times 10^{-3}(B + 0.42)$

k_c, k_ϕ, n – constants for a particular soil condition which are measured by plate sinkage tests (parameters introduced by Bekker, 1960)

n – is "ellipse squareness"

p_{CS} – average pressure transmitted by the carcass at $p_i = 0$ (bar)

P_i – tyre inflation pressure (bar)

P_C – tyre mean contact pressure (bar)

P_{CS} – tyre carcass stiffness (bar)

P_D – contact pressure in a particular point (bar)

$P_{\max}$ – tyre maximum contact pressure (bar)

PR – ply rating

r – tyre radius (mm)

R – radius of the circle area (mm)

q – dry bulk density of the soil (t/m^3)

Q – vertical point load (kN)

Q_d – soil compactability (t/m^3)

S – tyre section height (mm)

T – tyre numeric (parameter introduced by Krick, 1969)

w – water content (%)

W – tyre axle load applied (tonne)

z – soil sinkage (mm)

ρ – the respective distance of the relation point from the centre of the circle area (for the pressure distribution equations introduced by Söhne, 1958; mm)

σ_r – polar principal stress (kPa)

σ_z – vertical compressive stress (kPa)

ϑ and r – polar coordinates (Boussinesq, 1885; ^{o} and m, respectively)

1 INTRODUCTION

1.1 Background to study

To ensure maximum crop yields for agricultural production, it is critical that soil bulk densities are within a particular density range (Soane and Ouwerkerk, 1994). This provides good soil-water-air relationship which promotes optimum growth. Introducing loads onto the soil via machinery increases the soil bulk density producing compaction and damage to the soil-water-air-plant system, as shown in Figure 1.1 from the work by Negi *et al.* (1981). If the soil bulk density falls below the optimum density range and there is insufficient root-soil contact, then the plant yield also decreases. However, this effect is small compared to the higher densities which have the most detrimental effect.

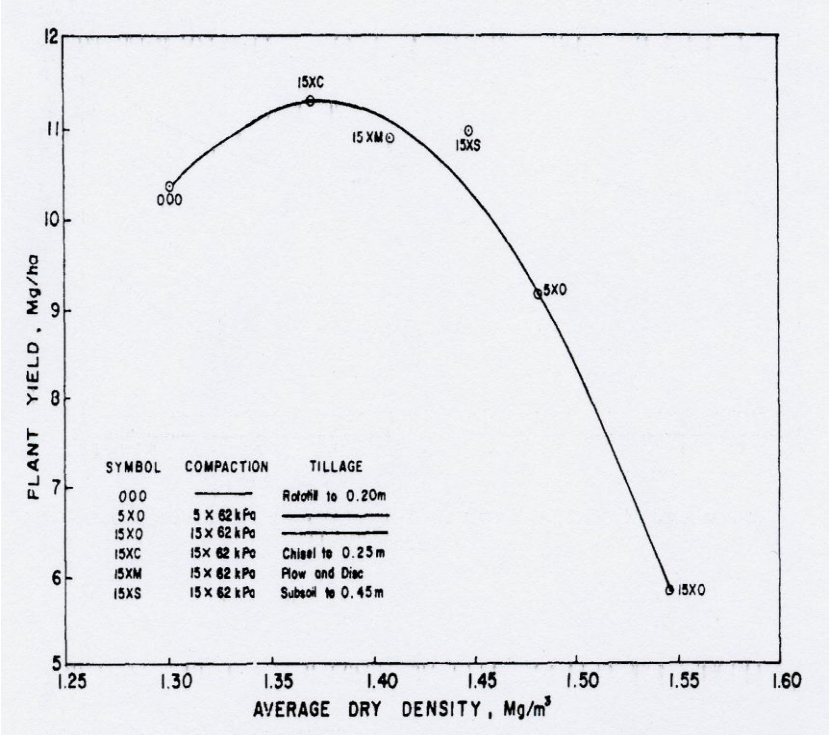

Figure 1.1 Effects of soil compaction on plant yield in a sandy loam soil (Negi *et al.*, 1981)

Over the last few decades, farm machinery has increased substantially in weight increasing the loads on soil and exacerbating compaction problems (Horn *et al.*, 2006).

Compacted soils, therefore, require effective management strategies to return them to an optimum physical condition improving quality and yield of crops, and also to reduce the risk of further compaction and the likelyhood of erosion. Biological methods to restore damaged soil include rotating crops and/or growing break crops giving a range of root patterns. Soil compaction can also be reversed by tillage which loosens the compacted soil (Spoor and Godwin, 1978). Any of these techniques require additional time and costs. Therefore, there is a need to find an approach that could reduce costs and energy use for compaction alleviation.

A better understanding of load transfer to the soil via agricultural tyres is therefore essential to provide improved solutions to tyre selection, as wheel traffic is the major cause of soil compaction (Soane and Ouwerkerk, 1994).

The negative effect of field traffic on soil properties has a long history. When horses were the primary source of power, it was observed that the 'passage of horse's hooves' was causing soil compaction. Kuipers and van de Zande (1994) assumed that a hoofprint has about the same contact area as a footprint and they found a typical value of the average contact pressure on the soil for a 0.750 tonne horse to be about 0.75 bar for a standing horse. For a walking horse the pressure was found to be about 1.5 bar and even more for a draught animal. Horse footprints had a smaller effect on soil compaction than agricultural vehicles because of their scattered distribution.

Steam engines were the first machines used to replace horse power on the field. They were extremely heavy, however, they did not cause soil compaction, as they did not travel over the fields, as they remained on the field headland. Later, steam engines became smaller, more manoeuvrable and versatile and were then introduced to till agricultural soil (Figure 1.2). They were still relatively heavy and often became 'bogged down' in fields under their own considerable weight (Vaughan, 2006), causing soil compaction. The introduction of smaller lighter tractors with internal combustion engines greatly reduced soil compaction damage. The evolution of these comparatively light tractors was a step towards improved soil management (Carpenter, 2003).

Figure 1.2 Steam tractor

The steady increase in machine power and weight over the recent decades has caused a negative effect on soil structure, workability, crop development and yield by increasing soil denisty. These heavier and more powerful machines were developed to improve mechanisation efficiency, reduce costs and improve the timeliness for crop management (Heuer *et al*., 2006). During the last 3 to 4 decades the mass of most agricultural and forestry machinery has increased by at least 4-fold (Horn *et al.*, 2006), which has resulted in an increase of soil compaction and damage. Wheel loads as high as 15 tonnes have been reported by Håkansson and Reeder (1994).

There is a need, therefore, to develop a management scenario which reduces soil damage and compaction. In order to do this, a better understanding of the soil contact pressure resulting from agricultural tyres is required.

Soil compaction occurs when soil particles are pressed together (usually by loading), reducing the pore space between them. Heavily compacted soils, therefore, contain few large pores and have a reduced rate of both water infiltration and drainage through the compacted layers, this occurs because large pores are the most effective in moving water through the soil. In addition, the exchange of gases is reduced in compacted soils, causing an increase in the likelihood of aeration related problems. Finally, soil compaction increases soil strength, making tillage more difficult and costly, and reduces the ability of roots to develop as they must exert greater force to penetrate the compacted layer. Lower numbers of roots in the soil consequently reduce yields (Brady and Weil, 2008).

The study on soil compaction began to intensify in the 1950s coinciding with the increase in agriculture mechanisation. Strutt (1970) in his report considered the state of soil damage and compaction. He found some soils to "suffer from dangerously low organic matter levels and they could not be expected to sustain the farming systems which have been imposed upon them". This resulted in several studies being undertaken into the issue of soil damage. Dwyer (1983) suggested that to minimize soil compaction it is necessary to keep ground pressure as low as possible. He went on to argue that to avoid excessive soil compaction tyres should be chosen to prevent deep sinkage.

The degree of surface compaction is largely determined by the ground contact pressure. Contact pressure can be reduced by having a larger contact area which can be achieved using dual wheels, radial tyres, low ground pressure tyres or tracks. Also an increase in tyre diameter or width creates a larger foot print so the area carrying the load is increased. As a consequence, tyre inflation pressure can be decreased resulting in a reduced contact pressure and thus less compaction (Ansorge, 2005). Surface compaction can also be reduced by trafficking when soil is in a less compactable state (has low moisture content and is not freshly cultivated) and loading tractors to give about 10% wheel slip (Department of Primary Industries and Water, 2007).

Another researched method of reducing compaction damage is to minimise the number of tillage operations. This has in many cases been adopted in the form of zero and/or minimum tillage systems (Chamen *et al.*, 1987; Douglas, 1990).

It has also been found that, the first pass of a vehicle or implement causes 70 - 80% of the total compaction in the soil. Controlled traffic farming systems have been introduced which involve confining many tillage and traffic operations to the same wheel tracks and separating the traffic lanes from the soil in which the crop grows. This has proven to have great potential benefits for the reduction of soil damage and compaction. Similarly soil compaction has been minimised by maintaining suitable stocking rates (Department of Primary Industries and Water, 2007).

Subsoil compaction is usually caused by heavy vehicle traffic on the field (Figure 1.3 shows sugar beet harvest: approximately 50 tonne harvester and 20 tonne trailer). Deep compaction is difficult to reduce as it is primarily determined by the axle load, which is defined by the weight of the tractor, any added ballast and load transfered under draft. Subsoil compaction can only be reduced by decreasing axle loads, however, this cannot be obtained in many situations. Subsurface compaction is difficult to overcome with tillage. The subsoil compaction effect can be repaired through deep tillage operations. A wide range of implements are used for this purpose including chisel tines, subsoilers, slant tines and oscillating tines. Spoor and Godwin (1978) assessed the quality of deep loosening using a range of rigid tines at different working depths and also with attached wings. They concluded that the attachment of wings to the tine foot and the use of shallow tines to loosen the surface layers in front of the deep tine allows more effective soil loosening. Overall, deep loosening is expensive and if carried out incorrectly can result in further soil compaction rather than loosening. Hakansson and Reeder (1994) reported that at depths > 0.4 m, the compaction may persist for a long period of time or even permanently so it is a serious threat to the soil productivity.

Figure 1.3 Heavy vehicle traffic on the field – sugar beet harvest

Despite the considerable amount of research on soil compaction conducted over recent years, soil compaction continues to be a problem. This is in part due to the fact that each of the soil management methods aiming at reducing compaction has some disadvantages. Sometimes controlled traffic or minimum tillage are not an option. Often large contact area tyres are not suitable for the purpose and tracks do not necessarily share the load equally over the entire

track. Up till now, soil compaction is not controlled and it has been recognised as a great problem of present agriculture.

Extensive research work has been carried out on the subject of agricultural tyres and rubber tracks considering their effect on soil compaction (e.g. Soane *et al.*, 1979; Soane *et al.*,1981; Smith and Dickson, 1988; Weise, 1990; Horn and Lebert, 1994; Ansorge, 2005; Ansorge and Godwin, 2006; Ansorge and Godwin, 2007) and the effects of soil compaction on field conditions and yield (Bateman, 1963; Flocker *et al.*, 1958; McKyes *et al.*, 1979; Negi *et al.*, 1981; Soane, 1983; Gunjal and Raghavan, 1986; Mander and McMullan, 1986; Voorhees, 1986; Stadie, 1987; Douglas, 1990; Soane and Ouwerkerk, 1994; Heuer *et al.*, 2006; Reintam *et al.*, 2006). However, little has been done on the matter of soil contact pressure appearing at the soil – tyre interface. Therefore, the assessment of the contact parameters is of great importance because of its consequences on soil compaction.

Chancellor (1976), Plackett (1983 and 1986) and Plackett *et al.* (1987) investigated the factors causing soil compaction. They found that the major factor was high soil contact pressure. They looked at the contact pressure resulting from agricultural tyres and then related it to the inflation pressure and carcass stiffness. They indicated that mean ground pressure could probably be defined as inflation pressure plus carcass pressure:

$$P_C = P_i + P_{CS} \qquad \text{Equation 1.1}$$

Chancellor's studies (1976) consider different factors affecting the relationship between soil pressure and compactability. The factors are as follows: moisture content, soil texture, vibration, repeated loading, loading speed and period. No experimental work of Chancellor was found to support his analysis and conclusions.

Plackett's experiment (1983) provides data for front and rear agricultural tyres showing the variation in contact area for increasing loads up to the maximum load for the minimum inflation pressure. His research indicates a simple method of measuring hard surface ground contact area. For most of his experiments, the mean ground pressure computed from the tyre load divided by the contact area was found not to be less than the inflation pressure of the

tyre. He suggests that the tyre carcass stiffness contributes to the ground pressure, and that this contribution is constant over the deflection range studied. The contribution of the tyre carcass stiffness was predicted by examining the load – deflection curves for a tyre. It was concluded that the carcass pressure added to the inflation pressure of the tyre correlates well with the mean ground pressure obtained in the test.

Additionally, Bekker (1956) cites that the pressure distribution in the case of an ideally elastic tyre and rigid surface would be uniform and equal to the pressure of inflation. However, the presence of the tyre treads and the stiffness of the carcass changes this relationship. He presents a simple contact pressure distribution for a solid rubber tyre and pneumatic tyre, both on a hard surface. The contact pressure distribution found for a tyre is not constant and varies depending on the stiffness of a tyre.

At present, there is not an agreed standard for determining the contact area or ground pressure of loaded agricultural tyres and there is limited information available which allows comparison to be made between different agricultural tyres in terms of the soil pressure they create. With the general increase in the size and power of tractors and a better understanding of the factors affecting plant growth there is a need for further detailed research on soil contact pressure caused by vehicular traffic on the land and for a more up-to-date investigation into the variety of agricultural tyres to allow the best tyre selection.

Few investigations of ground contact pressure resulting from agricultural tyres have been carried out. Chancellor (1976) and Plackett (1982, 1983, and 1986) investigated ground pressure resulting from agricultural tyres and then related it to the inflation pressure and carcass stiffness. Plackett's experiments (1983 and 1987) were conducted only on a hard surface and did not cover the whole range of working inflation pressure and load of the tyres tested. Additionally, these tests were carried out over twenty years ago and they covered relatively low loads, tyres manufactured in that era and static conditions. The considerations of Chancellor (1976) were only theoretical and were not proven experimentally. Bekker (1956) presented pressure distribution patterns under a solid rubber and pneumatic tyres but again only on a hard surface.

The problem of a pneumatic tyre running on a soil surface was investigated by a number of researchers (e.g. Söhne, 1953 and 1958; VandenBerg and Gill, 1962; McLeod *et al.*, 1966; Karafiath and Nowatzki, 1978; Diserens, 2006; Schjonning *et al.*, 2006b), but they did not fully consider this subject. This is probably due to the complexity of soil contact pressure determination and lack of any standard method of determining the contact area or contact pressure of a tyre operating in soil. The majority of these tests were carried out over twenty years ago when the researchers did not have adequate equipment to measure precisely the contact pressure distribution under a tyre. The continued increase in the size and weight of agricultural machines and knowledge obtained by the previous researchers indicate a need for a new concern about soil contact pressure caused by vehicular traffic.

As it was previously mentioned, the passage of agricultural vehicles over land transfers stresses through the soil profile via the tyre contact area, which results in soil compaction. The assessment of the contact pressure is of great importance because of its consequences on soil compaction. The studies include investigations of the soil pressures resulting from loaded agricultural tyres, which enable an improved tyre selection for better soil management.

Tyre contact pressure was considered to be an indicator of the potential to cause compaction in the upper layers of the soil (VandenBerg and Gill, 1962; Plackett 1984). It was due to the fact that soil compaction can result from high contact pressure and/or low soil strength (Soane *et al.*, 1981).

The contact pressure is a combination of tyre inflation pressure and the carcass stiffness of the tyre (Chancellor, 1976; Plackett, 1983). Therefore, determination of the contact pressure allowed for an estimation of the tyre carcass stiffness, which was considered as an equivalent pressure resulting from tyre carcass stiffness.

This work is a follow up to the earlier study on the effect of tyres and rubber tracks at high axle loads on soil compaction by Ansorge and Godwin (2007), which emphasises the importance of contact pressure distribution with respect to soil compaction changes. The previous study considers soil displacement, dry bulk density and penetrometer resistance which were measured to assess soil damage resulting from loaded tyres and tracks. It proved

that tracks cause less soil compaction than tyres and it confirmed that axle loads are less important than how they are distributed on the ground. Ansorge (2007) highlights the importance of soil contact pressure distribution, where he argues that a smooth pressure distribution is essential for reduction of soil compaction and it also agrees with the findings of Schjonning *et al.* (2008). In his work Ansorge (2007) also proposes a novel "in-situ" method to derive virgin compression line parameters where contact pressure was assumed to be uniform and was calculated as load over the area and reports on the need to have a full understanding of pressure distribution over the area of contact.

1.2 Project aim

To determine an effective method to measure the vertical pressure distribution on a hard surface and at a range of depths in the soil profile resulting from pneumatic agricultural tyres. From which the effect of the tyre carcass can be estimated and related to predictive methods.

1.3 Project objectives

(1) To develop a method to determine tyre contact pressure distribution on both hard surface and in the soil profile.

(2) To evaluate the influence of tyre inflation pressure, ply rating, tread pattern and load on the resulting hard surface and soil pressure.

(3) To determine the carcass stiffness of a number of agricultural tyres loaded to manufacturer's specification for different conditions.

(4) To investigate alternative methods to predict the carcass stiffness of the agricultural tyres and to attempt to develop an improved technique.

1.4 Outline methodology

The experiments involved determination of contact area and contact pressure for a range of tyres of differing ply ratings, tread pattern, inflation pressures and applied loads. It allowed an investigation of the effects of normal load, inflation pressure, tread pattern and ply rating on the resulting soil pressures to be conducted.

The experiments were carried out on a hard surface and in soil profile. They covered static and dynamic tests. For the hard surface tests, the tyres were loaded against a flat steel plate,

while the soil experiments were conducted in a sandy loam soil in controlled laboratory conditions to a series of soil depths above Tekscan sensors laid on a 70 mm steel plate. The aim of the hard surface tests was to determine the tyre deflection, contact area and surface pressure in the simplest form in a controlled environment. The contact pressure and deflection results obtained on a hard surface were used to estimate carcass stiffness of the tyres tested. The aim of the soil testing was to investigate soil pressure distribution resulting from agricultural tyres in the profile.

The work was carried out in two phases as shown in Table 1.1, which also refers to the relevant chapters for the results. The reader is also reffered to Table 3.1 which also includes the load and inflation pressure ranges. Phase 1 involved surface contact pressure investigations which were carried out on the hard surface. Phase 2 involved pressure distribution measurements in the soil profile conducted in the soil bin. Both phases involved different methods of measuring the pressure resulting from tyres. A simple ink technique (Plackett, 1983) was employed to determine the static contact patch of the range of agricultural tyres on a hard surface. This involved coating the tyre with black ink and pressing it onto a white card placed on a steel plate. A new application of Tekscan piezo-electric pressure mapping system allowed the real-time pressure distribution to be viewed across the contact patch using a sensor array. This was conducted by placing sensor mats on a hard surface and then loading the tyre onto the surface. Tekscan sensors were also used for pressure measurements in the soil profile, where they were buried in the soil. The system has not previously been used in soil contact pressure experiments with agricultural tyres, so there was a need to improve the performance of Tekscan sensors by designing a bespoke calibration and evaluation procedure.

Tekscan pressure study on the hard surface allowed tyre carcass stiffness to be determined and compared to the results obtained from the tyre deflection measurements and ink study. The results were also compared to a method based on the tyre manufacturer's data, which was developed in this project. Determination of the soil pressures below the tyres enabled an evaluation of the pressure transfer through the soil profile.

Table 1.1 Summary of the experimetal methodology

Phase	Experiment	Tyre	Size
Phase 1 Hard surface (reported in Chapter 5, 6 and 7)	Tyre deflection measurements and tyre contact area estimation using the ink method (static tests)	Inner tube	600/700/750R16
		Front tractor tyre	9.0-16
		Rear combine tyres: smooth and treaded	600/55R26.5
		Implement tyres: 5 ply ratings	11.5/80-15.3
	Pressure distribution measurements using Tekscan method (dynamic tests)	Front tractor tyre	9.0-16
		Rear combine tyres: smooth and treaded	600/55R26.5
		Implement tyres: 5 ply ratings	11.5/80-15.3
Phase 2 Soil profile (reported in Chapter 8)	Pressure distribution measurements using Tekscan method at a range of depths (dynamic tests)	Rear combine tyres: smooth and treaded (25, 100, 250, 400 and 550mm depth)	600/55R26.5
		Implement tyres: 5 ply ratings (100 and 250mm depth)	11.5/80-15.3

A critical review of literature relating to the subject of soil pressure with an emphasis on the previous methods for contact pressure determination – empirical and existing prediction models – used to determine the tyre contact pressure of agricultural tyres was carried out. Consideration of alternative ways of contact pressure prediction enabled development of an improved model for the estimation of pressure below agricultural tyres. At the end, recommendations for field practice were developed to improve soil management.

2 LITERATURE REVIEW

Compaction of agricultural soil by pneumatic tyres is a significant problem for agriculture as will be seen from the following literature review. Whilst there has been a significant volume of work on the subject, the interactions between soil and agricultural tyres are still not fully understood. The review of the current literature identifies previous work that is directly relevant to the study. It mainly reviews works on the topic of soil pressure and soil compaction resulting from loaded agricultural tyres.

Tyre manufacturers and users still do not completely understand the pressure that a pneumatic tyre applies to the soil surface in a range of conditions and the effect of "carcass stiffness". Therefore, there was a need for this research to review the previous methods used, investigate the soil contact pressure using modern measurement systems and a range of agricultural tyres and to develop a prediction model for the contact pressure estimation.

2.1 Introduction to tyres, soil stress and soil compaction

2.1.1 Tyre – definition and functions

A tyre is a rubber covering, typically inflated or surrounding an inflated inner tube, placed round a wheel to form a soft contact with the road (Soanes and Hawker, 2005). It is a heterogeneous and discontinuous object that is made from cords, wires and elastomers. It has complex elastic, plastic and viscous properties to operate under mechanical and thermal stress. Pneumatic tyres and balloons are a special case of structure where the tension in their skin is the reaction of the pressure of the gas or liquid inside (Gordon, 2006).

Inns and Kilgour (1978) identify the tyres to have four basic functions. These are as follows:

1) To support a load while both moving with minimum resistance and exerting low ground pressure.
2) To produce forces, at its contact with the ground, to provide tractive, braking or steering action.
3) To absorb shock loads and provide a degree of suspension.
4) To resist the abrading and cutting action of the surface over which they operate.

Gordon (1978) calls a pneumatic tyre a more important invention than the internal combustion engine, as *"the tyre has greatly changed the face of land transport"*. The first pneumatic tyres for agricultural purpose were fitted to two wheel carts by Dunlop in 1932. At present, manufacturers provide a wide variety of different tyre types, each intended to suit particular set of functional requirements. Each tyre is usually available in a range of sizes to allow the capacity of the tyre to be matched to the size and power of the machine. Tyre tread pattern and the size of the tyre are mainly influenced by the functional requirements of the tyre. These features give a good visual guide to intended use. Off-road tyres operate on a soft, deformable surface where the coefficient of friction between the tyre and surface may be low. Usually, its tread depth is increased and the tread density decreased giving distinct lugs, with spaces between. Lug action is not necessary on sand and concrete but is necessary on a slippery surface (VandenBerg and Reed, 1962), as the lugs enable the tread to penetrate and grip the soil. Bekker (1956) showed that thread design is of paramount importance in securing a firm grip between a tyre and a slippery hard surface. The thrust which the tyre can produce is more dependent on the strength of the soil in shear and less on tyre to soil friction. Soft soil tyres are prone to more rapid wear on road surfaces and the big separate lugs cause excessive noise and vibration (Inns and Kilgour, 1978). The basic rule of the tyre selection, given by Dwyer and Febo (1987), is: *"tractive performance is improved by fitting larger tyres and reducing inflation pressure and the improvement is greater the worse the ground conditions"*. Also heavier wheel loads improve tractive efficiency but that also leads to soil compaction. Generally, regarding tyres main importance on roads has safety, wear and comfort, while off-road (fields) – soil protection and draught transference.

There are two types of a pneumatic tyre construction – radial ply and cross ply, as presented in Fig 2.1 Inns and Kilgour (1978) describe tyre construction – cross ply tyres have both side wall and tread pattern that are substantially rigid to longitudinal and side loads. Their degree of rigidity depends on the angle of plies. This construction for agricultural tyres was used in the past. More popular at present, radial ply construction provides relatively flexible side walls and possibly lower carcass stiffness (which carry lower forces) with a very well braced tread. They have a longer tread life on hard surface and a lower drift angle for a given side load. The load capacity of the tyre depends on the strength of the tyre casing as indicated by the ply rating of the tyre. Originally the ply rating specified the number of layers of cotton

used in tyre construction. Now other materials with a higher tensile strength than cotton are used. Therefore, the ply rating is an expression for the strength on the tyre carcass which indicates the ratio of tyre strength to cotton strength and it does not necessarily state the number of plies. The ply rating value determines the maximum air pressure and carrying capacity of the tyre. At present, this has been superseded by the terms 'load index' and 'speed symbol'. These give the maximum load per tyre for the given speed rating.

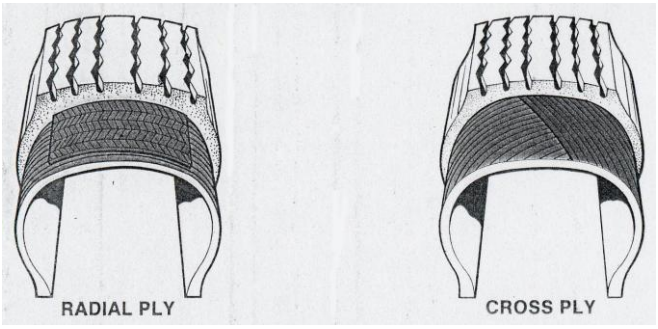

Figure 2.1 Ply construction of tyres (Inns and Kilgour, 1978)

The relationship between the load and contact area on a hard surface was investigated by Abeels (1976) who compared contact areas resulting from loading 12.4-36 6PR tyre of cross-ply to the same size tyre of radial construction. At a load of 10 kN the radial tyre was found to have 42% higher contact area than the cross-ply.

Karafiath and Nowatzki (1978) state that many theoreticians propose to use the rigid wheel as a model of the pneumatic tyre because they say that the pneumatic tyre behaves as a rigid wheel. However, they judge this statement to be suspect and being made in the interest of the simplicity of the research than in the interest of correct information on tyre behavior. The truth is that under some conditions pneumatic tyres behave as rigid wheels.

In return Plackett (1985) confirms that when the tyre is brought into contact with the soil, it can act in two different ways. It behaves as a rigid wheel if the stiffness of the tyre is greater than the maximum soil stress, calculated assuming that the tyre does not deflect. Alternatively, if the stiffness of the tyre is less than the maximum normal stress, then the tyre will deflect.

2.1.2 Soil stress

Movement of a wheel or track over the soil surface creates a pattern of stress within the soil mass that is caused by the compressive and shearing stress at the contact patch and dependant on various characteristics of the soil (Inns and Kilgour, 1978). The stresses normal to the contact surface are generally described as pressure, while the tangential stresses to the surface are referred as shearing stresses. Stress at the contact area effects the axle load and the tractive and steering action which the wheel is providing. The stress present between a tyre and the soil determines the amount of traction the device develops and the amount of soil compaction that may occur. The distribution and magnitude of the pressure and shearing stress over the contact area establish the capabilities of a particular tractive device for maximum traction and minimum compaction. A full knowledge of the factors affecting stress distribution would permit designing a moving device for maximum traction with minimum soil compaction (VandenBerg and Gill, 1962).

Boussinesq (1885) developed a number of equations for predicting the stress in the soil based upon a point load at the surface. The increase in stress within a uniform soil due to the application of a surface load may be estimated from the original elastic theory of Boussinesq or from modifications of the theory to account for the plastic behavior of the soil and non-uniformly distributed loads. The studies of Boussinesq are valid only for a solid, homogeneous, elastic, isotropic and semi-infinite mass which follows Hooke's law. Therefore, Boussinesq made the assumptions that the soil medium has all the patterns as elasticity, homogeneity, isotropy and semi-infinity. For the other assumptions of this theory see Jumikis (1962). The theory of Boussinesq says that if a force Q is applied at one point at the surface of a semi-infinite solid mass then the vertical compressive stress σ_z in any volume element, having the polar coordinates r and ϑ, is described by the following formula (see Figure 2.2 for an explanation of the symbols):

$$\sigma_z = \frac{3Q}{2\pi r^2}\cos^3\vartheta \qquad \text{Equation 2.1}$$

In Figure 2.2 (right) the polar principal stress σ_r is shown, that is found by the formula as follows:

$$\sigma_r = \frac{3Q}{2\pi r^2}\cos\vartheta \qquad \text{Equation 2.2}$$

So the vertical compressive stress σ_z also equals:

$$\sigma_z = \sigma_r \cos^2 \vartheta \qquad \text{Equation 2.3}$$

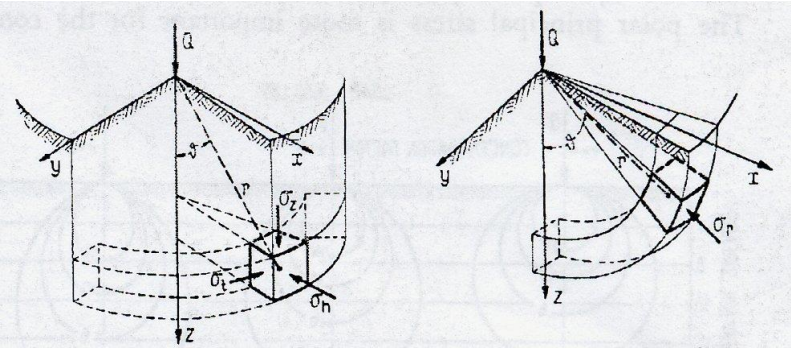

Figure 2.2 Vertical compressive stress (left) and principal compressive stress (right) in a volume element by a point load in a semi-infinite solid (Söhne, 1958)

Söhne (1953) developed a numerical procedure for calculating the vertical stresses in the soil caused by tyre loads. Following from the work of Boussinesq (1885), he concluded that a tyre does not transfer its load to a single point but to the whole soil-wheel contact area. To account for this, Söhne came up with the idea of dividing the contact area in a number of elements and assumed that point loads act in the centers of the elements.

Basic work concerning stress distribution in the soil due to surface loadings was done by Söhne (1958). He discusses the theory of Boussinesq and says that the numerous pressure measurements showed that there is a deviation in pressure distribution in the soil from the pressure distribution in a homogeneous isotropic mass. The compressive stress in the soil has a tendency to concentrate around the load axis. This tendency becomes greater when soil is more plastic due to increased moisture content and when the soil is less cohesive. He states that Fröhilch (1934) has considered this by introducing a concentration factor to Boussinesq's formulas referring to a homogenous isotropic mass. Söhne (1958) found different concentration factors for soils of different soil strengths and calculated stresses under a tyre load. Figure 2.3 shows the vertical compressive stress at the concentration factors ν =3 to 6 under a single load Q at the depth z. The lower curve ν =3 shows the distribution in an elastic isotropic mass according to the Boussinesq's theory. The curves ν =4 to 6 represent

distributions as they appear in soil. So the pressure distribution in soil can be calculated from the following equation:

$$\sigma_z = \frac{\nu Q}{2\pi z^2}\cos^{\upsilon+2}\vartheta = k\frac{Q}{z^2} \qquad \text{Equation 2.4}$$

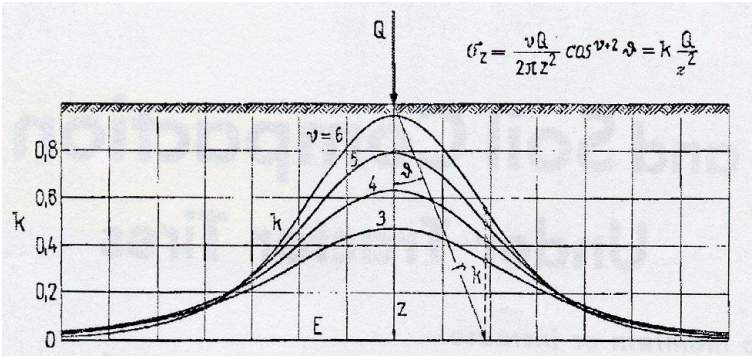

Figure 2.3 Vertical pressure stress at different concentration factors (Söhne, 1958)

An appropriate concentration factor has to be selected from experience and according to the measurements. The more the stresses concentrate around the axis of the load, the larger the factor should be. The work also showed that soil stress close to the surface is determined by the inflation pressure whereas soil stress in deeper layers depends upon the amount of wheel load. Discussing this, Schafer *et al.* (1992) concluded that the most significant limitation of these approaches was the assumption that soil has linear-elastic material properties. They add that agricultural soils rarely behave in a linear-elastic manner, therefore improved methods of predicting soil stress due to surface force are required. They must take into account non-linear stress-strain behavior.

The theories indicate that stress increases are greatest near the soil surface where they are most dependent upon the mean contact stress (ground pressure) between the load and the soil. With increasing depth, the increases in stress become increasingly dependent upon the magnitude of the load and less dependent upon the ground pressure (Smith and Dickson, 1988). The relevance of these theories to the compaction of soil due to the passage of agricultural vehicles has been reported by Blackwell and Soane (1981), Soane (1983) and Smith (1985).

The stress transmission in soil resulted from loading was also studied by Lamande *et al.* (2006a) who used load cells to measure soil pressure in the profile below the loaded area. One of the project aims was to evaluate the Boussinesq – Fröhlich theory of stress transmission in a soil by comparison of measured stresses in the soil profile and calculated stresses with the Boussinesq – Fröhlich equation. The quality of the soil stress prediction was not equivalent for all the treatments investigated. As shown in Figure 2.4, the prediction was better for the low rather than the high load. It probably happened due to larger vertical deformations in soil. Stresses are overestimated for a low contact stress and underestimated for a high contact stress but are of the right order of magnitude. That shows that the model for stress prediction has to be improved for a more accurate prediction.

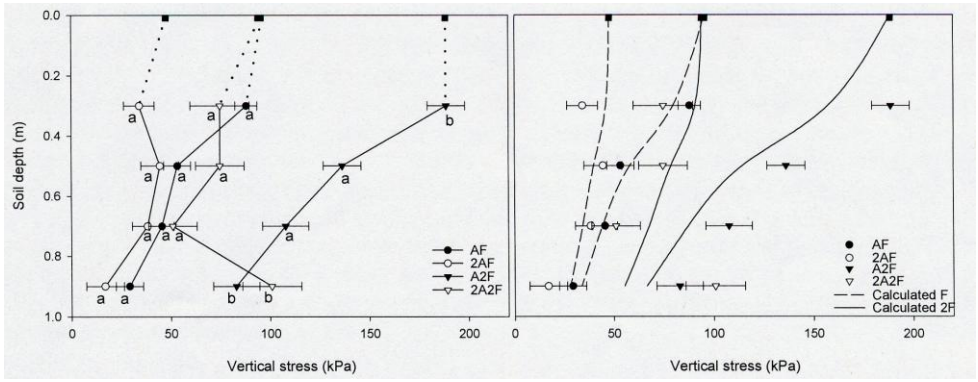

Figure 2.4 Vertical stress in the soil profile – average measured stress (left) and average measured stress with predicted stress (lines, right) for four loading treatment: AF – defined contact area and load, 2AF – doubling the contact area, 2A2F – doubling the contact area and load (Lamande *et al.*, 2006a)

When Söhne (1958) investigated the basic theories of the pressure distribution in agricultural soil, he cited that the stress created in the soil under external load depends on the size and shape of the area into which the force is introduced, the elasticity of the body transmitting the force and on the soil magnitudes, i.e. the grain size distribution, the pore volume and the moisture content. Additionally, the soil stress may vary with the duration of the load. It, therefore, differs to some extent from the stress distribution in solid, elastic bodies. Figure 2.5 shows pressure distribution under tractor wheels on hard loam soil for the different loads. Despite equal load per unit area on the surface, the lines of equal pressure stress reach down to a greater depth under the larger wheels with a higher load.

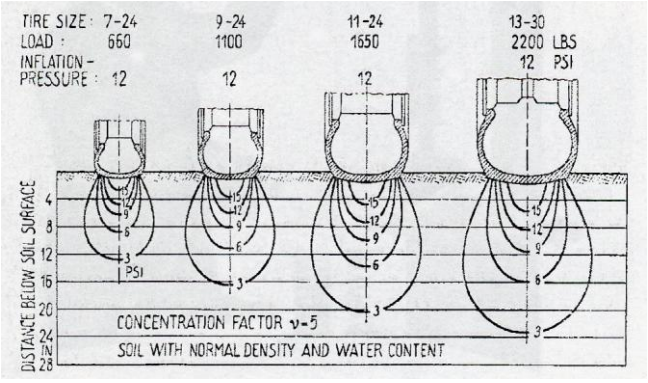

Figure 2.5 Curves of equal pressure under a range of tractor tyres (calculated values) (Söhne, 1958)

The shape of the pressure "bulbs" depends on the firmness of the soil as it is illustrated in Figure 2.6. In the case of hard, cohesive soil the bulbs are round, whereas in pliable, moist ground, the soil once more deflects to the sides and the pressure is concentrated at the centre. In soft soil the pressure bulbs become slimmer and reach to a greater depth.

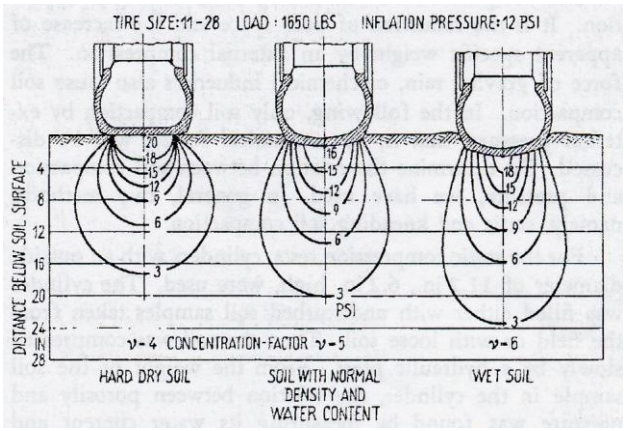

Figure 2.6 Curves of equal pressure under a tractor tyre for different soil conditions (calculated values) (Söhne, 1958)

The research carried out by Keller and Arvidsson (2004) lead to the similar conclusion on the factors of the soil stress that was concluded to be a function of the following factors: wheel load, wheel arrangement, tyre inflation pressure, contact stress distribution and soil conditions.

The inflation pressure, tyre size and carcass strength were considered by Soane *et al.* (1981) to control distribution of the forces at the tyre-soil interface, which is influenced by the initial strength of the soil. Therefore, the forces over the area of contact with the soil and the initial soil strength control the magnitude and distribution of stresses in the soil under the tyre.

2.1.3 Soil compaction due to tyres

The compressive stress occurring in the soil causes compaction. There are many definitions of soil compaction. The most appropriate definition appears to be given by Craig (1997), who defines soil compaction as *"the process of increasing the density of a soil by packing the particles closer together with a reduction in the volume of air but with no change in the volume of water"*. The process continues until the soil solid particles are forced into a dense state where they cannot be compacted further by compression alone (Inns and Kilgour, 1978). Schafer *et al.* (1992) say that soil is compacted when a force system exceeds the strength of the soil. Figure 2.7 compares soil structure for a non-compacted and compacted soil, where soil particles were squashed closer together and it drastically reduced spaces between them. The plant, therefore, does not have the same access to the water, air and nutrients and may suffer as a result (Agricultural Training Board, 1989).

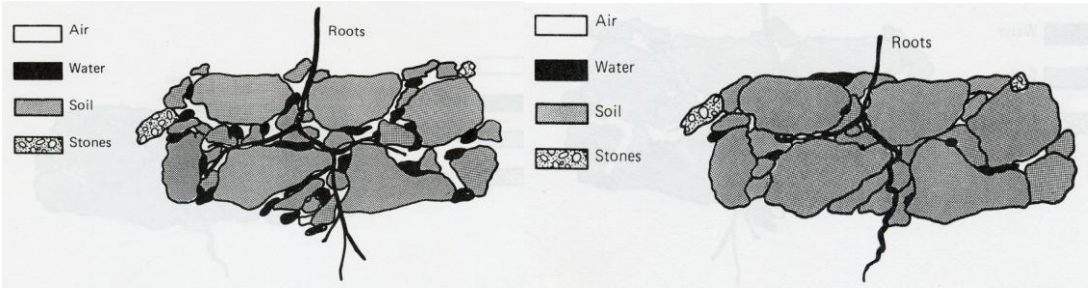

Figure 2.7 Mechanism of soil compaction (Agricultural Training Board, 1989)

The degree of compaction of a soil is measured in terms of dry bulk density that is the mass of solids only per unit volume of soil as given by Craig (1997):

$$Q_d = \frac{q}{1+w} \qquad \text{Equation 2.5}$$

Schafer *et al.* (1992) defined three functions of soil compaction management in crop production, which are: to provide optimum mobility and traction for the movement of

machines on the fields, to provide an optimum environment for plants and to provide for optimum conservation of soil and water resources. Soil compaction can be caused by a number of factors. Chancellor (1976) points out factors, which can be classify as natural forces, animals, heavy machinery and tillage tools. The last two factors cause the majority of soil compaction and are completely within man's control. Agricultural Training Board (1989) says that 90% of soil damage in terms of soil compaction is caused by agricultural tyres. Soil compaction changes physical and mechanical characteristics of soil which severely inhibit the capability of the soil to provide proper water uptake to the plant root system. Wheel traffic in fields is a major source of forces causing soil compaction (Soane *et al.*, 1981 and 1982, Taylor and Gill, 1984).

Whitlow (2001) states that the compaction is dependent on the following factors:

- The nature and type of soil,
- The water content,
- The amount of compaction attainable under field conditions,
- The type of machinery causing compaction.

Soil is especially susceptible to compaction when it is at the optimum water content. As water is added to a dry soil, it is absorbed and creates films around the soil particles. As the absorbed water films increase in thickness the particles become lubricated and are able to pack more closely together, so the density increases. At a certain point the porewater pressure in absorbed films tends to push the particles apart and so with further increases in water content the density decreases. The maximum dry bulk density, therefore, occurs at optimum water content as shown in Figure 2.8.

Soil loading inducing lower stresses than the soil precompression stress cause mainly elastic deformations, while loading giving greater stress causes soil compaction (Koolen and Kuipers, 1983). So Horn and Lebert (1994) argue that the risk of soil compaction could be minimised if the applied stress is lower than the soil precompression stress at any depth as in such a situation all deformations are elastic. However, that was not always found to be true. Keller (2004) analysed data from a number of tyre loading experiments and found that soil deformations were also created when measured stress was smaller than the precompression

stress. Also Kirby (1991) concludes that compaction damage can appear when the normal stress exerted by a tyre or track exceeds a value smaller than the precompression stress. A number of authors showed that the value of precompression stress is dependent upon several factors including the method of its determination (Koolen, 1974; Lebert e*t al.*, 1989; Arvidsson and Keller, 2004; Keller *et al.*, 2004). Therefore, soil compaction cannot be fully avoided by reducing the applied load to value of the precompression stress (Keller and Arvidsson, 2006).

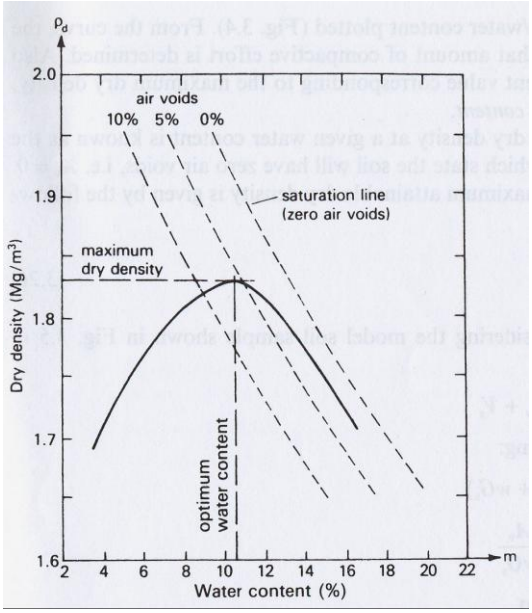

Figure 2.8 Dry bulk density vs. water content relationship

In consideration how to manage soil compaction, Schafer *et al.* (1992) points out the following issues which should be thought of: the sources of the force systems which cause compaction, distribution of the stresses which are caused by these forces, response of the soil to the stresses and consequences of the compaction to the cropping system. Schjonning *et al.* (2008) stated that to their knowledge, construction of agricultural tyres is based on empirical experience on tyre durability and traction, not on an overall aim of reducing soil compaction.

2.2 Effects of soil compaction

Trukmann *et al.* (2006) considers soil compaction as potentially a major threat to agricultural productivity and the main form of soil degradation in Europe. Mechanical methods are mostly used to eliminate compacted soil layers, however they are expensive and energy-consuming.

Raper *et al.* (1995b) highlight it by saying that soil compaction not only affects crop yields, but also increases energy usage to till compacted layers. Soil compaction can also affect water quality when infiltration is reduced and thus soil erosion is increased. The degree of compaction desired for crop production varies depending on biological, chemical and physical soil properties, crop requirements and management systems (Boone, 1988).

2.2.1 Influence of soil compaction on crop growth and yield

There are different opinions on the actual effect of soil compaction on yield. Most researchers recognise agriculture practices as a degradation of soil and causing increasing risks of diminished capacity for productive cropping. However, some authors say that crop yield does respond to compaction in a very complicated way. These problems were studied in a range of projects.

Inns and Kilgour (1978) report that excessive compaction may lead to poor soil aeration, delayed drainage, difficult root penetration and clod formation. The general rule declares that plant growth and yield usually suffer appreciably if the soil porosity is reduced below 10 – 15%.

Past field research on the plant response to a compactive force acting on the soil was reviewed by Voorhees (1986). The general rule from his research is that if axle loads are less than 5 tonne, compaction will be limited to the surface 300 mm of soil. Axle loads less than 5 tonne are typical for most field operations except harvest and transporting. Generally, the research confirms that surface layer compaction can significantly affect crop yield depending on soil texture and climatic conditions. Yields will be likely increased by a moderate increase in the soil compaction level during relatively dry conditions. Yields will be decreased by increasing compaction during wet seasons. Generally, soils with high clay content experience greater crop yield response to compaction (negatively or positively) than coarse textured soils, which was also found by Negi *et al.* (1981). Harvest and transport equipment is generally much heavier and its axle loads range between 10 and 20 tonne/axle. The effect of subsoil compaction from high axle loads on crop yield has not been researched as much as surface compaction effects. However, it was investigated that crop yield response to compaction in subsoil is also sensitive to texture and climatic conditions but appears to be mostly a negative

response. Axle loads greater than 10 tonne can cause compaction to a depth of 600 mm and result in significant yield decreases. The experiments covering a range of soil textures and crop species clearly show the significance of subsoil compaction from heavy axle loads (Figure 2.9). These findings agree with Dwyer (1983), who says that to avoid compaction of the subsoil, the maximum axle weight should not exceed 6 tonne. While to minimise compaction of the topsoil, vehicles should be fitted with tyres which are big enough to carry the maximum load at inflation pressure not higher than 1 bar when operating on firm soils and 0.5 bar for operation on soft soils.

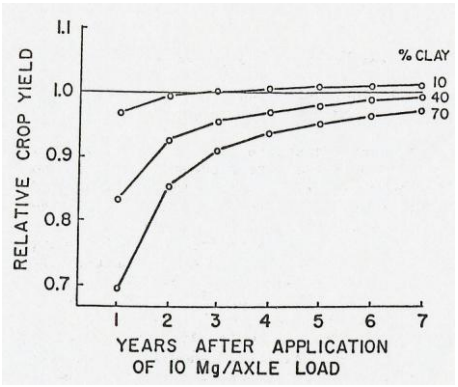

Figure 2.9 Relative crop yield as an effect of 10 tonnes load application (Voorhees, 1986)

Figure 2.9 presents the pronounced effect of soil texture on the crop yield. Soils with 10% clay showed only a slight initial yield reduction, an effect that lasted only one year. As percent clay increased to 40 and 70%, initial yields were decreased by 17 and 30%, respectively, and took longer to recover. A 70% clay soil was still showing a yield reduction 7 years after initial application of high axle loads. Additionally, Voorhees (1986) states that deep mechanical loosening of compacted soil can be detrimental because subsequent wheel traffic on the loosened soil can recompact the subsoil to a higher bulk density than its original value. That confirms a need for a modern investigation of the variety of agricultural tyres to allow the best tyre selection. Some similar findings were quoted by Chancellor (1976) after Das (1972 – unpubl.), who concluded that the main problem caused by soil compaction is restricted root penetration during early stages of plant growth. That prevents plants from using water stored in the soil at the greater depths.

Dense soil has a tendency to hold moisture more tightly, so plants have to exert greater stress to extract the water from the soil (Bodman and Constantin, 1965). That is why soil compaction results in increased moisture stress in plants and large amount of the soil moisture content which is held at tension beyond the extractive capacity of plant roots (Warkentin, 1971).

Research of Gunjal and Raghavan (1986) shows that yield of green peas decreased at the beginning and then increased with the continuous increase of contact pressure. The investigation proposes the theory that the maximum yield can be obtained if the optimum machine size is used for a given area.

Chancellor (1976) cites his personal communication with Carter, who conducted an experiment of controlled wheel traffic application, but it did not show significant differences in yield. Similar conclusions were obtained by Fountaine *et al.* (1952) who looked at the effect of compaction on yield of grain and straw. Also Heuer *et al.* (2006) found that the repeated passes of a combine sugar beet harvester caused subsoil compaction, although, beet growth and yield did not react. Conversely Flocker *et al.* (1958) found that stands of legume and brome grass cover crops were reduced by soil compaction, but yields were affected only at the highest compaction level (see Table 2.1).

Table 2.1 Effect of soil compaction on crop performance and soil conditions (Flocker *et al.*, 1958)

Compaction treatment	Dry bulk density 0-2.4 inch depth	Air-filled pore space	Water infiltration rate	Cover crop stand	Cover crop yield
	g/cm^3	percent	cm/hr	percent	g/ cm^2
Light	1.25	30.8	4.17	58.4	0.0444
Moderate	1.40	22.6	0.97	49.1	0.0442
Severe	1.56	13.6	0.10	36.5	0.0337

A similar pattern was found by Bateman (1963) who measured corn yields on two soils that were treated with various combinations of compaction and tillage methods. The results proved that only the most severe compacting treatment resulted in significant corn yield

reduction on one soil only. All other treatments did not show any pattern of significant yield differences.

The effect of various levels of contact pressure on the yield of grassland was investigated by Stadie (1987). Increased contact pressure caused plastic flow of the soil allowing ruts to be formed. The results showed that the increase of the contact pressure causes yield losses increase. An increase in yield on some treatments indicated an optimum level of contact pressure. This finding agrees with the concept of optimum levels of compaction that was proved by Soane (1983) and described in Section 2.3.

A similar experiment was carried out by Mander and McMullan (1986), who were also comparing the effect of contact pressure on the yield of grassland. The results also showed the same tendency with the yield losses at the high contact pressures of the standard tyres, while the lower pressure treatments of dual wheels and Terra-Tyres produced no losses, and in some cases provided an increase in yield. The effect of soil density at the moisture content on the silage corn yield was studied by McKyes *et al.* (1979) and is presented in Figure 2.10.

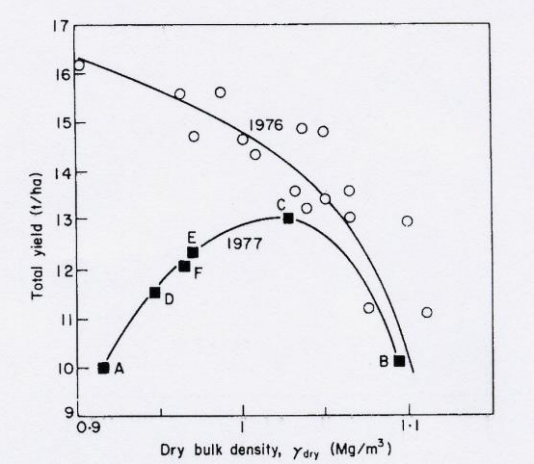

Figure 2.10 The effects of soil dry bulk density on yield (1976–wetter year, 1977–drier year) McKyes *et al.* (1979)

Douglas (1990) compared soil and crop responses in a conventional grassland traffic system with two alternative systems – a zero traffic system and a reduced ground pressure system. It was found that total dry matter yield was significantly greater after zero and reduced ground traffic system than a conventional traffic system.

Also Chamen *et al.* (1987) carried out an experiment to monitor the effects on soil and winter wheat crop responses of three levels of tyre/soil contact pressure, in conjunction with direct drilling and shallow cultivation. The tests were conducted on a clay soil with wheeling treatments varying in pressure from 0 to 2.5 bars. Three levels of tyre/soil pressure were provided by:

- Conventional tractors and equipment which ran on standard tyres at 1.0 bar to 2.5 bars inflation pressure (called Normal treatment),
- Modified tractor and machines with additional and sometimes oversize tyres at inflation pressure not exceeding 0.55 bar (called Low Ground Pressure treatment),
- A zero traffic system which operated with 2.4 m track tractors and machines used on uncropped permanent tramlines (called Zero Traffic treatment).

Measurements of soil bulk density and cone penetration resistance showed that the Normal and Low Ground Pressure systems returned the highest values, while the Zero Traffic system – the lowest. However, there was no significant difference in yield recorded between Normal, Low Ground Pressure and Zero Traffic direct drilled treatments. Only the combination of the Zero Traffic and shallow cultivation led to some drop in yield. Therefore, the authors conclude that the crop performance is more likely to be reduced by under-compaction than over-compaction in the wheeling pressure range 0 to 2.5 bars.

In summary, the relation between soil compaction and yield is not straightforward. It involves some interactions of soil, water and air as it influences various stages of plant development. In this discussion it is necessary to remember that an optimum soil compaction is required for appropriate seed germination. Each species has an optimum soil bulk density where gives maximum yield. The densities lower and higher than the optimum cause yield reduction. At present agricultural equipment is getting larger, has higher capacity, applies higher loads and pressures, therefore, its harmful effect on the soil – plant relationship tends to increase.

An irregular loading pattern which occurs in the field results in a spatial difference in the severity of soil compaction. It may also provide the reason for understanding individual reactions of plants to these spatial differences (Kuipers and van de Zande, 1994).

2.2.2 Effects of soil compaction on soil irrigation and drainage

One of the main effects of soil compaction is to reduce the size of pore space, which reduces the water flow in soil. Compacted soil also tends to have lower hydraulic conductivity, that is why it is more prompted to flood for long periods. The reduced infiltration capacity of soil may also lead to higher erosion susceptibility. When Chancellor (1976) was discussing this subject he pointed out the problem of compacting flooded soil, that causes further compaction and reduced drainage rates. Gebhardt *et al.* (2006) looked at the soil stress – deformation behaviour and its change in saturated hydraulic conductivity as a function of load. Mechanical stress results have shown that fine textured soils are susceptible to greater decreases in saturated hydraulic conductivity after compaction than coarse textured soils. It was due to already very low fraction of macro-pores in the primary conditions prior to compaction. Coarse textured soils show primarily high hydraulic conductivities and due to that part of their macro-porosity remains unaffected by compaction.

Another problem is that more compact soil also requires more frequent irrigation and the irrigation costs become greater on compacted soils than on non-compacted soils (Chancellor, 1976). The data obtained by Flocker *et al.* (1958) and presented in Table 2.1 indicate how extreme effects compaction can have on the infiltration rate. It is due to breaking up the largest pores through which water flows more freely and to reducing the space by compaction.

2.2.3 Soil tillage resistance and cloddiness affected by soil compaction

Compacted soil has a higher resistance to tillage forces and after tillage it has a tendency to be more cloddy. Chancellor (1976) says that intensive tillage can break down the clods, but leaves the soil with structure that is susceptible to compaction and cloddiness. Additionally, when he discussed this subject, he quoted findings of Bateman (1959) who noticed that compacting soil with four passes of a truck with tyres inflated to 5 bar caused a 92% increase in soil tillage resistance. Also Lyles and Woodruff (1963) looked at the response of soil to compaction in terms of the tillage resistance and cloddiness. Their experimental data shows a four times increase in draft force if the soil bulk density rises 0.29 t/m^3. Additionally, the same soil density increase caused an increase in cloddiness from 5% to 65%. As well as an increase of clods, the resistance of the clods to mechanical breakdown also increased. These

effects were less when the soil was drier. The same pattern was found by Flocker *et al.* (1958) as presented in Table 2.2.

Table 2.2 Effect of soil compaction on cloddiness and clod strength (Flocker *et al.*, 1958)

Compaction treatment	Dry bulk density 0 - 2.4 inch depth	Clod population	Clod density	Clod shear strength
	g/cm^3	grams	g/cm^3	g/cm^2
Light	1.25	8 440	1.49	492.6
Moderate	1.40	21 770	1.50	745.9
Severe	1.56	43 680	1.64	865.6

2.3 Options for reducing compaction under wheels

As stated by Plackett (1984), soil compaction is mainly a function of the pressure applied to the soil surface. Therefore, the amount and type of tillage required to loose compacted soil is closely dependent on the amount and type of traffic imposed on the soil during the previous crop season (Soane, 1983).

Soane *et al.* (1982) quotes that there are three primary ways of reducing the overall compaction of field soil by agricultural vehicles:

- reduction of the number of passes of conventional machinery,
- reduction of the vehicle mass and the contact pressure of wheel system,
- confinement of traffic to permanent or temporary wheel tracks (controlled traffic).

A diagrammatic representation of these options in relation to the types of vehicles is shown in Figure 2.11 (Soane *et al.*, 1979). Traffic reduction can be achieved by combining in one pass operations such as cultivation and seeding or certain types of harvesting operations using currently available machinery and common sense attitudes to machinery management. Ground contact pressure can be minimised by reducing the load on the wheels and increasing the contact area. Weight may be decreased by removing ballast to the minimum. Alternatively, contact area may be increased by lowering inflation pressure to the permissible minimum or by increasing tyre size or by fitting dual wheels.

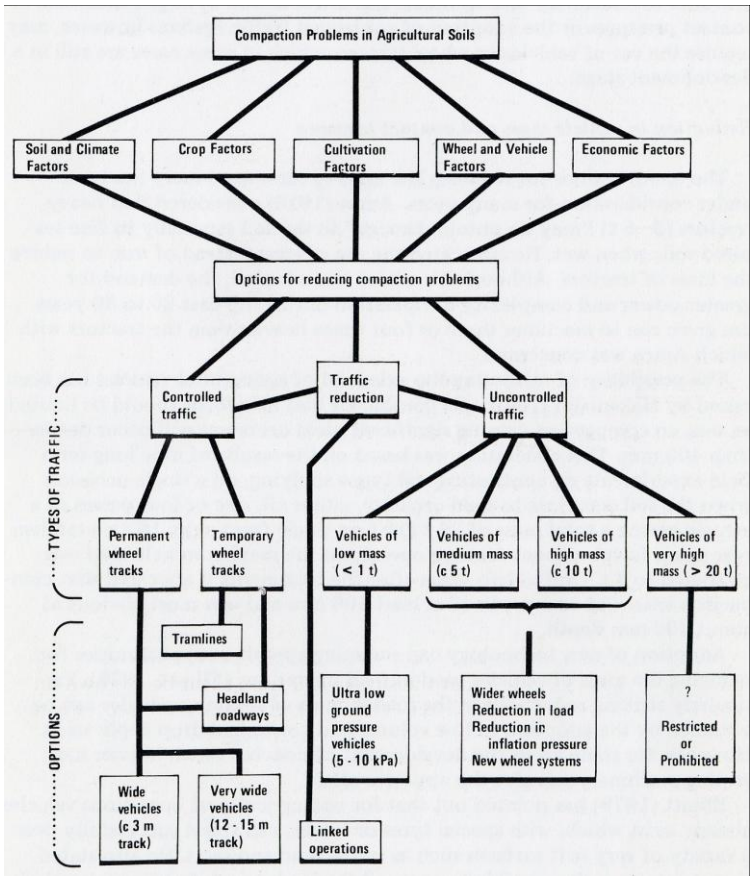

Figure 2.11 Diagram of the options for reducing soil compaction (Soane *et al.*, 1979)

Chancellor (1976) adds that in case of increasing the contact area, the total volume of compaction does not necessarily reduce, however, most of the soil receiving most of the compaction will be near the surface where soil density can more easily be decreased through conventional tillage. Additionally, Inns and Kilgour (1978) point out that confining field operations, that produce high soil pressure, to times when the soil is dry, leads to the minimization of soil compaction.

Soil compaction caused by a tyre at a given load and soil condition depends on tyre carcass stiffness, inflation pressure, diameter and section width. If the tyre carcass is more flexible, then more load is carried by the rolling surface and less on the edges of the carcass. Low inflation pressure of the tyre results in an increase in the contact area and tyre flexibility (Ansorge, 2005). The effects of tyres and tracks at high axle loads were studied by Ansorge and Godwin (2007), where soil compaction resulting from loaded tyres and tracks was assessed. The study proved that TerraTrac system causes less soil damage than tyres (at an

overall load of 12 tonne for the tracks and 10.5 tonne for the tyres). From that a conclusion was made that the way of load distribution to the ground is very important. Antille *et al.* (2008) also looked at the effects of tyre size on soil compaction and provided an indicator for tyre selection for combine – harvester tyres at high axle load and a range of inflation pressure. Their results show that increased tyre size and low inflation pressure reduced both soil deformation and the increase in soil bulk density beneath the tyres. After one passage of tyres on the soil the increases in soil bulk density was approximately 25% for the low bulk density soil (1.20 t/m^3) and only 2.3 – 5% for the high bulk density soil (1.60 t/m^3). The authors also found the advantage of increasing tyre size (i.e. contact patch area) and lowering inflation pressure where the tyre with the highest inflation pressure gave a significantly higher increase in penetration resistance obtained from drop-cone penetrometer compared with the tyres with lower inflation pressures. This study also highlights the importance of tyre contact pressure distribution, as it shows that a high load can be transferred to the soil with or without extremely harmful effect, which depends on the ground pressure distribution.

Dawson and Pearson (1985) proved that compaction is caused by a high contact pressure at the tyre/soil interface and, to a lesser extent, wheelslip and discussed that both of these factors can be minimised by a good tyre selection and usage of a central tyre inflation system which permits the vehicle tyre pressures to be regulated while on the move when there are variations in tyre loading. The system relates to the general tractor tyre rule that it should be as large as possible and at the minimum pressure for the load it is carrying in accordance with manufacturers' recommendations.

Weise (1990) carried out an investigation of soil deformation resulting from loaded rolling tyres in the controlled conditions of a soil bin. The experimental results let him analyze the effects of load, ground pressure and tyre type on soil compaction. The relationships were found between tyre load and rut dimensions. However wheel type appeared to be the most significant. Weise also studied the effect of splitting a load into two and showed a significant reduction in the size of the rut and in the extent of the soil displacement but just a little reduction in the maximum soil density obtained. The optimum split ratio was found to be 50% / 50%. However, the author states that greater benefits in reducing soil compaction could be achieved by reducing tyre inflation pressure or by using more favorable / suitable tyres.

2.4 Contact pressure under wheel – investigations

Determination of a tyre contact area is a way to conclude an average surface pressure under a wheel. When a pneumatic tyre is loaded on a flat rigid surface, it deflects as in Figure 2.12 (left). Thus, on a rigid surfaces tyre deflection defines the contact area (Plackett, 1984). This area is a function of tyre deformation that relies on tyre size, carcass stiffness, tread design, inflation pressure and axle load. On deformable surfaces the patch area is also dependant on the soil strength (Sharma and Pandey, 1996). At the first view, rigid surfaces do not appear to be of any interest in agriculture, however, Plackett (1984) says that when a pneumatic tyre is loaded against soil it can act in two ways. In the first case when the stiffness of the tyre is greater than the maximum suitable normal stress for the soil, then the tyre will behave as a rigid wheel as presented in Figure 2.12 (middle). In case when the tyre stiffness is less than the surface, the tyre will deflect as shown in Figure 2.12 (right). In both cases soil deformation causes the formation of a rut, however, as the rut depth decreases then the case of a tyre running on soil approaches that of a tyre running on a hard surface.

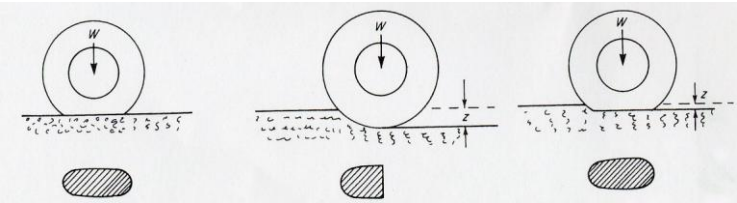

Figure 2.12 Tyre deflection schemes – on a hard surface (left), a rigid wheel on soft soil (middle) and a pneumatic tyre on soft soil (right) after Plackett (1984)

Koolen (1995) considers three types of soil behaviour under wheels: non-deforming, hardening and plastic flow. Non-deforming situation was described above as the hard surface scheme, when the soil stresses resulting from a loaded wheel are lower than the soil strength. Hardening and plastic flow happen when the wheel-induced soil stresses exceed soil strength. In case of hardening type behaviour the soil deforms and becomes more compacted until a new state of soil strength is reached which is able to support the stresses resulting from loaded tyre. Flow type behaviour occurs when a loading induces soil flow without volume change.

For simplicity, the contact area of tyres is often assumed to be circular and the contact pressure is uniformly distributed (Kirby *et al.*, 1997; Arvidsson *et al.*, 2002; Poodt *et al.*,

2003). The contact area of tyres has usually a rectangle, ellipse or torus shape (Karafiath and Nowatzki, 1978). For these shapes Eberan-Eberhorst (1965) derived relationships between tyre deflection and contact area for a range of inflation pressure. Hallonborg (1996) proposed a description of the contact area as a super ellipse, which describes the shape and size of different tyre-ground contact areas ranging from circles over ellipses to squares and rectangles. The super ellipse can assume a wide range of shapes for each quadrant of the contact area. Several researchers showed that tyre contact pressure is not uniform (Bekker, 1956; VandenBerg and Gill, 1962; McLeod *et al.*, 1966; Burt *et al.*, 1989; 1992; Gysi *et al.*, 2001; Trautner, 2003; Way and Kishimoto, 2004). Way *et al.* (2000) concluded that distribution of soil-tyre contact pressures on lugs of radial tractor tyre on loose soil are more uniform if the tyre is used at load and inflation pressure recommended by the manufactures in comparison to overinflated or underinflated tyre, which was also confirmed by Schjonning *et al.* (2008).

Karafiath and Nowatzki (1975) observed and reported a general schematic representation of the relationship between soil strength, tyre stiffness, sinkage and deflection (Figure 2.13). Relaying on the figure it is possible to determine tyre deflection and sinkage from input values of tyre stiffness and soil strength. Figure 2.13 shows two examples. The bottom part of the graph illustrates a flexible tyre operating on strong soil where small sinkage and large tyre deformation appears. The top of the diagram demonstrates an opposite soil and tyre conditions resulting in small tyre deflection and large sinkage.

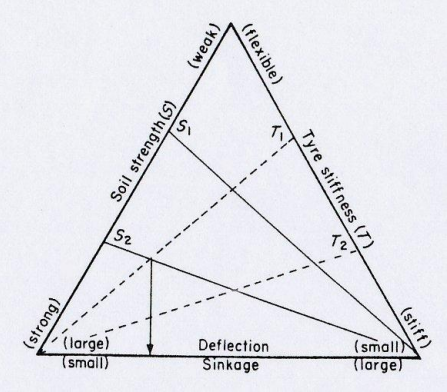

Figure 2.13 Schematic representation of the relationship between soil strength, tyre stiffness, deflection and sinkage (Karafiath and Nowatzki, 1975)

2.4.1 Contact pressure under a wheel on a hard surface

Stresses measured on an unyielding surface represent the upper limit of stresses that would develop in a soil that yields relatively little under the tyre load. At the Waterways Experiment Station (Waterways Experiment Station, 1964) tyre interface stress measurements were carried out with some sensors placed on the hard surface. The general pattern of stress distribution observed in these tests demonstrated a fairly uniform stress distribution over the center of the contact area and stress concentration at the perimeter of the contact area, called "edge stresses". The researchers stated that the magnitude of the stress in the center of the contact area is related to the tyre inflation pressure, while these edge stresses are related to the stiffness of the tyre sidewall.

Inns and Kilgour (1978) state that a lattice plot can be used to present information on the relationship between contact area, load and inflation pressure for a tyre operating on a hard surface. An example of the lattice curves is presented in Figure 2.14.

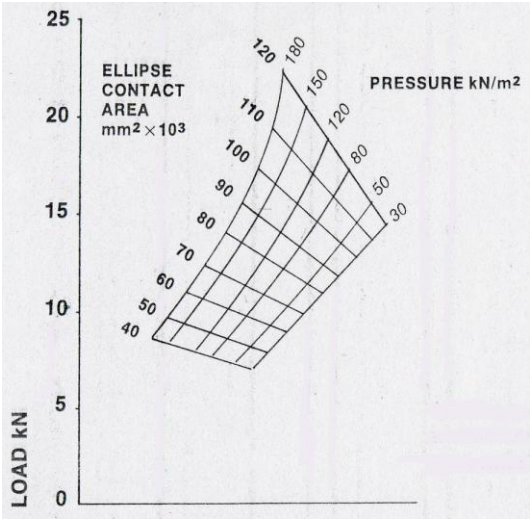

Figure 2.14 Contact area vs. load and inflation pressure (Inns and Kilgour, 1978)

They also report that the dynamic characteristics of tyres are slightly different to static. The dynamic stiffness is on average 10% greater than static for rear traction tyres. However, at high pulls and low speed, when the tangential load due to traction is in the same order as the vertical load, the dynamic stiffness of the tyre is reduced by about 10%. Additionally, old tyres have about 25% lower stiffness.

Chancellor (1976) discussed a general principle, reported previously by Bekker (1956), that *"the pressure existing between a pneumatic tyre and the surface on which it rolls is approximately equal to the inflation pressure of the tyre"*. He explains that if the vertical load on a tyre increases, then the contact pressure remains constant while the tyre flattens so the product of the average pressure and contact area is equal to the vertical load. The other possible situation is when the load on the tyre is constant and the inflation pressure is reduced. In this case, the tyre will flatten to increase the contact area just enough so the principle that the average pressure and contact area are equal to the vertical load is obtained again. These findings are illustrated by Söhne (1952) in Figure 2.15.

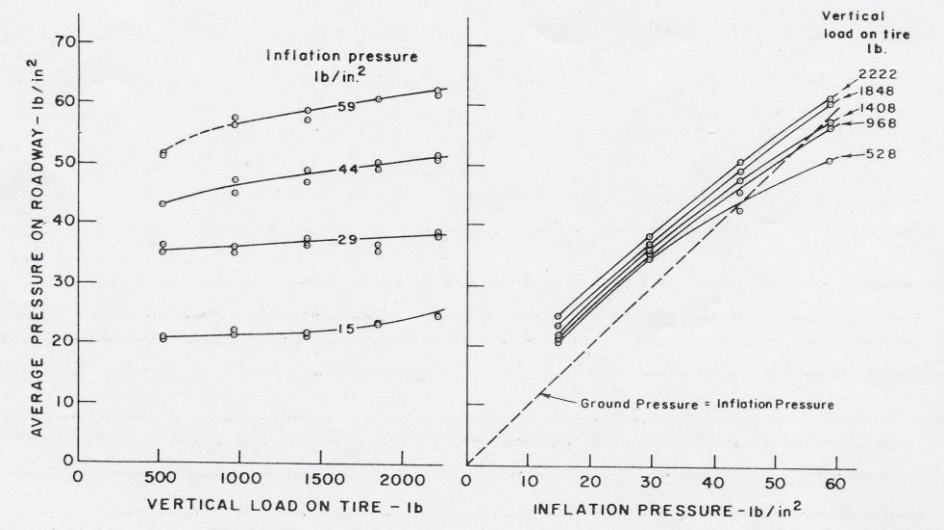

Figure 2.15 Relationship between the tyre vertical load / inflation pressure and the average surface pressure obtained on a firm roadbed (Söhne, 1952)

Factors that could cause the tyre contact pressure to deviate from inflation pressure, reported by Chancellor (1976), are following:

- The carcass stiffness of the tyre walls transmits some forces to the surface. Those forces tend to be concentrated around the edge of the contact area. This pattern was also reported by VandenBerg and Gill (1962).
- When a tyre rolls on a very soft soil, the soil near the front of the contact patch does not have enough strength to deflect the tyre against the inflation pressure, then the contact pressure is lower than the inflation pressure in this zone. If a tyre is rolled more than once over the same soil area, then the soil on the later passes affects the tyre

as would a more firm soil. This was illustrated in Figure 2.16 by Söhne (1952). Sometimes if the tyre inflation pressure is very high and soil is very soft, then the pneumatic tyre will behave like a rigid wheel. In this case tyre-soil contact pressure may all be below inflation pressure.

- Tyres equipped with lugs have usually higher pressure at the surface of lugs than the inflation pressure and the area of lug contact is much smaller than the area of tyre-soil contact patch. Trabbic *et al.* (1959) proved that by measuring pressure on the interface between tractor tyre lugs and soil (Figure 2.17). The pressure concentration on the lugs is most pronounced on a firm surface, while on a soft surface the tyre undertread surface holds substantial load. However, Chancellor (1976) states that the pressure concentration effect mainly occurs at the soil surface and upper soil layer, while at greater depths there is little difference between pressures created by lugged and smooth tyres.

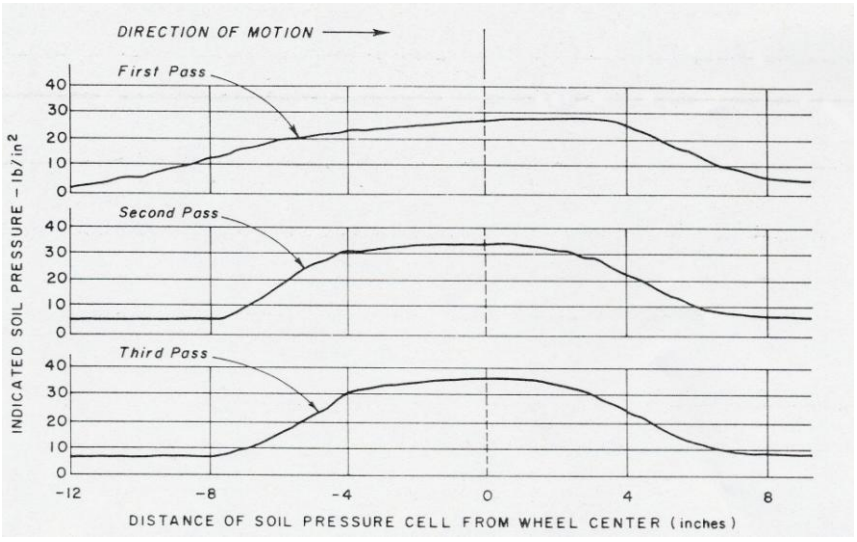

Figure 2.16 Pressure measurements in an agricultural soil at a depth of 75 mm – Firestone 9 – 40 loaded to 0.7 tonne at 2.5 bar (Söhne, 1952)

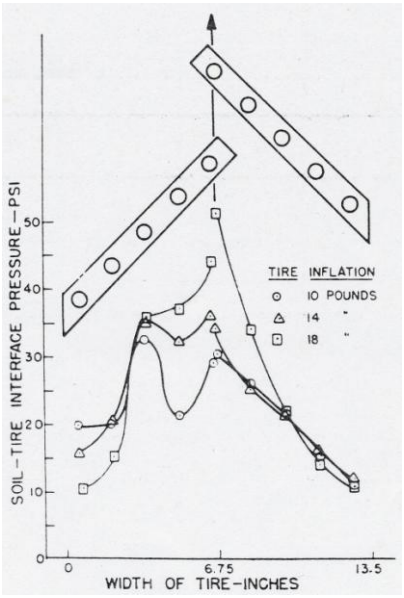

Figure 2.17 Contact pressure on the interface between tractor lugs and soil (left) and on the carcass between the lugs (right) (Trabbic *et al.*, 1959)

Similar conclusion were found by Bekker (1956) who says that the pressure distribution in case of an ideally elastic tyre and rigid surface would be uniform and equal to the inflation pressure. However, he states, the presence of tyre treads and the carcass stiffness change the picture. He gave a solid rubber tyre and pneumatic tyre (both on a hard surface) a careful consideration. Starting from a solid rubber tyre (Fig. 2.18a) and assuming that the local tyre pressure is proportional to the tyre deflection, the contact pressure is proposed by the equation:

$$P_C = c_r f \qquad \text{Equation 2.6}$$

Similarly, the maximum pressure in the centre would be:

$$P_{\max} = c_r f_{\max} \qquad \text{Equation 2.7}$$

Then the maximum contact pressure was modified as a function of the wheel load and maximum deflection, as follows:

$$P_{\max} = \frac{0.53W}{ab\sqrt{f_{\max}\frac{D}{2}}} \qquad \text{Equation 2.8}$$

Burt *et al.* (1992) studied different approaches of the peak tyre contact pressure estimation and compared them to the values obtained in their experiments. The research gave a conclusion that the peak pressures measured on compacted soils are much higher than mean pressures obtained from measurements and much greater than pressure calculated as load divided by contact area. On compacted soil, maximum pressures were found to be equal to the inflation pressure. Söhne (1958) showed that the maximum pressure at the soil-tyre interface for tractor tyres with no high lugs is equal to 1.4 to 2 times the mean pressure. While, Kolobov (1966) stated that the peak pressure for a tyre lug on firm soil is three to four times the tyre inflation pressure. Later Burt *et al.* (1989) reported that the normal stress distribution on loose and firm soil above a hardpan was found to be very non-uniform and the maximum pressures were two to three times the inflation pressure. Rusanov (1994) advise that the maximum contact pressure can be estimated by multiplying the mean ground pressure by a factor of 1.5. Recently, Lamande and Schjonning (2008) in their investigation found that the maximum stress (measured at 100 mm depth) exceeded the mean ground pressure by a factor of 1.7 – 2.4 for trailer tyres.

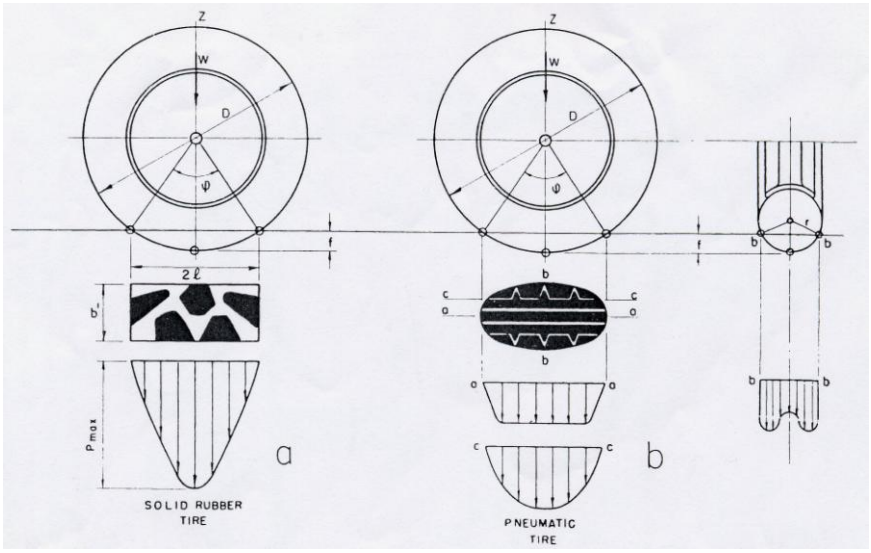

Figure 2.18 Contact pressure distribution for a solid and pneumatic tyre on a hard surface (Bekker, 1956)

According to further considerations of Bekker (1956), the problem of the maximum contact pressure for pneumatic tyres appears to be very complex since the pressure distribution depends not only on the inflation but also on the stiffness of the tyre carcass. Figure 2.18

shows pressure distribution in the various sections. In this case the following semi-empirical equation was proposed:

$$W = (P_i + P_{CS}) \frac{f_{\max}{}^2}{f_{\max} + 1} \sqrt{2Dr - 2 f_{\max} (\frac{D}{2} + r)} \qquad \text{Equation 2.9}$$

Concluding, Figure 2.18 illustrates the complexity of pressure distribution on the hard surface.

Plackett (1983) conducted contact area studies for agricultural tyres to determine tyre ground pressure on a hard surface. His research indicates a simple method of measuring hard surface ground contact area. The contact area of the tyre is determined by painting the tread with black ink and loading on to a piece of white card placed on the loading platform. The experiment provides data for agricultural tyres showing the variation in contact area for increasing loads up to the maximum load for the minimum inflation pressure. Plackett says that the mean ground pressure computed from the tyre load defined by the contact area is never less than the inflation pressure of the tyre. Additionally, mean ground pressure is constant over the deflection range studied. It suggests that the tyre carcass contributes to the ground pressure, and that this contribution is constant over the deflection range studied. This finding proves the theory of Chancellor (1976).

The contribution of the tyre carcass stiffness was predicted by examining the load deflection curves for a tyre. Figure 2.19 illustrates a set of load deflection curves for one type of tyre. It shows that as inflation pressure decreases, the slope of the load deflection curve also declines. If a tyre had no carcass stiffness, then the slope of the load – deflection curve would be zero at zero inflation pressure, as the carcass would not be able to support any load. Therefore, plotting the slope of the load – deflection characteristic against deflection pressure, as presented in Figure 2.20, and extrapolation of the curve allowed to find the carcass stiffness at zero inflation pressure (x value) and the pressure at which the carcass stiffness is zero (y value). The latter value was considered by Plackett (1983) to represent tyre carcass stiffness. It was concluded that the carcass pressure added to the inflation pressure of the tyre correlates well with the mean ground pressure obtained in the test. Plackett (1983) also suggested that

inflation pressure was a good indicator of mean ground pressure in the absence of mean ground pressure measurements.

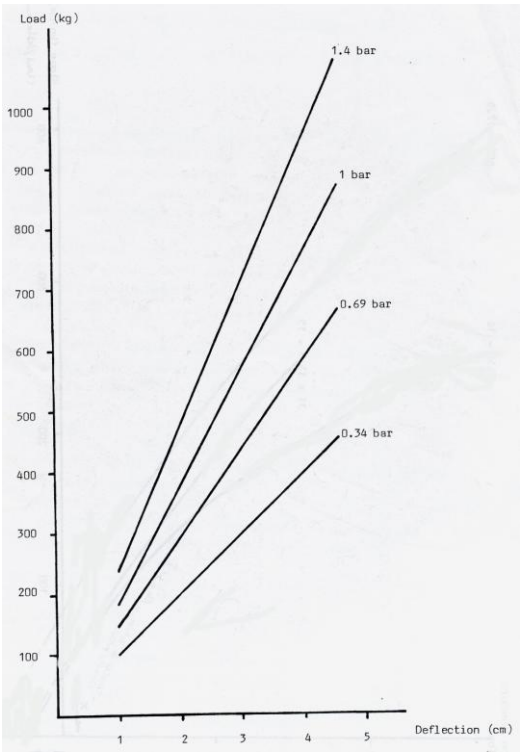

Figure 2.19 Load vs. deflection curve (Plackett, 1983)

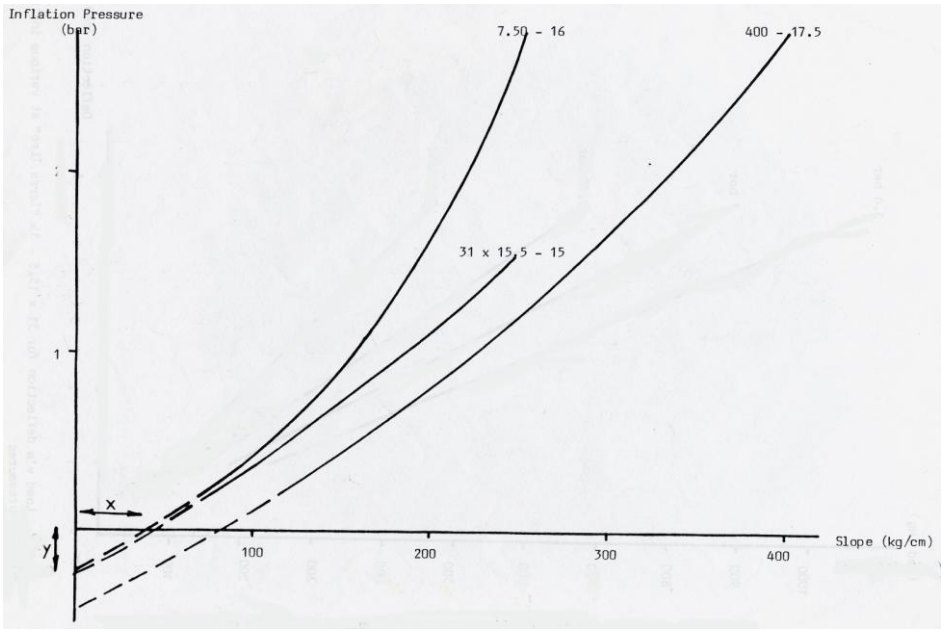

Figure 2.20 Carcass stiffness estimation from the inflation pressure vs. slope of load – deflection curve (Plackett, 1983)

Plackett (1983) concluded saying that it is likely that in the future mean ground pressure could be defined as inflation pressure plus carcass pressure. This would have the advantage that once the carcass pressure for a particular tyre is known, manufacturers would only have to quote a single value of carcass pressure for each tyre. Mean ground pressure could then be calculated from the inflation pressure for any particular application. Unfortunately, the contact area results obtained by Plackett (1983) represent static and hard surface conditions only, so the contact pressure on deformable surfaces was not fully investigated here.

Plackett *et al.* (1987) also carried out research on the ground pressure of agricultural tyres. He used tyres from different manufactures and a specially designed laboratory rig to measure contact area and convert obtained values into ground pressure. The investigation was conducted for tractor driving wheel tyres, trailer/implement tyres, low pressure flotation tyres and other types of agricultural tyres. Several different sizes of tyre were used for each machine type. Maximum permitted loads corresponding to the minimum and maximum allowable inflation pressures were applied. The research provides experimental data obtained for the wide range of agricultural tyres. That is why this reference is relevant in terms of the range of expected results. It has some limitation because there is no detailed description of the research method, its conditions and the results obtained in the investigation are not discussed.
The ink method of hard surface contact area measurements (1983) was also employed by Williams (1987), who investigated a range of aspects affecting a lightweight self-propelled crop treatment vehicle. His results showed that the mean contact pressure is never less than inflation pressure. This would seem to suggest that the tyre carcass contributes to the mean contact pressure that proves again Chancellor's theory. This carcass stiffness contribution appears to be constant over the range of loads and inflation pressures studied. The tyre carcass stiffness was determined as the carcass pressure at zero inflation pressure. At the end of the study, Williams (1987) compared his results to the figures obtained from the algorithms for calculating the tyre-soil contact pressure proposed by Rowland (1972) and Dwyer (1983). The magnitude of both Rowland's and Dwyer's relationships showed no agreement with the hard surface mean ground contact pressure found in the experiment of Williams (Table 2.3 and 2.4).

Table 2.3 Contact pressure comparison for Goodyear 29x12.00-15 tyre (Williams, 1987)

Inflation pressure (bar)	Mean maximum pressure after (Rowland, 1972) (bar)	Ground pressure index (Dwyer, 1983) (bar)	Mean contact pressure as load divided by area (Williams, 1987) (bar)	Inflation pressure + carcass stiffness (Plackett, 1983) (bar)
0.33	0.39	0.55	0.50	0.49
0.50	0.43	0.59	0.67	0.66
0.67	0.47	0.65	0.84	0.83
1.00	0.55	0.75	1.17	1.16
1.33	0.58	0.81	1.49	1.49

Table 2.4 Contact pressure comparison for Michelin 375/R75-20 tyre (Williams, 1987)

Inflation pressure (bar)	Mean maximum pressure after (Rowland, 1972) (bar)	Ground pressure index (Dwyer, 1983) (bar)	Mean contact pressure as load divided by area (Williams, 1987) (bar)	Inflation pressure + carcass stiffness (Plackett, 1983) (bar)
0.33	0.25	0.34	0.63	0.66
0.50	0.26	0.35	0.80	0.82
0.67	0.28	0.39	0.88	0.99
1.00	0.32	0.44	1.21	1.32
1.33	0.34	0.47	1.60	1.66

The same method of contact area determination was employed by Kumar and Dewangan (2004) when investigating contact characteristics of a power tiller tyre. Their results showed that both deflection and contact area varied linearly with inflation pressure in the range of normal loads selected for the study. Also mean contact pressure was found to be almost linear to the inflation pressure. The ground pressure obtained in the research was greater than the inflation pressure at low inflation pressures, which indicates the tyre carcass contribution to the contact pressure at lower inflation pressure. However, as the inflation pressure was increased, the ground pressure was found to be less than the inflation pressure at all normal loads.

Also Walczyk (1995, 2000, 2001) and Walczykova and Walczyk (1999) investigated deformation characteristics of agricultural pneumatic tyres using the same method for contact area determination with employment of video camera and computer image analysis program

for data processing. The measurements of tyre deflection and contact pressure were done for a number of tyres and on the basis of the results specific equations for calculating deflection and contact pressure of each tyre were developed (dependant on tyre load and inflation pressure). Also tyre stiffness was considered, which was calculated as the ratio of the wheel load and deflection on a rigid surface.

Upadhyaya and Wulfsohn (1990) conducted simulation studies to predict the effect of tyre size, load and inflation pressure on the contact geometry of a rigid surface. They showed that for small tyre deflections the contact patch is elliptical, but as the deflection increases the width of tyre-soil contact is limited by the tread width and the contact area becomes more rectangular with curved edges. Figure 2.21 illustrates their finding.

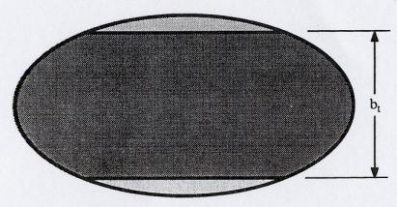

Figure 2.21 Contact area for a tyre on a rigid surface (Upadhyaya and Wulfsohn, 1990)

Plackett's method (1983) of hard surface contact patch determination was modified and applied by Oliver (2002) who investigated contact pressure of a 4x4 tyres on hard and sand surfaces. To measure the contact patch on a steel plate he applied a film of oil on the contact area of the tyre and then it was deflected to a given load on to a sheet of paper. The oil soaked into the paper under pressure providing a contact patch. Then the paper was scanned and contact patch was cut out and weighted on a precision balance. Tyre contact length and width were determined from the image. A similar method was used to obtain the static contact area on sand soil, which was discussed in Section 2.4.2.

A simple method of contact area measurements was also used by Wheeler and Kilgour (1994), who conducted an investigation leading to improve the self cleaning ability of Airboss segmented tyres in wet clay conditions. One part of the study concentrated on the measurements of total and tread only areas, both on soil and hard surfaces. For the hard surface tests glass plate with a grid and raised edge that retained milk was used. When the tyre

was loaded on the plate, the milk clearly showed the contact patch pattern. The area was observed by filming the underside of the glass.

Goodyear and Dunlop used extensively Tekscan pressure sensing system to measure contact pressure distribution below tyres on hard surfaces. Their measurements were often attached by under tyre photography through glass plates allowing them to verify TekScan system's suitability to this application (Eatough, 2002). Additionally, Eatough, (2002) evaluated Tekscan ability to be used on a soil surface (Section 2.4.2).

Gill and VandenBerg (1968) state that in another method of measuring soil stress distribution, small metal strips were placed under the loaded tyre while it was standing on a flat plate. The force needed to pull the strips from underneath the tyre was related to the normal load by means of the coefficient of friction of the strips. Depending on the location of the strips, the normal pressure could be estimated for various areas beneath the tyre. He also discusses the method of the contact area measurements in the dynamic conditions. A common method used is to roll a tyre through the soil and then stop and lift from the soil. However due to the ability of a pneumatic tyre to reform its original shape when it is unloaded, and any decrease in the load on a tyre causes it to move while it is still in contact with the soil. Thus, this method may lead an error. The proposed technique that overcomes this difficulty is to place solidifying material inside the tyre and maintain the deformation of the tyre until it has set. In this case, even if the tyre may try to reform, the cast retains the loaded shape of the carcass.

2.4.2 Contact pressure under wheel on a soil surface

Measurements of soil surface pressure in yielding soils have been undertaken by several investigators. As the soil deforms under the tyre load, the contact area increases and a natural reduction of the average value of the contact pressure occurs. Additionally, yielding of the soft soil levels the high peaks in the contact stress distribution at the perimeter of the contact area that occur at the hard surface. Therefore, the average pressure measured on a rigid surface represents an upper limit to the average stress in soft soil (Karafiath and Nowatzki, 1978).

In the discussion on pneumatic tyre-soil interactions Karafiath and Nowatzki (1978) offer the general relationship between the average contact stress and inflation pressure proposed by various researchers. The equation is as follows:

$$P_C = c_1 P_i + p_{CS} \qquad \text{Equation 2.10}$$

Bekker and Janosi (1960) proved that p_{CS} does not depend on the inflation pressure, as suggested in the equation above. Besides they concluded that the equation works for both soft and hard surfaces. For the tyre they tested p_{CS} was found to vary from 0.16 bar to 0.33 bar depending on the load and c_1 was 1. Several other investigators, that determined contact pressure below tyres, also found c_1 and p_{CS} values. For example, Simon (1964) indicated that c_1 is 0.6 for high inflation pressure, in return Ageikin (1959) found that c_1 is from 0.9 to 1.0 and p_{CS} from 0.41 bar to 0.69 bar depending upon the construction of tyre.

Bekker (1960) proposed soil pressure-sinkage relationship which results from civil engineering soil mechanics and has a form of:

$$P_C = [k_c / b + k_\phi] z^n \qquad \text{Equation 2.11}$$

Inns and Kilgour (1978) quote that relationship between contact patch area, load and inflation pressure in soft off-road conditions is very complex. Soft soil deforms and the contact area increases reducing the deflection of the tyre for a given load and inflation pressure. They say that it is often convenient to assume that the contact area is rectangular and its dimensions are close to:

$$width = 0.87b \qquad \text{Equation 2.12}$$

$$length = 0.31D \qquad \text{Equation 2.13}$$

However, these formulas are simplistic and do not even include parameters describing soil conditions or tyre inflation pressure.

Methods of measuring the contact stress and deformation of a pneumatic tyre operating in soil were reviewed by Plackett (1986). The review shows how difficult it is to determine the

dimensions of ground contact area. The assessment covers three possible positions of transducer location, these are:

(i) on soil surface,

(ii) on a sheet situated at an interface,

(iii) in the carcass of a tyre.

The author proves that the technique of installing transducers in the ground surface is suitable only for hard surface measurements, since the transducers can be rotated and moved during the passage of a wheel, giving inaccurate results. Alternatively, pressure measuring mats have some advantages that they are portable, easy to mount and give a quick answer. However, their accuracy is limited (especially on a soft surface). Plackett considered embedding transducers into a tread of tyre as the best method of measuring contact stress. However, the following problems may be associated with this technique:

(i) The transducer has to be isolated from stress caused by bending of a tyre carcass.

(ii) The application of eccentric loads on a transducer causes measurement errors.

(iii) The transducer sensing face must be mounted flush with the surrounding tread.

There is also another problem not mentioned by Plackett, which is the fact that the sensing element will most likely be made of a material with different properties to that of the tyre so this will change the behaviour of the tyre in the sensor location. The problems highlighted above were not overcome by Plackett (1986) and attempts to find a small transducer mounted in the tread of a pneumatic tyre and measuring contact pressure were not successful. He has not been able to carry out any experimental work to measure tyre contact pressure on soil surface. However, Plackett (1982) states that values of contact area measured directly on a hard surface are often quoted by the manufacturers as contact area in soil.

The stress distribution between a flexible traction device and a soil surface are more difficult to measure. Stress transducers register them when they are in contact with the surface. Correlating their registration with their position indicates the contact surface and pressure. If transducers are used, their orientation is rarely known when the tyre deforms, so direction of the force and contact area cannot be determined (Gill and VandenBerg, 1968). However, the Plackett's review of tyre deformation methods proves that a displacement transducer mounted into the air cavity of the tyre is the most suitable method of measuring tyre deflection. The

experiment carried out with a linear variable displacement transformer (LVDT) mounted into the air cavity of a agricultural drive tyre lets compare the tyre deformation at the three inflation pressures used on both hard and soft surface. The results show that for a high inflation pressure tyre deformation is greater on the hard surface. As inflation pressure is reduced, the levels of tyre deformation for the soft and hard surfaces are more comparable. Therefore, this indicates that soil deformation decreases significantly with reduced inflation pressure, causing tyre deformation and not soil deformation. In all cases tyre deformation increased when the inflation pressure decreased (Plackett, 1986).

Gill and VandenBerg (1968) state that at the Waterways Experiment Station (1961) stress transducers were embedded in a rigid steel wheel and the stress along the dynamic area of contact could be determined. The location of the wheel was associated with the location and orientation of the transducers at all the experimental time. Therefore, the normal pressure obtained was converted to a vertical pressure. The experiment was conducted in a clay soil and the pressure distribution seemed to have the maximum pressure in front of the center of the wheel. There appeared to be some discrepancy between the total weight applied to the wheel and the weight obtained from the vertical pressure distribution. It was probably due to the fact that the tangential components also support the tyre and they were not measured by the type of transducer used. Transducers that measure normal as well as tangential pressure should be employed there.

Pytka (2006) proposed a new idea for off-road contact pressure determination. He correlated tractive forces with the mean stresses in soil generated under a vehicle's load. In the experiment he used truck vehicles and SSTs (stress state transducers) designed by himself and buried in the soil to measure the soil pressure (Figure 2.22). It is a grouping of six strain gage type pressure transducers positioned relative to each other. In that new case the pressures captured can be calculated into a complete stress state.

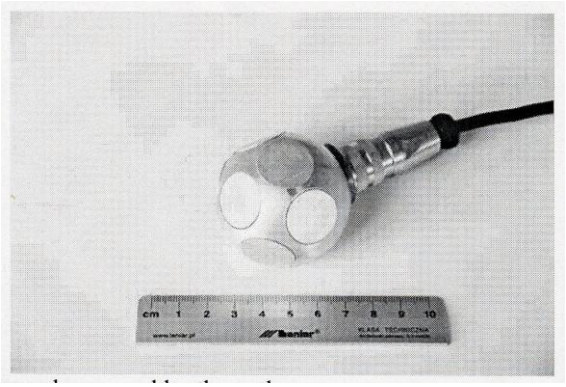

Figure 2.22 A stress pressure transducer used by Pytka (2006)

Oliver (2002) carried out exploratory studies to investigate the effect of wheel load, inflation pressure and slip on a tyre deflection and contact area under static and dynamic conditions. The studies were carried out on a steel plate (see Section 2.4.1) and sand surface using the tyres available for 4x4 Sports Utility Vehicles. The contact area measurements on sand are more difficult that other types of soil due to the "fluid" nature of the sand. In the experiment Oliver (2002) used a fine film of oil that he applied on the tyre. When the tyre was loaded on the sand surface the sand stuck to the contact area and then it was measured directly from the tyre using a measuring tape. The length was measured in the center and at 30 mm intervals, width – also at the center and 50mm intervals. Oliver used these dimensions to make an approximation of the tyre contact area. For the dynamic conditions the author looked at the tyre deformation measured with transducers placed inside the tyre. As the location of the transducer was known, it was possible to measure the contact length of the rolled tyre. Oliver (2002) explored the influence of wheel load, inflation pressure and slip on the tyre deflection and contact area. The size and shape of the contact patch and their relationship with tyre deflection was used in a performance of prediction model. The studies evaluated tyre stiffness to be the most influential criteria in determining the tyre contact area. It was shown that the contact area can be maximised on sand by reducing the stiffness of the tyre by reducing inflation pressure. The shape of contact area of the tested tyres was between rectangular and elliptical, depending on the tyre properties and the operating conditions. The author of this project converted the contact area results obtained by Oliver into the average contact pressure data under a loaded tyre. According to Chancellor (1976) *"pressure existing between a pneumatic tyre and a surface on which it rolls is approximately equal to the inflation pressure of the tyre"*. That was true for the hard surface where the average contact pressure was higher

than the tyre inflation pressure. However, in sand the average contact pressure was lower than the inflation pressure. The reasons for this appear to be two facts which are: for soft soil, the soil can flow aside the tyre and soil deformation which gives larger contact area and pressure non-uniformity at the contact patch.

Smith and Dickson (1984) estimated the static tyre/soil contact area by spraying kaolin powder liberally on the soil around the boundary between the tyre and the soil. Then the tyre was removed by reversing the vehicle. After that a rigid plastic sheet with a 40mm square grid was used to determine the area. The results obtained in this technique allowed calculation of a mean tyre/soil contact stress for a range of agricultural vehicles. For most of the vehicles mean contact stresses were significantly lower than the tyre inflation pressure which was explained in the paragraph above. The same technique for the contact area estimation on the soil was used by Wheeler and Kilgour (1994) and Schwanghart (1991).

Also Diserens (2006) measured contact area of agricultural trailer tyres in the field. The average contact pressure calculated as load over the area was found to be below inflation pressure which was already discussed. Inflation pressure was found not to be sufficient for estimation of ground pressure. Size of the tyre and load were also proven to be essential variables in assessing soil contact pressure resulting from wheeled traffic.

Some other data on the distribution of pressures under agricultural tyres loaded in a soft soil have been established by experimental work of VandenBerg and Gill (1962) and McLeod *et al.* (1966). They investigated various wheels at varying inflation pressure and produced pressure distribution graphs. VandenBerg and Gill (1962) used five strain gauged pressure cells of 2 inch diameter installed into a firm sand soil in a line parallel to the direction of tyre travel. The cells were placed flush with the soil surface and the smooth tyre was slowly driven over the line of cells. No soil deformation occurred during the passage of a wheel because the soil was very compact. They also embed transducers into the tread rubber of pneumatic tyres. The smooth tyre was driven on five different soft soils (sand, silt loam, sandy loam, silty clay loam, clay). Location and orientation of the pressure cells used is shown on Figure 2.23. The results obtained by the pressure cells in the tyre were compared to that obtained on a firm soil surface, and they appeared to be similar.

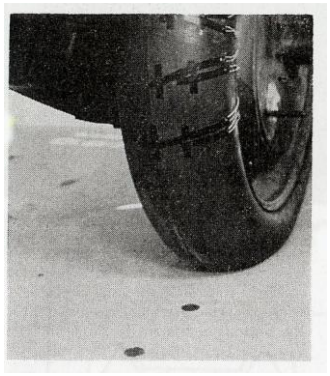

Figure 2.23 Location of pressure cells in the tyre and soil (VandenBerg and Gill, 1962)

Figure 2.24 shows typical pressures obtained in their experiments at different experimental conditions. The effect of tyre sinkage can be noticed on soft soil. It causes some extension of the pressure pattern. In front part of such pattern soil compression is lower and it is not sufficient to cause the average contact pressure equal to tyre inflation pressure, thus the tyre does not deflect distinctly in this zone.

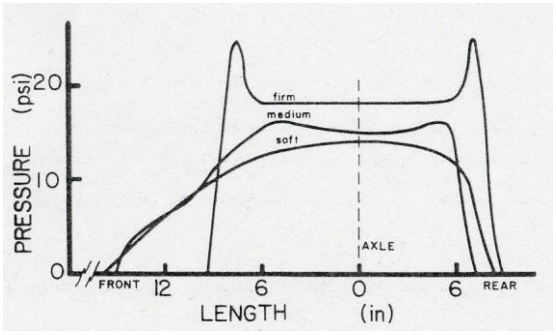

Figure 2.24 Longitudinal pressure distribution under centre of 11-38 smooth tyre inflated to 1 bar in a sandy soil at 3 soil conditions (VandenBerg and Gill, 1962)

Complete pressure distribution was recorded for firm sand test (Figure 2.25). On a firm surface stress concentration occurred at the perimeter and the pressure over the center of the contact area was relatively uniform and varied with the inflation pressure. The experiment shows an influence of sidewall stiffness that specially becomes evident at the lower inflation pressure.

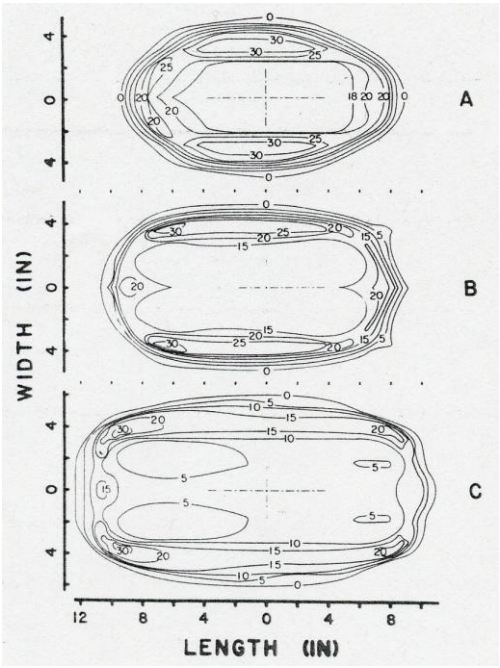

Figure 2.25 Contact pressure distribution under the smooth tyre on sandy soil for 3 inflation pressures – (A) 1 bar, (B) 0.69 bar, (C) 0.41 bar (VandenBerg and Gill, 1962)

In addition, as a check on the accuracy of the pressure results, the total load on a tyre was calculated from the pressure data and compared to the total tyre load. All of the calculated loads were within 15% of the measured loads. The experiment covered comparison of the static and dynamic contact areas. Static area was measured from ink print (surface type not defined). The dynamic contact area appeared to be bigger than static area. This probably results from the extra flexibility when the tyre rolls. Gill and VandenBerg (1968) reviewing this experiment states that due to the rigidity of the tyre carcass, the stress applied by a tyre is generally greater than tyre inflation pressure. If a very flexible tyre such as a low-ply low-inflation pressure tyre was used, the surface pressure distribution would by fairly uniform and the pressure applied to the soil would be close to the tyre inflation pressure.

The research of McLeod *et al.* (1966) covered assessing soil compaction and vertical soil stresses beneath a conventional rear tractor tyre, dual conventional tyres and a wide low pressure tyre. To measure soil pressure strain-gauge pressure cells were placed in the sandy loam soil. As Figure 2.26 shows, stresses are the lowest under the Terra-Tyre, increasing significantly in the order of the dual and single tyres. However, the authors discuss that even though the Terra-Tyre and the dual tyre cause lower soil stress and compaction than the single

tyre, but differences are not necessarily such that they would be significant in crop yield response.

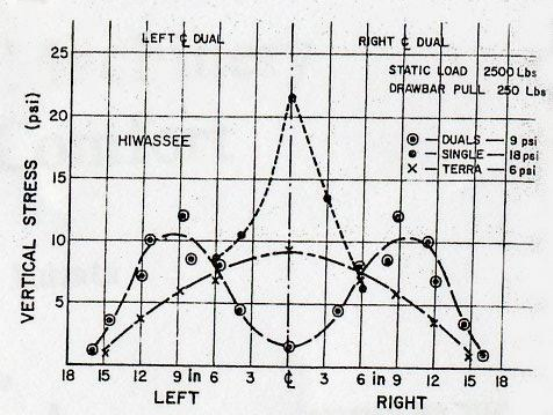

Figure 2.26 Lateral distribution of vertical soil stress at the approximate depth of 150mm under the tyre axle (McLeod *et al.*, 1966)

Two methodologies of measuring vertical stress in soil were developed by Lamande *et al.* (2006b). One method considers the distribution of the vertical stress in the tyre – soil interfaced (contact area method), and the other covers the measurements of vertical stress and displacement in soil profile (profile method). They developed new stress transducers to be used for the determination of the soil pressure under agricultural machinery. For the contact area method a rubber blanket with 17 cylindrical stress transducers glued was designed to be installed perpendicular to the direction of driving. The example is shown on Figure 2.27. Each transducer consists of a steel cylinder (ϕ 50 mm, 32 mm high) in which a load cell is installed and activated by a steel piston. The battery of transducers is to be placed into soil at 100 mm depth. The profile method records the stress distribution at the soil profile using cylindrical steel transducer housing (ϕ 52 mm, 80 mm long), which accommodate a cell and a small oil-holding container (Figure 2.28). Pressure transducers are to be connected to the container through an oil-filled plastic tube and can record the vertical displacement. The shape of the transducer housings is also new. They were constructed to behave as a wedge to ensure a good contact with soil.

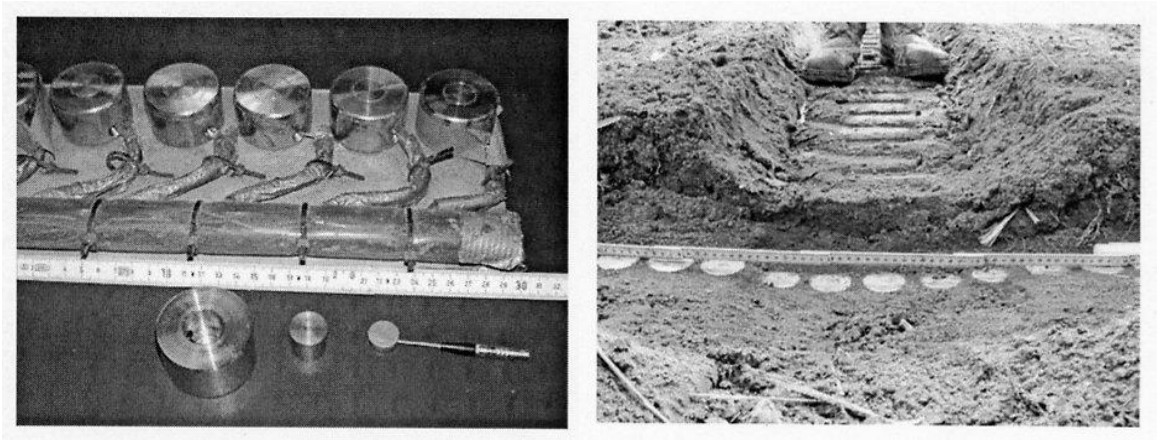

Figure 2.27 Stress transducers (left) with their application of soil pressure measurements (right) (Lamande *et al.*, 2006b)

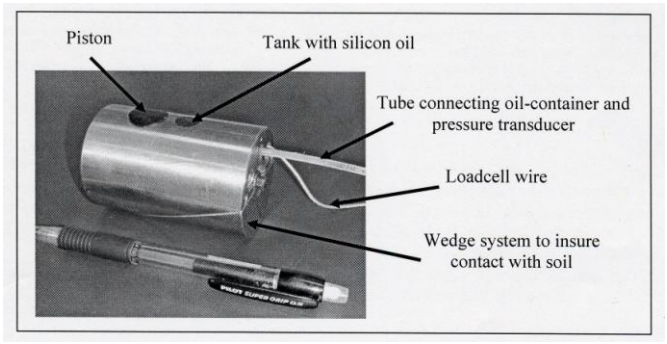

Figure 2.28 Cylindrical transducer (Lamande *et al.*, 2006b)

The novel approach of the vertical stress measurements developed by Lamande *et al.* (2006b) was implemented in the investigation carried out by Schjonning *et al.* (2006a), who employed the contact area method for the vertical stress below two radial-ply agricultural trailer tyres measurements. The tyres had low lugs and mainly differed in the width and aspect ratio. The tyre footprints were described by a super ellipse, which is given by:

$$\left|\frac{x}{a'}\right|^{n} + \left|\frac{y}{b'}\right|^{n} = 1 \qquad \text{Equation 2.14}$$

Measured and predicted characteristics of the tyre footprint and the contact pressure distribution were analysed. Obtained results indicated presence of the carcass stiffness, because the peak stress was higher than the inflation pressure in all cases as given (in kPa):

$$P_{\max} = 1.03P_i + 88.6 \qquad \text{Equation 2.15}$$

Therefore, the measured peak stress was generally about 90 kPa higher than tyre inflation pressure. However, the contact average pressures were in most of the cases lower than the tyre inflation pressure (especially for the high inflated tyres), which was already discussed. Additionally, it was noticed that the narrower tyre with higher aspect ratio was reflected in a longer contact patch than the wider tyre with low aspect ratio. This may be related to a higher carcass flexibility derived from the higher aspect ratio.

The effect of reduced inflation pressure on soil-tyre interface stresses was investigated by Raper *et al.* (1995a), who used Sensotec pressure transducers. They were placed on the tyre lug and in the under-tread area (Figure 2.29). The results confirmed that tyre inflation pressure greatly affects the soil-tyre interface stresses across the surface of the tyre, especially on the lug. The changes in inflation pressure caused the peak soil-tyre contact pressures to behave differently on dissimilar parts of the lug. As the inflation pressure was decreased, the contact stresses also decreased near the center of the tyre. Stress decreases were also noticed near the outside edge of the tyre in most of the cases, however it was more variable and less significant. The reason for that was a sidewall stiffness, which became a factor near outside edge. In a lug near an edge of tyre, the load was the main significant factor on the contact stress. In the under-tread area, inflation pressure was not very important factor for the contact stress, while a load was.

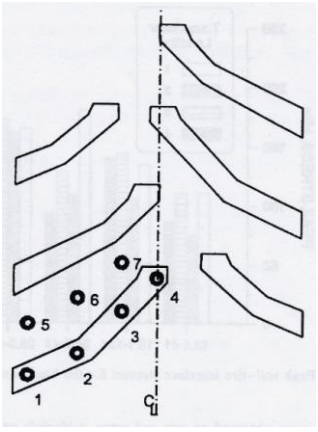

Figure 2.29 Locations of the soil-tyre interface transducers (Raper *et al.*, 1995a)

The same pressure transducers were used by Way and Kishimoto (2004) who looked at the tyre contact pressure on structured and loose soils. They found that on structured clay soil,

contact pressures on lugs were considerably greater than tyre inflation pressure and the pressures between the lugs were substantially lower than inflation pressure. While, on a loose sandy loam and loose clay loam, some contact pressure on lugs where higher than inflation pressure by only small amount and the others were smaller than inflation pressure by a small amount, whereas pressures between the treads were less than inflation pressure.

Söhne (1953) considered pressure distribution in a soil profile. He cited that in hard, dry soil the tyre tread carries over the whole weight and the surface pressure under the tread is 3 – 4 times as high as the surface load. However, at the depth 60 – 90 mm pressure is distributed over a whole load surface. Conversely, in a yielding soil a load is distributed over the tread and in between, and the pressure under tread is not so much higher than under grooves of the tread. Finally, very soft soil in wet conditions forms a strong plasticity that results in a very small pressure difference under a tyre tread and between.

The study of tyre rut dimensions was carried out by Painter (1981) who developed apparatus for measuring contact area dimensions. The experiment was conducted for one tyre and suggested an empirical equation for contact area:

$$A = \frac{\pi}{4} a_1 a_3 D^{a_2} C^{a_2} f^{2-(a_2+a_4)} \qquad \text{Equation 2.16}$$

A dominant factor affecting pressure in a loaded soil profile found by Taylor and Burt (1987) was an axle load applied to a tyre. They used pressure cells installed in the soil profile to measure the stress caused by a passage of a tyre. The experiments were undertaken in two soil types, sandy loam and clay loam. From the research they conclude that if a traffic pan is present in the soil then the pressures below the pan are lower and above it are higher than in the soil with uniform density.

Also Söhne (1952) conducted an investigation comparing the surface pressure under tyres in soft and hard surface conditions. The pressure on the hard surface was found to be almost uniform and above the inflation pressure. While the contact pressure on the soil surface was less uniform and lower than the inflation pressure (especially for the high inflation pressures) as presented in Figure 2.5.

Stress distribution in the soil due to surface loads of agricultural tyres (with and without lugs) was extensively researched by Söhne (1958). He noted that the maximum and mean contact pressures are smaller than the inflation pressure when narrow tyres produce deep tracks. Conversely the pressures under wide tyres and twin tyres with low inflation pressures are higher than the inflation pressure (Figure 2.30).

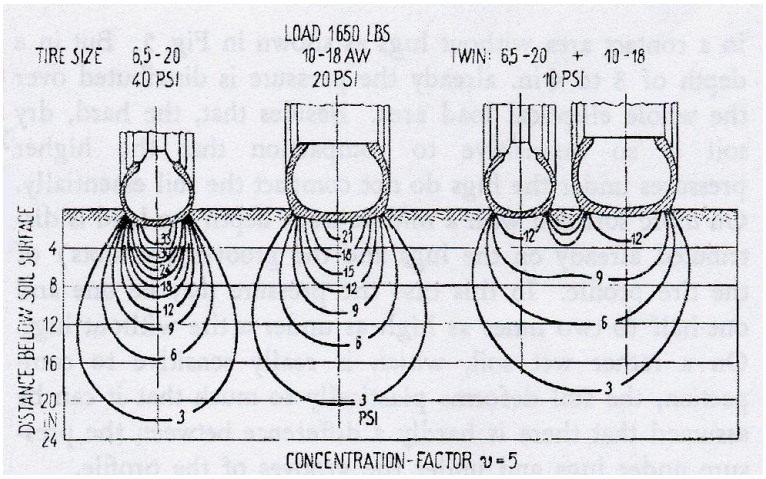

Figure 2.30 Calculated curves of equal pressure below narrow, wide and twin trailer tyres (Söhne, 1958)

The investigation of Söhne also showed an approximately equal pressure over the entire contact area when large-volume tyres without lugs were in contact with a hard dry surface. Figure 2.31 shows that this is not true for plastic and soft soils.

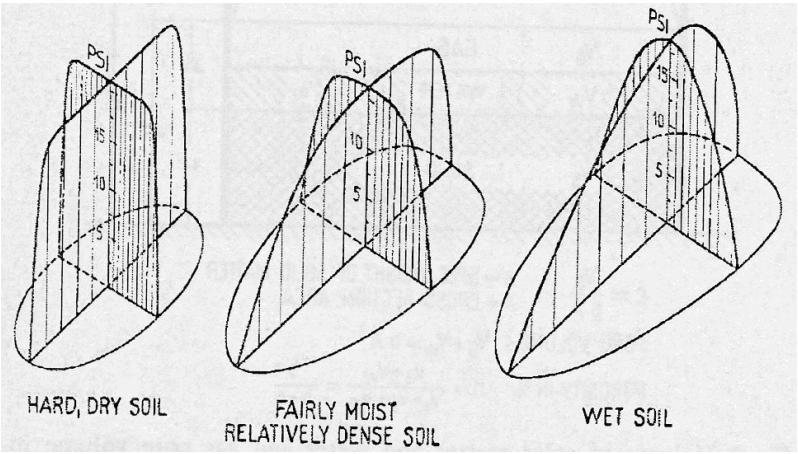

Figure 2.31 Pressure distribution at the contact area between tyre and soil (Söhne, 1958)

The research leads to prediction of pressure distribution for three cases shown in Figure 2.31. It can be calculated as follows:

- Hard dry soil – circle contact area:

$$P_D = P_{\max}[1-(\rho^{16}/R^{16})] \qquad \text{Equation 2.17}$$

$$P_{\max} = 1.125P_C \qquad \text{Equation 2.18}$$

- Fairly moist relatively dense soil – contact area follows a parabola of the fourth degree:

$$P_D = P_{\max}[1-(\rho^{4}/R^{4})] \qquad \text{Equation 2.19}$$

$$P_{\max} = 1.5P_C \qquad \text{Equation 2.20}$$

- Wet soil – contact area follows a quadratic parabola shape:

$$P_D = P_{\max}[1-(\rho^{2}/R^{2})] \qquad \text{Equation 2.22}$$

$$P_{\max} = 2P_C \qquad \text{Equation 2.23}$$

The pressure distribution for tyres having high lugs changes significantly. On a hard dry soil the tyre lugs carry the whole load. The pressure in the contact area of the lugs is three times higher than in a contact area without lugs. However, 100 mm below the surface it is already distributed over the whole elliptical load area. On more soft soil the load is distributed on the lugs and the grooves (or slots). In this case the pressure may be one to two times higher than under the tyre without lugs. Wet soil deforms plastically so much that it can be assumed that there is hardly a difference between the pressure under lugs and under the tyre carcass. Additionally, according to Söhne findings, soil stress increases due to surface load are the greatest near the soil surface. He also states that the soil stress close to a surface is determined by the inflation pressure and soil deformation (i.e. the size of contact area), while soil stress in deeper layers depends on a tyre load. These findings were also supported by Smith and Dickson (1990).

Krick (1969) and Kolobov (1966) both used pressure transducers embedded within the wheel to measure the stress distribution on the surface. Their investigations differ in the tyre types that they used. Krick used rigid wheels and pneumatic tyres in sandy loam, while Kolobov worked with a tractor tyre. Both of these studies were conducted only for one tyre and that is why their results are very limited. Krick (1969) developed a small membrane transducer

which allowed to measure of the pressure, tangential and lateral stress in the surface of both agricultural tyres and rigid wheels. When studying a yielding soil, he used plaster of Paris to make a model of the deformed surface. Then the contact patch was determined from the set cast. Using dimensional analysis techniques he established relationships between tyre deflection, load carrying capacity and contact area. He also compared pressure distribution under the rigid and pneumatic tyre which was found to be more uniform. Kolobov (1966) concluded that tyre tractive properties depend on the magnitude and nature of contact pressure distribution. He also confirmed that a reduction of inflation pressure results in an improvement in the pressure distribution and tractive performance.

Burt *et al.* (1987) also proposed a technique for measuring normal and tangential stresses at the soil-tyre interface for pneumatic tractor tyres on firm and soft soils. They developed a measuring system installed in the air cavity of a pneumatic tyre for measuring stress values and direction of the stresses. A number of pressure transducers were mounted in the tyre, flush with its surface, in lugs and between lugs. Sound emitters were used for the measurements of the direction of stresses.

An alternative approach to measure contact stress is to place a flexible mat measuring pressure between the tyre and the soil surface. There is very little evidence found showing this technique to be used to measure soil pressure. This is due to a mat's disadvantage that it cannot conform to the soil surface.

The Tekscan pressure sensing system was used by Eatough (2002) to measure pressure distribution under 4x4 tyres on the two types of soil. He performed the pilot experiment to verify the suitability of the Tekscan system using the three most potentially suitable pressure mats with the pressure range 0 – 690 kPa (5051 mat, 6300 mat and 6911 mat). A free rolling PT 235/70 R16 smooth tyre and split rim inflated to 2.21 bar and mounted on a Land Rover hub with a 0.65 tonne load were utilized in the test. The mats were fastened within plastic sleeves and glued to the tyre. The soil used for the verification tests was compacted sandy loam and its deflection was very low. It was a novel use of the Tekscan system as an investigative technique on deformable surface. Previously this system was used beneath rolling tyres only on hard surfaces by Goodyear and Dunlop (Eatough, 2002). The experiment

showed some suitability of the Tekscan to this application. In the investigation of normal stress on sand only the 6300 mat was used as it was long enough to cover the full contact width. Unfortunately, constant flexing and high strains damaged the mat's electrical connections very quickly. As the sandy loam surface tested upon was relatively rigid and the speed was comparatively low, the results did not show significant pressure distribution variations at the tyre – surface interface, although slight pressure reductions were found at the rear of the contact area, where the contact with the ground reduced as the tyre lifted off. However, in the sand tests, which were performed at higher speed, the pressures measured were found to be unevenly distributed. Reduced pressures were observed at the tyre entry and exit points, and increased pressures were noted over the second quarter of the contact length and at the edge of the tread.

These two patterns agree with the findings of a number of previous researchers (Gill and Vanden Berg, 1968; Bekker, 1969; Oida *et al.*, 1988). Contact pressure also tended to be reduced along the central width of the contact area and increased closer to the edge of contact patch. The sand tests also employed three different tread designs (lateral, longitudinal, 45 degree backward facing treads). Ignoring the influence of the treads, pressure distribution patterns found for all these tyres were similar to the smooth tyre. Additionally, the pressures recorded on the treads were greater than on the groove on the edges of the treads that were closer to the front of the contact patch. The surface pressures results, obtained by Eatough (2002) in the sandy loam verification test and in the main contact pressure experiment on the sand, have shown an agreement with the average contact pressures calculated as load over the area. They also show a similar tendency to the results obtained by Oliver (2002) - the average contact pressures were always lower than the tyre inflation pressure as previously discussed. However, the peak contact pressures results under the tyres loaded on sand were found to be higher than the inflation pressure.

Also, Keller and Arvidsson (2004) gained similar findings, when measuring vertical soil stress in different depth of soil. Maximum stress directly under a tyre, measured at 0.1 m depth, was considerably higher than tyre inflation pressure. It was also found to be unevenly distributed, both in driving direction and perpendicular to driving direction. They found that reducing tyre inflation pressure reduces stresses and displacements in the topsoil and in the upper subsoil.

A very different technique for the determination of dynamic three-dimensional soil – tyre interface profile was developed by Wulfsohn and Upadhyaya (1992). The method involves measuring incremental lateral arc lengths of the profile at discrete locations along the contact length, and then fitting the coefficients of a model of soil deformation at the soil – tyre contact profile to the experimental data using a nonlinear constrained optimization algorithm. The measurements were done with the transducer consisting of a thin wire covered within a flexible cable placed perpendicular to the direction of tyre travel on the soil surface. The wire was connected to a spring-loaded potentiometer measuring the linear extension of the wire when a tyre ran over it and when it deformed with the soil under the tyre. In that way the contact area was determined for two different sized dynamic tractor tyres at two levels of inflation pressure and in two soil conditions. The results obtained in the experiments were used to determine the contact area, which was then compared to the static contact area results obtained on a hard surface. It was found that the contact area becomes wider and shorter with decreased soil stiffness.

Tyre deflection and contact area studies carried out by Abeels (1976) were conducted in both static and dynamic conditions upon rigid plates and on deformable surfaces. The author of the research concluded that a stiffness coefficient of a tyre is defined as ply rating and inflation pressure, while the ratio of height to width under load specifies a tyre deformation coefficient, a squash rate and a flattening rate. These three parameters were proved to characterize the elasticity of the tyre and to be related to the tyre – soil contact area.

2.4.3 Pressure transfer in the soil profile

Soil pressure in the soil profile under a dynamic tractor track and tractor tyre was analysed by Reaves and Cooper (1960). Strain-gage pressure cells were employed to measure stresses within silt loam soil. The authors concluded that the soil pressure under a pneumatic tyre is at least twice as great as under a track (see Figure 2.32). This is reasonable because contact length for the tyre is approximately 600 mm, while that for the track is 1500 mm (for caring the same dynamic load). Besides that, it was also noticed that the stress (pressure) under a tyre is more constant than under a crawler track.

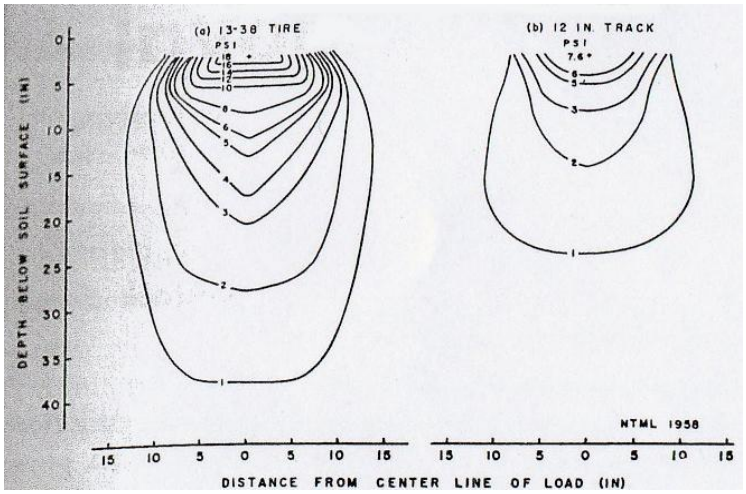

Figure 2.32 Soil pressure transfer in the soil (Reaves and Cooper, 1960)

Christov (1969) measured pressure distribution in the soil profile resulting from a passage of a tyre. He buried pressure transducers in the soil below the centre of a tyre at 3 depths. Then a tractor was driven above the sensors. The front tractor wheel (6.00-18) was inflated to a constant pressure of 2.5 bar and loaded to 0.82 tonne, while the rear wheel (13-28) was loaded to 2.19 tonne at 3 inflation pressures of 1.6 bar, 1.2 bar and 0.8 bar. Figure 2.33 presents the results obtained, where pressure decreases with an increase of sensor depth for each tyre. Also, the stresses in the soil increased as inflation pressure of the rear tyre increased. The maximum pressures recorded below the rear tyre at 100 mm were found to be larger than tyre inflation pressures; this was not the same for the front tyre.

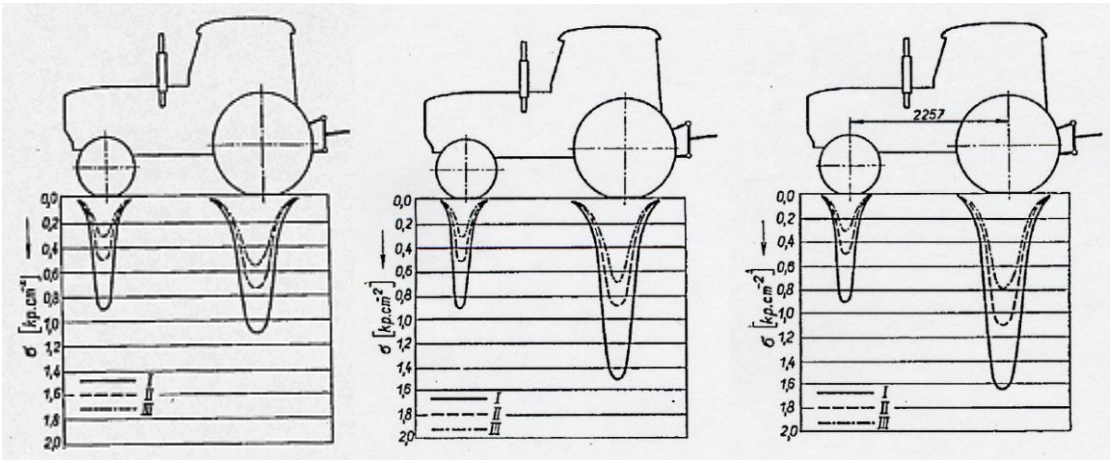

Figure 3.33 Pressure resulting from passage of a tractor (front tyre inflated to 2.5 bar, rear tyre: 0.8 bar – left, 1.2 bar – middle, 1.6 bar – right, sensor buried at: I – 150 mm, II – 250 mm, III – 250 mm; Christov, 1969)

The pressures acting on buried pseudo archaeological items were investigated by Dresser *et al.* (2006). The studies involved measuring the pressure on buried plates (to simulate the upper surface of walls) and cylinders with pressure sensors mounted flush on surface. The pressure transducers used were 19 mm diameter 10 bar ceramic membrane type. The soil with features buried at the different depths was loaded by a range of tillage implements used in farming and a variety of farm vehicles (tractors, harvesting machines, trailers and trucks). The results obtained show that the tyre and track loads produce much higher pressures than the tillage implements. The peak pressures at 250 mm depth resulted from tractors, trailers, harvesters and tracks loads varied from 0.5 to 7.5 bar, depending on the load, inflation pressure and machinery type (Figure 2.34). The pressures under the tyres measured at the depth of 250 mm were very close to the air pressure in the tyre. It is clearly seen that tyre inflation pressure has a greater influence on the soil pressure than the load. Additionally, it was proved again that tracks generate much lower soil pressure than tyres and they should be used where it is possible.

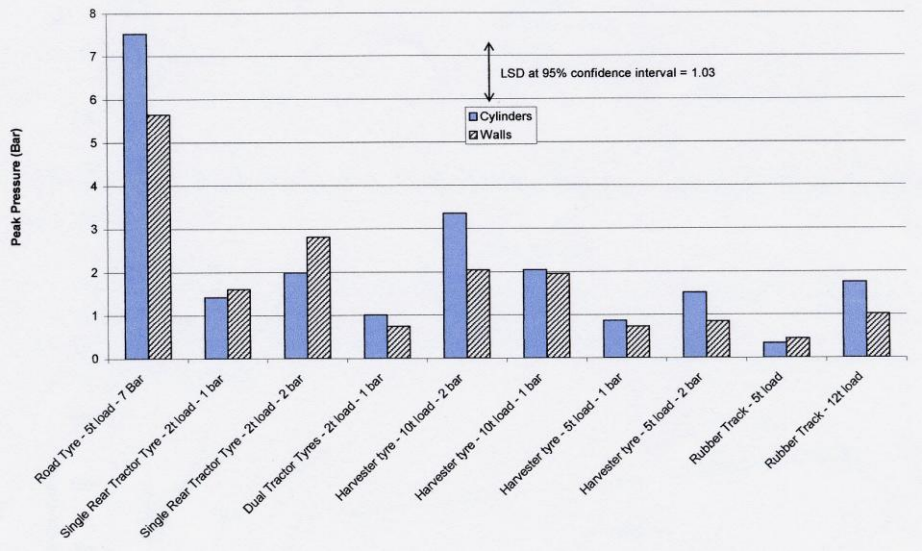

Figure 2.34 Tyre and track peak pressures at 0.25 m depth (Dresser *et al.*, 2006)

Figure 2.35 clearly shows a reduction of the peak pressures with depth resulted from the surface load. The shallowest transducer was placed at the 250mm depth and soil surface pressure was not recorded. However, it would be possible to extrapolate the pressure vs. depth curves to obtain the pressure at the soil surface, that could be done with a better confidence if the peak pressures were measured at more depths of the soil profile.

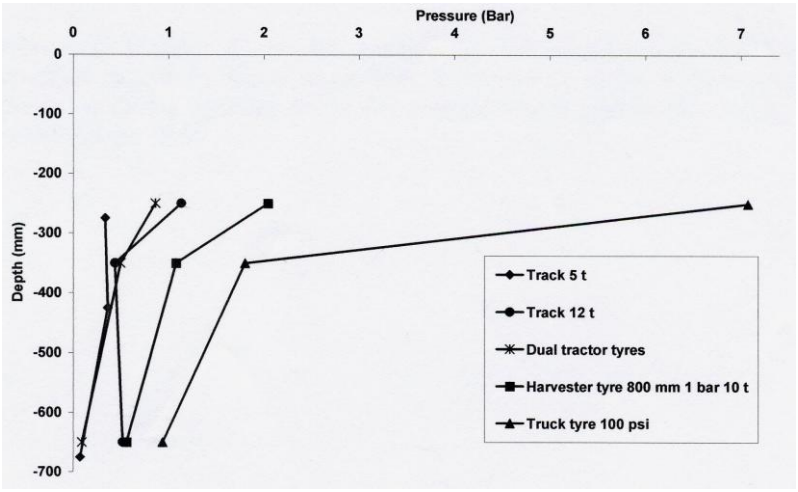

Figure 2.35 Peak pressure vs. soil depth for tyre and track loads (Dresser *et al.*, 2006)

Soil pressure transfer resulting from agricultural tyres was also studied by Weissbach (2001), who used hosepipe sensors for the pressure measurements. He found that at 100mm depth the pressure under the tyres was very close to the air pressure in the tyre. Figure 2.36, presenting pressures in the ground under the number of tyres with the same load and varying inflation pressures, shows that low air pressure leads to sustainable less ground pressure over the whole soil depth studied.

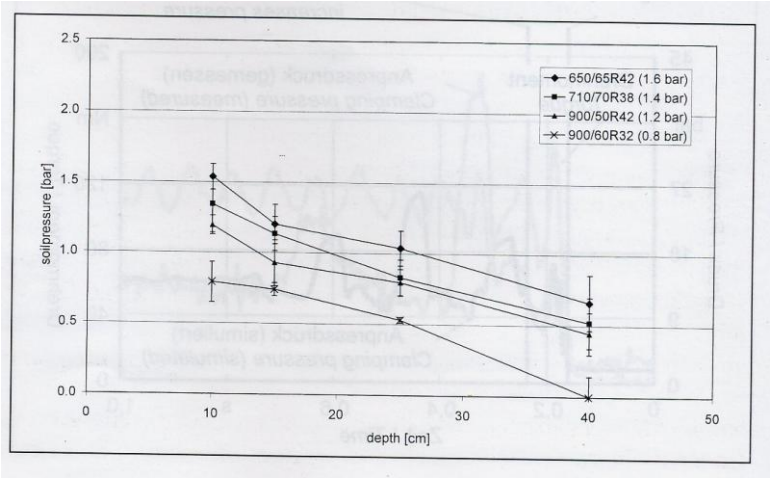

Figure 2.36 Soil pressure in the soil profile (Weissbach, 2001)

Weissbach (2001) also concluded that the maximum contact pressure is decisive for the soil compaction rather than the average contact pressure. The study brings also a conclusion that

tyre inflation pressure and ground pressure are directly related (Figure 2.37) and soil protection can be achieved with the suitable air pressure selection.

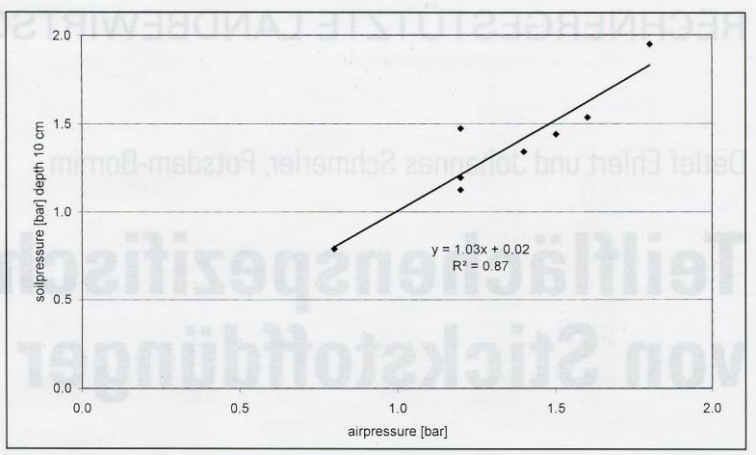

Figure 2.37 Soil pressure at 100mm depth vs. tyre inflation pressure (Weissbach, 2001)

2.5 Tyre deflection under load

Radial tyre deformation is usually measured in a static condition and is called deflection. It appears to be a measure of the flexibility of a pneumatic tyre (Gill and VandenBerg, 1968). Tyre deflection depends on the following factors: inflation pressure, load, tyre stiffness and character of the supporting surface (Tijink, 1994).

Correct tyre inflation pressure is crucial for an appropriate tyre performance. To prevent carcass damage tyre manufactures design all tyres to run at a set amount of deflection, as presented in Figure 2.38. Tyre over-inflation reduces the contact patch, reduces grip and increases the risk of shock damage to the tyre, whereas, under-inflation gives excessive deflection and distortion of the casing which may cause premature failure of the tyre. Correct inflation pressure results in a good tyre grip, optimum performance, long tyre life and comfort (Agricultural Training Board, 1989).

Normal agricultural tyres (aspect ratio H/B of about 0.8) should be operated at up to 20% deflection. Tyres with a smaller aspect ratio have a greater deflection limit which is 25%. Some tyres can be used for short durations at deflection of 35% (Tijink, 1994). Browne *et al.* (1981) found tyre deflection to be the most important factor influencing tyre contact area. Saarilahti (2002) discussed that tyre deflection is dependent on the load applied, inflation

pressure, carcass stiffness and tyre type (radial/cross-ply). Srivastava *et al.* (1993) concluded that typical agricultural tyres deflect by approximately 19% of their section width when they are loaded to their maximum recommended load for a particular inflation pressure. This agrees with Gee-Clough *et al.* (1978) who stated that tyres deflect by 20%.

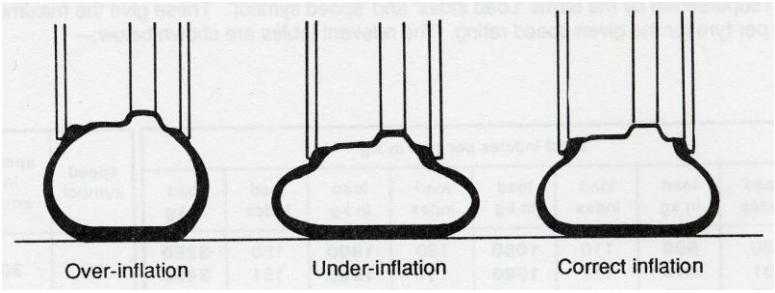

Figure 2.38 Tyre deflection (Agricultural Training Board, 1989)

According to the experimental data of the most commonly used tyres at this time, Krick (1969) proposed the following empirical equation for predicting tyre deflection:

$$\frac{f}{S} = 0.67T^{-0.8} \qquad \text{Equation 2.24}$$

$$T = \frac{P_i Db}{W} \qquad \text{Equation 2.25}$$

The equation for predicting tyre deflection above was evaluated by Godbole *et al.* (1993) and slightly changed.

Another empirical equation for estimating tyre deflection was given by Painter (1981):

$$W = A_0 + A_5 f + A_6 P_i f^{2-(A_2+A_4)} \qquad \text{Equation 2.26}$$

Komandi (1976) proposed the following relationship of tyre deflection on hard surface:

$$f = C_1[W^{0.85}/(b^{0.7} D^{0.43} P_i^{o.6})]K \qquad \text{Equation 2.27}$$

2.6 Tyre stiffness

Many researchers consider tyre stiffness as the ratio of the wheel load and deflection on a rigid surface (Lines, 1991; Lines and Murphy, 1991; Tijink, 1994; Walczykowa, 1999). Tijink (1994) discusses that carcass stiffness is not constant for a tyre and typical values are

250kN/m and 450kN/m at inflation pressures of 80 kPa and 200 kPa, respectively. Lines and Murphy (1991) showed that inflation pressure and tyre volume (size) significantly affect the stiffness of agricultural tyres. Tyre stiffness increases almost linearly with inflation pressure. Walczykowa and Walczyk (1999) studied the effect of load on stiffness of 6-16 (PR 6) front tractor tyre and found that wheel load increase resulted in decrease in tyre stiffness.

In this project, however, tyre carcass stiffness is considered as the equivalent pressure resulting from the tyre carcass when transmitting the load to the underlying surface and is calculated in pressure units. Carcass stiffness was considered as a pressure for the practical reason of estimating the tyre contact pressure by a number of researchers (Söhne, 1952; Bekker, 1956; VandenBerg and Gill, 1962; Abeels, 1976; Chancellor, 1976; Karafiath and Nowatzki, 1978; Plackett, 1983, 1984, 1985, 1986; Williams, 1987; Raper *et al.*, 1995a, Schjonning *et al.*, 2006a, Schjonning *et al.*, 2008). However, only Bekker (1956), Karafiath and Nowatzki (1978) and Plackett (1983) devised methods for predicting the equivalent pressure resulting from tyre carcass stiffness, which are presented in Section 2.4. Tijink (1994) concluded that an increase in inflation pressure at a constant load results in a decrease in carcass stiffness, so it is also not a constant value. For a tyre inflated to a high inflation pressure carcass stiffness can have a negative value. An increase of wheel load at constant inflation pressure results in a small increase in tyre carcass stiffness (Söhne, 1952). Plackett (1983) developed the load – deflection method to estimate carcass stiffness of agricultural tyres (section 2.4.1). His results are as shown below:

- Front tractor/implement ribbed tyre (7.5-16): 0.35 bar
- Trelleborg tyre (400-17.5): 0.44 bar
- Trelleborg tyre (600-30.5): 0.38 bar
- Terra tyre (31x15.5-15): 0.25 bar
- Terra tyre (67x44.00-25): 0.06 bar
- Radial tractor tyre (12.0-18): 0.32 bar
- Radial tractor tyre (16.9-34): 0.21 bar
- Cross-ply tractor tyre (16.9-34): 0.21 bar

Schjonning *et al.* (2008) measured the vertical stress distribution across a contact area at 100 mm soil depth for two radial trailer agricultural tyres (650/65R30.5 and 800/50R34) and

concluded that for both tyres the peak stresses measured increased significantly with tyre inflation pressure and were generally about 90 kPa higher than tyre inflation pressure, which could be considered as the equivalent pressure from tyre carcass stiffness.

When representatives of tyre manufactures were asked about values for carcass stiffness, they said it is approximately equal to 1 – 2% of tyre inflation pressure for radial tyres and 3 – 4 % for cross-ply tyres. Tijink (1994) says that in the Netherlands a quick rule of thumb is used for estimating the average contact pressure on a hard surface which is $P_C = 1.25P_i$, which means that 25% of inflation pressure was assumed to be carcass stiffness. German advisory services assumed that carcass stiffness for cross-ply tyres equal to 30 kPa and for radial tyres 20 kPa.

Steiner (1979) developed two equations for estimation of contact area of cross-ply and radial tyres on a hard surface. He did not include ply rating parameter in his equations as he found that it improves R^2 by 1% only.

2.7 Critical review of missing aspects

The review of the literature describing studies on soil pressure and soil compaction resulting from agricultural vehicles reveals that a wide variety of studies were carried out in the past. However, it mainly covers an extensive research work on agricultural tractor tyres that was carried out mainly over the past 20 years. It also shows that much more attention was paid to soil compaction, theories of soil behaviour and the effects of soil compaction to field conditions and yield than to soil contact pressure.

Only Bekker (1956), Chancellor (1976) and Plackett (1982, 1983, 1986) investigated contact pressure resulting from agricultural tyres and then related it to the inflation pressure and carcass stiffness. They indicated that mean ground pressure could probably be defined as inflation pressure plus carcass pressure. However, it was done only at the hard surface and was never fully proved. This is probably due to a complexity of soil contact pressure determination and lack of any standard method of determining the contact area or contact pressure of a tyre operating in soil. Concluding the consideration, it is worth seeing that most of the off-road agricultural transport is performed by means of wheeled vehicles and relays entirely on pneumatic tyres running on the soil. The performance of a wheel depends fully on

the soil-tyre interaction. The contact area is the only part of the interaction, therefore the geometry of contact area, magnitude and distribution of stresses are crucial (Tijink, 1994). The review proves that the mechanics of the relation between soil and pneumatic tyre is not fully known. Therefore, it was decided to investigate more thoroughly the aspect of pressure resulting from loaded agricultural tyres on both hard and soil surfaces. That will provide a valuable indicator for appropriate tyre selection. The selection of tyre size and inflation pressure for a particular load and soil conditions are crucial to minimising soil compaction and ensuring soil sustainability. Generally, an increase in tyre size is accompanied by a decrease in tyre inflation pressure to support a given axle load. This also improves tractive performance and reduces soil deformation (Antille *et al.*, 2008).

A major reason for the initiation of this project resulted from the work of Plackett who worked on the tyre carcass stiffness concept. His work was used as the initial guidelines for the investigation and made it easier to understand the subject and to conduct this investigation into a variety of agricultural tyres.

Tekscan pressure sensing system is required to measure the surface pressure resulted to loaded agricultural tyres on hard and deformable surfaces. The verification of the pressure mapping system conducted by Eatough (2002) demonstrates its poor ability for the soil surface application. However, an appropriate selection of the Tekscan sensors and their specific application could lead to the new findings that previous investigators were not able to find due to the instrumentation they used.

Most of the research on agricultural tyres have been undertaken in the field, but there was very little done of modelling of soil behaviour under the agricultural tyres that could lead to the correct prediction of the results. Additionally, the static investigations do not actually indicate the dynamic stress beneath the tyre while it is rolling, since following Gill and VandenBerg (1968), the magnitude and distribution probably differ for dynamic and static situations. Therefore, it was decided, in accordance with the literature review, to obtain data for various conditions – hard and soil surface, that could lead to a better understanding of the soil surface pressure resulting from agricultural tyres and would allow a determination of tyre carcass stiffness and its effect onto the contact pressure.

3 INSTRUMENTATION AND EXPERIMENTAL METHODOLOGY

3.1 Introduction

This chapter describes the methodology for the experimental component of the project. The main aim of the experimental work was to measure the pressures resulting from loaded agricultural tyres both on a hard surface and at a range of depths in the soil profile. A range of agricultural tyres, from those fitted to tractors, trailers and implements to combine harvesters, were used to investigate the effects of normal load, inflation pressure and carcass stiffness, on the resulting soil pressures both at or near the surface and at depth in the soil profile.

The experiments were conducted in two phases:
Phase 1 covered surface contact pressure measurements carried out on the hard surface and
Phase 2 involved assessments of the surface contact pressure and pressure distribution in the soil profile.

Phase 1 involved measuring tyre contact area, surface pressure and deflection on a hard surface which was assumed to be the simplest form of a controlled environment. A simple ink method, previously employed by Plackett (1983), was used for the contact area determination. The tyre contact areas obtained using this method were then used for the calculation of mean contact pressure as tyre load divided by contact area. A piezo-electric pressure mapping system, Tekscan, was employed for the tyre contact pressure distribution measurements.

Phase 2 examined soil pressure distribution resulting from loaded tyres in the soil profile at varying depths. Tekscan pressure measuring sensors were used to measure the pressure. In order to do this they were buried horizontally in the soil at varying depths.

Both phases were conducted in the Soil Dynamics Laboratory, in the soil bin facility at the Silsoe Campus. As Phase 2 involved using a sandy loam soil (Godwin, 1974 and Misiewicz, 2005), a number of laboratory tests were conducted to measure the properties of the soil in the packing state selected for the work. The feasibility of Tekscan pressure mats for the project application was preliminarily tested.

The analyses of the wheel parameters and soil conditions were necessary to provide distinct treatments that would lead to results and would deliver the aims of the project. The sandy loam soil was chosen for the experiment, as it is a relatively common type, readily suffers from compaction and has a single grain structure which makes it relatively easy to use for this form of investigation. The following variable factors were selected:

- Tyre type: size, tread pattern and stiffness ranging from an unsupported inner tube to a range of tyres differing in "ply" ratings,
- Inflation pressure,
- Normal load.

A variety of facilities and instrumentation systems were required for the studies, they are described following the experimental methodology.

3.2 Experimental facilities

3.2.1 Soil dynamic laboratory

Pressure measurement experiments on a hard surface and in the soil were conducted in the soil bin laboratory, developed by Godwin *et al.* (1987), which provides controlled soil conditions which are essential for these studies. It consists of a below floor level soil bin and a travelling soil processor which is moved along the bin for the soil preparation. The processor contains a grab bucket, a scraper, a roller and a scorer. It works under complete control of the operator who either sits on board or controls it from a remote control room. The tank is 20 m long, the depth is 0.8 m and the width is 1.65 m (Figure 3.1). The soil used in the bin is sandy loam of the Cotternham series (King, 1969) with 17.1% clay, 17.2% silt and 65.7% sand (6.1% coarse sand, 34.9% medium sand, 24.7% fine sand) determined by the pipette method as described by Avery and Bascomb (1982). The water content was maintained between 9 – 10% dry base and the soil was prepared uniformly to a dry bulk density of approximately 1.5 t/m^3 which was selected to represent a common soil condition for agricultural fields with a relatively low bearing capacity.

Figure 3.1 Soil bin laboratory

The hard surface experiments required preparation of the dense soil conditions in the soil bin and placing a 50 mm steel plate on the soil surface providing an un-deformable surface. Then, depending on the method of contact pressure assessment, white paper sheets or pressure sensing sensors were placed on the plate (Section 3.4.1). After that the tyres were loaded on the plate statically or dynamically using the most appropriate single wheel tester, as described in Section 3.2.3.

The soil experiments were carried out in the soil bin in order to limit the amount of variability in soil conditions (in comparison to field conditions where soil is heterogenic) and to be able to evaluate the effect of tyre stiffness, inflation pressure and load on the soil pressure. The use of the soil bin facility allows repeatable tests under controlled conditions and significantly reduces the inherent variability in soil preparation that is common in field conditions. The soil experiments required an accurate soil preparation. It was done relying on the technician's knowledge and experience gained by assisting in other projects and checked by the author. The machine presented in Figure 3.2 was used to shift and compact the soil. Soil present in the soil bin was scraped by the blade in 25 mm layers and place at the end of the bin. Then using, both, the grab and blade, the same soil was transported and spread uniformly along the

soil bin. Approximate soil densities were achieved by compaction of the soil in 50 mm layers using the roller. After the compaction of each layer, water was applied to replace that lost in processing and to help to bond the soil layers together, the surface was then "scored" to avoid planes of weakness in the soil profile. The soil was prepared to required depths, then the steel plate with the pressure sensing sensors (Section 3.4.2 and Chapter 4) was placed on the soil surface and the soil preparation was continued to the required "top" surface level.

Core sampling measurements provided wet and dry soil bulk densities, porosity and moisture content of the soil. The samples were taken before each test at four random locations. The core sampling tests were conducted as described by Day (2001). Further analyses were based on the mean values that were calculated.

Figure 3.2 Soil preparation in the soil bin (left: soil spreading, right: soil compacting)

3.2.2 Test tyres and speed

Table 3.1 shows the range of tyres used in the project with their specifications and types of experiment performed. As presented in the table, nine tyres representing variations in type, use, size and tread pattern were selected. The selection also included five tyres which are the same size but vary in tyre ply rating. The tyres used are shown in Figure 3.3.

Phase	Experiment	Tyre	Size	Ply rating	Load (tonne) / inflation pressure (bar) range
Phase 1 Hard surface	Tyre deflection measurements and tyre contact area estimation using the ink method (static tests)	Inner tube	600/700/750R16	n/a	Combinations of loads of 0.01, 0.02, 0.03, 0.04, 0.05, 0.06, 0.07, 0.08 with inflation pressures of 0.07bar, 0.08bar, 0.1bar.
		Front tractor tyre – cross–ply	9.0-16	10	Combinations of loads of 0.5, 1.0, 1.5, 2.0 with inflation pressures of 1.0, 2.0, 3.0, 4.0.
		Rear combine tyres (smooth and treaded) – radial	600/55R26.5	-	1.8/0.5, 1.8/1.0, 2.5/0.5, 2.5/1.0, 2.5/1.5, 2.5/2.0, 2.5/2.5, 2.665/0.5, 3.5/1.5, 3.765/1.0, 4.5/1.5, 4.5/2.0, 4.5/2.5, 4.822/1.5, 5.92/2.0, 6.5/2.5, 6.885/2.5
		Implement tyres – cross–ply	11.5/80-15.3	8 10 12 14 16	1.19/1.5, 1.42/2.0, 1.63/2.5, 1.7/2.7 1.19/1.5, 1.42/2.0, 1.7/2.7, 1.95/3.4 1.19/1.5, 1.7/2.7, 1.95/3.4, 2.18/4.1 1.19/1.5, 1.7/2.7, 1.95/3.4, 2.18/4.1, 2.43/4.8 1.2/1/5, 1.7/2.7, 1.95/3.4, 2.18/4.1, 2.575/5.4
	Pressure distribution measurements using Tekscan method (dynamic tests)	Front tractor tyre – cross–ply	9.0-16	10	1.0/1.0, 1.0/1.5, 1.0/2.0, 1.0/2.5, 1.0/3.0, 1.0/3.5, 1.5/2.0, 1.5/2.5, 1.5/3.0, 1.5/3.5, 2.0/2.0, 2.0/2.5, 2.0/3.0, 2.0/3.5
		Rear combine tyres (smooth and treaded) – radial	600/55R26.5	-	1.8/0.5, 1.8/1.0, 2.5/0.5, 2.5/1.0, 2.5/1.5, 2.5/2.0, 2.5/2.5, 3.5/1.5, 3.765/1.0, 4.5/1.5, 4.5/2.0, 4.5/2.5, 6.5/2.5, 6.885/2.5
		Implement tyres – cross–ply	11.5/80-15.3	8 10 12 14 16	1.7/2.7 1.7/2.7 1.7/2.7 1.7/2.7 1.2/1/5, 1.7/2.7, 1.95/3.4, 2.18/4.1, 2.575/5.4
Phase 2 Soil profile	Pressure distribution measurements using Tekscan method (dynamic tests)	Rear combine tyres (smooth and treaded) – radial	600/55R26.5	-	Smooth: 2.5/2.5, 4.5/2.5, 6.5/2.5, 2.5/0.5, 2.5/1.0, 2.5/1.5, 2.5/2.0, 2.5/2.5, 4.5/1.5, 4.5/2.0, 4.5/2.5, 6.5/2.5 Treaded: 6.5/2.5
		Implement tyres – cross–ply	11.5/80-15.3	8 10 12 14 16	1.7/2.7 1.7/2.7 1.7/2.7 1.7/2.7 1.2/1/5, 1.7/2.7, 1.95/3.4, 2.18/4.1, 2.575/5.4

Table 3.1 Tyre selection

Figure 3.3 Range of agricultural tyres used in the study (from top left: inner tube, front tractor tyre, smooth and treaded combine tyre, implement tyres)

The following tyre types were investigated to find the influence of the following aspects on the resulting pressure:

A. Presence or absence of tyre tread
B. Differing tyre ply rating
C. Standard tyre to compare these results with the studies by Plackett (1983)
D. "Purely" flexible inner tube with little or no carcass stiffness

A. Agricultural tyres often have aggressive tread patterns which are made up of lugs or ribs. The presence of a distinct tread may significantly change the pattern of pressure distribution in the contact area. In order to observe the effect of tyre tread and obtain a true and simplified picture of the force distribution, the 600/55-R26.5 Trelleborg rear combine tyre was examined both without and with 30 mm high lugs.

B. To evaluate the effect of tyre ply rating on the resulting pressure five tyres of the same dimensions and tread pattern but varying in ply rating were selected. These were Goodyear implement tyres (11.5/80-15.3) with ply rating varying from PR8 to PR16.

C. In order to compare the current results to the work previously carried out by Plackett (1983) a 9.0-16 Firestone front tractor tyre was selected for testing in a pilot study.

D. A "purely" flexible inner tube with no tread pattern was selected for a pilot study as it was expected it would behave as a "perfect" balloon where contact pressure is equal to inflation pressure and there is little or no carcass stiffness.

All the tyres were examined at their "design" pressure – load specification and a selection of tyres were also tested beyond normal manufacture specification. The purpose of which was to characterise their behaviour over a wider range of conditions. This enabled the effect of using the tyres at a range of inflation pressures and loads on the tyre contact pressure to be studied. N. B. This range should not be considered a recommendation for normal commercial practice.

All the tyres were included in the hard surface experiments where black ink was employed for indication of the contact area (A, B, C and D groups). Tyre deflection tests were conducted for all the tyres tested apart from the inner tube (A, B and C groups). For the contact pressure measurements, employing Tekscan system, A, B and C groups were used for the hard surface studies and A and B groups for the soil experiments, as presented in Table 3.1.

A number of researchers have investigated the effect of tyre speed on magnitude of soil compaction. Stafford and de Carvalho Mattos (1981) proved that the effect of speed on soil compaction is greater at the shallower depths for sandy clay loam and clay soils, where there was no effect of speed at 200 mm depth although there was an increase in soil bulk density at all the speeds tested. The effects of speed on soil compaction found by Stafford and de Carvalho Mattos were not large, especially at low forward speeds. They are more significant under initial loose soil conditions, where an increase of speed of a vehicle can reduce compaction up to 50%. Horn and Lebert (1995) also concluded that the speed of the tyre has a small effect on the contact pressure distribution and soil compaction. However, they had a

different opinion on the effect of speed on soil vertical stresses. Aboaba (1969) and Ansorge (2007) investigated the influence of speed of roller and tyre travel pulled on a loose soil, respectively. They both proved that with increasing speed soil displacement in the profile decreased. Therefore, as the soil is slightly more subject to compaction at slow speeds, the current study experiments, which were conducted dynamically, were performed at low speeds.

The ink tests and deflection measurements on the hard surface could be only carried out in static conditions. The dynamic tests were carried out at a constant speed of 0.085 m/s, which was measured using a stopwatch. This slow speed, in comparison to real field working operations carried out usually at 1.5 – 2 m/s, was selected as Tekscan sensors were expected to be more accurate at a slower speed as the errors were expected to with higher speeds (Chapter 4). Soil compaction was considered to be greater at slow speeds, therefore, this gives the worst case scenario.

As a tyre passes, it induces stresses in the soil, which have both compressive and shear elements. In these studies for simplicity the wheels were towed rather than driven. This was done to avoid the effects of wheel slip which would lead to higher shear stresses in the upper soil layers, which could not be measured.

3.2.3 Test frames

Three different loading frames were used to carry different tyres. They were required for carrying tyres, towing them and for load application. They were selected depending on the tyre size and the maximum load applied. All the tests, hard surface and soil tests, were conducted in the soil bin at the Soil Dynamics Laboratory. The soil bin was selected in order to be able to have controlled and repeatable soil conditions. The frames were used rather than full scale machinery as the soil bin accommodates the frames more easily and enables a wide range of normal loads to be selected. They were connected to the soil processor (described in section 3.2.1) for both static and towed dynamic tests. Using frames in the soil bin provided an accurate control of forward speed, load and soil parameters much better than it would have been done in field conditions with full scale machinery.

The larger tyres – two rear combine tyres and five implement tyres were loaded using the load frame designed by Ansorge (2005) as shown in Figure 3.4. This equipment transfers the normal load from the mass of the frame onto the wheel by using a vertical hydraulic ram. Hence, wheel loads can be easily changed as the load is a function of the pressure applied to the ram. The hydraulic ram is also used for lifting and lowering a wheel. In this rig wheels are exchanged or removed through the rear of the frame. The loading weights supplying the counterforce of the ram are spread equally over the frame. The tyres were towed using the processor shown in Figure 3.1.

Figure 3.4 The 12 tonne loading frame designed by Ansorge (2005) for large agricultural tyres

The medium sized front tractor tyre was carried and loaded with another smaller frame (5 tonne) shown in Figure 3.5. The frame was stabilised by the soil processor with a “hinged” pivot point connection (shown to the left of the Figure 3.5). The loads were applied on this frame were in the form of static weights (ranging from 5 kg to 500 kg) which were equally placed in the loading brackets on both sides of the frame.

Figure 3.5 The 5 tonne loading frame for medium agricultural tyres attached via a hinged pivot point to the soil processor

A 0.25 tonne frame (Figure 3.6) was built for testing the inner tube. This frame was also stabilized by the soil processor with a hinged pivot point and it was loaded by the number of weights placed on the frame (1 kg, 5 kg, 10 kg, 20 kg).

Figure 3.6 The 0.25 tonne loading frame for small agricultural tyres attached via a hinged pivot (far left) to the soil processor

3.3 Instrumentation

This section describes the instrumentation required to measure tyre normal load, pressure (tyre inflation pressure and pressure in the Tekscan calibration device, see Chapter 4), tyre deflection, contact patch area and pressure distribution resulting from the loaded tyres. All the equipment used was calibrated prior to its use, Appendix B contains a detailed description of the calibration process for each measuring instrument with the results. A summary of the instrumentation used and the calibration factors are given in Table 3.2.

For all the tests the following datalogger was used: FE-366-TA dual microanalogue transducer amplifier (produced by Fylde Electronic Laboratories Ltd).

Table 3.2 Calibration parameters of the instrumentation

Parameter	Device	Calibrated range	Calibration coefficient	Datalogger gain	Coefficient of determination R^2	Hysteresis (%)
Normal load	Hydraulic pressure gauges (models A&B)	A: 0 – 2.7t A: 0 – 6.6t B: 0 – 12t	1.931V/t 0.941V/t 0.063V/t	1:100 1:50 1:100	1.000 0.999 1.000	9.21 4.62 3.21
	Tension link dynamometer	0–0.5t 0–2.5t	N/A	N/A	0.999 1.000	0.06 0.05
	Extended octagonal ring transducers	0–3t 0–9t	3.382V/t 0.670V/t	1:100 1:200	1.000 1.000	0.03 0.05
Inflation pressure	Air line pressure gauge	0–2b	N/A	N/A	0.982	13.14
	Digitron pressure gauge	0–2b	N/A	N/A	1.000	1.42
	Druck pressure gauge	0–20b	N/A	N/A	1.000	0.005
Tyre deflection	Draw string transducers (1000mm & 2000 mm long)	1000mm: 0–550mm 2000mm: 0–550mm	0.009V/mm 0.005V/mm	1:1 1:1	1.000 1.000	0.01 0.03
Contact area	Canon digital camera	N/A	9.227 pixels/mm^2	N/A	1.000	N/A

3.3.1 Normal load measuring equipment

The normal loads applied to the tyres were measured using a range of instruments as follows: hydraulic pressure transducer, tension link dynamometer and extended octagonal ring transducer (Figure 3.7). The selection was dependant on the maximum load applied and frame used for loading a particular tyre.

- Extended octagonal ring transducers (EORT)

There were two extended octagonal ring transducers (with the maximum capacity of 5 tonne and 10 tonne, respectively), designed by Godwin (1975) and Godwin *et al.* (1987), used in the experiments. The 5 tonne transducer was used in the application described below. The 10 tonne device was used for load measurements during the tyre deflection tests and for calibrating the pressure gauge on the 12 tonne loading system. Figure 3.7 (right) presents a tyre being loaded onto the EORT for calibration which was further described in Appendix B. The EORTs were calibrated against the Avery Universal testing machine which is rated to 50 tonne with the accuracy of 0.2%.

- Hydraulic pressure transducer (Sun Hydraulics)

For all the tyres mounted to 12 tonne frame, a load applied was a function of the pressure applied to a hydraulic ram. The ram has a transducer which measures the pressure in the top of the ram cylinder. Two hydraulic pressure transducers were used. Calibration of the system gave the relationships between the pressure in the ram and the load applied to a tyre.

- Tension link dynamometer (Staightpoint Ltd)

The loads applied, during the static hard surface contact area experiments, to all the tyres tested in the 5 tonne and 0.25 tonne frames, were measured using the tension link dynamometer with the maximum capacity of 5 tonne. The load cell was mounted between the lifting crane and the load being measured. For the loads up 2.5 tonne the frame was lifted by the crane at the centre of tyre axle. Due to the fact that the maximum working load of the crane is 2.5 tonne, the loads above this value were measured by lifting the loading frame on one side. In this case the reading measured by the load cell indicated half of the normal load applied to a tyre. For a higher accuracy, a 5 tonne extended octagonal ring transducer was installed vertically on the processor where a frame was connected. That allowed measuring vertical force applied on the pivot point while loading the tyres.

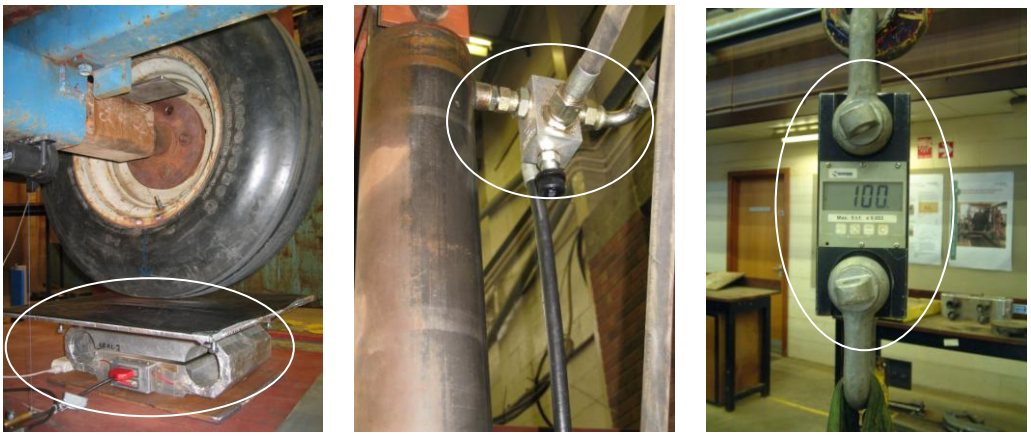

Figure 3.7 Load measuring equipment (left: extended octagonal ring transducer, middle: hydraulic pressure transducer, right: tension link dynamometer)

3.3.2 Inflation pressure measurements (tyres and pneumatic rig)

A number of pressure gauges were used in the project. The gauges employed differ in their application and pressure range that they work at. They were used for measuring tyre inflation pressure and determination of the pressure in the Tekscan calibration device. The devices are described below and presented in Figure 3.8, and calibrated as described in Appendix B.

- Air line pressure gauge (Sealey)

This gauge was initially used but was found to be not accurate enough. It is rated up to 10 bars and it was located at the air line providing pressured air.

- Digitron 2086P pressure gauge

Digitron 2086P is an electronic pressure gauge which works in the range between 0 - 10 bars. It was eventually adopted for most of the tests other than the calibration of Tekscan sensors which employed Druck pressure gauge.

- Druck DPI 104 pressure gauge

Druck DPI 104 is a digital pressure gauge working at the range of 0 – 20 bars pressure. It was used for determining the pressure applied to the pneumatic apparatus designed and constructed to calibrate the Tekscan sensors.

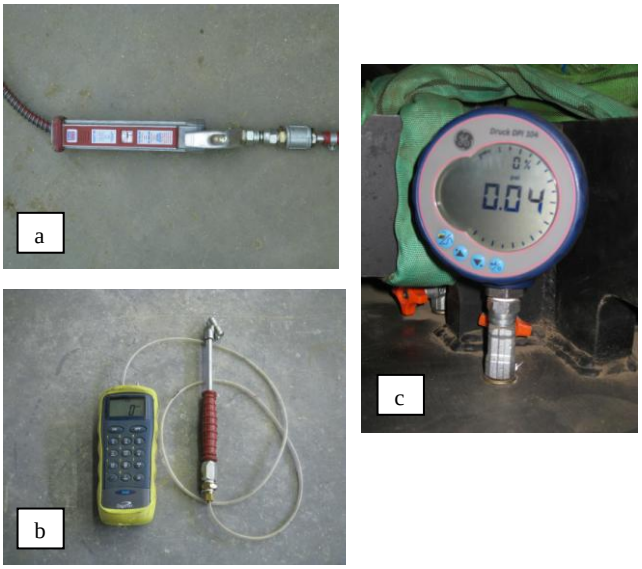

Figure 3.8 Equipment for pressure measurements: a – air line pressure gauge (Sealey), b – Digitron 2086P pressure gauge, c – Druck DPI 104 pressure gauge

3.3.3 Tyre deflection measurements

Vertical deflection of the tyres was measured using draw string transducers. They were used in order to observe how the tyres deflect during load and inflation pressure changes.

The vertical deflections were measured in a static situation when the tyres were loaded onto a hard surface, as a benchmark reference position. The tests were conducted using two draw string transducers (manufactured by UniMeasure, total length of 1000 mm and 2000 mm) mounted outside the tyre as shown in Figure 3.9. The maximum vertical deflection was obtained by measuring both the loaded and unloaded radius and subtracting the difference. The transducers were placed on the each side of a tyre at the centre of axle and a data logger was used to enable measurement of the deflection on each side and the mean value of deflection was calculated. The accuracy of tyre deflection measurements depends on the fittings of the tyres to the rim and their uniformity. To minimise this effect, the same part of a tyre was brought in contact for each deflection test.

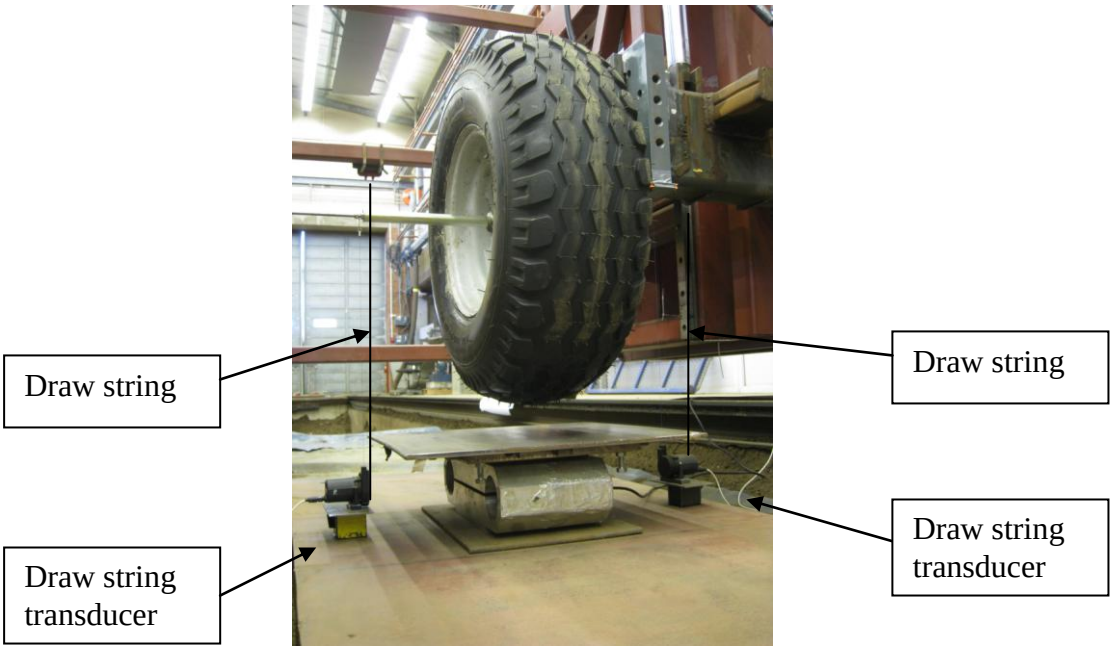

Figure 3.9 Draw string transducers and EORT for measuring tyre vertical deflection and load

3.3.4 Contact patch (ink)

To determine the tyre contact area on a hard surface under static conditions a simple procedure used previously by Plackett (1983), here after known as Plackett's technique, involves the use of black ink and white paper, where the tyre is coated with black ink and loaded onto a sheet of white paper. It is a simple method, usually applied statically, because a rolling inked footprint does not contain any information about the shape of the leading and trailing edge of the footprint (Pottinger, 2006). Figure 3.10 shows an example of the contact area ink patch, the area of which was then measured using a digital planimeter or digitalised and processed in Matlab software (Matlab, 2005) for the tyre contact area measurement as discussed in Appendix A.

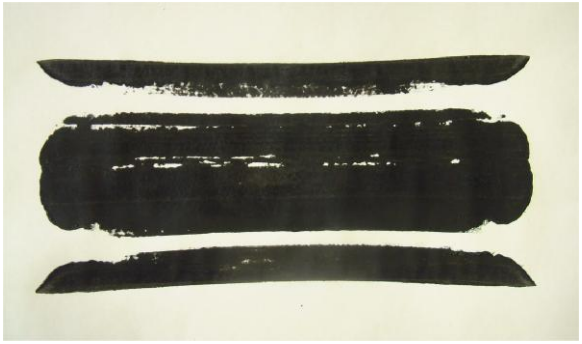

Figure 3.10 Contact area ink patch (front tractor tyre with two grooves)

3.3.4.1 Planimiter Placom

In the initial stage of the project a digital planimeter Placom was used for the measurements of tyre contact areas obtained in the ink tests. However, it was found to be time-consuming so a method involving image processing was developed.

3.3.4.2 Method of measuring contact area using image processing

In order to be able to measure the contact area more efficiently, an image analysis method was developed. It employs a Canon PowerShot S45 digital camera and a Matlab program. The method involves taking pictures of each tyre ink patch. These images were imported to Matlab software and a script was developed for counting the black pixels and determining the contact area. The camera was calibrated by taking a number of pictures of known areas and the new technique for the area measurement was tested against the planimeter method. The accuracy of the digital image analysis method was found to be similar to the planimeter's technique. The error for the image processing method was found to be 0.28 – 0.53%, while for the planimeter it equals to 0.16 – 0.23%. The image processing method was selected for the contact area measurements, as it is less time-consuming. The image processing procedure and evaluation of its accuracy is presented in Appendix A.

3.3.5 Measurements of tyre contact pressure

After the evaluation of the alternative methods of pressure measurements (Chapter 4), the system developed by Tekscan was found to be the most appropriate for measuring pressure distribution across the contact area on the hard surface and in the soil profile below rolling tyres.

Tekscan sensors were chosen for soil pressure measurements as they react similarly to the soil as they are not hard and rigid and did not cause stress concentration. There was also no effect of bridging over the transducers, which would result in inaccurate measurement results. If a sensor film was placed on the soil surface or buried in the soil profile it would behaved as soil reinforcement as its flexibility is different to that of the soil. It would result in incorrect soil pressure values. Additionally, if the sensor mats were located in the soil without any support, when the tyres travelled over the sensors, the soil would deform, and the orientation and direction of the forces would have been difficult to determine. It was, therefore, decided to

use a smooth non-deformable steel plate buried in the soil at a range of depths and the sensors were then placed on it. The plate gave controlled conditions and was used to mimic the environment where a soil hard pan is present in the profile of an agricultural soil. The plate in the soil placed close to the surface was used to mimic conditions of dry grassland where the soil is almost un-deformable due to the inherent soil strength and presence of roots in the topsoil. The results showed the effect of soil depth above a given "level" on reducing the vertical stress and its distribution.

3.4 Experimental methodology

Phase 1 involved a series of experiments carried out with a range of agricultural tyres (see Table 3.1) loaded onto a hard surface. For Phase 2 a selection of the agricultural tyres (see Table 3.1) were towed along the soil surface. The procedures of these studies are described below and their results presented in Chapters 5 – 8.

3.4.1 Phase 1 - hard surface experiments

The aim of Phase 1 was to investigate the effect of load, inflation pressure, presence of tread patter and ply rating on the resulting contact pressure on a hard surface. In order to achieve this, a range of tyres was evaluated at a number of loads and inflation pressures (Table 3.1). The experiments involved measuring tyre contact area, surface pressure and deflection on a hard surface to determine these three parameters in the simplest form in a controlled environment. The contact pressure and deflection results were obtained in order to estimate carcass stiffness of the tyres tested. The study of tyre behaviour on a rigid flat surface represents its behaviour on a heavily compacted soil and prepares the way for further study of tyre performance on soil which is the main aim of this project.

The first method of surface contact pressure determination employed the Tekscan pressure mapping system (described in Chapter 4 and Section 3.3.5) which allowed dynamic pressure measurements. This method enabled tyre contact area and surface pressure distribution (with maximum and mean contact pressure) to be measured. The experiments were carried out in the soil bin as described in Section 3.2.1. Three steel plates (each 2.5 m long x 1.5 m wide x 70 mm thick) were placed in the soil bin at the top of the compacted soil to provide a uniform flat surface. Tekscan sensors were placed on a sheet of aluminum (1.5 m long x 1.5 m wide x

10 mm thick) and located on the middle steel plate. The appropriate Tekscan sensors were selected for each test depending on the size and tread pattern of the tyre and also the pressure range required as described in Chapter 4. The sensors were covered with a layer of plastic film to prevent puncturing of the sensors by tyre treads or soil particles. Then the tyres were loaded onto the hard surface and rolled freely straight-ahead in the soil bin at a constant speed of 0.085 m/s. The Tekscan system was used for contact pressure measurements at a frequency of 100 Hz. The pressure distribution at the tyre – surface interface was recorded as a movie. Each test was carried out three times and the testing variables are presented in Table 3.1. Data recorded by Tekscan system was then transferred and processed in Matlab software (Chapter 4). The contact pressure data was then used for determination of the tyre carcass stiffness, as the difference between the mean/maximum contact pressure and tyre inflation pressure.

The second method involved contact area experiments which were carried out in static conditions following a procedure previously used by Plackett (1983). A steel plate was used in the soil bin to provide a uniform flat surface to load the tyres onto. Three frames, presented in Section 3.2.3, were used to load and move the tyres. Plackett's technique for contact area measurements involved coating the tyres with black ink and loading them onto a white paper placed on the hard surface. Each individual experimental situation was carried out once plus one test for each tyre was repeated three times to ensure repeatability of the results.

There are two types of contact patch results, obtained from the ink tests, depending on the tread pattern of the tyre. The category of the contact area results can be described as follows:

- Tread contact area – actual contact area given by "a single ink print" (tread blocks only for the tread tyres, carcass – for the smooth tyres),
- Projected contact area – total projected area obtained by "a rotation ink print" for the treaded tyres obtained by loading and rotating a tyre a number of times (tread blocks and voids).

For the treadles tyres only the single ink print method was employed. While for the treaded tyres two methods of data collection were employed – the single and rotation ink print. Thus, the area results – tread and projected contact areas – gave two contact pressures for each test.

Tyre ink prints were measured using the electronic planimeter or the images were imported to a computer and the areas were estimated using Matlab software (Section 3.3.4 and Appendix A). Average contact pressure was calculated as load divided by the contact area. The data obtained, was used in order to determine the difference between the mean contact pressure and tyre inflation pressure, which was then compared to the tyre carcass stiffness evaluated using the Tekscan system.

Tijink (1994) considers the mean contact pressure parameter obtained in the ink tests as extremely useful when designing and selecting tyres and machinery as it is commonly used by tyre manufactures for a quick assessment of the compaction capability of the tyre. Table 3.1 shows the variables considered in the contact area measurements on the hard surface. Some of the experimental treatments were the same as the tyres and inflation pressures studied by Plackett (1983, 1987). This enabled a direct comparison of the data. Gill and VandenBerg (1968), however, questioned the usefulness of this method suggesting it is limited since it is only applicable for static conditions. Pottinger (2006) discussed the difference between the rolling and static footprint shapes and pressure distribution for car passenger tyres on the roads. He concluded that for a rolling tyre the normal stresses on the shoulder are higher and the stresses on the crown are lower (in comparison to a static tyre). The change in stress pattern is associated with changes in lateral stress, which generally get reduced in rolling. This is due to the fact that the shoulders move inwards while the crown tends to deform away from the surface; this results in a reduction of the magnitude of crown normal stress.

Tyre deflection experiments were also conducted while the tyres were loaded onto the hard surface. Draw string transducers (Section 3.3.3) were used for the vertical deflection measurements. These tests were carried out statically for all the tyres tested in this project as presented in Table 3.1. The tyre load – deflection data enabled an evaluation of the Plackett's technique for the tyre carcass stiffness estimation (Plackett, 1983) described in Chapter 2.

3.4.2 Phase 2 - soil experiments

Phase 2 considered soil pressure determination in the soil profile at varying depths, as it was conducted in the controlled soil conditions of the soil bin. The aim of this phase was to determine the effect of tyre load, inflation pressure, presence of tread pattern, ply rating and

soil depth on the resulting soil pressure. In order to achieve this, a range of tyres (Table 3.1) were loaded at varying loads and inflation pressures and run over the soil at a constant speed of 0.085 m/s. The tyres were rolled freely straight-ahead. Tekscan sensors (Section 3.3.5 and Chapter 4) were used, buried horizontally at varying depths (from 25 to 550 mm), to measure the pressure in the soil with the frequency of 100 Hz.

Tekscan sensors were covered with a layer of plastic film in order to prevent their puncturing by soil clods or stones. The sensors were placed on a sheet of aluminum (1.5 m long x 1.5 m wide x 10 mm thick) and positioned on the steel plate (2.5 m long x 1.5 m wide x 70 mm thick), which was used as a reaction plate. The soil above the sensors was sieved and then it was uniformly prepared by the soil processor (as described in Section 3.3.4) to a certain soil bulk density. Prior to each test the following soil parameters were measured: dry bulk density and moisture content. Then the tyres at a range of loads and pressures (Table 3.1) were mounted to one of the load frames and run over the soil. Sandy loam soil was used for the tests. Soil moisture content was kept at 9 – 10% – citied by Day (2001), while the dry bulk density was maintained at 1.5 g/cm^3. Pressure data recorded by Tekscan sensors was then processed using Matlab scripts as discussed in Chapter 4.

In order to observe the soil pressure distribution through the soil profile and the depths to which the parameters investigated have an effect, the soil pressures were measured at a range of different depths. Van den Akker (2004) considered the problem of soil compaction to be mainly the subsoil, as compaction of the subsoil requires a great effort to remedy and in some cases is irreversible when it is at depth beyond economical repair. However, as topsoil compaction is also a problem, therefore, the pressures were investigated through the soil profile from 25 to 550 mm.

3.5 Statistical analysis

As preparation of the experiments and data collection procedure was time-consuming, hence, it was impossible to replicate all the treatments. Some treatments of the ink experiments were carried out only once, however, to ensure repeatability of the results, one treatment for each tyre and each experimental set up was carried out three times. It confirmed that the results were repeatable and gave some idea on the variations obtained. The Tekscan hard surface

contact pressure experiments and vertical deflection measurements were carried out with three replications; it was completed in order to evaluate the repeatability of the measuring system and investigate the data variations. The Tekscan soil contact pressure tests were conducted once for each treatment, as the procedure was time-consuming. To insure the repeatability of the data, at least one treatment for each tyre was carried out three times. For some cases continuous variables were considered, therefore it was possible to conduct a regression analysis. As explained in Chapter 4, the data collected using Tekscan system contains a number of data sets recorded by each row of Tekscan sensor for each treatment. This data was used to determine a mean contact patch, which was further used in the analysis. Time limitations did not permit to do any statistical analysis on the data collected by each sensor row.

For statistical analysis Statistica 9 software (2009) was used. Appendixes G – J and M contain results obtained in the statistical analysis. For some analysis the variables were not continuous, however, the graphs provided by the software show a continuous change, which was not the case. When linear relationships were obtained for a continuous variable, a linear regression analysis was performed. In other cases, an analysis of variance (ANOVA) was conducted in order to assess if the factors and their correlations have significant effects on the variables measured. Where possible a factorial ANOVA was performed, for some cases only a one way ANOVA was possible to conduct. A confidence level of 95% was selected, which means that the probability for receiving the tested results from a random population was less than 5%. Before the data was statistically analysed, it was verified if it was normally distributed.

For the combine and implement tyres, the analysis of variance considered only one factor which was a combination of tyre load and inflation pressure. This was due to the fact that as tyre load increases, its inflation pressure has to be increased. Therefore, at each inflation pressure, the tyres were not studied at all the same loads. This was the case for the smooth and treaded combine tyres, while the implement tyres were tested at the range of inflation pressure and only the corresponding maximum loads.

4 TEKSCAN PRESSURE MAPPING SYSTEM

4.1 Introduction

This chapter summarises options available for pressure measurements which were reviewed in Chapter 2 and concentrates on pressure mapping systems which can provide a pattern of pressure distribution. As the Tekscan pressure mapping system was found to be the most appropriate for the tyre contact pressure measurements on both surfaces and in the soil profile, this is described in more detail. No earlier literature, either in the public domain or the Tekscan company, was found on the subject of measurements of soil pressures resulting from agricultural tyres. Therefore, it was necessary to evaluate and improve the performance of Tekscan system, which is the main focus of this chapter.

4.2 Alternative approaches to accessing soil pressure

A number of approaches for the measurement of contact and soil pressure employed by a range of researchers were discussed in Chapter 2. Having a pressure sensor installed in the soil was considered by Horn and Lebert (1994) to be one of the main problems of determination of the soil stresses. In general, pressure sensors are a foreign body in the soil with different deformation properties from those of soil. Horn and Lebert (1994) suggested that if a pressure sensor is weaker than the soil, then the recorded stresses will be underestimated in comparison to the 'real' stresses. Whilst, for a stronger sensor the stresses will concentrate at the transducer as it is more rigid. This will result in an overestimation of the 'real' soil pressure. In theory, the elasticity of the transducer should be the same as the elasticity of the soil surrounding the sensor. However, they considered it extremely difficult to obtain this relationship in practice.

There are two types of pressure sensors: (a) those that deform plastically and (b) those which deform elastically. Plastic sensors are built using pneumatic or hydraulic bodies and they change volume according to the applied stresses. Usually they are weaker than the soil and tend to underestimate stresses. Elastic stress transducers consist of piezo-electric materials or strain gauges placed on an aluminium or steel diaphragm, they overestimate the real stresses (Horn and Lebert, 1994).

For this project a pressure mapping system containing a large number of small pressure transducers was required. Pottinger (2006) indicated that it is possible to measure normal stress over a large area using 1-D transducers employing printed circuit technology which generate an array of small force sensors. A matrix of small elastic piezo-electric transducers was selected as the aim of this project is to develop an understanding of pressure distribution across the tyre contact patch. The width of the sensors required to be above 600 mm in order to be able to test all the tyres selected. The expected maximum contact pressure was approximately 5 bar, so sensors with a range as high as this were required. When selecting a pressure mapping system, its accuracy and spatial resolution was required to be as high as it was possible.

4.3 Validation of the available pressure mapping systems

Initially, the experiments investigating the contact pressure under the tyre on a hard surface using ink for contact area determination were carried out. They only allowed an estimation of the mean contact pressure by dividing the total load by the contact area. Many researchers showed that tyre contact pressure is not uniform (Bekker, 1956; VandenBerg and Gill, 1962; McLeod *et al.*, 1966; Burt *et al.*, 1989, 1992; Gysi *et al.*, 2001; Trautner, 2003; Way and Kishimoto, 2004). VandenBerg and Gill (1962) investigated pressure distribution under loaded agricultural tyres using five strain gauged pressure cells of 2 inch diameter installed into a firm sand soil in a line parallel to the direction of tyre travel. There is a need for a better technique that could lead to a good understanding of the pressure distribution under a tyre on both hard and soil surfaces. It was, therefore, recognised that a pressure mapping system would be a better tool for achieving the aims of the research. A review of the available pressure mapping systems was carried out in two stages. The first stage covered consideration of three available systems and took into account their specification. The second stage involved preliminary testing of Tekscan system which was found to be the most suitable.

Stage 1: Three following suppliers were considered:

1. A.D.S. Ltd. – Tekscan (I-Scan system with Conformat system)

   Tekscan is a piezo-electric pressure mapping system which allows monitoring and comparison of real-time contact area and pressure distributions over time. It dynamically

measures the interface pressure between two surfaces. Tekscan contains thin sensing mats built as multi-sensor array varying is size, shape, spacing resolution and pressure range.

2. Sensor Products Inc. – PressureX – pressure sensitive film

Pressurex is a mylar based thin pressure sensitive film that contains a layer of tiny microcapsules. It permanently captures contact area, contact pressure distribution and its magnitude between any two contacting surfaces, as the application of force on the film causes the microcapsules to rupture. The conception of the film is similar to Litmus paper, as Pressurex changes colour in direct proportion to the amount of force applied. It captures an individual image of pressure distribution and cannot be used dynamically. If the film is used dynamically, it captures the maximum pressure that it is exposed to. There are number of films which vary in pressure range and can be cut to match any size and shape.

3. Interface Force Measurements Ltd. - Xsensor Pressure Mapping System

Xsensor sensors are also pressure imaging mats which allow contact area and pressure distributions over time to be monitored and recorded. Their construction is similar to Tekscan sensors and they are available in a range of dimensions, speeds, special resolutions and pressure ranges.

The following parameters were considered in the evaluation of the best system: flexibility (non-rigid flexible membrane), size, pressure resolution, ability to upgradeable the system (replace parts of the system with ones that provide better performance), customizability (make parts of the system according to individual requirements), reusability, static vs. dynamic application, test-monitoring capability, modularity and cost. The characteristics of the available systems are presented in the Table 4.1 below with a comparison of the three products for each of the above parameters. The table allows visual evaluation of each product and its potential for use within the project. Tekscan pressure mapping systems and related components supplied by A.D.S. Ltd. are shown to be the most suitable for the planned work of measuring pressure distribution across the contact area on the hard surface and also in the soil profile below rolling agricultural tyres. The Tekscan pressure mats were tested in the second stage of the validation. This involved loading one of the agricultural tyres onto a range of sensors placed on a hard and soil surface. The performance of the sensors was found to be satisfactory and the system was purchased.

Table 4.1 Evaluation of pressure mapping systems

Systems		Flexibility	Size	Pressure resolution	Upgradeable	Customizable	Reusable	Static vs. dynamic application	Test monitoring capability	Modular	Total Cost
A.D.S. Ltd. – TekScan	**Standard I-Scan system** – 2 handle USB pressure measurement system includes 2 sensor mats and 5 sensors (2 of 6300 strap, pressure rating 50psi, size 264 x 34mm and 2 of 9830 '11 strap', pressure rating 10psi, size 188.6 x 203.2 mm) **ConforMat system** – Software system + ConforMat (5330, pressure rating 6psi, size 471mm x 471mm)	✓	✓	✓	✓	✓	✓	BOTH	✓	✓	£28,857.00
Sensor Products Inc. – Pressurex	**Topaq system** – for data analysis; **10 rolls** – ultra-low pressure films (pressure rating 28 - 85psi, roll dimension 270mm x 5m)	✗	✗	✗	✗	✗	✗	STATIC	✗	✗	$17,775.75
Interface Force Measurments Ltd. – Xsensor	**Xsensor System software** **Standard sensor** – flexible, high pressure (pressure rating 10 – 200psi, size 290mm x 290mm)	✓	✓	✗	✓	✗	✓	BOTH	✓	✗	£19,163.00 * discounted £22,545.00 * regular

4.4 Introduction to Tekscan system

The Tekscan system is a piezo-electric pressure mapping system (Figure 4.1) which allows the real-time contact area and pressure distribution to be viewed across a multi-sensor array (Tekscan, 2008b). The system records information, statically and dynamically, for further analysis and it consists of:

- Piezo-electric pressure sensitive mats called sensors,
- Data acquisition handle that communicates through USB port,
- Data acquisition software,
- Sensor software map.

Tekscan thin-film sensors consist of two thin, flexible polyester sheets which have electrically conductive electrodes placed in varying patterns. They also contain a thin semi-conductive ink coating as an intermediate layer between the electrical contacts. The ink provides the electrical resistance at each of the intersection points (called sensels) and this resistance changes as the stress across the cell changes. By measuring the changes in current flow at each intersecting point, the applied force distribution pattern can be measured and recorded by the Tekscan system. The lattice of the mat allows the software to determine the location of the load. Each sensor mat has different dimensions and pressure rating. Therefore, each mat requires a different sensor software map program containing information about size and spatial resolution to properly correlate any recorded nodal pressures to their correct physical location. The Tekscan system has an 8-bit output, which means that each individual sensing element reads a raw value from 0 – 255 giving a resolution of 0.4%. This raw data corresponds to the force applied to the sensel and should be calibrated. The thin construction (0.1 mm) of the mat allows it to be gently deformed and permits minimally intrusive/invasive surface pressure measurements. The Tekscan handle gathers data from the sensor, processes it and sends it to a computer (Tekscan, 2008a).

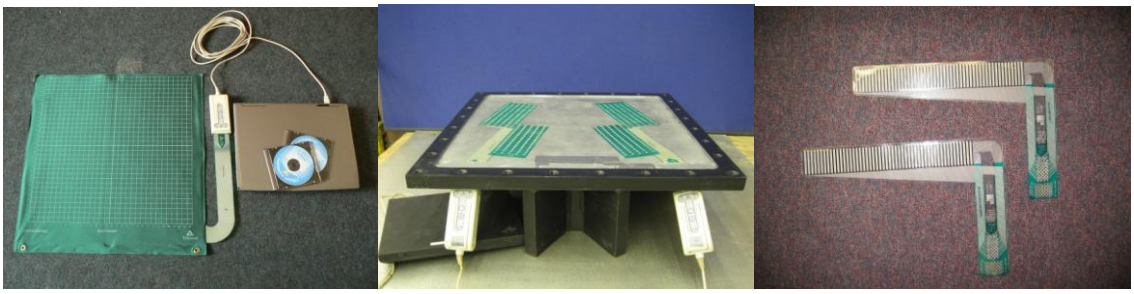

Figure 4.1 Tekscan pressure mapping system (left: Conformat 5330 sensor, middle: 9830 sensor, right: 6300 sensor)

The following sensors were used:

- Conformat system: Conformat 5330 'early production'
    - standard pressure range: 0 to 8 psi (0 to 0.55 bar) which can be increased/decreased by factor of 10
    - sensing area: 471.4 mm x 471.4 mm
    - number of sensing elements: 1024
- I-Scan system: Sensors 9830_A and 9830_B
    - standard pressure range: 0 to 10 psi (0 to 0.7 bar) which can be increased/decreased by factor of 10
    - sensing area: 188.6 mm x 203.2 mm
    - number of sensing elements: 176
- I-Scan systems: Sensors 6300_A and 6300_B
    - standard pressure range: 0 to 50 psi (0 to 3.45 bar) which can be increased/decreased by factor of 10
    - sensing area: 264.2 mm x 33.5 mm
    - number of sensing elements: 2288

The methodology for using Tekscan sensors in the investigation of measuring pressures resulting from tyres was described in Section 3.4. The majority of the experiments involved using 9830_A and 9830_B sensors. They were selected as it was possible to cut them and place across the soil bin as a narrow band. They were used in all soil experiments with the range of tyres and the hard surface tests with the smooth and treaded rear combine tyres. As the 6300_A and 6300_B sensors have a higher special resolution and they work at a higher pressure range, they were selected to be used in the hard surface experiments on the

implement tyres. For the implement tyre, the sensors were put one next to the other across the soilbin to "cover" the whole width of the tyres. Due to the large lugs of the treaded rear combine tyre, the sensors were place on one side of the tyre contact area in order to record contact pressure distribution across the lug. The contact patch was build with the assumption that the tyre was centrally loaded and the pressure on the other side of the contact patch was the same.

4.5 Previous reported experience using the Tekscan system

Rose and Stith (2004) employed Tekscan sensors for vertical pressure measurements in railroad tracks. They investigated the problem of drift and calibration technique using a hydraulic compression and tensile machine. The calibration tests showed that the level of sensors' accuracy was satisfactory under similar loading pressures, times and materials. Non-linearity of the sensors was confirmed by the application of a number of loads and consideration of the total raw outcome. A power log equation was established as the best fit of the calibration relationship. Multiple calibration curves were found to give better accuracy.

Calibration of the Tekscan system was also considered by Brimacombe *et al.* (2005), who proposed calibration routines which provide more accurately calibrated force measurements than the Tekscan built-in calibration function. The I-Scan sensor was used in these experiments and four different calibration methods were evaluated: two Tekscan linear calibrations (performed at two different scales namely 20% and 80% of the maximum applied load), a Tekscan power calibration (carried out at 20% and 80% of the maximum applied load), a user-defined 10-point cubic calibration and a user-defined 3-point quadratic calibration. All the calibration passed through point (0, 0). Figure 4.2 shows the output calibrated using the five calibrations against Instron load cell measurements. When comparing the three Tekscan software implemented calibrations, the power calibration was the most accurate. The two linear calibrations, conducted at 20% and 80% of the maximum load, and the power calibration (20% and 80% of the maximum load) gave the following errors of 24.4%, 10.5% and 2.7%, respectively. The user-defined polynomial calibrations were found to be more accurate giving force measurement error (difference between calibrated Tekscan output and applied load against the tested sensor range) of 1.5% and 0.6% for the quadratic and cubic calibrations, respectively. These results confirmed that determining your own

specific calibration curves gives the possibility of obtaining a higher accuracy of the system, therefore it is advised to calibrate data externally. Similar was found by DeMarco *et al.* (2000).

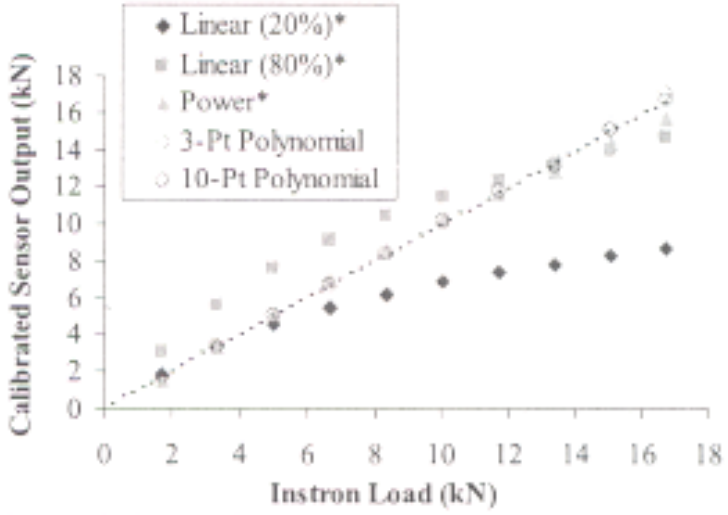

Figure 4.2 Typical sensor output after Tekscan and user-defined calibrations (Brimacombe *et al.*, 2005)

The Tekscan power calibration used by Wilson *et al.* (2003) was reported to give a comparable error of 4.4%. Buis and Convery (1997) reported in their study an average variation of +/- 2% with a maximum variation of +/- 10% for an individual sensing element.

Maurer e*t al*. (2003) evaluated the F-socket Tekscan system and assessed errors associated with sensor drift, surface curvature, cell scatter and loading rate. It was proved that sensor equilibration, which accounts for some variations between the individual sensing elements of a sensor, is effective in reducing inter-cell variation. Accuracy of the system was checked by applying known loads to the sensor and comparing them to the Tekscan output. After a 9-point equilibration and 2-point calibration (20% and 80%) pressures were underestimated and overestimated by a maximum of 10.9% and 1.1%, respectively. The results were most accurate when the sensor calibration was conducted at the same loading rate as the pressure application during the tests. In this case, the sensor output was found not to be influenced by surface curvature.

The accuracy of the Tekscan system in determining contact area was investigated by Drewniak *et al.* (2007). An approach aiming to improve the accuracy of the contact area measurements collected by the system was evaluated. The experiments involved applying circular indenters/discs (a foam-rubber pad between the sensor and the intender) of varying known sizes to a Tekscan sensor. The system recorded contact areas and they were compared with the actual areas. The Tekscan data was post-processed to filter out sensel signal intensity values that were at least two standard deviations from the average sensel signal intensity values of the sensor matrix. From this an adjusted area was calculated. Unprocessed Tekscan results gave area percent errors ranging from 5% to 27%. The filtering algorithm reduced most errors to less than 1%. The errors were found to be influenced by the size of the area loaded, where the smaller the area the larger the contact area percent error. This results from the "edge effect", where the sensels along the perimeter provided an output despite the fact that they were not in direct contact with the indenter. An unexpected finding was the trend for a greater percent error in contact area with an increase in the applied load. Loading the sensor with a pressure above the saturation pressure greatly decreased the accuracy of contact area measurements. Drewniak *et al.* (2007) pointed out one weakness of the Tekscan system, which is that if any part of a loading object comes into contact with a sensel, the area for the entire sensel will be added to the total contact area, hence, overestimating contact area.

The repeatability and accuracy of a Tekscan sensor measuring facet joint loads, pressures and contact areas were investigated by Wilson *et al.* (2006). They also studied the effect of the calibration protocol on the measured parameters. The repeatability of the system in the force, pressure and area measurement varied between 4 – 10%. Their results show that accuracy is influenced by the type of calibration used and that measurements made using a linear calibration were more repeatable and more accurate than those made with a two-point calibration. The linear calibration method overestimated the applied load by an error of 18% +/- 9% (mean +/- standard deviation) up to 50% +/- 9%, while the two-point method overestimated the loads by 35% +/- 16% to 56% +/- 10% depending on the load. The limited accuracy of the sensor could be influenced by the fact that the applied loads were small (5 – 15%) relative to the sensor's measurement range. This is supported by the finding that accuracy was improved for higher applied loads. The authors, however, pointed out the advantages of Tekscan system compared to the other comparable methods. They highlight its

possibility for pressure distribution measurements, electronic recording of results, ability to measure the area of load distribution and a simple experimental setup.

Research on Tekscan system application in the medical industry was also carried out by Ferguson-Pell *et al.* (2000) who evaluated the suitability of Tekscan sensors for application in low pressure measurements. Drift, repeatability, linearity and hysteresis were tested. The drift was found to be 1.7 – 2.5%/logarithmic time and the repeatability was 2.3 – 6.6%. The linearity was 1.9 – 9.9% and hysteresis was on average 5.4%. The drift results suggest that the system is most accurate for static measurements. The sensors are also suitable for dynamic experiments but a compatible calibration method needs to be used.

Harris *et al*. (1999) compared Tekscan system sensors to the Fuji pressure-sensitive film. The contact areas measured using the Fuji film were found to be 11 – 36% smaller than the values obtained with Tekscan sensors. They also point out some other limitations of the pressure sensitive film as handling, sensitivity to shear stress and the fact that it captures only one movement in time. While the Tekscan system is easier to use and continuously records data with time. Additionally, one sensor can be used for a number of tests and the data collected with Tekscan system had a smaller standard deviation than with Fuji pressure-sensitive film. Overall, Tekscan system was found to be easier to use and a more reliable technique in comparison to Fuji film.

The Tekscan system was also validated for static and dynamic pressure measurements in human femorotibal joints by Wirz *et al.* (2002). For the static investigations, Tekscan was compared with the Fuji measuring system. No significant differences were found in maximum pressures and contact areas between the two systems. However, the Tekscan system can be used for many tests, while the Fuji film can only be used once, this also permits the Tekscan to make dynamic pressure measurements. Sumiya *et al.* (1998) concluded that the Tekscan system does not measure the normal pressures accurately enough for a high level of certainty in terms of absolute values, but it allows for relative comparisons of pressure distributions. The system, therefore, can be valid for evaluation of factors affecting pressure distribution.

The review of the literature describing studies on the Tekscan pressure mapping system clearly highlights the problems associated with the system which are as follows: drift, repeatability and hysteresis. It also points out the importance of the appropriate calibration of the sensors in order to reduce the uncertainties in the results.

4.6 Calibration of the Tekscan system

Both from the principles of good science and the above literature, it is paramount that the sensor mats need to be calibrated and their performance evaluated. In order to provide fundamental and independent calibration of the Tekscan sensors a pneumatic rig was designed and constructed to allow the application of uniform pressure to all sensing elements being simultaneously calibrated. The calibration of Tekscan sensors is required in order to convert their digital output into engineering units. There are some variations between individual sensing elements of any given sensor. The output inaccuracies related to the sensor variations can be minimised by applying a uniform pressure across the entire sensor; this process is called equilibration.

The calibration was conducted by two methods which were then compared. Firstly, the sensors were equilibrated and calibrated following the Tekscan guidelines from the Tekscan (2006). Their performance was evaluated by comparison of the real and recorded data using Matlab software (Matlab, 2005) and the errors of each pressure element calculated. The second method involved recording directly the raw values available from the Tekscan system when applying a number of uniform pressures in increasing increments to the sensels. This was conducted in order to locate the erroneous sensors and apply a calibration to each individual sensel. The performance of the sensors calibrated using the second method was also evaluated (Matlab software, Matlab, 2005) and found to provide more accurate results, although there were still some residual variations but they are lower than the variations obtained following the Tekscan recommended calibration. The new Tekscan calibration was initiated by Misiewicz *et al.* (2008) and continued in this project.

4.6.1 Design of the calibration device

The device (shown in Figure 4.3 and 4.4), designed and built at Cranfield University, was used for conditioning, equilibrating and calibrating Tekscan pressure mapping sensors. The

detailed design of the calibration device with stress analysis and its detailed drawings are given in Appendix C.

Calibration/equilibration system components are shown in Figure 4.3 and 4.4. The sensor is placed on the smooth ground upper surface of the bottom plate, and then the diaphragm is placed on the sensor followed by the top plate. The plates are bolted together by 28 M16 set-screws torqued to 200 Nm. Pressure is applied inside the device from the top into the plenum chamber and recorded using the digital pressure gauge Druck (Chapter 3). The maximum pressure that can be applied using the device is 34.5 bars. Air can be used to pressurise the device up to 8 bars, whilst oil is recommended for pressures above 8 bars. A flexible rubber membrane or polythene sheet was used as a diaphragm. This allows a uniform pressure application to the entire sensor. The entire system weights 0.28 tonne.

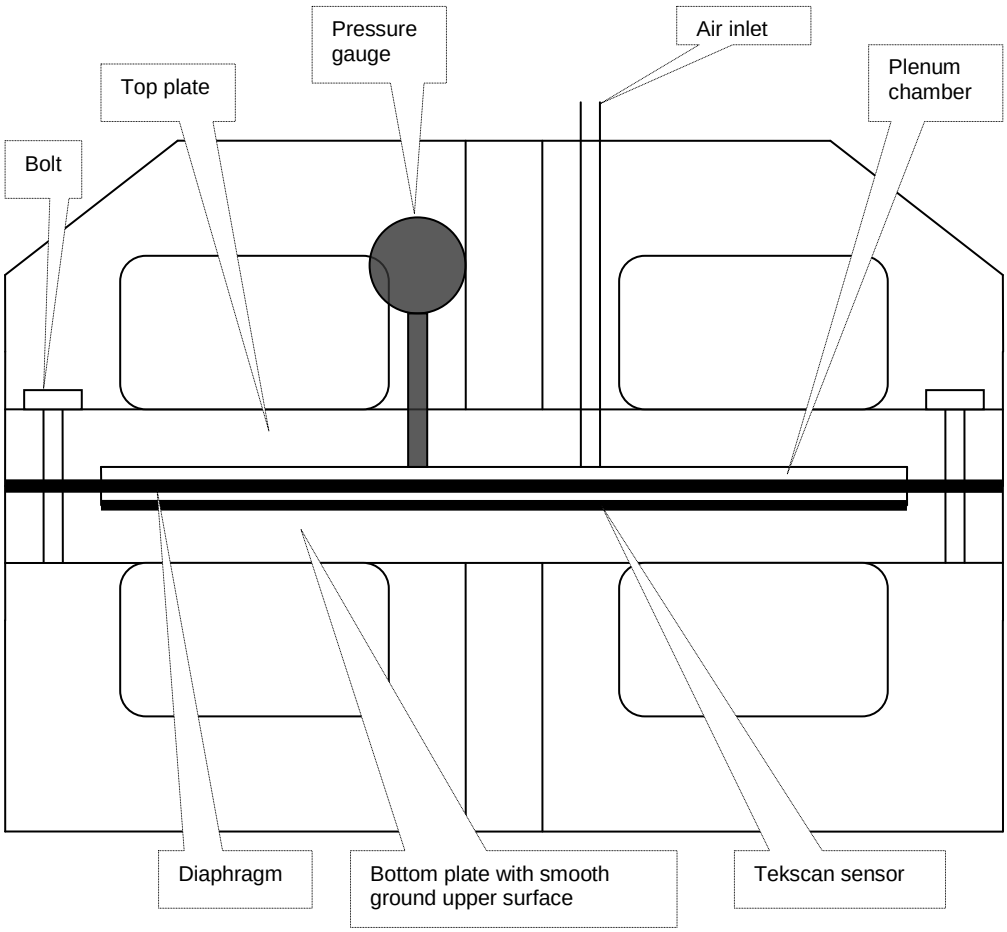

Figure 4.3 Components of the Tekscan calibration device

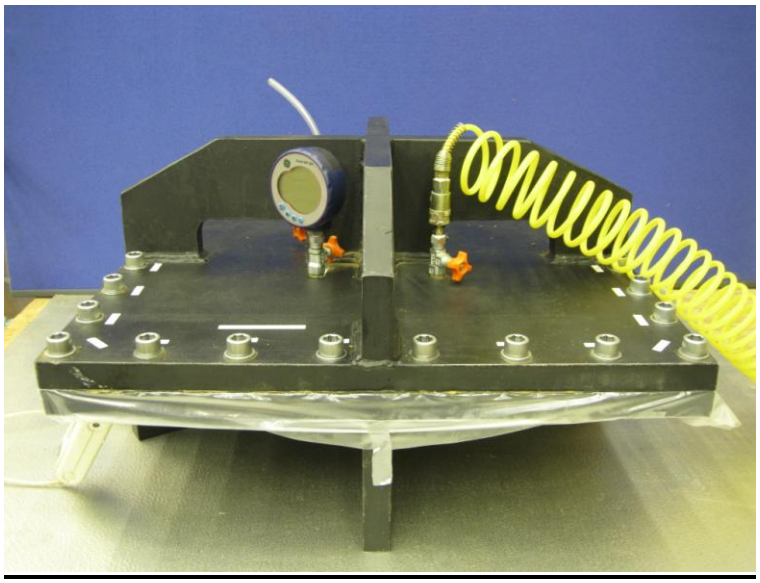

Figure 4.4 Tekscan calibration device

BPMS Research ver. 5.84C (English) software was used for working with the Conformat sensor (hardware driver version 5.21, language DLL version 5.84). For using the I-Scan sensors, I-Scan ver. 5.83l (English) was employed with a hardware driver version 5.21 and language DLL version 5.83.

4.6.2 Tekscan recommended calibration

The manual of Tekscan software (Tekscan, 2006) provides two methods of calibrating sensors, a one point calibration or a two point calibration. These two calibration methods are applicable depending on the application, the expected results and the materials used. A one point calibration assumes a linear output from the sensor with zero force (pressure) applied resulting in zero total raw sum of output. In this case the I-Scan system uses two points to calculate the calibration relationship. This type of calibration is desirable for applications where similar loads are applied in the tests. The other type of calibration is a two point calibration, which takes into account the non-linearity of the sensels. It also uses the zero force equals to zero output assumption and then determines a power logarithmic curve using two other calibration points. As the one point calibration assumes a linear output, it gives the variation of the cells output accurately, which presents an accurate pressure distribution with higher and lower pressure areas shown to scale. However, total loads could vary from the calibration load and it may be over or underestimated. Rose and Stith (2004) found that the two point calibration underestimates the lower pressure areas and overestimates the higher

pressure areas, but gives accurate total load. It was, therefore, decided that the two – point calibration method is more appropriate for this project, especially as the loads measured in the experiments were expected to vary widely.

Following Tekscan recommendations, the sensors were conditioned by loading them five times before they were calibrated. This procedure helps to lessen the effect of drift and hysteresis (Tekscan, 2006). They were loaded with uniform pressure to values approximately 20% greater than the expected during the tests. For the calibration and equilibration uniform pressures were applied to the sensor as follows:

1). The equilibration was conducted in 10 increments when pressure was increased. Prior to this process a minimum pressure was applied to the sensor for one minute to establish an equilibrium condition.

2). During the calibration process, a scale factor established during the equilibration process was applied to each sensing element to make the output uniform between sensels. A two – point calibration was performed by applying two different loads to the sensor (20% and 80% of the expected maximum test load). The loads were applied for one second to allow the pressure to stabilise. Using these data Tekscan software performs a power law interpolation for overall sensor based on zero load and the two known calibration loads.

Mean pressure indication

In order to evaluate the Tekscan calibration, a number of uniform pressures were applied to each sensor after it was equilibrated and calibrated. The mean, minimum and maximum Tekscan values were calculated and compared to the applied pressures as indicated with the Druck pressure gauge. The data were presented in Table 4.2. This shows that the mean overall sensel pressures, obtained by Tekscan sensors, were found to be a good indication of the pressure applied to a sensor. However, a large variation of pressures across the sensor was found, especially for the high pressures.

Table 4.2 Tekscan accuracy in the mean pressure measurements

Sensor	Pressure applied (bar)	Tekscan results			Error of the mean pressure (%)	Max deviation against full scale (%)
		Mean pressure (bar)	Maximum pressure (bar)	Minimum pressure (bar)		
Conformat 5330 'early production'	0.689	0.669	0.756	0.559	2.9	3.9
	1.386	1.395	1.498	1.282	0.6	3.3
	2.101	2.164	2.392	2.015	3.0	8.7
	2.759	2.805	3.343	1.903	1.7	25.6
6300_A	0.689	0.705	1.231	0.307	2.2	17.4
	1.379	1.385	1.988	0.635	0.5	24.8
	2.068	2.059	3.019	1.206	0.4	31.8
	2.758	2.789	3.019	1.822	1.1	32.0
6300_B	0.689	0.678	0.916	0.394	1.6	8.2
	1.379	1.381	1.626	1.157	0.2	7.0
	2.068	2.050	2.424	1.804	0.9	10.7
	2.758	2.730	3.485	2.344	1.0	21.6
9830_A	0.138	0.132	0.196	0.084	4.0	7.7
	0.276	0.256	0.298	0.221	7.3	5.1
	0.414	0.440	0.478	0.407	6.3	4.6
	0.552	0.621	0.716	0.600	12.6	11.5
9830_B	0.138	0.145	0.233	0.090	5.5	15.6
	0.276	0.265	0.303	0.230	4.0	6.7
	0.414	0.385	0.414	0.354	6.8	5.5
	0.552	0.557	0.563	0.495	1.0	11.0

Pressure drift

Tekscan sensors do not have a constant output when a constant load is applied. The output drifts as the load is applied statically. A test was conducted for 9830_A pressure mat to quantify the amount of drift associated with the sensor. It consisted of uniformly loading the entire sensor for 90 seconds and analyzing the percentage increase in the total applied pressure due to drift as a function of time (Figure 4.5). To minimize the effect of drift, calibration process was conducted over a similar time period to the experiments, by using a one second loading period for both the sensor calibration and the experimental tests.

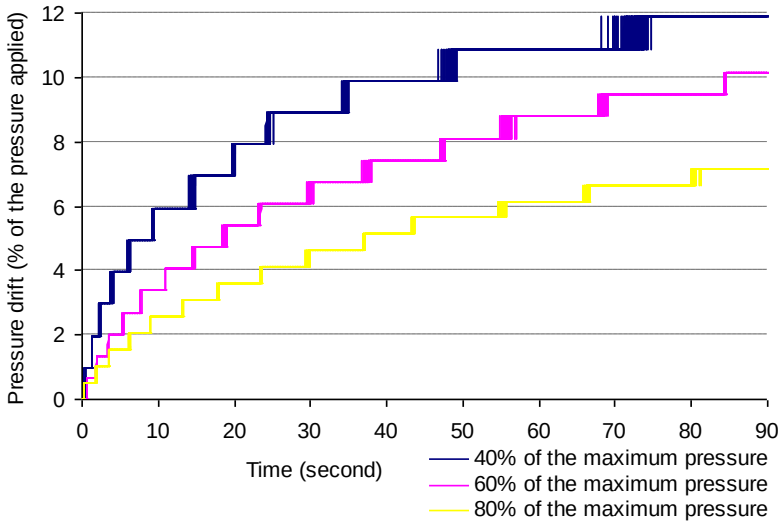

Figure 4.5 Pressure drift for the 9830_A sensor

Compliance factor

Another problem arose from the types of materials being used in the tests. Tekscan sensors have a varied output that depends on the materials that apply the force to the sensor (Tekscan, 2006). During the calibration operation, the sensor was placed on the smooth ground surface of steel plate, a flexible rubber diaphragm or polythene film was then placed over the sensor. Air pressure was uniformly applied to the diaphragm. Both, the hard surface and soil experiments, will involve a smooth aluminium plate loaded by a pneumatic tyre and Tekscan sensor placed at the interface either directly or through the soil. Materials as similar as possible were used in both the calibration and experiments. The rubber and polythene film membrane, used in the calibration, were expected to distribute the pressure similarly to the tyre. Using soils (sandy loam and sand) as pressure transferring medium was tried, however, the pressure was not found to be sufficiently uniform due to the presence of soil particles and their 'interlocking' and 'bridging'. In order to check similarity of the compliance factor during the calibration and experiments, a comparison of the weight computed from the Tekscan vertical pressure distribution and the total weight applied to a tyre was investigated.

Pressure distribution

In order to evaluate the responses of the individual sensing element, the data obtained for each sensor mat, when a range of uniform pressures were applied, were stored in a matrix called 'Tekscan calibrated pressure'. A second matrix containing the true pressure values applied to

a sensor and measured with calibrated pressure gauge (‘applied pressure’) was also constructed.

Construction of two matrices followed calculation of errors as the comparison of two matrixes – ‘Tekscan calibrated pressure’ and ‘applied pressure’ against the full scale of each sensor. The errors confirmed the necessity of improving the calibration performed by Tekscan software. The errors calculated for each sensor tested were plotted as histograms (Figure 4.6). Each histogram presents all the errors obtained for all the sensels for each sensor tested at a range of pressures. Several outliers were found for each sensor, which give evidence of presence of failed sensels. The most frequent values (modes) of errors occurring in the collections of data were found to be 0 or to be relatively close to it. Histogram distributions also show that the 6300_A, 6300_B, 9830_A and 9830_B give errors up to +/- 20%. The Conformat 5330 ‘early production’ was found to have a tendency to over-read the pressure with the errors mostly below 10%.

Table 4.3 shows percentage of sensing area giving an error smaller than the levels of error chosen. The Conformat 5330 ‘early production’ has the best accuracy with 100% of the area providing an error below 10% and 98% of the area giving error less than 5%. The other four sensors are generally associated with larger errors and only 64% - 86% of the area has less than 5% error and 92% - 98% of the sensing area giving errors lower than 10%.

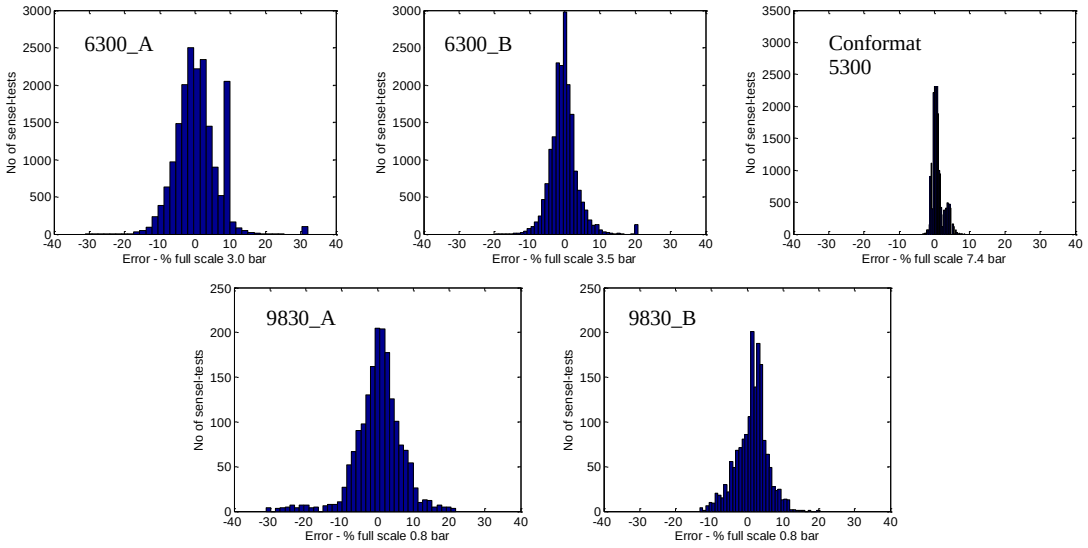

Figure 4.6 Errors of Tekscan sensors

Table 4.3 Sensing area giving errors lower than quoted errors (%) after the application of the Tekscan calibration

Sensor	Error (%)	% of sensing area giving error lower than quoted error (%)
Conformat 'early production' 5330	< 1	58.7
	< 3	89.3
	< 5	98.0
	< 7	99.9
	< 10	100.0
6300_A	< 1	15.2
	< 3	44.6
	< 5	65.1
	< 10	94.8
	< 20	99.3
6300_B	< 1	28.6
	< 3	67.5
	< 5	85.8
	< 10	97.9
	< 20	99.3
9830_A	< 1	16.1
	< 3	44.6
	< 5	63.5
	< 10	90.7
	< 20	97.8
9830_B	< 1	15.6
	< 3	49.6
	< 5	77.5
	< 10	96.4
	< 20	99.9

The evaluation of Tekscan accuracy in the pressure distribution measurements, after the Tekscan calibration was applied, was conducted using Matlab software (Matlab, 2005). The Matlab code written for the evaluation of the Tekscan calibration is presented in Appendix D.

The errors can be classified into two types: random error and systematic error. Random error is caused by inherently unpredictable fluctuations in the readings of a measurement apparatus or in the experimenter's interpretation of the instrumental reading, whereas systematic error is predictable, and typically constant or proportional to the true value. If the cause of the systematic error can be identified, then it can usually be eliminated (Clarke and Cooke, 2004).

Calibration problems

After the sensors were calibrated and equilibrated following the Tekscan calibration procedure, the experiments involving loading the tyres on the soil surface and rolling it over the Tekscan sensors buried in the soil bin soil were started as discussed in Chapter 3. Figure 4.7 illustrates pressure profiles (cross–section) found in the centre of a tyre contact patch. The data was collected by two sensors which were overlapping in the centre. The results collected at the overlapping area were found to differ significantly by up to 26% (Figure 4.7 left), which was not expected. The raw data (un-calibrated and un-equilibrated) from the same test was plotted in Figure 4.7 (right). The raw outputs collected by the same two sensors from the overlapping area were found to be similar, which indicated an issue with the Tekscan calibration and equilibration procedure. The reason for this was the fact that some of the Tekscan sensels are erroneous or are not functioning and Tekscan calibration includes the faulty sensels which results in high errors. While a number of uniform pressures are applied to the sensor, the software reads the pressure applied as a load. When some erroneous sensels give higher results, automatically therefore the good sensels record lower values than it should have recorded, which happens in order to counterbalance the load applied. In case if some dead sensels are present, the good sensels record pressures that are too high.

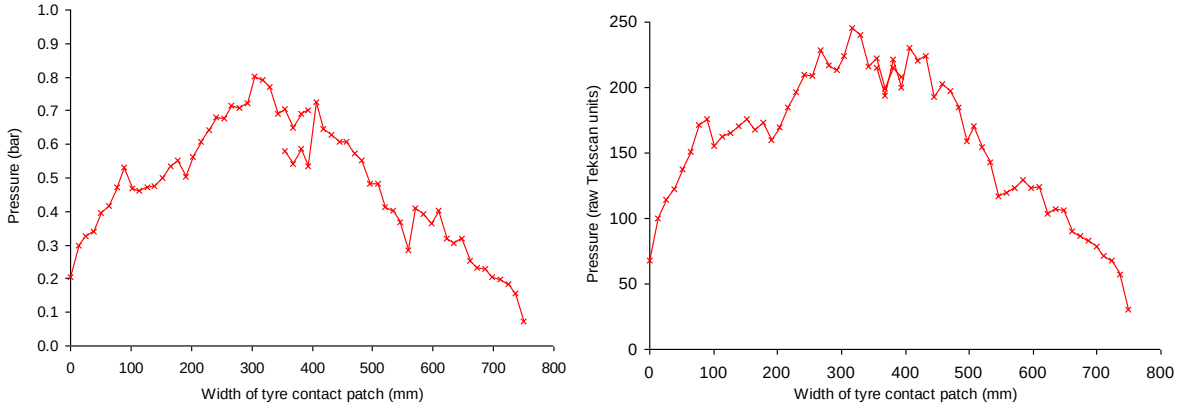

Figure 4.7 Profiles of tyre contact pressure (left: data calibrated and equilibrated following Tekscan procedure, right: un-calibrated and un-equilibrated data)

To improve the performance of the sensors and overcome the problem of Tekscan calibration, the raw Tekscan data obtained by loading the sensors with a number of uniform pressures in the calibration device was used for the further analysis.

4.6.3 Regression models for the non-calibrated data

As Tekscan calibration involves establishing one power law regression curve for a sensor, which is an average value for all the sensing elements, it was required to verify the raw output data of each individual sensel in order to verify it they have the same characteristic. The Tekscan sensors were placed in the calibration device and loaded with a number of uniform pressures. The raw output data (non-calibrated and non-equilibrated) and equilibrated data were recorded and plotted against the applied pressure, as shown for the 9830_A sensor in Figure 4.8. It was verified that the calibration characteristic varies between the sensels, however, the equilibration procedure was found to account for the different calibration characteristics to a great extent. Following Tekscan (2006), power best-fit functions were established to visualise the extreme differences in the sensor performance. After the equilibration was applied to the Tekscan raw output, the maximum variation was found to decrease from 130% to 6%. In order to further increase the accuracy of Tekscan system, a multi-point per sensel calibration was designed (Section 4.6.4).

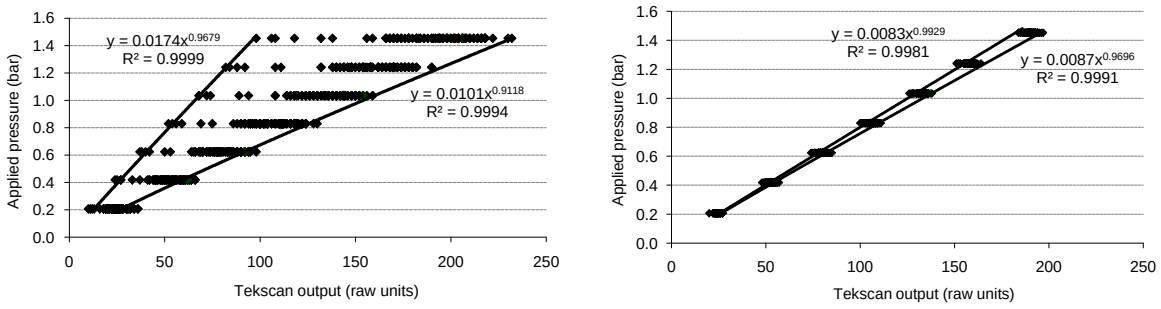

Figure 4.8 Pressure applied vs. Tekscan output for each sensing element of the 9830_A sensor (left: non-calibrated and non-equilibrated data, right: non-calibrated but equilibrated data, N.B. data was plotted using Tekscan convention for calibration)

The relationships between the applied pressure and Tekscan raw output were plotted for each sensing element of 9830_A and 9830_B sensors. A range of regression curves were established using a linear, power, 2nd, 3rd and 4th order polynomial functions. The variability of the Tekscan data obtained by application of the uniform pressure was accounted by calculating the coefficient of determination (R^2) values of each regression curve. The mean R^2 value and standard deviation were calculated and presented in Table 4.4. In order to obtain these values, the raw Tekscan data was processed in Matlab and the scripts developed are

attached in Appendix E. The results showed that the power function gives the smallest coefficient of determination amongst the functions considered, while the polynomial curves give higher R^2 values. The 4^{th} order polynomial was found to be marginally better than the lower order polynomial functions. It benefits over the linear function only 0.3% which is close to the resolution of the system. However, as it was simple to establish a fourth order polynomial function using Matlab software, it was selected as the best fit.

Table 4.4 Coefficient of determination and standard deviation for a range of model functions

Sensor	Model	Mean R^2	Standard deviation of R^2
9830_A	Linear	0.9964	0.0040
	Power	0.9873	0.0116
	2^{nd} order polynomial	0.9989	0.0009
	3^{rd} order polynomial	0.9992	0.0006
	4^{th} order polynomial	0.9994	0.0005
9830_B	Linear	0.9969	0.0028
	Power	0.9874	0.0108
	2^{nd} order polynomial	0.9988	0.0011
	3^{rd} order polynomial	0.9992	0.0008
	4^{th} order polynomial	0.9995	0.0005

Figure 4.9 and 4.10 present histograms of the coefficient of determination for each sensor after the different models were established. The figures show how the coefficient varied between the sensing elements. The majority of the sensels were found to have a good agreement with each model function so their coefficient of determination values were found to be relatively close to 1. The power function gave the largest range of R^2 vales for both sensors which varied from 0.95 to 1. The polynomial functions provided significantly higher coefficient of determination values which were above 0.975 for the linear function and above 0.992 for the 2^{nd}, 3^{rd} and 4^{th} order polynomial, with the 4^{th} order polynomial giving the highest R^2 values. It was, therefore, confirmed that the 4^{th} order polynomial model is the best fit for the Tekscan data.

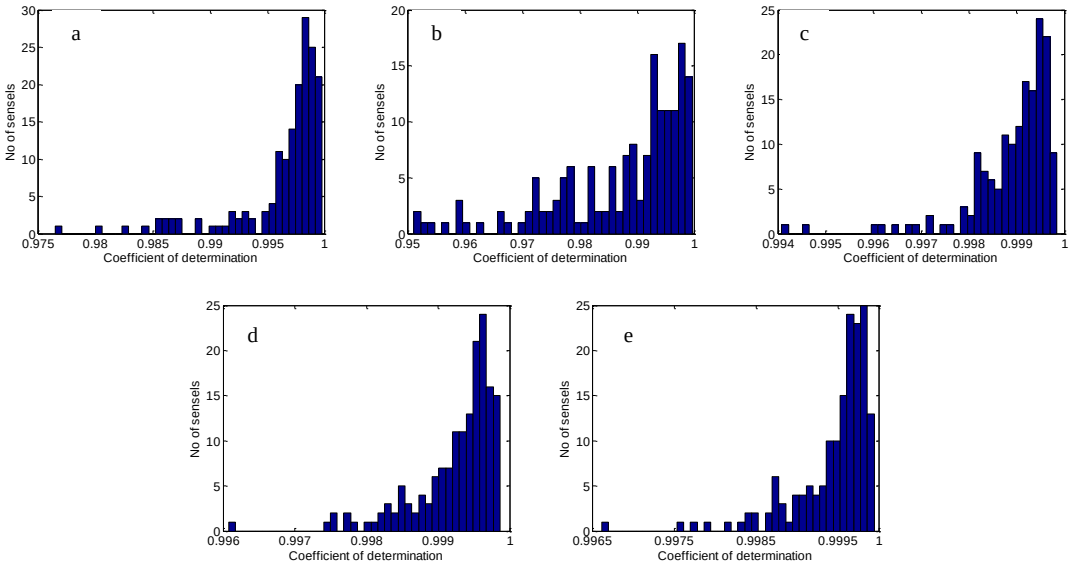

Figure 4.9 Coefficient of determination for the 9830_A sensor (a: linear, b: power, c: 2nd, d: 3rd and e: 4th order polynomial calibration function)

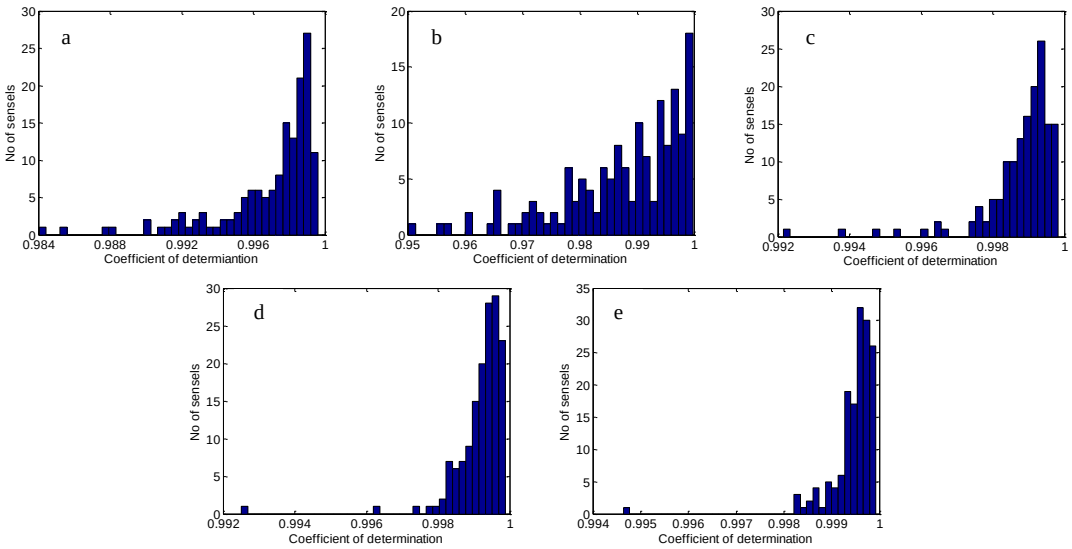

Figure 4.10 Coefficient of determination for the 9830_B sensor (a: linear, b: power, c: 2nd, d: 3rd and e: 4th order polynomial calibration function)

4.6.4 Multi-point per sensel calibration with sensel selection

The mulit-point per sensel calibration involved working directly from the raw values available from the Tekscan system. It included deleting erroneous sensors and applying a multi-point per sensel calibration in a controlled way.

The multi-point calibration of the Tekscan sensors was previously used by DeMarco *et al.* (2000) and Brimacombe *et al.* (2005), where it was found to significantly reduce the amount of error given by the system. In this project the multi-point calibration involved an application of 10 pressures uniformly distributed across the sensor in increasing increments from 10% to 100% of the maximum pressure expected for each sensor, which was conducted in the calibration device. Each pressure was applied for one second, then Tekscan raw data was recorded and processed in Matlab (Appendix E).

Processing the data involved:

1. Loading the data

The raw Tekscan data was loaded and stored in a matrix called 'Tekscan pressure' and a second matrix contained the true pressure values applied to a sensor and measured with the calibrated pressure gauge ('applied pressure') was also stored.

2. Construction of the relationship between 'Tekscan raw data' and 'applied pressure'

A relationship between the 'Tekscan raw data' and 'applied pressure' was established by plotting the best fit curve. The following regression lines were created: linear, power, second, third and fourth polynomials. The regression lines were constructed for each sensel, their characteristic was saved and used for evaluating the multi-point per sensel calibration (point 4 and 5) where the best regression characteristic was selected and further used in calibrating the test data.

3. An identification of the erroneous and dead sensels

The identification of the erroneous and dead sensels was required in order to eliminate them before the calibration was applied. The selection was done on the following basis:

- dead sensels: the sensels giving zero output when loaded;
- erroneous sensels: visual selection.

The third possible way of identifying erroneous sensels was recognised as selection according to coefficient of determination R^2 values. This method was considered but was not further used as the multi-point per sensel calibration with the sensel selection as described above was found to give satisfying results as discussed in (4) and (5) below. In

the future, coefficient of determination could be used for an identification of the sensel giving less confident data. An acceptable boundary for R^2 would have to be chosen and sensels having R^2 greater or equal to the number chosen would be selected as 'good' sensels. The others would be assumed to be faulty and would be ignored in further analyzes. The number of sensels selected as those giving 'good' results would be dependent on the R^2 limit chosen. A number of selection levels could be used: slight selection could exclude only the worse sensels and give an overview of contact pressures across the sensor, severe selection could exclude more sensels and leave less but more accurate data points. Severe sensel selection may result in an occurrence of 'holes' in the data, but improves confidence in the results. This method of sensel selection could be required in some further studies if the accuracy of the Tekscan system was not found to be satisfactory.

4. Calculation of statistical residuals

In order to evaluate the mulit-point calibration, the per sensel calibration characteristic was applied to the 'Tekscan raw data' and the residual errors were calculated as comparison of two matrices – 'Tekscan pressure' and 'applied pressure' against the full scale for each sensor. The data obtained for 9830_A and 9830_B sensors was selected for the evaluation of the multi-point per sensel calibration as these two sensors were used for most of the experimental work. The residual errors were plotted as histograms for each type of regression curve analysed (Figures 4.11 and 4.12). The results confirmed that the design of the multi-point per sensel calibration significantly improved the accuracy of Tekscan pressure measurements by reducing the residual errors below 7% for the linear calibration, below 5% for the 2^{nd} order polynomial calibration and below 4% for the 3^{rd} and 4^{th} order polynomials. The power function was found to have the worse effect in reducing the errors as the residuals were found to vary from -10% to +20% for the 9830_A sensor and from -15% to + 15% for the 9830_B sensor. Therefore, the findings confirmed that the 4^{th} order polynomial is the best fit to Tekscan data and significantly improves the accuracy of the system.

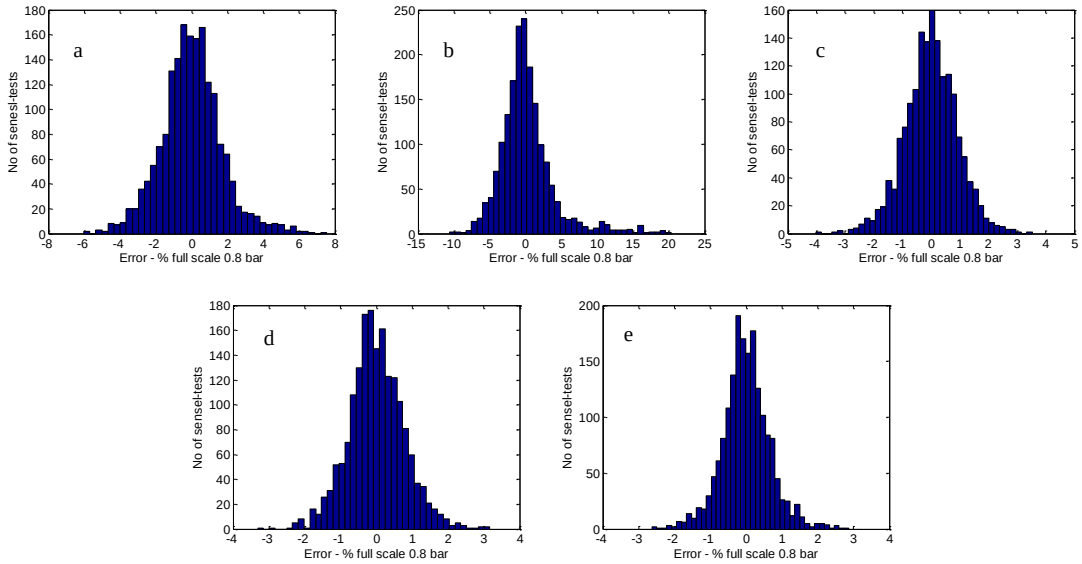

Figure 4.11 Residual errors for the 9830_A sensor after multi-point per sensel calibration (a: linear, b: power, c: 2nd, d: 3rd and e: 4th order polynomial)

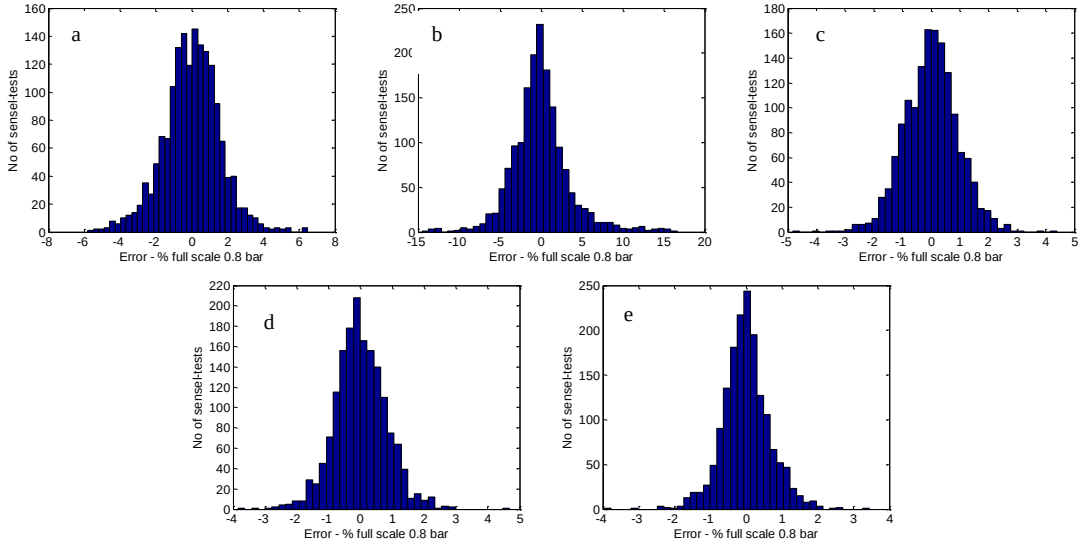

Figure 4.12 Residual errors for the 9830_B sensor after multi-point per sensel calibration (a: linear, b: power, c: 2nd, d: 3rd and e: 4th order polynomial)

Table 4.5 shows the percentage of sensing area giving residual errors lower than quoted for each calibration. It was again confirmed that the 4th order polynomial regression curve gives the best accuracy of the data with the residual errors below 3% for almost all sensing elements.

Table 4.5 Sensing area giving residual errors lower than quoted error (%) after the application of the multi-point per sensel calibration

Sensor	Residual error (%)	% of sensing area giving residual error lower than quoted error (%) for a range of calibration functions				
		Linear	Power	2nd order polynomial	3rd order polynomial	4th order polynomial
9830_A	< 1	51.0	31.6	73.3	81.6	87.8
	< 3	91.7	70.7	99.7	99.8	100.0
	< 5	98.7	87.7	100.0	100.0	100.0
	< 10	100.0	96.5	100.0	100.0	100.0
	< 20	100.0	99.9	100.0	100.0	100.0
9830_B	< 1	51.8	32.3	71.4	80.3	87.6
	< 3	93.6	70.7	99.5	99.8	99.8
	< 5	99.3	87.6	100.0	100.0	100.0
	< 10	100.0	97.6	100.0	100.0	100.0

5. Calculation of statistical errors

In order to further check the accuracy of the multi-point calibration, statistical errors were calculated. A set of raw Tekscan data were obtained by loading 9830_A and 9830_B sensors and the results are presented in Figure 4.13 and 4.14, and Table 4.6.

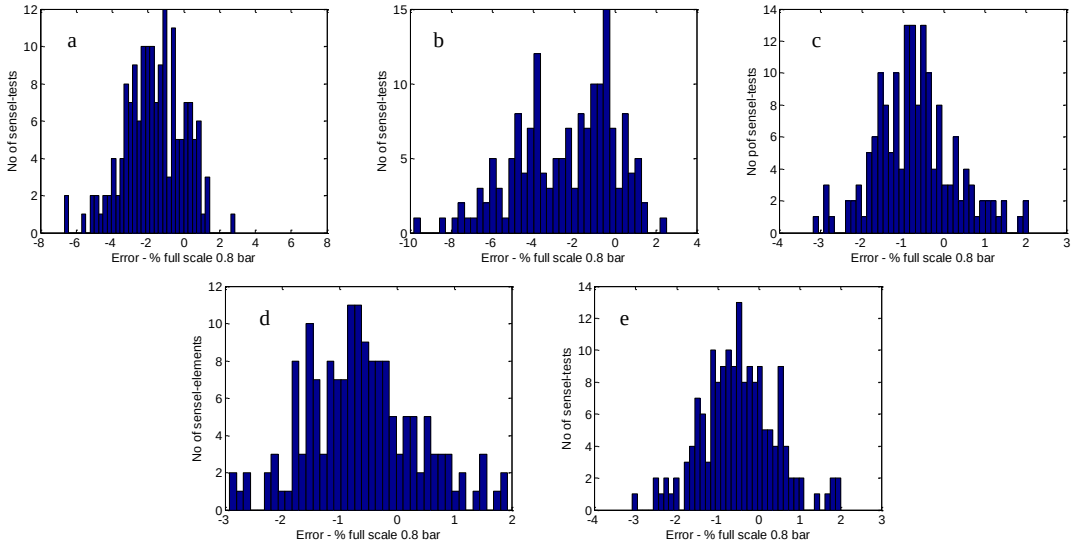

Figure 4.13 Statistical errors for 9830_A sensor after the multi-point per sensel calibration (a: linear, b: power, c: 2nd, d: 3rd and e: 4th order polynomial)

c

d e

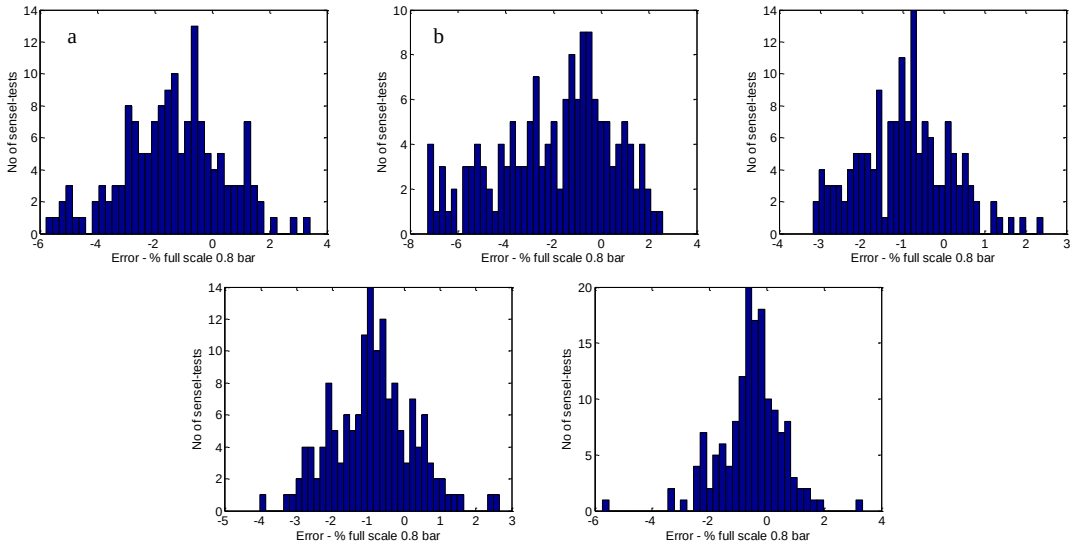

Figure 4.14 Statistical errors for 9830_B sensor after the multi-point per sensel calibration (a: linear, b: power, c: 2nd, d: 3rd and e: 4th order polynomial)

Generally, the results were found to slightly underestimate the pressures. The highest errors were found again for the power function which was from approximately -10% to +3%. For the 2nd order polynomial the error range was the smallest and it only varied from -3% to +2.5%. However, the results in Table 5 confirmed that the 4th order polynomial gives the largest amount of sensing area that has the statistical error lower than 1%. It was found to be 67.1% and 70.2% of the sensing area, depending on the sensor, while for the linear and power functions it was approximately 30% of the area.

Table 4.6 Sensing area giving statistical errors lower than quoted error (%) after the application of the multi-point per sensel calibration

Sensor	**Statistical error (%)**	**% of sensing area giving statistical error lower than quoted error (%) for a range of calibration functions**				
		Linear	**Power**	**2nd order polynomial**	**3rd order polynomial**	**4th order polynomial**
9830_A	**< 1**	32.3	30.5	58.5	59.2	67.1
	< 3	79.9	60.4	99.4	100.0	99.4
	< 5	97.0	85.4	100.0	100.0	100.0
	< 10	100.0	100.0	100.0	100.0	100.0
	< 20	100.0	100.0	100.0	100.0	100.0
9830_B	**< 1**	32.4	31.8	49.0	53.0	70.2
	< 3	83.4	69.5	97.4	97.4	97.4
	< 5	96.7	85.4	100.0	100.0	99.3
	< 10	100.0	100.0	100.0	100.0	100.0

4.7 Processing and interpreting Tekscan data

Each Tekscan test required a large amount of data to be collected. It needed to be processed in order to give an understanding of pressure distribution across the contact patch. A procedure for processing the data and building a pressure contact patch which was present during the test under the tyre was developed in Matlab software and the code written is shown in Appendix F. The data processing was necessary as the sensors were placed across the soilbin as a narrow band perpendicular to the tyre travel direction and did not cover the whole length of the contact patch. The scripts for "shifting" the data, presented in the appendix, were specially designed for the 9830 sensors which were used for the majority of contact pressure tests as shown in Figure 4.15. The other scripts can be also used for all other sensors. In order to use the script for time shifting data obtained from other sensors, the code for shifting was slightly modified depending on the dimensions and orientation of the sensors.

Figure 4.15 The 9830_A and 9830_B Tekscan sensors placed in the soilbin

The processing procedure involved the following steps:

Step 1: Read the raw Tekscan data files.

Step 2: Recognition of the faulty sensels and application of the 4th order polynomial multi-point per sensel calibration.

Step 3: Realignment of the data according to the orientation of the sensors (Figure 4.17).

Step 4: Time shift of the data to get all the points to a single line across the contact patch (Figure 4.16). The time shift procedure was analysed in Matlab as its accuracy was essential for precise contact patch construction using the Tekscan data obtained in the experiments. The time shift was required in order to align four sensing mats and build the contact patches (Figure 4.16). The estimation of number of sensel columns per frame was carried out by looking at the tyre movement. Two methods were considered: observation of the data (looking how pressure travels across the sensors) and calculation according to the tyre speed measured. The data observation involved:

- visual observation how the pressure travelled across the sensor (pressure gradient was only observed when tyre entered and left the sensor, in the middle section of the contact patch a clear pressure gradient was not observed),
- consideration of the speed of the maximum pressure travel across the whole sensor carried out in Matlab (it was necessary to assume that the contact patches were rectangular, while in reality they had a shape of ellipse; which introduced an error),
- estimation of the speed of the maximum pressure travel only for three rows located in the centre of tyre using Matlab (there was too much noise found when considering only three rows in the center of tyre).

Concluding, the consideration of the above did not give a good estimation of the tyre speed which was due to a large variability of the pressure data across the sensor and a relatively small amount of sensing elements used. A larger number of smaller sensing elements would allow for a better estimation of the tyre speed when considering the contact pressure data changes. Therefore, the number of sensel columns per frame was estimated according to tyre speeds measured as discussed in Chapter 3.

Step 5: Selection of single lines of sensing elements.

Step 6: Build a contact patch for the individual row of data by placing together a series of snapshots recorded by the same line of sensing elements at adequate time interval. Build the contact patches for all the single lines of sensels.

Step 7: A mean contact pressure patch construction using the contact patches built up for individual sensing rows (Figure 4.17). Then, according to the mean contact patch, both the mean pressure over the patch and the maximum pressure were determined.

Appendix F contains the scripts developed in Matlab software for interpreting the data.

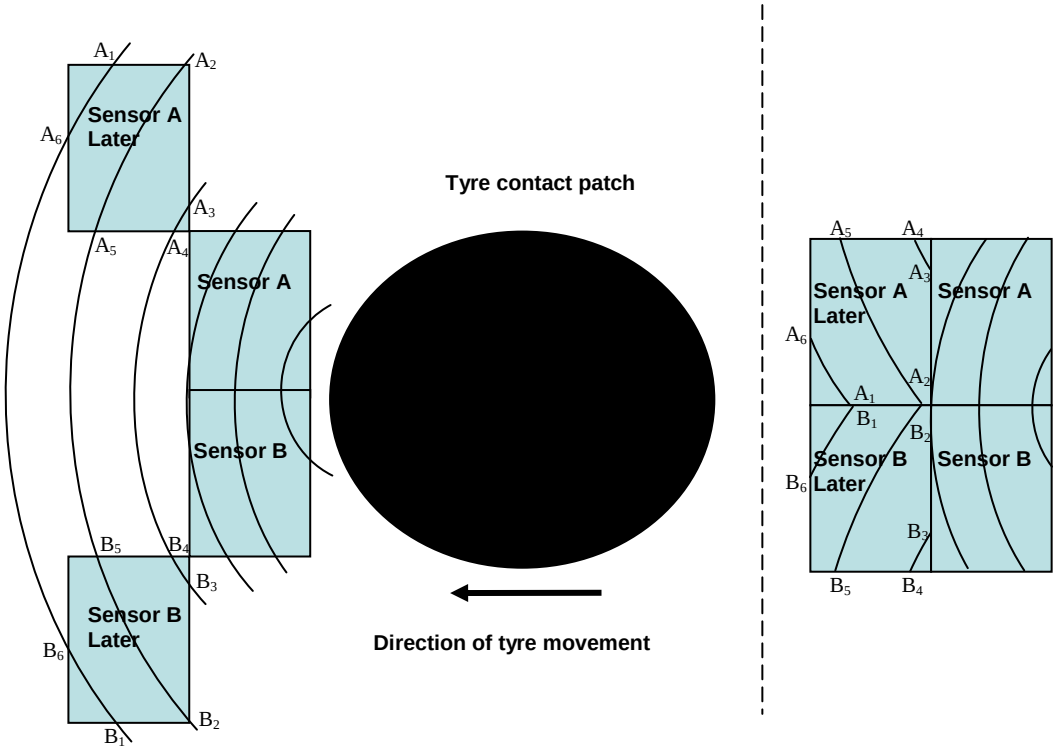

Figure 4.16 Orientation of the 9830 sensors for testing (left: real sensor arrangement, right: data arrangement the way that the Tekscan software records it)

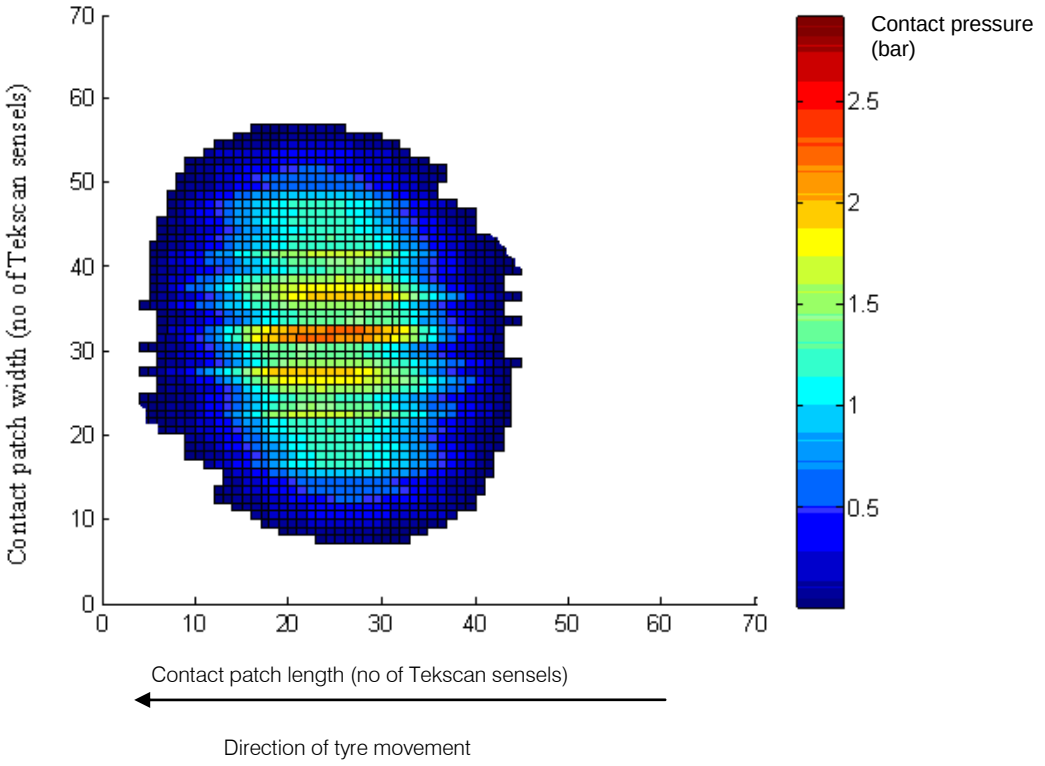

Figure 4.17 Example of tyre contact patch with contact pressure distribution

4.8 Correction of the multi-point per sensel calibration with sensel selection

As described in Section 4.6.4, Tekscan sensors were calibrated in the calibration device and a multi-point per sensel calibration was established according to the calibration data. However, the calibration was conducted under different conditions than those used when the tyre pressures were measured (on a hard surface and buried in the soil). The main difference was using different loading materials: air for calibrating, rubber and soil for testing. In order to calibrate the sensors, they were placed on a smooth machined steel surface and loaded with uniform air pressure through a polythene diaphragm. Tyre hard surface experiments involved placing the sensors on a smooth steel plate, covering them with a polythene sheet and loading with a range of agricultural tyres. The experiments conducted in soil employed the same materials as the hard surface study, the extra medium introduced was sandy loam soil layer placed at the top of the polythene sheet. The tyres were, therefore, loaded on to the soil. Due to different compliance factors of the materials used, it was expected that a correction factor may need to be applied to the tyre contact pressure data.

In order to evaluate the requirement for a correction factor, two sets of experiments were conducted. These were as follows:

1). Comparison of the calibration and test environments in small scale controlled study

These were conducted using 9830 sensors as they where used in the majority of the experiments. Additionally, 9830 sensors were selected as being those which might produce the greatest discrepancy with the known load due to a relatively large non-active areas (ratio of non-active/active area for a 9830 sensor is approximately equal to 4). Initially a multi-point per sensel calibration with selection of faulty sensels was established, which was based on data obtained when loading the sensors in the calibration device. This calibration was used for three sets of tests:

- The sensors were loaded with a number of uniform pressures in the calibration device (with a polythene diaphragm).
- In order to simulate the hard surface tyre loading environment, the sensors were covered with a polythene sheet a number of sensing elements were selected randomly (excluding any faulty sensels) and 50 – 500 g laboratory weights were individually applied to each selected sensel through a 2mm thick rubber pad of the size of the active area (Figure 4.18, left and middle).

- To simulate the soil conditions, the small rubber pad was replaced with a cube of sandy loam soil confined in a larger rubber pad with a square cut off (with the same dimensions as sensel's active area). The 50 – 500 g laboratory weights were applied to the soil cube placed on the selected sensels (Figure 4.18, right). In order to minimise drag on the walls of the rubber, 2mm thick rubber was used which resulted in having a shallow layer of soil (2 mm).

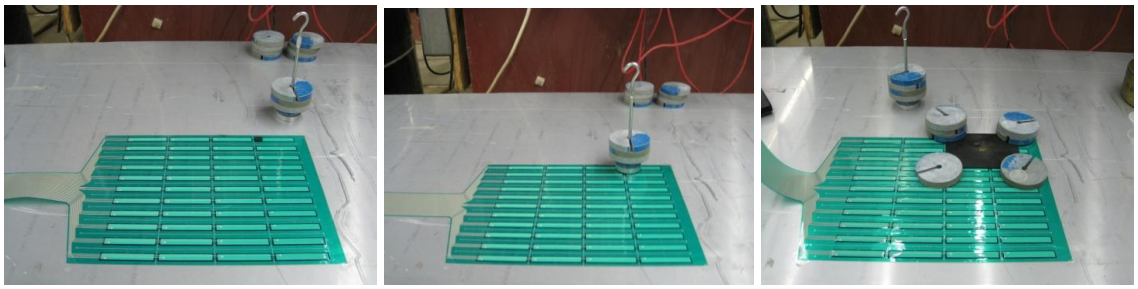

Figure 4.18 Small scale controlled study using Tekscan sensors (rubber pad tests – left and middle picture, soil cube test – right picture)

The loads applied to the sensels using the three different media were recorded by Tekscan and compared as shown in Figure 4.19 and Figure 4.20. The figures present data obtained for one random sensing element. Other randomly selected sensels showed the same relationships. The tests conducted in the calibration device provided Tekscan recorded data that agree with the applied values. Which confirms that the data obtained when loading the sensor in the calibration device agree with the calibration conducted previously using the same device. The relationship between the applied and recorded load was found to be linear, however, the data recorded by Tekscan when the loads were applied through the rubber pad or soil cube were found to be smaller than the applied load. The average ratio between the applied and measured load equalled to 1.87 and 1.76 for the rubber pad and soil cube study, respectively. This proved a requirement for correction factor to be used for the hard and soil contact pressure data obtained using 9830 sensors. To confirm this, further investigation involved using each individual experimental data set obtained when the range of tyres were loaded onto both hard and soil surface. This involved comparison of the pressure results from each tyre load applied and the load recorded by Tekscan system.

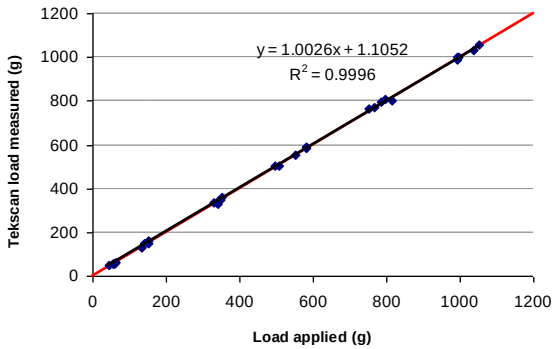

Figure 4.19 Tekscan measured load vs. applied load (9830 sensor loaded in the calibration device, results obtained for one randomly selected sensel; 1:1 line in red)

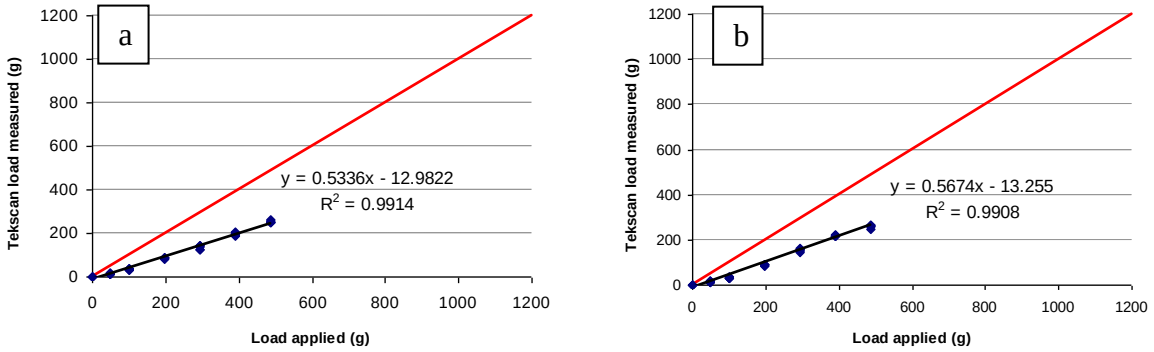

Figure 4.20 Tekscan measured load vs. applied load (a: load applied through a rubber pad, b: load applied through a soil cube; 1:1 line in red)

2). Comparison of the load applied to tyres and recorded by Tekscan system

In order to further evaluate the above finding, the loads applied to tyres and those recorded by the Tekscan sensors were compared. The data collected by the three types of sensors (9830, 6300, 5330) were evaluated as given below:

A. 9830 sensors (used in soil experiments with all the tyres and hard surface experiments with the smooth and treaded combine tyres)

Figure 4.21 presents the ratio of the applied and recorded load for all the tyre tests conducted for both the hard surface and the soil using the 9830 sensors. The loads applied were considerably higher than the recorded loads. The ratio of the applied load and recorded load varied from 1.5 to 2.3, which was found to be close to the results obtained in the small scale controlled study discussed above.

It was concluded that the difference between the applied loads and recorded values resulted from the fact that different loading materials were used for the calibration and testing. Air is the most deformable medium, so when the sensors are loaded with air during the calibration, the pressure is uniform as the air follows the shape of Tekscan sensors. Soil and rubber are less deformable, this is why they do not follow the shape of Teksan sensors that well. As the Tekscan recorded loads were considerably lower than the loads applied, it suggests that part of the load applied concentrated on the non-active areas of the sensors. In order to evaluate the reason of that, the thickness of active and non-active parts of the sensors was compared. The active parts of the 9830 sensors were found to be thicker than the non-active areas. However, the thickness difference was small. This indicates that the non-active parts of the sensors are less flexible than the active areas, and when the load is applied to the sensors, the active areas deform more and carry less load.

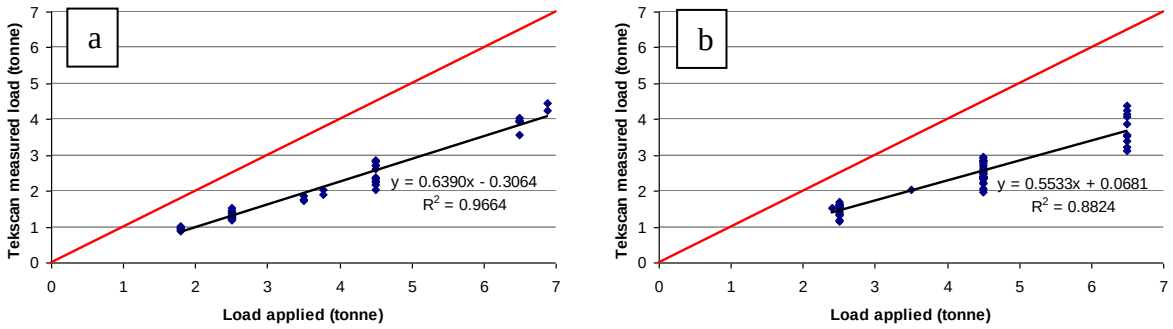

Figure 4.21 Tekscan measured load vs. applied load (results obtained for the 9830sensor when loaded by the smooth and treaded combine tyres; a: hard surface, b: soil; 1:1 line in red)

The variation of the ratio obtained could be associated with changes in tyre properties at different loads and inflation pressures. Also the following inaccuracies could have influence on the applied or measured load:

- Measurements of the load applied
- Measurements of tyre rolling speed
- Tekscan contact pressure measurements
- Soil preparation

In order to correct the performance of the 9830 sensor, all individual tyre contact pressure data points obtained using the sensors were increased by correction factors calculated as

applied load/recorded load for each test in order for the Tekscan recorded load to agree with the load applied to the tyres.

B. 6300 sensors (used for experiments on implement tyres on a hard surface)

The 6300 sensors have a better spatial resolution than the 9830 sensors (Chapter 4). Comparison of the loads applied to the tyres and measured by Tekscan, when testing the implement tyres using 6300 Tekscan sensors, agreed within +/- 10% which is illustrated by Figure 4.22. A correction factor was not applied to the data recorded by the 6300 sensors as the differences between the load applied and measured were found to be relatively small.

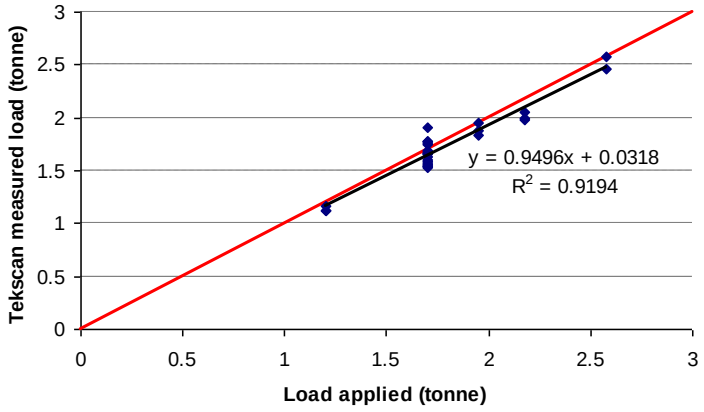

Figure 4.22 Tekscan measured load vs. applied load (results obtained for the 6300 sensor when it was loaded with the implement tyres on the hard surface; 1:1 line in red)

C. Conformat 5330 sensor (used for experiments on the front tractor tyre)

The loads recorded were compared to the loads applied and an agreement was found with a maximum variance up to +/- 12% (Figure 4.23). The pressure data recorded by the Conformat 5330 Tekscan sensor did not require correction.

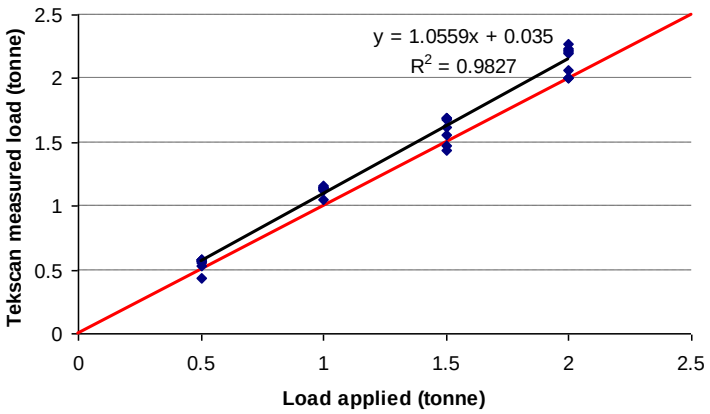

Figure 4.23 Tekscan measured load vs. applied load (results obtained for the 5330 sensor when it was loaded with the front tractor tyre on the hard surface; 1:1 line in red)

5 PILOT STUDY INTO AN EVALUATION OF A RANGE OF METHODS TO DETERMINE TYRE CARCASS STIFFNESS ON HARD SURFACES

5.1 Introduction

This chapter considers the results obtained during the pilot study conducted on a hard surface using an inner tube commonly used in agricultural tyres (600/700/750R16) and a Firestone front tractor tyre (9.0-16). The inner tube, shown in Figure 3.3, was selected for the study as it is a "purely" flexible material with no tread pattern and effectively behaves as a "perfect" balloon where contact pressure is equal to inflation pressure and there is little carcass stiffness. Further, the 9.0-16 front tractor tyre, presented in Figure 3.3, was selected for a comparison with the 7.5-16 front tractor tyre, tested previously by Plackett (1983).

The evaluation of the methods for tyre carcass stiffness determination was considered in the following three chapters. This chapter evaluates the methods using the inner tube and front tractor tyre. The evaluation of the tyre carcass stiffness determination methods continues further in Chapter 6 and Chapter 7 where carcass stiffness was determined for the other tyres. Details of the experimental procedure with the full description of the methods used are given in Chapter 3. In order to evaluate alternative methods of carcass stiffness estimation and determine carcass stiffness of the tyres tested, the tyre contact area, mean contact pressure, pressure distribution and maximum vertical deflection of each of the tyres was measured. Tyre mean and maximum carcass stiffness was determined. The mean value was determined according to the mean contact pressure for a tyre contact patch, while the maximum carcass stiffness was calculated from the maximum contact pressure found for each tyre contact patch. The tyres used in the investigation were studied at a range of the working inflation pressures and loads up to the maximum recommended values as given by the manufacture (as shown in Table 3.1). From the results, it was possible to evaluate the effects of tyre load, inflation pressure, ply rating and presence of tread on the resulting contact pressure.

For the purpose of this work, following that of Bekker (1956), Chancellor (1976) and Plackett (1983), the term tyre carcass stiffness is considered to be the equivalent contact pressure derived from tyre carcass measured at the contact patch. As discussed in Chapter 2, Chancellor (1976) considered a general principle, reported previously by Bekker (1956), that

"the pressure existing between a pneumatic tyre and the surface on which it rolls is approximately equal to the inflation pressure of the tyre". This was further explained by Chancellor (1976) suggesting that as a load is applied to the tyre, the tyre deflects keeping the contact pressure constant. Therefore, the contact patch increases. However, there is a point at which the tyre cannot deflect anymore and the contact pressure exceeds the inflation pressure. Bekker (1956) and Chancellor (1976) both stated that the presence of tyre treads and the carcass stiffness further contribute to the contact pressure. Plackett (1983, 1986 and 1987) studied the contact pressure resulting from agricultural tyres and then related it to the inflation pressure and tyre carcass stiffness. He indicated that mean tyre contact pressure could be defined as inflation pressure plus carcass pressure as described in Equation 1.1. Plackett (1983) reported that the results of his studies showed that tyre carcass contribution to the overall contact pressure is effectively constant.

In the discussion on pneumatic tyre-soil interactions, Karafiath and Nowatzki (1978) offered a different relationship between the average contact stress and inflation pressure, presented by Equation 2.10, which suggests the difference between tyre contact pressure and its inflation pressure is not constant but it varies with changes in inflation pressure.

In order to determine the carcass stiffness of a tyre a number of approaches, previously considered by Misiewicz *et al.* (2007), were considered including:

1. The pressure difference method (A) to measure both mean and maximum contact pressure using Tekscan (Section 3.4.1)
2. The pressure difference method (B) using ink to estimate the size of the contact patch and hence mean contact pressure (Section 3.4.1)
3. Tyre load - deflection method (Section 3.4.1)
4. Tyre manufacture specification data method
    a. an inflation pressure at zero load
    b. a load at zero inflation pressure

A requirement for an understanding of contact pressure distribution was discussed in Chapter 2. The method considering Tekscan contact pressure results is the most fundamental approach to carcass stiffness determination. The mean and maximum contact pressures were

determined using the Tekscan pressure mapping system. The pressures at the tyre contact patch on a hard surface were reported to be unevenly distributed which agrees with the findings of some previous researchers as discussed in Chapter 2. Tyre mean carcass stiffness was calculated as the difference between the mean contact pressure and tyre inflation pressure. Trautner (2003) stated that soil compaction mainly results from the maximum contact pressure. Therefore, the maximum tyre carcass stiffness was calculated as maximum contact pressure minus tyre inflation pressure. The carcass stiffness results obtained using the pressure difference method according to Tekscan data were compared to the values obtained using the other three methods.

The second technique was proposed by Plackett (1983) and is based on the assumption that tyre carcass stiffness is a constant value for a tyre which agrees with Bekker (1956) and was further discussed by Chancellor (1976). This method of carcass stiffness estimation looks at the difference between the mean contact pressure and tyre inflation pressure. Tyre contact patches were found by loading the range of tyres on the hard surface with white paper and black ink. The average contact pressures under a tyre were obtained by dividing tyre load by contact area. As described in Chapter 3, two contact area results were obtained, these were:

- tread contact area and
- projected contact area

They relate to the rotational and single ink print methods, respectively. The projected contact area results represent a situation where a tyre was loaded onto firm soil and the treads penetrated the soil. The tread contact areas illustrate a case where the loading surface is stiff and does not allow the tyre to penetrate. This is less common in the off-road environment. The mean contact pressures were calculated for the both cases.

The tyre load – deflection method was proposed by Plackett (1983) who suggested that the contribution of the tyre carcass stiffness may be predicted by examining the load – deflection characteristic for a tyre. As described in Chapter 2, this method involves examining the tyre load - deflection relationship for a tyre at a range of tyre inflation pressures and it leads to estimation of tyre sidewall stiffness. Therefore, in order to use this method, tyre maximum vertical deflection was measured for the range loads and inflation pressures. The relationships obtained were plotted as load vs. deflection and the relationships were found to be almost

linear for the loads and pressure ranges recommended by tyre manufacture (Figure 2.19). Plackett (1983) concluded that as tyre inflation pressure decreases, the slope of the load – deflection curve also decreases. Further, he concluded that if a tyre had zero carcass stiffness, then the slope of the load – deflection relationship would be zero at zero inflation pressure, as the carcass would not support any load. Therefore, plotting the slope of the load – deflection curve against inflation pressure, as shown in Figure 2.20, and extrapolation of the relationship to the inflation pressure axis gives an estimation of the carcass strength at zero inflation pressure (x value) and the pressure at which the carcass strength is zero (y value). Plackett (1983) suggested that the negative value of inflation pressure at zero load – deflection is an indication of tyre carcass stiffness.

The method based on tyre manufacture specification data is a speculative technique using the currently available tyre manufacture data. This is a method to investigate the possibility of using the currently available manufacture data for tyre carcass stiffness estimation. To develop this possible method, tyre manufacture's specification graphs were used to estimate tyre remaining stiffness by plotting the maximum load against inflation pressure for a number of forward speeds as shown in Figure 5.1. This presents a series of relationships which were extrapolated using both linear and 2nd order polynomial functions in order to provide two selected points:

a. an inflation pressure at zero load and
b. a load at zero inflation pressure

Where:

a. The consideration of the inflation pressure at zero load provides tyre remaining stiffness which could be a speculative indicator of tyre carcass stiffness. This method is very simple as it does not require any experiments to be conducted other than those already published by the manufacturers.

b. The load which can be supported by a tyre when there is no inflation pressure provides data that can be converted into a pressure applied over the tyre contact area. This method of tyre remaining stiffness estimation requires the tyre contact area to be measured at the recommended load and inflation pressure. It was shown that tyres maintain at a constant contact area, when they are loaded with the maximum load for a given inflation pressure,

according to tyre manufacture specification. Therefore, only one contact area experimental test for a tyre is required. The contact areas for this project were measured in the ink and Tekscan experiments and the results obtained using the two methods were found to be in a good agreement.

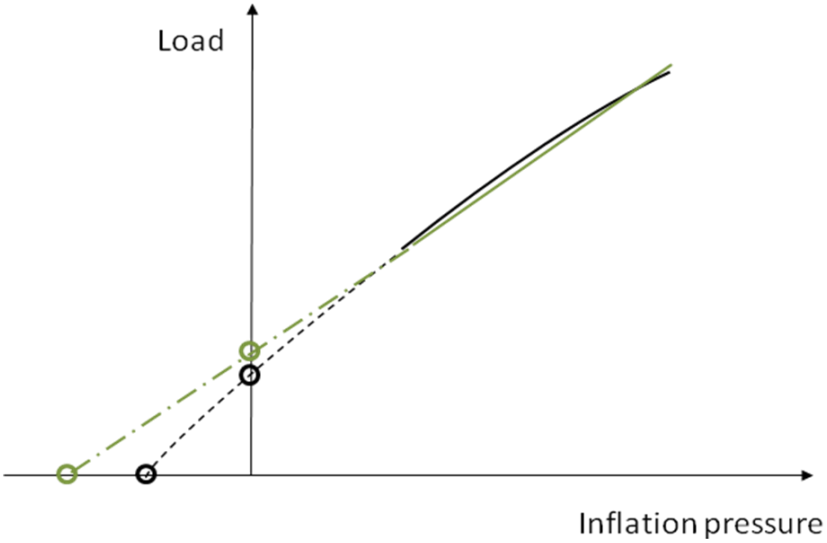

Figure 5.1 Tyre carcass stiffness estimation according to the method based on tyre manufacture specification data (green: linear extrapolation, black: polynomial extrapolation)

As discussed in Chapter 3, the tyres were placed into four groups as follows:

A. Presence or absence of tyre tread
B. Differing tyre ply rating
C. Standard tyre to compare these results with the studies by Plackett (1983)
D. "Purely" flexible inner tube with little or no carcass stiffness

The tests conducted on the inner tube and front tractor tyre were considered as the pilot study and the results obtained are presented in this chapter. The aspect of the presence of tyre tread was evaluated in Chapter 6 according to the data obtained for the 600/55R26.5 smooth and treaded rear combine tyres. Chapter 7 considers the effect of tyre ply rating on the resulting contact pressure. Further evaluation of the effect of tyre tread and ply rating was conducted in the soil where resulting pressures in soil profile were considered. Each chapter both presents and discusses the results obtained for each group of tyres, from which the final conclusions were drawn.

The pilot study started with the hard surface experiments using the inner tube and it involved determination of the contact area and mean contact pressure using the Plackett's ink method. The study was conducted to assess the ink method used for its ability of the mean contact pressure determination. The results obtained where then used to determine the stiffness of the tube. Following this, the load – deflection experiments were conducted and the results obtained were employed to find the stiffness of the tube, according to the Plackett's technique (1983). As the inner tube expanded during the study, it was not possible to continue the study with the contact pressure distribution measurements using the tube. Hence, the pilot study moved to the front tractor tyre. For this tyre, the study involved an evaluation of the four methods of carcass stiffness estimation, described above.

5.2 The inner tube with minimum carcass stiffness

This section contains the study conducted on the inner tube inflated to a number of pressures at a range of loads. The tube is a "purely" flexible material with no tread pattern and it was expected it would behave as a "perfect" balloon where contact pressure is equal to inflation pressure and there is little or no carcass stiffness.

5.2.1 The pressure difference method (B) using ink to estimate the size of the contact patch and hence mean contact pressure

Figure 5.2 (upper) shows the contact area results obtained when the inner tube was experimentally studied (solid lines) and contact area determined by dividing the tyre load by the corresponding inflation pressure (called further theoretical data - dotted line). The latter values were calculated assuming the tube has no carcass stiffness and its contact pressure is equal to the inflation pressure. However, while the experimental results agree with the contact area data calculated theoretically at higher inflation pressures (0.1 bar), at lower inflation pressures the tyre experimental contact area was found to be lower than the theoretical area. This proves that even the inner tube has a carcass stiffness as its sidewalls reinforce the tube and prevent it from total deflection. A load increase resulted in an increase in the contact area and the analysis of variance showed that effect of load is significant on the contact area at 95% confidence level (Appendix G.1). The inflation pressure also appeared to have an effect on contact area but it was not necessary to replicate this for statistical analysis, as this was considered as a pilot study.

Figure 5.2 (lower) presents the results of the mean contact pressure against tyre inflation pressure; the mean values were calculated according to the contact areas obtained in the experiments. The mean contact pressures were found to be close to tyre inflation pressure (as indicated by the 1:1 line). They were found to rise with increasing inflation pressure and load. As for the lowest load (0.01 tonne), the theoretical mean contact pressure is approximately 0.009 bar lower than the experimental results, therefore, the mean contact pressures is lower than the inflation pressures. The reasons for which are explained below. When the inner tube was loaded with loads above 0.02 tonne, the mean contact pressure was found to be higher than the inflation pressure. The maximum values were found for 0.08 tonne load, where the difference between the mean contact pressure and inflation pressure varied between 0.028 – 0.008 bar. This shows that even the most flexible of tyre membranes has a very small carcass stiffness, the magnitude of which tends to reduce with inflation pressure and load.

A peculiarity was found in the data obtained in the ink tests for the inner tube. If a tyre does not have any carcass stiffness, it is expected that its contact area is equal to the theoretical area, calculated assuming the mean contact pressure is equal to its inflation pressure. While, when a tyre has some carcass stiffness, its contact area should be smaller than the theoretical area, as the reinforcement prevents the tyre from deflecting. If tyre contact area is greater than the theoretical area, tyre carcass stiffness is negative and the tyre deflects more than necessary in order to carry the load applied, which is impossible. This peculiarity was found for the inner tube at high inflation pressures, where contact areas were found to be greater than the theoretical contact areas. Also other researchers found the same abnormality for data obtained in the ink tests (Ansorge, 2007).

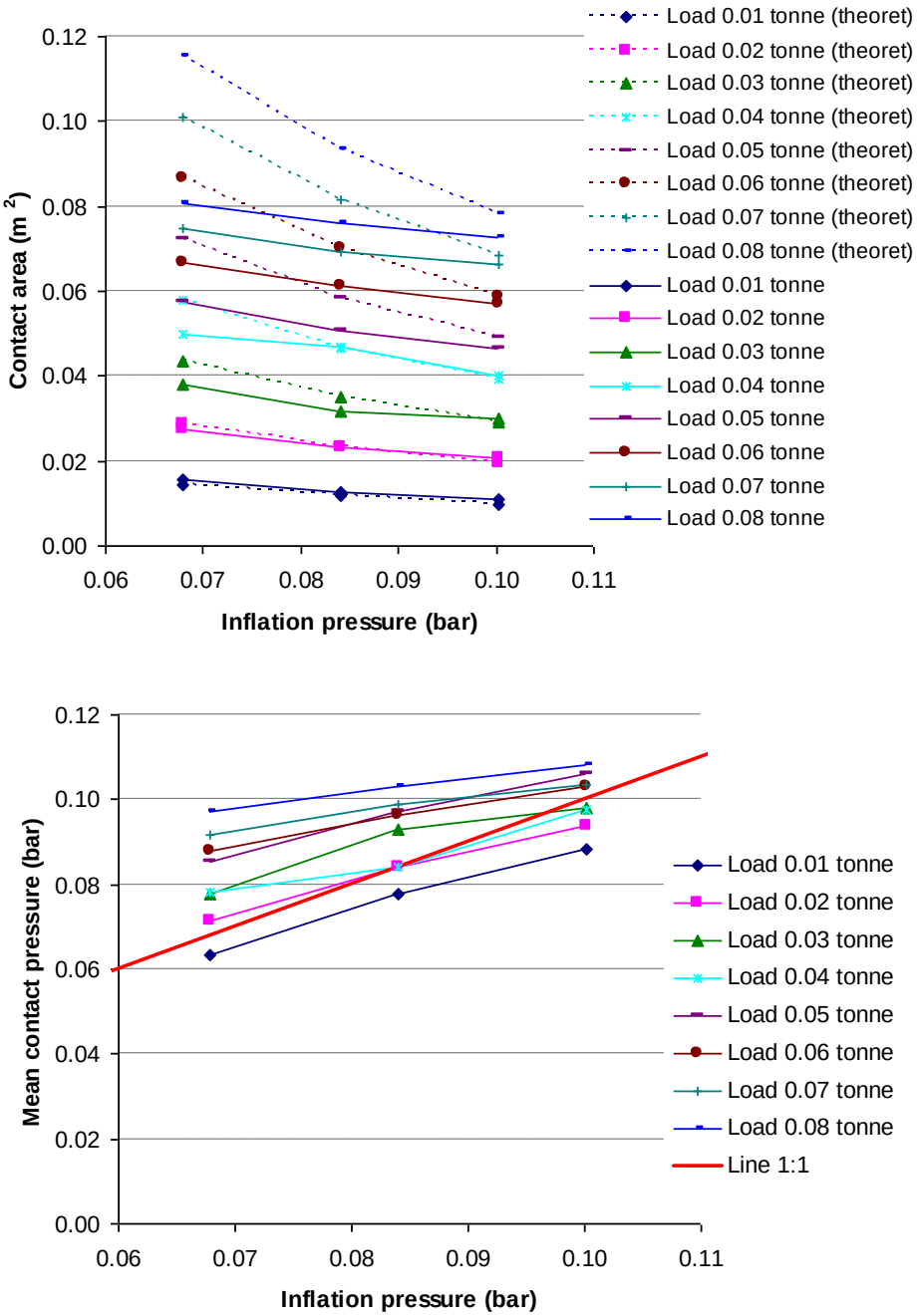

Figure 5.2 Contact area (upper) and contact pressure (lower) vs. inflation pressure based on the ink data – Tyre inner tube (solid line: experimental data, dotted line: theoretical data)

The above indicates that the assessment of the contact area (using the ink method), provides a tyre area which is in contact with the surface, but does not necessarily transfer any load as shown in Figure 5.3. The resulting error has a greater effect at high inflation pressures, as at high inflation pressures tyre contact areas are smaller. It is also expected that tyre contact

pressure is not uniformly distributed across the contact patch (Bekker, 1956; VandenBerg and Gill, 1962; McLeod *et al.*, 1966; Burt *et al.*, 1992; 1989; Gysi *et al.*, 2001; Trautner, 2003; Way and Kishimoto, 2004 and as it shall be observed later in Chapter 5) and at high inflation pressures it concentrates in the central contact patch, while, at low inflation pressures tyre sidewalls carry significant amount of load, therefore, the maximum contact pressures should be found below tyre sidewalls. Also tyre architecture could have an effect on the fact that tyres at high inflation pressures some parts of the tyre have contact with the ground but do not transfer any load. From the above, it can be concluded that determination of the tyre contact area gives an indication of the area which has contact with the ground, but not necessarily transfers any load. Furthermore, this indicates that this method does not provide any information on tyre contact pressure distribution and can give an erroneous indication of the mean contact pressure.

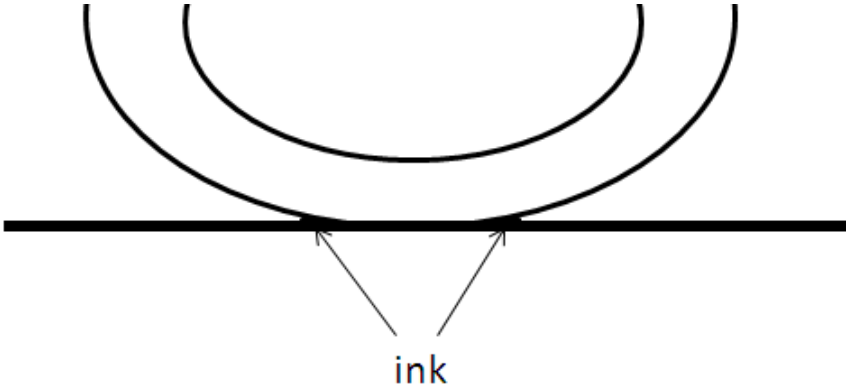

Figure 5.3 Tyre contact area determination according to the ink method

Another disadvantage of the ink method is that it provides a "history" of the tyre contact patch area rather than the actual contact patch, as it indicates the contact area which is in contact while tyre load is increased (from zero to the test load). If tyre buckles in the centre of contact patch with an increase of tyre load, the method will show the contact area obtained while loading the tyre and this will not reflect the tyre buckling.

5.2.2 Tyre load – deflection method

The load – deflection relationship of the inner tube at the range of inflation pressures is shown in Figure 5.4, where the effect of load and inflation pressure can be seen. As the inflation pressure increases, the tube deflects less, while, a load increase results in a greater deflection.

Following the Plackett's method of carcass stiffness estimation (1983), the slopes of the load – deflection relationships where plotted against the inflation pressure as presented in Figure 5.5. A linear extrapolation of the obtained characteristic to the inflation pressure axis enabled the effective carcass stiffness to be determined as suggested by Plackett (1983), which was found to be – 0.001 bar.

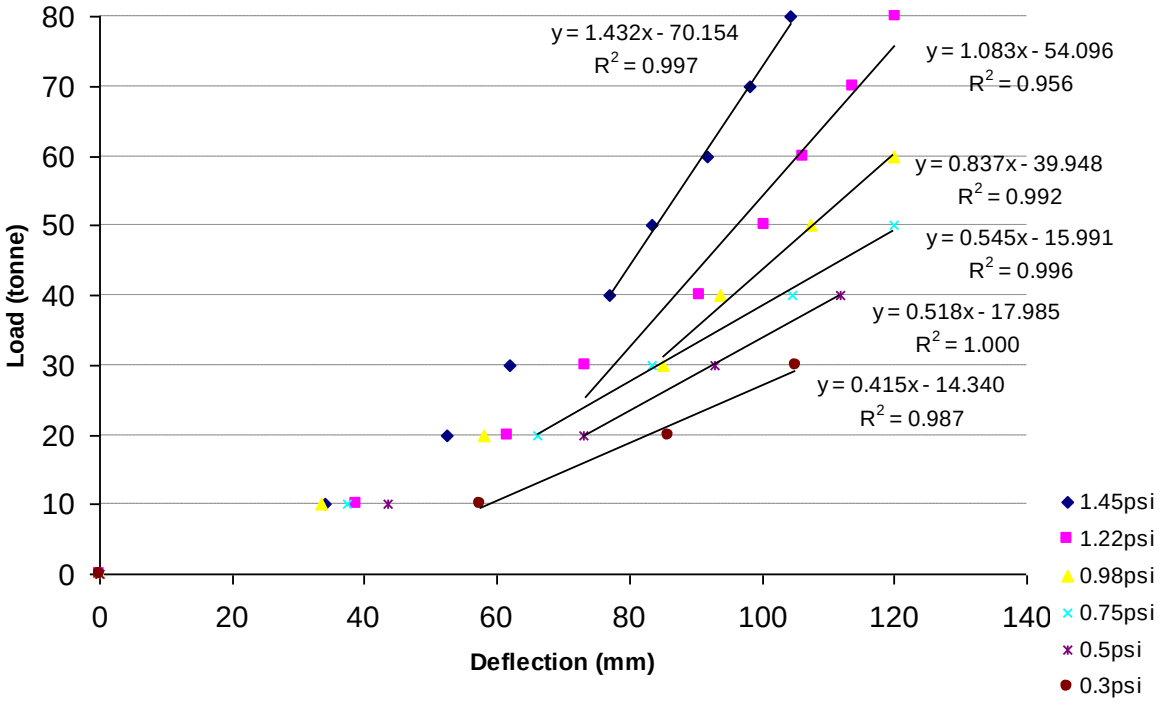

Figure 5.4 Load – deflection relationship for the inner tube

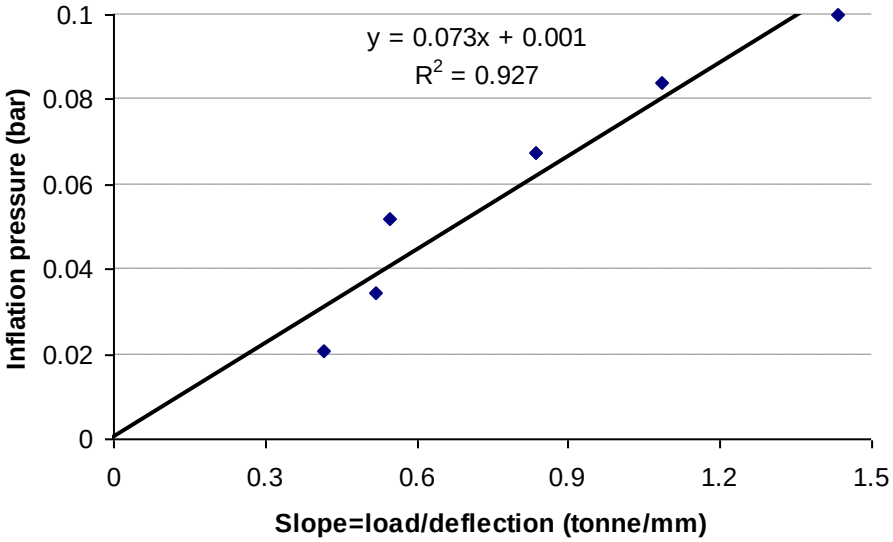

Figure 5.5 Inflation pressure vs. slope of load – deflection relationship for the inner tube

5.3 Front tractor tyre with a comparison of the current and previous results

This section concentrates on a 9.0-16 front tractor tyre (Firestone), presented in Figure 3.3, which was selected for a comparison with the 7.5-16 front tractor tyre, tested previously by Plackett (1983). The front tractor tyre currently tested at the range of load and inflation pressures (shown in Table 3.1). This made it possible to observe the effect of load and inflation pressure on tyre contact area and pressure. In order to be able to compare the results of the tyre currently tested to the 7.5-16 front tractor tyre, the tests using the 9.0-16 front tractor tyre were replicated in the same manner as the study by Plackett. The only difference was the loading and inflation pressure specification, as the tyre tested previously was only loaded up to 0.5 tonne, while the tyre studied currently can carry loads up to 1.5 tonne (Figure 5.15) and was even studied above its recommended load up to 2 tonne. This, however, confirms that present agricultural vehicles are much heavier than the ones used in the past and their tyres are required to carry considerably greater loads.

5.3.1 The pressure difference method (A) to measure both mean and maximum contact pressure using Tekscan

Figure 5.6 presents tyre contact pressure distribution for the 9.0-16 front tractor tyre recorded using Tekscan system. This shows that increasing both inflation pressure and load results in a rise in the mean and maximum contact pressures. It also shows that the tyre contact area increases with load and decreases with an increase in inflation pressure. The pressure distribution was not found to be uniform and pressure concentration was found at the sidewall edges of tyre contact patches for the tyre at low inflation pressures, while an increase in inflation pressure resulted in a pressure concentration movement from the sidewall edges to the central area of the contact patch. Histograms of the frequency distribution of the contact pressures are evaluated in Section 6.1 for the combine tyre, which is more typical of these in current use.

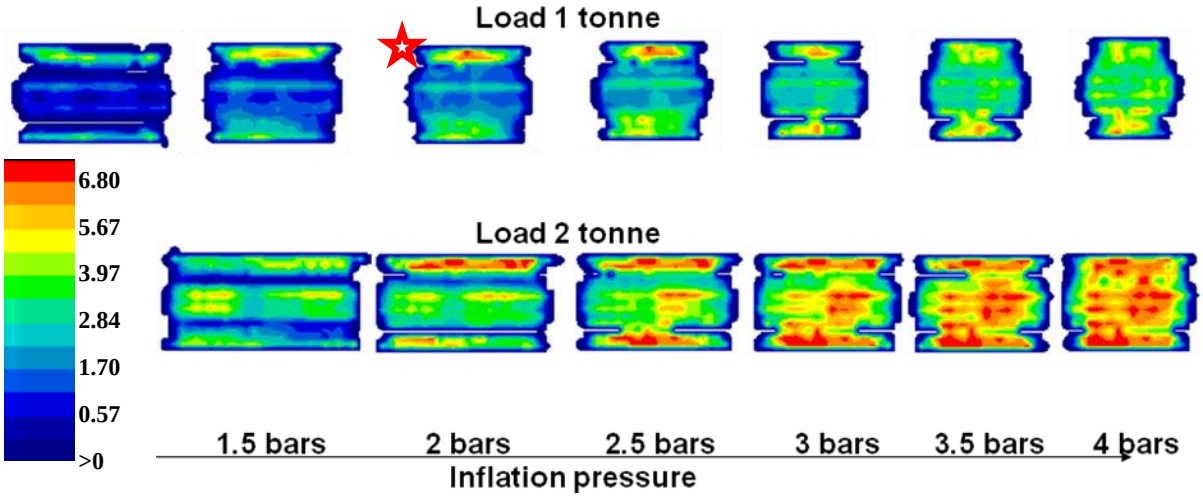

Figure 5.6 Contact pressure distribution (bar) for the 9.0-16 front tractor tyre at the range of loads and inflation pressures (★ - rated load and inflation pressure)

Figure 5.7 shows relationships between tyre contact area and inflation pressure for different loads, where an increase of inflation pressure results in a decrease of the tyre contact area. Tyre load, inflation pressure and interaction between load and inflation pressure have significant effect on contact area at 95% confidence level as shown in Appendix G.2. The contact areas for the two rated loads and inflation pressures were found to be similar.

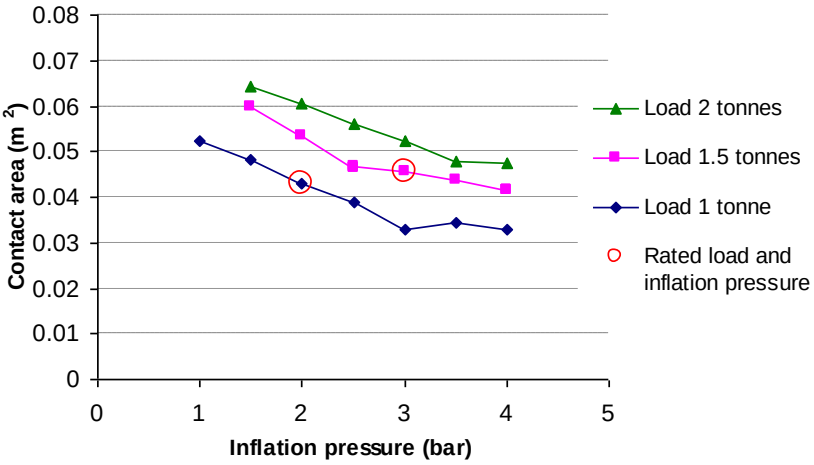

Figure 5.7 Tyre contact area obtained according to the Tekscan method vs. inflation pressure for the 9.0-16 front tractor tyre (LSD at 95% confidence level = 0.0012m^2)

Figure 5.8 presents contact pressure data for the front tractor tyre. As in some experiments with this tyre the Tekscan sensor became saturated, it was not possible to investigate how the

overall mean and maximum contact pressure varied with change of tyre inflation pressure and load. It was only possible to consider pressure in the central area of the contact patch. This is shown in Figure 5.8 which presents both mean and maximum contact pressures for the middle section of contact patch plotted against tyre inflation pressure. An increase of inflation pressure resulted in an increase in both the mean and maximum contact pressure. The mean contact pressure was also found to be higher than tyre inflation pressure and the difference between the mean contact pressure. The mean pressure was found to be influenced by tyre load, as expected with the 1 tonne data being close to 1:1 line. The maximum contact pressures were found to be higher than the mean pressures and also influenced by tyre load (see Figure 5.8 right).

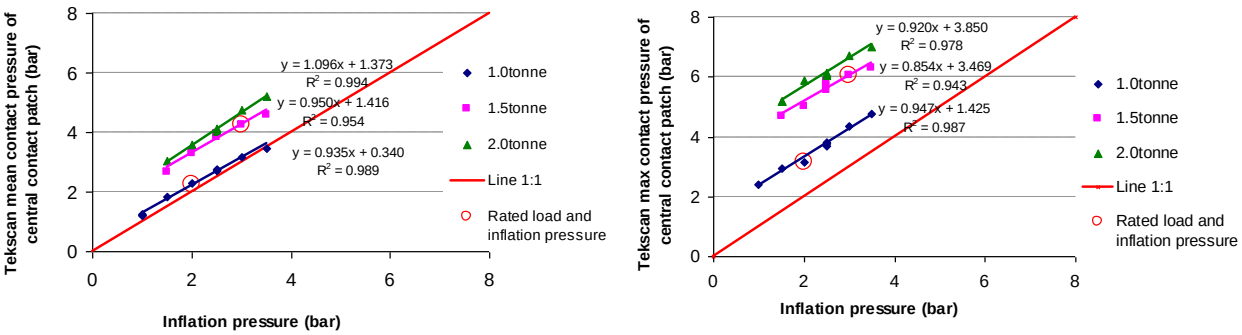

Figure 5.8 Mean contact pressure vs. tyre inflation pressure (left) and maximum contact pressure vs. tyre inflation pressure (right) for the front tractor tyre from Tekscan tests (left: LSD at 95% confidence = 0.094 bar, right: LSD at 95% confidence = 0.125 bar)

As the relationships between the contact pressures and tyre inflation pressures were found to be close to linear functions, a linear regression analysis was carried out on the mean and maximum contact pressure data (Appendix J.1 and J.2). The analyses proved that tyre load and inflation pressure have a significant effect on the mean and maximum contact pressure of the front tractor tyre.

Further, 't' tests showed that the slopes of the mean and maximum contact pressure are significantly different from 1. This proves that the difference between the contact pressure and inflation pressure, considered as tyre carcass stiffness, is not a constant value but it changes with inflation pressure and load. The analysis provided the following regression

equations for a determination of the mean and maximum contact pressure of the front tractor tyre studied:

$$\textbf{Mean } P_C = -0.85 + 0.83xP_i + 1.49xW \qquad \text{Equation 5.1}$$

$$\textbf{Max } P_C = -0.17 + 0.72xP_i + 2.33xW \qquad \text{Equation 5.2}$$

The mean and maximum contact pressure equations above fit the experimental data with R^2 of 96% and 91%, respectively.

Further consideration of carcass stiffness of the front tractor tyre, according to the Tekscan results, is illustrated in Figure 5.9. The mean carcass stiffness equals to 0.21 bar, 1.29 bar and approximately 1.61 bar for loads of 1.0 tonne, 1.5 tonne and 2.0 tonne, respectively. The overall mean value was found to be 0.99 bar, while for the rated load and inflation pressure the carcass stiffness was found to be 0.20 bar and 1.26 bar for 1.0 tonne and 1.5 tonne loads, respectively. Consideration of the carcass stiffness as an extrapolation of the mean contact pressure to zero inflation pressure, provided the following values: 0.34 bar, 1.42 bar and 1.37 bar, respectively.

The maximum carcass stiffness was found to be 1.29 bar, 2.10 bar and 3.66 bar depending on tyre loads of 1.0 tonne, 1.5 tonne and 2.0 tonne, respectively. The overall mean maximum carcass stiffness is 2.68 bar. For the rated load and inflation pressure the maximum carcass stiffness was found to be 1.17 bar and 3.06 bar for 1.0 tonne and 1.5 tonne, respectively. While, an extrapolation of the maximum contact pressure to zero inflation pressure gave the maximum carcass stiffness of 1.42 bar, 3.47 bar and 3.85 bar, respectively.

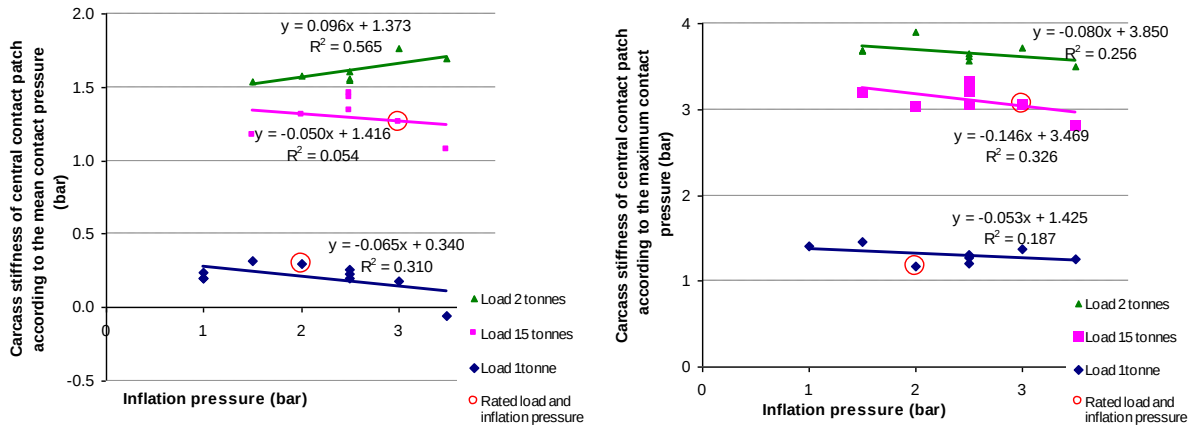

Figure 5.9 Tyre carcass stiffness vs. tyre inflation pressure for the front tractor tyre from Tekscan data – according to mean (left) and maximum (right) contact pressure

5.3.2 The pressure difference method (B) using ink to estimate the size of the contact patch and hence mean contact pressure

Figure 5.10 shows the relationships obtained between the contact area (left: tread contact area, right: projected contact area) and tyre inflation pressure for the front tractor tyre tested using the ink method. Figure 5.10 (right) also presents the contact area data calculated as tyre load divided by inflation pressure (dotted line). This is tyre contact area which would have a contact with the ground if the tyre did not have any carcass stiffness. However, due to stiffness of the tyre sidewalls and the fact that tyre is constrained by its physical construction, the contact area found in the experiments was smaller than the theoretical values at low inflation pressures for a purely flexible tyre. At the high inflation pressures, contact areas determined were found to be slightly greater than the theoretical values. This was discussed in Section 5.2 and was concluded to be related to the fact that the ink method also provides tyre contact area that has contact with a ground but does not necessarily transmits any load.

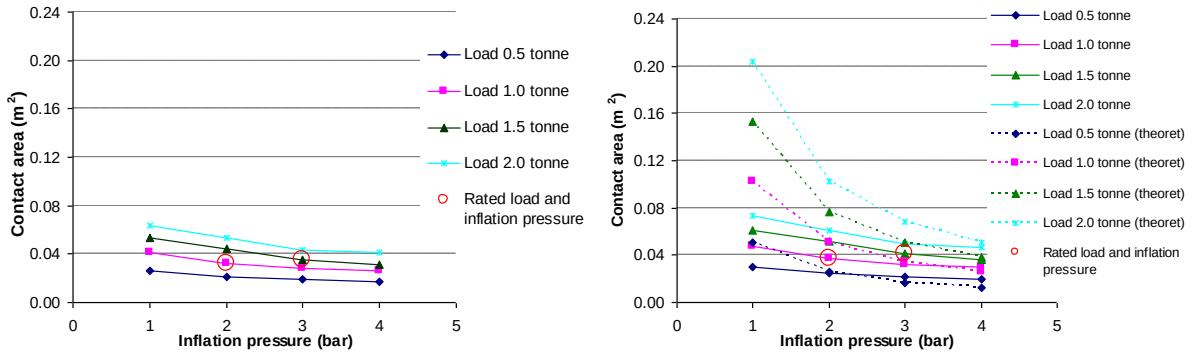

Figure 5.10 Contact area vs. inflation pressure obtained using the ink method - Front tractor tyre 9.0-16 (left: treaded area, right: projected area)

As shown in Figure 5.10, the tread contact areas and projected areas obtained in the experiments for a range of inflation pressure show similar trends with the tread areas being always smaller. The ratio of a projected / tread contact area varied depending on the tyre. For the front tractor tyre the projected areas were 12 – 17% greater than the treaded areas. The difference was relatively small as the tractor tyre had only two grooves on the tyre surface.

Tyre inflation pressure and load were both found to have a significant effect at 95% confidence level on both treaded and projected contact patch for the front tractor tyre

(Appendix G.3 and G.4). An increase in load produces an increase in the contact area, while an increase in inflation pressure results in a decrease in the area. The interaction between the load and inflation pressure is not significant to both treaded and projected contact area.

Contact area data obtained for the front tractor tyre using Tekscan system (Figure 5.7) was compared with the results obtained using the ink method (Figure 5.10 (left)) and a good agreement of the data was found and presented in Figure 5.11 and Misiewicz *et al.* (2008). The Tekscan method provided marginally greater (up to 12%) contact area results, which was expected. This is related to the edge effect, as if some sensels are partially loaded, the system assumes that the whole area of the sensel is loaded. For this part of the study, 9830 Tekscan sensors were used; they have worse spatial resolution than 6300 sensors used in other parts of the project (as quoted in Chapter 4). A relatively good agreement between the two methods, however, proves that the contact areas determined by Tekscan system also do not represent only the areas of contact that transmit the load but also the areas that have contact with the surface but do not transmit any significant load as discussed in Section 5.2. Therefore, it is not recommended to use the contact areas determined using Tekscan system or the ink method to calculate the mean contact pressure. Especially, as it was confirmed that the tyre contact pressure is not uniform, but highly variable across the contact patch (Figure 5.6).

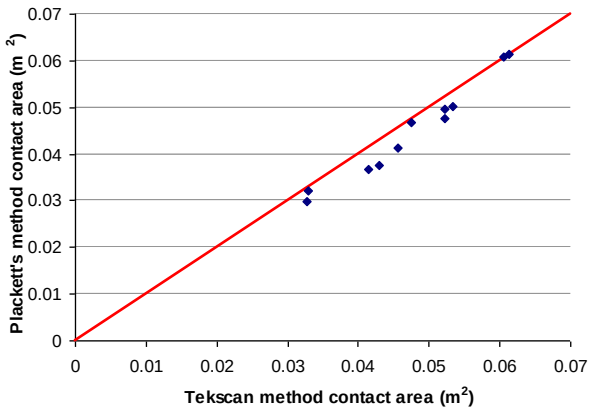

Figure 5.11 Comparison of Tekscan and ink methods for tyre contact area determination (1:1 line in red)

Figure 5.12 illustrates the mean contact pressure results obtained for the front tractor tyre 9.0-16. For a better visualisation and comparison of the mean contact pressure and tyre inflation

pressure, the 1:1 line was added to all figures presenting relationships between tyre inflation pressure and mean contact pressure.

The significant effects of inflation pressure and load on contact pressure were found for the front tractor tyre as presented in Appendix G.5 and G.6. An increase in inflation pressure leads to a contact pressure increase and the load increase also results in the contact pressure rise. The fact of mean contact pressures, derived from tyre contact area, being lower than the inflation pressure at high inflation pressures was previously discussed in Section 5.2.

The difference between the mean projected contact pressure and tyre inflation pressure was found not to be constant but to decrease with an increase in tyre inflation pressure and increase with an increase in tyre load. The difference was found to vary from 0.6 bar and 1.7 bar to negative and 0.2 bar values for the 0.5 tonne and 2.0 tonne load, respectively. The overall mean carcass stiffness value was found to be 0.32 bar, which is much lower than the mean carcass stiffness obtained in the Tekscan study. If carcass stiffness was considered as the mean tyre contact pressure at zero inflation pressure, then it would be 1.37 bar, 1.72 bar, 1.82 bar and 2.19 bar for the 0.5 tonne, 1.0 tonne, 1.5 tonne and 2.0 tonne load, respectively. When considering carcass stiffness as the difference between the mean tread contact pressure and tyre inflation pressure, the results were found to be greater and they varied from 0.9 bar and 2.1 bar to negative value and 0.8 bar when the tyre was loaded to 0.5 tonne and 2.0 tonne, respectively. The mean maximum carcass stiffness was found to be 0.71 bar, which is again considerably lower than the value determined in the Tekscan experiments. While the maximum tyre contact pressure at zero inflation pressure was found to be 1.57 bar, 1.98 bar, 2.06 bar and 2.55 bar, for the 0.5 tonne, 1.0 tonne, 1.5 tonne and 2.0 tonne load, respectively. The two tests conducted at the tyre rated values of 1.0 tonne/2.0 bar and 1.5 tonne/3.0 bar showed similar difference between the contact pressure and inflation pressure. They were found to be 0.61 bar and 0.57 bar when considering the mean values and the maximum values were equal to 1.00 bar and 1.12 bar. These values are, however, different to the carcass stiffness obtained when the front tractor tyre was tested at the rated load and inflation pressures using Tekscan system.

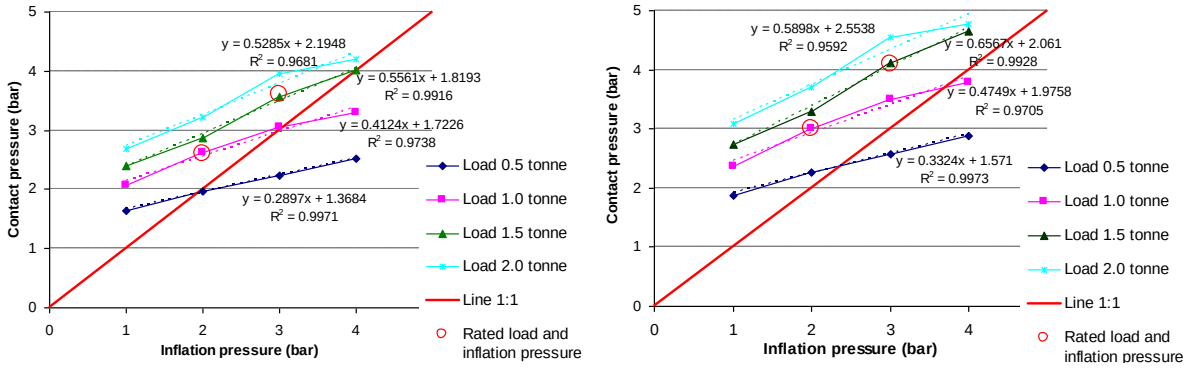

Figure 5.12 Contact pressure vs. inflation pressure according to the ink method data – Front tractor tyre 9.0-16 (left: mean contact pressure calculated according to the tread area, right: mean contact pressure calculated according to the projected area)

The contact pressure results calculated according to the ink tests for the tractor tyre at higher inflation pressures, therefore, do not agree with the results obtained using Tekscan system and and findings of Chancellor (1976) and Plackett (1983) who reported that the tyre carcass contributes to the ground pressure, and that this contribution is constant. According to the mean contact pressure results obtained using the ink method tyre carcass contribution to the ground pressure was not found to be constant over the range of inflation pressure tested. However, it could have been associated with the fact that the mean contact pressure cannot be determined according to the contact area, but needs to be measured.

5.3.3 Tyre load - deflection method

Tyre – load deflection relationships of the front tractor tyre at different inflation pressures are presented in Figure 5.13. The load - deflection relationships were found to have some small non-linear characteristics, hence a linear regression equation was fitted to the complete load range to estimate the slope (all equations resulted in R^2>0.99). The slope of the regression equation when plotted against inflation pressure is given in Figure 5.14; it resulted in an estimation of the carcass stiffness value as 0.35 bar.

According to the load - deflection method, the 7.5-16 front tractor tyre, tested previously by Plackett (1983), was found to have carcass stiffness equal to 0.35 bar, which agrees with the carcass stiffness result of the front tractor tyre currently tested.

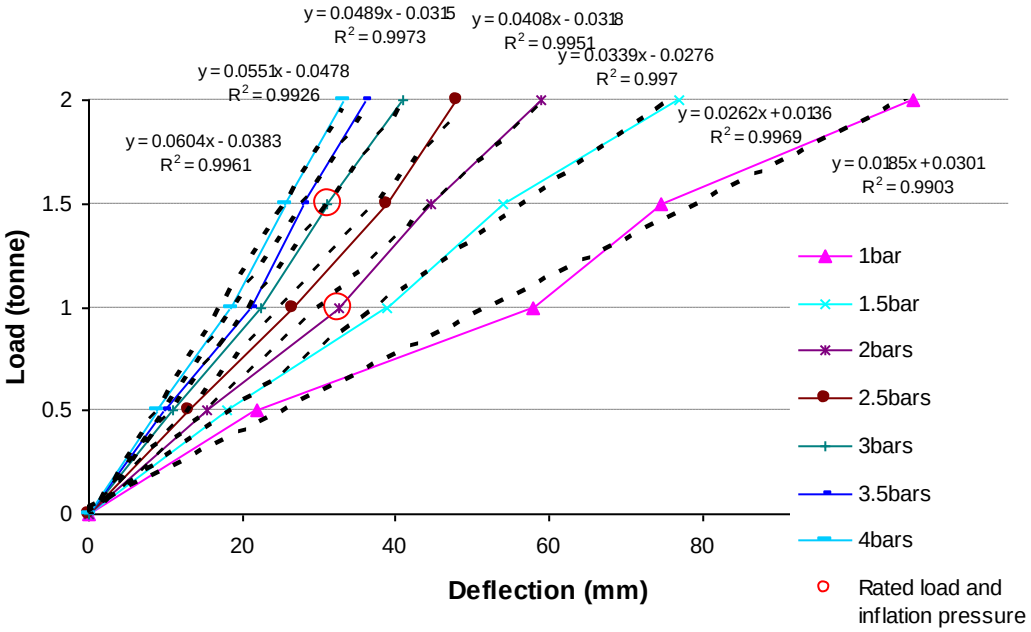

Figure 5.13 Load – deflection relationship for the front tractor tyre

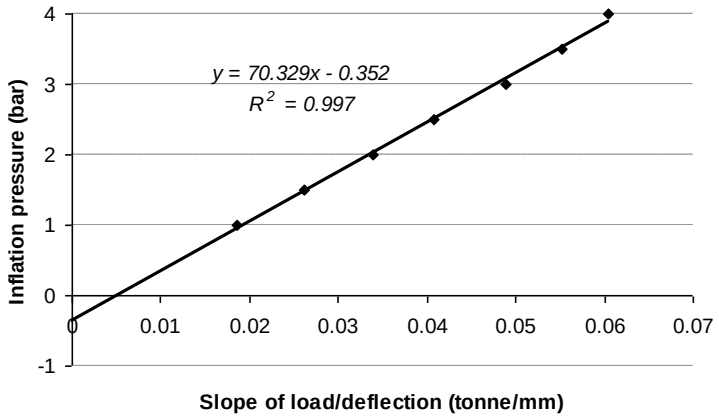

Figure 5.14 Inflation pressure vs. slope of load – deflection curve for the front tractor tyre

5.3.4 Tyre manufacture specification data method

Tyre manufacture data for the front tractor tyre together with linear and 2nd order polynomial functions established is presented in Figure 5.15. The extrapolation to the inflation pressure to the x axis gave carcass stiffness of 1.36 bar and 0.75 bar for both the 10 mph and 30 mph tyre speed for the linear and polynomial function, respectively. While extrapolation of the same functions to the load axis at zero inflation pressure, with an assumption that tyre contact area was 0.045 m^2 (which was obtained in the Tekscan and ink tests) provided carcass stiffness

values of 1.03 bar and 0.76 bar for the linear and polynomial regression functions, respectively (for 10 mph forward speed). Speed increase to 30 mph resulted in carcass stiffness decline to 0.90 bar and 0.66 bar, respectively.

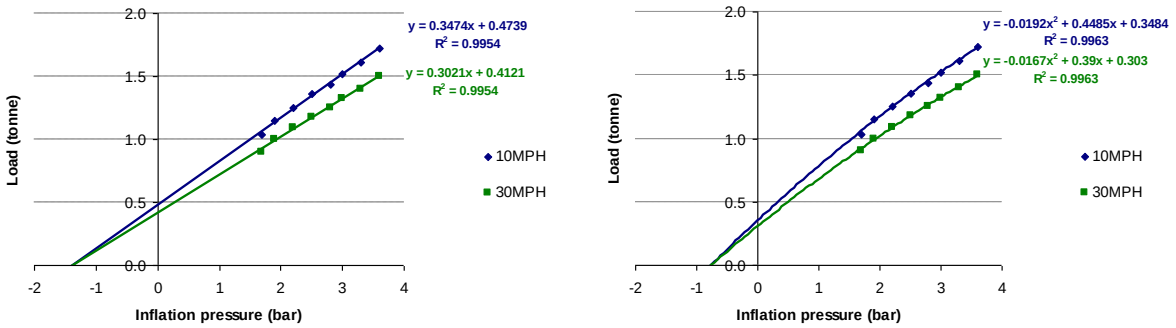

Figure 5.15 Inflation pressure vs. load with linear (left) and 2nd order polynomial (right) regression lines – Front tractor tyre (manufacture specification for 10 mph and 30 mph forward speeds)

5.4 Comparison of the results

The preliminary study conducted on the inner tube involved the ink and deflection experiments. They were done in order to determine the carcass stiffness of the flexible inner tube. The method based on tyre manufacture data was not possible to be conducted as the studies involved evaluation of the inner tube's carcass stiffness, rather than tyre's. Due to expansion of the inner tube during the preliminary study, it was not possible to continue the study involving its contact pressure distribution measurements using the tube. Hence, the study moved to the front tractor tyre for which the study involved an evaluation of the four methods of carcass stiffness estimation described above.

Table 5.1 contains data obtained for the inner tube according to the ink and deflection methods. The mean contact pressure was determined for the tube according to the ink data obtained. Further, the carcass stiffness of the tube was evaluated. The results obtained in the ink methods, showing the relationship between the mean contact stress and inflation pressure for different loads agree with the relationship proposed by Karafiath and Nowatzki (1978) and presented by Equation 2.10. The mean carcass stiffness values for each load were determined, from those an overall mean value was calculated, as presented in Table 5.2.

The results showed that the inner tube effectively does not have any carcass stiffness, as the difference between the mean contact pressure and inflation pressure varied from – 0.01 bar to 0.03 bar depending on the load and inflation pressure, with the mean carcass stiffness of 0.01 bar. The mean contact pressures under the inner tube at low load and high pressures, determined using the ink contact areas, were found to be lower than the inflation pressure, which was considered to be impossible. This indicates that the ink method should not be used for the mean pressure estimation, as it only gives an indication about the area that has contact with the loading surface, but does not necessarily transfer any load. This, then, results in an under-estimation of the mean contact pressure. This method does not provide any real indication about the pressures applied.

From the above it was concluded, that the ink method should not be used for an estimation of the mean tyre contact pressure. Therefore, there is a need to use a better and more advanced technique for the contact pressure distribution determination. In order to gain a better understanding of the relationship between the tyre characteristic and contact pressure the Tekscan pressure mapping system was used for measuring distribution of the contact pressure across the contact patch. This allowed the mean contact pressure to be accurately determined. The Tekscan pressure mapping system was used to determine contact pressure distribution for a range of tyres, which provided mean and maximum contact pressure values and also enabled the contact area to be determined, which was compared to the results obtained using the ink method.

The method of the carcass stiffness estimation, looking at the load – deflection characteristic, also confirmed that the inner tube is a "purely" flexible material with no carcass stiffness. The value obtained in this method was found to be – 0.001 bar.

Table 5.1 Relationship between the mean contact pressure and inflation pressure obtained for the inner tube at different loads following the relationship proposed by Karafiath and Nowatzki (1978)

Load (tonne)	Mean contact pressure according to the ink data	
	c_1	P_{CS} (bar)
0.01	0.78	0.01
0.02	0.70	0.02
0.03	0.63	0.04
0.04	0.60	0.04
0.05	0.63	0.04
0.06	0.47	0.06
0.07	0.37	0.07
0.08	0.34	0.07

Table 5.2 Estimation of the inner tube carcass stiffness

Load (tonne)	Pressure difference method according to the ink data		Load – deflection method P_{CS} (bar)
	Mean P_{CS} (bar)	Overall mean P_{CS} (bar)	
0.01	-0.01	0.01	- 0.001
0.02	0		
0.03	0.01		
0.04	0		
0.05	0.01		
0.06	0.01		
0.07	0.01		
0.08	0.02		

The relationships between the contact pressures and tyre inflation pressures obtained in the Tekscan in the pilot on the 9.0-16 Firestone front tractor tyre were found to be close to linear functions. The linear regression analysis proved that both tyre load and inflation pressure have a significant effect on both mean and maximum contact pressure as presented in Equation 5.1 and 5.2. The ‘t’ tests showed that the slopes of the mean and maximum contact pressure are significantly different from 1. This proves that the mean and maximum tyre carcass stiffness of this tyre is not a constant value but it changes with inflation pressure and load.

Table 5.3 presents tyre carcass stiffness data obtained for the front tractor tyre using different methods as presented in Section 5.3.1 – 5.3.4. Also the mean carcass stiffness values for each load were determined, following that an overall mean value was calculated.

Table 5.3 Estimation of the tyre carcass stiffness of the front tractor tyre (Firestone 9.0-16)

P_{CS}	Tyre load (tonne)	Pressure difference method A (Tekscan)			Pressure difference method B (ink)			Load – defl. method P_{CS} (bar)	Tyre manufacture specification data method (low tyre rolling speed)	
		Mean P_{CS} (bar)	Overall mean P_{CS} (bar)	P_{CS} at rated load and pressure (bar)	Mean P_{CS} (bar)	Overall mean P_{CS} (bar)	P_{CS} at rated load and pressure (bar)		An inflation pressure at zero load (linear/2nd polynomial) (bar)	A load at zero inflation pressure (linear/2nd polynomial) (bar)
Mean P_{CS}	0.5 1.0 1.5 2.0	0.21 1.29 1.61	0.99	0.20 1.26	-0.41 0.25 0.71 1.02	0.32	0.61 0.57	0.35	1.36 / 0.75	1.03 / 0.76
Max P_{CS}	0.5 1.0 1.5 2.0	1.29 2.10 3.66	2.68	1.17 3.06	-0.10 0.66 1.20 1.53	0.71	1.00 1.12			

It is understood that in order to determine tyre maximum carcass stiffness it is necessary to measure tyre contact pressure distribution which will provide the maximum contact pressure. The ink technique provided projected and tread contact area, which were then used to calculate the mean contact pressures over the projected and tread contact areas. The carcass stiffness, calculated as a difference between the mean tread contact pressure and inflation pressure, was called maximum carcass stiffness. However, it was expected that it would be considerably lower than the maximum carcass stiffness determined in Tekscan study, which was the case.

Contact pressure measurements using Tekscan system showed non-uniform contact pressure distribution below the front tractor tyre. Not all the pressure distribution data sets were found to be normally distributed. At low inflation pressure it was positively skewed (right-skewed) with a large amount of values at low pressures and with relatively few high values. At high inflation pressure the pressure distribution was found to be negatively skewed (left-skewed)

as there are only few low values and a large amount of high values. When the tyre was loaded following the tyre manufacture specification, the contact pressure distribution was found to be more uniformly distributed with a normal distribution.

According to the contact pressure data obtained using Tekscan, tyre carcass stiffness was determined for the front tractor tyre as the difference between tyre contact pressure and inflation pressure. Mean and maximum carcass stiffness was considered. The carcass stiffness evaluated for the front tractor tyre was found to increase with a load increase and decrease with an increase in tyre inflation pressure. According to mean contact pressures, the mean carcass stiffness of the front tractor tyre was found to be 0.21 bar, 1.29 bar and approximately 1.61 bar for 1.0 tonne, 1.5 tonne and 2.0 tonne loads, respectively. The overall mean value was found to be 0.99 bar, while for the rated load and inflation pressure the carcass stiffness was found to be 0.20 bar and 1.26 bar for 1.0 tonne and 1.5 tonne, respectively. While, the mean maximum carcass stiffness was found to be 1.29 bar, 2.10 bar and 3.66 bar depending on tyre loads of 1.0 tonne, 1.5 tonne and 2.0 tonne, respectively. The overall mean maximum carcass stiffness is 2.68 bar. For the rated load and inflation pressure the maximum carcass stiffness was found to be 1.17 bar and 3.06 bar for 1.0 tonne and 1.5 tonne, respectively. The maximum carcass stiffness was found to be more than two times greater than the mean carcass stiffness. This, however, did not consider the effect of the sidewall edges, where the maximum carcass stiffness could be higher.

The carcass stiffness data obtained for the front tractor tyre in the ink method are considerably lower than the values above. The carcass stiffness results obtained in the Tekscan study were found to be approximately 1.5 – 2.5 times greater than the values form the ink tests. This agree with the findings of the study on the inner tube, which concluded that the mean contact pressure should not be estimated from the contact area but should be measured. This is associated with the finding that the pressure is not uniform below a tyre. Furthermore, Plackett's ink method for mean contact pressure estimation indicates the area where a tyre touches a surface. It does not demonstrate any pressure distribution below a tyre. An average contact pressure obtained by this method is only an estimation of the contact pressure between the surface and tyre. It was found that the mean contact pressure obtained by this method is lower than the actual mean pressure, since at the edges of the contact patch or the middle area

(depending on tyre inflation pressure and load) may only touch the surface and not apply any significant load. Such a case is not recognised by the Plackett's ink method. Therefore, in order to determine tyre carcass stiffness, it is recommended to measure tyre contact pressure distribution rather than contact area.

The tyre load – deflection characteristic of the front tractor tyre provided carcass stiffness of 0.35 bar, which agrees with the previous study of Plackett (1983) on the 7.5-16 front tractor tyre. However, the carcass stiffness result obtained is approximately three times lower than the mean values obtained in Tekscan study. This is probably due to the fact that this method provides only stiffness of the tyre sidewalls as it is based on the load – deflection characteristic. While the Tekscan method considering the difference between the contact pressure and inflation pressure, takes into account both sidewall and tyre belt stiffness. The method based on tyre load – deflection relationship appears to be sensitive to error in experimental results, as a small error was found to give a great change in the carcass stiffness value. Also a linear fit for the load - deflection curves does not seem to be a good assumption.

The method based on tyre manufacture specification data provided carcass stiffness of 1.36 bar / 0. 75 bar and 1.03 bar / 0.76 bar depending on the technique used (method a: an inflation pressure at zero load (linear / 2nd order polynomial) and method b: a load at zero inflation pressure (linear / 2nd order polynomial)). The results obtained are in a closer agreement with the carcass stiffness of the front tractor tyre which was found to be 0.99 bar and 1.26 bar, respectively (Tekscan study). This method, therefore, gives an indication of the mean and rated carcass stiffness values of the front tractor tyre. The technique based on a load at zero inflation pressure (method b) with a linear fit gave the closest result which differs 4% from the mean value and 22% from the rated value. The method looking at the inflation pressure at zero load (method a), according to the linear fit, provided values that agree within 37% and 8% with the mean carcass stiffness and the carcass stiffness at rated load and inflation pressure, respectively.

A comparison of the results of carcass stiffness estimation for the front tractor tyre obtained by the ink, load – deflection and tyre manufacture methods to the values obtained in the pressure distribution measurements was conducted. This was done in order to find a simple

method of carcass stiffness estimation, so there would not be a need to conduct the pressure distribution study, which is more time-consuming and require more sophisticated experimental equipment. The method based on tyre manufacture data was found to be a relatively good indication of the mean carcass stiffness of the front tractor tyre. The ink and load – deflection methods gave significantly lower values. The maximum carcass stiffness was not successfully indicated by any of the techniques used apart from the Tekscan study. It could, however, be estimated as a relative value to the mean carcass stiffness. For the front tractor tyre the maximum carcass stiffness was found to be approximately 2.5 – 3 times greater than the mean carcass stiffness.

5.5 Conclusions

The preliminary study using the "purely" flexible inner tube lead to the following conclusions:

1. Some mean contact pressures under the inner tube, determined using the ink contact areas, were found to be lower than the inflation pressure, which is impossible. This indicates that the ink method should not be used for the mean pressure estimation.
2. According to the ink method, the inner tube effectively does not have any carcass stiffness, i.e. 0.01 bar.
3. The load – deflection method also indicated that the inner tube does not have carcass stiffness as this technique provided a value of – 0.001 bar.

The study based on the 9.0-16 Firestone front tractor tyre gave the following findings:

1. Tyre contact pressure distribution of the front tractor tyre was found to be non-uniform. The pressure concentration was found at the sidewall edges of tyre contact patches for the tyre at low inflation pressures, while an increase in inflation pressure resulted in a pressure concentration movement from the sidewall edges to the central area of the contact patch.
2. According to the Tekscan contact pressure experiments, the mean carcass stiffness of the front tractor tyre was found to vary with tyre load and vary slightly with tyre inflation pressure. The carcass stiffness is 0.21 bar, 1.29 bar and 1.61 bar for 1.0 tonne, 1.5 tonne and 2.0 tonne loads, respectively. The mean value was found to be 0.99 bar. The fact that tyre carcass stiffness is not constant with inflation pressure

changes does not agree with previous findings of Bekker (1956) and Plackett (1983).

3. According to the Tekscan contact pressure experiments, the maximum carcass stiffness of the front tractor tyre was also found to vary with tyre load and vary slightly with tyre inflation pressure. The mean maximum values are 1.29 bar, 2.10 bar and 3.66 bar depending on tyre loads of 1.0 tonne, 1.5 tonne and 2.0 tonne, respectively. The mean maximum value is 2.68 bar. The maximum carcass stiffness was found to be approximately 2.5 – 3 times greater than the mean carcass stiffness.
4. The mean contact pressure results obtained in the ink tests were found to be considerably lower than the mean data obtained in the Tekscan study. The Tekscan method gave the mean carcass stiffness approximately 1.5 – 2.5 times higher carcass stiffness values than the ink study. This proves that the ink method should not be recommended for determination of the mean contact pressure.
5. According to the load – deflection method, the 9.0-16 front tractor tyre was found to have carcass stiffness of 0.35 bar, which agrees with the previous study of Plackett (1983) on the 7.5-16 front tractor tyre. However, the result given by this method is considerably lower than the real carcass stiffness of the front tractor tyre (the results are approximately smaller by a factor of 3). Further, this method appears to be sensitive to error in experimental results. Particularly, a linear fit for the load - deflection curves does not seem to be a good assumption.
6. The method based on tyre manufacture specification data provided carcass stiffness between 1.36 bar / 0. 75 bar and 1.03 bar / 0.76 bar depending on the technique used. The technique based on a load at zero inflation pressure with a linear fit gave the closest result which differs 12% from the ‘real’ value.
7. Comparing the results of carcass stiffness estimation for the front tractor tyre obtained by the ink, load – deflection and tyre manufacture methods, the technique based on the tyre manufacture data was found to give results which are in a closer agreement with the measured mean carcass stiffness obtained in the Tekscan study.

6 THE EFFECT OF TYRE TREAD ON TYRE CARCASS STIFFNESS (SMOOTH AND TREADED COMBINE TYRES)

This chapter also evaluates the range of methods to determine tyre carcass stiffness on a hard surface. Here, the data from the 600/55-R26.5 Trelleborg smooth and treaded rear combine tyres, presented in Figure 3.3, were considered. Tyre mean and maximum carcass stiffness was determined. The mean value was calculated according to the mean contact pressure for a tyre contact patch, while the maximum carcass stiffness was based on the maximum contact pressure found for each tyre contact patch. These tyres were also selected in order to investigate the effect of tyre treads on the contact pressure distribution. They were both tested at or below their maximum recommended load at a range of inflation pressures according to the tyre manufacture specification data given in Figure 6.16. The ink and deflection tests were conducted statically, while Tekscan study was dynamic and the tyres were rolled at speed of 0.085 m/s (0.03 km/h).

6.1 The pressure difference method (A) to measure both mean and maximum contact pressure using Tekscan

Contact pressure distribution was evaluated for the 600/55-R26.5 Trelleborg smooth combine tyre, which was also investigated by Misiewicz *et al.* (2009). The tyre was loaded at a range of inflation pressures and at or below the maximum recommended load. In general non-uniform pressure distribution was detected below the smooth combine tyre. The contact pressure distribution of the combine tyre was normally distributed only for rated load and inflation pressure. In other cases it was found to be skewed. Appendix K presents graphical display of the pressure distribution data as histograms, which confirm non-uniform pressure distribution across the contact patch. The pressure distribution was found not to be normally distributed when under and over – loading the tyre. At lower inflation pressures (below 1.5 bar), significant pressure concentrations were found at the sidewall edges of tyre contact patch as presented in Figure 6.1. For those cases pressure distribution was positively skewed (right-skewed) with a large amount of values at low pressures and relatively few high values.

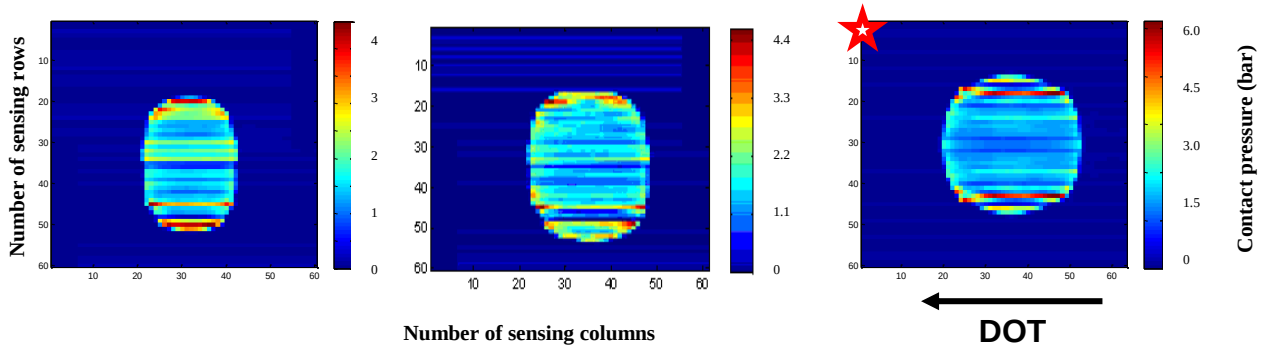

Figure 6.1 Contact pressure distribution (bar) for the tyre at 1.0 bar inflation pressure at a range of loads (from left: 1.8 tonne, 2.5 tonne, 3.765 tonne; direction of travel from right to left; ★ - rated load and inflation pressure)

As the smooth combine tyre inflation pressure was increased to 1.5 bar, which was the recommended inflation pressure for 4.5 tonne load, the contact pressure distribution was found to be more normally distributed with relatively greater pressures in the central area of contact patches. The pressures close to the sidewall edges were found to decrease as illustrated in Figure 6.2. Further increase in inflation pressure without any change in load, resulted in a negatively skewed pressure distribution (left-skewed) with a great amount of high values and few low values.

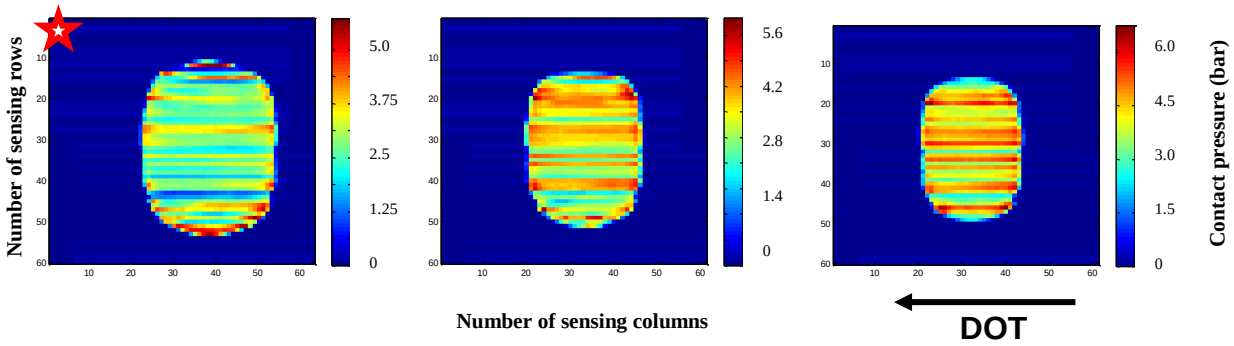

Figure 6.2 Contact pressure distribution (bar) for the tyre loaded to 4.5 tonne at different inflation pressure (from left: 1.5 bar, 2.0 bar and 2.5 bar; direction of travel from right to left; ★ - rated load and inflation pressure)

Tyre contact areas obtained in the Tekscan experiments for the smooth and treaded combine tyres are presented in Figure 6.3. Both tyres were tested up to their maximum recommended load for a range of pressures. The results showed that the maximum contact area remains

approximately constant. The smooth tyre was found to have greater contact areas than the treaded tyre, which was expected as the area obtained for the treaded tyre represents only contact of the treads. The combination of tyre inflation pressure and load was found to have a statistically significant effect on contact area of the smooth and treaded tyres at 95% confidence level (Appendix H.1 and H.2). The analysis of variance also proved that the effect of tyre tread has a significant effect on the resulting tyre contact area (Appendix H.3).

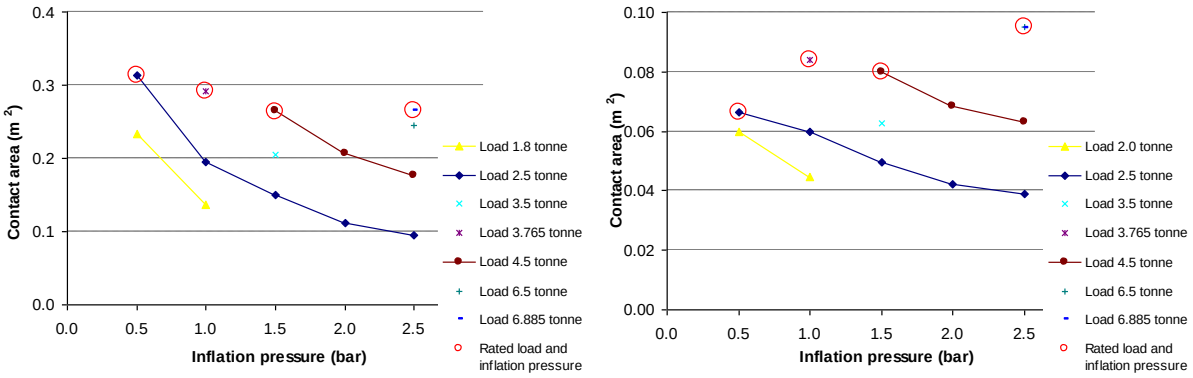

Figure 6.3 Tyre contact area vs. inflation pressure for the combine tyres obtained using the Tekscan method (left: total contact area for the smooth combine tyre, right: tread contact area for the treaded combine tyre)

Figure 6.4 shows the mean contact pressure vs. inflation pressure for the smooth and treaded tyre obtained using Tekscan system. The maximum contact pressure for both tyres was presented in Figure 6.5. The data confirmed that as inflation pressure increases there is an increase in both the mean and maximum contact pressure for both smooth and treaded tyres. Also a load increase resulted in an increase in the mean and maximum pressure. The mean and maximum contact pressures were found to be higher than the tyre inflation pressure over the range studied (see Figure 6.4 and 6.5).

Overall, the maximum contact pressures were found to be significantly higher than the mean contact pressure. The results also confirm that when a tyre is equipped with lugs, pressure at the surface of the lugs is considerably higher than the inflation pressure and it is also much greater than the pressure at the surface of a smooth tyre. The effect of tyre tread was also significant at 95% confidence to the mean and maximum contact pressures (Appendix H.4 and H.5). The pressure concentration effect was expected on firm surface. It is expected to be

less significant on soils where tyre carcass between the tread bars both carry some of the load, the effect of which will be studied in greater detail in Chapter 8.

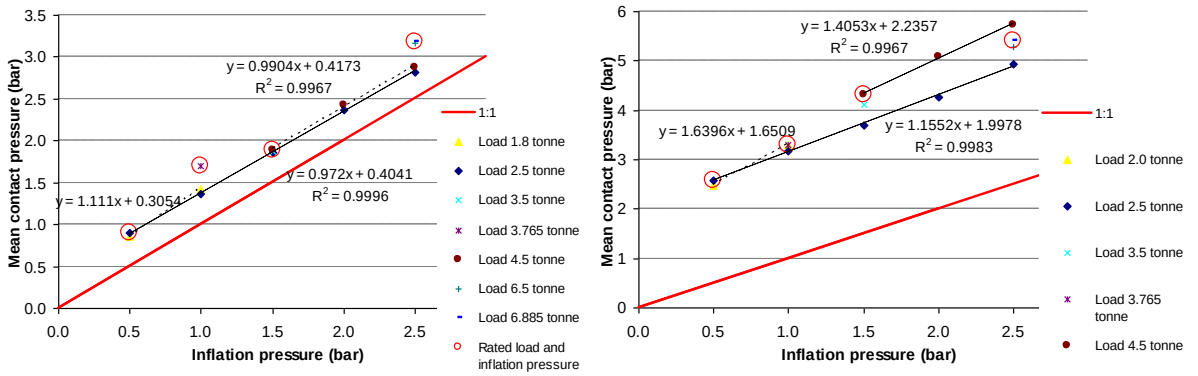

Figure 6.4 Mean contact pressure vs. tyre inflation pressure for the smooth (left) and treaded (right) combine tyres for a range of safe working loads

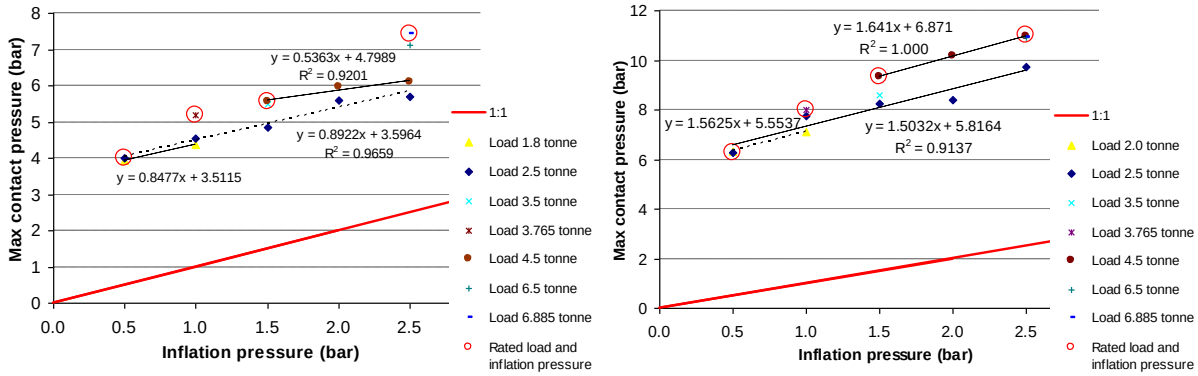

Figure 6.5 Maximum contact pressure vs. tyre inflation pressure for the smooth (left) and treaded (right) combine tyres for a range of safe working loads

The mean contact pressure results for the smooth combine tyre (Figure 6.4 (left)) approximately follow the model proposed by Plackett (1983) as the difference between the mean contact pressure and inflation pressure appears to be a constant value over the range studied. However, a regression analysis discussed below confirms that the trends presented in Figure 6.4 and 6.5 follow the model proposed by Karafiath and Nowatzki (1978) as the difference between the contact pressure and inflation pressure varies with inflation pressure.

As the relationships between the contact pressures and tyre inflation pressures were found to

be close to linear for both the smooth and treaded combine tyres, a linear regression analysis was carried out and presented in Appendix J.3 – J.6. The analysis confirmed that tyre load and inflation pressure have significant effect on the mean and maximum contact pressure of the smooth tyre. For the treaded tyre, only inflation pressure has an influence on the resulting contact pressures. The 't' tests, based on the results obtained in the regression analysis for both tyres, showed that the slope of the inflation pressure is significantly different from 1. This means that the contact pressure does not increase at the same rate as tyre inflation pressure. Therefore, tyre carcass stiffness is not a constant value but it changes with inflation pressure. Also the effect of load on the carcass stiffness was found but it was found to be significant only for the smooth tyre.

The analysis provided the following regression equations:

- Smooth combine tyre:

$$\textbf{Mean } P_C = 0.27 + 0.92 \times P_i + 0.08 \times W \qquad \text{Equation 6.1}$$

$$\textbf{Max } P_C = 3.37 + 0.39 \times P_i + 0.42 \times W \qquad \text{Equation 6.2}$$

- Treaded combine tyre:

$$\textbf{Mean } P_C = 1.86 + 1.41 \times P_i \qquad \text{Equation 6.3}$$

$$\textbf{Max } P_C = 5.94 + 1.84 \times P_i \qquad \text{Equation 6.4}$$

The mean and maximum contact pressure linear regressions obtained for the smooth combine tyre fit the experimental data in 99% and 75%, respectively. The regression line established for the mean and maximum contact pressure obtained below the treaded tyre fits the data in 85% and 61%, respectively.

The difference between the contact pressure and inflation pressure, considered as carcass stiffness, was further studied and presented for both the smooth and treaded combine tyres in Figure 6.6 and 6.7. The mean value for the smooth tyre varies between 0.3 bar – 0.7 bar and the maximum varies between 3 bar – 5 bar. The overall mean values of mean and maximum carcass stiffness of the smooth combine tyre were found to be 0.44 bar and 3.81 bar, respectively. While for the rated loads and inflation pressures, the means of the mean and maximum carcass stiffness were 0.54 bar and 4.46 bar, respectively.

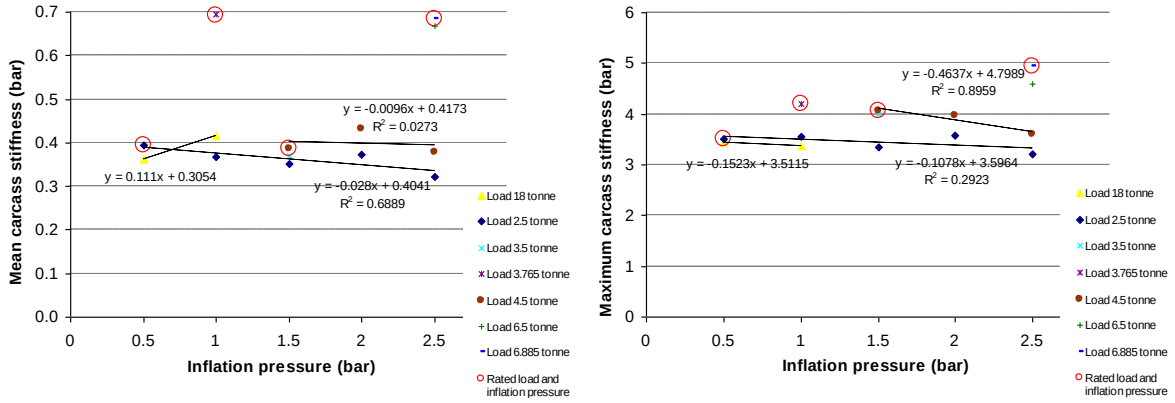

Figure 6.6 Tyre carcass stiffness vs. tyre inflation pressure for the smooth combine tyre according to mean (left) and maximum (right) contact pressure

The carcass stiffness of the treaded combine tyre, presented in Figure 6.7 was found to be significantly greater than the carcass stiffness of the same size smooth tyre. The mean values were found to vary between 2.0 – 3.2 bar. While the maximum carcass stiffness varies between 5.9 – 8.4 bar. The overall mean values of mean and maximum carcass stiffness of the treaded combine tyre tested are equal to 2.51 bar and 7.16 bar, respectively. While for the rated loads and inflation pressures, the means of the mean and maximum carcass stiffness are 2.53 bar and 7.25 bar, respectively.

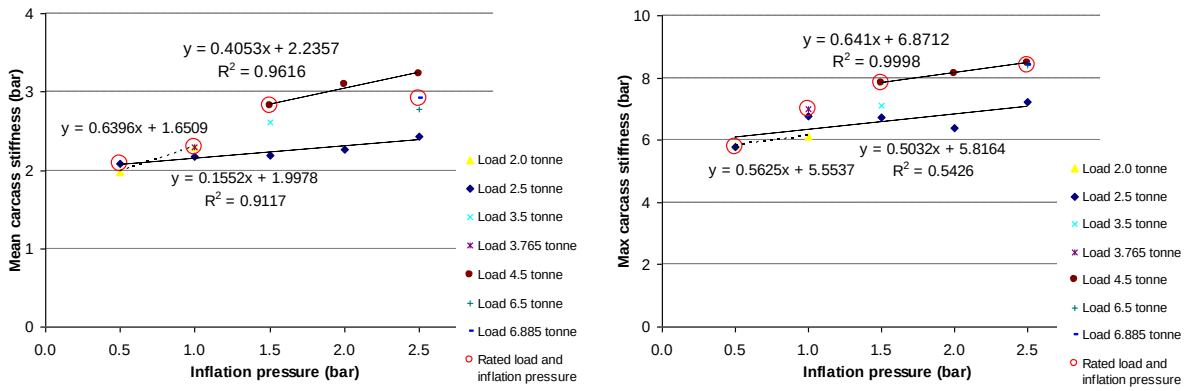

Figure 6.7 Tyre carcass stiffness vs. tyre inflation pressure for the treaded combine tyre according to mean (left) and maximum (right) contact pressure

Both, the mean and maximum carcass stiffness of the treaded tyre were found to be greater than the values obtained for the smooth tyre. The analysis of variance proved that tyre tread

has a significant effect on the mean and maximum carcass stiffness (Appendix H.6 and H.7).

6.2 The pressure difference method (B) using ink to estimate the size of the contact patch and hence mean contact pressure

The contact area results obtained for the treaded combine tyre are presented in Figure 6.8 (left: projected area, right: tread area). Figure 6.9 (left) shows contact area data for the smooth combine tyre. Figure 6.9 (right) illustrates a comparison of the contact area data for the smooth and treaded tyre. As both tyres were tested up to their maximum recommended load for a range of pressures, it was shown that tyre maximum contact area remains approximately constant which was also the case for the results obtained in the Tekscan study. Figure 6.9 (right) shows that the smooth tyre had larger contact areas than the projected area of the treaded tyre. This confirms that tyre treads increase an overall tyre carcass stiffness so the tyre requires a smaller contact area to carry the same amount of load. The combination of tyre load and inflation pressure was found to have a significant effect on the treaded and projected contact area of the treaded combine tyre as shown in Appendix H.8 and H.9 (at 95% confidence level). The analysis of variance could not be conducted for the smooth tyre as the experiments were not replicated.

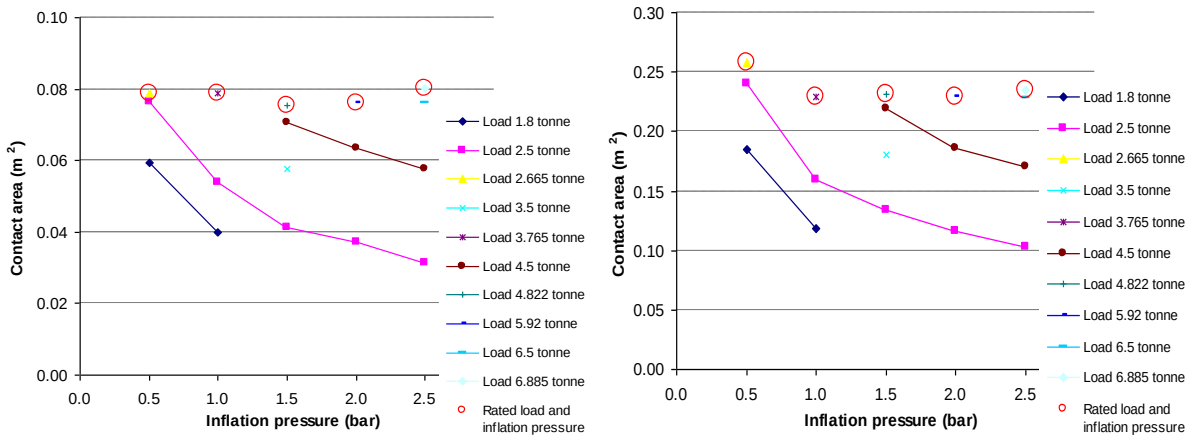

Figure 6.8 Tyre contact area vs. inflation pressure according to the ink data – Treaded combine tyre (left: projected area, right: tread area)

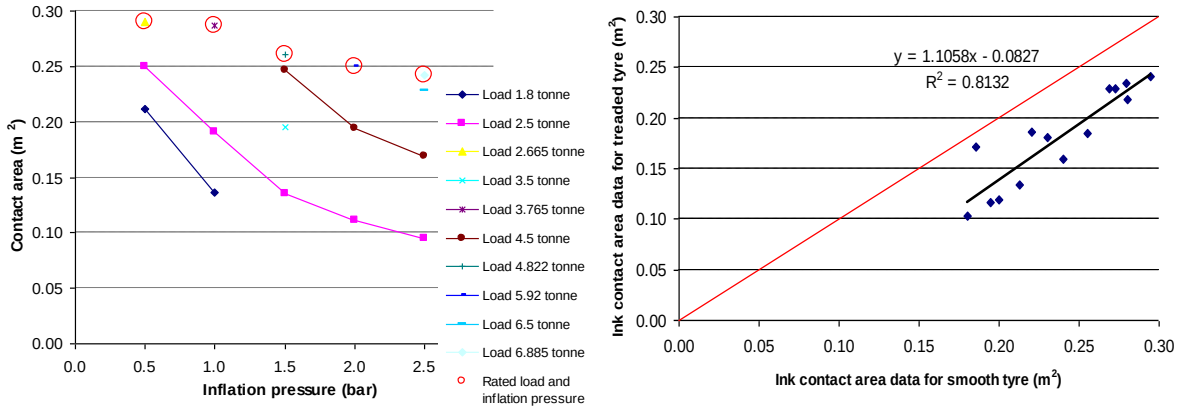

Figure 6.9 Tyre contact area according to the ink data – Smooth combine tyre (left: contact area vs. inflation pressure, right: comparison of the data for the smooth and treaded tyre)

The contact area results obtained in the ink experiments (Figure 6.8 (right) and Figure 6.9 (left)) were compared to the values obtained in the Tekscan experiments (Figure 6.3) and they were found to be in relatively close agreement as presented in Figure 6.10. The Tekscan results were found to be up to 20% greater than the ink contact areas. However, the majority of the data was in agreement within 10%. It agrees with the data obtained for the front tractor tyre (Chapter 5). Additionally, it is necessary to remember that the ink tests were carried out statically, while the Tekscan study was dynamic.

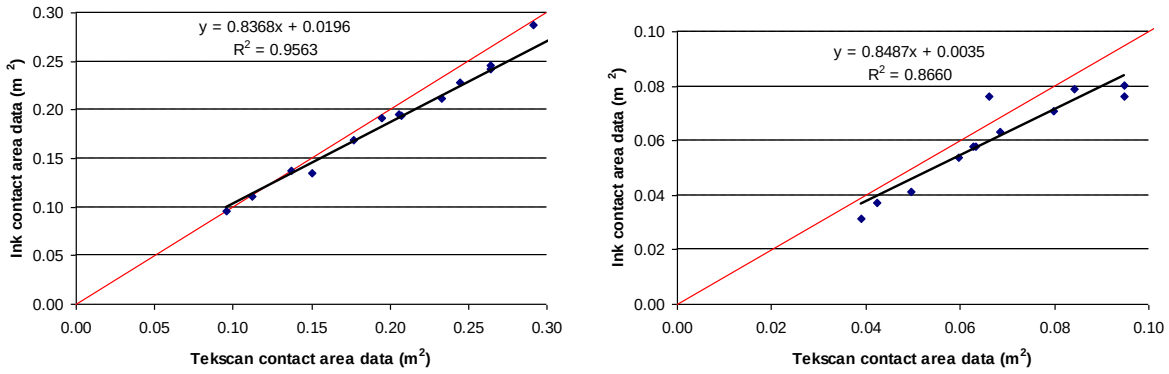

Figure 6.10 Comparison of the ink and Tekscan methods for tyre contact area measurement (left: smooth combine tyre, right: treaded combine tyre)

According to the contact area values obtained in the ink experiments, tyre mean contact pressures were calculated by dividing tyre load by contact area obtained in the ink tests. This

was discussed before to be not a good practice, however, it was decided to implement this practice in order to evaluate the data obtained in the ink experiments on the smooth and treaded combine tyres. The mean contact pressures are presented in Figure 6.11 and 6.12 for the smooth and treaded combine tyre, respectively. An increase in inflation pressure was found to result in a rise in the mean contact pressure for both smooth and treaded tyres. The load did not appear to have an effect on the mean contact pressure for both smooth and treaded combine tyres. The ANOVA, however, showed that the combination of tyre load and inflation pressure has a significant effect on the mean contact calculated according to the tread and projected areas (Appendix H.10 and H.11).

The mean contact pressure calculated according to the contact area was found to be always greater than the inflation pressure for both tyres. This confirms that the combine tyres have a different architecture than the previously tested tyres, so the contact area determined are not considerably greater than the areas that truly transfer the load. However, as the mean contact pressures determined according to the ink contact areas were found to be lower than the values provided by Tekscan. This, therefore, means that the contact areas provided by the ink method also include the areas where the tyres have contact with the surface but do not support any load, which leads to an underestimation of the mean contact pressure.

According to the ink method, the difference between the mean contact pressure and tyre inflation pressure for the smooth combine tyre (Figure 6.11) was found to vary from 0.5 bar to 0.1 bar with a mean value of 0.28 bar. This relationship follows the model of Karafiath and Nowatzki (1978) who suggested that tyre carcass stiffness is influenced by its inflation pressure. It was found to reduce with inflation pressure and to be independent of load. However, the Tekscan study, evaluated in Section 6.1, showed the effect of load on the mean and maximum contact pressure and resulting carcass stiffness.

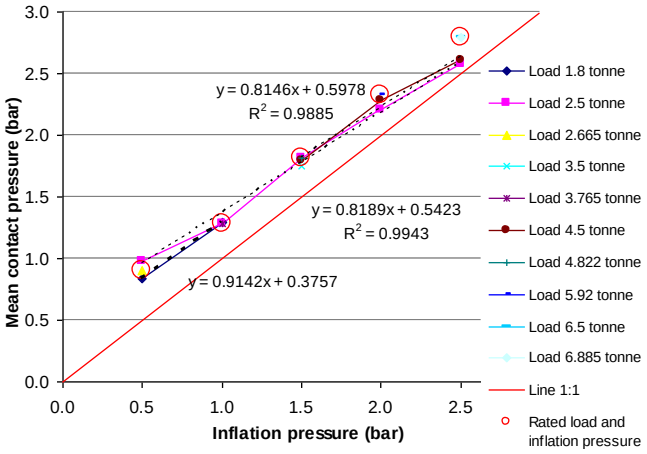

Figure 6.11 Contact pressure vs. inflation pressure according to the ink data – Smooth combine tyre

The mean difference between the mean contact pressure and inflation pressure for the treaded combine tyre is 0.41 bar, however, it was found to vary depending on tyre inflation pressure. The difference between the mean contact pressure, according to the tread contact area, and tyre inflation pressure was found to be greater with the mean value of 4.38 bar and vary from 2.75 bar to 5.5 bar depending on tyre inflation pressure. The relationships presented in Figure 6.12, follow the model of Karafiath and Nowatzki (1978), as contact pressure tends to change with inflation pressure and the relationships were found to be independent of load.

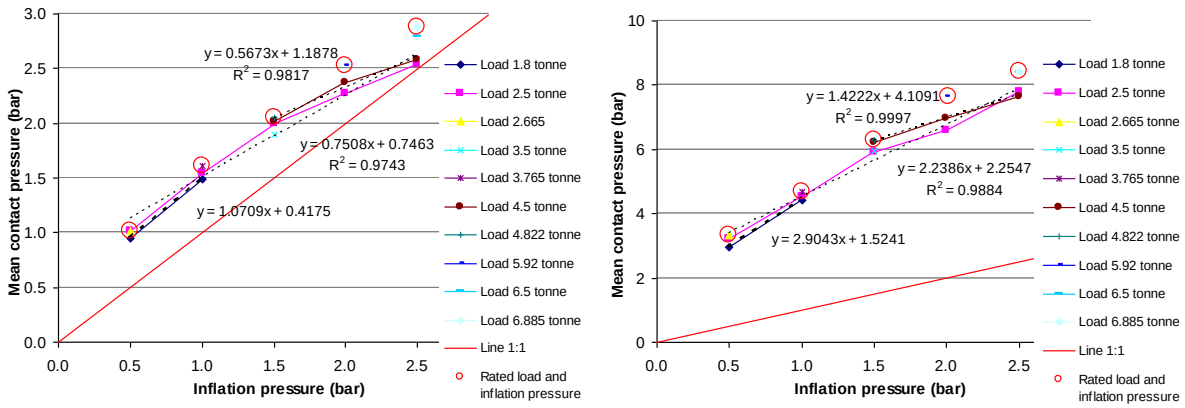

Figure 6.12 Contact pressure vs. inflation pressure according to the ink data – Treaded combine tyre (left: mean contact pressure calculated according to the projected area, right: mean contact pressure calculated according to the tread area)

6.3 Tyre load - deflection method

Figure 6.13 and 6.14 show data collected for both the smooth and treaded rear combine tyres. An increase in tyre load results in an increase in tyre deflection for both tyres. While, as inflation pressure decreases the slope of the load - deflection curve also decreases. The slopes of the load – deflection relationships for the same inflation pressures are approximately the same for the smooth and treaded tyres. Only the intercepts of the relationships are different as the smooth combine tyre was found to deflect more than the treaded tyre. Therefore, it was shown that tyre tread has an effect on tyre vertical deflection, however, it does not have an effect on the slope of the load – deflection characteristic. The difference in the deflection was, however, found to be relatively small. This is understandable as it is the tyre walls that effectively deflect. Following Plackett's procedure, the slopes of these relationships were plotted against inflation pressure, as shown in Figure 6.15. The relationships were found to be linear and were extrapolated to find the carcass stiffness as the intercept on the inflation pressure axis. This method of carcass stiffness estimation gives a value of 0.83 bar for the both smooth and treaded combine tyres.

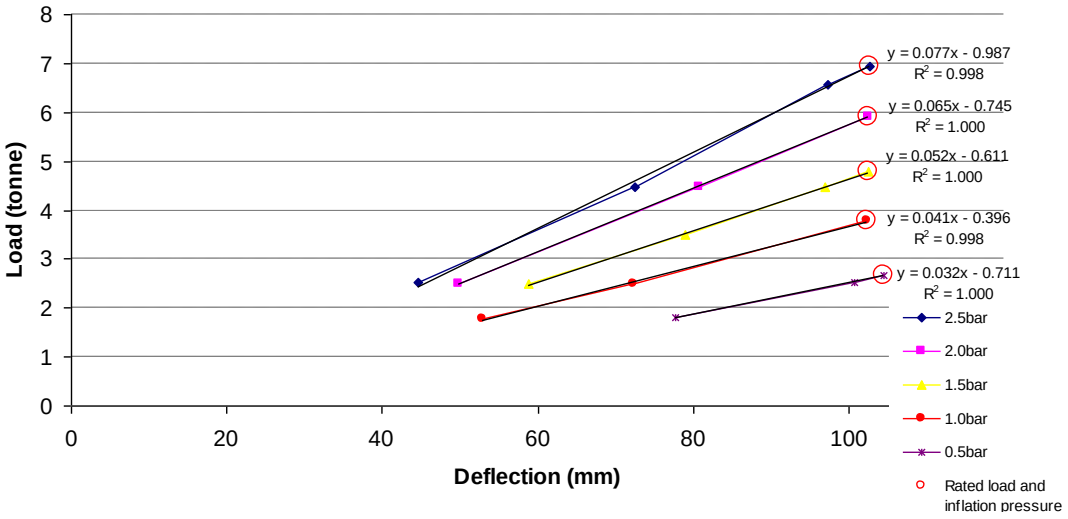

Figure 6.13 Load vs. deflection curve – Smooth combine tyre

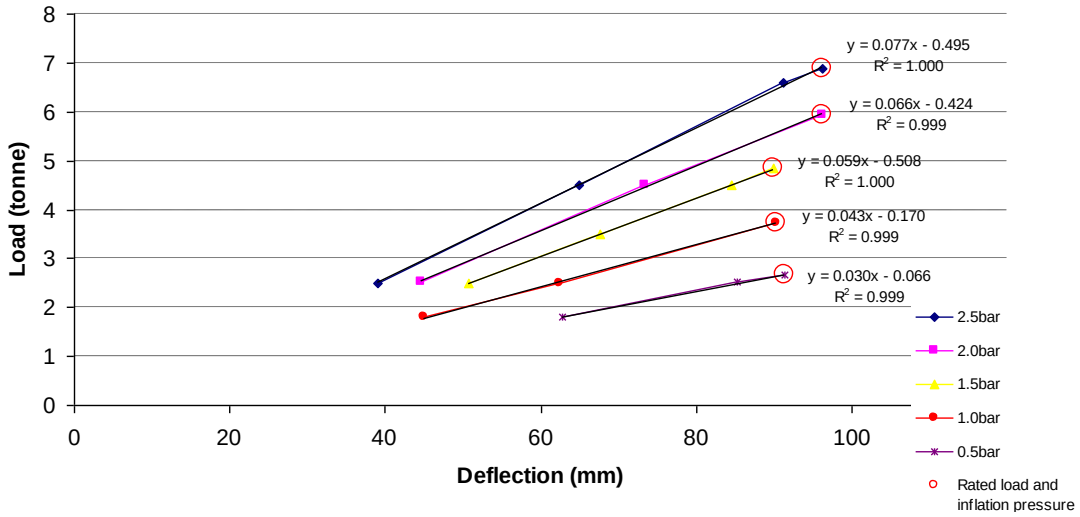

Figure 6.14 Load vs. deflection curve – Treaded combine tyre

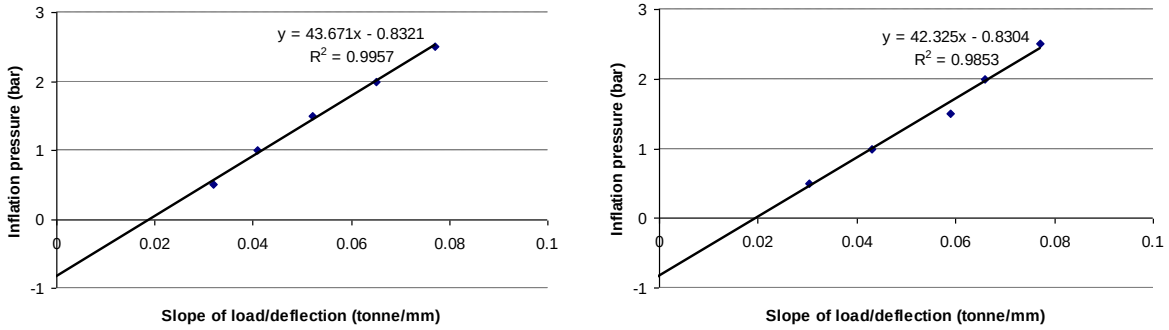

Figure 6.15 Inflation pressure vs. slope of load – deflection curve – Smooth combine tyre (left) and treaded combine tyre (right)

6.4 Tyre manufacture specification data method

Figure 6.16 and 6.17 present tyre manufacture load vs. inflation pressure data extrapolated using a linear and 2nd order polynomial regression, respectively, for the rear combine tyre. According to the inflation pressure at zero load the carcass stiffness results for the free rolling rear combine tyre (FR) at the speed of 10 km/h were found to be 0.79 bar or 0.65 bar according to linear and 2nd order polynomial regression functions, respectively. Using the data for a driven tyre (D) at 50 km/h speed the carcass stiffness decrease only to 0.68 bar and 0.59 bar. This shows that tyre speed and driving/rolling have a small effect on the tyre inflation pressure at no load for this combine tyre. Only for the cyclic driven tyre, the pressure at zero load is considerably greater as it is 0.98 bar and 0.81 bar, respectively.

Studying the tyre load which can be carried by a non-inflated tyre, according to linear or 2nd order polynomial regression functions the carcass stiffness was also estimated. The tread and projected contact areas, required in order to convert the load that the tyres are able to carry with no pressure, where determined using the Tekscan and ink method, respectively. According to this method, based on a linear or 2nd order polynomial function, respectively, the carcass stiffness of the free rolling rear combine tyre at 10 km/h was found to be:

- for the smooth combine tyre: 0.63 bar or 0.57 bar (mean contact area 0.026 m^2)
- for treaded combine tyre: 2.04 bar or 1.83 bar (mean tread contact area 0.08 m^2)
- for treaded combine tyre: 0.71 bar and 0.65 bar (mean projected contact area 0.23 m^2)

Increasing the tyre driven speed to 50 km/h results in the carcass stiffness decrease from the values above to the following:

- for the smooth combine tyre: 0.28 bar or 0.26 bar (mean contact area 0.026 m^2)
- for treaded combine tyre: 0.92 bar or 0.86 bar (mean tread contact area 0.08 m^2)
- for treaded combine tyre: 0.32 bar and 0.30 bar (mean projected contact area 0.23 m^2)

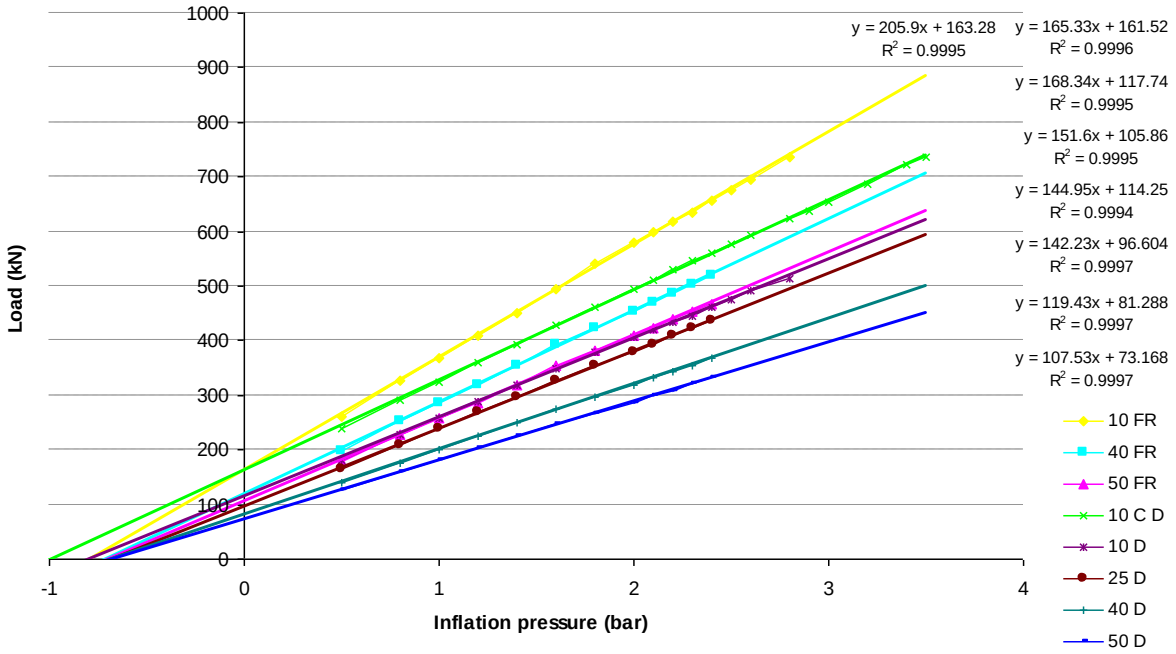

Figure 6.16 Inflation pressure vs. load with linear regression functions – Rear combine tyre (tyre manufacture specification data for free rolling (FR), cyclic driven (CD) and driven (D) tyre as a range of speeds in km/h)

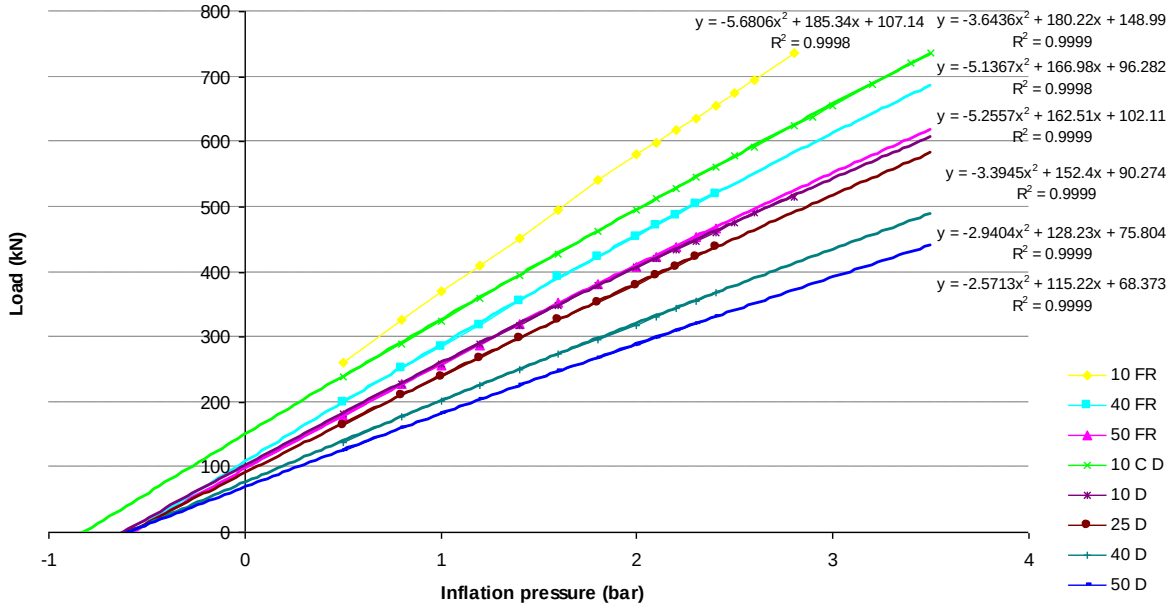

Figure 6.17 Inflation pressure vs. load with 2nd order polynomial functions – Rear combine tyre (tyre manufacture specification data for free rolling (FR), cyclic driven (CD) and driven (D) tyre as a range of speeds in km/h)

6.5 Comparison of the results

Tyre contact pressure distribution of the smooth combine tyre was found to be non-uniform. The data showed that in order to have the contact pressure normally distributed (almost uniformly) it is crucial to inflate the tyre correctly for a given load. Loading tyres above and below the maximum values recommended by tyre manufacturers should be avoided. When the tyres were loaded at lower inflation pressures than these ones recommended by the tyre manufacturer, significant pressure concentrations were found at the sidewall edges of tyre contact patch. For those cases pressure distribution was positively skewed, as a lot of low pressure results were found in comparison to very few high values. Further increase in inflation pressure above its recommended value without any change in load, resulted in a negatively skewed pressure distribution with a greater proportion of high values and few low values.

The over-loading tyres is not recommended due to a danger of tyre damage resulted from buckling of the carcass and ultimately failure or reduced working life. Tyre under-loading

causes a reduction of contact area and non-uniformity of the contact pressure distribution. It may result in soil compaction and worse tyre performance. A decrease in tyre load should, therefore, be associated with a reduction of tyre inflation pressure for a tyre contact area and deflection to be maintained.

Tyre contact area data obtained in both ink and Tekscan experiments for the smooth and treaded combine tyres were found to agree between the two methods. Both tyres were tested up to their maximum recommended load for a range of pressures. The results showed that the maximum contact area remains approximately constant, which also agrees with the deflection results which show that the tyres loaded to a range of rated loads and inflation pressures obtain the same maximum deflection . The smooth tyre was found to have greater contact areas than the treaded tyre, this was due to the fact that the treaded tyre transferred its load to the surface only through its treads. This confirms that tyre treads influence tyre carcass stiffness making it possible for a smaller contact area to support the same load. This resulted in higher contact pressures under the treaded tyre than the smooth tyre. According to the data obtained in the Tekscan study, tyre carcass stiffness of the treaded tyre was found to be greater than for the smooth tyre. The statistical analysis showed that tyre tread has a significant effect at 95% confidence level on the tyre contact area, mean and maximum contact pressure for the combine tyres studied.

Regression analysis conducted using the mean and maximum contact pressure data obtained, confirmed that tyre load and inflation pressure both have a significant effect on the contact pressure of the smooth tyre. For the treaded tyre, only inflation pressure has a statistically significant influence on the resulting contact pressures. This is illustrated by Equations 6.1 – 6.4. The ‘t’ tests for both tyres, showed that the slope of the inflation pressure is significantly different from 1. This means that the contact pressure do not increase at the same rate as tyre inflation pressure, therefore, the difference between the contact pressure and inflation pressure, considered as tyre carcass stiffness, is not a constant, as suggested by Bekker (1956), Chancellor (1976) and Plackett (1983, 1986 and 1987), but it changes depending on tyre inflation pressure and load. Karafiath and Nowatzki (1978) proposed a relationship between the contact pressure and inflation pressure, which shows that the difference between these two is not constant but is influenced by the inflation pressure as given in Equation 2.10.

Also the effect of tyre load was found for the smooth combine tyre, however, it was not previously considered by Karafiath and Nowatzki (1978).

Table 6.1 presents the results obtained for different methods of carcass stiffness estimation. According to the Tekscan results, the mean carcass stiffness of the smooth tyre varies between 0.3 bar – 0.7 bar and the maximum varies between 3 bar – 5 bar. Both, the mean and maximum values were found to be dependent on combination of tyre inflation pressure and load. The overall mean values of mean and maximum carcass stiffness of the smooth combine tyre were found to be 0.44 bar and 3.81 bar, respectively. While for the rated loads and inflation pressures they are 0.54 bar and 4.46 bar.

As discussed above, the carcass stiffness of the treaded combine tyre determined, using the Tekscan contact pressure data, was found to be considerably greater than the carcass stiffness of the same size smooth tyre. The mean values were found to vary between 2.0 bar – 3.2 bar, while the maximum carcass stiffness varies between 5.9 bar – 8.4 bar. An increase in tyre inflation pressure results in a rise in the mean and maximum carcass stiffness. The load was not found to have a statistically significant effect at 95% confidence level. The overall mean values of mean and maximum carcass stiffness of the treaded combine tyre tested are equal to 2.51 bar and 7.16 bar, respectively. Whilst for the rated loads and inflation pressures they are 2.53 bar and 7.25 bar, respectively.

According to the ink method, the difference between the mean contact pressure and tyre inflation pressure for the smooth combine tyre varies from 0.5 bar to 0.1 bar with a mean value of 0.28 bar. The mean difference between the mean contact pressure and inflation pressure for the treaded combine tyre is 0.41 bar. The difference between the mean contact pressure, according to the tread contact area, and tyre inflation pressure was found to be greater with the mean value of 4.38 bar and vary from 2.75 bar to 5.5 bar depending on tyre inflation pressure. The carcass stiffness values provided by the ink method are considerably lower than the results obtained using Tekscan system.

Table 6.1 Comparison of carcass stiffness of the smooth and treaded rear combine tyres (600/55-R26.5) using a range of estimation methods (tyre carcass stiffness determined for the following tyre loads: 1.8 tonne/2.0 tonne (smooth/treaded), 2.5 tonne, 4.5 tonne)

Tyre	P_{CS}	Pressure difference method A (Tekscan)			Pressure difference method B (ink)			Load – defl. method P_{CS} (bar)	Tyre manufacture specification data method (low tyre rolling speed)	
		Mean P_{CS} (bar)	Overall mean P_{CS} (bar)	P_{CS} at rated load and pressure (bar)	Mean P_{CS} (bar)	Overall mean P_{CS} (bar)	P_{CS} at rated load and pressure (bar)		An inflation pressure at zero load (linear/2nd polynomial) (bar)	A load at zero inflation pressure (linear/2nd polynomial) (bar)
Smooth combine tyre	Mean P_{CS}	0.39 0.36 0.40	0.44	0.54	0.31 0.27 0.23	0.28	0.32	0.83	0.79 / 0.65	0.63 / 0.57
	Max P_{CS}	3.40 3.66 3.87	3.81	4.46	-	-	-			
Treaded combine tyre	Mean P_{CS}	2.13 2.23 3.05	2.51	2.53	0.47 0.37 0.32	0.41	0.52	0.83		0.71 / 0.65 (according to the projected area); 2.04 / 1.83 (according to the treaded area)
	Max P_{CS}	5.98 6.57 8.15	7.16	7.25	2.90 4.11 4.95	4.38	4.57			

Tyre load – deflection method gave carcass stiffness value of 0.83 bar for both smooth and treaded combine tyres. This is higher than the mean carcass stiffness of the smooth tyre and considerably lower than the mean carcass stiffness of the treaded combine tyre measured with the Tekscan method.

The method based on tyre manufacture specification data provided tyre carcass stiffness values which could be an indication of the mean carcass stiffness. Conversion of the load at zero inflation pressure (obtained using a linear fit on the tyre manufacture data, method b) using the contact area (at the tyre manufactures' recommended load and inflation pressure) for the smooth tyre and treaded tyre (tread area) lead to pressures of 0.63 bar and 2.04 bar, respectively. This agrees with the mean carcass stiffness values obtained in Tekscan study within 40% and 19% for smooth and treaded tyre, respectively. The rated values agree better as they differ by 17% and 19%, respectively. The technique looking at the inflation pressure at zero load (method a) using a polynomial regression line gave an estimate of the mean carcass stiffness of the smooth combine tyre within 32%, while the carcass stiffness of the

tyre at the rated load and pressure was approximated within 20%. Method (a) did not successfully give an indication of the mean carcass stiffness of the treaded tyre. The comparison of the results obtained different methods of carcass stiffness estimation showed that the method based on tyre manufacture data looking at a load at zero inflation pressure (with a linear fit) could be used for an estimation of carcass stiffness of the combine tyres studied.

The three methods of tyre carcass stiffness estimation evaluated were not successful in predicting the maximum tyre carcass stiffness of the combine tyres. Therefore, in order to determine the maximum carcass stiffness of these tyres, it is necessary to determine the contact pressure distribution resulting from loaded tyres, which can be obtained using Tekscan system. Alternatively, it can be estimated as 8 or 3 times greater than the mean carcass stiffness for the smooth or treaded tyre, respectively.

6.6 Conclusions

1. Tyre tread was found to have a significant effect at 95% confidence level on the tyre contact area, mean and maximum contact pressure for the 600/55-R26.5 Trelleborg rear combine tyres. The contact pressures generated under the treaded combine tyre on the hard surface were significantly greater than the ones under the smooth tyre.
2. Tekscan contact pressure distribution study proved that tyre contact pressure is not uniformly distributed even for a smooth relatively flexible tyre. The distribution was found to be normally distributed only if the tyre was loaded according to the tyre manufacture specification. Over-inflation for a carried load resulted in a negatively skewed distribution, while under-inflation gave a positively skewed distribution.
3. The carcass stiffness results obtained in Tekscan experiments indicate that the mean and maximum carcass stiffness of the smooth tyre are influenced by tyre load and inflation pressure. The overall mean value for the smooth tyre varies between 0.3 bar – 0.7 bar (mean value of 0.44 bar) and the maximum carcass stiffness varies between 3 bar – 5 bar (mean of 3.81 bar). The mean values for the treaded tyre were found to be greater and they vary between 2.0 bar – 3.2 bar

(mean of 2.51 bar), while the maximum carcass stiffness was found to be between 5.9 bar – 8.4 bar (mean of 7.16 bar). The mean and maximum carcass stiffness of the treaded tyre were found to be dependent on tyre inflation pressure, the effect of load was not significant. The maximum carcass stiffness of the smooth and treaded combine tyre was found to be approximately 8 and 3 times greater than the mean carcass stiffness, respectively.

4. The tyre carcass stiffness of both smooth and treaded combine tyres obtained using the ink method was significantly less than the values obtained by Tekscan study.
5. The results from tyre load – deflection method indicated that the maximum deflection of the smooth tyre was greater than deflection of the treaded tyre. This, however, had no significant effect on the carcass stiffness, which was based on the slope of the load – deflection relationships, as these were found to be approximately the same for both tyre. The load – deflection method provided carcass stiffness value of 0.83 bar for both the smooth and treaded combine tyres. However, this value did not compare to those obtained by Tekscan system.
6. According to the tyre manufacture data tyre carcass stiffness results, a load at zero inflation pressure (linear fit) for the smooth tyre and treaded tyre (tread area) lead to pressures of 0.63 bar and 2.04 bar, respectively. This agrees with the mean carcass stiffness values obtained in Tekscan study within 40% and 19% for smooth and treaded tyre, respectively. The rated values agree better as they differ by 17% and 19%, respectively.

7 EFFECT OF PLY RATING ON TYRE CARCASS STIFFNESS (IMPLEMENT TYRES)

This chapter evaluates five Goodyear implement tyres of the same size (11.50/80–15.3) but varying in ply rating (8, 10, 12, 14, 16), shown in Figure 3.3. The methods of carcass stiffness determination were assessed for these tyres. The five tyres were studied at a constant inflation pressure and corresponding maximum load, which allowed ply rating effect on the resulting contact pressure to be evaluated. Additionally, the highest ply rating implement tyre (16 PR) was tested over its whole range of inflation pressures and its maximum corresponding loads. Therefore, the implement tyres were only studied at their rated loads and inflation pressures. The tyre manufacture specification of the implement tyres is presented in Figure 7.17. The ink and deflection tests were carried out in static conditions, while the Tekscan contact pressure investigation was conducted dynamically with the tyres rolled at a constant speed of 0.085 m/s (0.03 km/h). Tyre mean and maximum carcass stiffness was determined according to the Tekscan study. The mean value was determined according to the mean contact pressure over the tyre contact area, while the maximum carcass stiffness was calculated using the maximum contact pressure found for each tyre contact patch.

7.1 The pressure difference method (A) to measure both mean and maximum contact pressure using Tekscan

Tyre contact pressure distribution plots, obtained for the implement tyres varying in ply rating subjected to a load of 1.7 tonne and at a constant inflation pressure of 2.7 bar, are presented in Figure 7.1. The figure shows that the tyres were not symmetrically loaded onto the contact patch and larger pressure concentrations were found on one side of the contact patch. This was due to the faults of the tyre loading frame used. As expected, the pressure distribution was not uniform. The ply rating was not found to influence the distribution. Appendix K presents graphical display of the pressure distribution data as histograms, which confirm non-uniform pressure distribution across the contact patch.

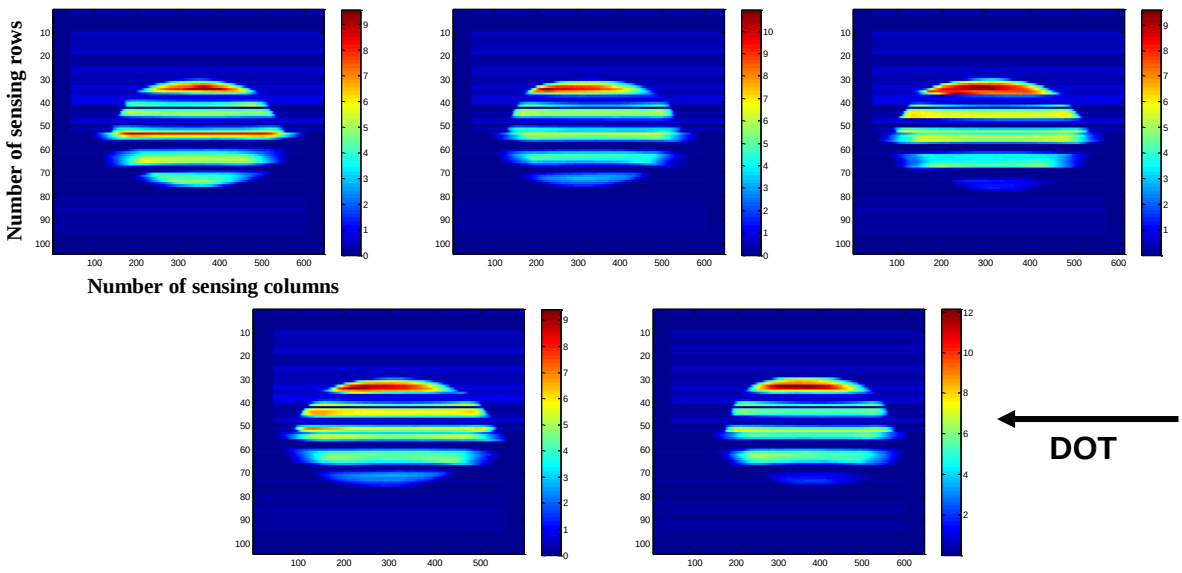

Figure 7.1 Tyre contact pressure distribution (bar) for the implement tyres varying in ply ratings (PR) at 1.7 tonne and 2.7 bar (from top left: PR 8, PR10, PR12, PR14, PR16) Please note change in both pressure colour range and length of x axis

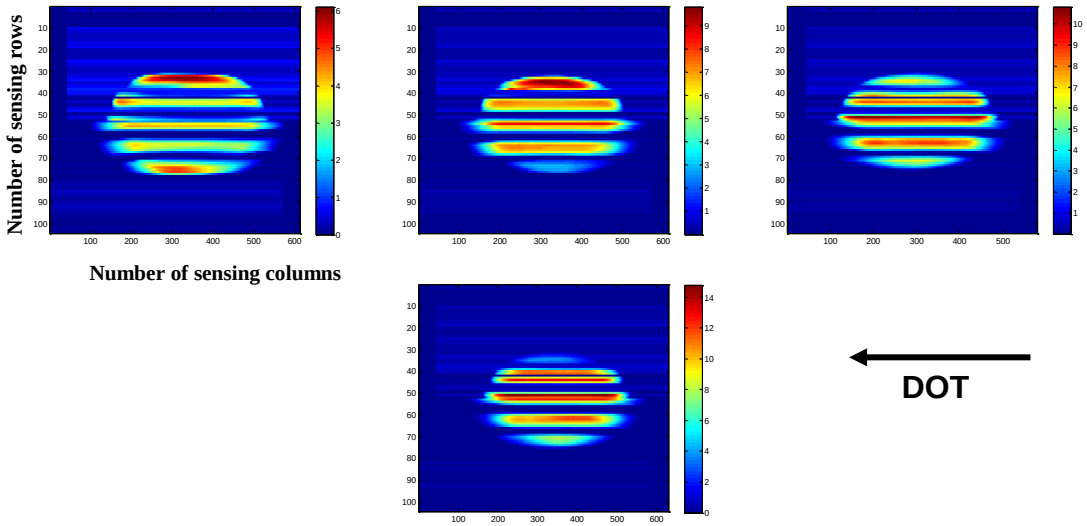

Figure 7.2 Tyre contact pressure distribution (bar) for the 16-ply implement tyre at varying loads and inflation pressures (from top left: 1.2 tonne + 1.5 bar, 1.95 tonne + 3.4 bar, 2.18 tonne + 4.1 bar, 2.575 tonne + 5.4 bar); Please note change in both pressure colour range and length of x axis

Figure 7.2 presents tyre contact pressure distribution of the 16-ply implement tyre at a range of loads and inflation pressures. The tyre was loaded approximately centrally during these

tests. In general, the pressure distribution was non-uniform (Appendix K). The distribution for the two lower loads and inflation pressures shows that the vertical stresses were found to concentrate at the sidewall edges of the contact patch. As the load and inflation pressure increased, pressure concentration moved to the central area of the contact patch. It can also be observed, that an increase in tyre load and inflation pressure resulted in a rise in vertical stresses without any considerable area change, which will be further studied in this chapter.

When the implement tyres with the same size but varying in ply rating were tested at a constant inflation pressure of 2.7 bar and a corresponding maximum load of 1.7 tonne, it was observed that the different ply rating tyres generated similar size contact patch (see Figure 7.3); on average this was found to be 0.036 m^2. The analysis of variance showed that tyre ply rating does not have a significant effect on the size of contact patch at 95% confidence level as presented in Appendix I.1.

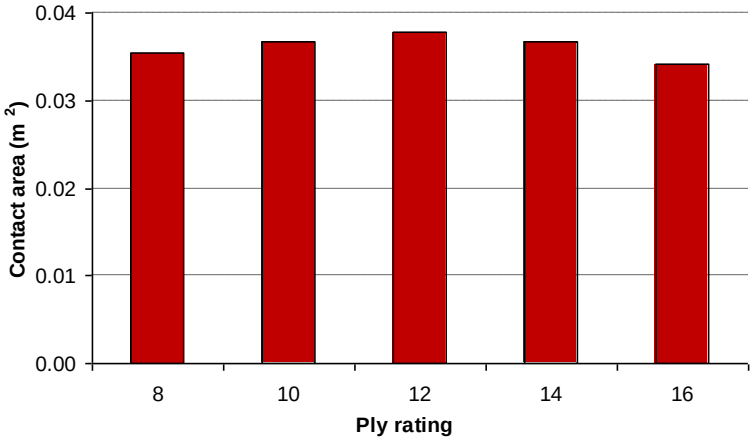

Figure 7.3 Tyre contact area vs. tyre ply rating for implement tyres based on the Tekscan study (LSD at 95% confidence level = 0.0041 m^2)

When the 16-ply implement tyre was tested at a range of inflation pressures and corresponding maximum recommended loads, an increase in inflation pressure and tyre load resulted in a decrease in the contact area, as shown in Figure 7.4. The decrease from 0.036 m^2 to 0.032 m^2, however, was found to be statistically insignificant at 95% confidence level (Appendix I.6). This was expected as when a tyre manufacture publishes the corresponding loads and inflation pressures, tyre contact area and deflection are kept relatively constant for the best tyre performance.

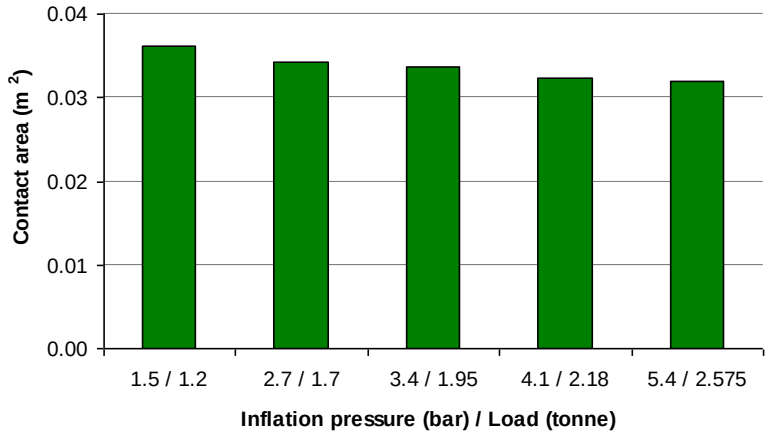

Figure 7.4 Tyre contact area vs. inflation pressure and load for 16-ply implement tyre according to the Tekscan tests (LSD at 95% confidence level = 0.0031 m^2)

Figure 7.5 shows the relationship between ply rating and the mean and maximum contact pressures for the implement tyres. A slight but non-significant increase in the mean contact pressure was found with an increase in the tyre ply rating. The maximum contact pressure was shown to be independent of ply rating. Statistically, the effect of ply rating was found to be insignificant on both mean and maximum contact pressure at 95% confidence (Appendix I.2 and I.3). The maximum contact pressures were approximately twice the mean contact pressures.

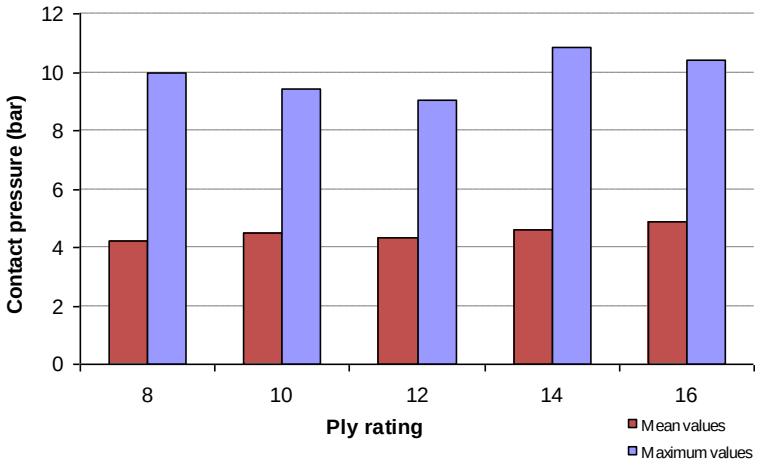

Figure 7.5 Mean/maximum contact pressure vs. ply rating for the implement tyres at a constant inflation pressure and load of 2.7 bar and 1.7 tonne from the Tekscan study (LSD at 95% confidence = 0.53bar for the mean values, LSD = 0.46bar for the maximum values)

When studying the 16-ply rating implement tyre, an increase in tyre inflation pressure and load gave a significant increase in the mean and maximum contact pressure at the range of inflation pressures and corresponding maximum loads, as presented in Figure 7.6. This was evaluated in the analysis of variance with 95% confidence presented in Appendix I.7 and I.8. The mean pressure was greater than tyre inflation pressure and the difference increased with an increase in inflation pressure. The maximum pressures were found to be approximately twice the mean contact pressures.

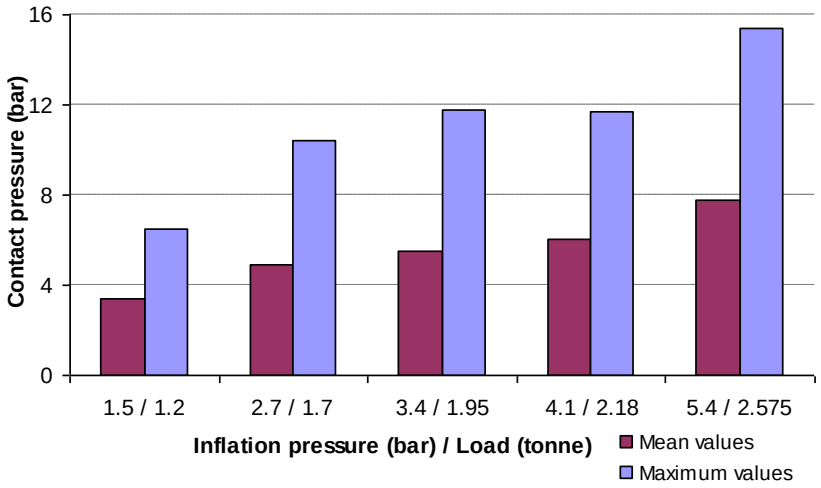

Figure 7.6 Mean and maximum contact pressure vs. tyre inflation pressure and load for the 16-ply implement tyre from Tekscan data (LSD at 95% confidence level = 0.46 bar for the mean values, LSD at 95% confidence level = 3.09 bar for the maximum values)

Figure 7.7 illustrates the relationship between tyre ply rating and carcass stiffness for the implement tyres. The relationship obtained for the mean and maximum carcass stiffness were both found to be independent of tyre ply rating at 95% confidence (Appendix I.4 and I.5). The mean stiffness was found to be in a range between 1.5 bar – 2.2 bar. The maximum carcass stiffness varied between 6.3 bar – 8.1 bar. It was shown that increasing the tyre ply rating resulted in a slight increase in the tyre carcass stiffness, considered as the difference between the mean/maximum contact pressure and tyre inflation pressure, but this increase was not found to be statistically significant.

Different methods of tyre reinforcement can be used to achieve different ply rating version tyres. In general, four different parameters can be combined and these are as follows: carcass

ply material, number of plies, construction configuration and bead reinforcement (Goodyear, 2009). Combinations of the four parameters are used in order to increase tyre load carrying capacity. The contact pressure results obtained for the implement tyres show that combination of these four parameters has no effect on the carcass stiffness of these tyres. Therefore, an increased tyre load carrying capacity of these tyres is not related to change in their carcass stiffness, understood as the difference between the resulting contact pressure and tyre inflation pressure.

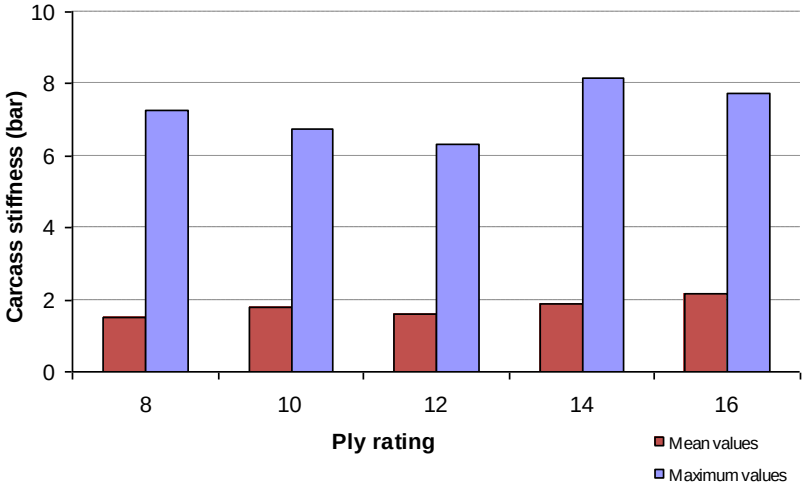

Figure 7.7 Tyre carcass stiffness vs. tyre ply rating for the implement tyres – according to mean and maximum contact pressure (Tekscan data)

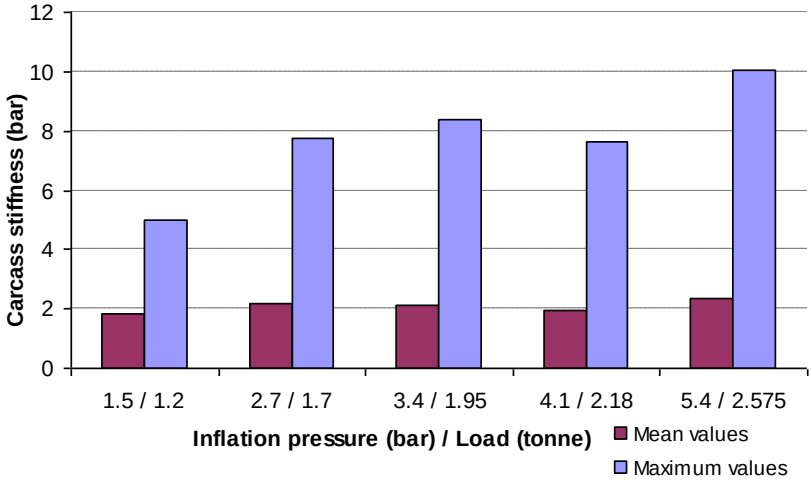

Figure 7.8 Tyre mean and maximum carcass stiffness vs. tyre inflation pressure and load for 16-ply implement tyre (Tekscan data)

The effect of tyre inflation pressure on carcass stiffness was also evaluated for the 16-ply implement tyre. Figure 7.8 shows results for the mean and maximum carcass stiffness. There is a trend for an increase in carcass stiffness with increasing inflation pressure and load, this is being greater for the maximum values. The mean carcass stiffness was found to vary between 1.9 bar and 2.3 bar, while the maximum carcass stiffness varied between 5 bar – 10 bar. The combination of tyre inflation pressure and load does not have a statistically significant effect on the mean and maximum carcass stiffness (Appendix I.9 and I.10).

7.2 The pressure difference method (B) using ink to estimate the size of the contact patch and hence mean contact pressure

Figure 7.9 presents tyre tread contact area vs. inflation pressure and load for the five implement tyres of different ply rating. Figure 7.10 shows the projected areas obtained for the same tyres at the range of inflation pressures and loads. Each tyre has a different maximum recommended inflation pressure and corresponding load. Therefore, for this part of the study, each of the tyres was tested at a range of inflation pressures and corresponding recommended loads (up to the maximum inflation pressure).

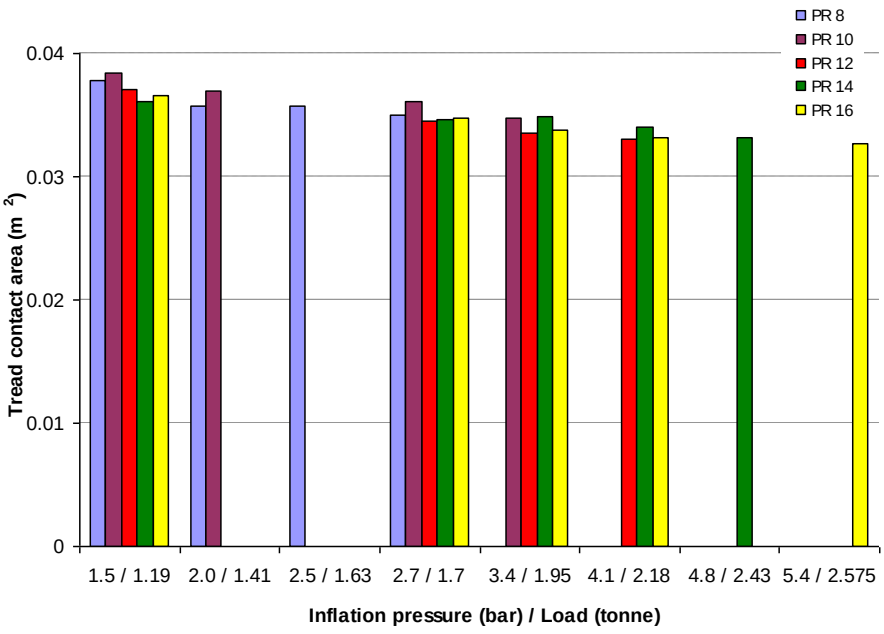

Figure 7.9 Tread contact area vs. inflation pressure and load from the ink tests – Implement tyres at the range of inflation pressures and maximum recommended loads

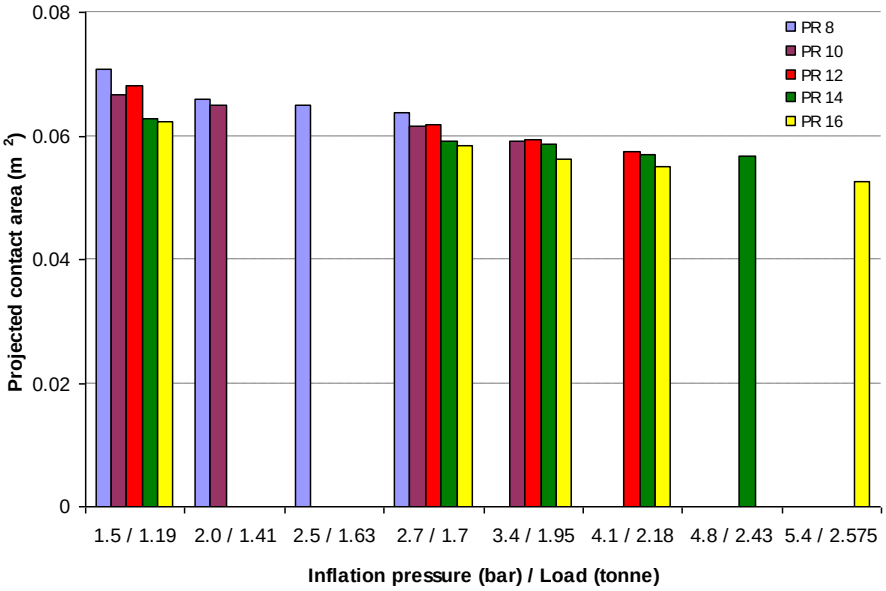

Figure 7.10 Projected contact area vs. inflation pressure and load from the ink tests – Implement tyres at the range of inflation pressures and maximum recommended loads

As shown in Figure 7.9 and 7.10, the projected contact area was found to be approximately twice the treaded contact area of the implement tyres. As expected, an increase in the inflation pressure with an accompanied increase of tyre load results in a decrease in the contact area. This was proven to be significant for both treaded and projected contact areas (Appendix I.11 and I.12). However, overall the contact area changes slightly with a change in tyre inflation pressure and load and the tread area varies from 0.038 to 0.033 m^2, while the projected area reduces from 0.071 to 0.053 m^2. Tyre ply rating does not appear to have an effect on tyre contact area, however, it was not evaluated statistically. For the tyre loaded to 1.7 tonne at 2.7 bar inflation pressure, the tread contact area remains approximately constant with changes of tyre ply rating with a mean value of 0.035 m^2, while the projected contact area shows a very small decrease (from 0.064 to 0.058 m^2) with increases in the ply rating from 8 to 16.

Contact area data obtained using the ink method (Figure 7.10) and the Tekscan method (Figure 7.3 and 7.4) showed a relatively good agreement between the two methods used as shown in Figure 7.11. However, at lower contact areas the results obtained in the ink method were found to be higher than the Tekscan areas up to 3%, while at the greater areas the ink contact areas were lower than the areas given by Tekscan up to 4%. The Tekscan tests

conducted for the implement tyres on the hard surface employed 6300 sensors, which have a better spatial resolution than the 9830 sensors previously used (Chapter 6). This is why the contact area data, obtained using the Tekscan and ink methods, was found to be in a good agreement.

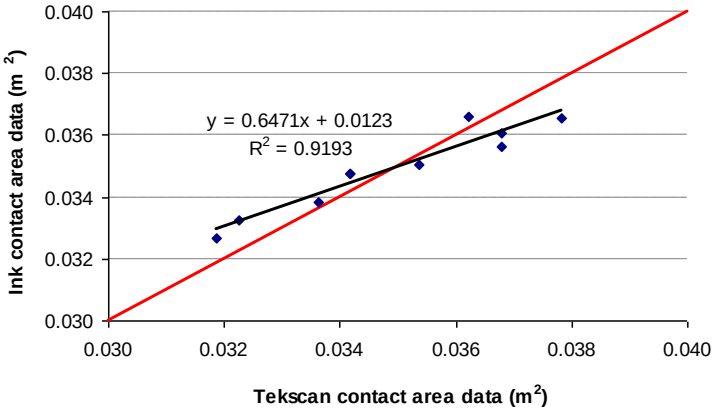

Figure 7.11 Comparison of Tekscan and ink methods for tyre contact area determination for the implement tyres (1:1 line in red)

Figures 7.12 and 7.13 present the relationship between tyre mean contact pressure (calculated by dividing tyre load by tread and projected contact area, respectively) and the combination of tyre inflation pressure and load for the range of implements tyres. Both, the tread and projected mean contact pressures were found to increase slightly with an increase in tyre ply rating for the same load and inflation pressure. They increased only marginally by approximately 0.2 bar over the ply rating range studied. As expected, the tread contact pressure was found to be significantly greater than the projected contact pressure. Increasing the inflation pressure and load results in an increase of the mean contact pressure for both the projected and tread pressure. This was evaluated statistically using analysis of variance at 95% confidence level and it was found to have a significant effect as presented in Appendix I.13 and I.14.

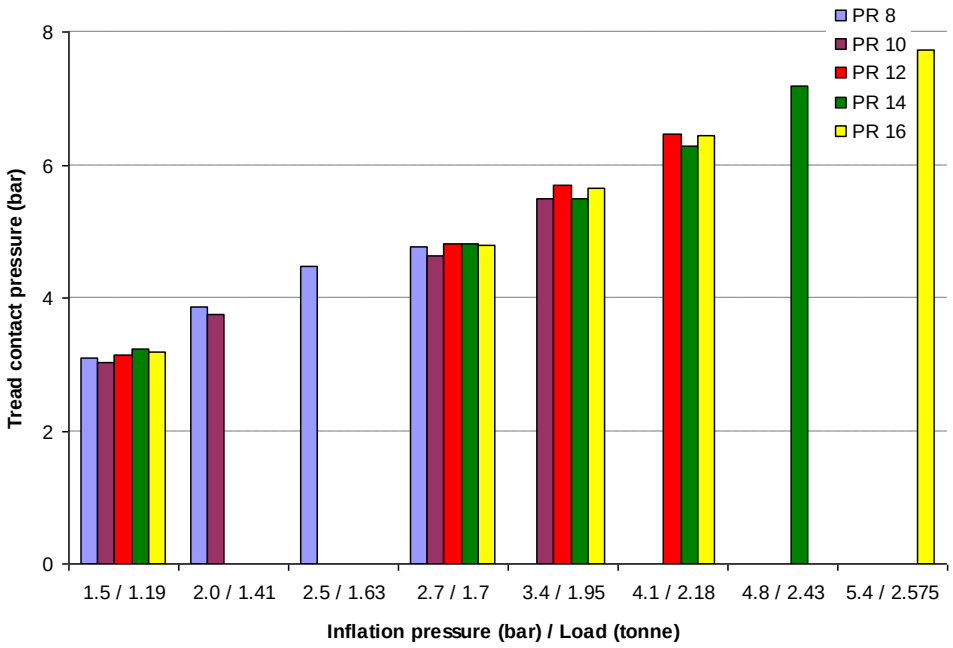

Figure 7.12 Mean tread contact pressure vs. inflation pressure and load from the ink tests – Implement tyres at the range of inflation pressures and maximum recommended loads

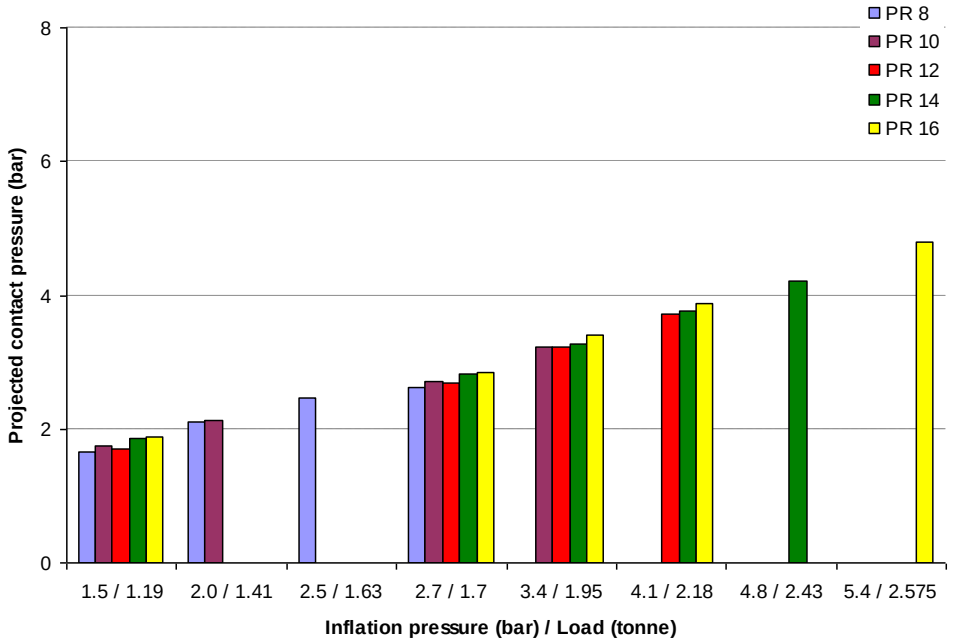

Figure 7.13 Mean projected contact pressure vs. inflation pressure and load from the ink tests – Implement tyre at the range of inflation pressures and maximum recommended loads

The mean projected contact pressure is marginally above the tyre inflation pressure only for the lower inflation pressures. It increases with an increase of the inflation pressure but at a

slower rate and it reaches a point from which it is marginally lower than the inflation pressure. This was found to be an anomaly as previously discussed in Chapter 5. The treaded contact pressure was found to be significantly higher than the inflation pressure for the whole inflation pressure range studied. The difference between the mean projected contact pressure and tyre inflation pressure was found to be up to 0.4 bar for lower inflation pressure and be negative for greater inflation pressures. Consideration of the carcass stiffness as the difference between the tread contact pressure and inflation pressure provided values between 1.5 – 2.4 bars depending on the combination of tyre load and inflation pressure, with the overall mean value of 2.06 bar.

7.3 Tyre load - deflection method

Figure 7.14 presents load - deflection relationships for the 16-ply implement tyre for a range of inflation pressures. Figure L.1 (Appendix L) presents the load – deflection data obtained for all five tyres differing in ply rating and shows that as tyre ply rating increases, the tyre deflection decreases.

Following Plackett's technique (1983), only the linear parts of the correlations were used for tyre carcass stiffness estimation. Similar relationships were obtained for the lower ply rating implement tyres and the slopes of the load – deflection relationships for different ply rating tyres were plotted and shown in Figure 7.15. It allowed the carcass stiffness to be estimated for the range of ply ratings as given in Figure 7.16. The carcass stiffness was found to vary between 0.02 bar for the 8 ply rating and 1.57 bar for the 14 ply rating, where the three highest ply ratings are similar and 8 is very small. The carcass stiffness results obtained using the load – deflection method do not change linearly with an increase in tyre ply rating.

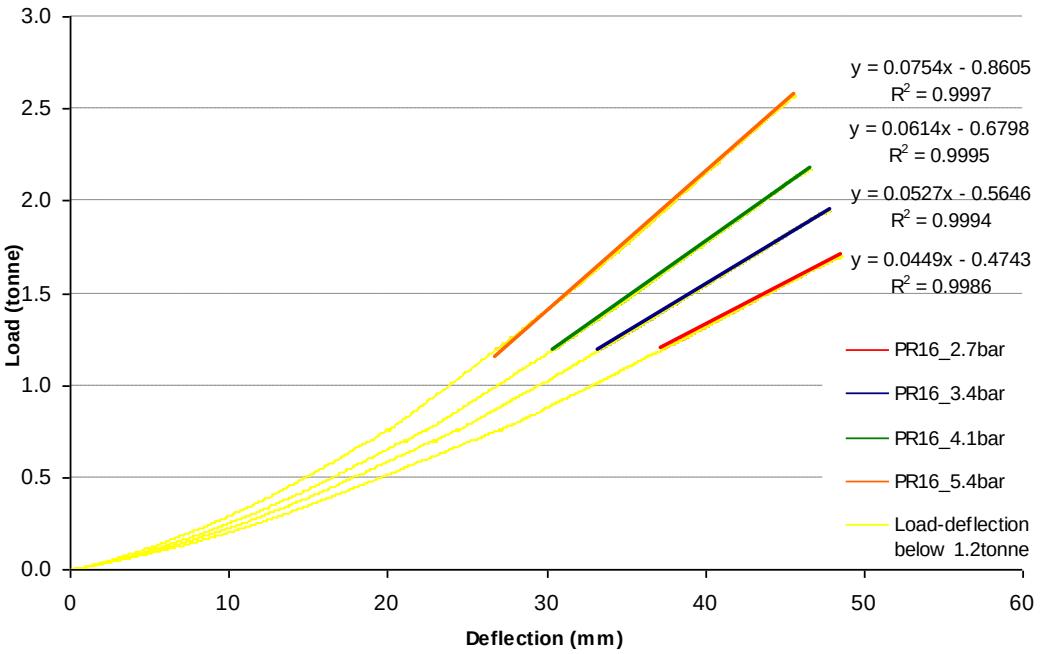

7.14 Load – deflection relationship for the 16-ply implement tyre

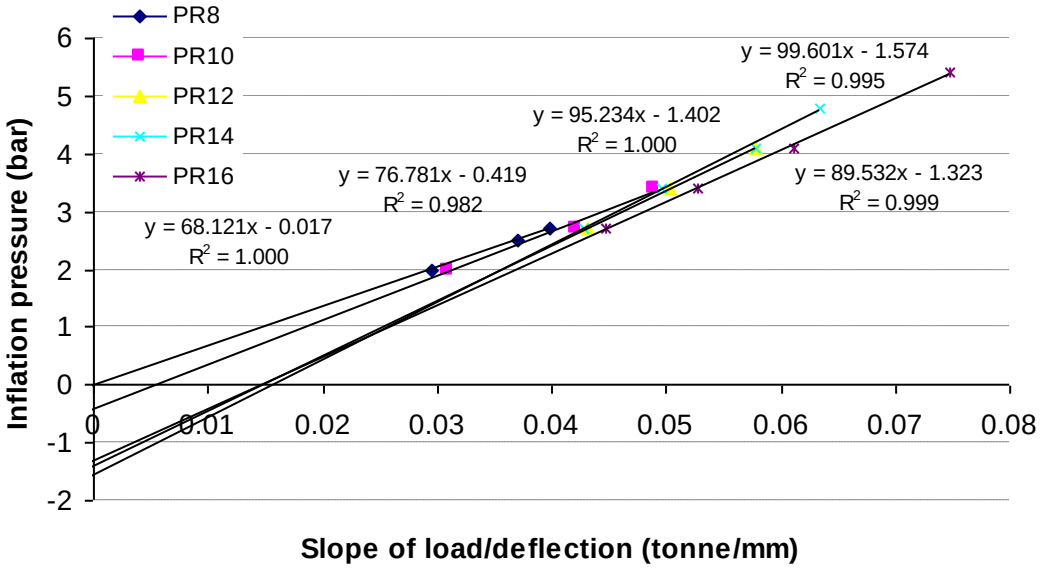

7.15 Inflation pressure vs. slope of load – deflection curve for 8, 10, 12, 14, 16-ply implement tyres

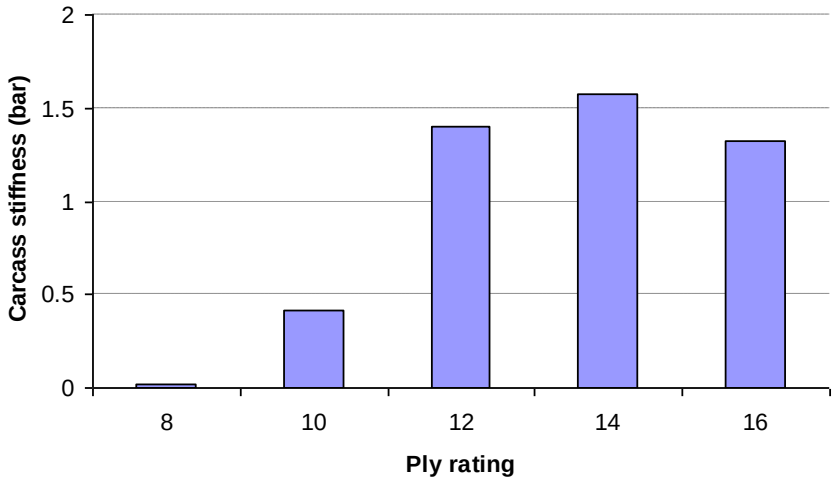

7.16 Tyre carcass stiffness vs. ply rating for implement tyres

7.4 Tyre manufacture specification data method

Figures 7.17 and 7.18 present load vs. inflation pressure relationship provided by the tyre manufacturer for the Goodyear 11.50/80-15.3 implement tyres of different ply rating. A linear and 2nd order polynomial regression lines were established using this data, respectively. According to the tyre manufacture data, for a given inflation pressure the tyres varying in ply rating are supposed to carry the same maximum load, however, the higher the ply rating is, the greater loads and inflation pressure the tyre is able to sustain. Only the 16PR driven wheel has a different load – inflation pressure characteristic, which is related to the fact that the other characteristics were established a rolled rather than driven tyre. From the tyre data, carcass stiffness was estimated as tyre inflation pressure at zero load and according to tyre maximum load at zero inflation pressure (Figure 7.19).

Figure 7.19 shows carcass stiffness values obtained from the linear and 2nd order polynomial regression line established using the load vs. inflation pressure data. Due to the curvature in the data, the 2nd order polynomial regression line gave lower values of carcass stiffness than the linear relationship. The polynomial function results varied from 0.33 bar for 8-ply to 0.96 bar for 16-ply and 1.01 bar for 14-ply tyre. The linear regression line gave carcass stiffness results from 1.27 bar to 2.11 bar for 8-ply and 16-ply, respectively. The overall mean values for the non-driven implement tyres are 1.73 bar and 0.74 bar according to the linear and polynomial regression lines, respectively. According to the linear and 2nd order polynomial

function, the inflation pressure values at zero load for the 16-ply driven wheel are 2.03 bar and 0.87 bar, respectively.

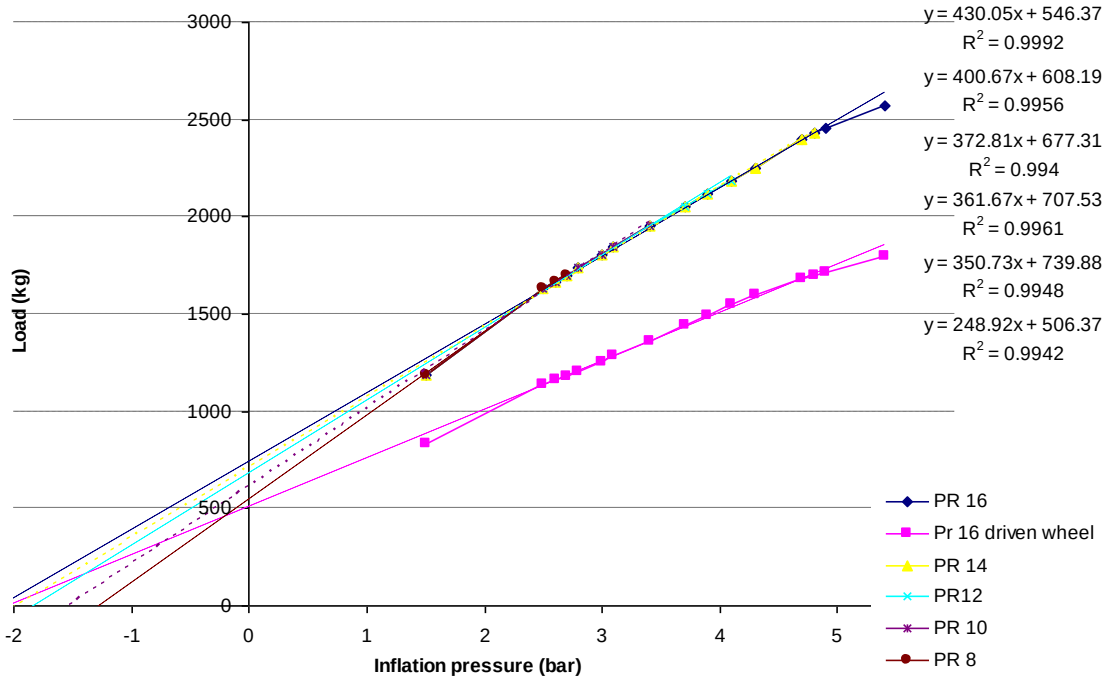

Figure 7.17 Inflation pressure vs. load with linear regression lines – Implement tyre (tyre manufacture specification)

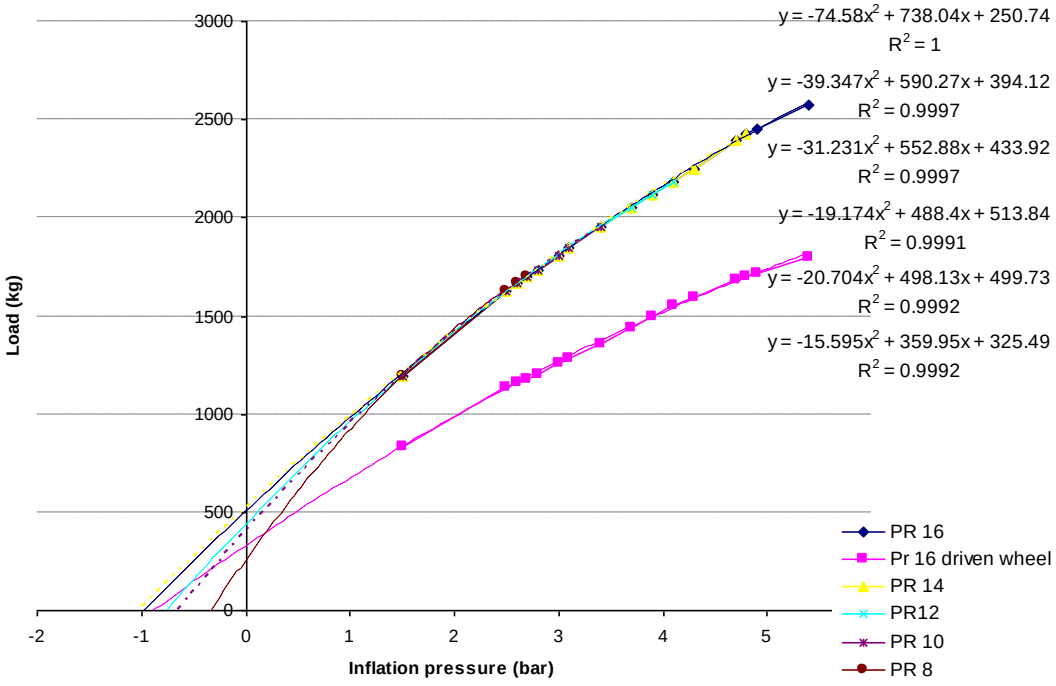

Figure 7.18 Inflation pressure vs. load with 2nd order polynomial regression lines – Implement tyre (tyre manufacture specification)

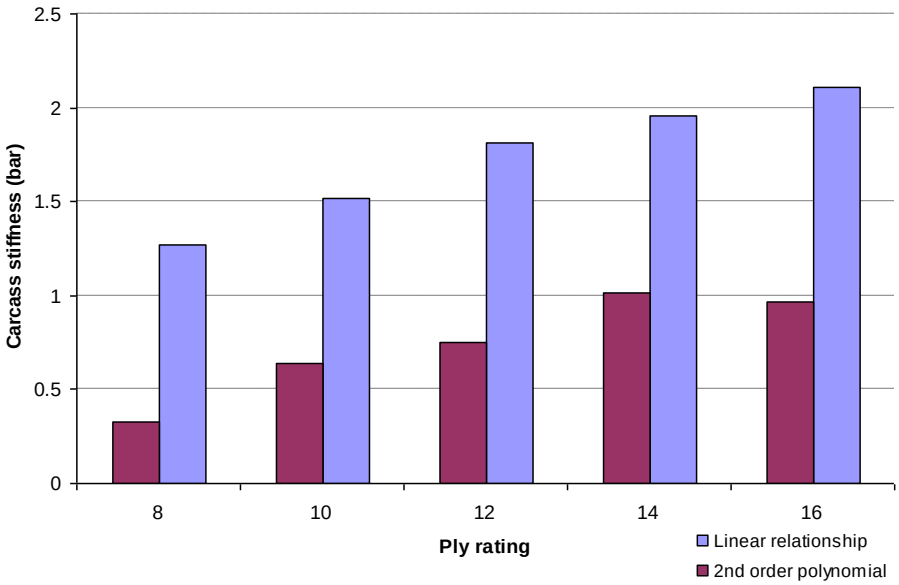

Figure 7.19 Tyre carcass stiffness vs. ply rating for the implement tyre (according to tyre inflation pressure at zero load)

The loads at zero inflation pressure (from Figure 7.17 and 7.18) were converted into pressure by dividing the maximum rated loads at zero inflation pressure by tyre mean tread contact area obtained in Tekscan experiments (0.036 m^2) and mean projected area from the ink tests (0.06 m^2). The carcass stiffness results obtained were plotted for the range of tyre ply ratings for the two regression relationships, as shown in Figure 7.20. The following results were obtained for the linear and 2nd order polynomial regression lines:

- according to treaded contact area: from 1.48 bar to 2.00 bar for the linear and from 0.76 bar to 1.39 bar for the polynomial function (overall mean of 1.78 bar and 1.13 bar, respectively)
- according to projected contact area: from 0.89 bar to 1.21 bar for the linear and from 0.41 bar to 0.84 bar for the polynomial function (overall mean of 1.07 bar and 0.68 bar, respectively)

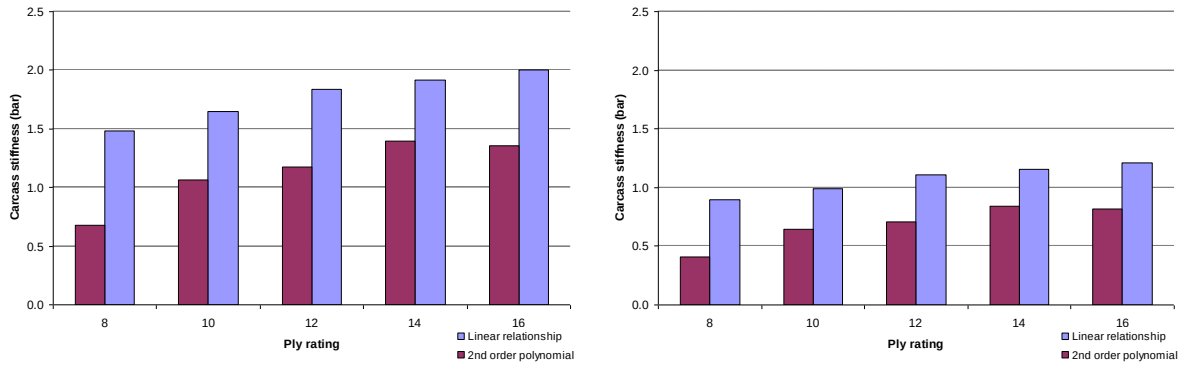

Figure 7.20 Tyre carcass stiffness vs. ply rating for the implement tyre (according to tyre load at zero inflation pressure for the tread contact area (left) and projected contact area (right))

7.5 Comparison of the results

Tyre contact pressure distribution of the implement tyres studied was found to be non-uniform and it was not normally distributed. All the tests were conducted at the rated loads and inflation pressures as recommended by the tyre manufacturer.

Tyre contact area data obtained in both ink and Tekscan experiments for the implement tyres were found to agree between the two methods within 4%. The contact area results showed that the contact area obtained for the five tyres, at the recommended load and inflation pressure, remains approximately constant. The higher the tyre ply rating, the less the tyre deflects under the same load. The maximum deflection of each tyre was found to be approximately constant for each tyre and was reached when the tyres were loaded with the maximum load for each inflation pressure.

Table 7.1 presents combined carcass stiffness data obtained for the implement tyres using different techniques. It was impossible to determine a relationship between the contact pressure and inflation pressure as the implement tyres were tested at a range of inflation pressure and their corresponding maximum recommended loads at these pressures. However, Tekscan studies provided mean tyre carcass stiffness values, for the tyres characterised by different ply rating, in a range between 1.5 bar – 2.1 bar, with the maximum carcass stiffness varying between 6.3 bar – 8.1 bar. The mean contact pressure results were found to increase slightly with ply rating but this was not significant as shown in the analysis of variance at 95% confidence level. Therefore, it was proved that increase of tyre ply rating was not

associated with a significant increase of tyre carcass stiffness. Further, Tekscan studies on 16-ply implement tyre at different inflation pressures and maximum load showed the effect of combination of tyre inflation pressure and load on the resulting mean and maximum contact pressure. An increase in contact pressure with inflation pressure and load was found for both the mean and maximum values. The mean carcass stiffness of the 16-ply implement tyre varies between 1.9 bar and 2.3 bar, while the maximum carcass stiffness was found to be between 5 bar and 10 bar over the range of inflation pressure from 1.5 bar to 5.4 bar.

Table 7.1 Evaluation of carcass stiffness estimation methods for the 11.50/80–15.3 implement tyres (bar)

P_{CS}	PR	Pressure difference method A (Tekscan)	Pressure difference method B (ink)	Load – deflection method	Tyre manufacture specification data method (low tyre rolling speed)	
		Mean P_{CS} (bar)	Mean P_{CS} (bar)	P_{CS} (bar)	An inflation pressure at zero load (linear/2nd polynomial) (bar)	A load at zero inflation pressure (linear/2nd polynomial) (bar)
Mean P_{CS}	16	2.10	-0.26	1.32	2.11 / 0.96	1.21 / 0.82
	14	1.90	-0.12	1.57	1.96 / 1.01	1.16 / 0.84
	12	1.61	-0.08	1.40	1.82 / 0.75	1.11 / 0.71
	10	1.78	0.05	0.42	1.52 / 0.64	0.99 / 0.64
	8	1.53	0.03	0.02	1.27 / 0.33	0.89 / 0.41
Max P_{CS}	16	7.75	2.22			(based on the projected area); 2.00 / 1.35
	14	8.15	2.10			1.92 / 1.39
	12	6.32	2.11			1.84 / 1.18
	10	6.74	1.82			1.65 / 1.07
	8	7.26	1.87			1.48 / 0.68 (based on the tread area)

According to the projected contact area from in the ink tests, the carcass stiffness was found to be significanlty lower than the mean carcass stiffness obtained using Tekscan. However, the tyre carcass stiffness, obtained according to the tread contact area, has a similar range as the mean carcass stiffness data obtained by Tekscan system for the implement tyres.

Tyre load – deflection method gave carcass stiffness between 0.02 bar for the 8 ply rating and 1.57 bar for the 14 ply rating, where the three highest ply ratings are almost the same and 8 is almost zero. These are significantly lower than the measured carcass stiffness data obtained in the Tekscan study.

The method based on tyre manufacture specification data provided tyre carcass stiffness values which could be an indication of the mean carcass stiffness. Conversion of the load at zero inflation pressure (method b), obtained by an extrapolation of the linear fit on the tyre manufacture data, gave the closest results to the mean values obtained in Tekscan study. The maximum difference between the results was 15%, however, most of the data agreed within 5%. An inflation pressure at zero load with a linear fit (method a) also gave a relatively good approximation of the carcass. Data obtained using this technique differed from the measured values up to 20% and most of the results differed by more than 10%. Therefore, if there was a case, when there was no possibility of measuring tyre contact area for the manufacturer recommended load and inflation pressure, then an inflation pressure at zero load could be used as an indication of tyre mean carcass stiffness.

The methods of carcass stiffness estimation evaluated for the implement tyres were not successful in predicting the maximum tyre carcass stiffness. Contact pressure distribution measurements would be the most accurate way of determining the maximum carcass stiffness. This, however, is time-consuming and requires pressure mapping system. Alternatively, the maximum carcass stiffness of the implement tyres can be approximately estimated as 4 times greater than the mean carcass stiffness of these tyres.

7.6 Conclusions

1. The contact pressure distribution study, using the Tekscan mapping system, showed that tyre contact pressures of the 11.50/80–15.3 Goodyear implement tyres are neither uniformly or normally distributed.
2. There was no significant effect of ply rating on the carcass stiffness of implement tyres obtained using the Tekscan studies. The mean carcass stiffness of the implement tyres was found to be in a range of 1.5 bar – 2.1 bar, while the maximum value varies between 6.3 bar – 8.1 bar.
3. The results of studies with a range of rated loads and inflation pressures using the 16-ply rating tyre, showed that inflation pressure and load had an effect on the mean and maximum carcass stiffness. The mean carcass stiffness of the 16-ply implement tyre varies between 1.9 bar and 2.3 bar, while the maximum carcass stiffness varies between 5 bar and 10 bar. The maximum carcass stiffness was

found to be approximately 4 times greater than the mean carcass stiffness.

4. The tyre carcass stiffness of the implement tyres calculated according to the projected contact areas obtained in the ink study was significantly less than the values obtained by Tekscan. However, tyre carcass stiffness obtained according to the tread contact area has a similar range as the data obtained by Tekscan system.
5. Tyre load – deflection method provided carcass stiffness values which were significantly lower than the results given by Tekscan study.
6. The method based on tyre manufacture specification could be used to give an indication of the mean carcass stiffness as it provided tyre carcass stiffness values which were found to be in the best agreement with the mean carcass stiffness data of the Tekscan study. The technique based on a load at zero inflation pressure with a linear fit gave the results that were most similar. The maximum difference between the two methods was 15%, however, most of the data agreed within 5%. Therefore, if there is no possibility of measuring tyre contact area at the recommended load and inflation pressure, it is advised to use the technique based on an inflation pressure at zero load (with a linear fit), as it provides data which differs from the measured value by less than 20%.

8 THE EFFECT OF LOAD, INFLATION PRESSURE, PRESENCE OF TREAD AND PLY RATING ON PRESSURE TRANSFER THROUGH SOIL

8.1 Introduction

This chapter contains the results obtained in all the tests that were conducted in order to determine pressures resulting from loaded agricultural vehicles in the soil. The experiments involved pressure measurements in the soil profile at different depths using Tekscan system. Details of the experimental set up and description of the method used are given in Chapter 3.

The area of tyre influence and resulting mean and maximum soil pressure over the area of influence and pressure distribution resulting from tyres were measured at the range of depths. The aim of the experiments was to determine the effect of tyre load, inflation pressure, presence of tyre tread, ply rating and soil depth on the resulting soil pressure. Sandy loam soil was used for the tests. Soil moisture content was remained between 9 – 10 % which is the optimum moisture content for sandy loam soils (Day, 2001), while the dry bulk density was maintained at approximately 1.5 t/m^3, which is a moderate soil density commonly found in agricultural fields.

As discussed in Chapter 3, two groups of tyre types were selected to be tested in soil. The tyre types were investigated to find the influence of the following aspects on the resulting pressure:

A. The presence or absence of tyre tread (as with Chapter 6)
B. The effect of differing tyre ply rating (as with Chapter 7)

The 600/55-R26.5 Trelleborg rear combine tyre was examined with lugs and without lugs which allowed an evaluation of the effect of tyre lug on the soil pressure. The soil pressure below the two rear combine tyres, smooth and treaded, was determined at five different soil depths as follows: 25 mm, 100 mm, 250 mm, 400 mm and 550 mm. The smooth rear combine tyre was tested at a range of the working inflation pressures and loads up to the maximum manufacture recommended values at shallow depths (25 mm and 100 mm). The loads and inflation pressures were the same as in the hard surface experiments (Chapter 6). At the greater depths (250 mm, 400 mm and 550 mm) the smooth tyre was tested at its maximum

permitted inflation pressure (2.5 bar) and a range of loads up to its maximum recommended load (2.5 tonne, 4.5 tonne and 6.5 tonne). The experimental work on the treaded combine tyre looked at the soil contact pressure through the soil profile when the treaded tyre was loaded to its maximum recommended load at the maximum permitted pressure of 6.5 tonne and 2.5 bar, respectively. The maximum load and inflation pressure were selected as the worse case scenario which would cause the most soil damage. In practice tyres are often used at their maximum loads and pressures. This allowed for the influence of load, inflation pressure, soil depth and presence of tyre tread on mean and maximum soil pressure and contact area to be evaluated.

Five Goodyear implement tyres of the same dimensions (11.50/80–15.3) and tread pattern but varying in ply rating, previously studied on the hard surface (Chapter 7), were used to evaluate the effect of tyre ply rating on the resulting soil pressure. All five tyres were tested at one inflation pressure and maximum corresponding load, which was the same for all five implement tyres. Additionally the stiffest tyre (PR 16) was examined at the range of inflation pressure and the maximum corresponding loads. For the implement tyres the soil pressure was determined at two depths (100 mm and 250 mm), this was due to time limitations.

8.2 The effect of tyre tread on soil pressure (smooth and treaded combine tyres)

This section discusses if tyre tread has an effect on the pressure resulting from loaded combine tyres (Trelleborg 600/55-R26.5). This was investigated by a comparison of the pressures in the soil profile generated by the smooth and treaded combine tyres. The study involved an examination of the area of tyre influence, pressure distribution across the area, mean and maximum pressure. It was done in two parts: one part looked at the effect of tyre tread, soil depth and load on the four parameters listed above, this was done considering the soil profile of 550 mm deep; the second part considered the effect of soil depth, inflation pressure and load, this part only involved shallow pressure measurements up to 250 mm on the smooth combine tyre.

8.2.1 Soil pressure distribution

Investigation on the pressure distribution involved a study of the distribution through the soil profile for the smooth tyre inflated to 2.5 bar and loaded with 4.5 tonne. Further, the pressure

distribution results obtained for the smooth and treaded combine tyres at 2.5 bar inflation pressure loaded to their maximum recommended load of 6.5 tonne were compared.

Figure 8.1 presents the pressure distribution data obtained when the smooth combine tyre at 2.5 bar inflation pressure was loaded on a hard surface with 4.5 tonne. The pressure was found to be approximately uniformly distributed in the central part of the contact area. Tyre sidewall edges do not carry considerable amount of load, they generate lower contact pressure than the central contact patch. The mean contact pressure is 2.88 bar with the maximum value of 6.09 bar, which is considerably greater than the tyre inflation pressure.

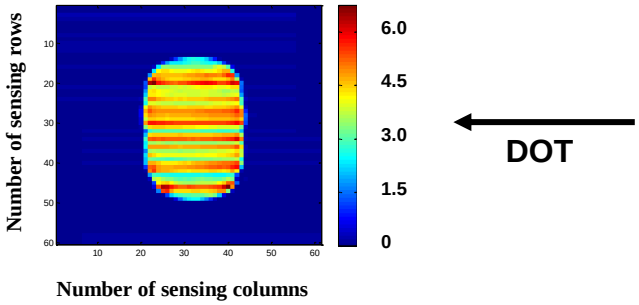

Figure 8.1 Contact pressure distribution (bar) for the smooth tyre inflated to 2.5 bar loaded with 4.5 tonne on a hard surface

The results obtained on the hard surface (Figure 8.1) can be compared to the data obtained in the soil as shown in Figure 8.2. The pressure distribution was found to be less uniform in the soil than it was found for the smooth combine tyre loaded on a hard surface. A pressure concentration was found in the centre of contact patch at each soil depth studied with an increase in contact area with soil depth. Tyre contact patch became longer with depth increase, while its width did not increase significantly. This was previously found by Ansorge (2007). An increase in tyre contact patch with soil depth results in a decrease in the mean and maximum pressures as the load transferred from the tyre through the soil is applied to greater areas. This will be further discussed in Section 8.2.2.

At 250 mm, the maximum pressure was found to be 2.81 bar, which is slightly greater than the inflation pressure of the tyre loaded. This suggests that most of the pressure resulting from tyre carcass stiffness dissipated in the top 250 mm layer of soil for the smooth combine tyre loaded with 4.5 tonne. At 550 mm depth, maximum pressures of 1.48 bar were recorded. This

confirms an ability of tyres to cause subsoil compaction of vulnerable soils, which could not be cultivated by the standard agricultural techniques, but would require an employment of tillage to depth in excess of 0.6 m. This agrees with Ansorge (2005 and 2007), who looked at the effect of axle loads carried on pneumatic combine wheels on soil bulk density increase. In his study, a significant soil displacement was found below heavy harvester tyres at 0.5 m soil depth.

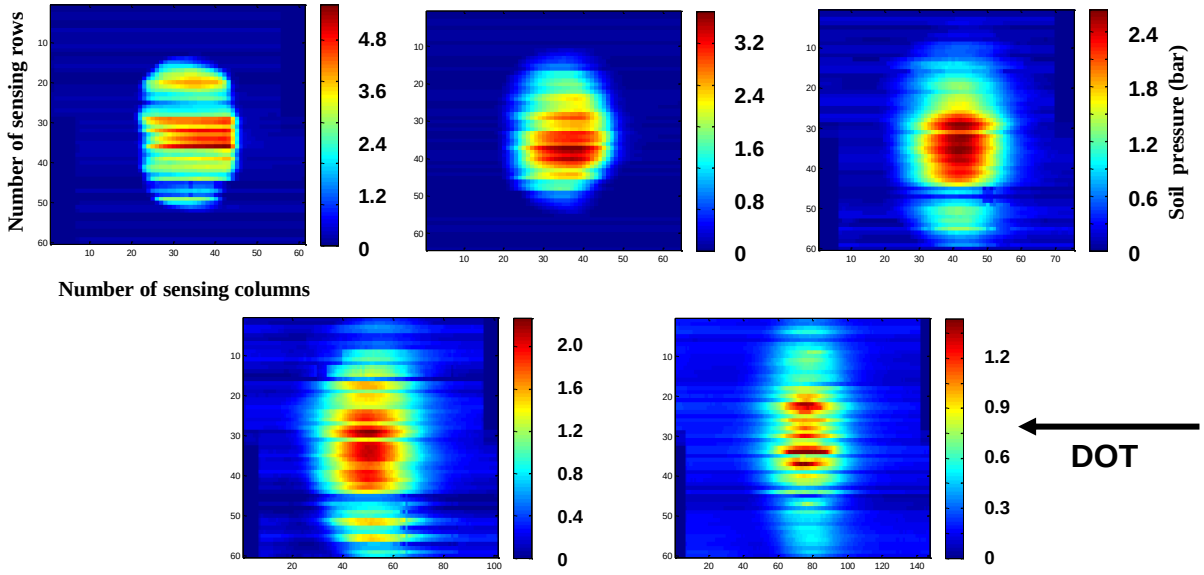

Figure 8.2 Pressure transfer through the soil profile (bar) for the smooth combine tyre inflated to 2.5 bar at 4.5 tonne (from top left: depth of 25mm, 100mm, 250mm, 400mm and 550mm) Please note change in both pressure colour range and length of x axis

Pressure distribution in the soil profile obtained for the smooth and treaded combine tyres loaded to the maximum recommended load of 6.5 tonne at 2.5 bar is shown in Figures 8.3 and 8.4, respectively. At the shallow depth of 25 mm, pressure is approximately uniformly distributed below the smooth tyre, while considerable pressure concentration was found at the sidewall edges of the treaded tyre. With an increase in soil depth, pressure was concentrated in the central contact patch at each soil depth for both tyres. Visually pressure distribution did not appear to vary greatly between the smooth and treaded tyre. However, the maximum pressures generated by the treaded tyre tended to be greater than the ones resulting from the smooth tyre, especially at the shallow depths. The effect of the tyre tread on the area of influence, mean and maximum pressure will be further evaluated in Section 8.2.2.

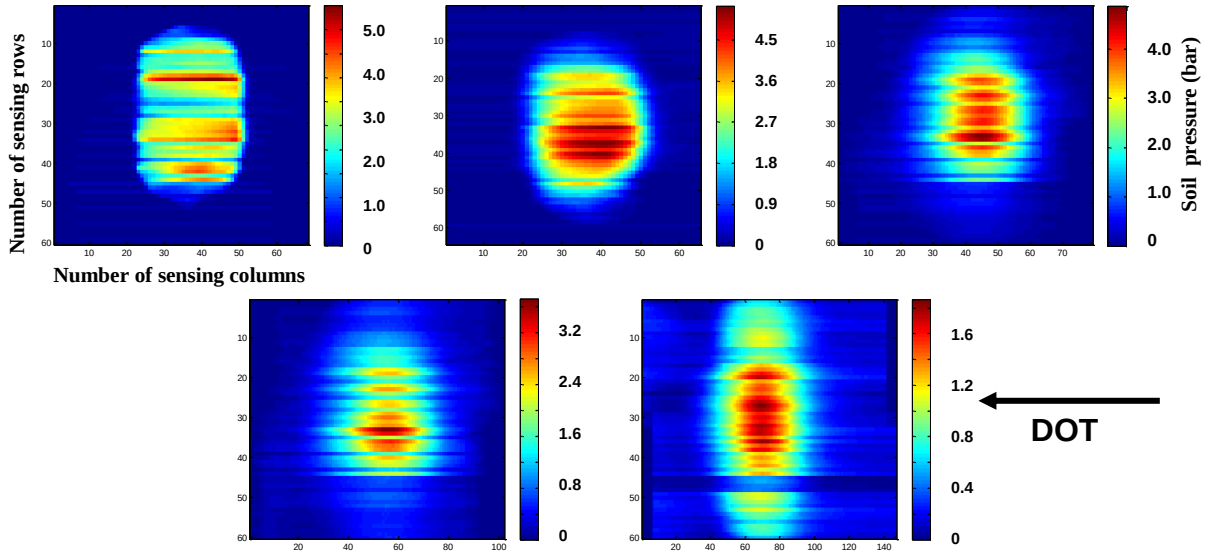

Figure 8.3 Pressure transfer through the soil profile (bar) for the smooth combine tyre inflated to 2.5 bar at 6.5 tonne (from top left: depth of 25mm, 100mm, 250mm, 400mm and 550mm) Please note change in both pressure colour range and length of x axis

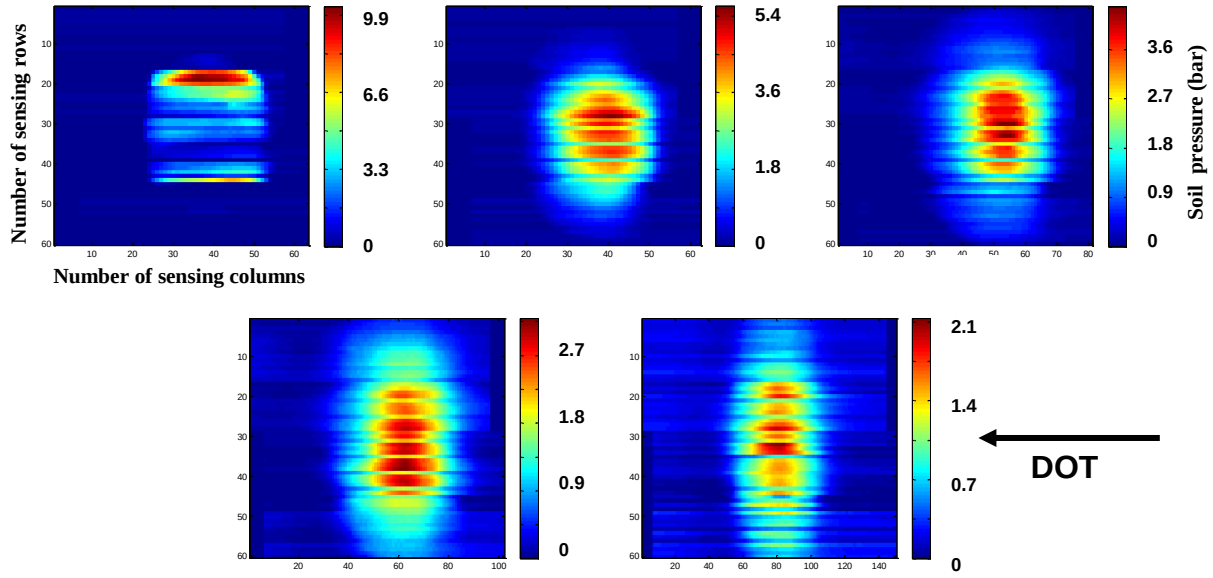

Figure 8.4 Pressure transfer through the soil profile (bar) for the treaded combine tyre inflated to 2.5 bar at 6.5 tonne (from top left: depth of 25mm, 100mm, 250mm, 400mm and 550mm) Please note change in both pressure colour range and length of x axis

8.2.2 Pressure transfer through the soil profile

As discussed in Chapter 2, Boussinesq (1885) developed equations for predicting pressures in the soil. They were further modified by Fröhilch (1934) by introduction of a correction factor to refer to varying soil strength. This was further considered by Söhne (1958), who determined the pressure distribution "bulbs" under pneumatic tyres running on soils varying in strength (hard, medium and soft). According to Söhne (1958), area of tyre influence changes in soil profile following a bulb shape, which means the area affected by a tyre increases with depth to some depth and then further in the soil profile the area decreases. The shape of the pressure bulbs depends on the firmness of the soil, as shown in Figure 2.6. Hard dry soils have round bulbs, while soft and wet soils have slimmer pressure bulbs which reach to a greater depth. Therefore, the change of the area of influence of a loaded tyre depends on soil hardness. Söhne (1958) also considered the effect of tyre load on the soil profile, as shown in Figure 2.5. It was illustrated that the greater the load is, the deeper the soil affected by the tyre.

In this study, the pressure transfer through the soil was studied for the smooth tyre inflated to its maximum inflation pressure of 2.5 bar and loaded with a range of loads up to its maximum recommended load. This was then compared to the pressures obtained below the treaded tyre at the maximum recommended load and the same inflation pressure.

Figure 8.5 shows how the area of influence changes with soil depth for the smooth and treaded tyre. At 0 mm soil depth, contact area data obtained on the hard surface for the tyres was also plotted. As the soil depth increases, the area of tyre influence also increases as the load spreads over a greater area. The increase was found to approximately follow a linear relationship for the smooth tyre loaded with three different loads up to 400 mm soil depth (with the R^2 values varying from 0.954 to 0.988), while for the treaded tyre the trend was found to be curve-linear. The contact areas at the hard surface were found to be considerably smaller than the areas in the soil profile, especially for the treaded tyre. This was expected, as the surface area of the treaded tyre includes only tyre treads, as the areas between the treads do not have any contact with the hard surface which leads to high pressures at the contact area. When a tyre rolls over the soil, it sinks and its load is applied to the soil through the treads and the areas between. This is why the areas of influence in the soil profile below the

surface under the treaded and smooth tyres are comparable. However, the contact area results obtained for the smooth combine tyre on the hard surface were found to follow the linear trends obtained in the soil profile.

The area results, presented in Figure 8.5, agree with the theoretical pressure bulb data obtained by Söhne (1958) for in the initial depth of the soil profile (Figure 2.5 and 2.6), as over the initial soil depth, the soil area of influence increases with soil depth in a near linear manner from the soil surface to 400 mm, after which the rate of increase declines. The lack of linearity from 400 mm could be due to a possible truncation of data, which might have happened due to a limited width of Tekscan sensors. In order to fully evaluate the soil pressure bulbs developed by Söhne (1958), it would be necessary to determine the areas affected by tyres below 400 mm soil profile using a wider set of Tekscan sensors. A nearly linear increase in the area of tyre influence in the soil profile might have been predominantly affected by the increase in the length of the area affected. As a consideration of the areas of influence of the smooth combine tyre indicated, that the width of the area did not change considerably with soil depth but was found to be approximately constant. This is in agreement with the results obtained by Ansorge (2007) who studied soil deformation resulting from loaded tyres. The soil deformation was found to show "punching failure", where the width of the area disturbed by tyres was not affected by soil depth (up to 600mm depth).

A linear regression analysis was carried out using the area of influence data obtained at the surface and in the soil profile below the smooth tyre at different loads (Appendix M.4). The analysis provided the following regression equations for a determination of the area affected by the smooth combine tyre at 2.5 bar inflation pressure in the soil profile:

$$\mathbf{A = -0.017 + 0.045xW + 0.0014xd} \qquad \text{Equation 8.1}$$

This proves that soil depth and tyre load have a significant effect on the soil area affected by the smooth combine tyre. The regression equation fit the experimental data in 98%.

The area of tyre influence at the depth of 550 mm is approximately 4 – 5 times greater than the area at 25 mm depth. This confirms that the load applied by a tyre and transferred in the soil spreads over a greater area with depth. The greater the load applied to the tyre, the greater

is the area affected. According to the analysis of variance at 95% confidence level, tyre tread, the interaction between soil depth and tyre tread, the interaction between soil depth and tyre load do not have a significant effect on the area of influence for the two tyres used in the study, which was proved in ANOVA at 95% confidence and presented in Appendix M.1. This confirms that there was no significant difference in the soil contact areas generated by the smooth and treaded combine tyres at any soil depth studied.

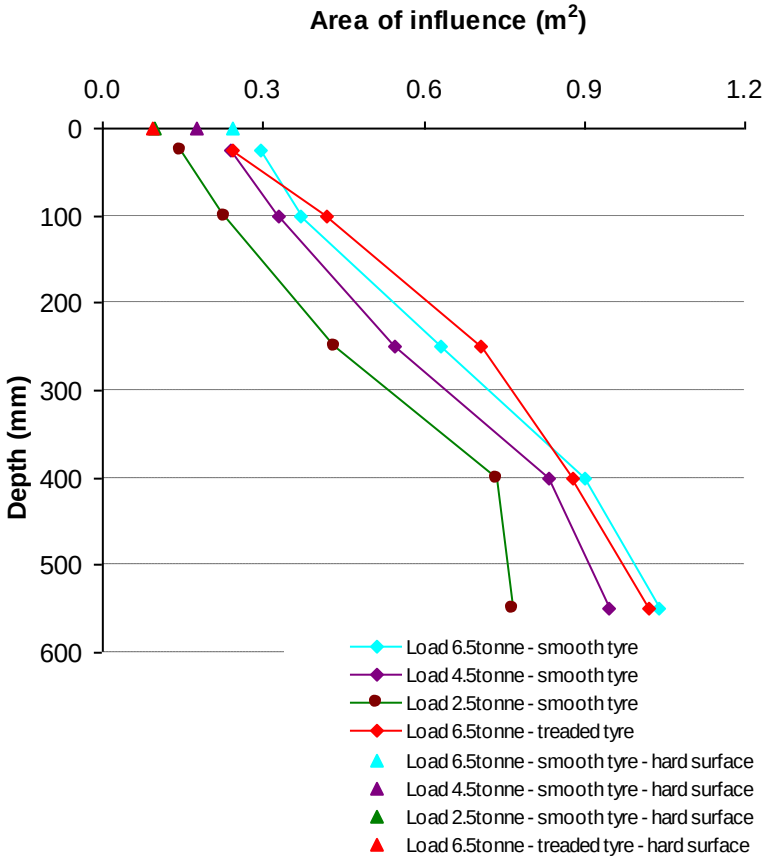

Figure 8.5 Area of influence of the loaded smooth and treaded combine tyres at 2.5 bar

The mean pressure transferred from the soil surface in the soil profile is presented in Figure 8.6. The pressures obtained when the tyres were loaded on the hard surface are indicated by triangular marks on the x axis. They are greater than the mean pressures in the soil profile. The magnitude of mean pressure in the soil decreases with soil depth. The relationships show a hyperbolic decrease in soil pressure with depth which was also found by Dresser *et al.* (2006), Lamande (2006a), Söhne (1958) and other researchers.

Figure 8.7 presents mean pressures calculated as load over area according to the areas of influence of the smooth tyre at different depths. The mean soil pressures obtained in this way agree with the measured values in the soil within 0.5%, while the surface pressures measured was 10 – 18% greater than the values calculated according to the areas of influence. This proves that, the mean soil pressure in the soil at a particular depth can be determined according to the soil area of influence of the tyre. This also agrees with the conclusions drawn according to the hard surface results that tyre contact area on the hard surface should not be used for determination of the mean contact pressure. The 0.5% difference between the measured and calculated mean soil pressures gives further confidence in Tekscan system, this is providing the recommended procedures for improving Tekscan performance are followed.

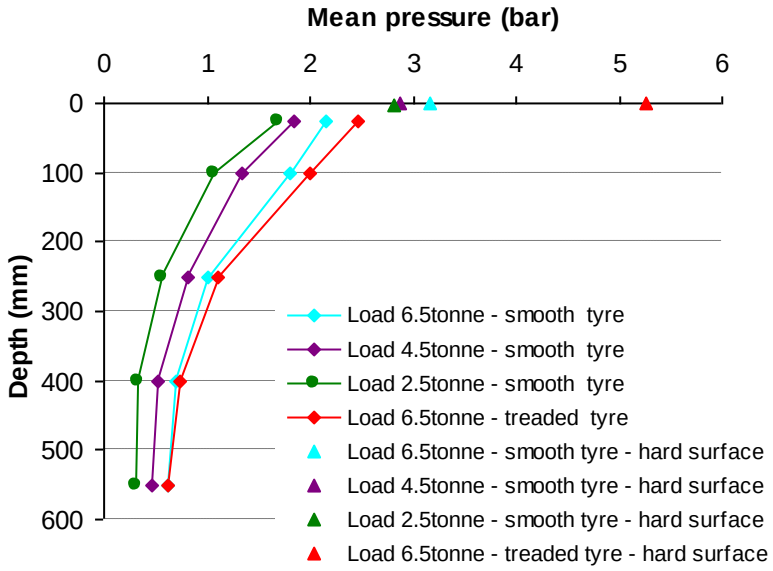

Figure 8.6 Transfer of the mean pressure through the soil profile for the smooth and treaded combine tyres inflated to 2.5 bar

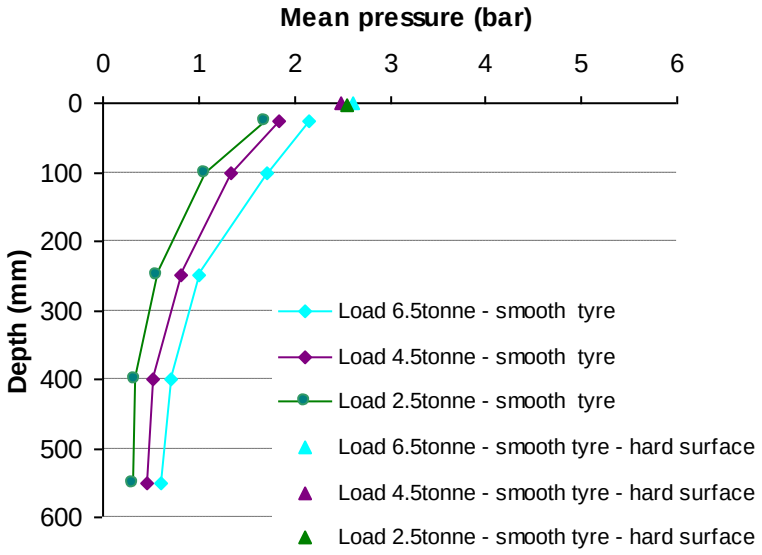

Figure 8.7 Transfer of the mean pressure through the soil profile for the smooth combine tyre inflated to 2.5 bar calculated according to the areas of tyre influence

As illustrated in Figure 8.6, tyre load also has an effect on the mean pressure, as a load increase results in a rise of the mean pressure. The effects of soil depth and tyre load were found to be significant on the mean soil pressure at 95% confidence level (as shown in Appendix M.5). The presence of tyre tread, interaction between soil depth and tyre tread, interaction between soil depth and tyre load do not have a significant effect on the mean pressure of the two tyres tested (Appendix M.2 and M.5). Nevertheless, up to 400 mm soil depth, the mean pressures under the treaded tyres were greater than below the smooth combine tyre. However, the differences were not statistically significant. This proves that tyre tread only has an effect on the mean soil pressure at the surface, further in the soil profile the pressure concentration below the tread dissipates.

The above proves, that in order to minimise the soil pressure, it is necessary to minimise tyre load. As the presence of tyre tread was not found to have a significant effect on the soil pressure in the soil profile, it is recommended to select tyres with the most appropriate tyre tread for traction and self-cleaning purposes.

In general, the mean pressures in the soil were found to be relatively high and some pressures were still detected at 550 mm depth. The soil pressures below the smooth combine tyres were

lower than the tyre inflation pressure (2.5 bar) through the whole soil profile studied. The shallowest test conducted at 25 mm provided mean pressures in the range of 1.7 – 2.2 bar. Below the treaded tyre, the mean pressure at 25 mm was equal to 2.5 bar which was the same as the tyre inflation pressure. As the pressure decreases through the soil profile, at 550 mm values in a range of 0.3 – 0.6 bar were detected, for both the smooth and treaded combine tyres.

The maximum pressures recorded through the soil profile and on the hard surface are shown in Figure 8.8. The highest pressures were detected close to the surface and they decrease with an increase in soil depth. The maximum contact pressure at 25 mm below the treaded tyre was approximately twice that of the smooth tyre at the same load. The tread was found to have an effect on the maximum contact pressure in the soil profile. The maximum soil pressures of the smooth and treaded tyre were, however, significantly different only up to 100 mm depth as shown in Appendix M.3.

Dain-Owens (2010) used the same smooth rear combine tyre in the same soil to determine peak subsurface pressures at 250 mm soil depth using a number of single ceramic strain gauge pressure transducers. As shown in Figure 8.7, the data from the soil profile was of a similar order of magnitude (4.3 bar : 3.2 bar) to that observed by Dain-Ownes (2010) using the same tyre at the same inflation pressure but at marginally different loads (6.5 tonne : 5.9 tonne, respectively). It was expected for Dain-Owens (2010) to obtain lower pressure result due to the tyre load difference. Generally, the pressure difference obtained in these two studies is not greater than two confidence intervals for the pressure data obtained the hard surface study.

Tyre load was found to have a statistically significant effect on the maximum soil pressure at 95% confidence level. The maximum pressures are, however, significantly different for different loads at the greater depths only below 100 mm, while close to the surface they do not differ statistically as presented in Appendix M.6.

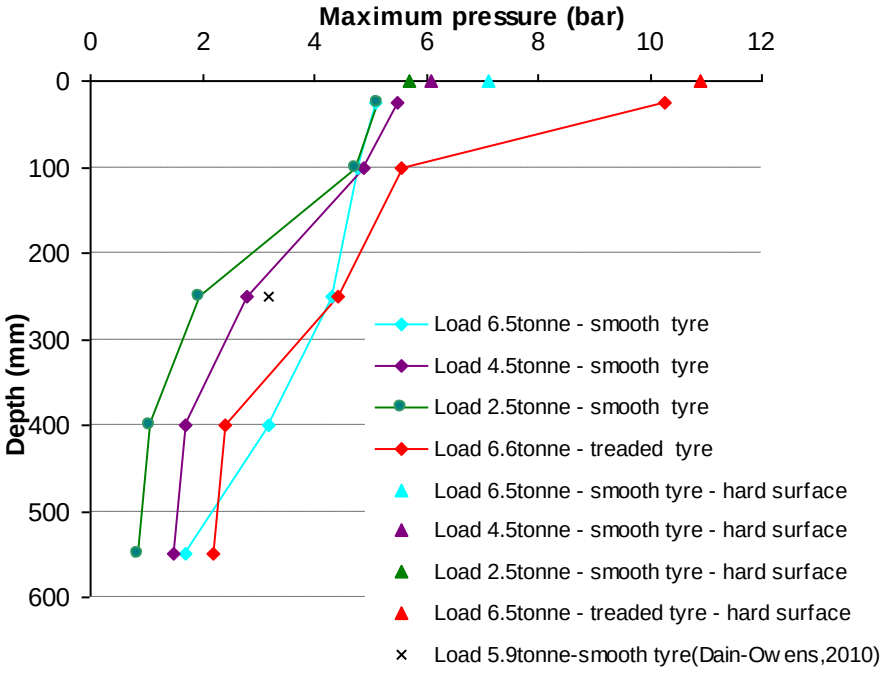

Figure 8.8 Transfer of the maximum pressure through the soil profile for the smooth and treaded combine tyres inflated to 2.5 bar

Overall, the results highlight the risk of compaction of vulnerable soils by agricultural traffic. Just below the soil surface, at 25 mm depth, the maximum pressures generated by the tyres are above 5 bars. For lower loads, the maximum pressures are smaller than below the heavily loaded tyres. This is why below the lightly loaded tyre (2.5 tonne) at 550 mm depth the maximum pressure is only 0.86 bar which is considerably lower than below the heavier tyres (above 1.5 bar). However, usually tyres are loaded up to or in some cases above their maximum recommended load at a given inflation pressure. For the tyres at the maximum recommended load of 6.5 tonne, the maximum pressure at 400 mm was found to be 3.19 bar and 2.39 bar for the smooth and treaded tyre, respectively. These values are close to the inflation pressure of 2.5 bar. This suggests that most of the pressure resulting from tyre carcass stiffness dissipated in the upper 400 mm soil layer when the tyres were loaded to its maximum load according to tyre manufacture specification. The pressures were found to be approximately 2 bar at the depth of 550 mm. This confirms that at greater depths the maximum pressures resulting from loaded tyres are still relatively high and may cause subsoil compaction of vulnerable soils which is difficult to alleviate. In order to minimise soil compaction, it is required to maintain low tyre load. This will then result in a lower maximum soil pressure in soil profile.

8.2.3 Effect of tyre inflation pressure and load on soil pressure close to the surface

This section evaluates the pressure results obtained at the shallow layer of soil up to 100 mm depth. The effect of soil depth, tyre inflation pressure and load on the resulting pressure generated by the smooth combine tyre is investigated here.

The areas influenced by the loaded smooth tyre at the range of loads and inflation pressures are presented in Figure 8.9. They were measured in the soil at two depths of 25 mm and 100 mm. In general, the areas at those depths are greater than the hard surface contact area for the same tyre at the same loads and inflation pressures (as compared to Figure 6.3 left). The areas in the soil increase with depth and the effect of soil depth was found to be significant which was shown in Appendix M.7. Further, an increase in tyre load causes an increase in contact area at both depths studied. As the inflation pressure increases, the area of influence decreases. At high inflation pressures, the area reaches approximately a constant value at each depth and under each tyre load. This is the minimum contact area, which is obtained when the tyre is loaded to rated load and inflation pressure. The effect of combination of load and inflation pressure was found to be statistically significant at 95% confidence interval (Appendix M.7).

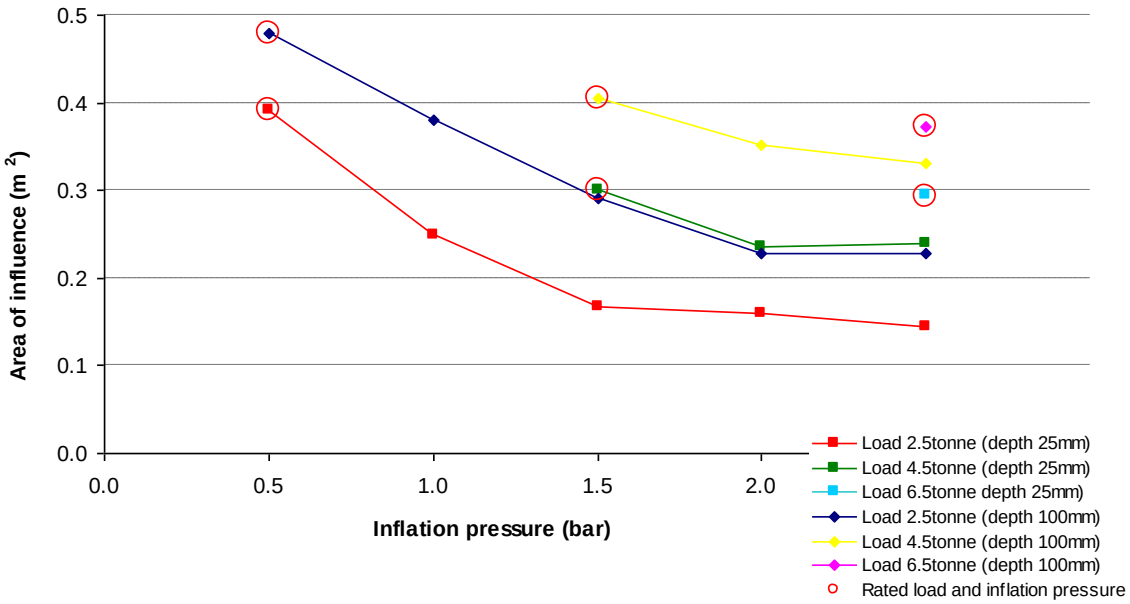

Figure 8.9 Area of influence vs. inflation pressure affected by the smooth combine tyre at 25 mm and 100 mm soil depth

The mean pressures obtained in the soil at 25 mm and 100 mm depth below the smooth

combine tyre are presented in Figure 8.10. As the tyre inflation pressure increases, the mean pressure also increases. Tyre load also has an effect on the mean soil pressure and as it rises, the pressure in the soil goes up. The combination of tyre load and inflation pressure has significant effect on the mean soil pressure (Appendix M.8). Therefore, in order to maintain low pressures in the soil profile it is recommended to keep tyre load and inflation pressure as low as possible.

When the tyre was loaded onto the soil at its lowest recommended inflation pressure (0.5 bar), the mean soil pressure at both depths was above the inflation pressure. This shows that tyre carcass stiffness of the smooth combine tyre contributes more when the tyre is at lower inflation pressure. Overall for all the higher inflation pressures, the mean soil pressures were found to be lower than tyre inflation pressure. The mean pressures were found to be lower at the greater depths, the soil depth has a significant effect on the mean pressure for the depths studied (Appendix M.8).

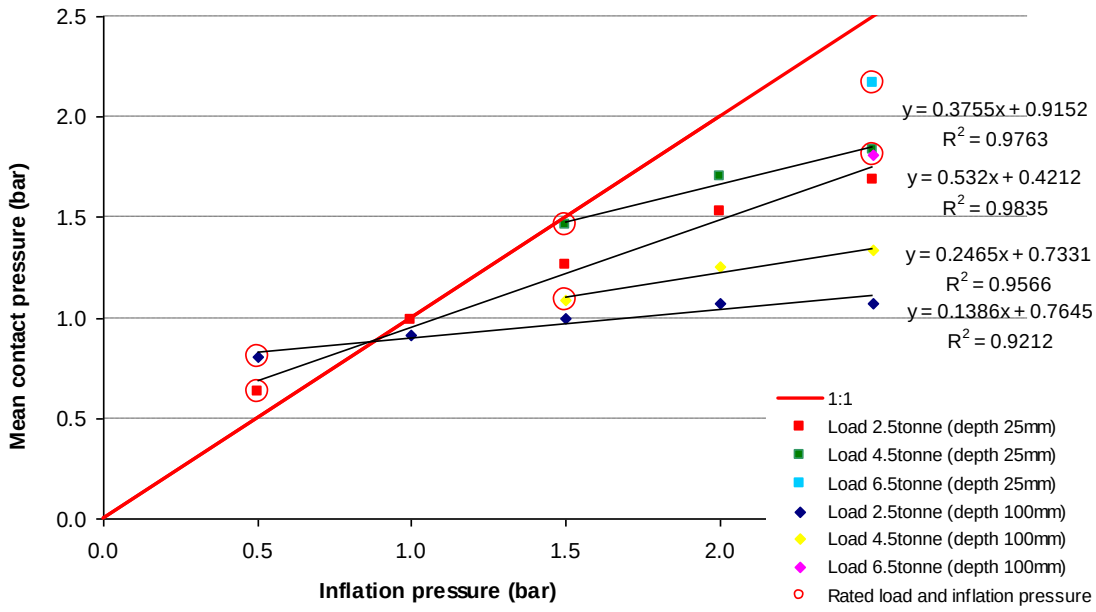

Figure 8.10 Mean pressure vs. inflation pressure resulting from the smooth combine tyre at 25 mm and 100 mm soil depth

The maximum pressures recorded below the smooth tyre at the range of loads and inflation pressure at 25 mm and 100 mm soil depth are presented in Figure 8.11. As for the mean pressures, the maximum pressures were found to be lower at greater soil depth and the soil

depth was found to have a significant effect on the maximum pressure at 95% confidence level (Appendix M.9). An increase in tyre load and inflation pressure resulted in an increase in the maximum soil pressures; the effect of combination of load and inflation pressure was found to have a significant effect on the maximum soil pressure in this study (Appendix M.9). The effect of inflation pressure was found to be approximately proportional. Therefore, in order for the soil maximum pressures to remain low in the upper 250 mm layer of the soil profile, it is recommended to reduce tyre inflation pressure and load.

Generally, all the values of maximum pressures at both depths, shown in Figure 8.11, are considerably greater than tyre inflation pressure. Overall, they were found to be high as they varied form 2 bar to 5.5 bar. This confirms that soil compaction can happen below loaded agricultural tyres in the topsoil layer.

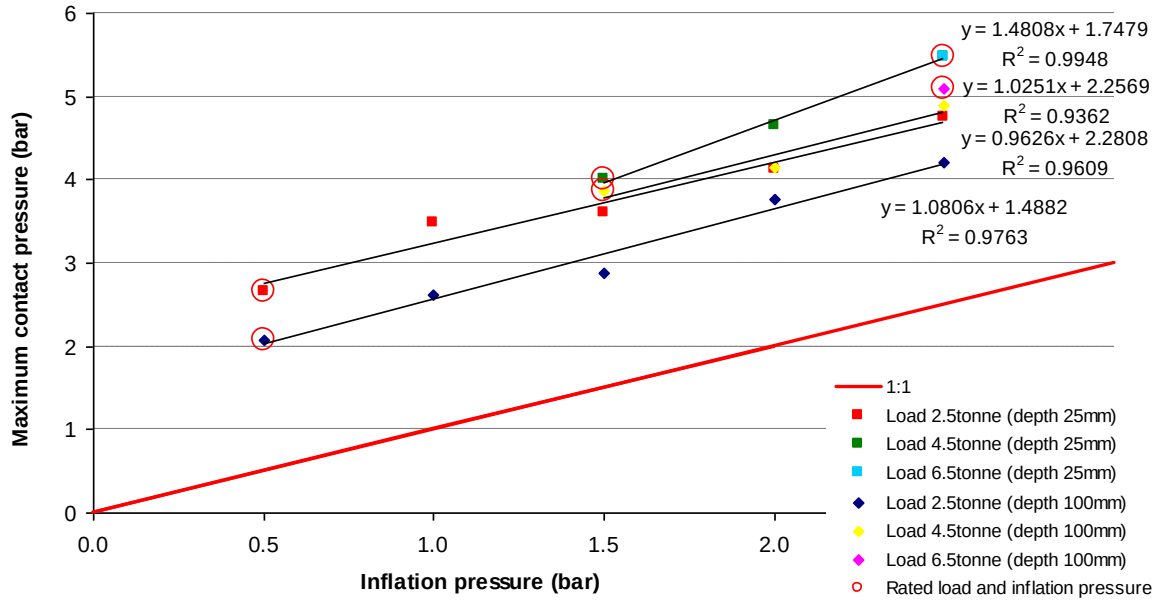

Figure 8.11 Maximum pressure vs. inflation pressure resulting from the smooth combine tyre at 25 mm and 100 mm soil depth

8.3 Effect of ply rating on soil pressure transfer (implement tyres)

The first part of this section examines the effect of tyre ply rating of the Goodyear implement tyres (11.50/80–15.3) on the resulting soil pressures. This was investigated by comparing the pressures in the soil profile below five implement tyres with different ply rating, studied previously on the hard surface in Chapter 7. The second part of the study involved an

investigation of the effect of correlation of tyre load and inflation pressure for one of the implement tyres. This was done using the 16-ply rating tyre at a number of inflation pressures and corresponding maximum loads. Both parts of the study involved an assessment of the area affected by the tyres, pressure distribution across the area, mean and maximum soil pressures. These parameters were measured at two depths of 100 mm and 250 mm. They were, then, compared with the relative values obtained for the same tyres on the hard surface.

8.3.1 Soil pressure distribution

The soil pressure distribution below the implement tyres at 250 mm soil depth is presented in Figure 8.12 and 8.13. Figure 8.12 shows the pressures obtained when the five implement tyres varying in ply rating were loaded onto the soil. While, pressure distribution below the 16-ply tyre at the range of inflation pressures and corresponding loads is illustrated in Figure 8.13.

Overall, the soil pressure distribution was found to be non-uniform for each test. Pressure cross-sections have approximately trapezoidal shape with peak values located in the central area of the contact patch. According to Figure 8.12, tyre ply rating was found to have a little effect on the resulting pressure with similar areas and pressures. The effect of ply rating was further analysed in an evaluation of its effect on the area of influence, mean and maximum soil pressures in Section 8.3.2. Figure 8.13 illustrates how the soil pressure distribution at 250 mm depth changes with the changes of tyre load and inflation pressure, where the magnitude of the maximum pressure increased with the tyre load and inflation pressure.

8.3.2 Effect of tyre ply rating on soil pressure

The effect of tyre ply rating on the area of influence of the range of implement tyres, at the range of depths, was investigated as shown in Figure 8.14. As discussed previously for the combine tyres, also for the implement tyres the area of tyre influence rises with the soil depth increase. The depth has a statistically significant effect on the area at 95% confidence level, while tyre ply rating was not found to have a significant effect (Appendix M.10). The area of influence at 100 mm is approximately 4.5 times greater than the hard surface contact area under the implement tyres. At 250 mm depth, the area increases further and it is 2.5 – 3 times greater than at 100 mm.

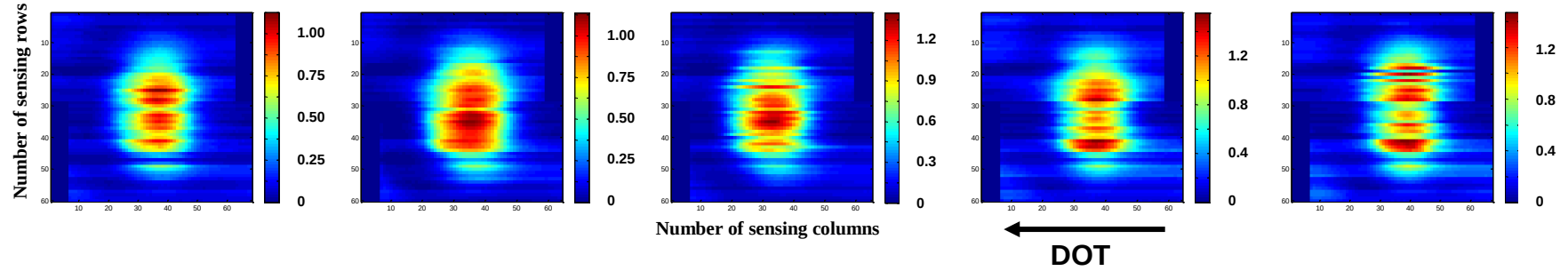

Figure 8.12 Soil pressure distribution (bar) below the implement tyres varying in ply rating at 1.7 tonne and 2.7 bar at 250 mm soil depth (from left: PR16, PR14, PR12, PR10, PR8) Please note change in both pressure colour range and length of x axis

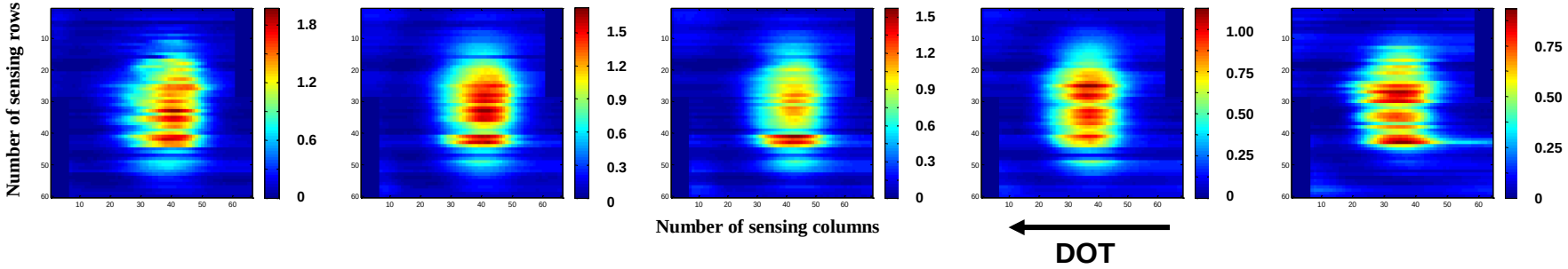

Figure 8.13 Soil pressure distribution (bar) below 16-PR implement tyre at the range of loads and inflation pressures at 250 mm soil depth (from left: 2.575 tonne + 5.4 bar, 2.18 tonne + 4.1 bar, 1.959 tonne + 3.4 bar, 1.7 tonne + 2.7 bar, 1.2 tonne + 1.5 bar) Please note change in both pressure colour range and length of x axis

The mean soil pressures obtained in the soil profile under the implement tyres varying in ply rating were plotted as shown in Figure 8.15. As the soil depth increased, the mean pressures decreased. This is due to fact that the soil pressures spread over greater areas, as shown in Figure 8.14. The depth has a significant effect on the mean soil pressures measured under these tyres. The mean pressures are not significantly influenced by the ply rating. Also the interaction between soil depth and tyre ply rating does not have a signifficnt effect on the mean soil pressure (Appendix M.11). The values obtained at the hard surface varied between 4.2 – 4.9 bar, at 100 mm soil depth they were between 0.95 – 1.1 bar, while at 250 mm they discipated to 0.38 – 0. 42 bar. This shows that the soil pressures at 100 mm approximately 4.5 times lower than the values obtained at the hard surface. At 250 mm the pressures disspated further and they were 2.5 – 3 times lower than at 100 mm. As tyre ply rating of the implement tyres does not have a significant effect on the mean soil pressure, the selection of tyre ply rating should be based on the loads that the tyre needs to carry. The stiffer tyres are able to carry greater loads at corresponding greater inflation pressures. However, at the same load and inflation pressure, they all resulted in approximately the same soil pressure in the soil profile.

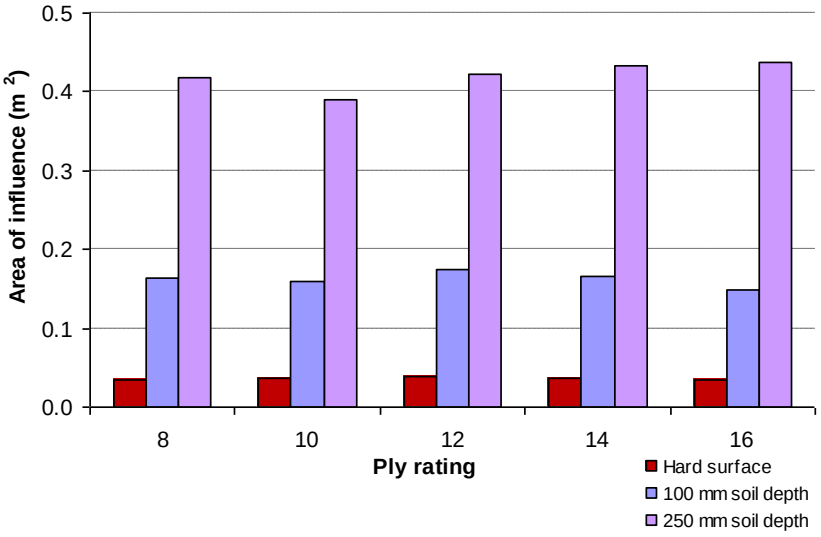

Figure 8.14 Area of influence below the implement tyres varying in ply rating at 1.7 tonne and 2.7 bar at the range of depths

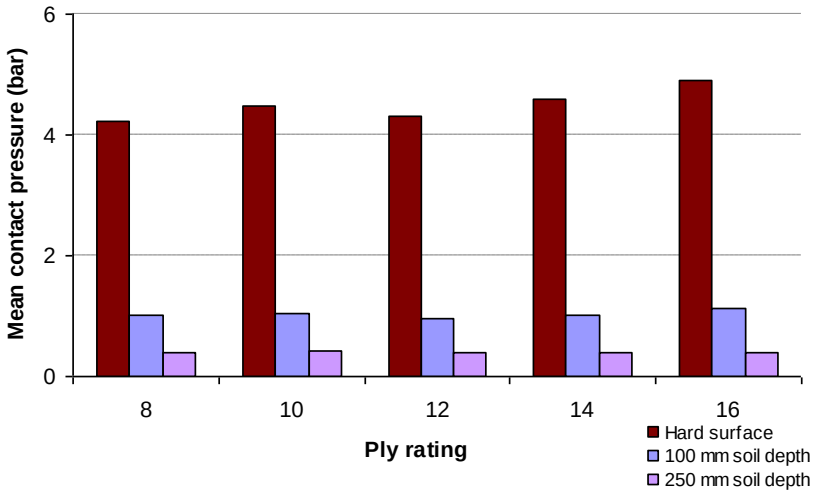

Figure 8.15 Mean soil pressure below the implement tyres varying in ply rating at 1.7 tonne and 2.7 bar at the range of depths

Figure 8.16 presents the maximum soil pressures obtained under the implement tyres varying in ply rating. The maximum soil pressure values were found to decrease with soil depth. At the hard surface, they were found to be signifficanly greater than in soil profile (Appendix M.18). At the hard surface the maximum pressures varied between 9.0 – 10.8 bar, while at 100 mm soil depth they were between 5.0 – 5.6 bar. Further in the soil profile, they disipated to 1.1 – 1.3 bar at 250 mm. This shows that at the depth of 100 mm the pressures were approximately 50% of the ones obtained on the hard surface. While at 250 mm depth, the maximum values were equal to 20 – 25% of the ones at 100 mm. Similarly, as for the mean soil pressures, the maximum soil pressure below the implement tyres was not found to be significantly influenced by their ply rating. Also the interaction between the soil depth and tyre ply rating does not have a significant effect on the maximum pressures below the implement tyres studied (Appendix M.12). It can be concluded that a change in tyre ply rating would not result in a significant reduction of soil pressures in the soil profile, therefore, it would not lead to a reduction in soil compaction.

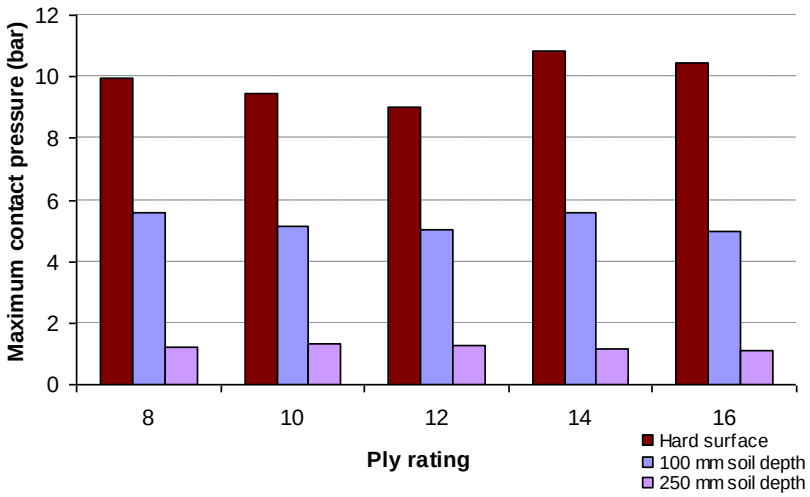

Figure 8.16 Maximum soil pressure below the implement tyres varying in ply rating at 1.7 tonne and 2.7 bar at a range of depths

8.3.3 Effect of the correlation between tyre inflation pressure and load on soil pressure

As discussed before, the area of tyre influence increases as the soil depth increases, which is presented in Figure 8.17. At hard surface, the contact area of the 16-ply rating implement tyre was approximately constant at the different loads and pressures studied. In the soil at 100 mm depth, the area influenced by the tyre varied but it was not found to be influenced by the combination of tyre load and inflation pressure. However, in the soil profile at 250 mm depth, it was found to change marginally with the combination of tyre load and pressure. The effect of depth, combination of inflation pressure and load and the correlation between depth and inflation pressure and load are statistically significant (Appendix M.13). An increase in load and inflation pressure, resulted in a slight increase in the area affected through the soil profile, however, some results were not significantly different between each other. The area of influence at 100 mm was found to be 4 – 6 times greater than the hard surface area. Further, the area at 250 mm was 2 – 3 times greater than the area at 100 mm. The greater the load and inflation pressure, the greater the ratio.

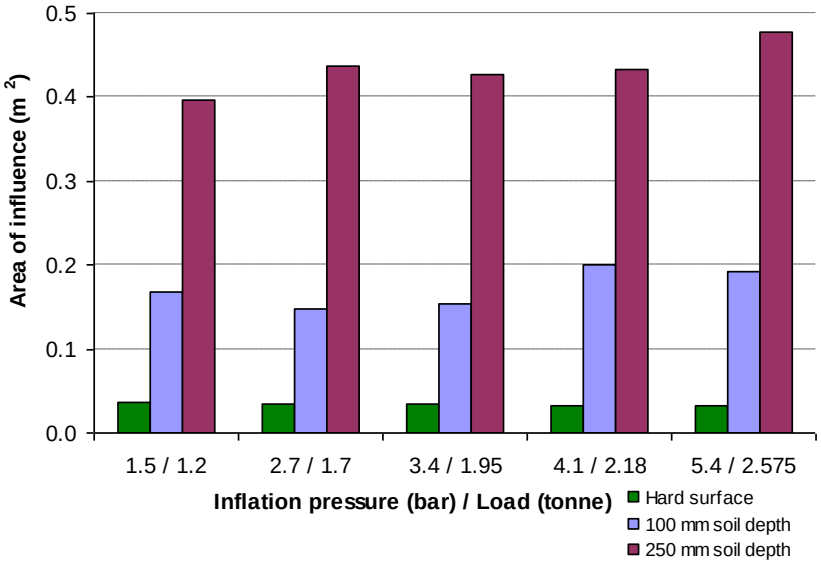

Figure 8.17 Area of influence below the 16-PR implement tyre at varying loads and inflation pressures at a range of depths

The mean soil pressures obtained under the 16-ply implement tyres at the range of inflation pressures and corresponding loads are presented in Figure 8.18. As for the previous figures, the data obtained on the hard surface was plotted with the results from the soil profile at two depths of 100 mm and 250 mm. The mean values were significantly influenced by soil depth (Appendix M.14), which agrees with the previous discussion. The mean pressures at the surface varied from 3.4 bar to 7.7 bar. At the depth of 100 mm the pressures were between 0.7 – 1.3 bar, while at 250 mm they fell to 0.3 bar to 0.5 bar. The pressures at the hard surface were found to be 4 – 6 times greater than at 100 mm soil depth. Then at 250 mm, the results were approximately 30 – 50% of the pressures at 100 mm depth.

An increase in tyre inflation pressure and corresponding tyre load (following the tyre manufacture specification) resulted in a rise in the mean soil pressures below the 16-ply implement tyre at the range of depths. The effect of combination of tyre load and inflation pressure had a significant effect on the mean pressure. Also the interaction between the soil depth and tyre inflation pressure and load were also found to have a signifficant effect on the mean values, nevertheless, some results were not

significantly different between each other (Appendix M.14). A pressure and load increase from the lowest recommended values of 1.5 bar and 1.2 tonne to the highest pressure and load of 5.4 bar and 2.575 tonne resulted in an increase of 126% in the mean pressure at the hard surface. At 100 mm soil depth it produced 86% increase, while at 250 mm the mean pressure increased by 67%. Therefore, in order to maintain a low mean contact pressure in the soil profile, it is necessary to keep both the tyre inflation pressure and load low.

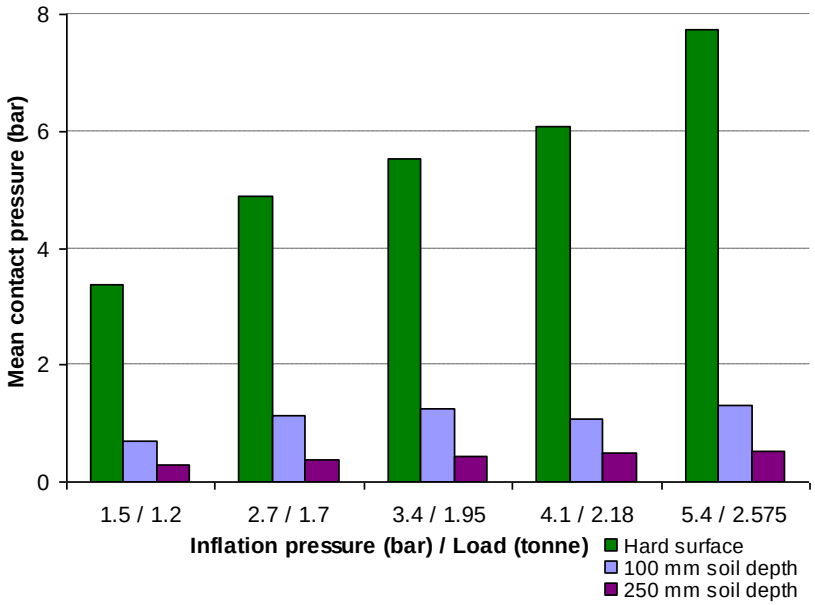

Figure 8.18 Mean soil pressure below the 16-PR implement tyre at varying loads and inflation pressures at a range of depths

Figure 8.19 shows the maximum soil pressures obtained under the stiffest implement tyre studied. The signifficant effect of soil depth on pressure was also found here, as the maximum pressures decreased with depth (Appendix M.15). The maximum values obtained at 100 mm soil depth were smaller than at the hard surface by approximately 30 – 50%. At 250 mm the soil pressures dissipated further and the maximum values were qual to 20 – 30% of the pressures at 100 mm.

Similarly, as it was observed for the mean pressures, the maximum pressures were found to be influenced by the combination between tyre inflation pressure and load. An increase in tyre inflation pressure and load resulted in a rise in the maximum soil pressures. At the hard surface the maximum pressures below the implement tyre varied from 6.5 bar to 15.4 bar. At 100 mm depth the maximum values detected were between 3.5 – 8.5 bar, while at 250 mm the soil pressures of 1.0 – 1.8 bar were recorded. The effect of combination of inflation pressure and load is statistically signifficant (with some results not significantly different between each other), while the interraction between those two and soil depth are not signifficant (Appendix M.15). Therefore, when the tyre is at lower inflation pressure and its corresponding load, it generates lower maximum soil pressures through the soil profile. An increase in the inflation pressure and load from 1.5 bar and 1.2 tonne to 5.4 bar and 2.575 tonne produced an increase in the mean pressure at the hard surface of 137%. At 100 mm soil depth, the increase was even more, as it was 145%. Deeper in the soil profile at 250 mm the mean pressure increased by 80%.

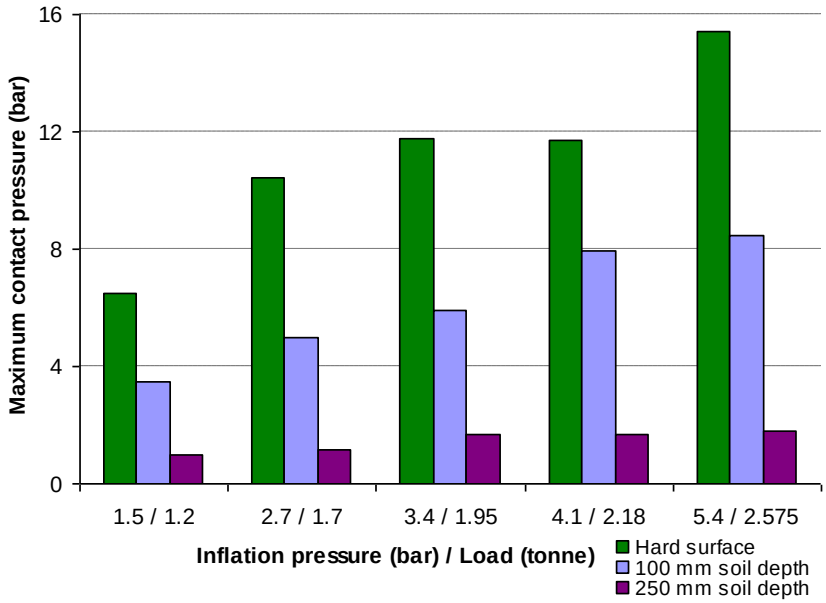

Figure 8.19 Maximum soil pressure below the 16-PR implement tyre at varying loads and inflation pressures at a range of depths

8.4 Comparison of the results

This chapter assesses the influence of tyre tread, ply rating, load and inflation pressure on the soil pressures created below agricultural tyres at a range of depths. The results obtained for the smooth and treaded combine tyre and five implement tyres varying in ply rating were studied here. The smooth and treaded combine tyre considered the effect of tyre tread, while the implement tyres allowed an evaluation of the effect of tyre ply rating. Further, the study conducted using all these tyres looked at the effect of tyre load and inflation pressure.

The smooth and treaded combine tyres were evaluated in terms of their soil pressure creation in the soil profile of 550 mm. The treaded tyre at the hard surface was only supported on the treads. Therefore, it had a smaller contact area than the smooth tyre, this resulted in greater mean and maximum pressures at the surface. Further in the soil profile the pressure concentrated below the treads dissipated. Tyre tread does not have a significant effect on soil area and mean pressures in the soil profile. However, the maximum contact pressure was found to be significantly influenced by tyre tread and the results obtained for the smooth and treaded tyre were found to be significantly different up to 100 mm soil depth. The treaded tyre had a smaller area of influence than the smooth tyre at 25 mm soil depth. The mean pressures below the treaded tyre were greater than under the smooth tyre up to 400 mm depth, but this was not statistically significant. At the greater depths of the soil profile, the resulting pressure and area of influence were found not to differ significantly.

The effect of tyre ply rating on the resulting soil pressure was investigated using the implement tyres at varying ply rating which were as follows: 8, 10, 12, 14 and 16. Comparable soil pressures were created in the soil profile of 250 mm under the implement tyres studied under a constant load and its corresponding inflation pressure, which was the same for the five tyres studied. Therefore, a change in ply rating does not lead to a change in the resulting soil pressures below the implement tyres employed in this study. This indicates that the implement tyres at varying ply rating, but a constant load and inflation pressure, would create the same amount of

compaction of agricultural soil. Following the tyre manufacture specification, the stiffer the implement tyre is the heavier loads it is able to carry. The greater the load to the tyre is applied, the greater inflation pressure is required. Therefore, when deciding on tyre ply rating, tyre selection should be based the maximum loading requirements. As discussed in Chapter 6, tyres should be prevented from under- and over-loading, as this leads to a less uniform pressure distribution across their tyre surface contact patch. Further, when selecting the tyres a consideration of a possibility of a minimum loading application should be considered. This would allow minimisation of the inflation pressure according to the tyre specification. A decrease in tyre inflation pressure and load results in a decrease in the mean and maximum soil pressure through the soil profile.

Soil pressure distribution determined at the range of depths below the agricultural tyres studied was found to be non-uniform. As the area affected by the tyre was found to get larger with soil depth, the soil pressures spread over the greater areas, therefore, the mean and maximum pressures decreased with soil depth. At the range of depths, the pressure was concentrated in the central part of the area of influence and decreased towards the edges. Pressure cross-section was found to have an approximately trapezoidal shape with peak pressures located in the central area of the contact patch.

The areas of tyre influence go up with the soil depth increase for all the tyres studied. The areas in the soil profile are significantly greater than at the hard surface. At 250 mm, it was approximately 2 – 3 times greater than close to the soil surface at 25 mm. At 550 mm, the area was 4 – 5 times greater than close to the soil surface. Reduction of tyre load resulted in an area decrease through the whole soil profile up to 550 mm. This proves that when a lower load is applied to a tyre, smaller area is affected by this tyre.

The area resulting from the smooth combine tyre was found to increase with soil depth in a linear manner from the soil surface to 400 mm, after this depth the rate of

increase declines. This partially agrees with the soil pressure bulbs developed by Söhne (1958), but it might have been related to data truncation as the width of Tekscan sensors was limited. In order to fully evaluate the findings of Söhne, it would be recommended to determine the areas of tyre influence at 550 mm depth and below. A nearly linear increase in the area of influence of tyre in the soil profile was considered to be mainly affected by the increase in the contact length of the area affected. The width of the area did not appear to change considerably with soil depth, which agrees with Ansorge (2007), who studied soil deformation resulting from loaded agricultural tyres. He found that the width of the area disturbed by tyres was not affected by soil depth and was approximatelty constant ("punching failure").

A linear regression analysis of the area of tyre influence of the smooth combine tyre proved that soil depth and tyre load have a significant effect on the area as shown in Equation 8.1. The regression equation fit the experimental data in 98% and could be used to determine area affected by the smooth combine tyre.

The areas obtained below the smooth combine tyre were further evaluated and they were converted into mean pressures by dividing the load applied by the area. The values obtained agreed with the soil pressures measured within 0.5%, while the difference between the mean contact pressures calculated and measured varied between 10 – 18%. This proves that the mean soil pressure can be determined according to the area of tyre influence, while the surface contact pressure needs to be measured as its determination according to the contact area leads to contact pressure under-estimation.

A linear increase in area of tyre influence with soil depth and an inverse proportionality between the tyre load and resulting area explain the hyperbolic decrease in pressure in soil profile found in this study and also previously by many other researchers (Dresser *et al.*, 2006; Lamande, 2006a; Söhne, 1958). This can be presented as:

$$y = \frac{1}{x} \qquad \text{Equation 8.2}$$

As the area of influence is inversely proportional to the pressure; this means that if the area at a particular depth is doubled then the soil pressure reduces by 50%.

The effect of tyres on the soil pressures was observed through the whole depth of the soil profile studied. For the combine tyres the effect was found up to the depth of 550 mm. When the treaded tyre was loaded according to its manufacture specifications, the mean pressure at 25 mm was equal to its inflation pressure. The mean soil pressures below the treaded tyre at the greater depths and below the smooth tyre at all the soil depths were considerably lower than the tyre inflation pressure. However, the maximum pressure at 100 mm depth was found to be considerably greater than the tyre inflation pressure. For both tyres the maximum pressures were found to be close to the inflation pressure at 400 mm depth. The implement tyres were studied up to 250 mm soil depth, as they usually carry smaller loads and their effect on the subsoil was expected to be lower. Their maximum pressures at 250 mm were greater than the inflation pressure. While the mean pressures at both depths studied, 100 mm and 250 mm were smaller than their inflation pressures. In order to maintain low soil pressures, it is required to keep tyre load as low as possible. This will allow the operator to reduce tyre inflation pressure according to the tyre manufacture specification.

The effect of tyre load and inflation pressure on soil pressure was studied for both the smooth combine tyre and 16-ply implement tyre. In case of the smooth combine tyre, the influence of load and inflation pressure was studied separately. While for the implement tyre the evaluation of these two parameters was conducted together, as this tyre was tested at the range of inflation pressures and their corresponding maximum loads. Tyre load increase was found to result in an increase in the mean and maximum soil pressures through the soil profile below the smooth combine tyre tested up to 550 mm soil depth. Also an increase in inflation pressure causes a rise in the soil pressures resulting from the combine tyre. This was, however, investigated for the top 100 mm soil depth. The above agrees with the results for the implement tyre, where as

inflation pressure and load were both increased, the soil pressures in the profile of 250 mm also increased. This proves that in order to maintain the soil pressures below agricultural tyres low, it is required to keep the tyres at low inflation pressure and load.

8.5 Conclusions

The following conclusions were drawn according to the soil pressure data discussed in this chapter:

1. Tyre tread was not found to have a significant effect on the area of influence and mean soil pressure in the soil profile below the 600/55-R26.5 Trelleborg combine tyres. However, the maximum contact pressure is significantly influenced by tyre tread and the results obtained for the smooth and treaded tyre were found to be significantly different up to 100 mm soil depth. The treaded tyre had a smaller area of influence than the smooth tyre at 25 mm soil depth. The mean pressures below the treaded tyre were greater than under the smooth tyre up to 400 mm depth, but this was not statistically significant.
2. Under the range of 11.50/80–15.3 Goodyear implement tyres varying in ply rating (from 8 to 16), similar soil pressures were created in the soil profile of 250 mm. Therefore, change in ply rating does not lead to a change in soil pressures. This leads to a conclusion that all the implement tyres at varying ply rating, but a constant load and inflation pressure, would create the same amount of soil compaction. According to the tyre manufacture specification, the stiffer the implement tyre is the heavier loads it can carry at a greater inflation pressure. This is why, when choosing tyre ply rating of these implement tyres, the tyre selection should be based on the loading requirements.
3. Soil pressure distribution at the range of depths below the tyres studied was found to be non-uniform. Pressure cross-section was found to have an

approximately trapezoidal shape with peak pressures located in the central area of the contact patch.

4. The areas of tyre influence increase with soil depth increase. For the smooth combine tyre, the area increases in an approximately linear manner from the soil surface to 400 mm soil depth. A linear regression equation describing the change of area depending on soil depth and tyre load was established. At greater depths, the rate of area increase decreases, this, however, requires further evaluation. The linear increase in the area could be related to an increase in length of the area, as the width of area tends approximately constant with soil depth. This however, requires further investigation.
5. Conclusion (4) explains the hyperbolic decrease in soil pressure with soil depth found in this and other studies.
6. The soil area of tyre influence of the smooth combine tyre was found to be a good indication of the mean soil pressure, as the mean soil pressures obtained using the two methods agreed within 0.5%. The difference between the mean surface pressures calculated and measured were between 10 – 18%. This demonstrate that the mean soil pressure can be determined according to the area affected by the tyre, while the surface contact pressure should not be determined according to the contact area but needs to be measured.
7. Up to soil depth of 550 mm, an effect of tyres on soil pressures was found. When the studied tyres were loaded according to their tyre manufacture specifications, the mean pressure at 100 mm was considerably lower than the tyre inflation pressure. Only below the treaded combine tyre the pressure at 100 mm was equal to its inflation pressure. The maximum pressures at this depth were found to be considerably greater than the tyre inflation pressure. Below combine tyres at 400 mm, the maximum pressures was found to be close to the inflation pressure. The implement tyres, studied up to 250 mm soil depth, had their maximum pressures greater than the inflation pressure at this depth. This confirms an ability of

agricultural tyres to cause subsoil compaction of vulnerable soils, which cannot be alleviated by the standard cultivation techniques, but requires an employment of deep tillage. In order to maintain low soil pressures, it is required to keep tyre load as low as possible. This will allow to reduce tyre inflation pressure according to the tyre manufacture specification.

8. An increase in tyre inflation pressure and load results in an increase in soil pressures through the soil profiles considered. In order to maintain low soil pressures below agricultural tyres, it is recommended to keep the tyres at low inflation pressure and load.

9 FINAL DISCUSSION

In order to determine an effective method to measure the vertical pressure distribution on a hard surface and at a range of depths in the soil profile resulting from pneumatic agricultural tyres, it was necessary to improve the performance of the Tekscan pressure mapping system. With this technique it has been possible to review earlier methods to estimate mean contact pressure and to determine the resulting pressure distribution both on a hard surface and at depth in the soil profile. From this it has been possible to estimate the tyre carcass stiffness effects. The soil pressure study illustrated how the pressure generated by pneumatic tyres distributes in the soil. The effect of tyre ply rating on the resulting contact pressure and carcass stiffness was evaluated using a range of implement tyres differing in ply rating; this was done both on the hard surface and in the soil profile. Further, the effect of tyre tread on the resulting pressures was assessed using both a treaded and smooth combine tyre.

The performance of Tekscan pressure sensing system was evaluated prior to its employment for the tyre pressure studies. Three Tekscan sensors were used in this study, these were 9830, 6300 and 5330 sensors, where the 9830 sensor has a low density of sensing elements (low spatial resolution), while the 6300 sensor is relatively small but has a high density of sensing elements (high spatial resolution). A diaphragm device, for calibrating Tekscan sensors, was designed to use air pressure which can be applied uniformly to the whole area of the sensor. Firstly, the calibration recommended by Tekscan was conducted and its outcome was evaluated. This calibration uses Tekscan software for calibration and it only requires 3 points to establish one regression characteristic for the whole sensor. It also involves multi-point equilibration which compensates for any differences between the sensors. The calibration conducted following Tekscan recommendation provided errors varying between +/- 20%.

The calibration process was modified by designing a multi-point per-sensel calibration with sensel selection. It involved the establishment of an individual

calibration relationship for each sensel using 10 data points. This was developed in Matlab software with a selection of sensing elements, which failed to meet calibration criteria, so the data recorded by these elements was discarded. This calibration process significantly improved the accuracy of Tekscan system and it was found to be an appropriate tool for the hard surface contact pressure and soil pressure determination resulting from agricultural tyres. A range of regression characteristics were evaluated in order to find the one which has the best ability to represent Tekscan data, these were: linear, power, 2^{nd} order polynomial, 3^{rd} order polynomial and 4^{th} order polynomial. The polynomial functions were found to give the best representation of the data and the 4^{th} order polynomial is the best fit of the data. Concluding, Tekscan multi-point per-sensel calibration with sensel selection allowed for the Tekscan sensors to provide a more accurate data as errors were lowered from +/- 20% to +/- 4%.

As the calibration was performed in different conditions than the tyre testing, normalising the sum of the recorded pressure to equal the known applied load was required, as discussed in Chapter 4. This was dependent on the spatial resolution of the sensors. Each Tekscan sensor contains a grid of sensing elements, therefore, a Tekscan mat consists both active and non-active areas. As the 9830 sensor has a low spatial resolution, it does not have a lot of sensing elements, and a larger part of this sensor includes the non-sensing area. Therefore, when using this sensor for a non-uniform pressure applications, it is possible to under-estimate the pressures, if the pressure concentrates on the non-active areas of the sensor. For the 6300 sensor, which has a high spatial resolution with a relatively small non-active area, a smaller proportion of pressure can concentrate on the non-active area. Therefore, it was found that, the normalising the pressures was only required for a low spatial resolution sensor as the 9830. It involved determination of the correction factor which was calculated as the load applied to the tyre and load measured by Tekscan. The factor has to be applied to the pressure data resulting from tyres to ensure that the two loads are equal to each other. Tekscan system produces a lot of data, therefore, a procedure for processing the data and building a pressure contact patch resulting from tyres was

developed in Matlab. Using techniques described above, it was possible to use Tekscan pressure mapping system to determine pressures resulting from agricultural tyres with an improved accuracy and spatial resolution.

In previous research, relatively large pressure transducers were used to measure soil pressures resulting from tyres. These transducers may have an effect on changing soil conditions as they are relatively large objects which are introduced into the soil and the pressure determined is less related to soil pressure as it is a pressure concentrated on a hard object (as discussed in Chapter 2). Also the spatial resolution of the transducers used in previous work was poorer. Dain-Owens (2010), Dresser *et al.* (2006), Pytka (2006) and Christov (1969) used only single pressure transducers buried in the soil below the centre of a tyre, which gave pressure indication in one point only. While, McLeod *et al*. (1966) and Lamande *et al*. (2006b) used a row of transducers placed in the soil perpendicularly to direction of tyre travel, but the sensors were spaced approximately 50 mm apart. This gave pressure in a particular point below tyres but did not give an indication on the soil pressure distribution below tyres. However, in this study a 2.5 m long x 1.5 m wide x 70 mm thick steel plate was used below the Tekscan sensors as a reaction plate. A comparison of the maximum pressure from this study to that obtained by Dain-Owens (2010), where the same tyre in the same soil and at the same inflation pressure but at 5.9 tonne load rather than 6.5 tonne resulted in maximum pressure of 3.2 bar compared to 4.3 bar. This difference is not greater than two confidence intervals for the pressure data from the hard surface study.

Tyre mean contact pressure, determined on a hard surface using Tekscan system, was found to be higher than tyre inflation pressure, further, it was found to be higher than the mean contact pressure determined according to the ink method. Tekscan study showed that an increase in inflation pressure and load results in an increase in both the mean and maximum tyre contact pressure. However, this increase is not constant, as suggested by Bekker (1956), Chancellor (1976) and Plackett (1983), but it is dependent on tyre inflation pressure and load. Pressures in the soil profile, also

measured using Tekscan system, were as expected, found to be lower than those recorded on the hard surface. However, pressures up to 2 bar were detected at a soil depth of 550 mm. An increase in tyre inflation pressure and load results in an increase in soil pressures through the soil profiles considered. This confirms that in order to maintain low soil pressures below agricultural tyres, it is recommended to keep the tyres at low inflation pressure and load.

Tyre carcass stiffness was estimated for the range of tyres tested using the four techniques which differed in the level of sophistication. These were as follows:

1. The pressure difference method (A) to measure both mean and maximum contact pressure using Tekscan,
2. The pressure difference method (B) using ink to estimate the size of the contact patch and hence mean contact pressure,
3. Tyre load - deflection method,
4. Tyre manufacture specification data method:
    a. an inflation pressure at zero load,
    b. a load at zero inflation pressure.

The pressure difference method employing pressure mapping system is the most appropriate way of carcass stiffness determination, as it provides the difference between tyre contact and inflation pressure. This method, however, involves tyre contact pressure distribution measurements which require sophisticated contact pressure mapping equipment. The other three methods – ink method, tyre load-deflection method and method based on tyre manufacture data – require simpler tyre tests. However, they all give a variation of carcass stiffness values.

The ink method and tyre load – deflection technique both were found to underestimate tyre carcass stiffness. The anomalies obtained using the ink method to determine tyre mean contact pressure disproved the ability of this technique to effectively indicate the mean tyre contact pressure and consistently under predicted the mean contact pressure. This was found to be contrary to the assumptions used by a

number previous researchers (eg. Plackett (1983), Williams (1987), Kumar and Dewangan (2004) and Ansorge (2007), who used the ink method to determine the mean contact pressure. As discussed in Chapter 5, contact area includes the area that has contact with the ground but does not transfer any significant load. This happens as tyre contact pressure is not distributed uniformly. Assumption that the contact area is greater than the "real" area that transfers the load leads to an error in the mean contact pressure, which is lower than the "real" value. The ink method, however, proved to provide tyre contact area which agrees with the area obtained in the Tekscan study. The agreement was found to be better for the data obtained using the 6300 Tekscan sensor, where the maximum difference was found to be 4%. As the 9830 sensors have a low spatial resolution, for the tests they were used, the results were found to differ within up to 20%, however, the majority of the data agreed within 10%. This was due to the edge effect when assessing contact area using Tekscan, which was previously investigated by Drewniak *et al.* (2007), who used Tekscan sensors for medical studies.

The lowest carcass stiffness results were obtained using the load – deflection method developed by Plackett (1983). This could be related to the fact that this technique provides only the stiffness of tyre sidewalls as it only considers tyre vertical deflection. Also the assumption that a relationship between tyre load and deflection is linear may not be correct.

The use of the data provided by the tyre manufacture was found to be an easy and relatively accurate method of carcass stiffness estimation giving results not too dissimilar to the results of the mean values from the Tekscan pressure mapping system. Two techniques were compared, namely:

i. tyre inflation pressure at zero load, and
ii. the maximum load that tyre can carry when it is not inflated which can be converted into pressure.

The first technique was a speculative method which only considers the tyre manufacture recommended data and does not require any experiments to be

conducted. The latter method also uses data provided by a tyre manufacture and it requires one experimental tyre test. The method based on the evaluation of tyre manufacture specification gives carcass stiffness results which are in closer agreement to the carcass stiffness values measured using Tekscan. While the use of a linear regression function between the load vs. inflation pressure tyre manufacture data was found to give a marginally poorer fit ($r^2 = 0.99$) than the 2nd order polynomial ($r^2 = 0.999$), however, it gave results which were closer to the real mean carcass stiffness values determined in tyre contact pressure experiments. The technique considering the load that tyre is able to support without any inflation pressure, was found to give the best approximation of the mean carcass stiffness values. There is some difference between the true carcass stiffness values and the results provided by this technique, however, the method gives a good indication of the mean tyre carcass stiffness within 20% for all the tyres studied.

The maximum carcass stiffness values were not estimated by either of the methods. In order to accurately determine the maximum carcass stiffness of a tyre, it is necessary to conduct tyre contact pressure distribution measurements. However, a quick approximation can be done according to the mean carcass stiffness, as the maximum carcass stiffness was generally found to be 2.5 – 4 times greater than the mean values. This is, however, dependant on tyre characteristics (architecture and tread pattern).

Concluding, the Tekscan method of contact pressure determination enables tyre carcass stiffness to be determined. This provides a combined tyre carcass stiffness which takes into account both sidewall and tyre belt stiffness. The other methods of carcass stiffness approximation, considered in this project, do not require sophisticated experimental techniques but provide results that vary from the measured pressure data. The method based on the tyre manufacture data provides the best estimation of the mean carcass stiffness of the tyres studied with an error up to +/- 20% as compared to the Tekscan method. In order to assist in the selection of tyres with the lowest mean contact pressure the carcass stiffness can be estimated from the tyre manufacture specification data method. It is also recommended that the pressure

intercept value for the zero load is included in the tyre manufacturer's specification data, so tyre mean contact pressure can be easily estimated.

As expected, the tyre contact pressure distribution obtained below the tyres tested using Tekscan system on the hard surface and resulting soil pressure showed non-uniform pressure distribution. This agrees with previous findings of Bekker, 1956; VandenBerg and Gill, 1962; McLeod *et al.*, 1966; Burt *et al.*, 1992; 1989; Gysi *et al.*, 2001; Trautner, 2003, Way and Kishimoto, 2004, who used different means of contact pressure measurements, which were discussed in Chapter 2. The pressure cross-section was found to have an approximately trapezoidal shape with peak pressures located in the central area of the contact patch, which agrees with findings of Pottinger (2006). Further, the pressure distribution was found not to be normally distributed when under – and over – loading the tyres. The pressure distribution was found to be normally distributed if the tyres were loaded to their recommended load and inflation pressure. The distribution was skewed positively or negatively depending if the tyres were underinflated or overinflated (for the load applied), respectively. This proves that, for reduction of the peak pressures, selection of the load and inflation pressure recommended by tyre manufacturers is essential. As stated by Trautner (2003), soil compaction mainly results from the maximum contact pressure, therefore, remaining the contact pressure to be as uniform as possible may lead to minimisation of soil compaction resulting from agricultural traffic.

The relationships between tyre mean/maximum contact pressure and inflation pressure on the hard surface were found to vary for the tyres tested depending on their architecture, e.g. shape, carcass construction and tread pattern. Therefore, depending on tyre architecture, the mean and maximum carcass stiffness was found to be influenced by inflation pressure and load. Generally, an increase in load resulted in an increase in the carcass stiffness. This was found to be true for all the tyres tested apart from the treaded combine tyre when considering the maximum carcass stiffness, as it was not found to be significantly influenced by tyre load. The inflation pressure had an effect on all the tyres testes, however, for the front tractor tyre and smooth

combine tyre an increase in inflation pressure lead to a decrease in tyre carcass stiffness, while for the treaded tyre it resulted in an increase in its carcass stiffness. This means that the contact pressure do not increase at the same rate as tyre inflation pressure, therefore, the difference between the contact pressure and inflation pressure, considered as tyre carcass stiffness, is not a constant, as suggested by Bekker (1956), Chancellor (1976) and Plackett (1983, 1986 and 1987), but it changes depending on tyre inflation pressure and load. Karafiath and Nowatzki (1978) proposed a relationship between the contact pressure and inflation pressure, which shows that the difference between these two is not constant but is influenced by the inflation pressure as following:

$$P_C = c_1 P_i + P_{CS} \qquad \text{Equation 2.5}$$

The effect of tyre load found was not previously considered by Karafiath and Nowatzki (1978) or any other researchers.

A lack of general consistency in the effect of tyre inflation pressure on carcass stiffness, agrees with Pottinger (2006), who concluded that tyre mechanics is influenced by tyre design and operating conditions. He discussed it further saying that each tyre design and operating condition is unique. The current study also showed that the maximum carcass stiffness of the tyres studied is considerably greater than the mean values, however, the ratio of the maximum/mean carcass stiffness was also found to be dependent on tyre architecture.

The soil studies showed how the soil area influenced by tyres and pressures distribute through the soil profile. The effect of tyres on soil pressures was found up to the soil depth of 550 mm. When the studied tyres were loaded according to their tyre manufacture specifications, the mean pressure at 100 mm was considerably lower than the tyre inflation pressure. Only below the treaded combine tyre the pressure at 100 mm was equal to its inflation pressure. The maximum pressures at 100 mm depths were found to be considerably greater than the tyre inflation pressure. Below combine tyres at 400 mm, the maximum pressures was found to be close to the inflation pressure. The implement tyres, studied up to 250 mm soil depth, had their

maximum pressures greater than the inflation pressure at this depth. This confirms an ability of agricultural tyres to cause subsoil compaction of vulnerable soils which may not be alleviated by standard cultivation techniques, but requires an employment of deep tillage. In order to maintain low soil pressures below agricultural tyres, it is recommended to keep the tyres at low inflation pressure and load.

The effect of soil depth on the area of soil influence by the smooth combine tyre (Trelleborg 600/55-R26.5) was studied in detail. It was found to increase in an approximately linear manner from the surface to a depth of 400 mm. At greater depths, the rate of increase in area declined. This could suggest that soil pressure distribution resulting from loaded tyres either:

i. follows the pressure bulb shape found by Söhne (1958) according to his theoretical consideration based on Boussinesq (1885), or
ii. was affected by the truncation of data which may have occured due to the limitations on the width of the Tekscan sensors.

This, however, requires further evaluation by soil pressure/area determination at 550 mm and greater depths.

The linear relationship between the area of tyre influence and soil depth is thought to result from the predominant increase in the length of the contact patch, as suggested in an earlier study on the soil deformation below agricultural tyres (Ansorge, 2007), where the area of soil disturbance did not increase in width with soil profile depth ("punching failure"). The characteristic of the changes in length and width of the area of tyre influence require further investigation.

A hyperbolic function, relating the decrease in soil pressure to soil depth, was found in this study. Whilst also shown by other research (Dresser *et al.*, 2006; Lamande, 2006a; Söhne, 1958), it has not been previously explained in relation to the area effects. This relationship is due to the area of influence being inversely proportional to pressure and it linearly increasing with soil depth. Therefore, this results in a hyperbolic relationship between the soil pressure and depth, which means that

incrementally doubling an area will result in a reduction in soil pressure by 50% which is illustrated by this equation:

$$y = \frac{1}{x} \qquad \text{Equation 8.2}$$

The areas obtained below the smooth combine tyre were converted into mean pressure according to the tyre load applied. The resulting pressure was found to be in a good agreement with the mean soil pressure measured by Tekscan as the results varied only up to 0.5%. Therefore, determination of the soil area of tyre influence allows determination of the soil mean pressure. The surface contact pressure, calculated according to the contact area obtained on the hard surface, was not found to be in a good agreement with the mean contact pressure determined using Tekscan (error between 10 – 17%). This confirms that determination of the contact pressure distribution is required as contact area does not provide a good indication of the mean contact pressure.

At the hard surface, the presence of tyre tread had an influence on contact area, mean and maximum soil pressures for the Trelleborg combine tyres studied (600/55-R26.5). The treaded tyre had a smaller contact area than the smooth tyre, which resulted in greater mean and maximum pressures. The presence of tyre tread was not found to have a significant effect on the resulting soil area and mean soil pressure in the soil profile. However, the tread had a significant effect on the maximum soil pressure down to a depth of 100 mm. At the greater depths of the soil profile, the resulting pressure were found not to differ significantly. Ansorge (2007) previously observed the effect of tyre cleat onto the soil bulk density changes. His research showed that this effect was found in the soil profile down to 150 mm.

Surprisingly, changing the tyre ply rating, from 8 to 16 ply, for the range of the 11.50/80–15.3 Goodyear implement tyres evaluated in this project, did not have a significant effect on the mean and maximum contact pressure and on the resulting soil pressures in the profile. We, therefore, have to conclude that the carcass stiffness for this range of tyres, considered as the difference between the contact pressure and

inflation pressure, is the same independent of ply rating. In order to reinforce pneumatic tyres four parameters can be used; these are: carcass ply material, number of plies, construction configuration and bead reinforcement (Goodyear, 2009). Usually, a combination of these parameters is used in order to increase tyre load carrying capacity. The results obtained in this study for the implement tyres show that an increase in the load carrying capacity of these tyres did not result in an increase in the resulting surface and subsurface pressures. This implies that an increased tyre load capacity of these tyres is not related to change in their carcass stiffness, understood as the difference between the resulting contact pressure and tyre inflation pressure. This confirms that there are different ways of increasing loading ability of tyres and that does not have to be associated with an increased resulting pressures. Therefore, this particular range of implement tyres with different ply ratings, but similar loads and inflation pressures, would have similar pressure distributions and ultimately result in similar amounts of soil compaction.

In order to maintain low soil pressures below agricultural tyres, it is recommended to keep the tyres at low inflation pressure and load. As change in tyre ply rating does not lead to a change in soil pressures below the 11.50/80–15.3 Goodyear implement tyres studied, therefore, selection of these tyres should be based on the loading requirement. As the presence of tyre tread was not found to have a significant effect on the soil pressure in the soil profile for the 600/55-R26.5 Trelleborg tyres, it is recommended to select these tyres with the most appropriate tyre tread for traction and self-cleaning purposes.

10 FINAL CONCLUSIONS

The following conclusions can be drawn, based on the work included in this thesis, which was aimed at determining an effective method to measure pressure distribution under a range of agricultural tyres. From this tyre carcass stiffness, surface contact pressures and resulting subsurface soil pressures were determined.

1. It has been possible to enhance the capabilities of a commercial pressure mapping system (Tekscan) to record the pressures resulting from a selection of agricultural tyres on hard surfaces and within the soil profile (placed on a 70 mm thick steel plate at the appropriate depth). This has enabled the pressures to be determined with improved accuracy and spatial resolution. The main system improvements are:
   i. the use of a purpose built pneumatic calibration device,
   ii. a multi-point per-sensel calibration using a 4^{th} order polynomial regression curve,
   iii. a sensel selection which discards any sensing elements that fail to meet calibration criteria (this together with (i) and (ii) above reduces the error of recording from +/- 20% to +/- 4%),
   iv. where appropriate, to take account of the spatial resolution of the sensors, normalising the sum of the recorded pressure to be equal to the known applied load, and
   v. a data processing method (using Matlab) to produce a plan of the pressure contact patch.

   The data from the soil profile was of a similar order of magnitude to that observed by a previous study using pressure transducers.

2. The Tekscan study confirmed that an increase in tyre inflation pressure and load, results in an increase in both tyre mean and maximum surface contact pressure and subsurface pressure through the soil profile.

3. Tyre carcass stiffness was determined according to the pressure difference method, where the mean and maximum contact pressures of the tyre footprint were measured using the Tekscan system. This allowed the following methods of carcass stiffness estimation to be evaluated:
    i. The pressure difference method using ink to estimate the size of the contact patch and hence mean contact pressure,
    ii. Tyre load - deflection method,
    iii. Tyre manufacture specification data method.

    Both methods (i) and (ii) were found to give lower results, which were approximately equal to 30 – 50% of the tyre carcass stiffness obtained by Tekscan system. The methods developed in this study, based on tyre manufacture specification data, gave a better estimation of the mean tyre carcass stiffness. The estimation of the tyre carcass stiffness according to the theoretical load that the tyre is able to sustain at zero inflation pressure, gave the best agreement with the mean carcass stiffness which was found to be within +/- 20% of that recorded by Tekscan.

4. It is not possible to estimate the maximum carcass stiffness from methods (i), (ii) and (iii) in (3) above. Tekscan system, however, can be used to determine the maximum carcass stiffness, which was found to be 2.5 – 4 times greater than the mean carcass stiffness.

5. Contrary to expectation and the trend in the experimental data, the changes in the tyre ply rating (from 8 to 16) of the particular size of implement tyre (Goodyear, 11.50/80–15.3) examined did not have a significant effect on the mean and maximum contact pressure and on the soil pressures in the profile under the implement tyres evaluated and hence, did not significantly influence carcass stiffness.

6. Tyre tread has a significant effect on the contact area, mean and maximum contact pressure generated on a hard surface by the rear combine tyres studied (Trelleborg, 600/55-R26.5). Tyre tread was found not to have an effect on the soil area and mean contact pressure in the soil profile. The maximum soil pressure, however, was found to be significantly influenced by the tyre tread. This effect was only significantly different in a soil profile of 0 – 100 mm.

7. For the smooth rear combine tyre (Trelleborg, 600/55-R26.5), the pressured area under the tyre in the soil profile increases in a near linear manner from the surface to 400 mm, after which the rate of increase starts to decrease. This could however, be related to the data truncation effect. The increase in area is thought to result from the predominant increase in the length of the affected area, as earlier suggested by Ansorge (2007), that the width of the disturbed area below agricultural tyres is not affected by soil depth. This relationship explains the hyperbolic decrease in soil pressure with depth found in this and many other studies.

8. Measuring the contact area on a hard surface using either the ink method or the Tekscan system method gave close agreement. It is argued, therefore, that either technique can be adopted for the determination of tyre "contact area". These methods, however, should not be used for an estimation of the mean contact pressure on a hard surface, as it is argued that the "edge effect" of the perimeter of the "indicated" contact patch, does not transmit any significant load to the underlying surface.

9. In order to provide practical assistance in the selection of tyres with the lowest mean contact pressure the carcass stiffness estimated from the tyre manufacturer specification data should be used. To make this more user-friendly the intercept data for the zero load should be included in the tyre manufacturer's specification.

REFERENCES

Abeels, P.F.J., 1976, Tyre deflection and contact studies, Journal of Terramechanics, 13(3), 183 – 196.

Aboaba, F.O., 1969, Effects of Time on Compaction of Soils by Rollers, Trans. ASAE 11, 302 – 304.

Ageikin, Y.S., 1959, Determination of the deformation and the ground pressure parameters in soft ground, in Russian, Automobilnaya Promyshlennost No. 5.

Agricultural Training Board, 1989, Tyres and traction Technical Note, 245.3/TN, 12/89.

Ansorge, D., 2005, Comparison of soil compaction below wheels and tracks, MSc by Research Thesis, Cranfield University, Silsoe, England.

Ansorge, D. and Godwin, R.J., 2006, High Axle Load – Track – Tire Comparison, In: Advances in GeoEcology, Soil Management for Sustainability, edited by Horn, R. *et al.*, CATENA VERLAG GMBH, Germany.

Ansorge, D., 2007, Soil reaction to heavily loaded rubber tracks and tyres, PhD thesis, Cranfield University, Silsoe, England.

Ansorge, D. and Godwin, R.J., 2007, The effect of tyres and a rubber track at high axle loads on soil compaction, Part 1: Single axle-studies, Biosystems Engineering, 98 (1), 115 – 126.

Antille, D.L., Ansorge, D., Dresser, M.L., Godwin, R.J., 2008, The effects of tyre size on soil deformation and soil bulk density changes, Paper Number: 083879, ASABE Annual International Meeting, Providence, Rhode Island (29 June – 2 July 2008).

Arvidsson, J., Keller, T., 2004, Soil precompression stress I: A survey of Swedish arable soils, Soil Tillage Research, 77(1), 85 – 95.

Arvidsson J., Trautner, A., Keller, T., 2002, Influence of tyre inflation pressure on stress and displacement in the subsoil, in: Pagliai, M., Jones, R., Sustainable land management – environmental protection. A soil physical approach, Advances in Geoecology 35, Reiskirchen: Catena Verlag, 331 – 338.

Autodesk Inventor Professional software, 2004, Inventor 9.0.

Avery, B.W., Bascomb, C.L., 1982, Soil survey laboratory methods, Soil Survey Technical Monograph No. 6.

Bateman, H.P., 1959, Effects of basic tillage methods and soil compaction on corn production, Bulletin No. 645, Agricultural Experiment Station, University of Illinois, USA.

Bateman, H.P., 1963, Effect of field machine compaction on soil physical properties and crop response, Transactions of ASAE, 6(1), 19 – 24.

Bekker, M.G., 1956, Theory of land locomotion: the mechanics of vehicle mobility, The University of Michigan Press, USA.

Bekker, M.G., 1960, Off-the-road locomotion, University of Michigan Press, Ann Arbor.

Bekker, M.G. and Janosi, Z., 1960, Analysis of towed pneumatic tires moving in soft ground, U.S. Army OTAC, Land Locomotion Laboratory Report RR-6.

Bekker, M.J., 1969, Introduction to terrain-vehicle systems, University of Michigan Press, Ann Arbor.

Blackwell P.S. and Soane B.D, 1981, A method of predicting bulk density changes in field soils resulting from compaction by agricultural traffic, Journal of Soil Science, 32, 51 – 65.

Bodman, G.B., Constantin, G. K., 1965, Influence of particle size distribution in soil compaction, Hilgardia, 36(15), 567 – 591.

Boone, F.R., 1988, Weather and other environmental factors influencing crop responses to tillage and traffic, Soil & Tillage Research, 11, 283 – 324.

Boussinesq, J., 1885, Application des potentiels á l'étude de l'équilibre et du mouvement des solides élastiques (Application of potential theory in a study of equilibrium and motion of elastic solids), Gauthier-Villars, Paris.

Brady, N.C. and Weil, R.R., 2008, The nature and properties of soils, published by Prentice Hall, 14th edition.

Brimacombe, J., Anglin C., Hodgson A., Wilson D., 2005, Validation of calibration techniques for Tekscan pressure sensors, Proceedings of the 20th International Society of Biomechanics, Cleveland, OH.

Browne, A., Ludema K.C., Clark, S.K., 1981, Contact between the tire and roadway, In: S.K. Clark, Editor, *Mechanics of Pneumatic Tires*, U.S. Department of Transportation, Washington, DC (1981), 315–317.

Buis, A.W.P., Convery, P., 1997, Calibration problems encountered while monitoring stump/socket interface pressures with force sensing resistors: techniques adopted to minimise inaccuracies, Prosthet Orthot Int, 21, 179 – 182.

Burt, E.C., Wood, R.K., Bailey, A.C., 1992, Some comparison of average to peak soil-tire contact pressures, Transactions of ASAE, 35(2), 401 – 404.

Burt, E., C., Wood, R., K., Bailey, A., C., 1989, Effects of dynamic load on normal soil-tire interface stresses. Transactions of ASAE, 32(6), 1843 – 1846.

Burt, E.C., Bailey, A.C., Wood, R.W., 1987, Effects of soil and operational parameters on soil-tire interface stress vectors. Journal of Terramechanics, 24(3), 235 – 246.

Carpenter, T, 2003, Horse power to traction power, Agricultural Heritage Museum, South Dacota State, hppt://www.agmuseum.com/horsetotractor.html (accessed on 15 December 2006).

Chamen, W.C.T., Chittey E.T., Howse, K.R., 1987, The effect of different tyre/soil contact pressures on soil and crop responses when growing winter wheat: year 3 – 1984 – 85, Div. Note DN 1432, AFRC IER, Silsoe, England.

Chancellor, W.J., 1976, Compaction of soil by agricultural equipment, Bulletin 1881, Div. Agric. Sci., University of California, Davis, USA.

Christov, I., 1969, Niektoré poznatky získané meraním napätia pôdy pod traktorovými kolesami (Some information obtained by soil stress measurement under tractor wheels), Acta. Tech. Ag., 4, 217 - 288, University of Agriculture, Nitra, Czechoslovakia.

Clarke and Cooke, 2004, A basic course in Statistics**,** Hodder Arnold Publication, London.

Craig, R.F., 1997, Soil mechanics, 6th edition, E & FN Spon.

Dain-Owens, A.P., 2010, The effect of soil pressures generated by surface traffic as indicated by damage to buried archaeological artefacts, PhD thesis, Cranfield University, UK.

Das, K.C., 1972, Dynamics of corn root growth as affected by compact subsoil and its influence on crop response to irrigation, Unpublished PhD thesis, University of California, Davis, USA.

Dawson, J.R., Pearson, G., 1985, An experimental central tyre inflation system, National Institute of Agricultural Engineering, Divisional Note DN 1257, England.

Day, R.W., 2001, Soil testing manual – procedures, classification data and sampling practices, McGraw-Hill, Inc.

DeMarco, A.L., Rust, D.A., Bachus, K.N., 2000, Measuring contact pressure and contact area in orthopedic applications: Fuji Film vs. Tekscan, 46th Annual Meeting of Orthopedic Research Society, 12 – 15 March, 2000, Orlando, Florida.

Department of Primary Industries and Water, Managing Natural Resources, http://www.dpiw.tas.gov.au/inter.nsf/WebPages/TTAR-5DSVB7?open (accessed in October 2007).

Diserens, E., 2006, Calculating the contact area of farming trailer tyres in the field, Proceedings of International Soil Tillage Research Organization 17th Triennial Conference, Kiel, Germany.

Douglas, J.T., 1990, Conventional, reduced ground pressure and zero traffic systems in ryegrass grown for silage, 1989, Dep. Note 34, Scott. Centre Agric. Engng, Penicuik.

Dresser, M.L., Blackburn, D.W.K., Stranks, S.N., Dain-Owens, A.P., Godwin, R.J., 2006, Effects of tillage implements and vehicle loads on buried archeology, Proceedings of International Soil Tillage Research Organization 17th Triennial Conference, Kiel, Germany.

Drewniak, E.I., Crisco, J.J., Spenciner, D.B., Fleming, B.C., 2007, Accuracy of circular contact area measurements with thin-film pressure sensors, Journal of Biomechanics, 40, 2569–2572.

Dwyer, M.J., 1983, Soil dynamics and the problems of traction and compaction, Agricultural Engineer, 38(3), 62 – 68.

Dwyer, M.J., Febo, P., 1987, Handbook of agricultural tyre performance, AFRC Institute of Engineering Research, Report no. 47.

Eatough, K., 2002, Tractive performance of 4x4 tyre treads on pure sand, Unpublished EngD. Thesis, Cranfield University, Silsoe, England.

Eberan-Eberhorst, R., 1965, Zur Theorie des Luftreifens, A.T.Z. Vol. 67, No. 8.

Ferguson-Pell, M., Hagisawa, S. and Bain, D., 2002, Evaluation of a Sensor for Low Interface Pressure Applications, Medical Engineering & Physics.

Flocker, W.J., Vomocil, J.A., Vittum, M.T., 1958, Response of winter cover crops to soil compaction, Proceedings, Soil Science Society of America, 22(2), 181 – 184.

Fountaine, E.R., Payne, P.C.J., Hawkins, J.C., 1952, The effect of tractors on volume weight and other soil properties, National Institute of Agricultural Engineering, Report No. C.S. 17, Silsoe, England.

Fröhilch, O.K., 1934, Druckverteilung im Baugrunde (Formulas of Boussinesq), Springer Verlag, Vienna.

Gebhardt, S., Fleige, H., Horn, R., 2006, Stress-deformation behavior of different soil horizons and their change in saturated hydraulic conductivity as a function of load,

Proceedings of International Soil Tillage Research Organization 17th Triennial Conference, Kiel, Germany.

Gee-Clough, D., McAllister, M., Pearson, G. And Evernden, D. W., 1978, The empirical prediction of tractor-implement field performance, Journal of Terramechanics, 15(2), 81 – 94.

Gill, W.R., VandenBerg, G.E., 1968, Soil dynamics in tillage and traction, Agriculture Handbook No. 316, Agricultural Research Service, United States Department of Agriculture, Washington DC.

Godbole, R., Alcock, R., Hettiaratch, D., 1993, The prediction of tractive performance on soil surface, Journal of Terramechanics, 30(6), 443 – 459.

Godwin, R.J., Magalhaes, P.S.G., Miller, S.M, Fry, R.K., 1987, Instrumentation to study the force systems and vertical dynamic behaviour of soil-engaging implements, Journal of Agricultural Engineering Research, 36, 301 – 310.

Godwin, R.J., 1975, An extended octagonal ring transducer for use in tillage studies, Journal of Agricultural Engineering Research 20 (4), 347-352.

Godwin, R.J., 1974, An investigation into the mechanics of narrow tines in frictional soils, In: *Ph.D. thesis*, University of Reading, Reading, UK.

Goodyear, 2009, Personal consultation with Goodyear.

Gordon, J.E., 2006, The new science of strong materials, or, Why you don't fall through the floor, Princeton University Press, page 52.

Gordon, J.E., 1978, Structures or Why things don't fall down, Pitman Publishing Limited, London.

Gunjal, K.R., Raghavan, G.S.V., 1986, Economic analysis of soil compaction due to machinery traffic, Applied Engineering in Agriculture, 2, 85 – 88.

Gysi, M., Maeder, V., Weisskopf P., 2001, Pressure distribution underneath tires of agricultural vehicles, Transactions of the ASAE, 44(6), 1385 – 1389.

Håkansson, I., Reeder, R., 1994, Subsoil compaction by vehicles with high axle load-extent, persistence and crop response. Special Issue: Subsoil compaction by high axle load traffic. Soil and Tillage Research. 29, 277 – 304.

Hallonborg, U., 1996, Super ellipse as tyre-ground contact area, Journal of Terramechanics, 33(3), 125 – 132.

Harris, M.L., Morberg, P., Bruce, W.J.M., Walsh, W.R., 1999, An improved method for measuring tibiofemoral contact areas in total knee arthroplasty: a comparison of K-Scan sensor and Fuji film, Journal of Biomechanics 32, 951–958.

Heuer, H., Tomanova, O., Koch, H. J., 2006, Effect of repeated passes of heavy agricultural machinery on soil structure and sugar beet growth in central Germany, Proceedings of International Soil Tillage Research Organization 17th Triennial Conference, Kiel, Germany.

Horn, R., Lebert, M., 1994, Soil compactability and compressibility. In: Soane, B. D., van Ouwerkerk, C., Soil compaction in crop production, Published by Elsevier Science B. V., The Netherlands, 45 – 69.

Horn, R., Fleige, H., Peth, S. and Peng, X., 2006, Soil management for sustainability, Advances in GeoEcology, The 17th Triennial International Soil Tillage Research Conference, CATENA VERLAG GMBH, Germany.

Inns, F.M., Kilgour, J., 1978, Agricultural tyres, Dunlop Limited, London.

Jumikis, A. R., 1962, Soil mechanics, D. Van Nostrand Company, Inc., Princeton, New Jersey.

Karafiath, L.L., Nowatzki, E.A., 1978, Soil mechanics for off-road vehicle engineering, 1st edition, Trans Tech Publications, Germany.

Karafiath, L.L., Nowatzki, E.A., 1975, Soil mechanics for off-road vehicles, Trans Tech Publications, Aedermannsdorf, Switzerland.

Keller, T., 2004, Soil compaction and soil tillage – studies in agricultural soil mechanics, Doctoral Thesis, Agraria 489, Swedish University of Agricultural Science, Uppsala, Sweden.

Keller, T. and Arvidsson, J., 2004, Technical solutions to reduce the risk of subsoil compaction: effects of dual wheels, tandem wheels and tyre inflation pressure on stress propagation in soil, Soil and Tillage Research, Vol. 79, No. 2, 191 – 205.

Keller, T. and Arvidsson, J., 2006, Prevention of traffic-induced subsoil compaction in Sweden: Experiences from wheeling experiments, Archives of Agronomy and Soil Science, 52(2), 207 – 222.

Keller, T., Arvidsson, J., Dawidowski, J. B., Koolen, A. J., 2004, Soil precompression stress II: A comparison of different compaction tests and stress-displacement behaviour of the soil during wheeling, Soil Tillage Research, 77(1), 97 – 108.

King, D.W., 1969, Soils of Bedford and Luton District, Soil Series of England and Wales, Harpenden, UK.

Kirby, J.M, 1991, Strength and deformation of agricultural soil: Measurement and practical significance, Soil Use Manage 7(4), 223 – 229.

Kirby, J.M., Blunden, B.G., Trein, C.R., 1997, Simulating soil deformation using a critical-state model: II. Soil compaction beneath tyres and tracks, European Journal of Soil Science, 48(1), 59 – 70.

Kolobov, G.G., 1966, Soil pressure measurements beneath tractor tyres, Journal of Terramechanics, 3(1), 9 – 15.

Komandi, G., 1976, The determination of the deflection, contact area, dimensions and load carrying capacity for driven pneumatic tires operating on concrete pavement, Journal of Terramechanics, 13(1), 15 – 20.

Koolen, A.J., 1995, Mechanics of soil compaction, In: Soane, B. D., van Ouwerkerk, C., Soil compaction in crop production, Published by Elsevier Science B. V., The Netherlands, 23 – 44.

Koolen, A.J., 1974, A method for soil compactability determination, Journal of Agricultural Engineering, 19(3), 271 – 278.

Koolen, A.J., Kuipers, H., 1983, Agricultural soil mechanics: Advanced series in agricultural science, Vol. 13, Heidelberg: Springer.

Krick, G., 1969, Radial and shear stress distribution under rigid wheels and pneumatic tyres operating on yielding soils with consideration of tyre deformation, Journal of Terramechanics, 3, 73 – 98, Pergamon Press.

Kuipers, H., van de Zande, J.C., 1994, Quantification of traffic systems in crop production, in Soane, B.D., van Ouwerkerk, C., Soil compaction in crop production, Developments in Agricultural Engineering 11, Published by Elsevier Science B. V., The Netherlands.

Kumar, P. and Dewangan, K.N., 2004, Deflection and contact characteristics of a power tiller tyre, Agricultural Engineering International: the CIGR Journal of Scientific Research and Development, Manuscript PM 03 006, January, 2004.

Lamande, M., Schjonning, P., Togersen, F. A., 2006a, Tests of basic aspects of stress transmission in soil, Proceedings of International Soil Tillage Research Organization 17th Triennial Conference, Kiel, Germany.

Lamande, M., Schjonning, P., Droscher, P., Steffensen, F.S.F., Rasmussen, S.T., Koppelgaard, M., 2006b, Measuring vertical stress and displacement in two dimensions in soil during a wheeling event, Proceedings of International Soil Tillage Research Organization 17th Triennial Conference, Kiel, Germany.

Lamande, M., Schjonning, P., 2008, The ability of agricultural tyres to distribute the wheel load at the soil-tyre interface, Journal of Terramechanics, 45, 109 – 120.

Lebert, M., Burger, N., Horn, R., 1989, Effects of dynamic and static loading on compaction of structured soils, In: Larson, W. E., Blake, G. R., Allmaras, R. R.,

Voorhees, W. B., Gupta, S., Mechanics and related processes in structured agricultural soils, NATO ASI Series E, Applied Science 172, Dordrecht: Kluwer Academic Publishers, 73 – 80.

Lines, J.A., 1991, The suspension characteristics of agricultural tyres, PhD thesis, Cranfield University.

Lines, J.A., Murphy, K., 1991, The stiffness of agricultural tractor tyres, Journal of Terramechanics, 28(1), 49 – 64.

Lyles, L., Woodruff, N.P., 1963, Effects of moisture and soil packers on consolidation and cloddiness of soil, Transactions of ASAE, 6(4), 273 – 275.

Mander, A.L., McMullan, T.A.G., 1986, Comparison of the effects of various levels of contact pressure on a yield of permanent grassland, Div. Note DN 1364, National Institute of Agricultural Engineering, Silsoe, England.

Matlab, 2005, Matlab software version 7.1, Natick, MA, The MathWorks, Inc.

Maurer, J.R., Loitz-Ramage, B., Andersen, M. at al., 2003, Prosthetic socket interface pressures: Customized calibration technique for the TEKSCAN F-socket system, Summer Bioengineering Conference, Florida, 2003.

McKyes, E., Negi, S., Douglas, E., Taylor, F., Raghavan, V., 1979, The effect of machinery traffic and tillage operations on the physical properties of a clay and on yield of silage corn, Journal of Agricultural Engineering Research, 24, 143 – 148.

McLeod, H.E., Reed, I.F., Johnson, W.H., Gill, W.R., 1966, Draft, power efficiency and soil compaction characteristics of single, dual and low pressure tyres, Transactions of ASAE, 41 – 44.

Misiewicz, P.A., 2005, An investigation into the performance and development of a simple prediction model for the Spira-Lock anchor system, MSc thesis, Cranfield University at Silsoe, UK.

Misiewicz, P.A., Richards, T.E., Hann, M.J., and Godwin, R.J., 2007, Techniques for estimating the equivalent pressure from tyre carcass stiffness, 495-502, Proc. XXXII CIOSTA – CIGR Section V Conf., Nitra, Slovakia (September, 2007).

Misiewicz, P.A., Richards, T.E., Blackburn, K., Brighton, J.L., Hann, M.J., and Godwin, R.J., 2008, Techniques for estimating contact pressure resulting from loaded agricultural tyres, Paper Number: 083511, ASABE Annual International Meeting, Providence, Rhode Island (29 June – 2 July 2008).

Misiewicz, P.A., Richards, T.E., Blackburn, K., Hann, M.J., and Godwin, R J., 2009, Evaluation of the contact pressure distribution of a rear combine tyre on a hard surface, Tire Society Conference, Akron, OH (15 – 16 September 2009).

Negi, S.C., McKyes, E., Raghavan, G.S.V. and Taylor, F., 1981, Relationships of field traffic and tillage to corn yields and soil properties, Journal of Terramechanics, Vol. 18, No. 2, 81 – 90.

Oida, A., Satoh, A., Itoh, H. and Triratanasirihai, K., 1988, Measurement and analysis of normal longitudinal and lateral stresses in the wheel-soil contact area, Proceedings of the 2nd Asia-Pacific Conference of the International Society for Terrain-Vehicle Systems.

Oliver, M.J., 2002, Contact patch dynamics of pneumatic tyres in pure sand, Unpublished EngD. Thesis, Cranfield University, Silose, England.

Painter, D, 1981, A simple deflection model for agricultural tyres, Journal of Agricultural Engineering Research, 26 (1), 9 – 20.

Plackett, C.W., 1982, The prediction of forces acting on off-the-road wheels – a review, National Institute of Agricultural Engineering, Divisional Note DN 1112, England.

Plackett C.W., 1983, Hard surface contact area measurement for agricultural tyres, National Institute of Agricultural Engineering, Divisional Note DN 1200, England.

Plackett, C.W., 1984, The ground pressure of some agricultural tyres at low load and with zero sinkage, Journal of Agricultural Engineering Research, 29, p. 159 – 166.

Plackett C.W., 1985, A review of force prediction methods for off-road wheels, Journal of Agricultural Engineering Research, 31, 1 – 29.

Plackett, C.W., 1986, Instrumentation to measure the deformation and contact stress of pneumatic tyres operating in soft soil, Div. Note DN 1322, National Institute of Agricultural Engineering, Silsoe, England.

Plackett C.W., Clemens K., Dwyer, M. J., Febo, P., 1987, The ground pressure of agricultural tyres, AFRC Institute of Engineering Research, Report No.49.

Poodt, M.P., Koolen, A.J., van der Linden, J.P., 2003, FEM analysis of subsoil reaction on heavy wheel loads with emphasis on soil preconsolidation stress and cohesion, Soil Tillage Res, 73(1-2), 67 – 76.

Pottinger, M.G., 2006, Contact patch (footprint) phenomena, In: The Pneumatic Tire, US Department of Transportation, National Highway Traffic Safety Administration.

Pytka, J., 2006, Correlation between tractive forces and soil stresses – a background for wheel – soil interaction modeling, Proceedings of International Soil Tillage Research Organization 17th Triennial Conference, Kiel, Germany.

Raper, R.L., Bailey, A.C., Burt, E.C., Way, T.R., Liberati, P., 1995a, The effects of reduced inflation pressure on soil-tyre interface stresses and soil strength, Journal of Terramechanics, Vol. 32, No. 1, 43 – 51.

Raper, R.L., Johnson, C.E., Bailey, A.C., Burt, E.C., Block, W.A., 1995b, Prediction of soil stresses beneath a rigid wheel, Journal of Agricultural Engineering Research, 61, 57 – 62.

Reaves, C.A., Cooper, A.W., 1960, Stress distribution in soils under tractor loads, Agricultural Engineering, 20 – 21.

Reintam, E., Kuht, J., Trukmann, K., Raats, V., 2006, Soil compaction and fertilization effect on weed community and nutrient uptake on spring barley field, article in R. Horn, H. Fleige, S. Peth, X. Peng, 2006, Soil management for sustainability, Edited by Advances in GeoEcology, Germany.

Rose, J. and Stith, J., 2004, Tekscan Sensors – Rail/Tie Interface Pressure Measurement in Railway Trackbeds, Proceedings of Railway Engineering, 7th International Conference and Exhibition, London, United Kingdom, June.

Rowland, D., 1972, Tracked vehicle ground pressure and its effect on soft ground performance, vol. 1, Proceedings 4th International Conference of International Society for Terrain-Vehicle Systems, 24 – 28 April 1972, Stockholm.

Rusanov, V.A., 1994, USSR standards for agricultural mobile machinery: permissible influences on soil and methods to estimate contact pressure and stress at depth 0.5m, Soil Tillage Research, 29, 249 – 252.

Saarilahti, M., 2002, Evaluation of the WES-method in assessing the trafficability of terrain and the mobility of forest tractors, University of Helsinki, Department of Forest Resource Management.

Schafer, R.L., Johnson, C.E., Koolen, A.J., Gupta, S.C., Horn, R., 1992, Future research needs in soil compaction, Transactions of the ASAE, 35(6), 1761 – 1770.

Schjonning, P., Lamande, M., Togersen, F. A., Arvidsson, J., Keller, T., 2006a, Distribution of vertical stress at the soil-tyre interface: effects of tyre inflation pressure and the impact on stress propagation in the soil profile, article in R. Horn, H. Fleige, S. Peth, X. Peng, 2006, Soil management for sustainability, Edited by Advances in GeoEcology, Germany.

Schjonning, P., Lamande, M., Togersen, F.A., Pedersen, J., Hansen, P.O.M., 2006b, Reduction of soil compaction. Magnitude and distribution of stress in the contact area between wheel and soil. Report No. Markburg 127. The Danish Institute of Agricultural Sciences, Tjele, Denmark (in Danish with English summary).

Schjonning, P., Lamande, M., Togersen, F.A., Arvidsson, J., Keller, T., 2008, Modelling effects of tyre inflation pressure on the stress distribution near the soi-tyre interface, Biosystems Engineering, 99, 119 – 133.

Schwanghart, H., 1991, Measurement of contact area, contact pressure, and compaction under tyres in soft soil, Journal of Terramechanics, 28(4), 309 – 318.

Sharma, A.K., Pandey, K.P., 1996, A review on contact area measurement of pneumatic tyres on rigid and deformable surfaces, Journal of Terramechanics, 33(5), 253 – 264.

Simon, M., 1964, Les compacteurs a pneus en construction routiers, Annales de l'Institut Technique du Batiment et des Travaux Public, No. 193.

Smith, D.L.O., 1985, Compaction by wheels: a numerical model for agricultural soils, Journal of Soil Science, 36, 621 – 632.

Smith, D.L.O., Dickson, J. W., 1984, On the contributions of ground pressure and vehicle mass to soil compaction for vehicles carrying high and low payloads, Dep. Note SIN/411, Scot. Inst. Agric. Engng, Penicuik.

Smith, D.L.O., Dickson, J. W., 1988, The contribution of vehicle weight and ground pressure to soil compaction, International Conference on Agricultural Engineering, Paris.

Smith, D.L.O., Dickson, J. W., 1990, Contribution of vehicle weight and ground pressure to soil compaction, Journal of Agricultural Engineering Research, 46, 13 – 29.

Soane, B.D., 1983, Compaction by agricultural vehicles, Scottish Institute of Agricultural Engineering (SIAE), Technical Report 5.

Soane, B.D, Blackwell, P.S., Dickson, J.W. and Painter, D.J., 1981, Compaction by agricultural vehicles: a review, I. Soil and wheel characteristics, Soil Tillage Res., 1, 207 – 237.

Soane, B.D., Dickson, J.W. and Blackwell, P.S., 1979, Some options for reducing compaction under wheels on loose soil, Proc. 8th Conf. Int. Soil Tillage Res. Organ., Stuttgart, 2, 347 – 352.

Soane, B.D., Dickson, J.W. and Campbell, D.J., 1982, Compaction by agriculture vehicles: a review, III. Incidence and control of compaction in crop production, Soil Tillage Res., 2, 3 – 36.

Soane, B.D. and Ouwerkerk, C., 1994, Soil compaction in crop production, published by Elsevier, The Netherlands.

Soanes, C. and Hawker, S., 2005, Oxford English Dictionary, Third Edition Oxford: Oxford University Press.

Söhne, W.H., 1952, Stress transmission between tractor tyres and arable soils, Grundlagen der Landtechnik, 3, 75 – 87.

Söhne, W.H., 1953, Pressure distribution in and deformability of agricultural soil, Translation 37 from Kolloid Zeitschrift, 131, 89-96, NIAE, Silsoe, England.

Söhne, W.H., 1958, Fundamentals of pressure distribution and soil compaction under tractor tyres, Agricultural Engineering, 39, 276 – 281, 290.

Spoor, G., Godwin, R.J., 1978, An experimental investigation into the deep loosening of soil by rigid tines, Journal of Agricultural Engineering Research, 23, 243 – 258.

Srivastava, A.K., Goering, C.E., Rohrback, R.P, 1993, Tires and Traction: Engineering Principles of Agricultural Machines, ASAE Textbook 6.

Stadie, A.L., 1987, The effect of tyre contact pressure on grass yield during spring application of fertilizer, Div. Note DN 1425, AFRC Inst. Engng Res., Silsoe, England.

Stafford, J.V., de Carvalho Mattos, P., 1981, The effect of forward speed on wheel-induced soil compaction: laboratory simulation and field experiments, Journal of Agricultural Engineering Research, 26, 333 – 347.

Statistica 9, 2009, Statistical analysis software, StatSoft, Inc., Tulsa, OK.

Steiner, M., 1979, Analyse, synthese und berechnungsmethoden der triebkraft-schlup-kurve von luftreifen auf nachgiebigem boden, Forschungsbericht Agrartechnik des Arbeitskreises Forschung und Lehre der Max-Eyth-Gesellschaft (MEG) 33. Dissertation, München.

Strutt, 1970, Modern Farming and the Soil, Report for MAFF.

Sumiya, T., Suzuki, Y., Kasahara, T. and Ogata, H., 1998, Sensing stability and dynamic response of the F-scan in-shoe sensing system: A technical note, Journal of Rehab. Res. Devel., 35, 192 – 200.

Trabbic, G.W., Lask, K.V., Buchele, W.F., 1959, measurement of soil-tyre interface pressures, Agricultural Engineering, 40(11), 678 – 681.

Taylor, J.H. and Gill, W.R., 1984, Soil compaction: State-of-art report, Journal of Terramechanics, 21(2), 195 – 213.

Tekscan, 2008a, Tekscan technology, available at: www.tekscan.com/technology.html (accessed on 12 March 2008).

Tekscan, 2008b, Tekscan home page, available at: www.tekscan.com (accessed on 15 June 2008).

Tekscan, 2006, Tekscan I-Scan User Manual, Tactile force and pressure measurements system, v. 5.8x, published by Tekscan Inc, South Boston, MA.

Tijink, F.G.J., 1994, Quantification of vehicle running gear, In: Soil compaction in crop production, Elsevier Science B. V., 391 – 415.

Trautner, A., 2003, On soil behaviour during field traffic, PhD thesis, Swedish University of Agricultural Sciences, Uppsala.

Trukmann, K., Reintam, E., Kuht, J., Raats, V., 2006, Growing of Mugwort (Artemisia vulgaris L.), Canadian Thistle (Cirsium arvense L.) and Yellow Lupine (Lupinus luteus L.) on compacted soil, article in R. Horn, H. Fleige, S. Peth, X. Peng, 2006, Soil management for sustainability, Edited by Advances in GeoEcology, Germany.

Upadhyaya, S.K., Wulfsohn, D., 1990, Relationship between tyre deflection characteristics and 2-D contact area, Transactions of ASAE, 33(1), 25 – 30.

Walczyk, M., 1995, Zastosowanie techniki wideo-komputerowej do określenia powierzchni śladu koła ogumionego (Application of video-computer technique for determination of tired wheel track surface area), Zeszyty Problemowe Postępow Nauk Rolniczych z. 426, 191 – 197.

Walczyk, M., 2000, Zastosowanie komputerowej analizy obrazu w pomiarach parametrów odkształcenia opon rolniczych, Inżynieria Rolnicza, 7, 189 – 194.

Walczyk, M., 2001, Measurements of deformation characteristics of agricultural pneumatic tyres, International Scientific Conference: Agricultural Engineering on the beginning of 21st century, 6 June 2001, Nitra, Slovakia.

Walczykova, M., Walczyk, J., 1999, Test stand for investigation of agricultural tyres operational parameters, Trends in Agricultural Engineering, 545 – 549, Prague.

Warkentin, B.P., 1971, Effects of compaction on content and transmission of water in soils in compaction of agricultural soils, ASAE monograph, Chapter 5, 126 – 153, St. Joseph, Michigan, ASAE.

Way, T.R., Kishimoto, T., 2004, Interface pressures of a tractor drive tyre on structured and loose soils, Biosystems Engineering, 87(3), 375 – 386.

Way, T.R., Kishimoto, T., Burt, E.C., Bailey, A.C., 2000, Soil-tire interface pressures of a low aspect ratio tractor tire, Advances in Geoecology 32, Reiskirchen, 82 – 92.

Waterways Experiment Station, 1964, Stresses under moving vehicles, U.S. Army Corps of Engineering Waterways Experiment Station Technical Report, No. 3-545.

Waterways Experiment Station, 1961, Tests with rigid wheels, Tech. Rpt. 3-565, Rpt. 1, Vicksburg, Miss.

Weise, 1990, Modelling soil response to a rolling tyre: a soil bin study, M. Phil. Thesis, Silose College, England.

Weissbach, M., 2001, New tyre concept for protection of soil structure, Landtechnik 56, 2, 72 – 73.

Wheeler, P.N. and Kilgour, J., 1994, An investigation to improve the self cleaning ability of Airboss segmented tyres in wet clay conditions, Silsoe College (unpubl.), England.

Whitlow, R., 2001, Basic soil mechanics, 4th edition, Harlow, Prentice Hall.

Williams, L., 1987, Design aspects affecting the off-road mobility of a four-wheel, lightweight transport vehicle, MPhil (Research) Thesis, Silsoe College, England.

Wilson D.R., Apreleva, M.V., Eichler, M.J., Harrold, F.R., 2003, Accuracy and repeatability of a pressure measurement system in the patellofemoral joint, Journal of Biomechanics, 36, 1909 – 1915.

Wirz D., Becker R., Li S.F., Friederich N.F., Muller W., 2002, Validation of the Tekscan system for statistic and dynamic pressure measurements of the human femorotibial joint, Biomed Tech, 47, 195–201.

Wulfsohn, D., Upadhyaya, S.K., 1992, Determination of dynamic three-dimensional soil-tyre contact profile, Journal of Terramechanics, 29(4/5), 433 – 464.

Van den Akker, J.J.H., 2004, SOCOMO: a soil compaction model to calculate soil stresses and the subsoil carrying capacity, Soil and Tillage Research, 79, 113 – 127.

VandenBerg, G.E., Gill, W.R., 1962, Pressure distribution between a smooth tyre and the soil, Transactions of ASAE, 5, 2, 105 – 107.

VandenBerg, G.E. and Reed. I.F., 1962. Tractive performance of radial-ply and conventional tractor tires. *Transactions of the ASAE* 5(2), 126 – 129, 132.

Vaughan, L, 2006, Early agricultural steam engines were not tractors, but stationery engines mounted on heavy beds with wheels for portability, Virtual Museum, Canada, http://www.virtualmuseum.ca/pm.php?id=record_detail&fl=0&lg=English&ex=00000174&rd=85068&hs=0 (accessed on 15 December 2006).

Voorhees, W.B., 1986, The effect of soil compaction on crop yield, 37th Annual Earthmoving Industry Conference, Society of Automotive Engineers, Technical Paper 860729, USA.

APPENDIX A

DATA PROCESSING FOR TYRE CONTACT AREA MEASUREMENTS

A method involving image processing was developed for determination of the tyre contact area on a hard surface. The area was obtained by coating a tyre with black ink and loading it onto white paper. A Canon PowerShot S45 digital camera and a Matlab program were used. The technique involves taking pictures of the tyre ink patches, the images are saved and processed in Matlab software. This technique was found to be more time efficient in comparison to a digital planimeter.

A Matlab script was developed for reading the images and counting the number of black and white pixels. The contact area is then determined in Excel according to the calibration. The camera was calibrated by taking a number of pictures of images with known areas and establishing a relationship between the number of pixels and the area (Chapter 3). The accuracy of this method of area determination was tested against the method employing an electronic planimeter. The accuracy of the digital image analysis method was found to be similar to the planimeter's technique. Therefore this method was used for the contact area measurements as it was found to be more time efficient.

After the images were read in to Matlab, all the pixels for each image were divided into 256 levels of gray as 8 bit gray scale was assumed. Number one accounts for fully black, while 256 - fully white. The data was plotted as a histogram for each image and the number of pixels that are black or white was counted. There were three ways of establishing the border between black and white, which were as follows:

- Method 1 – grouping on the following basis: lower half of the gray scale was assumed to be black and the higher scale to be white ("lower half = black", "upper half = white");
- Method 2 – grouping according to the minimum point as the deviser between black and white ("below minimum = black", "above minimum = white");
- Method 3 – finds two peaks on each histogram and does the grouping from the middle point between the two maximums

All the methods give similar results. Method 1 is the simplest way of dividing black and white pixels, but it can give some errors if pictures were taken a different amount of light than the calibration as the data set could be shifted in the gray scale. Method 2and 3 overcome this problem by looking at the histogram distribution. Method 2 was found to be too simplistic as sometimes the minimum value was not a good deviser as it was found in some random place. Method 3 was selected as it is accurate and appears to be the most effective way of overcoming the light issue described above.

Matlab image processing script is shown below:

```
% Histogram processing for tyre contact areas
% Read a scanned image and count the number of pixels that are
"black" or "white"
% Then post-process in Excel with calibration functions
clear output
fid=fopen('list.txt');
files=textread(['list.txt'],'%s','delimiter','\n','whitespace','');
fclose(fid);
 for i=1:length(files)
    % Read the image file in
    % Assumes 8 bit grayscale - eg tiff
    char(files(i))
    filedata=imread(char(files(i)));
    % Plot a histogram of the data (one bin per pixel level)
    temp=hist(single(filedata(:)),256);
    bar(temp,'hist')
    title(char(files(i)));
    % Save figures for later viewing
    saveas(gcf,[char(files(i)) '.fig']);
    saveas(gcf,[char(files(i)) '.jpg']);
    % Method 1: Crude grouping on "lower half" = black, "upper
      half" = white basis
    bins=histc(filedata(:),[0 128 256]);
    output(i,1)=length(filedata(:));
    output(i,2)=bins(1);
    % Method 2: grouping on "Below minimum=black", Above minimum
      =white"
    bins=histc(filedata(:),[0 output(i,4) 256]);
    output(i,3)=bins(1);
    % Method 3: Aims to find the top point of the two "peaks" in the
      distribution then take the area between them halfway between
      the peaks
    [a,topeak1]=max(temp(1:128));
    [a,topeak2]=max(temp(129:256));
    topeak2=topeak2+129;
    %Put the position in the output array
    output(i,4)=topeak1+((topeak2-topeak1)/2);
    disp (['Minimum Pixel level at: ' num2str(output(i,4))])
    line([output(i,4) output(i,4)],[0 max(temp(:))],'Color','R')
    pause
end
```

The data obtained by Matlab (number of black and white pixels) were then post-process in Excel by applying the calibration function and determining the contact areas.

The evaluation of the accuracy of this image processing method for the contact area determination was conducted using a number of approaches as follows:

- Measure how well a regression line approximates the real data points in the calibration data set (R^2 value)

A linear relationship was found between the area and number of pixels as presented in Figure 3.19 (Chapter 3). R^2 value of 1.000 confirmed a good agreement of the real data with the calibration values.

- Look at the repeatability of the calibration process

In order to check the repeatability of the calibration data, two images used for calibration were pictured three times and their results were compared. The average error was found to be 0.28% and 0.53% for the 10000 mm^2 square and the 70685.83 mm^2 circle, respectively. While for the planimeter resulted in 0.23% and 0.16%, respectively.

- Investigate the effect of the spatial accuracy by repeating image collection

In order to check the influence of spatial location of the images when pictures were taken two calibration images were used. Each of them had five pictures taken when located in different spatial locations of the image (centre, top left corner, top right corner, bottom left corner and bottom right corner). The results obtained for each image were compared to the real area and the maximum variation was found to be 1.6% and 0.9% for the 10000 mm^2 and 250000 mm^2 squares, respectively. When the pictures of images used for calibration and tyre contact patches were taken, they were located in the centre of the snapshot, but even if some were located some distance from it, it would not make a significant difference.

APPENDIX B

CALIBRATION OF THE TESTING EQUIPMENT

This section describes the procedures undertaken to calibrate the instrumentation (Section 3.4) used during the project together with the calibration data obtained. Because of its importance the calibration of the Tekscan sensors is presented in Chapter 4.

Normal load measuring equipment

- Extended octagonal ring transducers (EORT)

The extended octagonal ring transducers rated up to 5 tonne and 10 tonne (Godwin 1975 and 1987) were used for the tyre load measurements during the load – deflection tests and for the calibration of the hydraulic pressure sensor. The calibration of each EORT was performed by applying different known vertical loads and measuring the change of voltage when loading and unloading. It was carried out using the Avery Universal Testing machine as shown in Figure B.1. A datalogger was connected to the EORT for measuring the resulting output voltage of the EORT during the calibration. The EORT was placed in the Avery Universal Testing machine. Vertical loads were gradually applied to the transducers in 2 kN and 10 kN increments to the maximum of 30 kN and 90 kN for the 5 tonne and 10 tonne transducers, respectively, then reduced to zero in the same increments. The process of loading and unloading was repeated three times for each transducer in order to verify repeatability. Test data was collected, recorded by a computer and then plotted in Figure B.2.

Figure B.1 Calibration of the EORT on the Avery Universal device

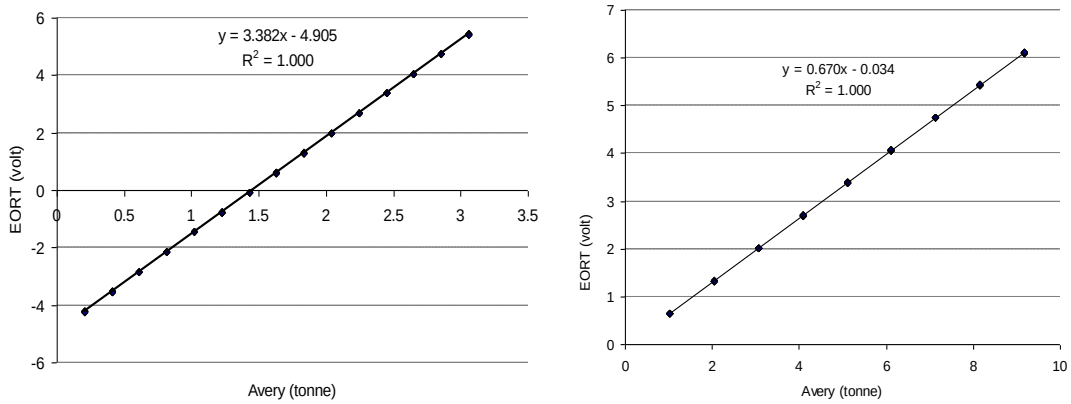

Figure B.2 EORT calibration (left: 5tonne transducer, right: 10tonne transducer)

The relationships obtained were also verified by plotting a curve that best fitted the data and the R^2 values calculated. For both extended octagonal ring transducers a close agreement was found between the resulting voltage and a given load for the three replications. A linear response was found for both transducers and very little hysteresis between the loading and unloading cycles, which were found to be 0.03% and 0.05%, for the 5 tonne and 10 tonne transducers, respectively. The R^2 values were found to be 1.000 for both transducers.

- Hydraulic pressure transducer (Sun Hydraulics)

Two hydraulic pressure transducers (Model A and B) were used for measuring normal load applied to the tyres tested in the 12 tonne loading frame. They were mounted on the hydraulic ram used on the frame for tyre load application. The calibrations were performed by applying a number of vertical loads to one of the agricultural tyres mounted in the rig using the hydraulic ram. A datalogger was connected to the pressure transducer and the EORT in order to measure the output voltage coming out of both devices. The calibration was performed with three different size tyres, one loaded up to 2.7 tonne (Model A), the other to 6.6 tonne (Model A) and the last one to 12.0 tonne (Model B). The loads applied to the tyres were continually increased up to the maximum value and then gradually decreased to zero. This process was repeated three times. Data collected was recorded and plotted as shown in Figure B.3.

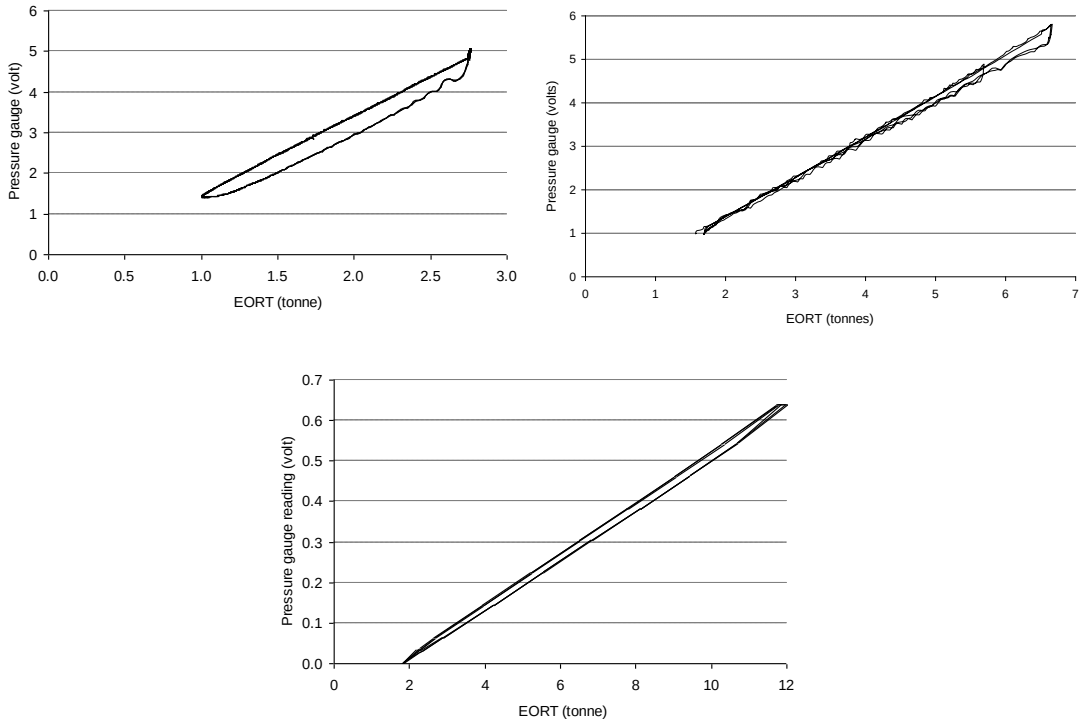

Figure B.3 Hydraulic pressure transducers calibration curves (left: maximum load of 2.7 tonne, right: maximum load of 6.6 tonne, bottom: maximum load of 12.0 tonne)

The load frame designed by Ansorge (2005) was especially designed for testing large agricultural tyres. It can be used for load application up to 12 tonne. Figure B.3 illustrates the hysteresis of the system when loading and unloading which results from drag on the linear bearing. The maximum hysteresis were found to be 9.2%, 4.6% and 3.2% of the maximum load for the lower, medium and higher load range, respectively. Figure B.4 presents regression curves that best fitted the data points obtained for each calibration test. Only values for tyres during loading were considered in the regression analysis as during the testing the tyres were loaded rather than unloaded. Linear relationships were found for both calibrations with the R^2 values being 1.000, 0.999 and 1.000 for the lower, medium and higher range calibrations, respectively. When loads were applied to the tyres, the error was from 0 to 0.25 tonne (9.21% of the maximum load), 0 to 0.30 tonne (4.62% of the maximum load) and 0 to 0.38 tonne (3.21% of the maximum load) for the lower, medium and higher calibration ranges, respectively.

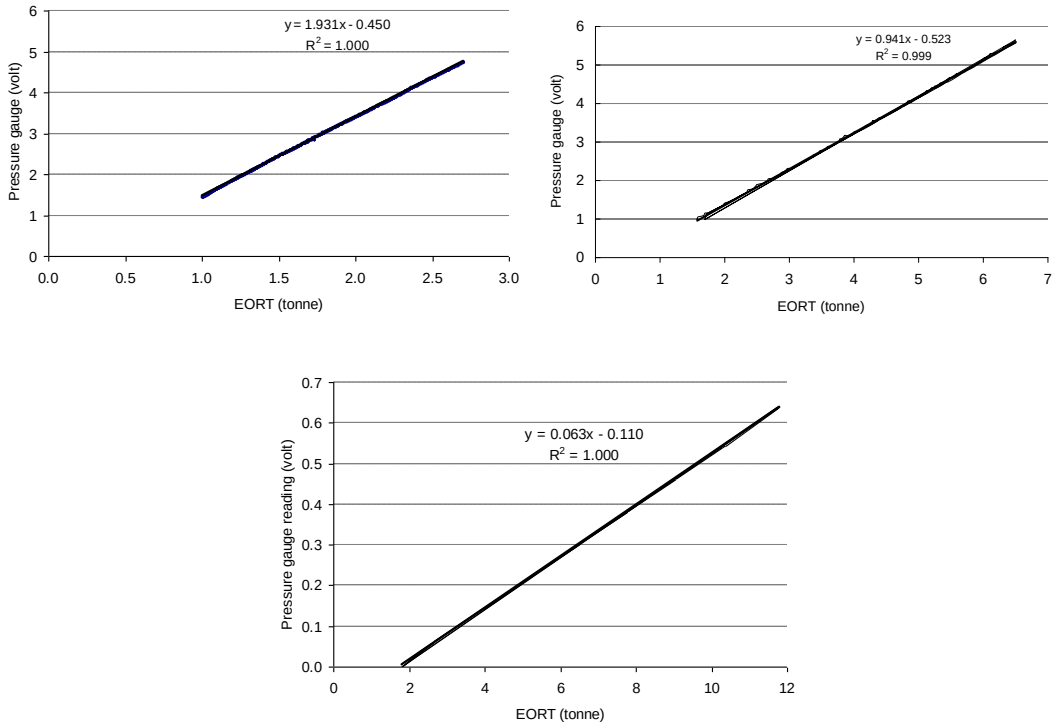

Figure B.4 Best fit curves according to the hydraulic pressure transducer calibrations (left: maximum load of 2.7 tonne, right: maximum load of 6.6 tonne, bottom: maximum load of 12.0 tonne)

- Tension link dynamometer (Staightpoint Ltd)

The dynamometer was used for tyre load measurements carried out using the 5 tonne and 0.25 tonne flames. It was calibrated twice as it needed to be used for two different pressure ranges. The calibrations were carried out by applying a range of loads to the dynamometer mounted in the Avery Universal Testing machine (calibrated yearly against a standard). The calibrations covered the range of 0 – 0.5 tonne and 0 – 2.5 tonne, with increasing and decreasing load in 0.1 tonne and 0.5 tonne increments, respectively. The procedure was repeated three times for each range and data was plotted as shown in Figure B.5.

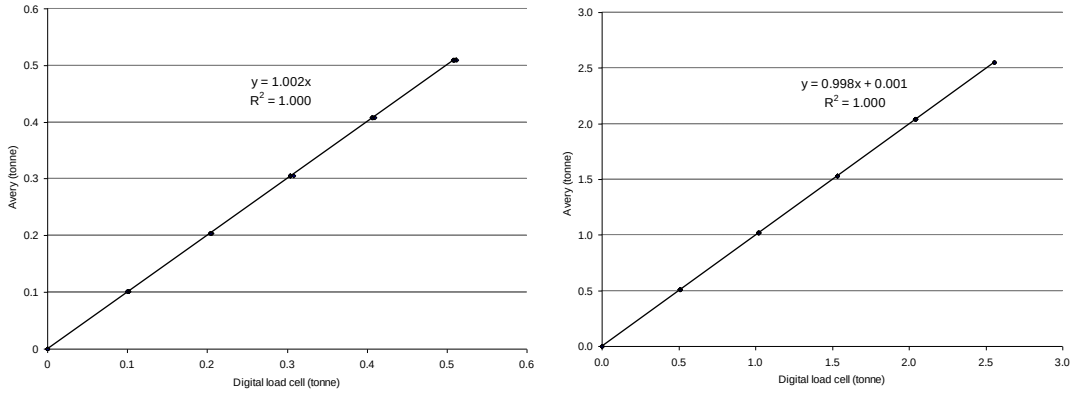

Figure B.5 Tension link dynamometer calibration curves (left: loas range 0 – 0.5 tonne, right: load range 0 – 2.5 tonne)

The calibration relationships were established using a regression analysis to the curve that best fitted the data points obtained for each calibration test. Linear relationships were found for both pressure ranges with the R^2 value of 1.000 for both calibrations. The hysteresis between the loading and unloading cycles was equal to 0.06% and 0.05%, for the calibration up to 0.5 tonne and 2.5 tonne, respectively.

The calibration curves for each instrument used for measuring tyre load were found to be linear. The EORT devices were found to be the most accurate and have the lowest hysteresis. However, due to the practical reasons it was not possible to use them for all the testing.

After the main calibration tests, simplified calibration tests were carried out for each instrument before each set of experiments. The comparisons of the results revealed no significant changes. During the experimental testing, the load measuring equipment was mainly used for the same ranges as it was calibrated but in some cases the regression lines were extrapolated.

Inflation pressure measuring equipment

- Air line pressure gauge (Sealey)

The air line pressure gauge was calibrated against a Lukas Hand Held Test Pump, which was calibrated against the Budenberg Standard (Figure B.6). The calibration of the air line gauge involved application of a number of pressures in approximately 0.3 bar increments from 0 up to 2.1 bar. The procedure was carried out three times and involved loading and unloading. The results recorded were plotted in Figure B.7 with the best fitted curve establishing the relationship. A significant difference was found between loading and unloading the pressure gauge. The calibration curve has an R^2 value of 0.982 with a hysteresis of 13.14%. Due to the large difference between loading and unloading characteristics this gauge was only used in the initial stage of the project and was discarded for the experimental studies.

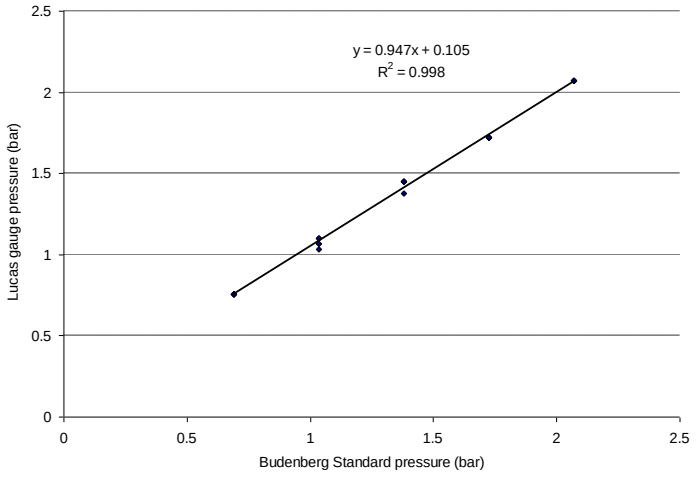

Figure B.6 Lukas Hand Held Test Pump calibration

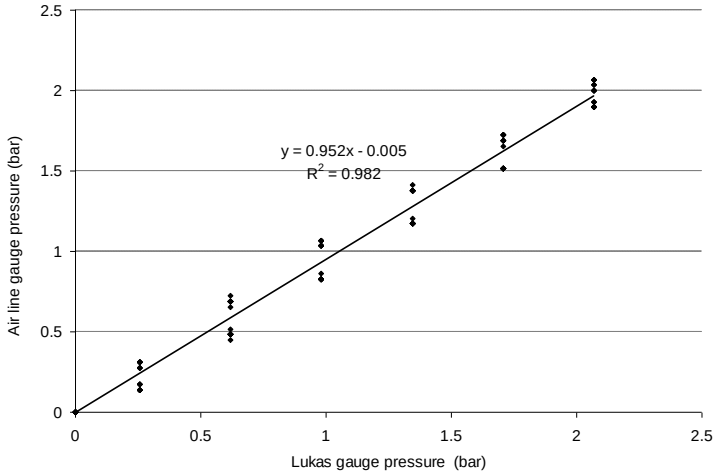

Figure B.7 Air line pressure gauge calibration

- Digitron 2086P pressure gauge

The Digitron pressure gauge was calibrated using a Lukas Hand Held Test Pump. The calibration of the Digitron pressure gauge involved applying a number of pressures in approximately 0.3 bar increments up to 2.1 bar. The procedure involved loading and unloading and was carried out three times. The results given by both pressure gauges were recorded and plotted in Figure B.8. The relationship was established by plotting the best fitted curve to the data points obtained for the three increasing and decreasing cycles. A close agreement of pressure data recorded by both pressure gauges was found. The calibration curve of Digitron was found to be linear with R^2 value of 1.000 and the maximum hysteresis of 1.42%.

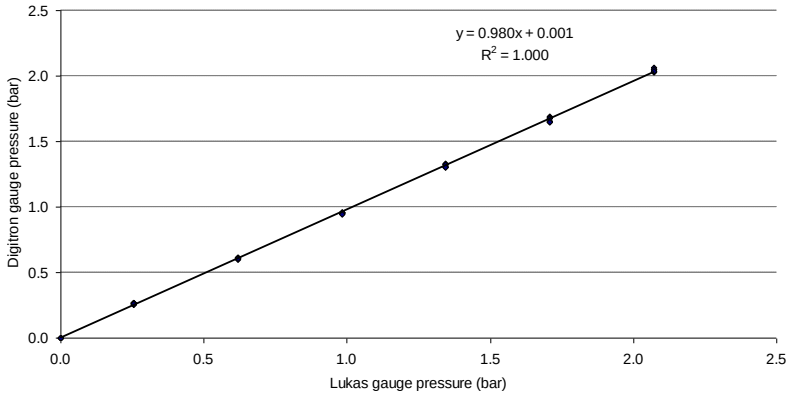

Figure B.8 Digitron pressure gauge calibration

- Druck DPI 104 pressure gauge

The Druck pressure gauge did not require to be calibrated as it has recently come from the manufacture with a calibration certificate. Figure B.9 was plotted according to the calibration data provided by the manufacturer. The relationship was found to be linear with R^2 value of 1.000 and the maximum hysteresis of 0.005%.

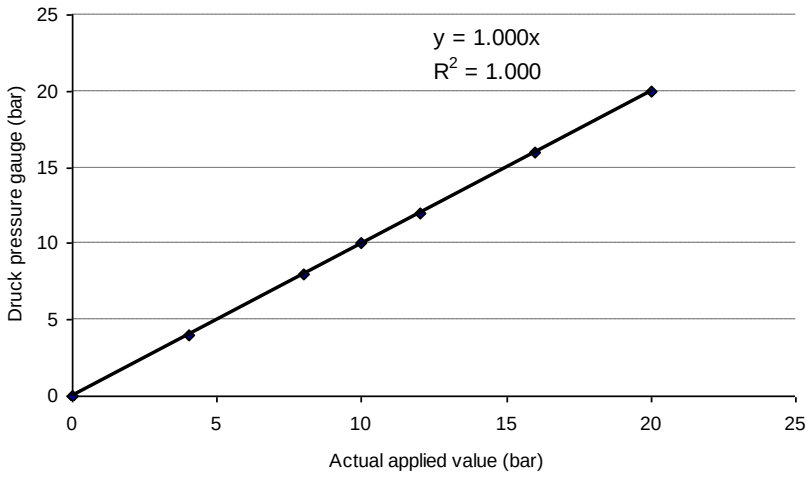

Figure B.9 Druck pressure gauge calibration

Draw string transducers

The draw string transducers were calibrated using a height gauge as shown in Figure B.10. They were connected to a datalogger measuring the output voltage which was recorded on a computer, then plotted (Figure B.11) against the measurement provided by the height gauge. The calibration of each transducer was performed by applying a range of vertical heights from 100 mm to 550 mm in 50 mm increments. The heights were gradually increased up to the maximum value and then decreased in the same increments. This process was repeated three times for each transducer.

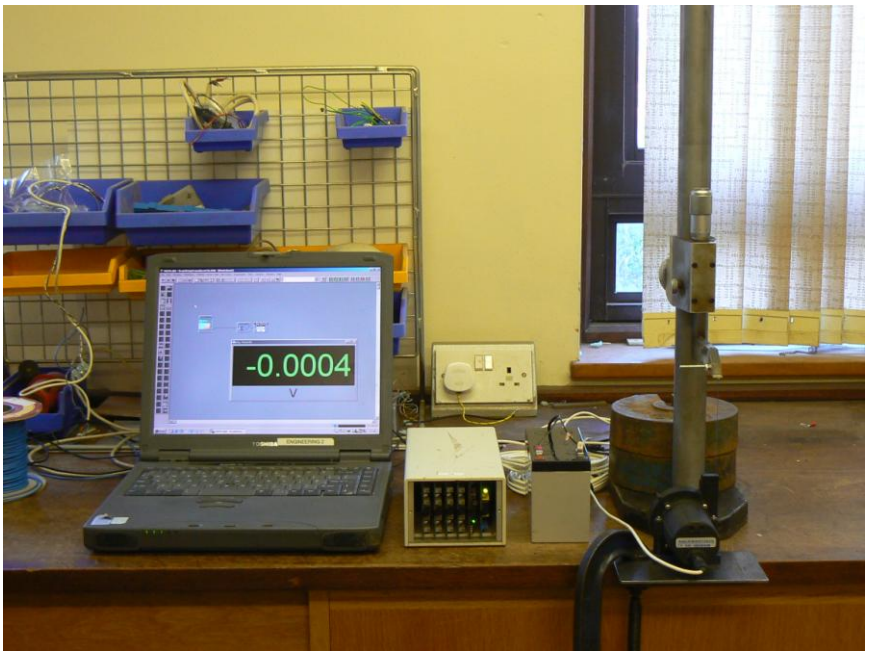

Figure B.10 Calibration of the draw string transducer

As shown in Figure B.11, the R^2 values were found to be 1.000 for both transducers with the hysteresis of 0.01% and 0.03% for the 1000 mm and 2000 mm long transducer, respectively.

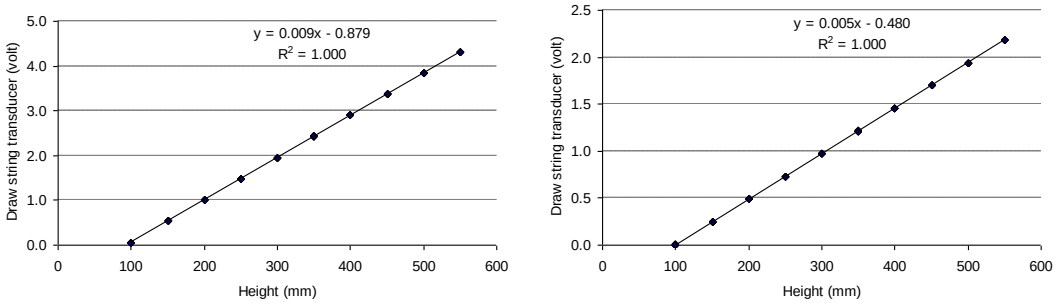

Figure B.11 Calibration of the draw string transducers (left: transducer 1000 mm long, right: transducer 2000 mm long)

Canon PowerShot S45 digital camera

Calibration of the Canon PowerShot S45 digital camera involved taking pictures of a number of black images printed on white paper located at a constant distance from the camera lens. They were a square and circle shape of known areas (250000 mm^2,

70685.83 mm^2, 40000 mm^2 and 10000 mm^2). It allowed for the relationship between the area and number of pixels to be established as shown in Figure B.12. A linear relationship was obtained with an R^2 value of 1.000. The correlation was then used for the tyre contact area determination. In order to do this, the tyre contact patches were pictured with the same camera and then the number of black pixels was calculated in Matlab (Matlab, 2005) and converted into area units (Appendix A).

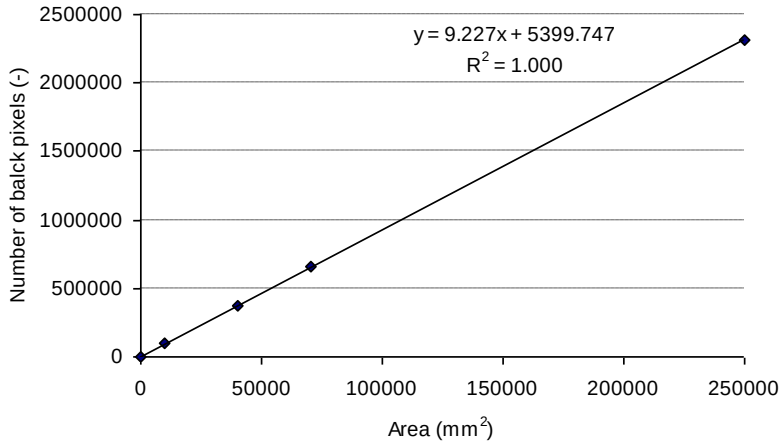

Figure B.12 Calibration of the Canon PowerShot S45 digital camera

APPENDIX C

DESIGN OF THE TEKSCAN CALIBRATION DEVICE

The device for calibrating Tekscan sensors was preliminarily designed using Autodesk Inventor Professional 9.0 software (2004). The design was followed by stress analysis carried out also using Autodesk Inventor. The software was used to simulate the behaviour of the two plates that account of the calibration device under structural loading conditions using Finite Element Analysis. The initial design was modified and the optimum design with relatively high safety factor was selected. As the safety factor, maximum stress and deflection were found to meet the standards, the final drawings were made in Autodesk Inventor and the apparatus was built.

The procedure for designing the calibration device is presented below and it is followed by the stress analysis report.

The calibration plates were required to be sufficiently large to accommodate the largest Tekscan sensor used. Therefore, the device was selected to have a square shape of 670 mm x 670 mm (external dimensions) with a square calibration area of 590 mm x 590 mm. A range of material thicknesses and strengths were evaluated in the stress analysis. Ultimately, the 30 mm thick mild steel material was selected. The device was designed to work up 34.5 bar. As it can be used for relatively high pressure, the safety and correctness of the design were essential. It was decided to use 'cross-shape' reinforcement on both plates in order to reduce any deflection of the plates when high pressures will be applied. The bottom plate was designed to have a 3mm recess so the sensors could be placed there for the calibration.

After the general shape and dimensions were decided, the amount of screws evenly distributed required to hold the two plates together was calculated, as shown:

- Maximum pressure: 34.5 bar
- As the pressurised area is to be 590 mm by 590 mm, the maximum force applied to the device will be: 1200 kN

- It was selected to have 24 screws distributed equally on four sides of the device, therefore, each screw will need to sustain the force of 50 kN
- The steel class for the screws was selected to be 10.9 (minimum 0.2% yield strength of 900 N/mm^2) and 16 mm nominal screw diameter was selected (tensile stress area of 157 mm^2)
- This type of screw is able to sustain 141 kN, which gives a factor of safety of 2.8 for the screw design.

The final design drawings were generated in Autodesk Inventor and presented in Figures C.1 – C.4.

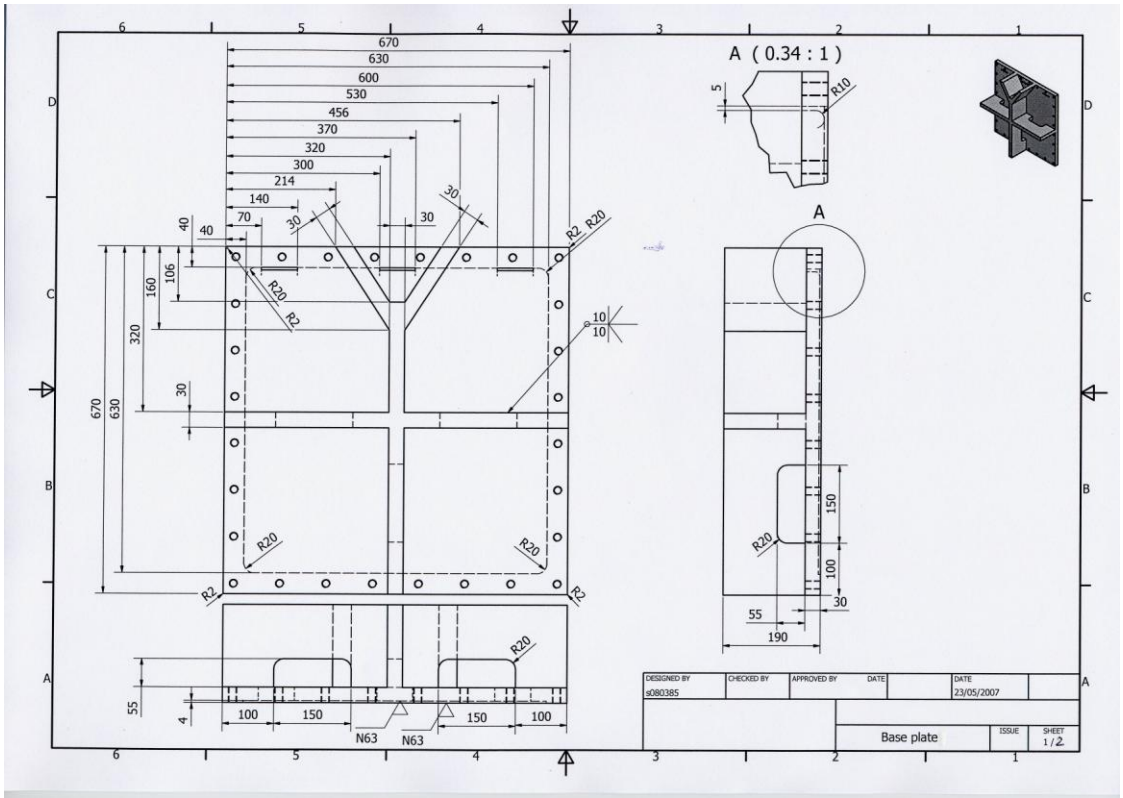

Figure C.1 Bottom plate – drawing no 1

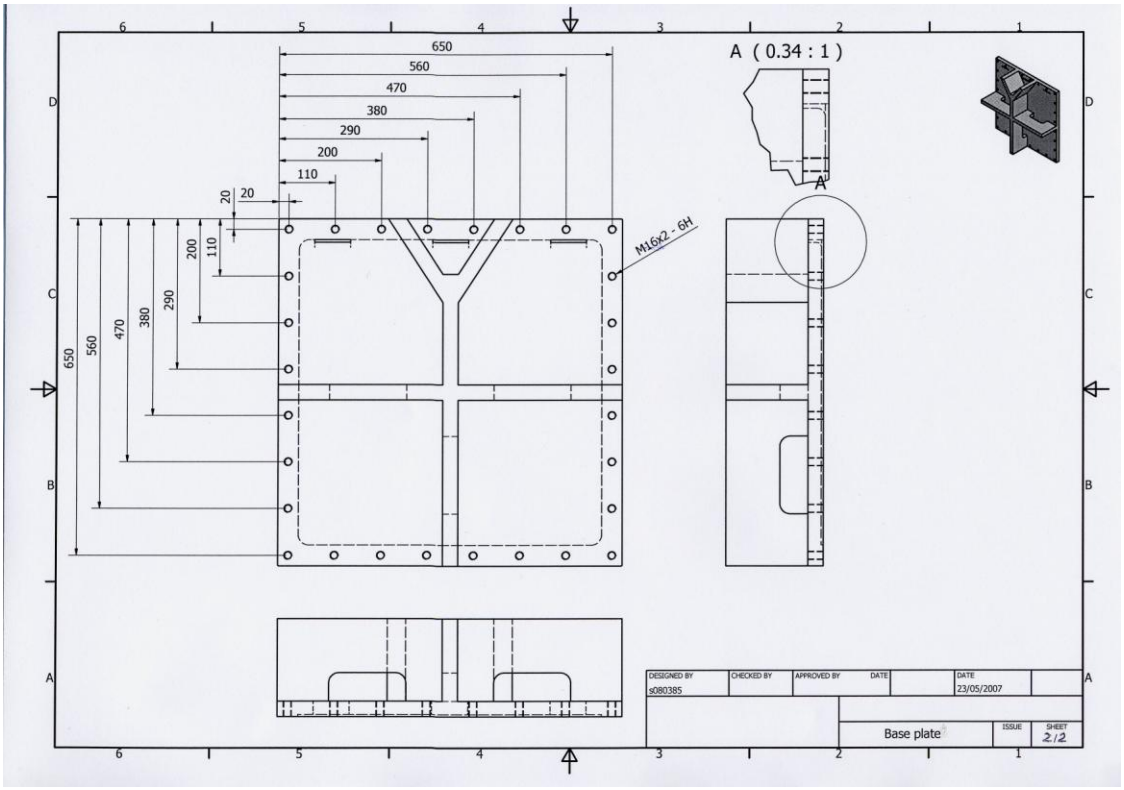

Figure C.2 Bottom plate – drawing no 2

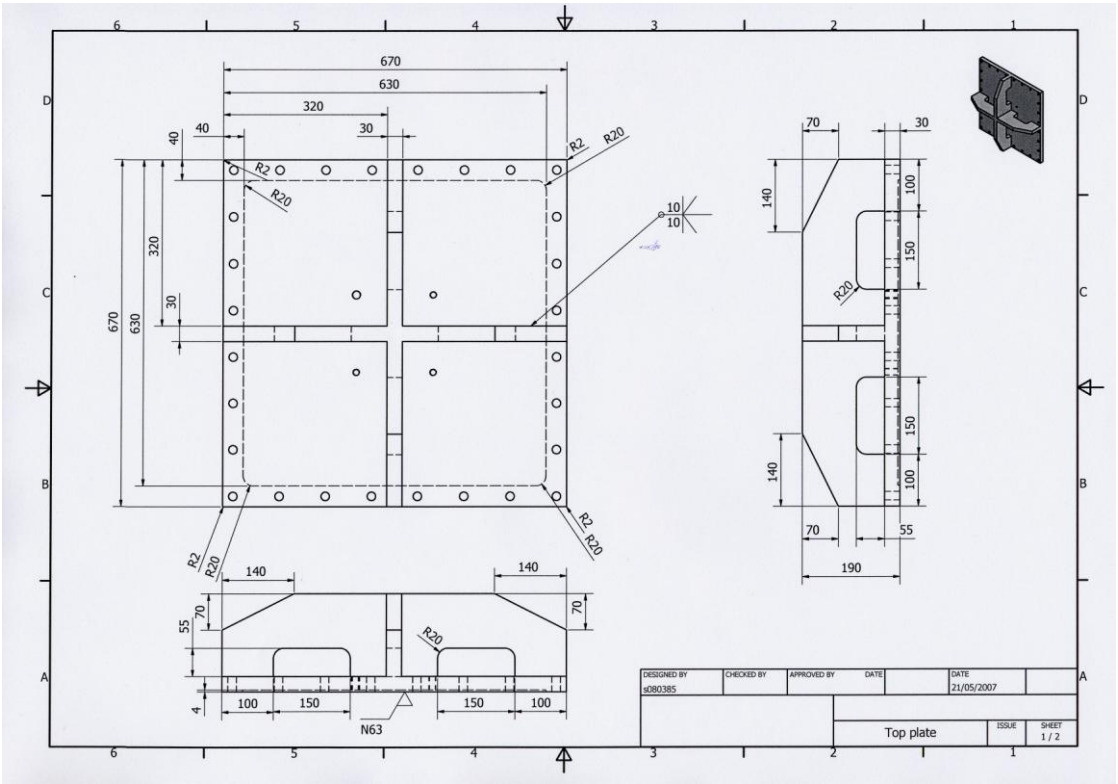

Figure C.3 Top plate – drawing no 1

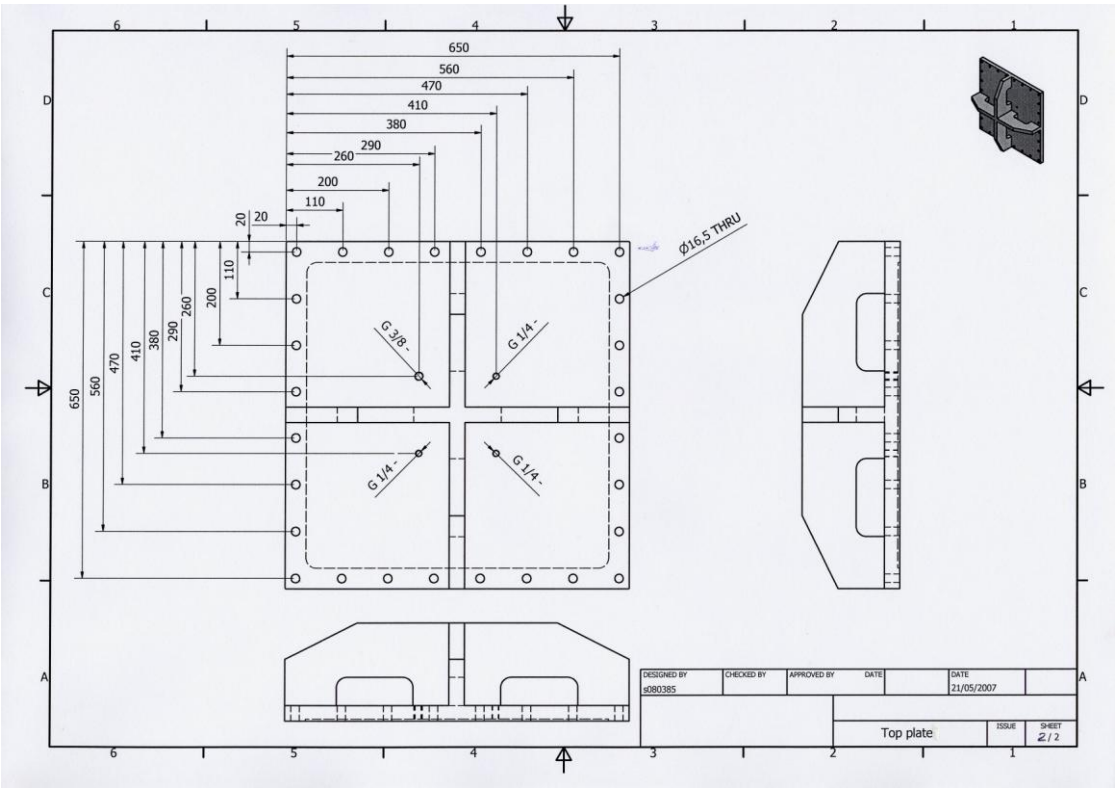

Figure C.4 Top plate – drawing no 2

Stress analysis report (generated in Autodesk Inventor)

1. Summary

The simulation was carried out separately for the two plates. The following scenario was considered for each plate:

- Scenario was based on the Inventor part *"Z:\Personal\bottomplate.ipt"* or *"Z:\Personal\topplate.ipt"*
- Considered the effect of structural loads
- Calculated the following safety factors maximum equivalent stress
- Calculated the structural results
- Plotted corresponding figures
- Provided additional details on the material characteristic

2. Bottom plate simulation

2.1 Design details

- The bounding box for the model measures 670.0 by 670.0 by 190.0 mm along the global x, y and z axes, respectively.
- The model weighs a total of 145 kg.
- *"Mesh"* contains 20231 nodes and 10657 elements.

Table 2.1 Bodies

Name	Material	Bounding Box (mm)	Mass (kg)	Volume (mm^3)	Nodes	Elements
"bottomplate.ipt"	*"Steel, Mild"*	670.0, 670.0, 190.0	145	1.85×10^{7}	20231	10657

2.2 Loads and constraints

The following table lists local loads and supports applied to specific geometry.

Table 2.2 Structural Loads

Name	Type	Magnitude	Vector	Reaction Force	Reaction Force Vector	Reaction Moment	Reaction Moment Vector
Pressure	Surface Pressure	3.45 MPa	N/A	N/A	N/A	N/A	N/A
Fixed Constraint	Surface Displacement	0.0 mm	[0.0 mm x, 0.0 mm y, 0.0 mm z]	1.19×10^{6} N	[-8.73×10^{-7} N x, 1.79×10^{-6} N y, -1.19×10^{6} N z]	3.79×10^{6} N mm	[3.78×10^{6} N mm x, 373,096.0 N mm y, 1.2×10^{-4} N mm z]

2.3 Results

2.3.1 Structural Results

Table 2.3 Values

Name	Scope	Minimum	Maximum	Alert Criteria
Equivalent Stress	*"Model"*	0.25 MPa	182.78 MPa	N/A
Deformation	*"Model"*	0.0 mm	0.28 mm	N/A

2.3.2 Equivalent Stress Safety

Table 2.4 Results				
Name	**Scope**	**Type**	**Minimum**	**Alert Criteria**
Stress Tool	*"Model"*	Safety Factor	1.13	N/A

2.3.3 Figures

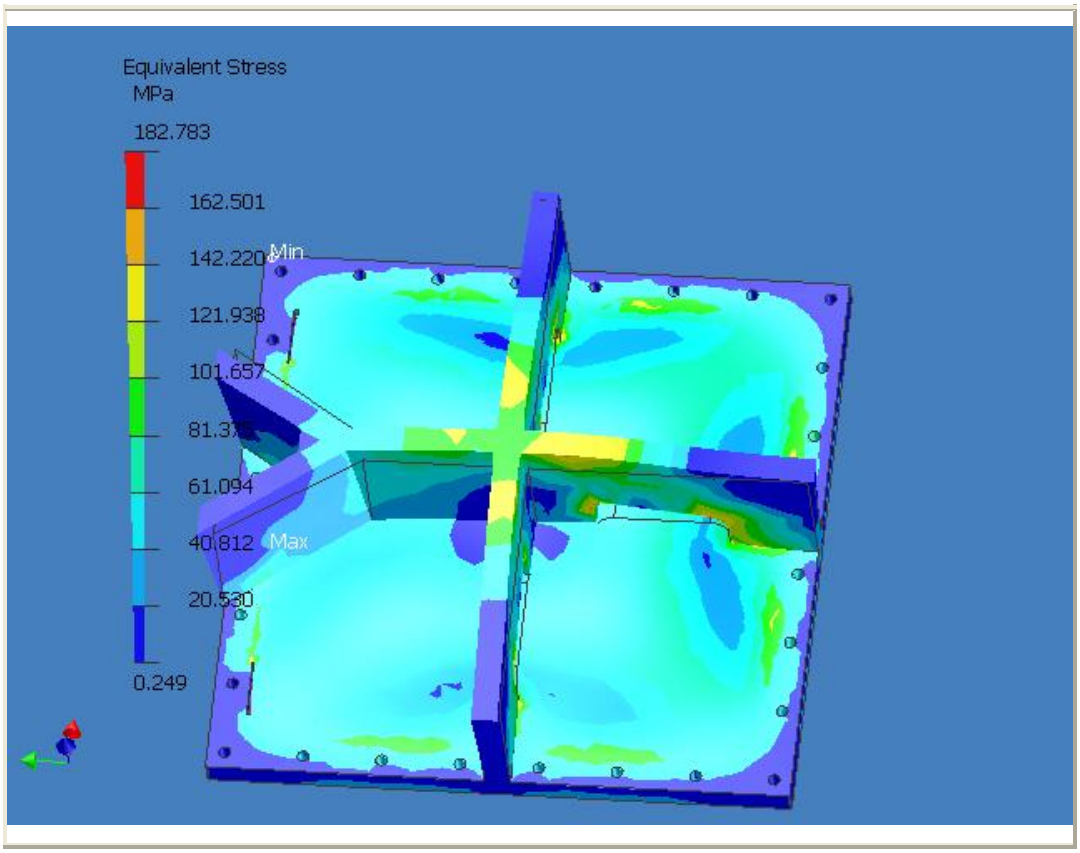

Figure 2.1 *"Equivalent Stress"* Contours (bottom plate)

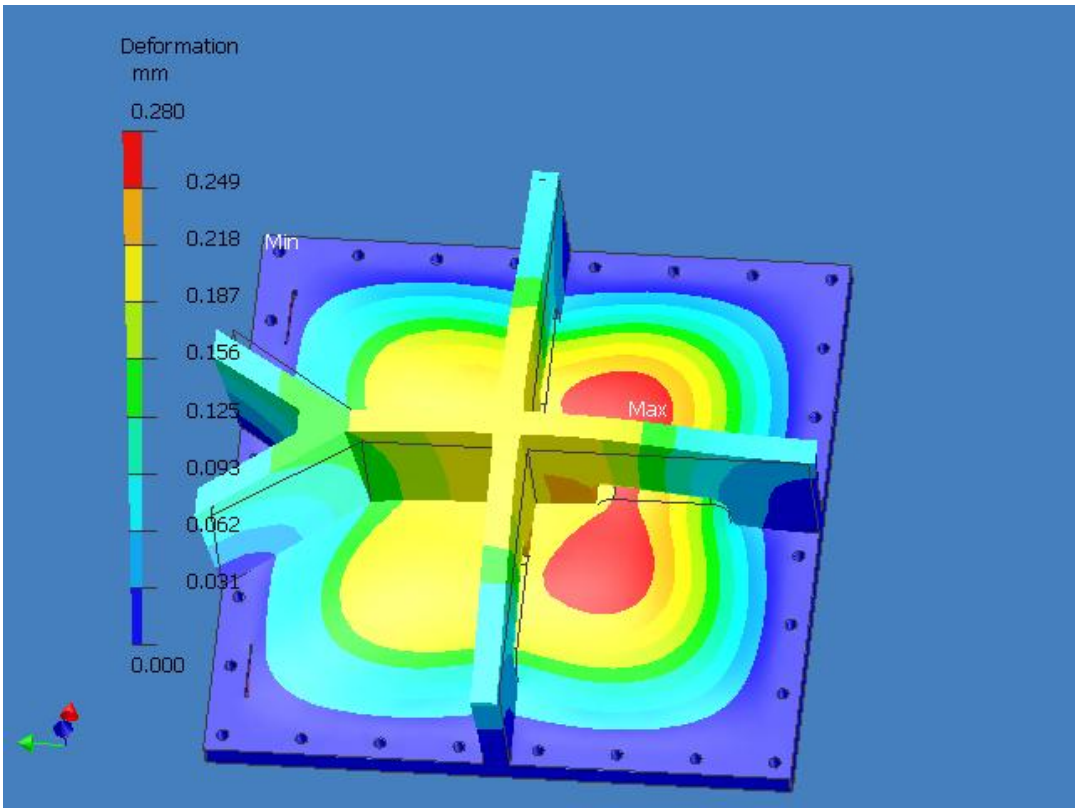

Figure 2.2 *"Deformation"* Contours (bottom plate)

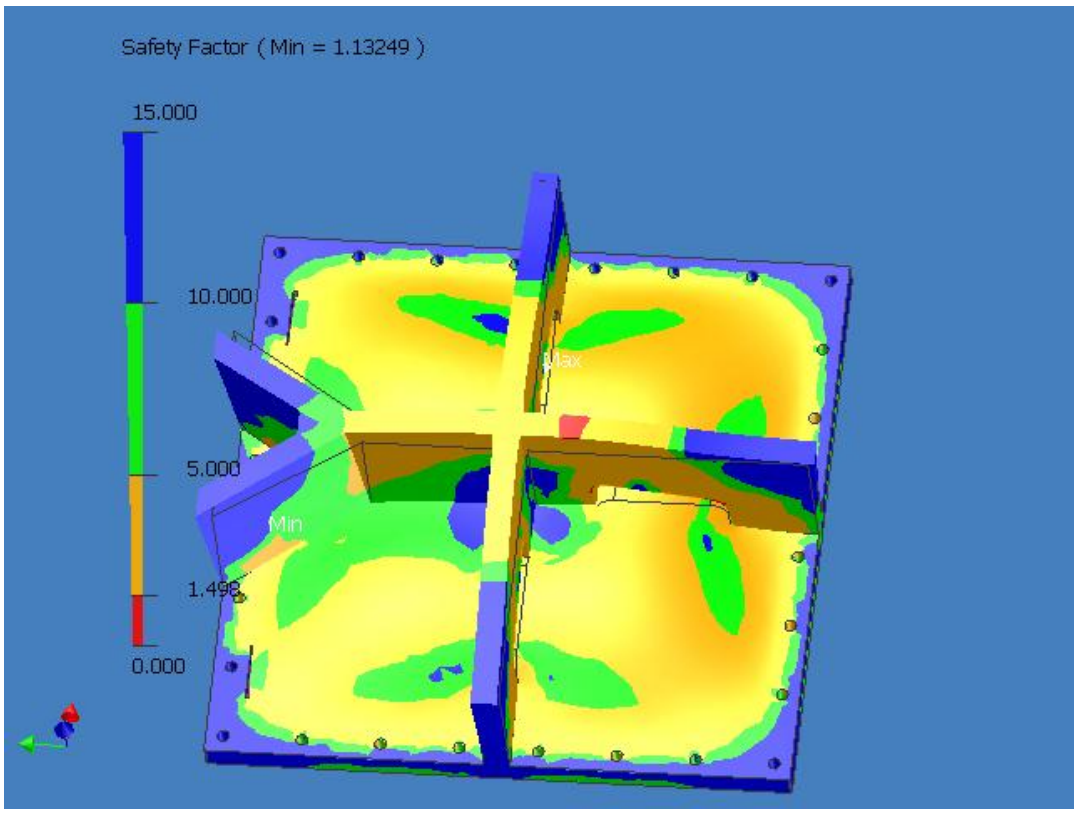

Figure 2.3 *"Safety Factor"* Contours (bottom plate)

3. Top plate simulation

3.1 Design details

- The bounding box for the model measures 670.0 by 670.0 by 190.0 mm along the global x, y and z axes, respectively.
- The model weighs a total of 131 kg.
- *"Mesh"* contains 22633 nodes and 12078 elements.

Table 3.1 Bodies

Name	Material	Bounding Box (mm)	Mass (kg)	Volume (mm^3)	Nodes	Elements
"topplate.ipt"	*"Steel, Mild"*	670.0, 670.0, 190.0	131	1.66×10^{7}	22633	12078

3.2 Loads and constraints

The following table lists local loads and supports applied to specific geometry.

Table 3.2 Structural Loads

Name	Type	Magnitude	Vector	Reaction Force	Reaction Force Vector	Reaction Moment	Reaction Moment Vector
Pressure	Surface Pressure	3.45 MPa	N/A	N/A	N/A	N/A	N/A
Fixed Constraint	Surface Displacement	0.0 mm	[0.0 mm x, 0.0 mm y, 0.0 mm z]	0.0 N	[0.0 N x, 0.0 N y, 0.0 N z]	0.0 N mm	[0.0 N mm x, 0.0 N mm y, 0.0 N mm z]

3.3 Results

3.3.1 Structural Results

Table 3.3.1.1 Values

Name	Scope	Minimum	Maximum	Alert Criteria
Equivalent Stress	*"Model"*	0.29 MPa	192.59 MPa	N/A
Deformation	*"Model"*	0.0 mm	0.29 mm	N/A

3.3.2 Equivalent Stress Safety

Table 3.3.2.2 Results

Name	Scope	Type	Minimum	Alert Criteria
Stress Tool	*"Model"*	Safety Factor	1.07	N/A

3.3.3 Figures

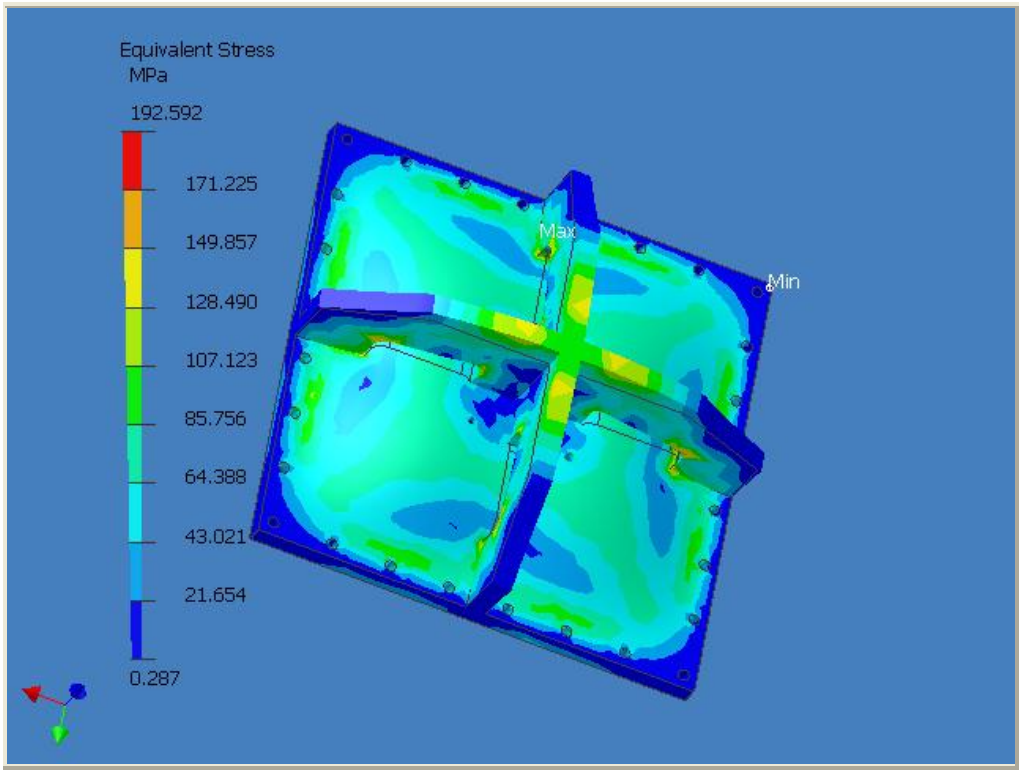

Figure 3.1 *"Equivalent Stress"* Contours (top plate)

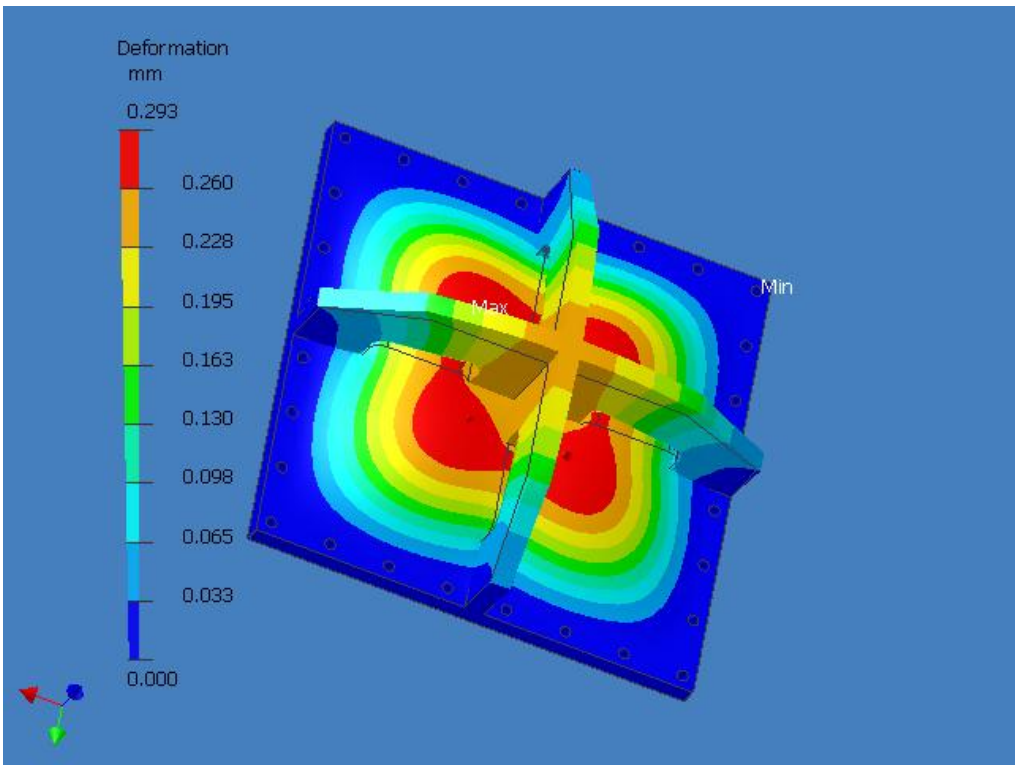

Figure 3.2 *"Deformation"* Contours (top plate)

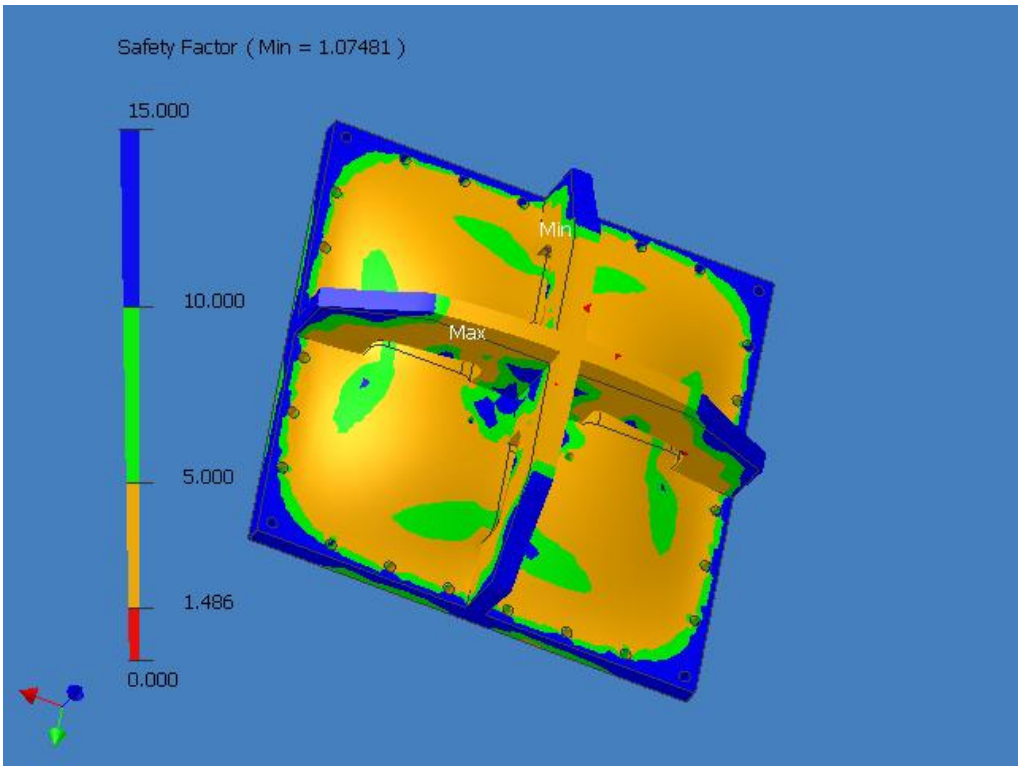

Figure 3.3 *"Safety Factor"* Contours (top plate)

4. Definition of mild steel

Table 4.1 *"Steel, Mild"* Properties		
Name	**Type**	**Value**
Modulus of Elasticity	Temperature-Independent	220,000.0 MPa
Poisson's Ratio	Temperature-Independent	0.28
Mass Density	Temperature-Independent	7.86×10^{-6} kg/mm^3

Table 4.2 *"Steel, Mild"* Stress Limits		
Name	**Type**	**Value**
Tensile Yield Strength	Temperature-Independent	207.0 MPa
Tensile Ultimate Strength	Temperature-Independent	345.0 MPa

APPENDIX D

MATLAB CODES FOR THE EVALUATION OF THE TEKSCAN CALIBRATION

The codes presented below were written in Matlab software version 7.1 (Matlab, 2005).

Procedure:

Load 'filelist' from Excel which contains a list of names of ASCII files (save it as filelist) and pressure applied (save it as pdata). The files and the pressure applied were recorded when the sensors were loaded with a range of uniform pressures in the calibration device after the Tekscan calibration was conducted.

Integrate the loaded data into one variable (filelist to be placed in column one, pdata to be placed in column two, the variable to be saved as filelist):

```
filelist=[filelist num2cell(pdata)]
```

Run the script:

```
% Load Tekscan contact pressure ASCII data files as listed in
'filelist' and call them 'recorded pressure'
data=readtek(char(filelist(1,1)));
datasize=[size(data,1),size(data,2)];
recordeddata=zeros([datasize,length(filelist)]);
for file=1:length(filelist)
    data=readtek(char(filelist(file,1)));
    recordeddata(:,:,file)=data;
end

% Build a matrix (the same size as the 'recorded pressure') and load
the applied pressure values into it and call them 'applied pressure'
appliedpressure=zeros(datasize(1),datasize(2),length(filelist));
for file=1:length(filelist)
appliedpressure(:,:,file)=ones(datasize)*cell2mat(filelist(file,2));
end

% Identify any dead sensors
deadsensors=zeros(datasize);
for row=1:datasize(1)
    for column=1:datasize(2)
%disp([row column]);
        xdata=recordeddata(row,column,:);
        ydata=appliedpressure(row,column,:);
        xdata=xdata(:);
        ydata=ydata(:);
        okflag=1;
        for i=1:length(xdata)
```

```
            if xdata(i)==0
                okflag=0;
            end
        end
        for i=1:length(ydata)
            if ydata(i)==0
                okflag=0;
            end
        end
        % deadsensor=1 means sensor has good data, deadsensor=0 means
        % mark this as unusable - dead sensor.
        if okflag==1
        deadsensors(row,column)=1;
        else
            deadsensors(row,column)=0;
        end
    end
end

% Convert the zero values for the dead sensels into NaN (not a
number)
deadsensors(deadsensors==0)=NaN

% Masking the applied pressure and recorded data arrays to remove
dead sensels
for file=1:length(filelist)
    appliedpressure(:,:,file)=appliedpressure(:,:,file).*deadsensors;
    recordeddata(:,:,file)=recordeddata(:,:,file).*deadsensors;
end

% Calculation of the errors against the full scale (0.77 bar is the
maximum pressure for the standard sensitivity of 9830 sensors)
clear error
error=recordeddata-appliedpressure;
error=error./0.77;
error=error*100;
error(not(isnan(error)))
hist(error(:),40)

% Calculation of sensing area giving errors lower than quoted
absolute errors (%)
test=abs(error)<20;
sum(test(:))
numel(test)
sum(test(:))/numel(test)
```

Script 'readtek' for reading ASCII single frame data in used in the script above:

```
% function to read Tekscan files
% only takes into account the rows and columns information (data)
function data=readtek(filename)
%filename='6300_B_Default_10psi_C&E.asf'
file=fopen (filename);
%process the header as appropriate
% DATA_TYPE MOVIE
```

```
line=fgetl(file);
% VERSION Tekscan Pressure Measurement System 5.83I
line=fgetl(file);
% HARDWARE 102-1891
line=fgetl(file);
% HWSENS 2
line=fgetl(file);
% FILENAME C:\Documents and
Settings\admindwp\Desktop\Tekscan\6300_B\6300_B_Default_10psi_C&E.fsx
line=fgetl(file);
% SENSOR_TYPE 6300
line=fgetl(file);
% ROWS 44
line=fgetl(file);
filerows=sscanf(line,'ROWS %d');
% COLS 52
line=fgetl(file);
filecols=sscanf(line,'COLS %d');
% ROW_SPACING 0.762 mm
line=fgetl(file);
% COL_SPACING 5.08 mm
line=fgetl(file);
% SENSEL_AREA 3.87096 mm2
line=fgetl(file);
% NOISE_THRESHOLD 3
line=fgetl(file);
% SECONDS_PER_FRAME 0.25
line=fgetl(file);
% MICRO_SECOND 0
line=fgetl(file);
% TIME 13 November 2007 15:31:12
line=fgetl(file);
% SCALE_FACTOR  0.0479536 PSI / raw
line=fgetl(file);
filescalefactor=sscanf(line,'SCALE_FACTOR %f PSI');
% EXPONENT 1.25608
line=fgetl(file);
fileexponent=sscanf(line,'EXPONENT %f');
% SATURATION_PRESSURE 50.5392 PSI (Exponential Extrapolation)
line=fgetl(file);
% CALIBRATION_POINT_1 0.488499 (KNewtons) 134468 (Raw Sum) 2288
(Number of Loaded Cells)
line=fgetl(file);
% CALIBRATION_POINT_2 1.9541 (KNewtons) 405462 (Raw Sum) 2288 (Number
of Loaded Cells)line=fgetl(file);
line=fgetl(file);
% CALIBRATION_INFO C:\Documents and
Settings\admindwp\Desktop\Tekscan\6300_B\6300_B_Default_10psi_C&E.fsx
line=fgetl(file);
% SENSITIVITY Default
line=fgetl(file);
% START_FRAME 1
line=fgetl(file);
startframe=sscanf(line,'START_FRAME %d');
% END_FRAME 1
line=fgetl(file);
endframe=sscanf(line,'END_FRAME %d');
```

```
% UNITS PSI
line=fgetl(file);
% MIRROR_ROW 0
line=fgetl(file);
% MIRROR_COL 0
line=fgetl(file);
% ASCII_DATA @@
line=fgetl(file);
fclose(file);

clear line

if endframe-startframe>0
    disp ('Warning - more than one frame detected - is this a movie
file?')
end

data=dlmread(filename,',',[30 0 30+filerows-1 filecols-1]);
return
```

APPENDIX E

MATLAB SCRIPTS FOR ESTABLISHMENT OF THE REGRESSION MODELS AND MULTI-POINT PER SENSEL CALIBRATION FOR THE NON-CALIBRATED TEKSCAN DATA

Procedure:

Load 'filelist' as described in the section above. For this use the raw data recorded when the sensors were loaded with a range of uniform pressures, in contrast to the pervious section where data calibrated using Tekscan procedure was used.

Integrate the loaded data into one variable (filelist to be placed in column one, pdata to be placed in column two, the variable to be saved as filelist):

```
filelist=[filelist num2cell(pdata)]
```

The following script is to be used for establishment of a fourth order polynomial regression model for each sensing element. Then the multi-point per sensel calibration is evaluated by the calculation of the coefficient of determination values and residual and statistical errors. As the fourth polynomial was found to be the best fit, the full script required for the establishment of this type of model was presented first. Following this, the code required to establish different types of regression functions is attached.

Run the 4th order polynomial regression model (it uses 'readtek' script as above):

```
% Load Tekscan contact pressure ASCII data files as listed in
'filelist' and call them 'recorded pressure'
data=readtek(char(filelist(1,1)));
datasize=[size(data,1),size(data,2)];
% Allocate memory for Tekscan recorded data
recordeddata=zeros([datasize,length(filelist)]);
% Read all data into array
for file=1:length(filelist)
    data=readtek(char(filelist(file,1)));
    recordeddata(:,:,file)=data;
end
```

```
% Build a matrix (the same size as the 'recorded pressure') and load
the applied pressure values into it and call them 'applied pressure'
appliedpressure=zeros(datasize(1),datasize(2),length(filelist));
% creating applied pressure array
for file=1:length(filelist)
appliedpressure(:,:,file)=ones(datasize)*cell2mat(filelist(file,2));
end

% Polynomial calibration coefficients (Identifies any dead sensors
and establishes regression curves for each well-working sensel)
% allocate memory for calibration coefficients
factor1=zeros(datasize);
factor2=zeros(datasize);
factor3=zeros(datasize);
factor4=zeros(datasize);
factor5=zeros(datasize);
% allocate memory for mask for dead sensels%
deadsensors=zeros(datasize);

for row=1:datasize(1)
    for column=1:datasize(2)
        %disp([row column]);
        xdata=recordeddata(row,column,:);
        ydata=appliedpressure(row,column,:);
        xdata=xdata(:);
        ydata=ydata(:);
        okflag=1;
        for i=1:length(xdata)
            if xdata(i)==0
                okflag=0;
            end
        end
        for i=1:length(ydata)
            if ydata(i)==0
                okflag=0;
            end
        end
        % if okflag is still 1 here, establish regression, otherwise
        % mark this as unusable - dead sensor.
        if okflag==1
            coeff=polyfit(xdata(:),ydata(:),4);
            factor1(row,column)=coeff(1);
            factor2(row,column)=coeff(2);
            factor3(row,column)=coeff(3);
            factor4(row,column)=coeff(4);
            factor5(row,column)=coeff(5);
            deadsensors(row,column)=1;
            % deadsensor=1 means sensor has good data,
              deadsensor=0 means bad data
        else
            deadsensors(row,column)=0;
        end
    end
end
```

```
% Convert the zero values for the dead sensels into NaN (not a
number)
deadsensors(deadsensors==0)=NaN

% Save the calibration files
save('sensorcalPolynomial4.mat','factor1','factor2','factor3','factor
4','factor5','deadsensors')

% Load calibration file
disp ('Loading calibration and deadsensors data from
sensorcalPolynomial4.mat')
load ('sensorcalPolynomial4.mat')

% Load faulty sensors file
disp ('Loading faulty sensors from faultysensors.xls')
faultysensors=xlsread('faultysensors.xls')

% Apply the calibration parameters to the raw data which will enable
to justify the regressions
% preallocate this for speed
recordedDataCalibratedPolynomial4=zeros(size(recordeddata));

for i=1:size(recordeddata,3)
      recordedDataCalibratedPolynomial4(:,:,i)=recordeddata(:,:,i).*
      deadsensors;
      recordedDataCalibratedPolynomial4(:,:,i)=recordedDataCalibrated
      Polynomial4(:,:,i).*faultysensors;
      recordedDataCalibratedPolynomial4(:,:,i)=(recordedDataCalibrate
      dPolynomial4(:,:,i).*recordedDataCalibratedPolynomial4(:,:,i).*
      recordedDataCalibratedPolynomial4(:,:,i).*recordedDataCalibrate
      dPolynomial4(:,:,i).*factor1)+recordedDataCalibratedPolynomial4
      (:,:,i).*recordedDataCalibratedPolynomial4(:,:,i).*recordedData
      CalibratedPolynomial4(:,:,i).*factor2+recordedDataCalibratedPol
      ynomial4(:,:,i).*recordedDataCalibratedPolynomial4(:,:,i).*fact
      or3+recordedDataCalibratedPolynomial4(:,:,i).*factor4+factor5;
end

% Save the calibrated data
disp ('Saving data...')
save('recordedDataCalibratedPolynomial4','recordedDataCalibratedPolyn
omial4')

% Calculate the coefficient of determination
for row=1:datasize(1)
    for column=1:datasize(2)
      recorded=reshape(recordedDataCalibratedPolynomial4(row,column,:
      ),size(recordedDataCalibratedPolynomial4,3),1);
      applied=reshape(appliedpressure(row,column,:),size(appliedpress
      ure,3),1);
      model=polyval(coeff,applied);
      ybar=mean(recorded);
      xbar=mean(applied);
      btemp=(applied-xbar).*(recorded-ybar);
      btemp=sum(btemp);
      btemp2=(applied-xbar);
      btemp2=btemp2.*btemp2;
```

```
        btemp2=sum(btemp2);
        b=btemp/btemp2;
        slrtemp=(applied-xbar).*(recorded-ybar);
        slrtemp=sum(slrtemp);
        slr=b.*slrtemp;
        stemp=(recorded-ybar);
        stemp=stemp.*stemp;
        s=sum(stemp);
        r2poly4(row,column)=slr/s;
    end
end

% Calculate the mean and standard deviation of coefficient of
determination and plot a histogram of the R2 values
tempr2poly4=r2poly4(not(isnan(r2poly4)))
m=mean(tempr2poly4)
s = std(tempr2poly4)
hist(tempr2poly4(:),40)

% Mask the applied pressure array to remove dead and faulty sensels
for file=1:length(filelist)
        appliedpressure(:,:,file)=appliedpressure(:,:,file).*deadsensor
        s.*faultysensors;
end

% Calculate the residual errors against the full scale (0.77 bar is
the maximum pressure for the standard sensitivity of 9830 sensors)
error=recordedDataCalibratedPolynomial4-appliedpressure;
error=error./0.77;
error=error*100;
error(not(isnan(error)))
hist(error(:),40)

% Calculate sensing area giving residual errors lower than quoted
absolute errors (%)
test=abs(error)<20;
sum(test(:))
numel(test)
sum(test(:))/numel(test)

% Calculate the statistical errors
% Load data from disc (Set of raw data obtained when loading the
sensor. The data should not be used previously for the establishment
of the calibration. Symbol X, used in the scripts below, represents
the date not previously used for the calibration.)
dataX=readtek('SensorD_6.10psi_Default.asf');

recordedCalibratedPoly4X=(dataX.*dataX.*dataX.*dataX.*factor1)+(dataX
.*dataX.*dataX.*factor2)+(dataX.*dataX.*factor3)+(dataX.*factor4)+fac
tor5;
recordedCalibratedPoly4X=recordedCalibratedPoly4X.*deadsensors.*fault
ysensors;

% Load an Excel file containing an array (size of row, column) of
applied pressure recorded when the analysed Tekscan snapshot was
recorded
disp ('appliedpressureX.xls')
```

```
appliedpressureX =xlsread('appliedpressureX.xls')
% Masking the applied pressure array to remove dead and faulty
sensels
appliedpressureX=appliedpressureX.*deadsensors.*faultysensors;

% Calculate the statistical errors against the full scale
errorX=recordedCalibratedPoly4X-appliedpressureX;
errorX=errorX./0.77;
errorX=errorX*100;
errorX(not(isnan(errorX)));
hist(errorX(:),40)

% Calculate sensing area giving statistical errors lower than quoted
absolute errors (%)
testX=abs(errorX)<20;
sum(testX(:))
numel(testX)
sum(testX(:))/numel(testX)
```

Linear regression model:

```
data=readtek(char(filelist(1,1)));
datasize=[size(data,1),size(data,2)];
actualdata=zeros([datasize,length(filelist)]);
for file=1:length(filelist)
    data=readtek(char(filelist(file,1)));
    actualdata(:,:,file)=data;
end

appliedpressure=zeros(datasize(1),datasize(2),length(filelist));
for file=1:length(filelist)
appliedpressure(:,:,file)=ones(datasize)*cell2mat(filelist(file,2));
end

slope=zeros(datasize);
intercept=zeros(datasize);
deadsensors=zeros(datasize);

for row=1:datasize(1)
    for column=1:datasize(2)
        xdata=actualdata(row,column,:);
        ydata=appliedpressure(row,column,:);
        xdata=xdata(:);
        ydata=ydata(:);
        okflag=1;
        for i=1:length(xdata)
            if xdata(i)==0
                okflag=0;
            end
        end
        for i=1:length(ydata)
            if ydata(i)==0
                okflag=0;
            end
        end
```

```
            if okflag==1
      [coefficients,S]=polyfit(actualdata(row,column,:),appliedpressu
      re(row,column,:),1);
      slope(row,column)=coefficients(1);
      intercept(row,column)=coefficients(2);
      deadsensors(row,column)=1;
        else
            deadsensors(row,column)=0;
        end
    end
end

deadsensors(deadsensors==0)=NaN
save('sensorcal.mat','slope','intercept')
load ('sensorcal.mat')
disp ('Loading faulty sensors from faultysensors.xls')
faultysensors=xlsread('faultysensors.xls')

actualDataCalibratedLinear=zeros(size(actualdata));
for i=1:size(actualdata,3)
        actualDataCalibratedLinear(:,:,i)=actualdata(:,:,i).*slope;
        actualDataCalibratedLinear(:,:,i)=actualDataCalibratedLinear(
        :,:,i)+intercept;
        actualDataCalibratedLinear(:,:,i)=actualDataCalibratedLinear(
        :,:,i).*deadsensors.*faultysensors
end

disp ('Saving data...')
save(['actualDataCalibratedLinear'],'actualDataCalibratedLinear')

for row=1:datasize(1)
    for column=1:datasize(2)
    actual=reshape(actualDataCalibratedLinear(row,column,:),size(actu
    alDataCalibratedLinear,3),1);
    applied=reshape(appliedpressure(row,column,:),size(appliedpressur
    e,3),1);
        model=polyval(coefficients,applied);
        ybar=mean(actual);
        xbar=mean(applied);
        btemp=(applied-xbar).*(actual-ybar);
        btemp=sum(btemp);
        btemp2=(applied-xbar);
        btemp2=btemp2.*btemp2;
        btemp2=sum(btemp2);
        b=btemp/btemp2;
        slrtemp=(applied-xbar).*(actual-ybar);
        slrtemp=sum(slrtemp);
        slr=b.*slrtemp;
        stemp=(actual-ybar);
        stemp=stemp.*stemp;
        s=sum(stemp);
        r2linear(row,column)=slr/s;
    end
end

tempr2=r2linear(not(isnan(r2linear)));
```

```
r2mean=mean(tempr2)
hist(tempr2(:),40)
s = std(tempr2)

dataX=readtek('SensorD_6.10psi_Default.asf');

recordedDataCalibratedLinearX=dataX.*slope;
recordedDataCalibratedLinearX=recordedDataCalibratedLinearX+intercept
;
recordedDataCalibratedLinearX=recordedDataCalibratedLinearX.*deadsens
ors.*faultysensors;
disp ('appliedpressureX.xls')
appliedpressureX =xlsread('appliedpressureX.xls')
appliedpressureX=appliedpressureX.*deadsensors.*faultysensors;

errorX= recordedDataCalibratedLinearX-appliedpressureX;
errorX=errorX./0.77;
errorX=errorX*100;
errorX(not(isnan(errorX)));
hist(errorX(:),40)

testX=abs(errorX)<20;
sum(testX(:))
numel(testX)
sum(testX(:))/numel(testX)
```

Power regression model:

```
data=readtek(char(filelist(1,1)));
datasize=[size(data,1),size(data,2)];
measuredData=zeros([datasize,length(filelist)]);
for file=1:length(filelist)
    data=readtek(char(filelist(file,1)));
    measuredData(:,:,file)=data;
end

appliedpressure=zeros(datasize(1),datasize(2),length(filelist));
for file=1:length(filelist)
appliedpressure(:,:,file)=ones(datasize)*cell2mat(filelist(file,2));
end

slope=zeros(datasize);
intercept=zeros(datasize);
deadsensors=zeros(datasize);
appliedLog=log(appliedpressure);
measuredLog=log(measuredData);

for row=1:datasize(1)
    for column=1:datasize(2)
        xdata=measuredData(row,column,:);
        ydata=appliedpressure(row,column,:);
        xdata=xdata(:);
        ydata=ydata(:);
        okflag=1;
        for i=1:length(xdata)
```

```
            if xdata(i)==0
                okflag=0;
            end
        end
        for i=1:length(ydata)
            if ydata(i)==0
                okflag=0;
            end
        end
        if okflag==1
            [coefficients,S]=polyfit(measuredLog(row,column,:),applie
            dLog(row,column,:),1);
            slope(row,column)=coefficients(1);
            intercept(row,column)=coefficients(2);
            deadsensors(row,column)=1;
        else
            deadsensors(row,column)=0;
        end
      measuredLogR=reshape(measuredLog(row,column,:),size(measuredLog
      ,3),1);
      appliedLogR=reshape(appliedLog(row,column,:),size(appliedLog,3)
      ,1);
        model=polyval(coefficients,appliedLogR);
        ybar=mean(measuredLogR);
        xbar=mean(appliedLogR);

        btemp=(appliedLogR-xbar).*(measuredLogR-ybar);
        btemp=sum(btemp);
        btemp2=(appliedLogR-xbar);
        btemp2=btemp2.*btemp2;
        btemp2=sum(btemp2);
        b=btemp/btemp2;

        slrtemp=(appliedLogR-xbar).*(measuredLogR-ybar);
        slrtemp=sum(slrtemp);
        slr=b.*slrtemp;

        stemp=(measuredLogR-ybar);
        stemp=stemp.*stemp;
        s=sum(stemp);

        r2power(row,column)=slr/s;
    end
end

intercept=exp(intercept)
deadsensors(deadsensors==0)=NaN

save('sensorcal.mat','slope','intercept')
load ('sensorcal.mat')

disp ('Loading faulty sensors from faultysensors.xls')
faultysensors=xlsread('faultysensors.xls')

measuredCalibratedPower=zeros(size(measuredData));
```

```
for i=1:size(measuredData,3)
      measuredCalibratedPower(:,:,i)=measuredData(:,:,i).^slope;
      measuredCalibratedPower(:,:,i)=measuredCalibratedPower(:,:,i).*
      intercept;
      measuredCalibratedPower(:,:,i)=measuredCalibratedPower(:,:,i).*
      deadsensors.*faultysensors
end

disp ('Saving data...')
save(['measuredCalibratedPower'],'measuredCalibratedPower')

tempr2=r2power(not(isnan(r2power)));
r2mean=mean(tempr2)
hist(tempr2(:),40)
s = std(tempr2)


dataX=readtek('SensorD_6.10psi_Default.asf');
recordedDataCalibratedPowerX=dataX.^slope;
recordedDataCalibratedPowerX=recordedDataCalibratedPowerX.*intercept;
recordedDataCalibratedPowerX=recordedDataCalibratedPowerX.*deadsensor
s.*faultysensors

disp ('appliedpressureX.xls')
appliedpressureX =xlsread('appliedpressureX.xls')
appliedpressureX=appliedpressureX.*deadsensors.*faultysensors;

errorX= recordedDataCalibratedPowerX-appliedpressureX;
errorX=errorX./0.77;
errorX=errorX*100;
errorX(not(isnan(errorX)));
hist(errorX(:),40)

testX=abs(errorX)<20;
sum(testX(:))
numel(testX)
sum(testX(:))/numel(testX
```

Second order polynomial regression model:

```
data=readtek(char(filelist(1,1)));
datasize=[size(data,1),size(data,2)];
recordeddata=zeros([datasize,length(filelist)]);
for file=1:length(filelist)
    data=readtek(char(filelist(file,1)));
    recordeddata(:,:,file)=data;
end

appliedpressure=zeros(datasize(1),datasize(2),length(filelist));
for file=1:length(filelist)
appliedpressure(:,:,file)=ones(datasize)*cell2mat(filelist(file,2));
end

factor1=zeros(datasize);
factor2=zeros(datasize);
factor3=zeros(datasize);
```

```
deadsensors=zeros(datasize);

for row=1:datasize(1)
    for column=1:datasize(2)
        xdata=recordeddata(row,column,:);
        ydata=appliedpressure(row,column,:);
        xdata=xdata(:);
        ydata=ydata(:);
        okflag=1;
        for i=1:length(xdata)
            if xdata(i)==0
                okflag=0;
            end
        end
        for i=1:length(ydata)
            if ydata(i)==0
                okflag=0;
            end
        end
        if okflag==1
            [coeff,S]=polyfit(recordeddata(row,column,:),appliedpress
            ure(row,column,:),2);
            factor1(row,column)=coeff(1);
            factor2(row,column)=coeff(2);
            factor3(row,column)=coeff(3);
            deadsensors(row,column)=1;
        else
            deadsensors(row,column)=0;
        end
    end
end

deadsensors(deadsensors==0)=NaN

save('sensorcalPower.mat','factor1','factor2','factor3','deadsensors'
)

disp ('Loading calibration and deadsensors data from
sensorcalPower.mat')
load ('sensorcalPower.mat')
disp ('Loading faulty sensors from faultysensors.xls')
faultysensors=xlsread('faultysensors.xls')


recordedDataCalibratedPoly2=zeros(size(recordeddata));
for i=1:size(recordeddata,3)
      recordedDataCalibratedPoly2(:,:,i)=recordeddata(:,:,i).*deadsen
      sors;
      recordedDataCalibratedPoly2(:,:,i)=recordedDataCalibratedPoly2(
      :,:,i).*faultysensors;
      recordedDataCalibratedPoly2(:,:,i)=(recordedDataCalibratedPoly2
      (:,:,i).*recordedDataCalibratedPoly2(:,:,i).*factor1)+recordedD
      ataCalibratedPoly2(:,:,i).*factor2+factor3;
end

disp ('Saving data...')
```

```
save('recordedDataCalibratedPoly2','recordedDataCalibratedPoly2')

for row=1:datasize(1)
    for column=1:datasize(2)
      recorded=reshape(recordedDataCalibratedPoly2(row,column,:),size
      (recordedDataCalibratedPoly2,3),1);
      applied=reshape(appliedpressure(row,column,:),size(appliedpress
      ure,3),1);
        model=polyval(coeff,applied);
        ybar=mean(recorded);
        xbar=mean(applied);
        btemp=(applied-xbar).*(recorded-ybar);
        btemp=sum(btemp);
        btemp2=(applied-xbar);
        btemp2=btemp2.*btemp2;
        btemp2=sum(btemp2);
        b=btemp/btemp2;
        slrtemp=(applied-xbar).*(recorded-ybar);
        slrtemp=sum(slrtemp);
        slr=b.*slrtemp;
        stemp=(recorded-ybar);
        stemp=stemp.*stemp;
        s=sum(stemp);
        r2poly2(row,column)=slr/s;
    end
end

tempr2poly2=r2poly2(not(isnan(r2poly2)))
m=mean(tempr2poly2)
hist(tempr2poly2 (:),40)
s = std(tempr2poly2)


dataX=readtek('SensorD_6.10psi_Default.asf');
recordedDataCalibratedPoly2X=(dataX.*dataX.*factor1)+dataX.*factor2+f
actor3;
recordedDataCalibratedPoly2X=recordedDataCalibratedPoly2X.*deadsensor
s.*faultysensors;

disp ('appliedpressureX.xls')
appliedpressureX =xlsread('appliedpressureX.xls')
appliedpressureX=appliedpressureX.*deadsensors.*faultysensors;

errorX=recordedDataCalibratedPoly2X-appliedpressureX;
errorX=errorX./0.77;
errorX=errorX*100;
errorX(not(isnan(errorX)));
hist(errorX(:),40)

testX=abs(errorX)<20;
sum(testX(:))
numel(testX)
sum(testX(:))/numel(testX
```

Third order polynomial regression model:

```
data=readtek(char(filelist(1,1)));
datasize=[size(data,1),size(data,2)];
recordeddata=zeros([datasize,length(filelist)]);
for file=1:length(filelist)
    data=readtek(char(filelist(file,1)));
    recordeddata(:,:,file)=data;
end

appliedpressure=zeros(datasize(1),datasize(2),length(filelist));
for file=1:length(filelist)
appliedpressure(:,:,file)=ones(datasize)*cell2mat(filelist(file,2));
end

factor1=zeros(datasize);
factor2=zeros(datasize);
factor3=zeros(datasize);
factor4=zeros(datasize);
deadsensors=zeros(datasize);

for row=1:datasize(1)
    for column=1:datasize(2)
        xdata=recordeddata(row,column,:);
        ydata=appliedpressure(row,column,:);
        xdata=xdata(:);
        ydata=ydata(:);
        okflag=1;
        for i=1:length(xdata)
            if xdata(i)==0
                okflag=0;
            end
        end
        for i=1:length(ydata)
            if ydata(i)==0
                okflag=0;
            end
        end
        if okflag==1
            coeff=polyfit(xdata(:),ydata(:),3);
            factor1(row,column)=coeff(1);
            factor2(row,column)=coeff(2);
            factor3(row,column)=coeff(3);
            factor4(row,column)=coeff(4);
            deadsensors(row,column)=1;
        else
            deadsensors(row,column)=0;
        end
    end
end

deadsensors(deadsensors==0)=NaN

save('sensorcalPolynomial3.mat','factor1','factor2','factor3','factor
4','deadsensors')
```

```
disp ('Loading calibration and deadsensors data from
sensorcalPolynomial3.mat')
load ('sensorcalPolynomial3.mat')
disp ('Loading faulty sensors from faultysensors.xls')
faultysensors=xlsread('faultysensors.xls')

recordedDataCalibratedPolynomial3=zeros(size(recordeddata));
for i=1:size(recordeddata,3)
      recordedDataCalibratedPolynomial3(:,:,i)=recordeddata(:,:,i).*d
      eadsensors;
      recordedDataCalibratedPolynomial3(:,:,i)=recordedDataCalibrated
      Polynomial3(:,:,i).*faultysensors;
      recordedDataCalibratedPolynomial3(:,:,i)=(recordedDataCalibrate
      dPolynomial3(:,:,i).*recordedDataCalibratedPolynomial3(:,:,i).*
      recordedDataCalibratedPolynomial3(:,:,i).*factor1)+recordedData
      CalibratedPolynomial3(:,:,i).*recordedDataCalibratedPolynomial3
      (:,:,i).*factor2+recordedDataCalibratedPolynomial3(:,:,i).*fact
      or3+factor4;
end

disp ('Saving data...')
save('recordedDataCalibratedPolynomial3','recordedDataCalibratedPolyn
omial3')

for row=1:datasize(1)
    for column=1:datasize(2)
      recorded=reshape(recordedDataCalibratedPolynomial3(row,column,:
      ),size(recordedDataCalibratedPolynomial3,3),1);
      applied=reshape(appliedpressure(row,column,:),size(appliedpress
      ure,3),1);
        model=polyval(coeff,applied);
        ybar=mean(recorded);
        xbar=mean(applied);
        btemp=(applied-xbar).*(recorded-ybar);
        btemp=sum(btemp);
        btemp2=(applied-xbar);
        btemp2=btemp2.*btemp2;
        btemp2=sum(btemp2);
        b=btemp/btemp2;
        slrtemp=(applied-xbar).*(recorded-ybar);
        slrtemp=sum(slrtemp);
        slr=b.*slrtemp;
        stemp=(recorded-ybar);
        stemp=stemp.*stemp;
        s=sum(stemp);
        r2poly3(row,column)=slr/s;
    end
end

tempr2poly3=r2poly3(not(isnan(r2poly3)))
r2mean=mean(tempr2poly3)
hist(tempr2poly3(:),40)
s = std(tempr2poly3)

dataX=readtek('SensorD_6.10psi_Default.asf');
```

```
recordedCalibratedPoly3X=(dataX.*dataX.*dataX.*factor1)+dataX.*dataX.
*factor2+dataX.*factor3+factor4;
recordedCalibratedPoly3X=recordedCalibratedPoly3X.*deadsensors.*fault
ysensors;

disp ('appliedpressureX.xls')
appliedpressureX =xlsread('appliedpressureX.xls')
appliedpressureX=appliedpressureX.*deadsensors.*faultysensors;

errorX=recordedDataCalibratedPoly3X-appliedpressureX;
errorX=errorX./0.77;
errorX=errorX*100;
errorX(not(isnan(errorX)));
hist(errorX(:),40)

testX=abs(errorX)<20;
sum(testX(:))
numel(testX)
sum(testX(:))/numel(testX
```

APPENDIX F

MATLAB SCRIPTS FOR PROCESSING AND INTERPRETING TEKSCAN DATA

The scripts for processing and interpreting the experimental data were written to work for Matlab software version 7.1 (Matlab, 2005). Here is the procedure required after the 4th order polynomial multi-point calibration was established (Appendix E).

Procedure:

Load 'filelist2' from Excel which contains a list of names of ASCII files and save it as filelist2. The files were recorded as raw movies when during the tyre contact pressure experiments.

Run 'readframes' script which loads the data from filelist2 and saves it as the original file names plus '-raw.mat':

```
% Readframes.m
% Read Tekscan video frames from ASCII data into 3d array
% filelist = cell array of file names for this script to process
for file=1:length(filelist2)
    filenameRaw=char(filelist2(file,1));
    disp (filenameRaw)
    handleFile=fopen(filenameRaw);
    modeMatch=0 ;
    % State variable - 0 = searching header, 1 = searching frame
    header, 2 = reading frame

    disp ('Headers...')
    while (feof(handleFile)==0)
        stringLineFile=fgetl(handleFile);
        if modeMatch==0  % header info
            if regexp(stringLineFile, '^ROWS (.+)')
                match=regexp(stringLineFile,'^ROWS (.+)','tokens');
                frameRowTotal=str2num(cell2mat(match{1}));
            elseif regexp(stringLineFile, '^COLS (.+)')
                match=regexp(stringLineFile,'^COLS (.+)','tokens');
                frameColTotal=str2num(cell2mat(match{1}));
            elseif regexp(stringLineFile, '^START_FRAME (.+)')
                match=regexp(stringLineFile,'^START_FRAME
(.+)','tokens');
                frameCountStart=str2num(cell2mat(match{1}));
            elseif regexp(stringLineFile, '^END_FRAME (.+)')
                match=regexp(stringLineFile,'^END_FRAME
(.+)','tokens');
                frameCountEnd=str2num(cell2mat(match{1}));
```

```
            elseif regexp(stringLineFile, '^Frame (.+)')
                match=regexp(stringLineFile,'^Frame (.+)','tokens');
                frameCountCurrent=str2num(cell2mat(match{1}));

                disp (['Data(' num2str(frameCountStart) ' - '
num2str(frameCountEnd) ')...'])
                pointerCurFrame=1;
                pointerFrameRow=1;

                  dataFileRaw=zeros(frameRowTotal,frameColTotal,(fram
                  eCountEnd-frameCountStart+1));
                modeMatch=2;
            end
        elseif modeMatch==1  % frame end - look for next frame
            if regexp(stringLineFile, '^Frame (.+)')
                match=regexp(stringLineFile,'^Frame (.+)','tokens');
                frameCountCurrent=str2num(cell2mat(match{1}));
                pointerFrameRow=1;
                modeMatch=2;
            end
        elseif modeMatch==2

% use Tekscan method as "split" method below isn't supported on all
versions of Matlab
            dataTemp=textscan(stringLineFile,'%n','delimiter',',');
            dataFileRaw(pointerFrameRow,:,pointerCurFrame)=dataTemp{1
            }';
            pointerFrameRow=pointerFrameRow+1;
            if pointerFrameRow > frameRowTotal
                pointerCurFrame=pointerCurFrame+1;
                pointerFrameRow=1;
                modeMatch=1;
            end
        end
    end

      fclose(handleFile);
      clear handleFile pointerLineData modeMatch pointerCurFrame
      frameCountCurrent dataLineFile pointerFrameRow stringLineFile

      disp ('Saving data...')
      save([filenameRaw '-
      raw.mat'],'dataFileRaw','filenameRaw','frameCountStart','frameC
      ountEnd')
end
```

Apply the 4th order polynomial calibration parameters to the experimental data and save the calibrated data:

```
% Load calibration file
disp ('Loading calibration and deadsensors data from
sensorcalPolynomial4.mat')
load ('sensorcalPolynomial4.mat')
```

```
% Load faulty sensors file
disp ('Loading faulty sensors from faultysensors.xls')
faultysensors=xlsread('faultysensors.xls')

% Load raw experimental data
for file=1:size(filelist2,1)
    filenameRaw=char(filelist2(file,1));
    load([filenameRaw '-raw.mat'])

    % Apply the calibration parameters to the experimental data
    caldata=zeros(size(dataFileRaw));
    for frame=1:size(dataFileRaw,3)
        rawdata=dataFileRaw(:,:,frame).*deadsensors;
        rawdata=rawdata.*faultysensors;

      caldata(:,:,frame)=(rawdata.*rawdata.*rawdata.*rawdata.*factor1
      )+(rawdata.*rawdata.*rawdata.*factor2)+(rawdata.*rawdata.*facto
      r3)+(rawdata.*factor4)+factor5;
    end
    clear rawdata

    disp ('Saving data...')
      save([filenameRaw '-
      cal.mat'],'filenameRaw','frameCountStart','frameCountEnd','cald
      ata')
end
```

Process the experimental data collected for one test at the time using two Tekscan sensors (lining up the data according to Figure 18):

```
% Assemble an image out of a single sensor row for each of the rows
and then combine it into a mean image
close all
% Load a selected experimental data and put into two identical arrays
- one for each sensor
load('Test13_sensorA_right_low3_uncal.asf-cal.mat')
caldataA=caldata;
clear caldata

load('Test13_sensorB_left_low3_uncal.asf-cal.mat')
caldataB=caldata;
clear caldata

% Select first and end frame in order to reduce the number of frames
which do not contain any data
firstFrame=3100;
endFrame=4300;

% Line up the data (shiftFrame and timeSenslelTravel depend on the
tyre speed and need to be adjusted for each data setup)
% Then build contact patch data sets out of a single sensor row for
each of the rows
shiftFrame = 109;
timeSenselTravel=18.16666666666667;
```

```
outFrameStrip=zeros(60,floor((endFrame-firstFrame)/18),6);
pointerOutFrameStrip=1;

for idealCurFrame=firstFrame:timeSenselTravel:endFrame
    pointerCurFrame=round(idealCurFrame);

    % Process data from Sensor A
    % take mean of ten frames to smooth the picture - original log at
    % 100hz is too fast for reality, convert it into 10hz
      tempFrameA=mean(caldataA(:,:,pointerCurFrame+shiftFrame:pointer
      CurFrame+3+shiftFrame),3);
      tempFrameALater=mean(caldataA(:,:,pointerCurFrame+(shiftFrame*2
      ):pointerCurFrame+3+(shiftFrame*2)),3);

    % Mask faulty sensels (Sensor A)
    % Mask for dead sensels
    % identify sensors below zero and set them to zero
    zeromask=tempFrameA>0;

    % Manual modification of frame data involving block out any
    % incorrect sensels
    % zeromask(:,6)=zeros(16,1);
    % zeromask(15,10)=0;

    % Apply mask to the frame data
    tempFrameA=tempFrameA.*double(zeromask);

    % Mask faulty sensels (Sensor A Later)
    % Mask for dead sensels
    % identify sensors below zero and set them to zero
    zeromask=tempFrameALater>0;

    % Manual modification of frame data involving block out any
    % incorrect sensels
    % zeromask(:,6)=zeros(16,1);
    % zeromask(15,10)=0;

    % Apply mask to the frame data
    tempFrameALater=tempFrameALater.*double(zeromask);

    % Integrate Frame A and Frame A Later data into one dataset
    bigFrameA=[zeros(16,1) flipud(tempFrameALater(:,1:5));
    tempFrameA(:,6:11)];
%%%%%%%
    % Process data from Sensor B
    % take mean of ten frames to smooth the picture - original log at
    % 100hz is too fast for reality, convert it into 10hz
      tempFrameB=mean(caldataB(:,:,pointerCurFrame:pointerCurFrame+3
      ),3);
      tempFrameBLater=mean(caldataB(:,:,pointerCurFrame+shiftFrame:po
      interCurFrame+3+shiftFrame),3);

     % Flip the data arrays left - right as the sensor was used
     upside down to the other match sensor
    tempFrameB=fliplr(tempFrameB);
```

```
    tempFrameBLater=fliplr(tempFrameBLater);

    % Mask faulty sensels (Sensor B)
    % Mask for dead sensels
    % identify sensors below zero and set them to zero

    zeromask=tempFrameB>0;

    % Manual modification of frame data involving block out any
    % incorrect sensels
    %zeromask(:,6)=zeros(16,1);
    %zeromask(15,10)=0;

    % Apply mask to the frame data
    tempFrameB=tempFrameB.*double(zeromask);

    % Mask faulty sensels (Sensor B Later)
    % Mask for dead sensels
    % identify sensors below zero and set them to zero
    zeromask=tempFrameBLater>0;

    % Manual modification of frame data involving block out any
    % incorrect sensels
    %zeromask(:,6)=zeros(16,1);
    %zeromask(15,10)=0;

    % Apply mask to the frame data
    tempFrameBLater=tempFrameBLater.*double(zeromask);

    % Integrate Frame B and Frame B Later data into one dataset
    bigFrameB=[zeros(16,1) flipud(tempFrameBLater(:,1:5));
    tempFrameB(:,6:11)];

    % Integrate all data from Sensor A and B
    hugeFrame=[bigFrameA; flipud(bigFrameB)];
    % Account for the middle overlapping section of the sensors (area
    overalping for the 9830 sensor was 4 x 16 sensing elements)
    hugeFrameX=hugeFrame(29:32,:);
    hugeFrameY=hugeFrame(33:36,:);
    xy=cat(3,hugeFrameX,hugeFrameY);
    xyMean=mean(xy,3);
    hugeFrame=[hugeFrame(1:28,:); xyMean(:,:); hugeFrame(37:64,:)];

    % Copy a single line of sensels into the output stripe
    for sensor=1:6
      outFrameStrip(:,pointerOutFrameStrip,sensor)=hugeFrame(:,sensor
      );
    end

    % Index on
    pointerOutFrameStrip=pointerOutFrameStrip+1;
end
close all
```

```
% Build contact patch data sets out of a single sensor row for each
of the rows
for i=1:size(outFrameStrip,3)
    outFrameStrip(:,:,i)=circshift(outFrameStrip(:,:,i), [0 i]);
end

outFrameStrip=outFrameStrip(:,size(outFrameStrip,3):size(outFrameStri
p,2),:);

% Plot individual images together
     for sensor=1:6
         subplot(3,2,sensor)
         image(outFrameStrip(:,:,sensor),'CDataMapping','scaled')
         colormap jet
     end
set(gcf,'NextPlot','new')
newplot

% Build a mean contact patch data set out of the contact patch data
sets constructed above
meanOutFrameStrip=zeros(size(outFrameStrip,1),size(outFrameStrip,2));

% Select the values above zero
 for ix=1:size(outFrameStrip,1)
     for iy=1:size(outFrameStrip,2)
         templist=outFrameStrip(ix,iy,1:6);
         meanOutFrameStrip(ix,iy)=mean(templist(templist>0));
     end
 end

% Load 'useFrameInMean' Excel file separate for each test masking
erroneous and dead sensels
disp ('Loading useFrameInMean_Test13.xls')
useFrameInMean_Test13=xlsread('useFrameInMean_Test13.xls')

% Calculate the mean contact pressure patch according to the
correctly working sensels
for row=1:size(meanOutFrameStrip,1)
    rowlist=zeros(1,size(outFrameStrip,2));
    for sensor=1:size(outFrameStrip,3)
        if useFrameInMean_Test13(row,sensor)==1
            rowlist=[rowlist; outFrameStrip(row,:,sensor)];
        end
    end
    meanOutFrameStrip(row,:)=mean(rowlist(2:size(rowlist,1),:),1);
end

% Plot the mean image
image(meanOutFrameStrip,'CDataMapping','scaled')
colormap jet
% Calculate contact area and mean contact pressure for individual
images
meanPressureOutFrameStrip=zeros(size(outFrameStripLast,3),1);
areaContactSenselsStrip=zeros(size(outFrameStripLast,3),1);
pointerSelectedPatches=zeros(size(outFrameStripLast,3),1);
```

```
dataSelectedPatches=zeros(size(outFrameStripLast,1)*size(outFrameStri
pLast,2),size(outFrameStripLast,3));

% Establish threshold mask
maskSlices=zeros(size(outFrameStripLast));
for slice=1:size(outFrameStripLast,3)
      dataPatchData=zeros(1,size(outFrameStripLast,1)*size(outFrameSt
      ripLast,2));
      pointerPatchData=1;
            for row=1:size(outFrameStripLast,1)
            dataRow=outFrameStripLast(row,:,slice);
            threshold=max(dataRow(1:15));
            goodValues=dataRow(dataRow>threshold);
            maskSlices(row,:,slice)=dataRow>threshold;
            if not(isempty(goodValues))
            dataPatchData(pointerPatchData:pointerPatchData+length(go
            odValues)-1)=goodValues;
            pointerPatchData=pointerPatchData+length(goodValues);
        end
    end

      meanPressureOutFrameStrip(slice)=mean(dataPatchData(1:pointerPa
      tchData-1));
      areaContactSenselsStrip(slice)=(pointerPatchData-1)*0.00021717;
      dataSelectedPatches(:,slice)=dataPatchData;
      pointerSelectedPatches(slice)=pointerPatchData-1;
end
clear dataPatchData pointerPatchData

% Find the maximum contact area of the individual images as some
images have some broken sensels and do not give a correct indication
of the contact area
areaForIndividualsLargest=max(areaContactSenselsStrip);

% Calculate maximum contact pressure for individual images
maxPressureOutFrameStrip=zeros(size(outFrameStrip,3),1);
for i=1:size(outFrameStrip,3)
          templist=outFrameStrip(:,:,i);
          maxPressureOutFrameStrip(i)=max(templist(:));
end

% Calculate the mean and maximum contact pressure for the mean image
templist=meanOutFrameStrip(:,:);
maxOfmeanPressure=max(templist(templist>maskForMean));
meanOfmeanPressure=mean(templist(templist>maskForMean));

% Calculate contact area for the mean image
areaForMean=numel(templist(templist>maskForMean));
areaForMean=areaForMean*0.00021717;
```

APPENDIX G

STATISTICAL ANALYSIS – HARD SURFACE RESULTS OF THE INNER TUBE AND FRONT TRACTOR TYRE (ANOVA)

G.1 Ink Tests: Inner tube – Contact area – effect of load (One-way ANOVA)

Effect	Univariate Tests of Significance for Average area (m2) (Spreadsheet7) Sigma-restricted parameterization Effective hypothesis decomposition				
	SS	Degr. of Freedom	MS	F	p
Intercept	0.055780	1	0.055780	3333.544	0.000000
Load (kg)	0.010547	7	0.001507	90.043	0.000000
Error	0.000301	18	0.000017		

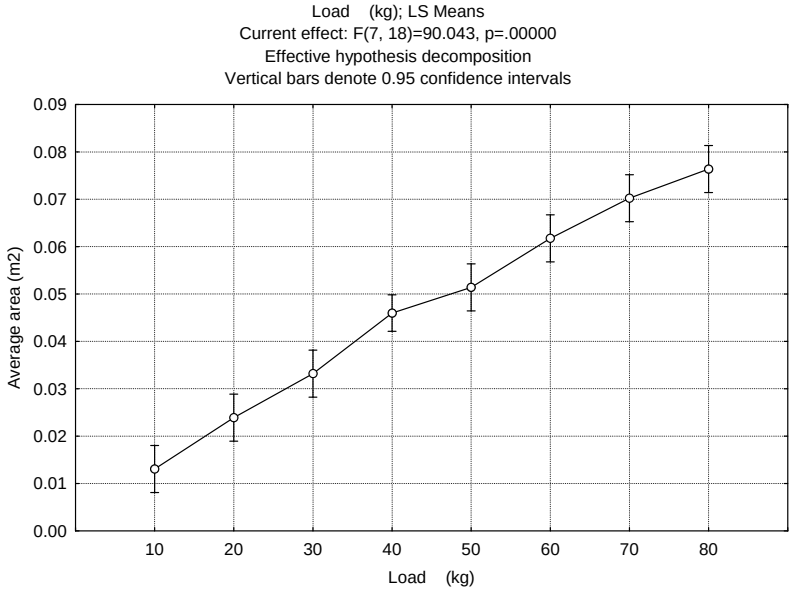

Cell No.	LSD test; variable Average area (m2) (Spreadsheet7) Probabilities for Post Hoc Tests Error: Between MS = .00002, df = 18.000								
	Load (kg)	1 .01308	2 .02391	3 .03319	4 .04599	5 .05140	6 .06174	7 .07022	8 .07638
1	10		0.004519	0.000011	0.000000	0.000000	0.000000	0.000000	0.000000
2	20	0.004519		0.012342	0.000001	0.000000	0.000000	0.000000	0.000000
3	30	0.000011	0.012342		0.000448	0.000035	0.000000	0.000000	0.000000
4	40	0.000000	0.000001	0.000448		0.086476	0.000051	0.000000	0.000000
5	50	0.000000	0.000000	0.000035	0.086476		0.006236	0.000024	0.000001
6	60	0.000000	0.000000	0.000000	0.000051	0.006236		0.020569	0.000359
7	70	0.000000	0.000000	0.000000	0.000000	0.000024	0.020569		0.081810
8	80	0.000000	0.000000	0.000000	0.000000	0.000001	0.000359	0.081810	

G.2 Tekscan Tests: Front Tractor Tyre – Contact area – effect of load and inflation pressure (Factorial ANOVA)

Effect	Univariate Tests of Significance for Contact area (m2) (Spreadsheet1) Sigma-restricted parameterization Effective hypothesis decomposition				
	SS	Degr. of Freedom	MS	F	p
Intercept	0.070790	1	0.070790	153750.1	0.000000
Load (kg)	0.001320	2	0.000660	1432.9	0.000000
Inflation pressure x 10 (bar)	0.002344	6	0.000391	848.4	0.000000
Load (kg)*Inflation pressure x 10 (bar)	0.000029	12	0.000002	5.3	0.000810
Error	0.000008	18	0.000000		

LSD at 95% confidence level = 0.0012m^3

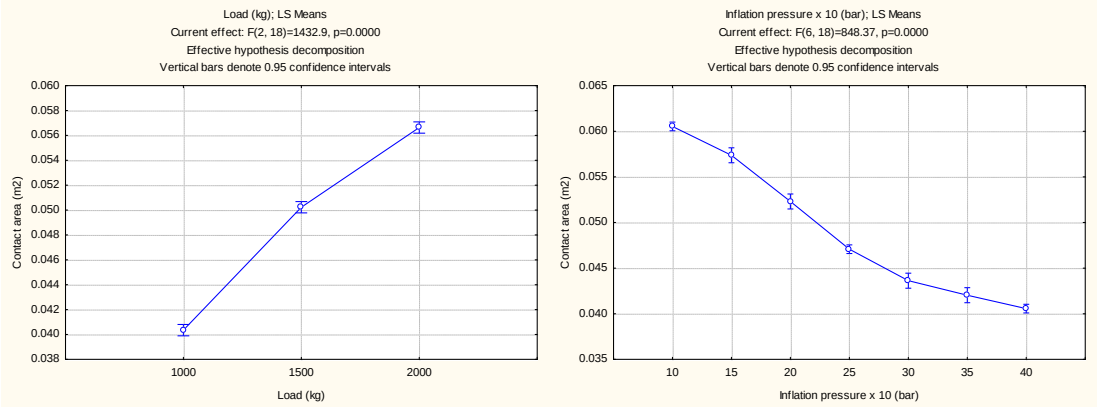

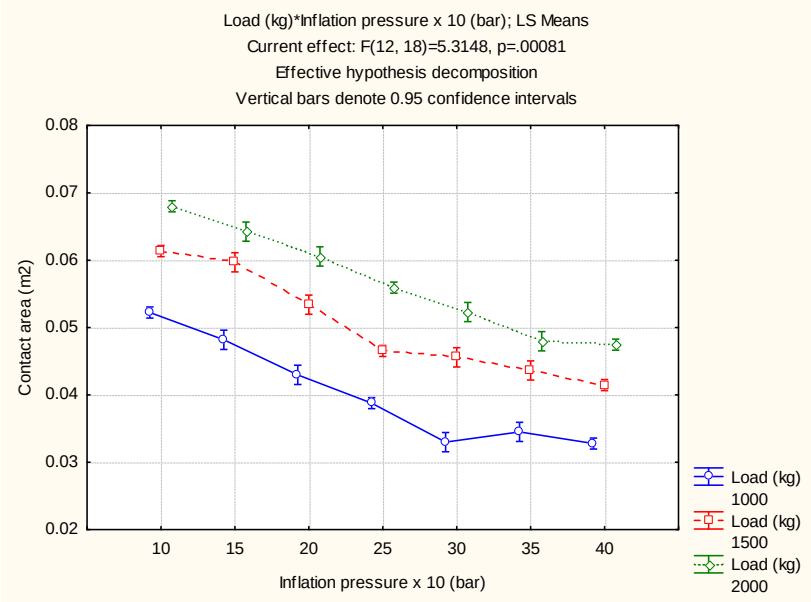

Cell No.	LSD test; variable Contact area (m2) (Spreadsheet1) Probabilities for Post Hoc Tests Error: Between MS = .00000, df = 18.000						
	Load (kg)	Inflation pressure x 10 (bar)	1 .05223	2 .04818	3 .04297	4 .03878	5 .03299
1	1000	10		0.000064	0.000000	0.000000	0.000000
2	1000	15	0.000064		0.000037	0.000000	0.000000
3	1000	20	0.000000	0.000037		0.000043	0.000000
4	1000	25	0.000000	0.000000	0.000043		0.000001
5	1000	30	0.000000	0.000000	0.000000	0.000001	
6	1000	35	0.000000	0.000000	0.000000	0.000036	0.130848
7	1000	40	0.000000	0.000000	0.000000	0.000000	0.784969
8	1500	10	0.000000	0.000000	0.000000	0.000000	0.000000
9	1500	15	0.000000	0.000000	0.000000	0.000000	0.000000
10	1500	20	0.156932	0.000037	0.000000	0.000000	0.000000
11	1500	25	0.000000	0.047848	0.000262	0.000000	0.000000
12	1500	30	0.000000	0.014234	0.014203	0.000000	0.000000
13	1500	35	0.000000	0.000160	0.506147	0.000008	0.000000
14	1500	40	0.000000	0.000000	0.068382	0.000134	0.000000
15	2000	10	0.000000	0.000000	0.000000	0.000000	0.000000
16	2000	15	0.000000	0.000000	0.000000	0.000000	0.000000
17	2000	20	0.000000	0.000000	0.000000	0.000000	0.000000
18	2000	25	0.000003	0.000000	0.000000	0.000000	0.000000
19	2000	30	0.927465	0.000433	0.000000	0.000000	0.000000
20	2000	35	0.000036	0.823646	0.000060	0.000000	0.000000
21	2000	40	0.000000	0.368121	0.000020	0.000000	0.000000

Cell No.	LSD test; variable Contact area (m2) (Spreadsheet1) Probabilities for Post Hoc Tests Error: Between MS = .00000, df = 18.000							
	6 .03451	7 .03277	8 .06135	9 .05968	10 .05339	11 .04652	12 .04558	13 .04362
1	0.000000	0.000000	0.000000	0.000000	0.156932	0.000000	0.000000	0.000000
2	0.000000	0.000000	0.000000	0.000000	0.000037	0.047848	0.014234	0.000160
3	0.000000	0.000000	0.000000	0.000000	0.000000	0.000262	0.014203	0.506147
4	0.000036	0.000000	0.000000	0.000000	0.000000	0.000000	0.000000	0.000008
5	0.130848	0.784969	0.000000	0.000000	0.000000	0.000000	0.000000	0.000000
6		0.039845	0.000000	0.000000	0.000000	0.000000	0.000000	0.000000
7	0.039845		0.000000	0.000000	0.000000	0.000000	0.000000	0.000000
8	0.000000	0.000000		0.047848	0.000000	0.000000	0.000000	0.000000
9	0.000000	0.000000	0.047848		0.000004	0.000000	0.000000	0.000000
10	0.000000	0.000000	0.000000	0.000004		0.000000	0.000000	0.000000
11	0.000000	0.000000	0.000000	0.000000	0.000000		0.245642	0.001661
12	0.000000	0.000000	0.000000	0.000000	0.000000	0.245642		0.056713
13	0.000000	0.000000	0.000000	0.000000	0.000000	0.001661	0.056713	
14	0.000000	0.000000	0.000000	0.000000	0.000000	0.000000	0.000053	0.012634
15	0.000000	0.000000	0.000000	0.000000	0.000000	0.000000	0.000000	0.000000
16	0.000000	0.000000	0.001665	0.000160	0.000000	0.000000	0.000000	0.000000
17	0.000000	0.000000	0.323322	0.377660	0.000001	0.000000	0.000000	0.000000
18	0.000000	0.000000	0.000000	0.000143	0.004634	0.000000	0.000000	0.000000
19	0.000000	0.000000	0.000000	0.000000	0.273036	0.000001	0.000002	0.000000
20	0.000000	0.000000	0.000000	0.000000	0.000023	0.081348	0.022896	0.000263
21	0.000000	0.000000	0.000000	0.000000	0.000001	0.106871	0.027411	0.000117

Cell No.	LSD test; variable Contact area (m2) (Spreadsheet1) Probabilities for Post Hoc Tests Error: Between MS = .00000, df = 18.000							
	14 .04145	15 .06800	16 .06424	17 .06055	18 .05592	19 .05230	20 .04796	21 .04746
1	0.000000	0.000000	0.000000	0.000000	0.000003	0.927465	0.000036	0.000000
2	0.000000	0.000000	0.000000	0.000000	0.000000	0.000433	0.823646	0.368121
3	0.068382	0.000000	0.000000	0.000000	0.000000	0.000000	0.000060	0.000020
4	0.000134	0.000000	0.000000	0.000000	0.000000	0.000000	0.000000	0.000000
5	0.000000	0.000000	0.000000	0.000000	0.000000	0.000000	0.000000	0.000000
6	0.000000	0.000000	0.000000	0.000000	0.000000	0.000000	0.000000	0.000000
7	0.000000	0.000000	0.000000	0.000000	0.000000	0.000000	0.000000	0.000000
8	0.000000	0.000000	0.001665	0.323322	0.000000	0.000000	0.000000	0.000000
9	0.000000	0.000000	0.000160	0.377660	0.000143	0.000000	0.000000	0.000000
10	0.000000	0.000000	0.000000	0.000001	0.004634	0.273036	0.000023	0.000001
11	0.000000	0.000000	0.000000	0.000000	0.000000	0.000001	0.081348	0.106871
12	0.000053	0.000000	0.000000	0.000000	0.000000	0.000002	0.022896	0.027411
13	0.012634	0.000000	0.000000	0.000000	0.000000	0.000000	0.000263	0.000117
14		0.000000	0.000000	0.000000	0.000000	0.000000	0.000000	0.000000
15	0.000000		0.000144	0.000000	0.000000	0.000000	0.000000	0.000000
16	0.000000	0.000144		0.001188	0.000000	0.000000	0.000000	0.000000
17	0.000000	0.000000	0.001188		0.000014	0.000000	0.000000	0.000000
18	0.000000	0.000000	0.000000	0.000014		0.000215	0.000000	0.000000
19	0.000000	0.000000	0.000000	0.000000	0.000215		0.000263	0.000008
20	0.000000	0.000000	0.000000	0.000000	0.000000	0.000263		0.526285
21	0.000000	0.000000	0.000000	0.000000	0.000000	0.000008	0.526285	

G.3 Ink Tests: Front Tractor Tyre – Tread contact area – effect of load and inflation pressure (Factorial ANOVA)

Effect	Univariate Tests of Significance for Tread contact area (m2) (Spreadsheet.sta) Sigma-restricted parameterization Effective hypothesis decomposition				
	SS	Degr. of Freedom	MS	F	p
Intercept	0.021727	1	0.021727	23877.07	0.000042
Load (kg)	0.001901	3	0.000634	696.30	0.001434
Inflation pressure (bar)	0.000712	3	0.000237	260.71	0.003824
Load (kg)*Inflation pressure (bar)	0.000081	9	0.000009	9.92	0.094873
Error	0.000002	2	0.000001		

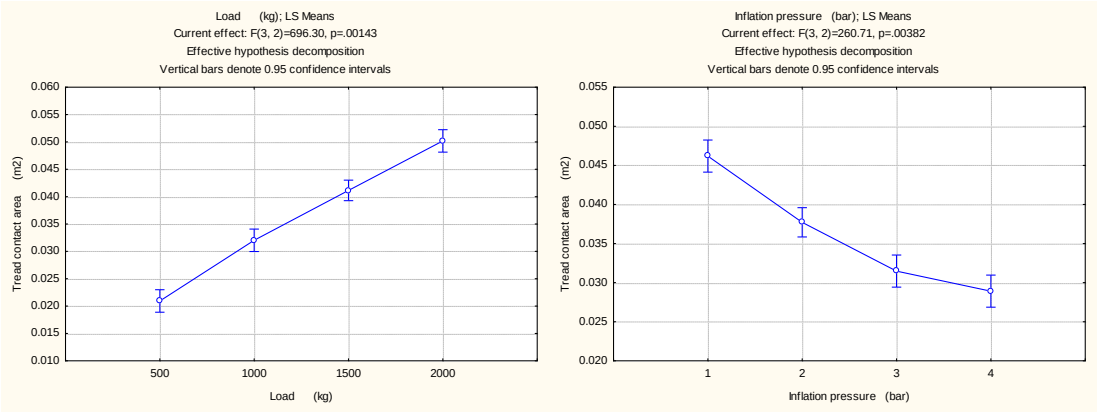

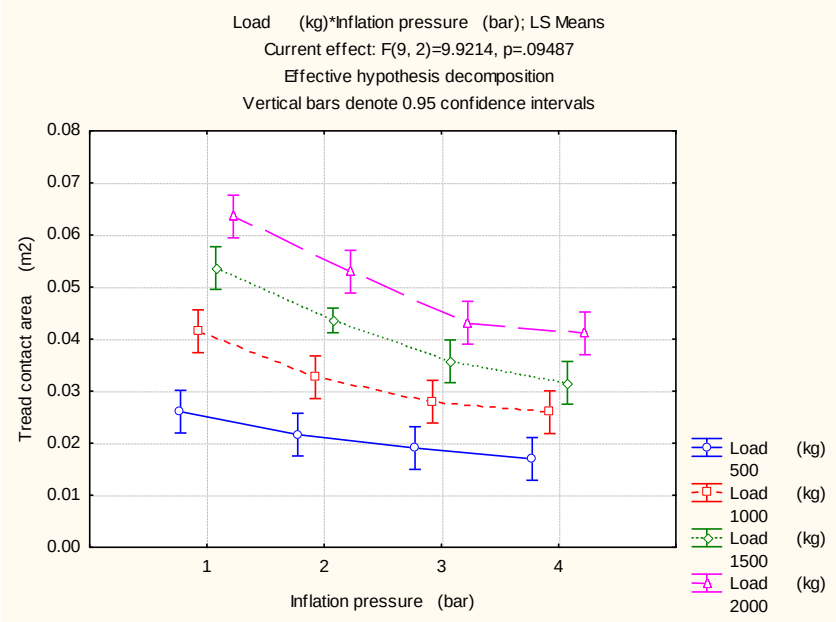

Cell No.	LSD test; variable Tread contact area (m2) (Spreadsheet.sta) Probabilities for Post Hoc Tests Error: Between MS = .00000, df = 2.0000								
	Load (kg)	Inflation pressure (bar)	1 .02606	2 .02166	3 .01906	4 .01699	5 .04150	6 .03267	7 .02797
1	500	1		0.082479	0.035256	0.021407	0.007541	0.039163	0.291877
2	500	2	0.082479		0.194676	0.074271	0.004588	0.014666	0.042732
3	500	3	0.035256	0.194676		0.263323	0.003595	0.009685	0.022181
4	500	4	0.021407	0.074271	0.263323		0.003014	0.007315	0.014749
5	1000	1	0.007541	0.004588	0.003595	0.003014		0.022547	0.009791
6	1000	2	0.039163	0.014666	0.009685	0.007315	0.022547		0.073381
7	1000	3	0.291877	0.042732	0.022181	0.014749	0.009791	0.073381	
8	1000	4	0.951137	0.085640	0.036165	0.021840	0.007452	0.038142	0.275272
9	1500	1	0.002381	0.001773	0.001518	0.001351	0.012105	0.004109	0.002748
10	1500	2	0.003926	0.002514	0.002012	0.001710	0.199507	0.010036	0.004940
11	1500	3	0.018881	0.009056	0.006484	0.005137	0.050582	0.151163	0.028882
12	1500	4	0.054435	0.017908	0.011382	0.008413	0.018055	0.510257	0.114812
13	2000	1	0.001292	0.001035	0.000918	0.000838	0.003724	0.001904	0.001435

Cell No.	LSD test; variable Tread contact area (m2) (Spreadsheet.sta) Probabilities for Post Hoc Tests Error: Between MS = .00000, df = 2.0000								
	Load (kg)	Inflation pressure (bar)	1 .02606	2 .02166	3 .01906	4 .01699	5 .04150	6 .03267	7 .02797
14	2000	2	0.002507	0.001853	0.001581	0.001404	0.013603	0.004396	0.002903
15	2000	3	0.006175	0.003918	0.003124	0.002649	0.347749	0.016190	0.007811
16	2000	4	0.007938	0.004775	0.003724	0.003113	0.797259	0.024628	0.010379

Cell No.	LSD test; variable Tread contact area (m2) (Spreadsheet.sta) Probabilities for Post Hoc Tests Error: Between MS = .00000, df = 2.0000								
	8 .02596	9 .05365	10 .04358	11 .03573	12 .03160	13 .06355	14 .05295	15 .04314	16 .04111
1	0.951137	0.002381	0.003926	0.018881	0.054435	0.001292	0.002507	0.006175	0.007938
2	0.085640	0.001773	0.002514	0.009056	0.017908	0.001035	0.001853	0.003918	0.004775
3	0.036165	0.001518	0.002012	0.006484	0.011382	0.000918	0.001581	0.003124	0.003724
4	0.021840	0.001351	0.001710	0.005137	0.008413	0.000838	0.001404	0.002649	0.003113
5	0.007452	0.012105	0.199507	0.050582	0.018055	0.003724	0.013603	0.347749	0.797259
6	0.038142	0.004109	0.010036	0.151163	0.510257	0.001904	0.004396	0.016190	0.024628
7	0.275272	0.002748	0.004940	0.028882	0.114812	0.001435	0.002903	0.007811	0.010379
8		0.002365	0.003885	0.018532	0.052786	0.001286	0.002489	0.006108	0.007841
9	0.002365		0.011755	0.005621	0.003721	0.018091	0.654824	0.016085	0.011367
10	0.003885	0.011755		0.019131	0.008343	0.003031	0.013545	0.728812	0.153622
11	0.018532	0.005621	0.019131		0.091989	0.002345	0.006084	0.031583	0.057637
12	0.052786	0.003721	0.008343	0.091989		0.001778	0.003968	0.013381	0.019542
13	0.001286	0.018091	0.003031	0.002345	0.001778		0.015829	0.004344	0.003595
14	0.002489	0.654824	0.013545	0.006084	0.003968	0.015829		0.018403	0.012728
15	0.006108	0.016085	0.728812	0.031583	0.013381	0.004344	0.018403		0.270188
16	0.007841	0.011367	0.153622	0.057637	0.019542	0.003595	0.012728	0.270188	

G.4 Ink Tests: Front Tractor Tyre – Projected contact area – effect of load and inflation pressure (Factorial ANOVA)

Effect	Univariate Tests of Significance for Projected contact area (m2) (Spreadsheet.sta) Sigma-restricted parameterization Effective hypothesis decomposition				
	SS	Degr. of Freedom	MS	F	p
Intercept	0.028677	1	0.028677	26413.73	0.000038
Load (kg)	0.002508	3	0.000836	770.02	0.001297
Inflation pressure (bar)	0.000937	3	0.000312	287.70	0.003466
Load (kg)*Inflation pressure (bar)	0.000108	9	0.000012	11.04	0.085811
Error	0.000002	2	0.000001		

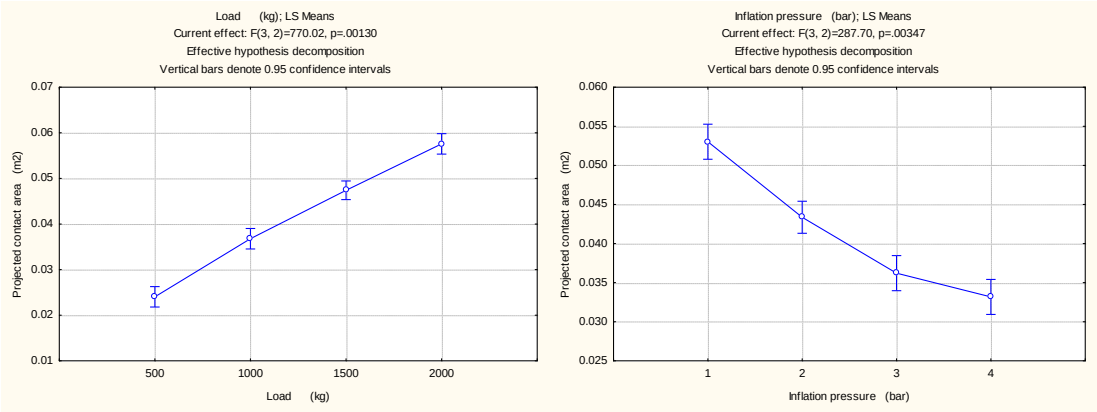

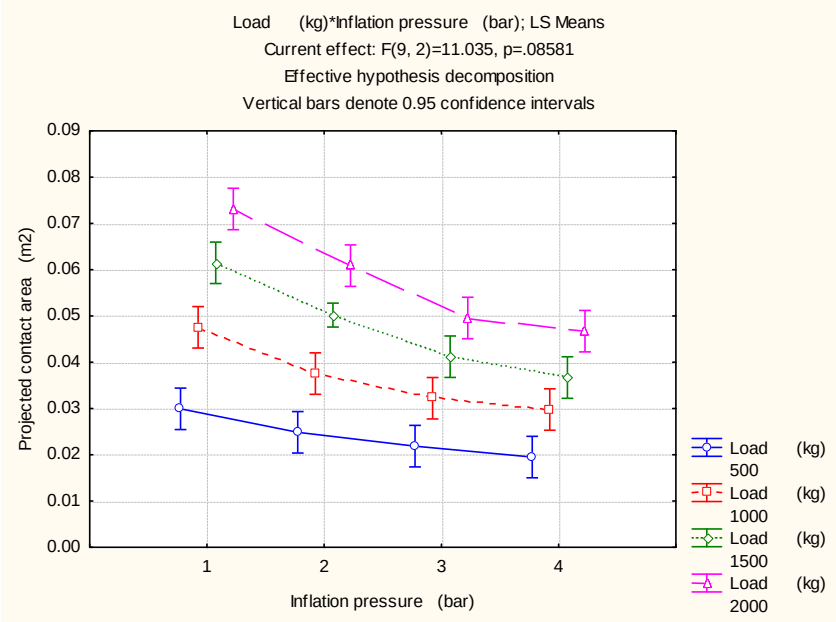

Cell No.	LSD test; variable Projected contact area (m2) (Spreadsheet.sta) Probabilities for Post Hoc Tests Error: Between MS = .00000, df = 2.0000								
	Load (kg)	Inflation pressure (bar)	1 .02993	2 .02486	3 .02186	4 .01951	5 .04755	6 .03754	7 .03222
1	500	1		0.075038	0.031811	0.019412	0.006916	0.035465	0.259910
2	500	2	0.075038		0.179449	0.068193	0.004188	0.013224	0.037776
3	500	3	0.031811	0.179449		0.250640	0.003274	0.008718	0.019649
4	500	4	0.019412	0.068193	0.250640		0.002749	0.006608	0.013166
5	1000	1	0.006916	0.004188	0.003274	0.002749		0.020983	0.009109
6	1000	2	0.035465	0.013224	0.008718	0.006608	0.020983		0.068848
7	1000	3	0.259910	0.037776	0.019649	0.013166	0.009109	0.068848	
8	1000	4	0.931381	0.078956	0.032917	0.019941	0.006806	0.034232	0.240026
9	1500	1	0.002172	0.001614	0.001380	0.001229	0.010990	0.003764	0.002524
10	1500	2	0.003508	0.002248	0.001800	0.001534	0.160027	0.008931	0.004454
11	1500	3	0.016645	0.008025	0.005754	0.004580	0.049881	0.130796	0.025858
12	1500	4	0.044336	0.015151	0.009733	0.007272	0.017907	0.621688	0.093655
13	2000	1	0.001161	0.000931	0.000825	0.000754	0.003304	0.001710	0.001295

Cell No.	LSD test; variable Projected contact area (m2) (Spreadsheet.sta) Probabilities for Post Hoc Tests Error: Between MS = .00000, df = 2.0000								
	Load (kg)	Inflation pressure (bar)	1 .02993	2 .02486	3 .02186	4 .01951	5 .04755	6 .03754	7 .03222
14	2000	2	0.002260	0.001670	0.001424	0.001266	0.012021	0.003966	0.002635
15	2000	3	0.005583	0.003537	0.002818	0.002394	0.305475	0.014690	0.007140
16	2000	4	0.007613	0.004512	0.003496	0.002919	0.628058	0.024828	0.010172

Cell No.	LSD test; variable Projected contact area (m2) (Spreadsheet.sta) Probabilities for Post Hoc Tests Error: Between MS = .00000, df = 2.0000								
	8 .02978	9 .06149	10 .05019	11 .04120	12 .03669	13 .07313	14 .06087	15 .04956	16 .04672
1	0.931381	0.002172	0.003508	0.016645	0.044336	0.001161	0.002260	0.005583	0.007613
2	0.078956	0.001614	0.002248	0.008025	0.015151	0.000931	0.001670	0.003537	0.004512
3	0.032917	0.001380	0.001800	0.005754	0.009733	0.000825	0.001424	0.002818	0.003496
4	0.019941	0.001229	0.001534	0.004580	0.007272	0.000754	0.001266	0.002394	0.002919
5	0.006806	0.010990	0.160027	0.049881	0.017907	0.003304	0.012021	0.305475	0.628058
6	0.034232	0.003764	0.008931	0.130796	0.621688	0.001710	0.003966	0.014690	0.024828
7	0.240026	0.002524	0.004454	0.025858	0.093655	0.001295	0.002635	0.007140	0.010172
8		0.002152	0.003459	0.016240	0.042629	0.001154	0.002239	0.005503	0.007486
9	0.002152		0.011135	0.005234	0.003511	0.015668	0.714132	0.014920	0.009801
10	0.003459	0.011135		0.017473	0.007853	0.002740	0.012444	0.656555	0.102189
11	0.016240	0.005234	0.017473		0.092046	0.002124	0.005567	0.029691	0.064590
12	0.042629	0.003511	0.007853	0.092046		0.001632	0.003693	0.012847	0.020916
13	0.001154	0.015668	0.002740	0.002124	0.001632		0.014152	0.003888	0.003099
14	0.002239	0.714132	0.012444	0.005567	0.003693	0.014152		0.016564	0.010666
15	0.005503	0.014920	0.656555	0.029691	0.012847	0.003888	0.016564		0.193103
16	0.007486	0.009801	0.102189	0.064590	0.020916	0.003099	0.010666	0.193103	

G.5 Ink Tests: Front Tractor Tyre – Tread contact pressure – effect of load and inflation pressure (Factorial ANOVA)

Effect	Univariate Tests of Significance for Contact pressure according to tread contact area (Spreadsheet6) Sigma-restricted parameterization Effective hypothesis decomposition				
	SS	Degr. of Freedom	MS	F	p
Intercept	185.0509	1	185.0509	34689.09	0.000029
Load (kg)	6.2440	3	2.0813	390.16	0.002558
Inflation pressure (bar)	5.3443	3	1.7814	333.94	0.002987
Load (kg)*Inflation pressure (bar)	0.3493	9	0.0388	7.27	0.126641
Error	0.0107	2	0.0053		

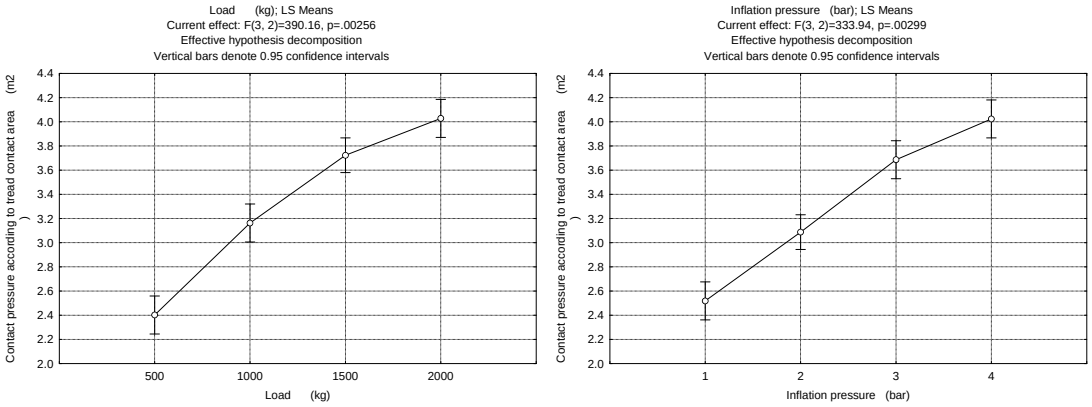

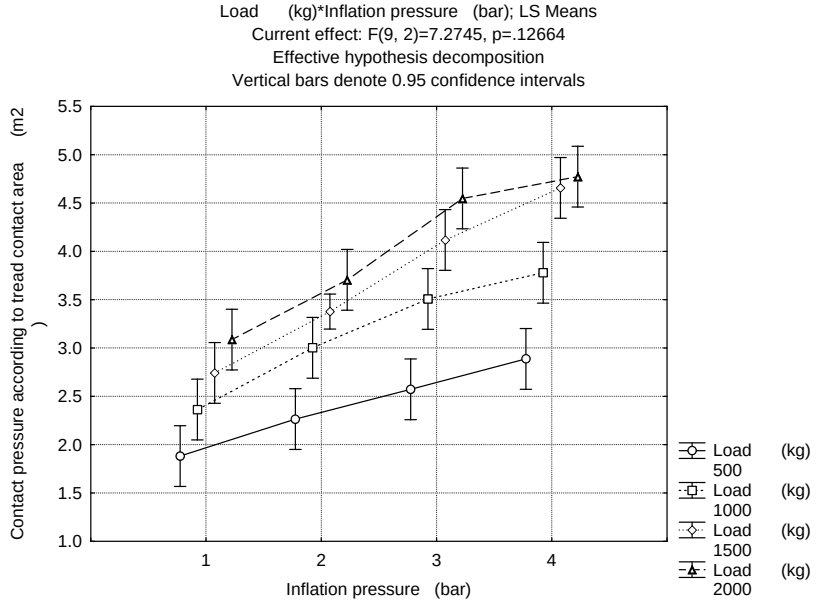

Cell No.	LSD test; variable Contact pressure according to tread contact area (Spreadsheet6) Probabilities for Post Hoc Tests Error: Between MS = .00533, df = 2.0000					
	Load (kg)	Inflation pressure (bar)	1 1.8824	2 2.2651	3 2.5730	4 2.8878
1	500	1		0.065766	0.021649	0.010390
2	500	2	0.065766		0.096502	0.026423
3	500	3	0.021649	0.096502		0.092881
4	500	4	0.010390	0.026423	0.092881	
5	1000	1	0.043113	0.440533	0.179923	0.036706
6	1000	2	0.008396	0.019055	0.053236	0.382227
7	1000	3	0.004017	0.006843	0.012002	0.026693
8	1000	4	0.002955	0.004626	0.007263	0.013187
9	1500	1	0.014115	0.043738	0.242292	0.294937
10	1500	2	0.003168	0.005700	0.010817	0.028428
11	1500	3	0.002128	0.003094	0.004441	0.006979
12	1500	4	0.001383	0.001860	0.002448	0.003393
13	2000	1	0.007267	0.015410	0.038022	0.192948
14	2000	2	0.003196	0.005104	0.008220	0.015595

Cell No.	LSD test; variable Contact pressure according to tread contact area (Spreadsheet6) Probabilities for Post Hoc Tests Error: Between MS = .00533, df = 2.0000					
	Load (kg)	Inflation pressure (bar)	1 1.8824	2 2.2651	3 2.5730	4 2.8878
15	2000	3	0.001499	0.002042	0.002726	0.003851
16	2000	4	0.001275	0.001692	0.002198	0.002989

Cell No.	LSD test; variable Contact pressure according to tread contact area (Spreadsheet6) Probabilities for Post Hoc Tests Error: Between MS = .00533, df = 2.0000							
	5 2.3637	6 3.0026	7 3.5073	8 3.7784	9 2.7426	10 3.3773	11 4.1178	12 4.6566
1	0.043113	0.008396	0.004017	0.002955	0.014115	0.003168	0.002128	0.001383
2	0.440533	0.019055	0.006843	0.004626	0.043738	0.005700	0.003094	0.001860
3	0.179923	0.053236	0.012002	0.007263	0.242292	0.010817	0.004441	0.002448
4	0.036706	0.382227	0.026693	0.013187	0.294937	0.028428	0.006979	0.003393
5		0.025153	0.008059	0.005288	0.066926	0.006851	0.003449	0.002023
6	0.025153		0.039421	0.017269	0.128180	0.047107	0.008470	0.003877
7	0.008059	0.039421		0.119681	0.017759	0.263098	0.027454	0.007980
8	0.005288	0.017269	0.119681		0.009798	0.041481	0.081460	0.013552
9	0.066926	0.128180	0.017759	0.009798		0.017202	0.005594	0.002900
10	0.006851	0.047107	0.263098	0.041481	0.017202		0.012724	0.004318
11	0.003449	0.008470	0.027454	0.081460	0.005594	0.012724		0.034838
12	0.002023	0.003877	0.007980	0.013552	0.002900	0.004318	0.034838	
13	0.019762	0.497534	0.055536	0.021628	0.079188	0.075247	0.009901	0.004305
14	0.005875	0.020933	0.195387	0.552289	0.011318	0.060221	0.057348	0.011583
15	0.002230	0.004441	0.009718	0.017565	0.003259	0.005155	0.053225	0.401291
16	0.001833	0.003388	0.006597	0.010619	0.002579	0.003633	0.023981	0.377764

Cell No.	LSD test; variable Contact pressure according to tread contact area (Spreadsheet6) Probabilities for Post Hoc Tests Error: Between MS = .00533, df = 2.0000			
	13 3.0875	14 3.7053	15 4.5475	16 4.7728
1	0.007267	0.003196	0.001499	0.001275
2	0.015410	0.005104	0.002042	0.001692
3	0.038022	0.008220	0.002726	0.002198
4	0.192948	0.015595	0.003851	0.002989
5	0.019762	0.005875	0.002230	0.001833
6	0.497534	0.020933	0.004441	0.003388
7	0.055536	0.195387	0.009718	0.006597
8	0.021628	0.552289	0.017565	0.010619
9	0.079188	0.011318	0.003259	0.002579
10	0.075247	0.060221	0.005155	0.003633
11	0.009901	0.057348	0.053225	0.023981
12	0.004305	0.011583	0.401291	0.377764
13		0.026836	0.004968	0.003736
14	0.026836		0.014711	0.009233
15	0.004968	0.014711		0.160931
16	0.003736	0.009233	0.160931	

G.6 Ink Tests: Front Tractor Tyre – Projected contact pressure – effect of load and inflation pressure (Factorial ANOVA)

Effect	Univariate Tests of Significance for Contact pressure according to projected contact area (Spreadsheet6) Sigma-restricted parameterization Effective hypothesis decomposition				
	SS	Degr. of Freedom	MS	F	p
Intercept	140.1507	1	140.1507	38709.85	0.000026
Load (kg)	4.7211	3	1.5737	434.66	0.002296
Inflation pressure (bar)	4.0423	3	1.3474	372.16	0.002681
Load (kg)*Inflation pressure (bar)	0.2507	9	0.0279	7.69	0.120249
Error	0.0072	2	0.0036		

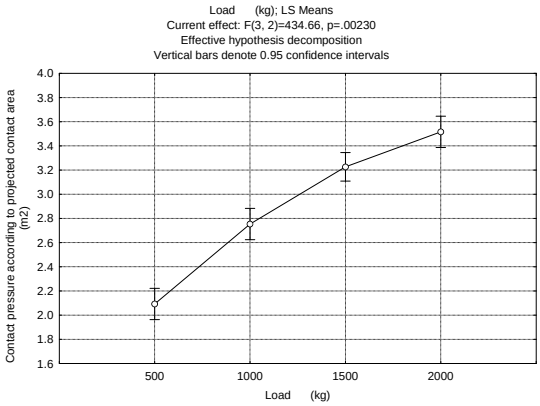

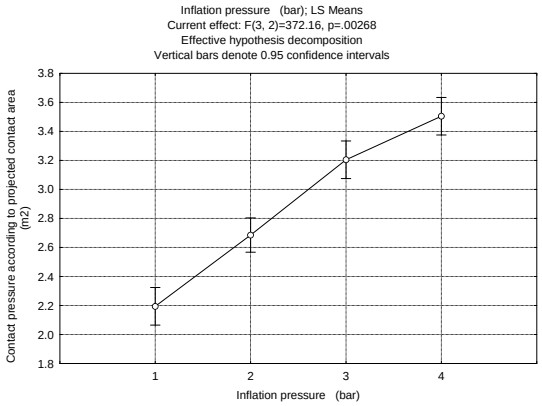

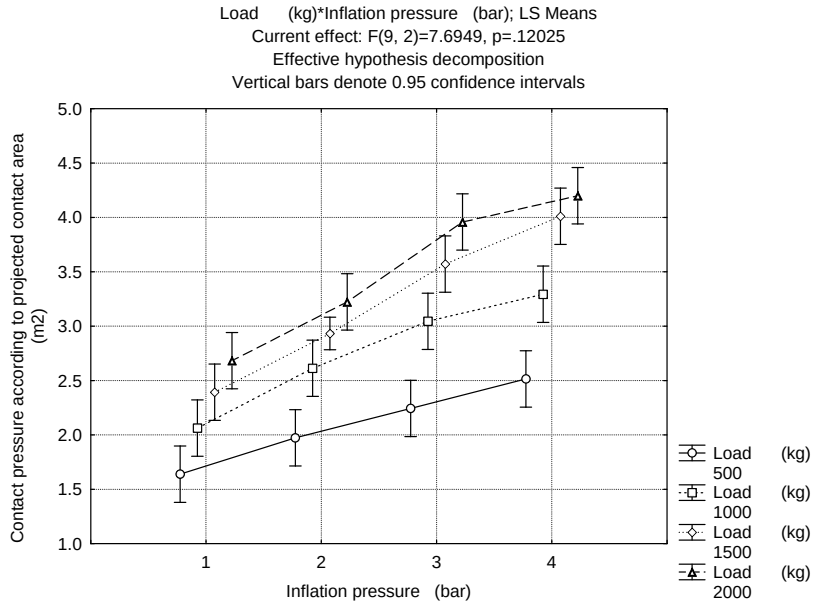

Cell No.	LSD test; variable Contact pressure according to projected contact area (Spreadsheet6) Probabilities for Post Hoc Tests Error: Between MS = .00362, df = 2.0000					
	Load (kg)	Inflation pressure (bar)	1 1.6390	2 1.9734	3 2.2435	4 2.5147
1	500	1		0.059062	0.019247	0.009310
2	500	2	0.059062		0.086598	0.023834
3	500	3	0.019247	0.086598		0.085917
4	500	4	0.009310	0.023834	0.085917	
5	1000	1	0.038008	0.403229	0.167918	0.033693
6	1000	2	0.007545	0.017241	0.049130	0.367166
7	1000	3	0.003645	0.006251	0.011093	0.024827
8	1000	4	0.002634	0.004128	0.006500	0.011722
9	1500	1	0.012501	0.038771	0.221102	0.288655
10	1500	2	0.002871	0.005204	0.010006	0.026520
11	1500	3	0.001934	0.002825	0.004083	0.006426
12	1500	4	0.001285	0.001740	0.002311	0.003220
13	2000	1	0.006578	0.014079	0.035498	0.186598
14	2000	2	0.002873	0.004604	0.007460	0.014123
15	2000	3	0.001343	0.001833	0.002453	0.003456
16	2000	4	0.001103	0.001458	0.001887	0.002541

Cell No.	LSD test; variable Contact pressure according to projected contact area (Spreadsheet6) Probabilities for Post Hoc Tests Error: Between MS = .00362, df = 2.0000							
	5 2.0629	6 2.6131	7 3.0447	8 3.2938	9 2.3929	10 2.9329	11 3.5712	12 4.0106
1	0.038008	0.007545	0.003645	0.002634	0.012501	0.002871	0.001934	0.001285
2	0.403229	0.017241	0.006251	0.004128	0.038771	0.005204	0.002825	0.001740
3	0.167918	0.049130	0.011093	0.006500	0.221102	0.010006	0.004083	0.002311
4	0.033693	0.367166	0.024827	0.011722	0.288655	0.026520	0.006426	0.003220
5		0.023099	0.007429	0.004746	0.060521	0.006319	0.003168	0.001903
6	0.023099		0.036744	0.015271	0.122537	0.044113	0.007797	0.003687
7	0.007429	0.036744		0.099574	0.016623	0.248756	0.025143	0.007672
8	0.004746	0.015271	0.099574		0.008805	0.035116	0.082618	0.013800
9	0.060521	0.122537	0.016623	0.008805		0.016160	0.005176	0.002756
10	0.006319	0.044113	0.248756	0.035116	0.016160		0.011641	0.004130
11	0.003168	0.007797	0.025143	0.082618	0.005176	0.011641		0.035509
12	0.001903	0.003687	0.007672	0.013800	0.002756	0.004130	0.035509	
13	0.018317	0.497632	0.051146	0.018863	0.076334	0.069385	0.009055	0.004083
14	0.005336	0.018905	0.170864	0.493914	0.010343	0.052781	0.054915	0.011477
15	0.002009	0.003977	0.008561	0.015999	0.002942	0.004558	0.045044	0.602116
16	0.001582	0.002864	0.005385	0.008709	0.002211	0.002995	0.017844	0.156470

Cell No.	LSD test; variable Contact pressure according to projected contact area (Spreadsheet6) Probabilities for Post Hoc Tests Error: Between MS = .00362, df = 2.0000			
	13 2.6830	14 3.2232	15 3.9584	16 4.1996
1	0.006578	0.002873	0.001343	0.001103
2	0.014079	0.004604	0.001833	0.001458
3	0.035498	0.007460	0.002453	0.001887
4	0.186598	0.014123	0.003456	0.002541
5	0.018317	0.005336	0.002009	0.001582
6	0.497632	0.018905	0.003977	0.002864
7	0.051146	0.170864	0.008561	0.005385
8	0.018863	0.493914	0.015999	0.008709
9	0.076334	0.010343	0.002942	0.002211
10	0.069385	0.052781	0.004558	0.002995
11	0.009055	0.054915	0.045044	0.017844
12	0.004083	0.011477	0.602116	0.156470
13		0.023930	0.004422	0.003133
14	0.023930		0.013131	0.007509
15	0.004422	0.013131		0.105192
16	0.003133	0.007509	0.105192	

APPENDIX H

STATISTICAL ANALYSIS – HARD SURFACE RESULTS OF THE COMBINE TYRES (ANOVA)

H.1 Tekscan Tests: Smooth Combine Tyre – Contact area – effect of combination of inflation pressure and load (One-way ANOVA)

Effect	Univariate Tests of Significance for Contact area (m2) (SmoothCombine_Tekscan.sta) Sigma-restricted parameterization Effective hypothesis decomposition				
	SS	Degr. of Freedom	MS	F	p
Intercept	1.790851	1	1.790851	117533.8	0.00
Combination of inflation pressure / load	0.172437	13	0.013264	870.5	0.00
Error	0.000427	28	0.000015		

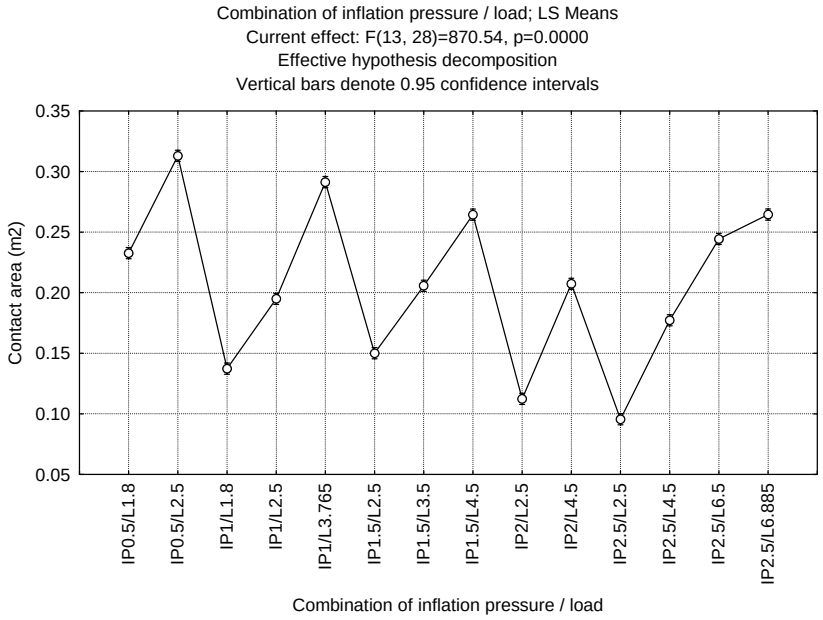

Cell No.	LSD test; variable Contact area (m2) (SmoothCombine_Tekscan.sta) Probabilities for Post Hoc Tests Error: Between MS = .00002, df = 28.000						
	Combination of inflation pressure / load	1 .23270	2 .31297	3 .13733	4 .19493	5 .29130	6 .15007
1	IP0.5/L1.8		0.000000	0.000000	0.000000	0.000000	0.000000
2	IP0.5/L2.5	0.000000		0.000000	0.000000	0.000000	0.000000
3	IP1/L1.8	0.000000	0.000000		0.000000	0.000000	0.000426
4	IP1/L2.5	0.000000	0.000000	0.000000		0.000000	0.000000
5	IP1/L3.765	0.000000	0.000000	0.000000	0.000000		0.000000
6	IP1.5/L2.5	0.000000	0.000000	0.000426	0.000000	0.000000	
7	IP1.5/L3.5	0.000000	0.000000	0.000000	0.002161	0.000000	0.000000
8	IP1.5/L4.5	0.000000	0.000000	0.000000	0.000000	0.000000	0.000000

Cell No.	LSD test; variable Contact area (m2) (SmoothCombine_Tekscan.sta) Probabilities for Post Hoc Tests Error: Between MS = .00002, df = 28.000						
	Combination of inflation pressure / load	1 .23270	2 .31297	3 .13733	4 .19493	5 .29130	6 .15007
9	IP2/L2.5	0.000000	0.000000	0.000000	0.000000	0.000000	0.000000
10	IP2/L4.5	0.000000	0.000000	0.000000	0.000563	0.000000	0.000000
11	IP2.5/L2.5	0.000000	0.000000	0.000000	0.000000	0.000000	0.000000
12	IP2.5/L4.5	0.000000	0.000000	0.000000	0.000006	0.000000	0.000000
13	IP2.5/L6.5	0.001036	0.000000	0.000000	0.000000	0.000000	0.000000
14	IP2.5/L6.885	0.000000	0.000000	0.000000	0.000000	0.000000	0.000000

Cell No.	LSD test; variable Contact area (m2) (SmoothCombine_Tekscan.sta) Probabilities for Post Hoc Tests Error: Between MS = .00002, df = 28.000							
	7 .20570	8 .26443	9 .11240	10 .20733	11 .09560	12 .17727	13 .24437	14 .26450
1	0.000000	0.000000	0.000000	0.000000	0.000000	0.000000	0.001036	0.000000
2	0.000000	0.000000	0.000000	0.000000	0.000000	0.000000	0.000000	0.000000
3	0.000000	0.000000	0.000000	0.000000	0.000000	0.000000	0.000000	0.000000
4	0.002161	0.000000	0.000000	0.000563	0.000000	0.000006	0.000000	0.000000
5	0.000000	0.000000	0.000000	0.000000	0.000000	0.000000	0.000000	0.000000
6	0.000000	0.000000	0.000000	0.000000	0.000000	0.000000	0.000000	0.000000
7		0.000000	0.000000	0.612338	0.000000	0.000000	0.000000	0.000000
8	0.000000		0.000000	0.000000	0.000000	0.000000	0.000001	0.983460
9	0.000000	0.000000		0.000000	0.000013	0.000000	0.000000	0.000000
10	0.612338	0.000000	0.000000		0.000000	0.000000	0.000000	0.000000
11	0.000000	0.000000	0.000013	0.000000		0.000000	0.000000	0.000000
12	0.000000	0.000000	0.000000	0.000000	0.000000		0.000000	0.000000
13	0.000000	0.000001	0.000000	0.000000	0.000000	0.000000		0.000001
14	0.000000	0.983460	0.000000	0.000000	0.000000	0.000000	0.000001	

H.2 Tekscan Tests: Treaded Combine Tyre – Contact area – effect of combination of inflation pressure and load (One-way ANOVA)

Effect	Univariate Tests of Significance for Contact area (m2) (Spreadsheet23) Sigma-restricted parameterization Effective hypothesis decomposition				
	SS	Degr. of Freedom	MS	F	p
Intercept	0.108183	1	0.108183	1331.842	0.000000
Combination of inflation pressure / load	0.009184	12	0.000765	9.422	0.005916
Error	0.000487	6	0.000081		

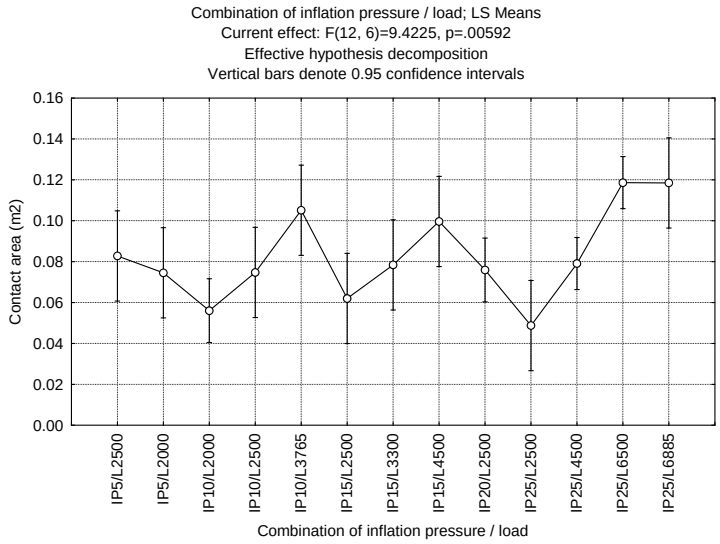

Cell No.	LSD test; variable Contact area (m2) (Spreadsheet23) Probabilities for Post Hoc Tests Error: Between MS = .00008, df = 6.0000						
	Combination of inflation pressure / load	1 .08280	2 .07455	3 .05603	4 .07475	5 .10515	6 .06199
1	IP5/L2500		0.541297	0.051489	0.550709	0.130074	0.153673
2	IP5/L2000	0.541297		0.144418	0.988144	0.053231	0.362601
3	IP10/L2000	0.051489	0.144418		0.140898	0.004329	0.608542
4	IP10/L2500	0.550709	0.988144	0.140898		0.054367	0.355639
5	IP10/L3765	0.130074	0.053231	0.004329	0.054367		0.014748
6	IP15/L2500	0.153673	0.362601	0.608542	0.355639	0.014748	
7	IP15/L3300	0.742676	0.771688	0.088879	0.782959	0.080780	0.244948
8	IP15/L4500	0.234078	0.096314	0.007514	0.098404	0.681791	0.025434
9	IP20/L2500	0.557662	0.903098	0.069118	0.916678	0.038268	0.252939
10	IP25/L2500	0.036854	0.089152	0.532693	0.087260	0.004438	0.338037
11	IP25/L4500	0.731763	0.679599	0.031182	0.692692	0.046110	0.152045
12	IP25/L6500	0.013736	0.005459	0.000268	0.005575	0.242485	0.001597
13	IP25/L6885	0.031143	0.013667	0.001308	0.013929	0.335393	0.004408

Cell No.	LSD test; variable Contact area (m2) (Spreadsheet23) Probabilities for Post Hoc Tests Error: Between MS = .00008, df = 6.0000						
	7 .07842	8 .09966	9 .07595	10 .04873	11 .07906	12 .11864	13 .11850
1	0.742676	0.234078	0.557662	0.036854	0.731763	0.013736	0.031143
2	0.771688	0.096314	0.903098	0.089152	0.679599	0.005459	0.013667
3	0.088879	0.007514	0.069118	0.532693	0.031182	0.000268	0.001308
4	0.782959	0.098404	0.916678	0.087260	0.692692	0.005575	0.013929
5	0.080780	0.681791	0.038268	0.004438	0.046110	0.242485	0.335393
6	0.244948	0.025434	0.252939	0.338037	0.152045	0.001597	0.004408
7		0.146628	0.830508	0.058670	0.952599	0.008314	0.019957
8	0.146628		0.075305	0.007149	0.095118	0.118010	0.189960
9	0.830508	0.075305		0.048691	0.718201	0.002037	0.008417
10	0.058670	0.007149	0.048691		0.026799	0.000529	0.001552
11	0.952599	0.095118	0.718201	0.026799		0.001698	0.009083

Cell No.	LSD test; variable Contact area (m2) (Spreadsheet23) Probabilities for Post Hoc Tests Error: Between MS = .00008, df = 6.0000						
	7 .07842	8 .09966	9 .07595	10 .04873	11 .07906	12 .11864	13 .11850
12	0.008314	0.118010	0.002037	0.000529	0.001698		0.989351
13	0.019957	0.189960	0.008417	0.001552	0.009083	0.989351	

H.3 Tekscan Tests: Treaded and Smooth Combine Tyres – Contact area – effect of tyre tread and combination of inflation pressure and load (Factorial ANOVA)

Effect	Univariate Tests of Significance for Contact area (m2) (Spreadsheet3) Sigma-restricted parameterization Effective hypothesis decomposition				
	SS	Degr. of Freedom	MS	F	p
Intercept	0.546373	1	0.546373	10634.62	0.000000
Combination of inflation pressure / load	0.046802	10	0.004680	91.10	0.000000
Tyre tread	0.096764	1	0.096764	1883.41	0.000000
Combination of inflation pressure / load*Tyre tread	0.015675	10	0.001567	30.51	0.000027
Error	0.000411	8	0.000051		

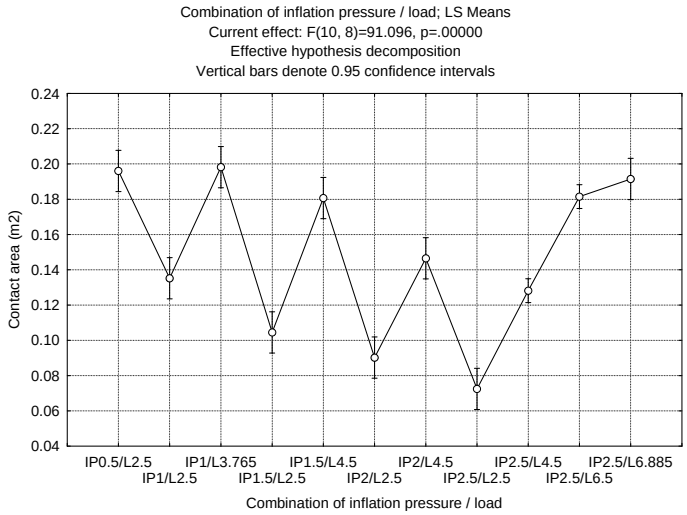

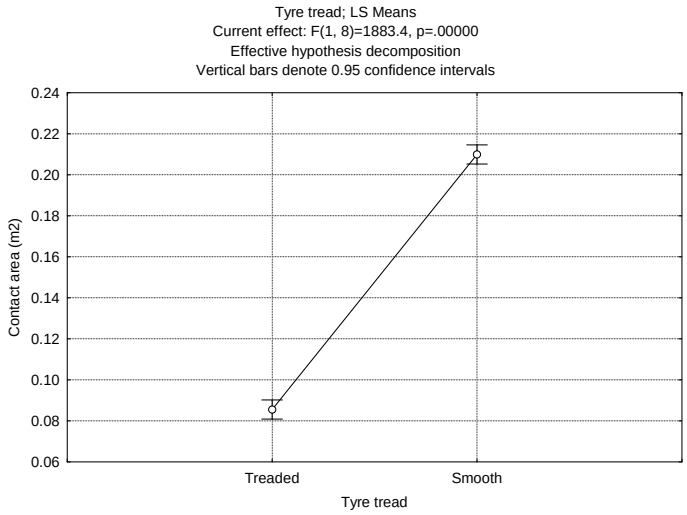

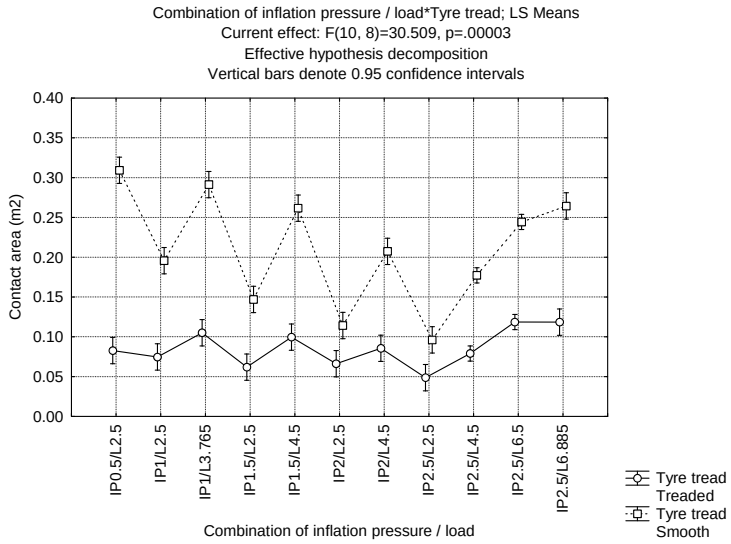

Cell No.	LSD test; variable Contact area (m2) (Spreadsheet3) Probabilities for Post Hoc Tests Error: Between MS = .00005, df = 8.0000					
	Combination of inflation pressure / load	Tyre tread	1 .08280	2 .30930	3 .07475	4 .19570
1	IP0.5/L2.5	Treaded		0.000000	0.449754	0.000004
2	IP0.5/L2.5	Smooth	0.000000		0.000000	0.000004
3	IP1/L2.5	Treaded	0.449754	0.000000		0.000002
4	IP1/L2.5	Smooth	0.000004	0.000004	0.000002	
5	IP1/L3.765	Treaded	0.058561	0.000000	0.017088	0.000020
6	IP1/L3.765	Smooth	0.000000	0.113691	0.000000	0.000013
7	IP1.5/L2.5	Treaded	0.074184	0.000000	0.243807	0.000001
8	IP1.5/L2.5	Smooth	0.000225	0.000000	0.000099	0.001348
9	IP1.5/L4.5	Treaded	0.134826	0.000000	0.039446	0.000013
10	IP1.5/L4.5	Smooth	0.000000	0.001550	0.000000	0.000186
11	IP2/L2.5	Treaded	0.141298	0.000000	0.426630	0.000001
12	IP2/L2.5	Smooth	0.014720	0.000000	0.004595	0.000042
13	IP2/L4.5	Treaded	0.786241	0.000000	0.313684	0.000005
14	IP2/L4.5	Smooth	0.000002	0.000008	0.000001	0.281724
15	IP2.5/L2.5	Treaded	0.009908	0.000000	0.033283	0.000001
16	IP2.5/L2.5	Smooth	0.222772	0.000000	0.067194	0.000010
17	IP2.5/L4.5	Treaded	0.663529	0.000000	0.616078	0.000001
18	IP2.5/L4.5	Smooth	0.000003	0.000000	0.000002	0.056547
19	IP2.5/L6.5	Treaded	0.002511	0.000000	0.000725	0.000014
20	IP2.5/L6.5	Smooth	0.000000	0.000050	0.000000	0.000370
21	IP2.5/L6.885	Treaded	0.007831	0.000000	0.002560	0.000062
22	IP2.5/L6.885	Smooth	0.000000	0.002228	0.000000	0.000140

Cell No.	LSD test; variable Contact area (m2) (Spreadsheet3) Probabilities for Post Hoc Tests Error: Between MS = .00005, df = 8.0000							
	5 .10515	6 .29130	7 .06199	8 .14700	9 .09966	10 .26170	11 .06626	12 .11420
1	0.058561	0.000000	0.074184	0.000225	0.134826	0.000000	0.141298	0.014720
2	0.000000	0.113691	0.000000	0.000000	0.000000	0.001550	0.000000	0.000000

Cell No.	LSD test; variable Contact area (m2) (Spreadsheet3) Probabilities for Post Hoc Tests Error: Between MS = .00005, df = 8.0000							
	5 .10515	6 .29130	7 .06199	8 .14700	9 .09966	10 .26170	11 .06626	12 .11420
3	0.017088	0.000000	0.243807	0.000099	0.039446	0.000000	0.426630	0.004595
4	0.000020	0.000013	0.000001	0.001348	0.000013	0.000186	0.000001	0.000042
5		0.000000	0.002771	0.003305	0.602949	0.000000	0.004969	0.398017
6	0.000000		0.000000	0.000001	0.000000	0.019289	0.000000	0.000000
7	0.002771	0.000000		0.000031	0.005904	0.000000	0.685055	0.000874
8	0.003305	0.000001	0.000031		0.001602	0.000003	0.000045	0.011953
9	0.602949	0.000000	0.005904	0.001602		0.000000	0.010933	0.189408
10	0.000000	0.019289	0.000000	0.000003	0.000000		0.000000	0.000000
11	0.004969	0.000000	0.685055	0.000045	0.010933	0.000000		0.001484
12	0.398017	0.000000	0.000874	0.011953	0.189408	0.000000	0.001484	
13	0.090518	0.000000	0.047916	0.000305	0.204089	0.000000	0.092164	0.022595
14	0.000008	0.000034	0.000001	0.000339	0.000005	0.000680	0.000001	0.000016
15	0.000531	0.000000	0.226941	0.000011	0.001021	0.000000	0.121974	0.000196
16	0.403039	0.000000	0.009719	0.001038	0.741553	0.000000	0.018315	0.113691
17	0.013560	0.000000	0.073071	0.000036	0.037597	0.000000	0.160378	0.002817
18	0.000023	0.000001	0.000001	0.006430	0.000014	0.000007	0.000001	0.000062
19	0.141750	0.000000	0.000132	0.009002	0.051015	0.000000	0.000226	0.606188
20	0.000000	0.000470	0.000000	0.000002	0.000000	0.069556	0.000000	0.000000
21	0.224437	0.000000	0.000526	0.022774	0.100231	0.000001	0.000871	0.682884
22	0.000000	0.029536	0.000000	0.000003	0.000000	0.789379	0.000000	0.000000

Cell No.	LSD test; variable Contact area (m2) (Spreadsheet3) Probabilities for Post Hoc Tests Error: Between MS = .00005, df = 8.0000							
	13 .08564	14 .20740	15 .04873	16 .09620	17 .07906	18 .17727	19 .11864	20 .24437
1	0.786241	0.000002	0.009908	0.222772	0.663529	0.000003	0.002511	0.000000
2	0.000000	0.000008	0.000000	0.000000	0.000000	0.000000	0.000000	0.000050
3	0.313684	0.000001	0.033283	0.067194	0.616078	0.000002	0.000725	0.000000
4	0.000005	0.281724	0.000001	0.000010	0.000001	0.056547	0.000014	0.000370
5	0.090518	0.000008	0.000531	0.403039	0.013560	0.000023	0.141750	0.000000
6	0.000000	0.000034	0.000000	0.000000	0.000000	0.000001	0.000000	0.000470
7	0.047916	0.000001	0.226941	0.009719	0.073071	0.000001	0.000132	0.000000
8	0.000305	0.000339	0.000011	0.001038	0.000036	0.006430	0.009002	0.000002
9	0.204089	0.000005	0.001021	0.741553	0.037597	0.000014	0.051015	0.000000
10	0.000000	0.000680	0.000000	0.000000	0.000000	0.000007	0.000000	0.069556
11	0.092164	0.000001	0.121974	0.018315	0.160378	0.000001	0.000226	0.000000
12	0.022595	0.000016	0.000196	0.113691	0.002817	0.000062	0.606188	0.000000
13		0.000002	0.006569	0.328152	0.449488	0.000004	0.004024	0.000000
14	0.000002		0.000000	0.000004	0.000000	0.006582	0.000005	0.002093
15	0.006569	0.000000		0.001575	0.006351	0.000000	0.000029	0.000000
16	0.328152	0.000004	0.001575		0.072170	0.000010	0.026603	0.000000
17	0.449488	0.000000	0.006351	0.072170		0.000000	0.000143	0.000000
18	0.000004	0.006582	0.000000	0.000010	0.000000		0.000008	0.000003
19	0.004024	0.000005	0.000029	0.026603	0.000143	0.000008		0.000000
20	0.000000	0.002093	0.000000	0.000000	0.000000	0.000003	0.000000	
21	0.011862	0.000022	0.000127	0.059039	0.001419	0.000102	0.986472	0.000000
22	0.000000	0.000491	0.000000	0.000000	0.000000	0.000006	0.000000	0.041038

Cell No.	LSD test; variable Contact area (m2) (Spreadsheet3) Probabilities for Post Hoc Tests Error: Between MS = .00005, df = 8.0000	
	21 .11850	22 .26450
1	0.007831	0.000000
2	0.000000	0.002228
3	0.002560	0.000000
4	0.000062	0.000140
5	0.224437	0.000000
6	0.000000	0.029536
7	0.000526	0.000000
8	0.022774	0.000003
9	0.100231	0.000000
10	0.000001	0.789379
11	0.000871	0.000000
12	0.682884	0.000000
13	0.011862	0.000000
14	0.000022	0.000491
15	0.000127	0.000000
16	0.059039	0.000000
17	0.001419	0.000000
18	0.000102	0.000006
19	0.986472	0.000000
20	0.000000	0.041038
21		0.000001
22	0.000001	

H.4 Tekscan Tests: Treaded and Smooth Combine Tyres – Mean contact pressure – effect of tyre tread and combination of inflation pressure and load (Factorial ANOVA)

Effect	Univariate Tests of Significance for Mean pressure (bar) (Spreadsheet3) Sigma-restricted parameterization Effective hypothesis decomposition				
	SS	Degr. of Freedom	MS	F	p
Intercept	268.4410	1	268.4410	1466.121	0.000000
Combination of inflation pressure / load	21.2142	10	2.1214	11.586	0.000986
Tyre tread	27.1454	1	27.1454	148.258	0.000002
Combination of inflation pressure / load*Tyre tread	1.5812	10	0.1581	0.864	0.594181
Error	1.4648	8	0.1831		

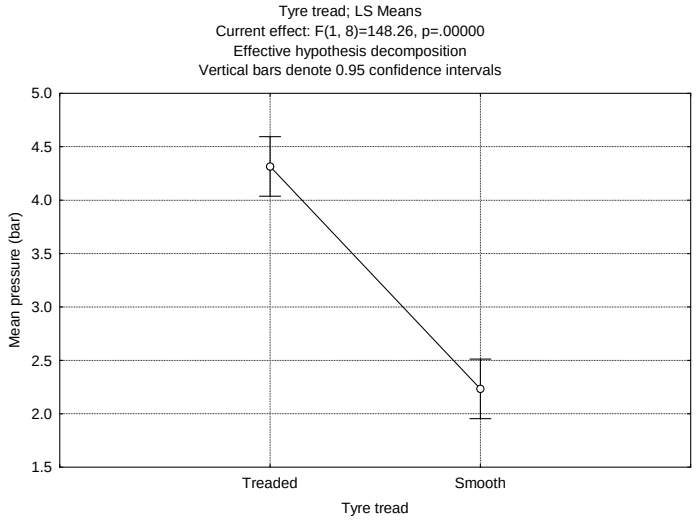

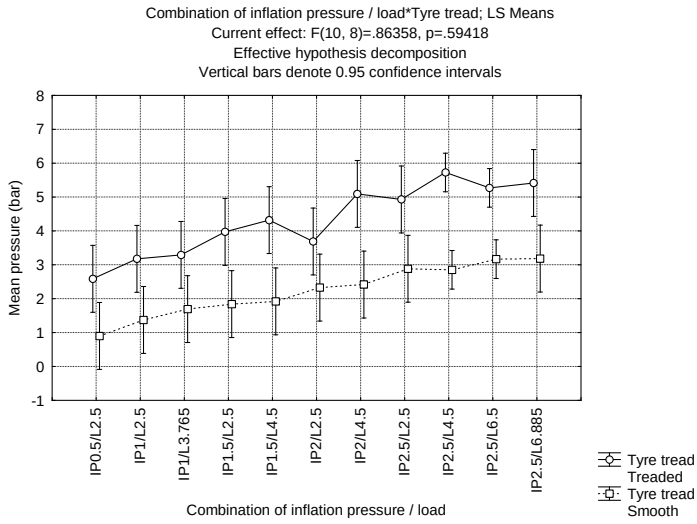

Cell No.	LSD test; variable Mean pressure (bar) (Spreadsheet3) Probabilities for Post Hoc Tests Error: Between MS = .18310, df = 8.0000					
	Combination of inflation pressure / load	Tyre tread	1 2.5875	2 .90096	3 3.1775	4 1.3732
1	IP0.5/L2.5	Treaded		0.023664	0.358154	0.079692
2	IP0.5/L2.5	Smooth	0.023664		0.005528	0.457591
3	IP1/L2.5	Treaded	0.358154	0.005528		0.017559
4	IP1/L2.5	Smooth	0.079692	0.457591	0.017559	
5	IP1/L3.765	Treaded	0.277130	0.004217	0.853089	0.013139
6	IP1/L3.765	Smooth	0.177815	0.226662	0.039792	0.611018
7	IP1.5/L2.5	Treaded	0.051409	0.000959	0.225500	0.002634
8	IP1.5/L2.5	Smooth	0.252406	0.158881	0.058226	0.461660
9	IP1.5/L4.5	Treaded	0.021039	0.000481	0.095640	0.001240
10	IP1.5/L4.5	Smooth	0.303441	0.130013	0.071710	0.390950
11	IP2/L2.5	Treaded	0.106241	0.001739	0.422583	0.005041
12	IP2/L2.5	Smooth	0.678999	0.046120	0.197852	0.153380
13	IP2/L4.5	Treaded	0.003251	0.000121	0.013281	0.000275
14	IP2/L4.5	Smooth	0.786160	0.036568	0.244730	0.122611

Cell No.	LSD test; variable Mean pressure (bar) (Spreadsheet3) Probabilities for Post Hoc Tests Error: Between MS = .18310, df = 8.0000					
	Combination of inflation pressure / load	Tyre tread	1 2.5875	2 .90096	3 3.1775	4 1.3732
15	IP2.5/L2.5	Treaded	0.004743	0.000160	0.020049	0.000372
16	IP2.5/L2.5	Smooth	0.637530	0.011242	0.640491	0.037157
17	IP2.5/L4.5	Treaded	0.000220	0.000010	0.000867	0.000022
18	IP2.5/L4.5	Smooth	0.605329	0.004228	0.530115	0.017191
19	IP2.5/L6.5	Treaded	0.000623	0.000021	0.002851	0.000048
20	IP2.5/L6.5	Smooth	0.273841	0.001782	0.985161	0.006661
21	IP2.5/L6.885	Treaded	0.001594	0.000072	0.006048	0.000156
22	IP2.5/L6.885	Smooth	0.352768	0.005437	0.991022	0.017250

Cell No.	LSD test; variable Mean pressure (bar) (Spreadsheet3) Probabilities for Post Hoc Tests Error: Between MS = .18310, df = 8.0000							
	5 3.2932	6 1.6935	7 3.9722	8 1.8411	9 4.3203	10 1.9220	11 3.6889	12 2.3277
1	0.277130	0.177815	0.051409	0.252406	0.021039	0.303441	0.106241	0.678999
2	0.004217	0.226662	0.000959	0.158881	0.000481	0.130013	0.001739	0.046120
3	0.853089	0.039792	0.225500	0.058226	0.095640	0.071710	0.422583	0.197852
4	0.013139	0.611018	0.002634	0.461660	0.001240	0.390950	0.005041	0.153380
5		0.029548	0.294395	0.043200	0.128077	0.053230	0.531525	0.149262
6	0.029548		0.005500	0.813419	0.002475	0.715482	0.010900	0.325236
7	0.294395	0.005500		0.007827	0.580930	0.009529	0.652175	0.026348
8	0.043200	0.813419	0.007827		0.003452	0.896899	0.015736	0.444557
9	0.128077	0.002475	0.580930	0.003452		0.004158	0.327265	0.010976
10	0.053230	0.715482	0.009529	0.896899	0.004158		0.019297	0.521496
11	0.531525	0.010900	0.652175	0.015736	0.327265	0.019297		0.054617
12	0.149262	0.325236	0.026348	0.444557	0.010976	0.521496	0.054617	
13	0.017752	0.000500	0.101109	0.000666	0.237382	0.000783	0.048881	0.001826
14	0.185987	0.265627	0.033191	0.368536	0.013721	0.436420	0.068869	0.885410
15	0.026924	0.000688	0.152405	0.000926	0.343731	0.001094	0.074542	0.002619
16	0.517781	0.084728	0.109794	0.123161	0.044977	0.150641	0.220052	0.384971
17	0.001160	0.000038	0.007523	0.000049	0.021670	0.000058	0.003334	0.000127
18	0.399217	0.046879	0.053335	0.074679	0.017893	0.096206	0.129245	0.318527
19	0.003937	0.000089	0.030265	0.000119	0.090611	0.000141	0.012584	0.000340
20	0.806328	0.017485	0.142254	0.027687	0.047998	0.035713	0.322553	0.127422
21	0.007983	0.000273	0.044122	0.000359	0.107748	0.000417	0.021339	0.000926
22	0.861896	0.039078	0.229256	0.057181	0.097363	0.070427	0.428724	0.194545

Cell No.	LSD test; variable Mean pressure (bar) (Spreadsheet3) Probabilities for Post Hoc Tests Error: Between MS = .18310, df = 8.0000							
	13 5.0932	14 2.4178	15 4.9293	16 2.8838	17 5.7256	18 2.8533	19 5.2708	20 3.1680
1	0.003251	0.786160	0.004743	0.637530	0.000220	0.605329	0.000623	0.273841
2	0.000121	0.036568	0.000160	0.011242	0.000010	0.004228	0.000021	0.001782
3	0.013281	0.244730	0.020049	0.640491	0.000867	0.530115	0.002851	0.985161
4	0.000275	0.122611	0.000372	0.037157	0.000022	0.017191	0.000048	0.006661
5	0.017752	0.185987	0.026924	0.517781	0.001160	0.399217	0.003937	0.806328
6	0.000500	0.265627	0.000688	0.084728	0.000038	0.046879	0.000089	0.017485

Cell No.	LSD test; variable Mean pressure (bar) (Spreadsheet3) Probabilities for Post Hoc Tests Error: Between MS = .18310, df = 8.0000							
	13 5.0932	14 2.4178	15 4.9293	16 2.8838	17 5.7256	18 2.8533	19 5.2708	20 3.1680
7	0.101109	0.033191	0.152405	0.109794	0.007523	0.053335	0.030265	0.142254
8	0.000666	0.368536	0.000926	0.123161	0.000049	0.074679	0.000119	0.027687
9	0.237382	0.013721	0.343731	0.044977	0.021670	0.017893	0.090611	0.047998
10	0.000783	0.436420	0.001094	0.150641	0.000058	0.096206	0.000141	0.035713
11	0.048881	0.068869	0.074542	0.220052	0.003334	0.129245	0.012584	0.322553
12	0.001826	0.885410	0.002619	0.384971	0.000127	0.318527	0.000340	0.127422
13		0.002223	0.793402	0.006486	0.236375	0.001916	0.728548	0.004568
14	0.002223		0.003207	0.463309	0.000154	0.403776	0.000417	0.167379
15	0.793402	0.003207		0.009640	0.145678	0.002990	0.509040	0.007351
16	0.006486	0.463309	0.009640		0.000428	0.952193	0.001303	0.581001
17	0.236375	0.000154	0.145678	0.000428		0.000036	0.229157	0.000082
18	0.001916	0.403776	0.002990	0.952193	0.000036		0.000122	0.393971
19	0.728548	0.000417	0.509040	0.001303	0.229157	0.000122		0.000317
20	0.004568	0.167379	0.007351	0.581001	0.000082	0.393971	0.000317	
21	0.608017	0.001114	0.444326	0.003060	0.548509	0.000836	0.776059	0.001874
22	0.013516	0.240761	0.020410	0.632636	0.000882	0.521473	0.002906	0.974169

Cell No.	LSD test; variable Mean pressure (bar) (Spreadsheet3) Probabilities for Post Hoc Tests Error: Between MS = .18310, df = 8.0000	
	21 5.4161	22 3.1845
1	0.001594	0.352768
2	0.000072	0.005437
3	0.006048	0.991022
4	0.000156	0.017250
5	0.007983	0.861896
6	0.000273	0.039078
7	0.044122	0.229256
8	0.000359	0.057181
9	0.107748	0.097363
10	0.000417	0.070427
11	0.021339	0.428724
12	0.000926	0.194545
13	0.608017	0.013516
14	0.001114	0.240761
15	0.444326	0.020410
16	0.003060	0.632636
17	0.548509	0.000882
18	0.000836	0.521473
19	0.776059	0.002906
20	0.001874	0.974169
21		0.006150
22	0.006150	

H.5 Tekscan Tests: Treaded and Smooth Combine Tyres – Maximum contact pressure – effect of tyre tread and combination of inflation pressure and load (Factorial ANOVA)

Effect	Univariate Tests of Significance for Max pressure (bar) (Spreadsheet3) Sigma-restricted parameterization Effective hypothesis decomposition				
	SS	Degr. of Freedom	MS	F	p
Intercept	1412.237	1	1412.237	2095.195	0.000000
Combination of inflation pressure / load	34.095	10	3.409	5.058	0.015383
Tyre tread	76.448	1	76.448	113.418	0.000005
Combination of inflation pressure / load*Tyre tread	7.119	10	0.712	1.056	0.478505
Error	5.392	8	0.674		

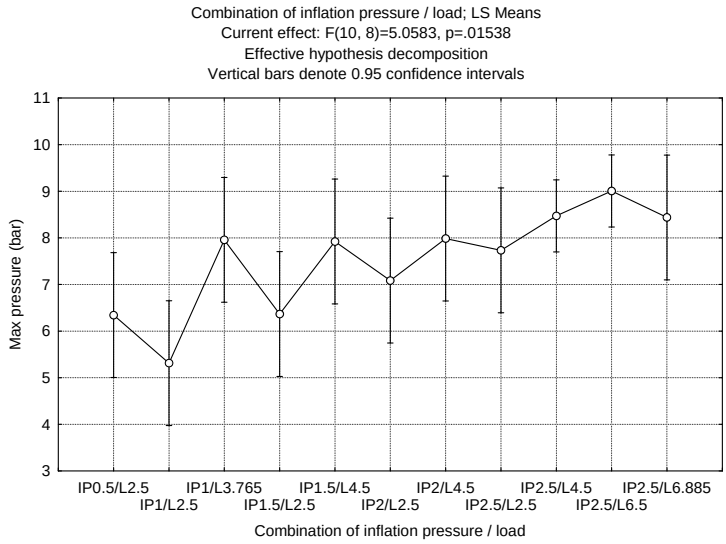

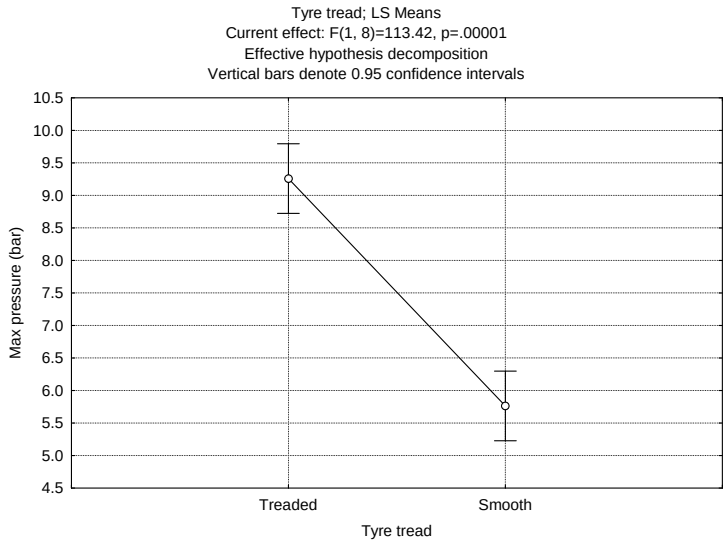

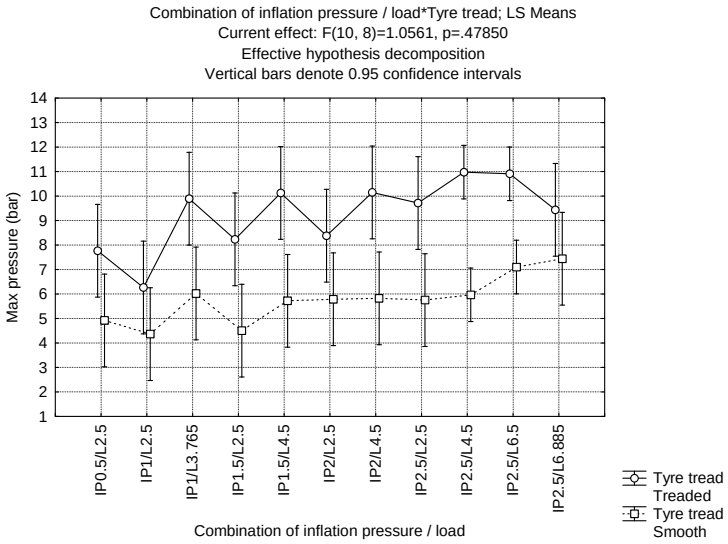

Cell No.	LSD test; variable Max pressure (bar) (Spreadsheet3) Probabilities for Post Hoc Tests Error: Between MS = .67404, df = 8.0000					
	Combination of inflation pressure / load	Tyre tread	1 7.7673	2 4.9213	3 6.2631	4 4.3629
1	IP0.5/L2.5	Treaded		0.039858	0.231264	0.018935
2	IP0.5/L2.5	Smooth	0.039858		0.281140	0.643462
3	IP1/L2.5	Treaded	0.231264	0.281140		0.140344
4	IP1/L2.5	Smooth	0.018935	0.643462	0.140344	
5	IP1/L3.765	Treaded	0.104778	0.002686	0.014129	0.001424
6	IP1/L3.765	Smooth	0.171423	0.370415	0.841369	0.190621
7	IP1.5/L2.5	Treaded	0.700530	0.021480	0.128666	0.010371
8	IP1.5/L2.5	Smooth	0.022783	0.727843	0.167945	0.907093
9	IP1.5/L4.5	Treaded	0.076879	0.002053	0.010456	0.001104
10	IP1.5/L4.5	Smooth	0.115901	0.510797	0.652580	0.276022
11	IP2/L2.5	Treaded	0.611569	0.017610	0.105615	0.008561
12	IP2/L2.5	Smooth	0.126508	0.477109	0.692639	0.254798
13	IP2/L4.5	Treaded	0.074406	0.001996	0.010134	0.001075
14	IP2/L4.5	Smooth	0.132201	0.460660	0.713278	0.244605
15	IP2.5/L2.5	Treaded	0.132087	0.003307	0.017805	0.001735
16	IP2.5/L2.5	Smooth	0.120482	0.495728	0.670146	0.266470
17	IP2.5/L4.5	Treaded	0.009574	0.000212	0.001091	0.000115
18	IP2.5/L4.5	Smooth	0.094068	0.302154	0.762572	0.129136
19	IP2.5/L6.5	Treaded	0.010630	0.000229	0.001192	0.000124
20	IP2.5/L6.5	Smooth	0.502624	0.050452	0.402092	0.020223
21	IP2.5/L6.885	Treaded	0.188656	0.004621	0.025745	0.002383
22	IP2.5/L6.885	Smooth	0.784627	0.061951	0.340760	0.029277

Cell No.	LSD test; variable Max pressure (bar) (Spreadsheet3) Probabilities for Post Hoc Tests Error: Between MS = .67404, df = 8.0000							
	5 9.8911	6 6.0231	7 8.2303	8 4.5027	9 10.124	10 5.7203	11 8.3808	12 5.7872
1	0.104778	0.171423	0.700530	0.022783	0.076879	0.115901	0.611569	0.126508
2	0.002686	0.370415	0.021480	0.727843	0.002053	0.510797	0.017610	0.477109

Cell No.	LSD test; variable Max pressure (bar) (Spreadsheet3) Probabilities for Post Hoc Tests Error: Between MS = .67404, df = 8.0000							
	5 9.8911	6 6.0231	7 8.2303	8 4.5027	9 10.124	10 5.7203	11 8.3808	12 5.7872
3	0.014129	0.841369	0.128666	0.167945	0.010456	0.652580	0.105615	0.692639
4	0.001424	0.190621	0.010371	0.907093	0.001104	0.276022	0.008561	0.254798
5		0.010363	0.190476	0.001664	0.845948	0.007062	0.229564	0.007681
6	0.010363		0.093822	0.226744	0.007708	0.800838	0.076776	0.844095
7	0.190476	0.093822		0.012416	0.141516	0.062613	0.900030	0.068493
8	0.001664	0.226744	0.012416		0.001286	0.324993	0.010230	0.300759
9	0.845948	0.007708	0.141516	0.001286		0.005290	0.171642	0.005744
10	0.007062	0.800838	0.062613	0.324993	0.005290		0.051147	0.955440
11	0.229564	0.076776	0.900030	0.010230	0.171642	0.051147		0.055962
12	0.007681	0.844095	0.068493	0.300759	0.005744	0.955440	0.055962	
13	0.830058	0.007475	0.137104	0.001252	0.983708	0.005134	0.166384	0.005574
14	0.008015	0.866166	0.071666	0.289079	0.005990	0.932989	0.058562	0.977486
15	0.882776	0.013013	0.237024	0.002032	0.733267	0.008824	0.283939	0.009608
16	0.007328	0.819875	0.065148	0.314101	0.005486	0.980297	0.053222	0.975122
17	0.285473	0.000798	0.020000	0.000134	0.395017	0.000545	0.025542	0.000592
18	0.003256	0.954099	0.044017	0.161089	0.002332	0.801417	0.034364	0.854490
19	0.314112	0.000870	0.022288	0.000144	0.431524	0.000592	0.028488	0.000644
20	0.018648	0.288059	0.268060	0.025383	0.012843	0.183114	0.214249	0.202925
21	0.705198	0.018730	0.329506	0.002804	0.569671	0.012611	0.390112	0.013755
22	0.067687	0.257332	0.514879	0.035306	0.049499	0.177026	0.440808	0.192598

Cell No.	LSD test; variable Max pressure (bar) (Spreadsheet3) Probabilities for Post Hoc Tests Error: Between MS = .67404, df = 8.0000							
	13 10.149	14 5.8210	15 9.7143	16 5.7499	17 10.976	18 5.9668	19 10.909	20 7.1019
1	0.074406	0.132201	0.132087	0.120482	0.009574	0.094068	0.010630	0.502624
2	0.001996	0.460660	0.003307	0.495728	0.000212	0.302154	0.000229	0.050452
3	0.010134	0.713278	0.017805	0.670146	0.001091	0.762572	0.001192	0.402092
4	0.001075	0.244605	0.001735	0.266470	0.000115	0.129136	0.000124	0.020223
5	0.830058	0.008015	0.882776	0.007328	0.285473	0.003256	0.314112	0.018648
6	0.007475	0.866166	0.013013	0.819875	0.000798	0.954099	0.000870	0.288059
7	0.137104	0.071666	0.237024	0.065148	0.020000	0.044017	0.022288	0.268060
8	0.001252	0.289079	0.002032	0.314101	0.000134	0.161089	0.000144	0.025383
9	0.983708	0.005990	0.733267	0.005486	0.395017	0.002332	0.431524	0.012843
10	0.005134	0.932989	0.008824	0.980297	0.000545	0.801417	0.000592	0.183114
11	0.166384	0.058562	0.283939	0.053222	0.025542	0.034364	0.028488	0.214249
12	0.005574	0.977486	0.009608	0.975122	0.000592	0.854490	0.000644	0.202925
13		0.005811	0.718131	0.005323	0.408114	0.002253	0.445457	0.012355
14	0.005811		0.010032	0.952633	0.000618	0.881614	0.000672	0.213622
15	0.718131	0.010032		0.009162	0.219866	0.004218	0.243002	0.024839
16	0.005323	0.952633	0.009162		0.000565	0.824755	0.000614	0.191649
17	0.408114	0.000618	0.219866	0.000565		0.000071	0.923041	0.000415
18	0.002253	0.881614	0.004218	0.824755	0.000071		0.000078	0.128845
19	0.445457	0.000672	0.243002	0.000614	0.923041	0.000078		0.000465
20	0.012355	0.213622	0.024839	0.191649	0.000415	0.128845	0.000465	
21	0.556335	0.014373	0.816435	0.013104	0.142851	0.006408	0.158709	0.039203
22	0.047898	0.200910	0.085720	0.183765	0.005780	0.158991	0.006397	0.731207

Cell No.	LSD test; variable Max pressure (bar) (Spreadsheet3) Probabilities for Post Hoc Tests Error: Between MS = .67404, df = 8.0000	
	21 9.4358	22 7.4392
1	0.188656	0.784627
2	0.004621	0.061951
3	0.025745	0.340760
4	0.002383	0.029277
5	0.705198	0.067687
6	0.018730	0.257332
7	0.329506	0.514879
8	0.002804	0.035306
9	0.569671	0.049499
10	0.012611	0.177026
11	0.390112	0.440808
12	0.013755	0.192598
13	0.556335	0.047898
14	0.014373	0.200910
15	0.816435	0.085720
16	0.013104	0.183765
17	0.142851	0.005780
18	0.006408	0.158991
19	0.158709	0.006397
20	0.039203	0.731207
21		0.123815
22	0.123815	

H.6 Tekscan Tests: Treaded and Smooth Combine Tyres – Mean carcass stiffness – effect of tyre tread and combination of inflation pressure and load (Factorial ANOVA)

Effect	Univariate Tests of Significance for Mean carcass stiffness (bar) (Spreadsheet3) Sigma-restricted parameterization Effective hypothesis decomposition				
	SS	Degr. of Freedom	MS	F	p
Intercept	56.46652	1	56.46652	308.3983	0.000000
Combination of inflation pressure / load	1.73833	10	0.17383	0.9494	0.540040
Tyre tread	27.14539	1	27.14539	148.2577	0.000002
Combination of inflation pressure / load*Tyre tread	1.58118	10	0.15812	0.8636	0.594181
Error	1.46477	8	0.18310		

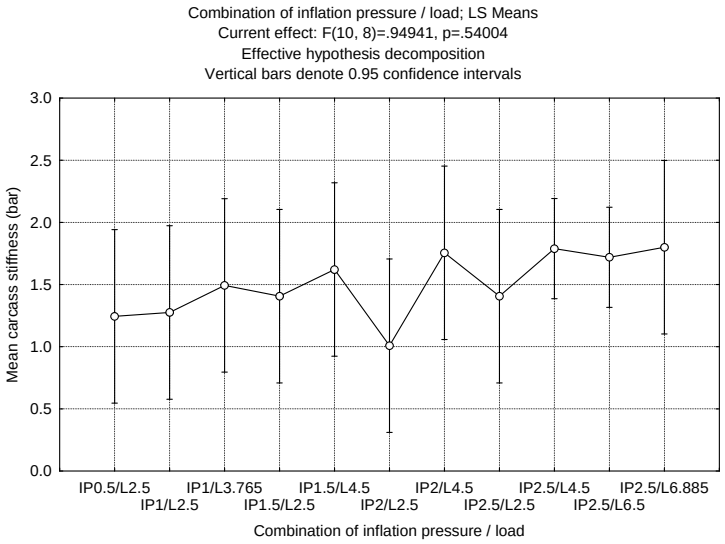
Combination of inflation pressure / load; LS Means
Current effect: F(10, 8)=.94941, p=.54004
Effective hypothesis decomposition
Vertical bars denote 0.95 confidence intervals
Mean carcass stiffness (bar)
3.0
2.5
2.0
1.5
1.0
0.5
0.0
IP0.5/L2.5
IP1/L2.5
IP1/L3.765
IP1.5/L2.5
IP1.5/L4.5
IP2/L2.5
IP2/L4.5
IP2.5/L2.5
IP2.5/L4.5
IP2.5/L6.5
IP2.5/L6.885
Combination of inflation pressure / load

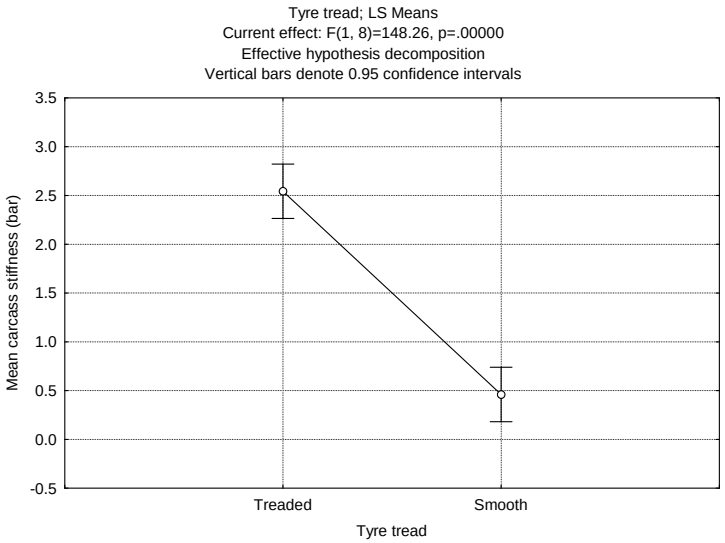
Tyre tread; LS Means
Current effect: F(1, 8)=148.26, p=.00000
Effective hypothesis decomposition
Vertical bars denote 0.95 confidence intervals
Mean carcass stiffness (bar)
3.5
3.0
2.5
2.0
1.5
1.0
0.5
0.0
-0.5
Treaded
Smooth
Tyre tread

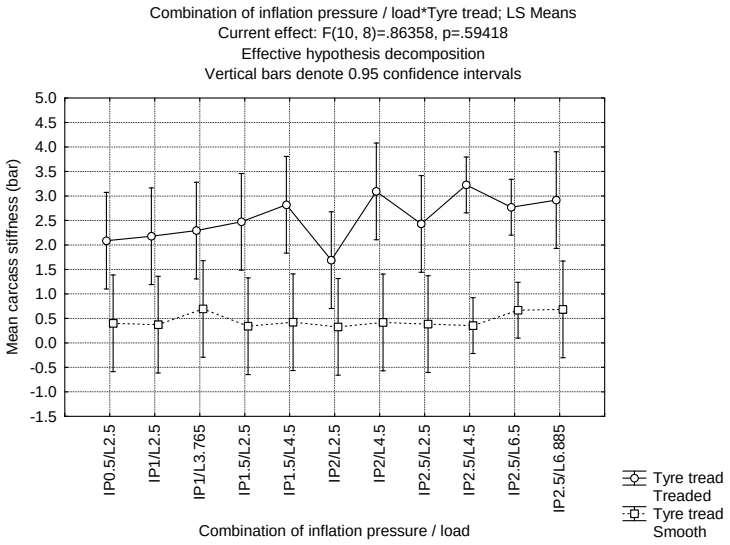
Combination of inflation pressure / load*Tyre tread; LS Means
Current effect: F(10, 8)=.86358, p=.59418
Effective hypothesis decomposition
Vertical bars denote 0.95 confidence intervals
Mean carcass stiffness (bar)
5.0
4.5
4.0
3.5
3.0
2.5
2.0
1.5
1.0
0.5
0.0
-0.5
-1.0
-1.5
IP0.5/L2.5
IP1/L2.5
IP1/L3.765
IP1.5/L2.5
IP1.5/L4.5
IP2/L2.5
IP2/L4.5
IP2.5/L2.5
IP2.5/L4.5
IP2.5/L6.5
IP2.5/L6.885
Combination of inflation pressure / load
Tyre tread
Treaded
Tyre tread
Smooth

Cell No.	LSD test; variable Mean carcass stiffness (bar) (Spreadsheet3) Probabilities for Post Hoc Tests Error: Between MS = .18310, df = 8.0000					
	Combination of inflation pressure / load	Tyre tread	1 2.0875	2 .40096	3 2.1775	4 .37324
1	IP0.5/L2.5	Treaded		0.023664	0.885500	0.022052
2	IP0.5/L2.5	Smooth	0.023664		0.018832	0.964592
3	IP1/L2.5	Treaded	0.885500	0.018832		0.017559
4	IP1/L2.5	Smooth	0.022052	0.964592	0.017559	
5	IP1/L3.765	Treaded	0.742671	0.014079	0.853089	0.013139
6	IP1/L3.765	Smooth	0.050182	0.641751	0.039792	0.611018
7	IP1.5/L2.5	Treaded	0.542731	0.009051	0.639301	0.008460
8	IP1.5/L2.5	Smooth	0.020324	0.923651	0.016194	0.958955
9	IP1.5/L4.5	Treaded	0.260471	0.003961	0.319117	0.003716
10	IP1.5/L4.5	Smooth	0.024972	0.973048	0.019864	0.937696
11	IP2/L2.5	Treaded	0.528583	0.065958	0.442796	0.061416
12	IP2/L2.5	Smooth	0.019646	0.906655	0.015659	0.941883
13	IP2/L4.5	Treaded	0.135129	0.002142	0.168701	0.002016
14	IP2/L4.5	Smooth	0.024700	0.978539	0.019649	0.943172
15	IP2.5/L2.5	Treaded	0.587731	0.010053	0.688288	0.009393
16	IP2.5/L2.5	Smooth	0.022654	0.978122	0.018034	0.986460
17	IP2.5/L4.5	Treaded	0.050201	0.000446	0.066684	0.000418
18	IP2.5/L4.5	Smooth	0.007962	0.925490	0.006112	0.968753
19	IP2.5/L6.5	Treaded	0.204098	0.001362	0.264203	0.001268
20	IP2.5/L6.5	Smooth	0.020734	0.603571	0.015700	0.567274
21	IP2.5/L6.885	Treaded	0.208111	0.003181	0.256978	0.002988
22	IP2.5/L6.885	Smooth	0.049034	0.651865	0.038882	0.620883

Cell No.	LSD test; variable Mean carcass stiffness (bar) (Spreadsheet3) Probabilities for Post Hoc Tests Error: Between MS = .18310, df = 8.0000							
	5 2.2932	6 .69349	7 2.4722	8 .34111	9 2.8203	10 .42205	11 1.6889	12 .32772
1	0.742671	0.050182	0.542731	0.020324	0.260471	0.024972	0.528583	0.019646
2	0.014079	0.641751	0.009051	0.923651	0.003961	0.973048	0.065958	0.906655
3	0.853089	0.039792	0.639301	0.016194	0.319117	0.019864	0.442796	0.015659
4	0.013139	0.611018	0.008460	0.958955	0.003716	0.937696	0.061416	0.941883
5		0.029548	0.774936	0.012131	0.409113	0.014841	0.347220	0.011735
6	0.029548		0.018728	0.576390	0.007908	0.665647	0.138596	0.562293
7	0.774936	0.018728		0.007827	0.580930	0.009529	0.231639	0.007578
8	0.012131	0.576390	0.007827		0.003452	0.896899	0.056536	0.982890
9	0.409113	0.007908	0.580930	0.003452		0.004158	0.098459	0.003348
10	0.014841	0.665647	0.009529	0.896899	0.004158		0.069635	0.879988
11	0.347220	0.138596	0.231639	0.056536	0.098459	0.069635		0.054617
12	0.011735	0.562293	0.007578	0.982890	0.003348	0.879988	0.054617	
13	0.222754	0.004145	0.334864	0.001880	0.664069	0.002244	0.048881	0.001826
14	0.014682	0.660742	0.009429	0.902341	0.004117	0.994506	0.068869	0.885410
15	0.827752	0.020880	0.945181	0.008685	0.536238	0.010588	0.255971	0.008407
16	0.013490	0.622674	0.008681	0.945443	0.003807	0.951197	0.063115	0.928396
17	0.095850	0.000902	0.165799	0.000388	0.435788	0.000468	0.014442	0.000376
18	0.004379	0.510561	0.002657	0.980963	0.001062	0.892733	0.026938	0.960023
19	0.362109	0.002979	0.562428	0.001168	0.922564	0.001439	0.059964	0.001129

Cell No.	LSD test; variable Mean carcass stiffness (bar) (Spreadsheet3) Probabilities for Post Hoc Tests Error: Between MS = .18310, df = 8.0000							
	5 2.2932	6 .69349	7 2.4722	8 .34111	9 2.8203	10 .42205	11 1.6889	12 .32772
20	0.011034	0.960137	0.006480	0.526804	0.002425	0.632013	0.072653	0.510472
21	0.333416	0.006282	0.484130	0.002779	0.878107	0.003337	0.077096	0.002697
22	0.028876	0.988532	0.018308	0.585949	0.007738	0.675940	0.135537	0.571719

Cell No.	LSD test; variable Mean carcass stiffness (bar) (Spreadsheet3) Probabilities for Post Hoc Tests Error: Between MS = .18310, df = 8.0000							
	13 3.0932	14 .41775	15 2.4293	16 .38384	17 3.2256	18 .35327	19 2.7708	20 .66801
1	0.135129	0.024700	0.587731	0.022654	0.050201	0.007962	0.204098	0.020734
2	0.002142	0.978539	0.010053	0.978122	0.000446	0.925490	0.001362	0.603571
3	0.168701	0.019649	0.688288	0.018034	0.066684	0.006112	0.264203	0.015700
4	0.002016	0.943172	0.009393	0.986460	0.000418	0.968753	0.001268	0.567274
5	0.222754	0.014682	0.827752	0.013490	0.095850	0.004379	0.362109	0.011034
6	0.004145	0.660742	0.020880	0.622674	0.000902	0.510561	0.002979	0.960137
7	0.334864	0.009429	0.945181	0.008681	0.165799	0.002657	0.562428	0.006480
8	0.001880	0.902341	0.008685	0.945443	0.000388	0.980963	0.001168	0.526804
9	0.664069	0.004117	0.536238	0.003807	0.435788	0.001062	0.922564	0.002425
10	0.002244	0.994506	0.010588	0.951197	0.000468	0.892733	0.001439	0.632013
11	0.048881	0.068869	0.255971	0.063115	0.014442	0.026938	0.059964	0.072653
12	0.001826	0.885410	0.008407	0.928396	0.000376	0.960023	0.001129	0.510472
13		0.002223	0.304538	0.002063	0.795364	0.000544	0.532384	0.001181
14	0.002223		0.010476	0.956680	0.000463	0.899393	0.001423	0.626161
15	0.304538	0.010476		0.009640	0.145678	0.002990	0.509040	0.007351
16	0.002063	0.956680	0.009640		0.000428	0.952193	0.001303	0.581001
17	0.795364	0.000463	0.145678	0.000428		0.000036	0.229157	0.000082
18	0.000544	0.899393	0.002990	0.952193	0.000036		0.000122	0.393971
19	0.532384	0.001423	0.509040	0.001303	0.229157	0.000122		0.000317
20	0.001181	0.626161	0.007351	0.581001	0.000082	0.393971	0.000317	
21	0.777347	0.003305	0.444326	0.003060	0.548509	0.000836	0.776059	0.001874
22	0.004060	0.671000	0.020410	0.632636	0.000882	0.521473	0.002906	0.974169

Cell No.	LSD test; variable Mean carcass stiffness (bar) (Spreadsheet3) Probabilities for Post Hoc Tests Error: Between MS = .18310, df = 8.0000	
	21 2.9161	22 .68452
1	0.208111	0.049034
2	0.003181	0.651865
3	0.256978	0.038882
4	0.002988	0.620883
5	0.333416	0.028876
6	0.006282	0.988532
7	0.484130	0.018308

Cell No.	LSD test; variable Mean carcass stiffness (bar) (Spreadsheet3) Probabilities for Post Hoc Tests Error: Between MS = .18310, df = 8.0000	
	21 2.9161	22 .68452
8	0.002779	0.585949
9	0.878107	0.007738
10	0.003337	0.675940
11	0.077096	0.135537
12	0.002697	0.571719
13	0.777347	0.004060
14	0.003305	0.671000
15	0.444326	0.020410
16	0.003060	0.632636
17	0.548509	0.000882
18	0.000836	0.521473
19	0.776059	0.002906
20	0.001874	0.974169
21		0.006150
22	0.006150	

H.7 Tekscan Tests: Treaded and Smooth Combine Tyres – Maximum carcass stiffness – effect of tyre tread and combination of inflation pressure and load (Factorial ANOVA)

Effect	Univariate Tests of Significance for Max carcass stiffness (bar) (Spreadsheet3) Sigma-restricted parameterization Effective hypothesis decomposition				
	SS	Degr. of Freedom	MS	F	p
Intercept	824.2636	1	824.2636	1222.878	0.000000
Combination of inflation pressure / load	14.4074	10	1.4407	2.137	0.147013
Tyre tread	76.4476	1	76.4476	113.418	0.000005
Combination of inflation pressure / load*Tyre tread	7.1188	10	0.7119	1.056	0.478505
Error	5.3923	8	0.6740		

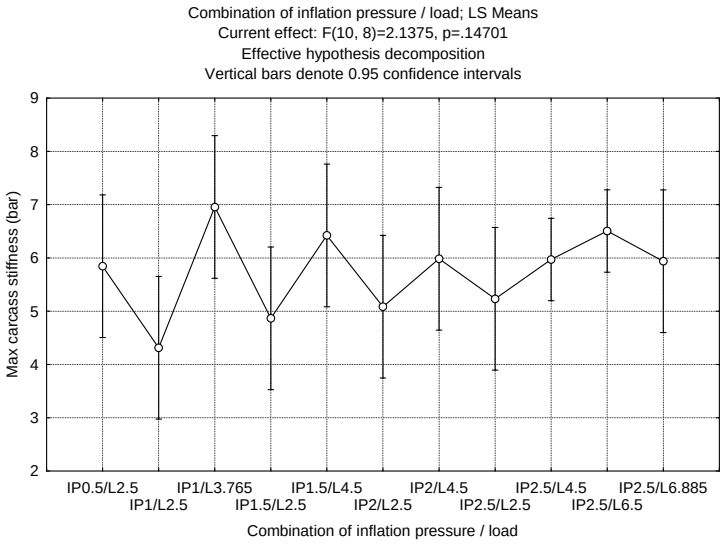
Combination of inflation pressure / load; LS Means
Current effect: F(10, 8)=2.1375, p=.14701
Effective hypothesis decomposition
Vertical bars denote 0.95 confidence intervals
Max carcass stiffness (bar)
9
8
7
6
5
4
3
2
IP0.5/L2.5
IP1/L2.5
IP1/L3.765
IP1.5/L2.5
IP1.5/L4.5
IP2/L2.5
IP2/L4.5
IP2.5/L2.5
IP2.5/L4.5
IP2.5/L6.5
IP2.5/L6.885
Combination of inflation pressure / load

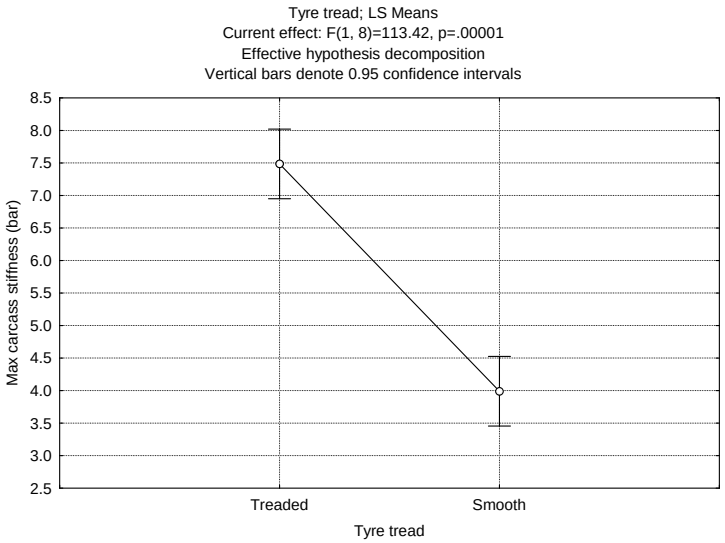
Tyre tread; LS Means
Current effect: F(1, 8)=113.42, p=.00001
Effective hypothesis decomposition
Vertical bars denote 0.95 confidence intervals
Max carcass stiffness (bar)
8.5
8.0
7.5
7.0
6.5
6.0
5.5
5.0
4.5
4.0
3.5
3.0
2.5
Treaded
Smooth
Tyre tread

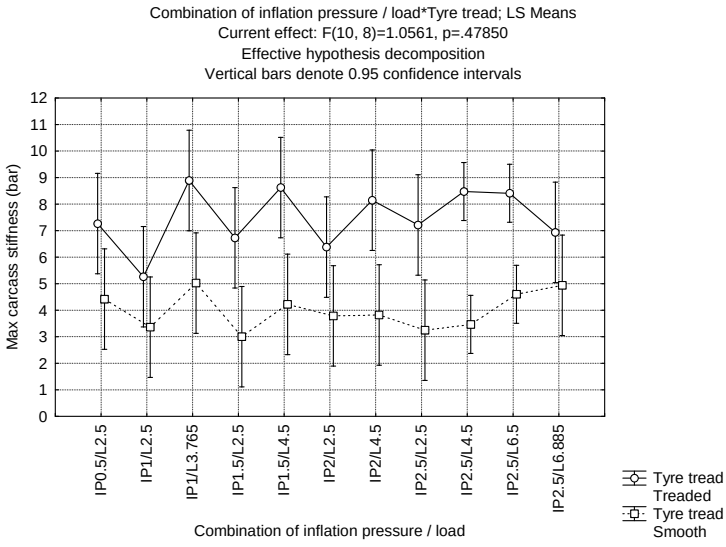
Combination of inflation pressure / load*Tyre tread; LS Means
Current effect: F(10, 8)=1.0561, p=.47850
Effective hypothesis decomposition
Vertical bars denote 0.95 confidence intervals
Max carcass stiffness (bar)
12
11
10
9
8
7
6
5
4
3
2
1
0
IP0.5/L2.5
IP1/L2.5
IP1/L3.765
IP1.5/L2.5
IP1.5/L4.5
IP2/L2.5
IP2/L4.5
IP2.5/L2.5
IP2.5/L4.5
IP2.5/L6.5
IP2.5/L6.885
Tyre tread
Treaded
Tyre tread
Smooth
Combination of inflation pressure / load

Cell No.	LSD test; variable Max carcass stiffness (bar) (Spreadsheet3) Probabilities for Post Hoc Tests Error: Between MS = .67404, df = 8.0000					
	Combination of inflation pressure / load	Tyre tread	1 7.2673	2 4.4213	3 5.2631	4 3.3629
1	IP0.5/L2.5	Treaded		0.039858	0.122591	0.009890
2	IP0.5/L2.5	Smooth	0.039858		0.489060	0.388651
3	IP1/L2.5	Treaded	0.122591	0.489060		0.140344
4	IP1/L2.5	Smooth	0.009890	0.388651	0.140344	
5	IP1/L3.765	Treaded	0.199517	0.004879	0.014129	0.001424
6	IP1/L3.765	Smooth	0.089316	0.618250	0.841369	0.190621
7	IP1.5/L2.5	Treaded	0.656002	0.081937	0.241944	0.019884
8	IP1.5/L2.5	Smooth	0.006282	0.256587	0.087421	0.764348
9	IP1.5/L4.5	Treaded	0.276230	0.006785	0.020054	0.001921
10	IP1.5/L4.5	Smooth	0.030443	0.866874	0.395314	0.481343
11	IP2/L2.5	Treaded	0.467066	0.129941	0.363915	0.031653
12	IP2/L2.5	Smooth	0.017141	0.599901	0.239380	0.724244
13	IP2/L4.5	Treaded	0.469643	0.012420	0.037807	0.003336
14	IP2/L4.5	Smooth	0.017919	0.619162	0.249390	0.703469
15	IP2.5/L2.5	Treaded	0.964699	0.042801	0.131366	0.010585
16	IP2.5/L2.5	Smooth	0.008566	0.342561	0.121146	0.924840
17	IP2.5/L4.5	Treaded	0.238059	0.002697	0.009511	0.000651
18	IP2.5/L4.5	Smooth	0.003900	0.343496	0.094712	0.915442
19	IP2.5/L6.5	Treaded	0.262783	0.002969	0.010560	0.000708
20	IP2.5/L6.5	Smooth	0.022786	0.853629	0.505249	0.227544
21	IP2.5/L6.885	Treaded	0.782463	0.062234	0.187661	0.015180
22	IP2.5/L6.885	Smooth	0.079871	0.667373	0.787307	0.211640

Cell No.	LSD test; variable Max carcass stiffness (bar) (Spreadsheet3) Probabilities for Post Hoc Tests Error: Between MS = .67404, df = 8.0000							
	5 8.8911	6 5.0231	7 6.7303	8 3.0027	9 8.6241	10 4.2203	11 6.3808	12 3.7872
1	0.199517	0.089316	0.656002	0.006282	0.276230	0.030443	0.467066	0.017141
2	0.004879	0.618250	0.081937	0.256587	0.006785	0.866874	0.129941	0.599901
3	0.014129	0.841369	0.241944	0.087421	0.020054	0.395314	0.363915	0.239380
4	0.001424	0.190621	0.019884	0.764348	0.001921	0.481343	0.031653	0.724244
5		0.010363	0.099771	0.000963	0.823904	0.003826	0.062593	0.002300
6	0.010363		0.179663	0.120033	0.014633	0.508857	0.275902	0.318207
7	0.099771	0.179663		0.012416	0.141516	0.062613	0.771111	0.034993
8	0.000963	0.120033	0.012416		0.001286	0.324993	0.019605	0.518317
9	0.823904	0.014633	0.141516	0.001286		0.005290	0.089435	0.003140
10	0.003826	0.508857	0.062613	0.324993	0.005290		0.099802	0.718847
11	0.062593	0.275902	0.771111	0.019605	0.089435	0.099802		0.055962
12	0.002300	0.318207	0.034993	0.518317	0.003140	0.718847	0.055962	
13	0.540362	0.027416	0.256660	0.002191	0.692867	0.009594	0.166384	0.005574
14	0.002391	0.330804	0.036617	0.500961	0.003268	0.739806	0.058562	0.977486
15	0.186695	0.095828	0.687716	0.006711	0.259295	0.032682	0.493267	0.018378
16	0.001258	0.165221	0.017134	0.836783	0.001691	0.427523	0.027215	0.655827
17	0.673184	0.006566	0.102792	0.000418	0.879846	0.002031	0.058061	0.001126
18	0.000443	0.139288	0.008792	0.637644	0.000616	0.449649	0.015258	0.744052
19	0.625034	0.007273	0.114492	0.000453	0.826446	0.002230	0.064804	0.001231

Cell No.	LSD test; variable Max carcass stiffness (bar) (Spreadsheet3) Probabilities for Post Hoc Tests Error: Between MS = .67404, df = 8.0000							
	5 8.8911	6 5.0231	7 6.7303	8 3.0027	9 8.6241	10 4.2203	11 6.3808	12 3.7872
20	0.001939	0.668608	0.054985	0.130116	0.002827	0.697825	0.097428	0.415150
21	0.130666	0.138098	0.863916	0.009536	0.183996	0.047505	0.645466	0.026585
22	0.009310	0.944163	0.161492	0.133912	0.013121	0.553026	0.249527	0.350179

Cell No.	LSD test; variable Max carcass stiffness (bar) (Spreadsheet3) Probabilities for Post Hoc Tests Error: Between MS = .67404, df = 8.0000							
	13 8.1485	14 3.8210	15 7.2143	16 3.2499	17 8.4761	18 3.4668	19 8.4093	20 4.6019
1	0.469643	0.017919	0.964699	0.008566	0.238059	0.003900	0.262783	0.022786
2	0.012420	0.619162	0.042801	0.342561	0.002697	0.343496	0.002969	0.853629
3	0.037807	0.249390	0.131366	0.121146	0.009511	0.094712	0.010560	0.505249
4	0.003336	0.703469	0.010585	0.924840	0.000651	0.915442	0.000708	0.227544
5	0.540362	0.002391	0.186695	0.001258	0.673184	0.000443	0.625034	0.001939
6	0.027416	0.330804	0.095828	0.165221	0.006566	0.139288	0.007273	0.668608
7	0.256660	0.036617	0.687716	0.017134	0.102792	0.008792	0.114492	0.054985
8	0.002191	0.500961	0.006711	0.836783	0.000418	0.637644	0.000453	0.130116
9	0.692867	0.003268	0.259295	0.001691	0.879846	0.000616	0.826446	0.002827
10	0.009594	0.739806	0.032682	0.427523	0.002031	0.449649	0.002230	0.697825
11	0.166384	0.058562	0.493267	0.027215	0.058061	0.015258	0.064804	0.097428
12	0.005574	0.977486	0.018378	0.655827	0.001126	0.744052	0.001231	0.415150
13		0.005811	0.444288	0.002919	0.738589	0.001137	0.790241	0.005696
14	0.005811		0.019215	0.635984	0.001178	0.718357	0.001288	0.433977
15	0.444288	0.019215		0.009162	0.219866	0.004218	0.243002	0.024839
16	0.002919	0.635984	0.009162		0.000565	0.824755	0.000614	0.191649
17	0.738589	0.001178	0.219866	0.000565		0.000071	0.923041	0.000415
18	0.001137	0.718357	0.004218	0.824755	0.000071		0.000078	0.128845
19	0.790241	0.001288	0.243002	0.000614	0.923041	0.000078		0.000465
20	0.005696	0.433977	0.024839	0.191649	0.000415	0.128845	0.000465	
21	0.326771	0.027811	0.816435	0.013104	0.142851	0.006408	0.158709	0.039203
22	0.024517	0.363730	0.085720	0.183765	0.005780	0.158991	0.006397	0.731207

Cell No.	LSD test; variable Max carcass stiffness (bar) (Spreadsheet3) Probabilities for Post Hoc Tests Error: Between MS = .67404, df = 8.0000	
	21 6.9358	22 4.9392
1	0.782463	0.079871
2	0.062234	0.667373
3	0.187661	0.787307
4	0.015180	0.211640
5	0.130666	0.009310
6	0.138098	0.944163
7	0.863916	0.161492

Cell No.	LSD test; variable Max carcass stiffness (bar) (Spreadsheet3) Probabilities for Post Hoc Tests Error: Between MS = .67404, df = 8.0000	
	21 6.9358	22 4.9392
8	0.009536	0.133912
9	0.183996	0.013121
10	0.047505	0.553026
11	0.645466	0.249527
12	0.026585	0.350179
13	0.326771	0.024517
14	0.027811	0.363730
15	0.816435	0.085720
16	0.013104	0.183765
17	0.142851	0.005780
18	0.006408	0.158991
19	0.158709	0.006397
20	0.039203	0.731207
21		0.123815
22	0.123815	

H.8 Ink Tests: Treaded Combine Tyre – Treaded contact area – effect of combination of inflation pressure and load (One-way ANOVA)

Effect	Univariate Tests of Significance for Tread contact area (m2) (Spreadsheet14) Sigma-restricted parameterization Effective hypothesis decomposition				
	SS	Degr. of Freedom	MS	F	p
Intercept	0.073431	1	0.073431	3008448	0.000000
Combination of inflation pressure / load	0.005804	16	0.000363	14861	0.000000
Error	0.000000	6	0.000000		

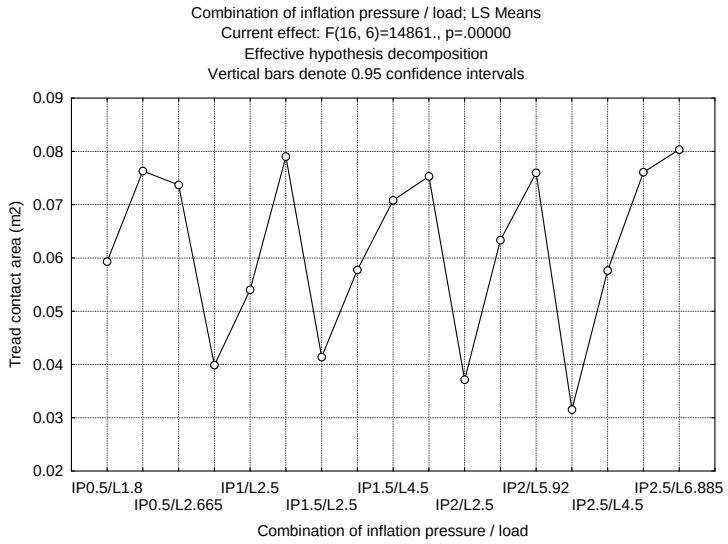

Cell No.	LSD test; variable Tread contact area (m2) (Spreadsheet14) Probabilities for Post Hoc Tests Error: Between MS = .00000, df = 6.0000						
	Combination of inflation pressure / load	1 .05933	2 .07631	3 .07370	4 .03987	5 .05402	6 .07900
1	IP0.5/L1.8		0.000000	0.000000	0.000000	0.000000	0.000000
2	IP0.5/L2.5	0.000000		0.000022	0.000000	0.000000	0.000019
3	IP0.5/L2.665	0.000000	0.000022		0.000000	0.000000	0.000000
4	IP1/L1.8	0.000000	0.000000	0.000000		0.000000	0.000000
5	IP1/L2.5	0.000000	0.000000	0.000000	0.000000		0.000000
6	IP1/L3.765	0.000000	0.000019	0.000000	0.000000	0.000000	
7	IP1.5/L2.5	0.000000	0.000000	0.000000	0.000476	0.000000	0.000000
8	IP1.5/L3.5	0.000385	0.000000	0.000000	0.000000	0.000003	0.000000
9	IP1.5/L4.5	0.000000	0.000000	0.000012	0.000000	0.000000	0.000000
10	IP1.5/L4.822	0.000000	0.003756	0.000351	0.000000	0.000000	0.000003
11	IP2/L2.5	0.000000	0.000000	0.000000	0.000005	0.000000	0.000000
12	IP2/L4.5	0.000002	0.000000	0.000000	0.000000	0.000000	0.000000
13	IP2/L5.92	0.000000	0.177395	0.000049	0.000000	0.000000	0.000009
14	IP2.5/L2.5	0.000000	0.000000	0.000000	0.000000	0.000000	0.000000
15	IP2.5/L4.5	0.000087	0.000000	0.000000	0.000000	0.000001	0.000000
16	IP2.5/L6.5	0.000000	0.232454	0.000012	0.000000	0.000000	0.000003
17	IP2.5/L6.885	0.000000	0.000002	0.000000	0.000000	0.000000	0.000996

Cell No.	LSD test; variable Tread contact area (m2) (Spreadsheet14) Probabilities for Post Hoc Tests Error: Between MS = .00000, df = 6.0000							
	7 .04139	8 .05776	9 .07080	10 .07530	11 .03713	12 .06335	13 .07597	14 .03153
1	0.000000	0.000385	0.000000	0.000000	0.000000	0.000002	0.000000	0.000000
2	0.000000	0.000000	0.000000	0.003756	0.000000	0.000000	0.177395	0.000000
3	0.000000	0.000000	0.000012	0.000351	0.000000	0.000000	0.000049	0.000000
4	0.000476	0.000000	0.000000	0.000000	0.000005	0.000000	0.000000	0.000000
5	0.000000	0.000003	0.000000	0.000000	0.000000	0.000000	0.000000	0.000000
6	0.000000	0.000000	0.000000	0.000003	0.000000	0.000000	0.000009	0.000000
7		0.000000	0.000000	0.000000	0.000000	0.000000	0.000000	0.000000

Cell No.	LSD test; variable Tread contact area (m2) (Spreadsheet14) Probabilities for Post Hoc Tests Error: Between MS = .00000, df = 6.0000							
	7 .04139	8 .05776	9 .07080	10 .07530	11 .03713	12 .06335	13 .07597	14 .03153
8	0.000000		0.000000	0.000000	0.000000	0.000000	0.000000	0.000000
9	0.000000	0.000000		0.000001	0.000000	0.000000	0.000000	0.000000
10	0.000000	0.000000	0.000001		0.000000	0.000000	0.022344	0.000000
11	0.000000	0.000000	0.000000	0.000000		0.000000	0.000000	0.000000
12	0.000000	0.000000	0.000000	0.000000	0.000000		0.000000	0.000000
13	0.000000	0.000000	0.000000	0.022344	0.000000	0.000000		0.000000
14	0.000000	0.000000	0.000000	0.000000	0.000000	0.000000	0.000000	
15	0.000000	0.583265	0.000000	0.000000	0.000000	0.000000	0.000000	0.000000
16	0.000000	0.000000	0.000000	0.005172	0.000000	0.000000	0.606515	0.000000
17	0.000000	0.000000	0.000000	0.000000	0.000000	0.000000	0.000001	0.000000

Cell No.	LSD test; variable Tread contact area (m2) (Spreadsheet14) Probabilities for Post Hoc Tests Error: Between MS = .00000, df = 6.0000		
	15 .05765	16 .07607	17 .08032
1	0.000087	0.000000	0.000000
2	0.000000	0.232454	0.000002
3	0.000000	0.000012	0.000000
4	0.000000	0.000000	0.000000
5	0.000001	0.000000	0.000000
6	0.000000	0.000003	0.000996
7	0.000000	0.000000	0.000000
8	0.583265	0.000000	0.000000
9	0.000000	0.000000	0.000000
10	0.000000	0.005172	0.000000
11	0.000000	0.000000	0.000000
12	0.000000	0.000000	0.000000
13	0.000000	0.606515	0.000001
14	0.000000	0.000000	0.000000
15		0.000000	0.000000
16	0.000000		0.000000
17	0.000000	0.000000	

H.9 Ink Tests: Treaded Combine Tyre – Projected contact area – effect of combination of inflation pressure and load (One-way ANOVA)

Effect	Univariate Tests of Significance for Projected contact area (m2) (Spreadsheet14) Sigma-restricted parameterization Effective hypothesis decomposition				
	SS	Degr. of Freedom	MS	F	p
Intercept	0.719519	1	0.719519	61546.18	0.000000
Combination of inflation pressure / load	0.050493	16	0.003156	269.94	0.000000
Error	0.000070	6	0.000012		

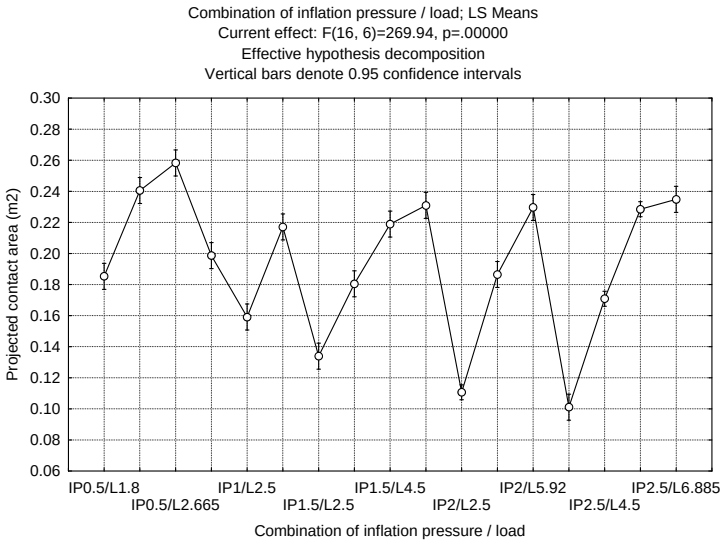

Cell No.	LSD test; variable Projected contact area (m2) (Spreadsheet14) Probabilities for Post Hoc Tests Error: Between MS = .00001, df = 6.0000						
	Combination of inflation pressure / load	1 .18530	2 .24051	3 .25826	4 .19864	5 .15912	6 .21708
1	IP0.5/L1.8		0.000027	0.000005	0.032906	0.001642	0.000594
2	IP0.5/L2.5	0.000027		0.010443	0.000131	0.000003	0.002868
3	IP0.5/L2.665	0.000005	0.010443		0.000017	0.000001	0.000144
4	IP1/L1.8	0.032906	0.000131	0.000017		0.000181	0.008812
5	IP1/L2.5	0.001642	0.000003	0.000001	0.000181		0.000020
6	IP1/L3.765	0.000594	0.002868	0.000144	0.008812	0.000020	
7	IP1.5/L2.5	0.000041	0.000001	0.000000	0.000011	0.001989	0.000002
8	IP1.5/L3.5	0.357966	0.000017	0.000004	0.009463	0.004478	0.000276
9	IP1.5/L4.5	0.000439	0.004266	0.000185	0.005713	0.000017	0.716609
10	IP1.5/L4.822	0.000080	0.095675	0.001324	0.000543	0.000006	0.028459
11	IP2/L2.5	0.000001	0.000000	0.000000	0.000001	0.000018	0.000000
12	IP2/L4.5	0.812604	0.000031	0.000006	0.045837	0.001305	0.000729
13	IP2/L5.92	0.000095	0.065254	0.001032	0.000682	0.000007	0.041093
14	IP2.5/L2.5	0.000002	0.000000	0.000000	0.000001	0.000020	0.000000
15	IP2.5/L4.5	0.010612	0.000002	0.000001	0.000412	0.024849	0.000023
16	IP2.5/L6.5	0.000035	0.022775	0.000283	0.000277	0.000002	0.027621
17	IP2.5/L6.885	0.000050	0.285126	0.002868	0.000294	0.000004	0.010443

Cell No.	LSD test; variable Projected contact area (m2) (Spreadsheet14) Probabilities for Post Hoc Tests Error: Between MS = .00001, df = 6.0000							
	7 .13391	8 .18048	9 .21892	10 .23096	11 .11065	12 .18650	13 .22962	14 .10110
1	0.000041	0.357966	0.000439	0.000080	0.000001	0.812604	0.000095	0.000002
2	0.000001	0.000017	0.004266	0.095675	0.000000	0.000031	0.065254	0.000000
3	0.000000	0.000004	0.000185	0.001324	0.000000	0.000006	0.001032	0.000000
4	0.000011	0.009463	0.005713	0.000543	0.000001	0.045837	0.000682	0.000001
5	0.001989	0.004478	0.000017	0.000006	0.000018	0.001305	0.000007	0.000020
6	0.000002	0.000276	0.716609	0.028459	0.000000	0.000729	0.041093	0.000000
7		0.000072	0.000002	0.000001	0.001062	0.000036	0.000001	0.000501

Cell No.	LSD test; variable Projected contact area (m2) (Spreadsheet14) Probabilities for Post Hoc Tests Error: Between MS = .00001, df = 6.0000							
	7 .13391	8 .18048	9 .21892	10 .23096	11 .11065	12 .18650	13 .22962	14 .10110
8	0.000072		0.000211	0.000045	0.000002	0.260186	0.000053	0.000003
9	0.000002	0.000211		0.047255	0.000000	0.000534	0.068996	0.000000
10	0.000001	0.000045	0.047255		0.000000	0.000093	0.791071	0.000000
11	0.001062	0.000002	0.000000	0.000000		0.000001	0.000000	0.051839
12	0.000036	0.260186	0.000534	0.000093	0.000001		0.000111	0.000002
13	0.000001	0.000053	0.068996	0.791071	0.000000	0.000111		0.000000
14	0.000501	0.000003	0.000000	0.000000	0.051839	0.000002	0.000000	
15	0.000084	0.050590	0.000019	0.000005	0.000001	0.007445	0.000006	0.000002
16	0.000000	0.000019	0.051451	0.556835	0.000000	0.000041	0.786893	0.000000
17	0.000001	0.000030	0.016608	0.453276	0.000000	0.000058	0.322146	0.000000

Cell No.	LSD test; variable Projected contact area (m2) (Spreadsheet14) Probabilities for Post Hoc Tests Error: Between MS = .00001, df = 6.0000		
	15 .17086	16 .22850	17 .23483
1	0.010612	0.000035	0.000050
2	0.000002	0.022775	0.285126
3	0.000001	0.000283	0.002868
4	0.000412	0.000277	0.000294
5	0.024849	0.000002	0.000004
6	0.000023	0.027621	0.010443
7	0.000084	0.000000	0.000001
8	0.050590	0.000019	0.000030
9	0.000019	0.051451	0.016608
10	0.000005	0.556835	0.453276
11	0.000001	0.000000	0.000000
12	0.007445	0.000041	0.000058
13	0.000006	0.786893	0.322146
14	0.000002	0.000000	0.000000
15		0.000001	0.000004
16	0.000001		0.159856
17	0.000004	0.159856	

H.10 Ink Tests: Treaded Combine Tyre – Tread contact pressure – effect of combination of inflation pressure and load (One-way ANOVA)

Effect	Univariate Tests of Significance for Tread contact pressure (bar) (Spreadsheet14) Sigma-restricted parameterization Effective hypothesis decomposition				
	SS	Degr. of Freedom	MS	F	p
Intercept	682.9422	1	682.9422	1966881	0.000000
Combination of inflation pressure / load	65.2467	16	4.0779	11744	0.000000
Error	0.0021	6	0.0003		

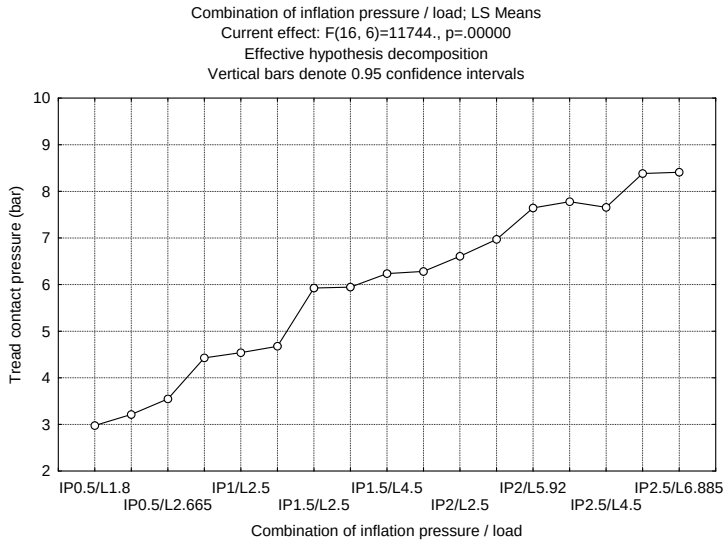

Cell No.	LSD test; variable Tread contact pressure (bar) (Spreadsheet14) Probabilities for Post Hoc Tests Error: Between MS = .00035, df = 6.0000						
	Combination of inflation pressure / load	1 2.9762	2 3.2138	3 3.5474	4 4.4284	5 4.5402	6 4.6752
1	IP0.5/L1.8		0.000104	0.000001	0.000000	0.000000	0.000000
2	IP0.5/L2.5	0.000104		0.000015	0.000000	0.000000	0.000000
3	IP0.5/L2.665	0.000001	0.000015		0.000000	0.000000	0.000000
4	IP1/L1.8	0.000000	0.000000	0.000000		0.005406	0.000084
5	IP1/L2.5	0.000000	0.000000	0.000000	0.005406		0.002179
6	IP1/L3.765	0.000000	0.000000	0.000000	0.000084	0.002179	
7	IP1.5/L2.5	0.000000	0.000000	0.000000	0.000000	0.000000	0.000000
8	IP1.5/L3.5	0.000000	0.000000	0.000000	0.000000	0.000000	0.000000
9	IP1.5/L4.5	0.000000	0.000000	0.000000	0.000000	0.000000	0.000000
10	IP1.5/L4.822	0.000000	0.000000	0.000000	0.000000	0.000000	0.000000
11	IP2/L2.5	0.000000	0.000000	0.000000	0.000000	0.000000	0.000000
12	IP2/L4.5	0.000000	0.000000	0.000000	0.000000	0.000000	0.000000
13	IP2/L5.92	0.000000	0.000000	0.000000	0.000000	0.000000	0.000000
14	IP2.5/L2.5	0.000000	0.000000	0.000000	0.000000	0.000000	0.000000
15	IP2.5/L4.5	0.000000	0.000000	0.000000	0.000000	0.000000	0.000000
16	IP2.5/L6.5	0.000000	0.000000	0.000000	0.000000	0.000000	0.000000
17	IP2.5/L6.885	0.000000	0.000000	0.000000	0.000000	0.000000	0.000000

Cell No.	LSD test; variable Tread contact pressure (bar) (Spreadsheet14) Probabilities for Post Hoc Tests Error: Between MS = .00035, df = 6.0000							
	7 5.9256	8 5.9449	9 6.2350	10 6.2821	11 6.6060	12 6.9684	13 7.6440	14 7.7775
1	0.000000	0.000000	0.000000	0.000000	0.000000	0.000000	0.000000	0.000000
2	0.000000	0.000000	0.000000	0.000000	0.000000	0.000000	0.000000	0.000000
3	0.000000	0.000000	0.000000	0.000000	0.000000	0.000000	0.000000	0.000000
4	0.000000	0.000000	0.000000	0.000000	0.000000	0.000000	0.000000	0.000000
5	0.000000	0.000000	0.000000	0.000000	0.000000	0.000000	0.000000	0.000000
6	0.000000	0.000000	0.000000	0.000000	0.000000	0.000000	0.000000	0.000000
7		0.491790	0.000023	0.000010	0.000000	0.000000	0.000000	0.000000

Cell No.	LSD test; variable Tread contact pressure (bar) (Spreadsheet14) Probabilities for Post Hoc Tests Error: Between MS = .00035, df = 6.0000							
	7 5.9256	8 5.9449	9 6.2350	10 6.2821	11 6.6060	12 6.9684	13 7.6440	14 7.7775
8	0.491790		0.000033	0.000014	0.000000	0.000000	0.000000	0.000000
9	0.000023	0.000033		0.124137	0.000002	0.000000	0.000000	0.000000
10	0.000010	0.000014	0.124137		0.000005	0.000000	0.000000	0.000000
11	0.000000	0.000000	0.000002	0.000005		0.000003	0.000000	0.000000
12	0.000000	0.000000	0.000000	0.000000	0.000003		0.000000	0.000000
13	0.000000	0.000000	0.000000	0.000000	0.000000	0.000000		0.002299
14	0.000000	0.000000	0.000000	0.000000	0.000000	0.000000	0.002299	
15	0.000000	0.000000	0.000000	0.000000	0.000000	0.000000	0.561734	0.001394
16	0.000000	0.000000	0.000000	0.000000	0.000000	0.000000	0.000000	0.000000
17	0.000000	0.000000	0.000000	0.000000	0.000000	0.000000	0.000000	0.000000

Cell No.	LSD test; variable Tread contact pressure (bar) (Spreadsheet14) Probabilities for Post Hoc Tests Error: Between MS = .00035, df = 6.0000		
	15 7.6573	16 8.3822	17 8.4092
1	0.000000	0.000000	0.000000
2	0.000000	0.000000	0.000000
3	0.000000	0.000000	0.000000
4	0.000000	0.000000	0.000000
5	0.000000	0.000000	0.000000
6	0.000000	0.000000	0.000000
7	0.000000	0.000000	0.000000
8	0.000000	0.000000	0.000000
9	0.000000	0.000000	0.000000
10	0.000000	0.000000	0.000000
11	0.000000	0.000000	0.000000
12	0.000000	0.000000	0.000000
13	0.561734	0.000000	0.000000
14	0.001394	0.000000	0.000000
15		0.000000	0.000000
16	0.000000		0.257008
17	0.000000	0.257008	

H.11 Ink Tests: Treaded Combine Tyre – Projected contact pressure – effect of combination of inflation pressure and load (One-way ANOVA)

Effect	Univariate Tests of Significance for Projected contact pressure (bar) (Spreadsheet14) Sigma-restricted parameterization Effective hypothesis decomposition				
	SS	Degr. of Freedom	MS	F	p
Intercept	71.32180	1	71.32180	15545.17	0.000000
Combination of inflation pressure / load	8.85785	16	0.55362	120.67	0.000004
Error	0.02753	6	0.00459		

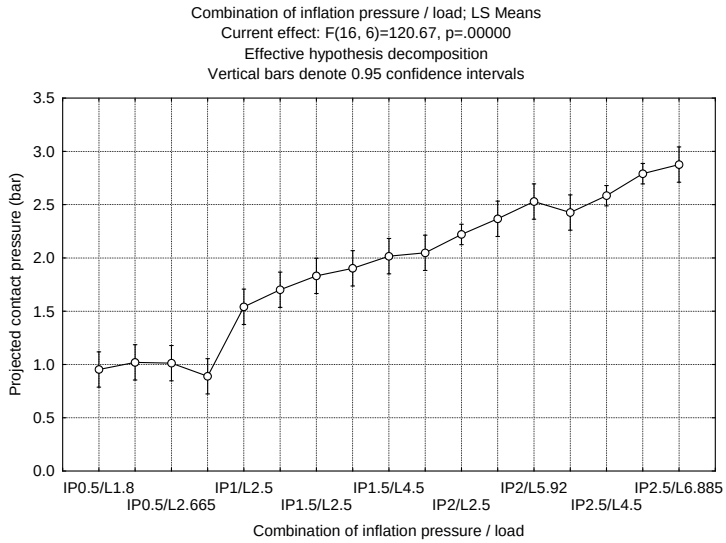

Cell No.	LSD test; variable Projected contact pressure (bar) (Spreadsheet14) Probabilities for Post Hoc Tests Error: Between MS = .00459, df = 6.0000						
	Combination of inflation pressure / load	1 .95296	2 1.0197	3 1.0123	4 .88896	5 1.5413	6 1.7014
1	IP0.5/L1.8		0.511939	0.558328	0.528919	0.000853	0.000232
2	IP0.5/L2.5	0.511939		0.940852	0.221216	0.001595	0.000387
3	IP0.5/L2.665	0.558328	0.940852		0.245299	0.001484	0.000365
4	IP1/L1.8	0.528919	0.221216	0.245299		0.000491	0.000147
5	IP1/L2.5	0.000853	0.001595	0.001484	0.000491		0.145717
6	IP1/L3.765	0.000232	0.000387	0.000365	0.000147	0.145717	
7	IP1.5/L2.5	0.000095	0.000148	0.000140	0.000064	0.023122	0.223313
8	IP1.5/L3.5	0.000061	0.000092	0.000088	0.000042	0.009295	0.080678
9	IP1.5/L4.5	0.000032	0.000046	0.000044	0.000023	0.002552	0.016637
10	IP1.5/L4.822	0.000027	0.000039	0.000037	0.000019	0.001845	0.011098
11	IP2/L2.5	0.000004	0.000005	0.000005	0.000003	0.000129	0.000565
12	IP2/L4.5	0.000006	0.000008	0.000008	0.000005	0.000134	0.000440
13	IP2/L5.92	0.000003	0.000004	0.000004	0.000003	0.000049	0.000132
14	IP2.5/L2.5	0.000005	0.000006	0.000006	0.000004	0.000091	0.000277
15	IP2.5/L4.5	0.000001	0.000001	0.000001	0.000001	0.000011	0.000029
16	IP2.5/L6.5	0.000000	0.000000	0.000000	0.000000	0.000004	0.000009
17	IP2.5/L6.885	0.000001	0.000001	0.000001	0.000001	0.000009	0.000018

Cell No.	LSD test; variable Projected contact pressure (bar) (Spreadsheet14) Probabilities for Post Hoc Tests Error: Between MS = .00459, df = 6.0000							
	7 1.8315	8 1.9024	9 2.0164	10 2.0482	11 2.2204	12 2.3671	13 2.5292	14 2.4259
1	0.000095	0.000061	0.000032	0.000027	0.000004	0.000006	0.000003	0.000005
2	0.000148	0.000092	0.000046	0.000039	0.000005	0.000008	0.000004	0.000006
3	0.000140	0.000088	0.000044	0.000037	0.000005	0.000008	0.000004	0.000006
4	0.000064	0.000042	0.000023	0.000019	0.000003	0.000005	0.000003	0.000004
5	0.023122	0.009295	0.002552	0.001845	0.000129	0.000134	0.000049	0.000091
6	0.223313	0.080678	0.016637	0.011098	0.000565	0.000440	0.000132	0.000277
7		0.487108	0.101714	0.064375	0.002522	0.001392	0.000341	0.000808

Cell No.	LSD test; variable Projected contact pressure (bar) (Spreadsheet14) Probabilities for Post Hoc Tests Error: Between MS = .00459, df = 6.0000							
	7 1.8315	8 1.9024	9 2.0164	10 2.0482	11 2.2204	12 2.3671	13 2.5292	14 2.4259
8	0.487108		0.278738	0.178898	0.006609	0.002848	0.000609	0.001565
9	0.101714	0.278738		0.751871	0.040270	0.010574	0.001740	0.005239
10	0.064375	0.178898	0.751871		0.069930	0.015818	0.002400	0.007597
11	0.002522	0.006609	0.040270	0.069930		0.109776	0.007550	0.039183
12	0.001392	0.002848	0.010574	0.015818	0.109776		0.141522	0.561889
13	0.000341	0.000609	0.001740	0.002400	0.007550	0.141522		0.322214
14	0.000808	0.001565	0.005239	0.007597	0.039183	0.561889	0.322214	
15	0.000072	0.000126	0.000349	0.000476	0.000595	0.032358	0.510846	0.089928
16	0.000018	0.000028	0.000061	0.000078	0.000049	0.001641	0.015580	0.003458
17	0.000035	0.000053	0.000107	0.000132	0.000157	0.001805	0.011073	0.003325

Cell No.	LSD test; variable Projected contact pressure (bar) (Spreadsheet14) Probabilities for Post Hoc Tests Error: Between MS = .00459, df = 6.0000		
	15 2.5839	16 2.7906	17 2.8761
1	0.000001	0.000000	0.000001
2	0.000001	0.000000	0.000001
3	0.000001	0.000000	0.000001
4	0.000001	0.000000	0.000001
5	0.000011	0.000004	0.000009
6	0.000029	0.000009	0.000018
7	0.000072	0.000018	0.000035
8	0.000126	0.000028	0.000053
9	0.000349	0.000061	0.000107
10	0.000476	0.000078	0.000132
11	0.000595	0.000049	0.000157
12	0.032358	0.001641	0.001805
13	0.510846	0.015580	0.011073
14	0.089928	0.003458	0.003325
15		0.009650	0.009656
16	0.009650		0.315862
17	0.009656	0.315862	

APPENDIX I

STATISTICAL ANALYSIS – HARD SURFACE RESULTS OF THE IMPLEMENT TYRES (ANOVA)

I.1 Tekscan Tests: Implement Tyres – Contact area – effect of PR (One-way ANOVA)

Effect	Univariate Tests of Significance for Contact area (m2) (Spreadsheet5) Sigma-restricted parameterization Effective hypothesis decomposition				
	SS	Degr. of Freedom	MS	F	p
Intercept	0.019641	1	0.019641	4352.813	0.000000
PR	0.000024	4	0.000006	1.344	0.319755
Error	0.000045	10	0.000005		

LSD at 95% confidence level = 0.0041 m^3

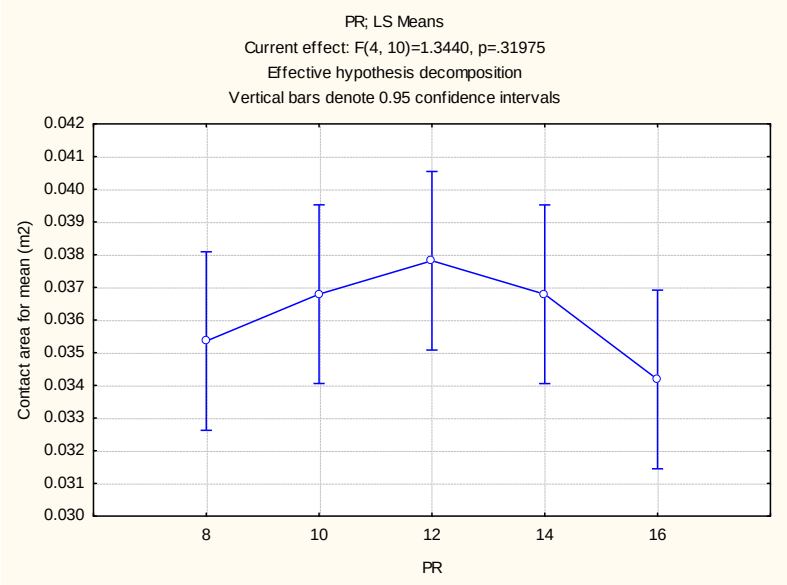

Cell No.	LSD test; variable Contact area (m2) (Spreadsheet5) Probabilities for Post Hoc Tests Error: Between MS = .00000, df = 10.000					
	PR	1 .03536	2 .03679	3 .03781	4 .03679	5 .03418
1	8		0.427393	0.186900	0.428242	0.513467
2	10	0.427393		0.568500	0.998780	0.163304
3	12	0.186900	0.568500		0.567489	0.062664
4	14	0.428242	0.998780	0.567489		0.163701
5	16	0.513467	0.163304	0.062664	0.163701	

I.2 Tekscan Tests: Implement Tyres – Mean contact pressure – effect of PR (One-way ANOVA)

Effect	Univariate Tests of Significance for Mean contact pressure (bar) (Spreadsheet5) Sigma-restricted parameterization Effective hypothesis decomposition				
	SS	Degr. of Freedom	MS	F	p
Intercept	304.1503	1	304.1503	3534.993	0.000000
PR	0.8105	4	0.2026	2.355	0.124007
Error	0.8604	10	0.0860		

LSD at 95% confidence level = 0.53 bar

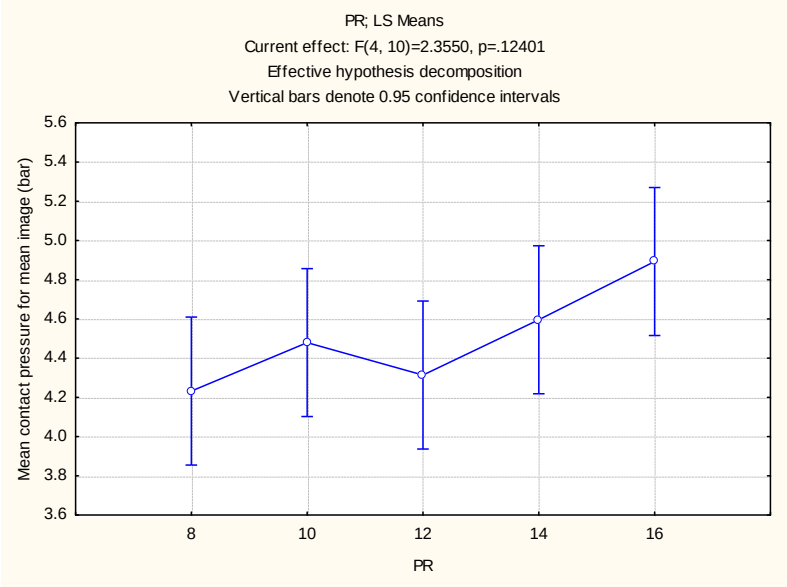

Cell No.	LSD test; variable Mean contact pressure (bar) (Spreadsheet5) Probabilities for Post Hoc Tests Error: Between MS = .08604, df = 10.000					
	PR	1 4.2324	2 4.4795	3 4.3140	4 4.5961	5 4.8928
1	8		0.326545	0.740475	0.159795	0.020212
2	10	0.326545		0.505244	0.636701	0.115058
3	12	0.740475	0.505244		0.266010	0.036243
4	14	0.159795	0.636701	0.266010		0.243672
5	16	0.020212	0.115058	0.036243	0.243672	

I.3 Tekscan Tests: Implement Tyres – Maximum contact pressure – effect of PR (One-way ANOVA)

Effect	Univariate Tests of Significance for Max contact pressure (bar) (Spreadsheet5) Sigma-restricted parameterization Effective hypothesis decomposition				
	SS	Degr. of Freedom	MS	F	p
Intercept	1481.912	1	1481.912	385.1536	0.000000
PR	6.473	4	1.618	0.4206	0.790477
Error	38.476	10	3.848		

LSD at 95% confidence level = 3.57 bar

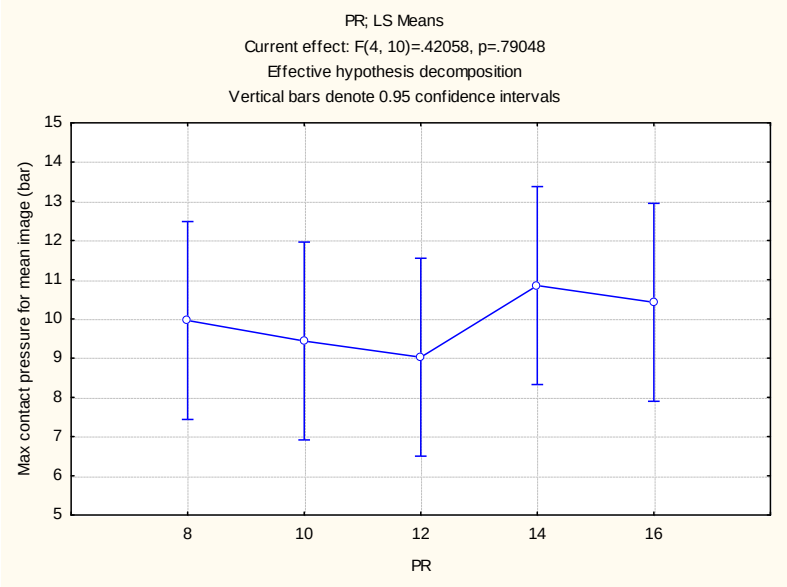

Cell No.	LSD test; variable Max contact pressure (bar) (Spreadsheet5) Probabilities for Post Hoc Tests Error: Between MS = 3.8476, df = 10.000					
	PR	1 9.9599	2 9.4380	3 9.0238	4 10.852	5 10.424
1	8		0.751204	0.571829	0.589869	0.777850
2	10	0.751204		0.801197	0.398082	0.551803
3	12	0.571829	0.801197		0.280313	0.402433
4	14	0.589869	0.398082	0.280313		0.794891
5	16	0.777850	0.551803	0.402433	0.794891	

I.4 Tekscan Tests: Implement Tyres – Mean carcass stiffness – effect of PR (One-way ANOVA)

Effect	Univariate Tests of Significance for Mean carcass stiffness (bar) (Spreadsheet5.sta) Sigma-restricted parameterization Effective hypothesis decomposition				
	SS	Degr. of Freedom	MS	F	p
Intercept	48.76019	1	48.76019	566.7163	0.000000
PR	0.81050	4	0.20263	2.3550	0.124007
Error	0.86040	10	0.08604		

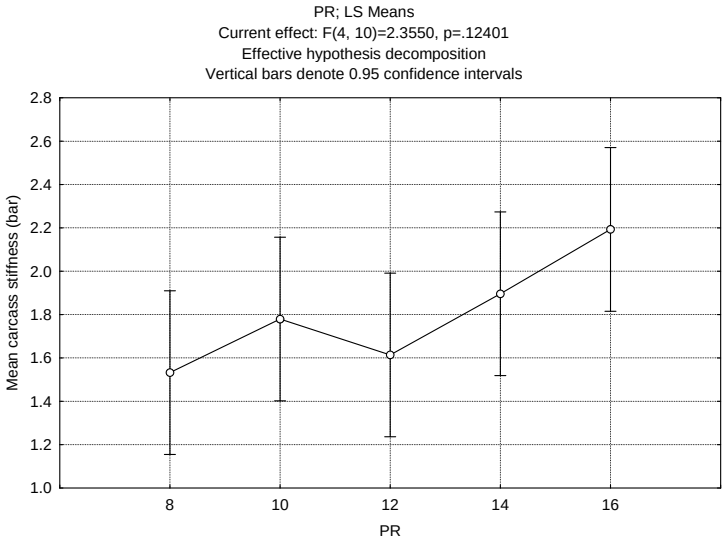

Cell No.	LSD test; variable Mean carcass stiffness (bar) (Spreadsheet5.sta) Probabilities for Post Hoc Tests Error: Between MS = .08604, df = 10.000					
	PR	1 1.5324	2 1.7795	3 1.6140	4 1.8961	5 2.1928
1	8		0.326545	0.740475	0.159795	0.020212
2	10	0.326545		0.505244	0.636701	0.115058
3	12	0.740475	0.505244		0.266010	0.036243
4	14	0.159795	0.636701	0.266010		0.243672
5	16	0.020212	0.115058	0.036243	0.243672	

I.5 Tekscan Tests: Implement Tyres – Maximum carcass stiffness – effect of PR (One-way ANOVA)

Effect	Univariate Tests of Significance for Maximum carcass stiffness (bar) (Spreadsheet5.sta) Sigma-restricted parameterization Effective hypothesis decomposition				
	SS	Degr. of Freedom	MS	F	p
Intercept	786.1609	1	786.1609	204.3256	0.000000
PR	6.4729	4	1.6182	0.4206	0.790477
Error	38.4759	10	3.8476		

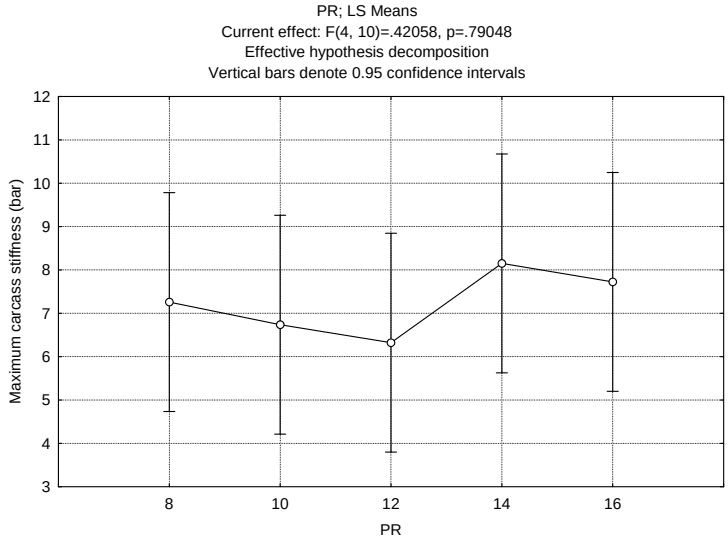

Cell No.	LSD test; variable Maximum carcass stiffness (bar) (Spreadsheet5.sta) Probabilities for Post Hoc Tests Error: Between MS = 3.8476, df = 10.000					
	PR	1 7.2599	2 6.7380	3 6.3238	4 8.1518	5 7.7242
1	8		0.751204	0.571829	0.589869	0.777850
2	10	0.751204		0.801197	0.398082	0.551803
3	12	0.571829	0.801197		0.280313	0.402433
4	14	0.589869	0.398082	0.280313		0.794891
5	16	0.777850	0.551803	0.402433	0.794891	

I.6 Tekscan Tests: Implement Tyres – Contact area – effect of inflation pressure and load combination (One-way ANOVA)

Effect	Univariate Tests of Significance for Contact area (m2) (Spreadsheet15.sta) Sigma-restricted parameterization Effective hypothesis decomposition				
	SS	Degr. of Freedom	MS	F	p
Intercept	0.015779	1	0.015779	5417.295	0.000000
Inflation pressure and load combination	0.000029	4	0.000007	2.510	0.108458
Error	0.000029	10	0.000003		

LSD at 95% confidence level = 0.0031 m^2

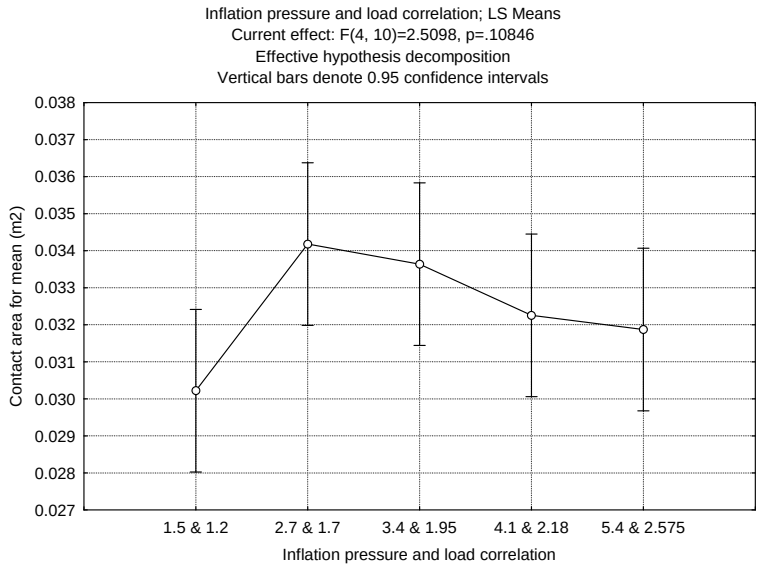

Cell No.	LSD test; variable Contact area (m2) (Spreadsheet15.sta) Probabilities for Post Hoc Tests Error: Between MS = .00000, df = 10.000					
	Inflation pressure and load combination	1 .03022	2 .03418	3 .03364	4 .03226	5 .03187
1	1.5 & 1.2		0.017488	0.034106	0.174709	0.263116
2	2.7 & 1.7	0.017488		0.705138	0.197363	0.128678
3	3.4 & 1.95	0.034106	0.705138		0.344791	0.233937
4	4.1 & 2.18	0.174709	0.197363	0.344791		0.788750
5	5.4 & 2.575	0.263116	0.128678	0.233937	0.788750	

I.7 Tekscan Tests: Implement Tyres – Mean contact pressure – effect of inflation pressure and load combination (One-way ANOVA)

Effect	Univariate Tests of Significance for Mean contact pressure (bar) (Spreadsheet15.sta) Sigma-restricted parameterization Effective hypothesis decomposition				
	SS	Degr. of Freedom	MS	F	p
Intercept	456.7550	1	456.7550	7056.329	0.000000
Inflation pressure and load combination	30.9097	4	7.7274	119.380	0.000000
Error	0.6473	10	0.0647		

LSD at 95% confidence level = 0.46 bar

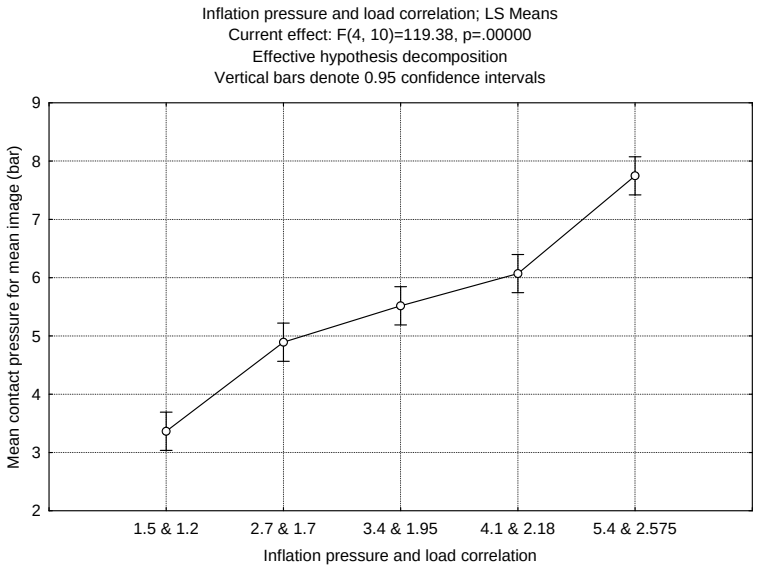

Cell No.	LSD test; variable Mean contact pressure (bar) (Spreadsheet15.sta) Probabilities for Post Hoc Tests Error: Between MS = .06473, df = 10.000					
	Inflation pressure and load combination	1 3.3643	2 4.8928	3 5.5168	4 6.0697	5 7.7472
1	1.5 & 1.2		0.000024	0.000001	0.000000	0.000000
2	2.7 & 1.7	0.000024		0.013259	0.000208	0.000000
3	3.4 & 1.95	0.000001	0.013259		0.023832	0.000001
4	4.1 & 2.18	0.000000	0.000208	0.023832		0.000011
5	5.4 & 2.575	0.000000	0.000000	0.000001	0.000011	

I.8 Tekscan Tests: Implement Tyres – Maximum contact pressure – effect of inflation pressure and load combination (One-way ANOVA)

Effect	Univariate Tests of Significance for Max contact pressure for mean image (bar) (Spreadsheet15.sta) Sigma-restricted parameterization Effective hypothesis decomposition				
	SS	Degr. of Freedom	MS	F	p
Intercept	1870.670	1	1870.670	649.5158	0.000000
Inflation pressure and load combination	123.674	4	30.919	10.7352	0.001216
Error	28.801	10	2.880		

LSD at 95% confidence level = 3.09 bar

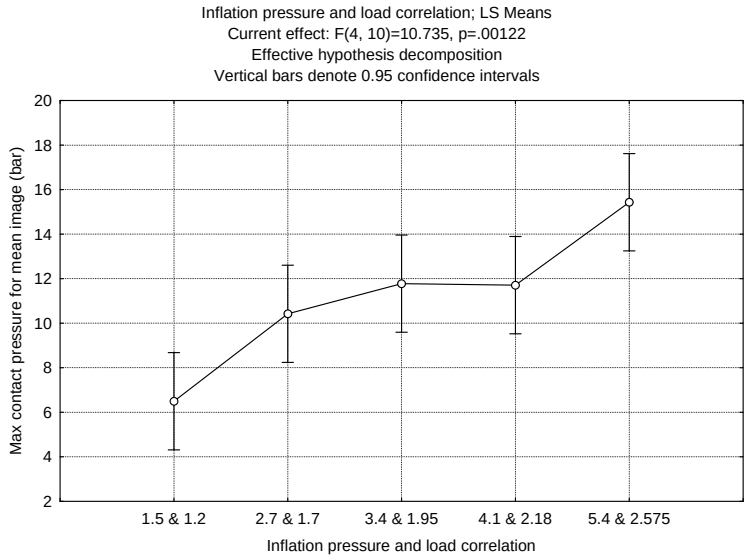

Cell No.	LSD test; variable Max contact pressure for mean image (bar) (Spreadsheet15.sta) Probabilities for Post Hoc Tests Error: Between MS = 2.8801, df = 10.000					
	Inflation pressure and load combination	1 6.4952	2 10.424	3 11.777	4 11.710	5 15.431
1	1.5 & 1.2		0.017686	0.003418	0.003703	0.000074
2	2.7 & 1.7	0.017686		0.351786	0.375447	0.004743
3	3.4 & 1.95	0.003418	0.351786		0.961883	0.024881
4	4.1 & 2.18	0.003703	0.375447	0.961883		0.022874
5	5.4 & 2.575	0.000074	0.004743	0.024881	0.022874	

I.9 Tekscan Tests: Implement Tyres – Mean carcass stiffness – effect of inflation pressure and load combination (One-way ANOVA)

Effect	Univariate Tests of Significance for Mean carcass stiffness (bar) (Spreadsheet15.sta) Sigma-restricted parameterization Effective hypothesis decomposition				
	SS	Degr. of Freedom	MS	F	p
Intercept	66.03550	1	66.03550	1020.171	0.000000
Inflation pressure and load combination	0.42764	4	0.10691	1.652	0.236673
Error	0.64730	10	0.06473		

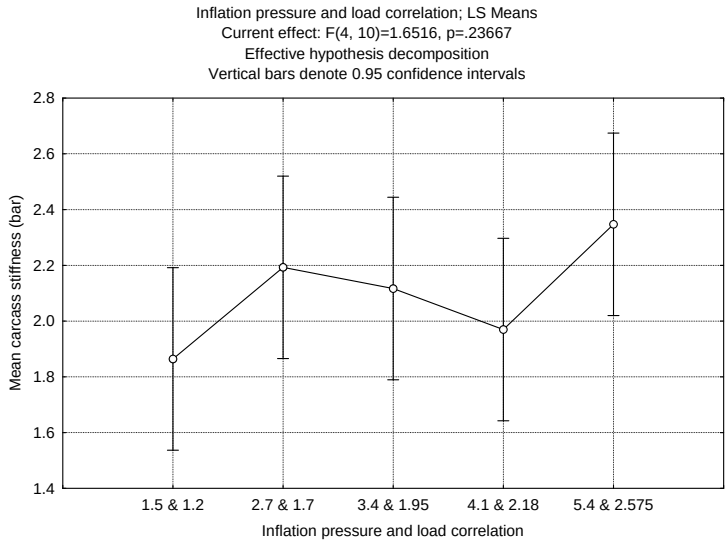

Cell No.	LSD test; variable Mean carcass stiffness (bar) (Spreadsheet15.sta) Probabilities for Post Hoc Tests Error: Between MS = .06473, df = 10.000					
	Inflation pressure and load combination	1 1.8643	2 2.1928	3 2.1168	4 1.9697	5 2.3472
1	1.5 & 1.2		0.144793	0.251999	0.622674	0.042417
2	2.7 & 1.7	0.144793		0.722008	0.308041	0.474475
3	3.4 & 1.95	0.251999	0.722008		0.495083	0.293328
4	4.1 & 2.18	0.622674	0.308041	0.495083		0.099229
5	5.4 & 2.575	0.042417	0.474475	0.293328	0.099229	

I.10 Tekscan Tests: Implement Tyres – Maximum carcass stiffness– effect of inflation pressure and load combination (One-way ANOVA)

Effect	Univariate Tests of Significance for Maximum carcass stiffness (bar) (Spreadsheet15.sta) Sigma-restricted parameterization Effective hypothesis decomposition				
	SS	Degr. of Freedom	MS	F	p
Intercept	900.3385	1	900.3385	312.6068	0.000000
Inflation pressure and load combination	39.6155	4	9.9039	3.4387	0.051494
Error	28.8010	10	2.8801		

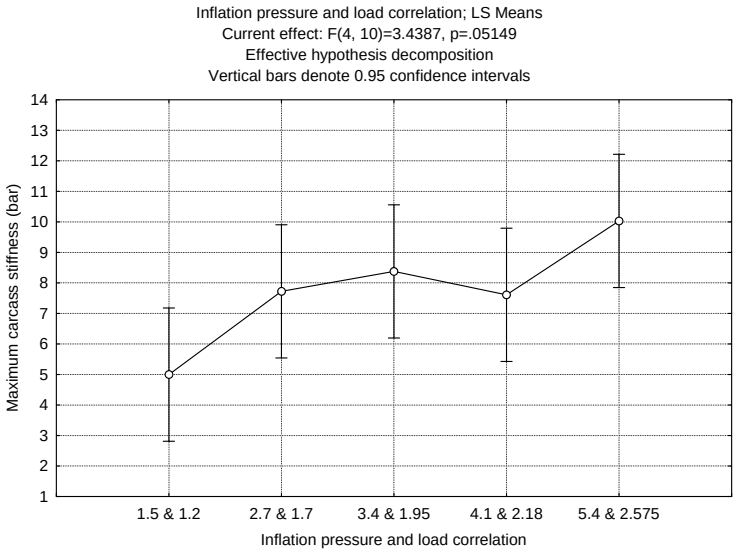

Cell No.	LSD test; variable Maximum carcass stiffness (bar) (Spreadsheet15.sta) Probabilities for Post Hoc Tests Error: Between MS = 2.8801, df = 10.000					
	Inflation pressure and load combination	1 4.9952	2 7.7242	3 8.3774	4 7.6095	5 10.031
1	1.5 & 1.2		0.077217	0.034796	0.088539	0.004581
2	2.7 & 1.7	0.077217		0.647432	0.935709	0.126955
3	3.4 & 1.95	0.034796	0.647432		0.591636	0.260334
4	4.1 & 2.18	0.088539	0.935709	0.591636		0.111153
5	5.4 & 2.575	0.004581	0.126955	0.260334	0.111153	

I.11 Ink Tests: Implement Tyres – Tread contact area – effect of inflation pressure and load combination (One-way ANOVA)

Effect	Univariate Tests of Significance for Tread area (m2) (Spreadsheet22) Sigma-restricted parameterization Effective hypothesis decomposition				
	SS	Degr. of Freedom	MS	F	p
Intercept	0.006883	1	0.006883	122719.2	0.000000
Inflation pressure and load combination (treatment)	0.000014	4	0.000003	62.1	0.003232
Error	0.000000	3	0.000000		

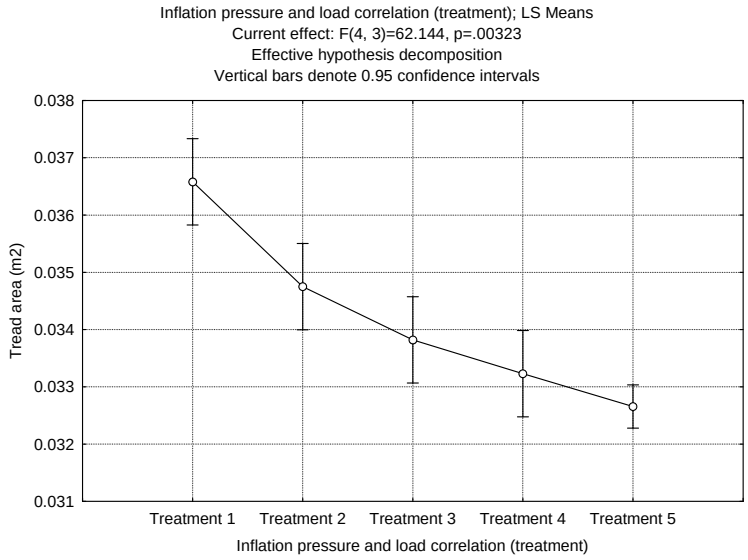

Cell No.	LSD test; variable Tread area (m2) (Spreadsheet22) Probabilities for Post Hoc Tests Error: Between MS = .00000, df = 3.0000					
	Inflation pressure and load combination (treatment)	1 .03658	2 .03475	3 .03382	4 .03323	5 .03266
1	Treatment 1		0.012049	0.003742	0.002127	0.000667
2	Treatment 2	0.012049		0.069180	0.020029	0.004219
3	Treatment 3	0.003742	0.069180		0.176358	0.021849
4	Treatment 4	0.002127	0.020029	0.176358		0.118983
5	Treatment 5	0.000667	0.004219	0.021849	0.118983	

I.12 Ink Tests: Implement Tyres – Projected contact area – effect of inflation pressure and load combination (One-way ANOVA)

Effect	Univariate Tests of Significance for Projected area (m2) (Spreadsheet22) Sigma-restricted parameterization Effective hypothesis decomposition				
	SS	Degr. of Freedom	MS	F	p
Intercept	0.019059	1	0.019059	945597.8	0.000000
Inflation pressure and load combination (treatment)	0.000087	4	0.000022	1072.9	0.000046
Error	0.000000	3	0.000000		

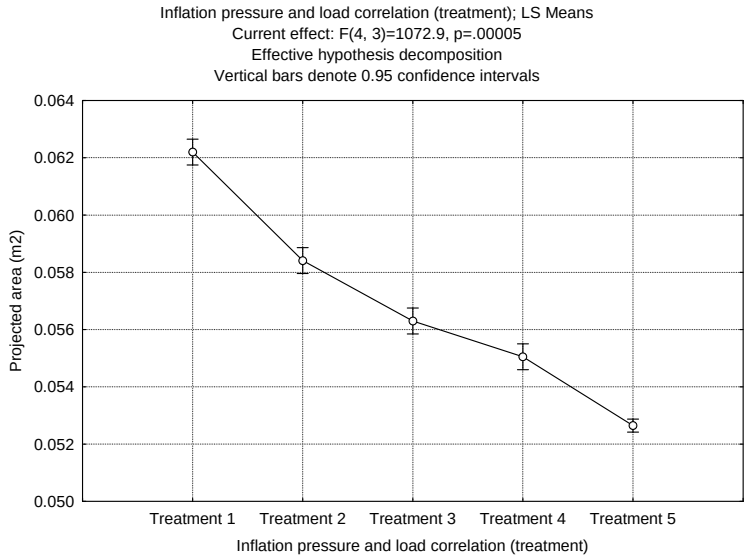

Cell No.	LSD test; variable Projected area (m2) (Spreadsheet22) Probabilities for Post Hoc Tests Error: Between MS = .00000, df = 3.0000					
	Inflation pressure and load combination (treatment)	1 .06220	2 .05841	3 .05630	4 .05505	5 .05265
1	Treatment 1		0.000325	0.000087	0.000049	0.000010
2	Treatment 2	0.000325		0.001840	0.000465	0.000046
3	Treatment 3	0.000087	0.001840		0.008355	0.000180
4	Treatment 4	0.000049	0.000465	0.008355		0.000625
5	Treatment 5	0.000010	0.000046	0.000180	0.000625	

I.13 Ink Tests: Implement Tyres – Tread contact pressure – effect of inflation pressure and load combination (One-way ANOVA)

Effect	Univariate Tests of Significance for Tread contact pressure (bar) (Spreadsheet4) Sigma-restricted parameterization Effective hypothesis decomposition				
	SS	Degr. of Freedom	MS	F	p
Intercept	182.0801	1	182.0801	57884.30	0.000000
Inflation pressure and load combination	20.5437	4	5.1359	1632.74	0.000025
Error	0.0094	3	0.0031		

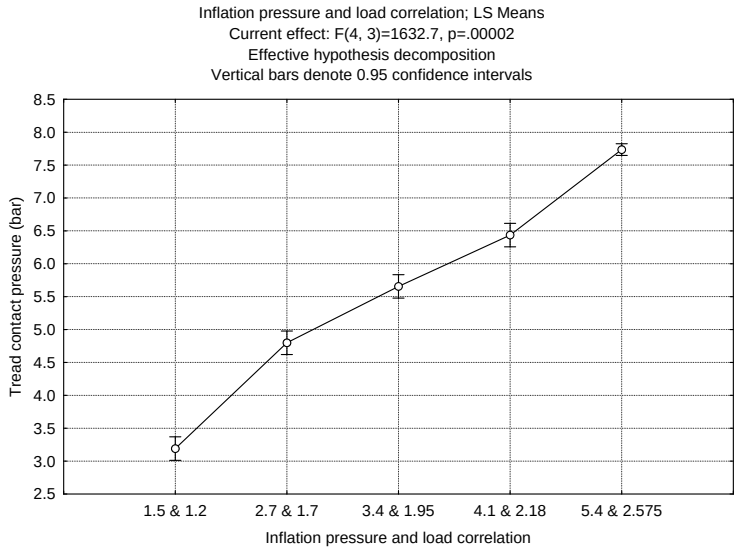

Cell No.	LSD test; variable Tread contact pressure (bar) (Spreadsheet4) Probabilities for Post Hoc Tests Error: Between MS = .00315, df = 3.0000					
	Inflation pressure and load combination	1 3.1913	2 4.7991	3 5.6563	4 6.4357	5 7.7356
1	1.5 & 1.2		0.000262	0.000073	0.000032	0.000006
2	2.7 & 1.7	0.000262		0.001695	0.000249	0.000021
3	3.4 & 1.95	0.000073	0.001695		0.002240	0.000060
4	4.1 & 2.18	0.000032	0.000249	0.002240		0.000246
5	5.4 & 2.575	0.000006	0.000021	0.000060	0.000246	

I.14 Ink Tests: Implement Tyres – Projected contact pressure – effect of inflation pressure and load combination (One-way ANOVA)

Effect	Univariate Tests of Significance for Projected contact pressure (bar) (Spreadsheet4) Sigma-restricted parameterization Effective hypothesis decomposition				
	SS	Degr. of Freedom	MS	F	p
Intercept	66.51035	1	66.51035	396019.3	0.000000
Inflation pressure and load combination	8.66435	4	2.16609	12897.4	0.000001
Error	0.00050	3	0.00017		

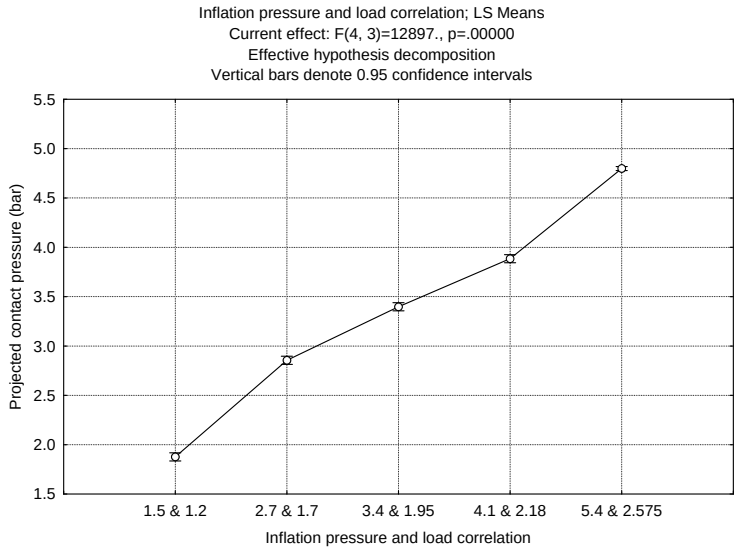

Cell No.	LSD test; variable Projected contact pressure (bar) (Spreadsheet4) Probabilities for Post Hoc Tests Error: Between MS = .00017, df = 3.0000					
	Inflation pressure and load combination	1 1.8768	2 2.8552	3 3.3978	4 3.8848	5 4.7982
1	1.5 & 1.2		0.000014	0.000004	0.000002	0.000000
2	2.7 & 1.7	0.000014		0.000085	0.000012	0.000001
3	3.4 & 1.95	0.000004	0.000085		0.000117	0.000002
4	4.1 & 2.18	0.000002	0.000012	0.000117		0.000009
5	5.4 & 2.575	0.000000	0.000001	0.000002	0.000009	

APPENDIX J

STATISTICAL ANALYSIS – HARD SURFACE RESULTS – LINEAR REGRESSION ANALYSIS

J.1 Tekscan Tests: Front Tractor Tyre – Mean contact pressure – effect of load and inflation pressure

Statistic	Summary Statistics; DV: Mean contact pressure (bar) (Spreadsheet11.sta)
	Value
Multiple R	0.982478743
Multiple R²	0.965264481
Adjusted R²	0.96333473
F(2,36)	500.201555
p	5.41911119E-27
Std.Err. of Estimate	0.217755442

N=39	Regression Summary for Dependent Variable: Mean contact pressure (bar) (Spreadsheet11.sta) R= .98247874 R²= .96526448 Adjusted R²= .96333473 F(2,36)=500.20 p<0.0000 Std.Error of estimate: .21776					
	b*	Std.Err. of b*	b	Std.Err. of b	t(36)	p-value
Intercept			-0.851074	0.154284	-5.51626	0.000003
Load (tonne)	0.543846	0.031062	1.495385	0.085411	17.50816	0.000000
Inflation pressure (bar)	0.818227	0.031062	0.827917	0.031430	26.34136	0.000000

$$t\ test\ of\ slope: \frac{1-0.8279}{0.0314} = 5.48 > t_{0.05}(36)$$

$$t_{0.05}(36) = 2.03$$

J.2 Tekscan Tests: Front Tractor Tyre – Maximum contact pressure – effect of load and inflation pressure

Statistic	Summary Statistics; DV: Max contact pressure (bar) (Spreadsheet11.sta)
	Value
Multiple R	0.958942614
Multiple R²	0.919570938
Adjusted R²	0.915102656
F(2,36)	205.7997
p	1.98350899E-20
Std.Err. of Estimate	0.382404028

N=39	Regression Summary for Dependent Variable: Max contact pressure (bar) (Spreadsheet11.sta) R= .95894261 R²= .91957094 Adjusted R²= .91510266 F(2,36)=205.80 p<0.0000 Std.Error of estimate: .38240					
	b*	Std.Err. of b*	b	Std.Err. of b	t(36)	p-value
Intercept			-0.175226	0.270942	-0.64673	0.521909
Load (tonne)	0.736919	0.047267	2.338462	0.149991	15.59066	0.000000
Inflation pressure (bar)	0.613613	0.047267	0.716542	0.055195	12.98194	0.000000

$$t\ test\ of\ slope: \frac{1-0.7165}{0.0552} = 5.14 > t_{0.05}(36)$$

$$t_{0.05}(36) = 2.03$$

J.3 Tekscan Tests: Smooth Combine Tyre – Mean contact pressure – effect of load and inflation pressure

Statistic	Summary Statistics; DV: Mean pressure (bar) (SmoothCombine_Tekscan.sta)
	Value
Multiple R	0.993205421
Multiple R²	0.986457008
Adjusted R²	0.985762496
F(2,39)	1420.35911
p	3.70198638E-37
Std.Err. of Estimate	0.0906369005

N=42	Regression Summary for Dependent Variable: Mean pressure (bar) (SmoothCombine_Tekscan.sta) R= .99320542 R²= .98645701 Adjusted R²= .98576250 F(2,39)=1420.4 p<0.0000 Std.Error of estimate: .09064					
	b*	Std.Err. of b*	b	Std.Err. of b	t(39)	p-value
Intercept			0.274138	0.037729	7.26590	0.000000
Inflation pressure (bar)	0.873830	0.024607	0.921606	0.025953	35.51111	0.000000
Load (tonne)	0.169964	0.024607	0.081617	0.011817	6.90706	0.000000

$$t\ test\ of\ slope: \frac{1-0.9216}{0.0259} = 3.03 > t_{0.05}(39)$$

$$t_{0.05}(39) = 2.02$$

J.4 Tekscan Tests: Smooth Combine Tyre – Maximum contact pressure – effect of load and inflation pressure

Statistic	Summary Statistics; DV: Max pressure (bar) (SmoothCombine_Tekscan.sta)
	Value
Multiple R	0.87146136
Multiple R²	0.759444901
Adjusted R²	0.747108742
F(2,39)	61.5625096
p	0.000000000000858388447
Std.Err. of Estimate	0.514995572

N=42	Regression Summary for Dependent Variable: Max pressure (bar) (SmoothCombine_Tekscan.sta) R= .87146136 R²= .75944490 Adjusted R²= .74710874 F(2,39)=61.563 p<.00000 Std.Error of estimate: .51500					
	b*	Std.Err. of b*	b	Std.Err. of b	t(39)	p-value
Intercept			3.368978	0.214377	15.71517	0.000000
Inflation pressure (bar)	0.273100	0.103708	0.388319	0.147462	2.63335	0.012058
Load (tonne)	0.668209	0.103708	0.432601	0.067141	6.44317	0.000000

$$t\ test\ of\ slope: \frac{1-0.3883}{0.1475} = 4.15 > t_{0.05}(39)$$

$$t_{0.05}(39) = 2.02$$

J.5 Tekscan Tests: Treaded Combine Tyre – Mean contact pressure – effect of load and inflation pressure

Statistic	Summary Statistics; DV: Mean pressure (bar) (TreadedCombine_Tekscan.sta)
	Value
Multiple R	0.930435709
Multiple R²	0.865710609
Adjusted R²	0.848924435
F(2,16)	51.5728368
p	0.000000105762958
Std.Err. of Estimate	0.446672152

N=19	Regression Summary for Dependent Variable: Mean pressure (bar) (TreadedCombine_Tekscan.sta) R= .93043571 R²= .86571061 Adjusted R²= .84892443 F(2,16)=51.573 p<.00000 Std.Error of estimate: .44667					
	b*	Std.Err. of b*	b	Std.Err. of b	t(16)	p-value
Intercept			1.757684	0.282891	6.213292	0.000012
Inflation pressure (bar)	0.823498	0.132817	1.258134	0.202917	6.200243	0.000013
Load (tonne)	0.140690	0.132817	0.095131	0.089808	1.059274	0.305205

Statistic	Summary Statistics; DV: Mean pressure (bar) (TreadedCombine_Tekscan.sta)
	Value
Multiple R	0.925361037
Multiple R²	0.85629305
Adjusted R²	0.8478397
F(1,17)	101.296296
p	0.0000000140870133
Std.Err. of Estimate	0.448272856

N=19	Regression Summary for Dependent Variable: Mean pressure (bar) (TreadedCombine_Tekscan.sta) R= .92536104 R²= .85629305 Adjusted R²= .84783970 F(1,17)=101.30 p<.00000 Std.Error of estimate: .44827					
	b*	Std.Err. of b*	b	Std.Err. of b	t(17)	p-value
Intercept			1.856055	0.268171	6.92116	0.000002
Inflation pressure (bar)	0.925361	0.091942	1.413760	0.140468	10.06461	0.000000

$$t\ test\ of\ slope: \frac{1.4138-1}{0.1405} = 2.94 > t_{0.05}(17)$$

$$t_{0.05}(17) = 2.11$$

J.6 Tekscan Tests: Treaded Combine Tyre – Maximum contact pressure – effect of load and inflation pressure

Statistic	Summary Statistics; DV: Max pressure (bar) (TreadedCombine_Tekscan.sta)
	Value
Multiple R	0.830393885
Multiple R^2	0.689554004
Adjusted R^2	0.650748254
F(2,16)	17.7693773
p	0.0000862757151
Std.Err. of Estimate	1.03448872

N=19	Regression Summary for Dependent Variable: Max pressure (bar) (TreadedCombine_Tekscan.sta) R= .83039388 R^2= .68955400 Adjusted R^2= .65074825 F(2,16)=17.769 p<.00009 Std.Error of estimate: 1.0345					
	b*	Std.Err. of b*	b	Std.Err. of b	t(16)	p-value
Intercept			5.564032	0.655173	8.492465	0.000000
Inflation pressure (bar)	0.532038	0.201942	1.238146	0.469954	2.634612	0.018026
Load (tonne)	0.359691	0.201942	0.370471	0.207994	1.781161	0.093877

Statistic	Summary Statistics; DV: Max pressure (bar) (TreadedCombine_Tekscan.sta)
	Value
Multiple R	0.792463073
Multiple R^2	0.627997721
Adjusted R^2	0.606115234
F(1,17)	28.6986448
p	0.0000522740193
Std.Err. of Estimate	1.0986037

N=19	Regression Summary for Dependent Variable: Max pressure (bar) (TreadedCombine_Tekscan.sta) R= .79246307 R^2= .62799772 Adjusted R^2= .60611523 F(1,17)=28.699 p<.00005 Std.Error of estimate: 1.0986					
	b*	Std.Err. of b*	b	Std.Err. of b	t(17)	p-value
Intercept			5.947122	0.657220	9.048913	0.000000
Inflation pressure (bar)	0.792463	0.147927	1.844200	0.344253	5.357112	0.000052

$$t\ test\ of\ slope: \frac{1.8442-1}{0.3442} = 2.45 > t_{0.05}(17)$$

$$t_{0.05}(17) = 2.11$$

APPENDIX K

PRESSURE DISTRIBUTION ANALYSIS OF TYRE CONTACT PATCH TEKSCAN DATA

Smooth combine tyre

1.8 tonne + 1.0 bar

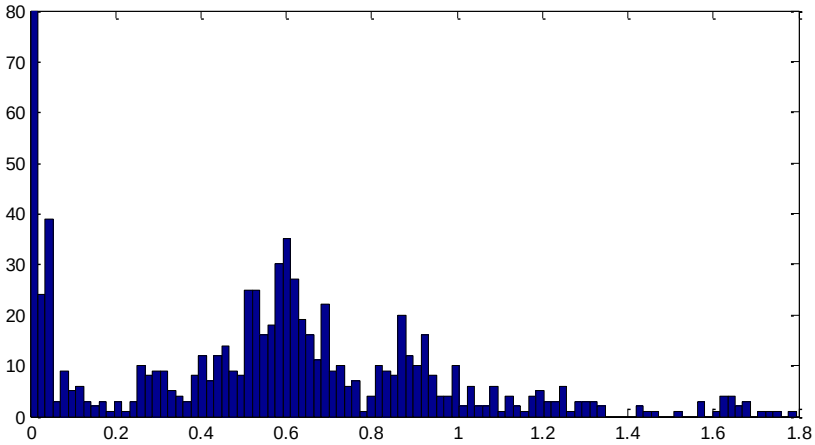

3.765 tonne + 1.0 bar

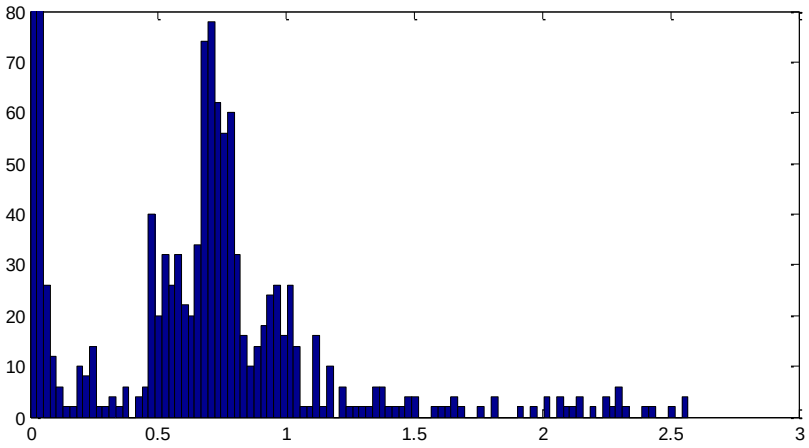

4.5 tonne + 1.5 bar

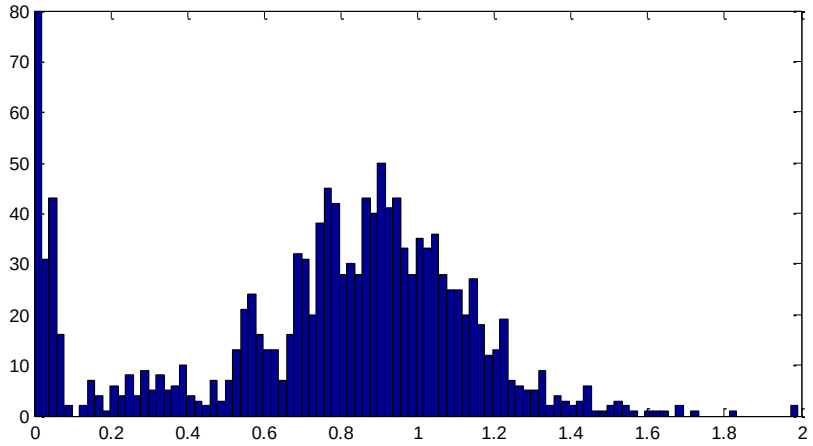

4.5 tonne + 2.0 bar

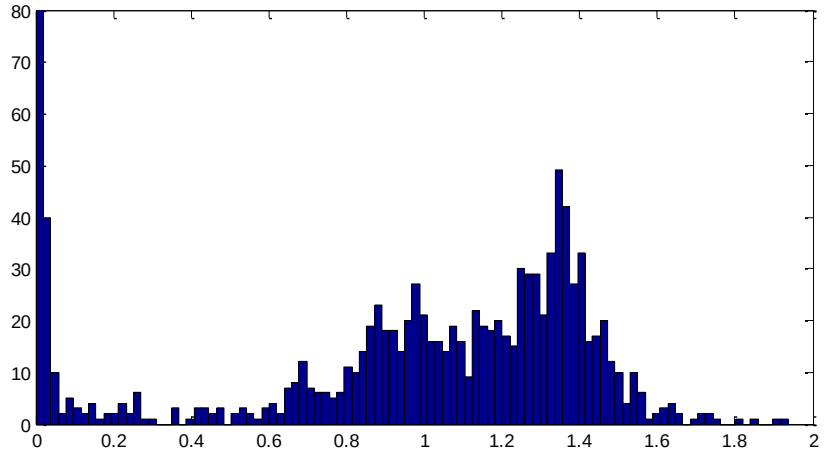

4.5 tonne + 2.5 bar

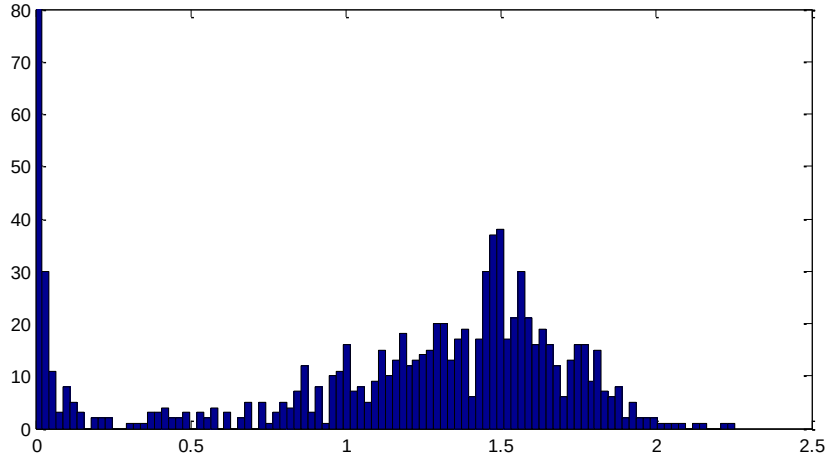

Implement tyres

1.2 tonne + 1.5 bar + PR16

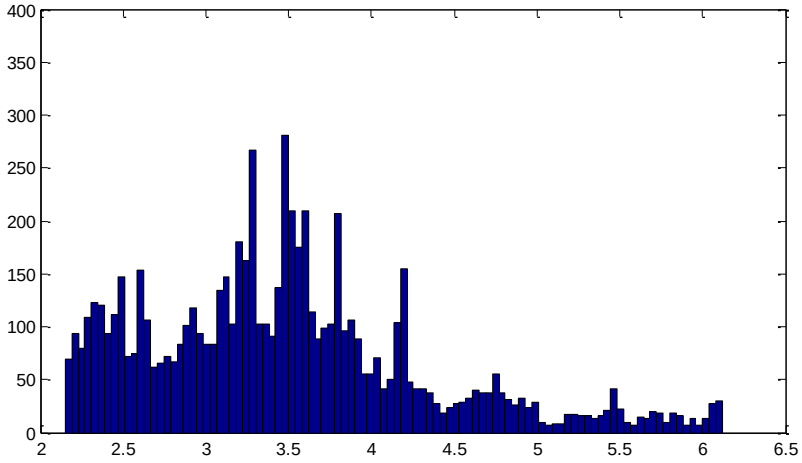

1.95 tonne + 3.4 bar + PR16

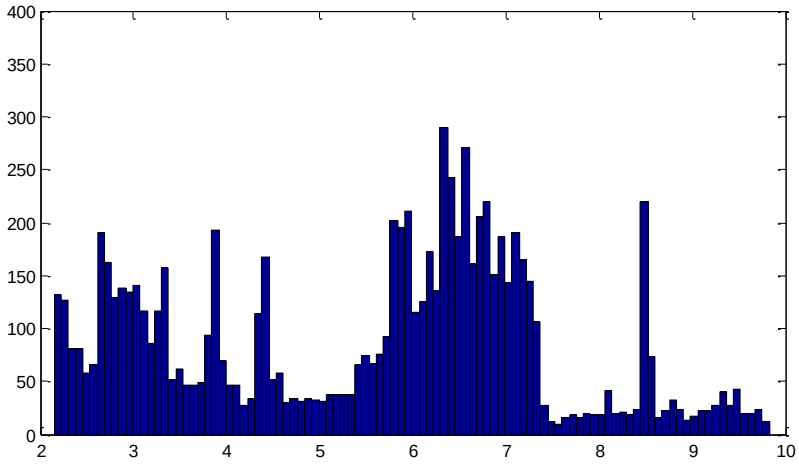

2.18 tonne + 4.1 bar + PR16

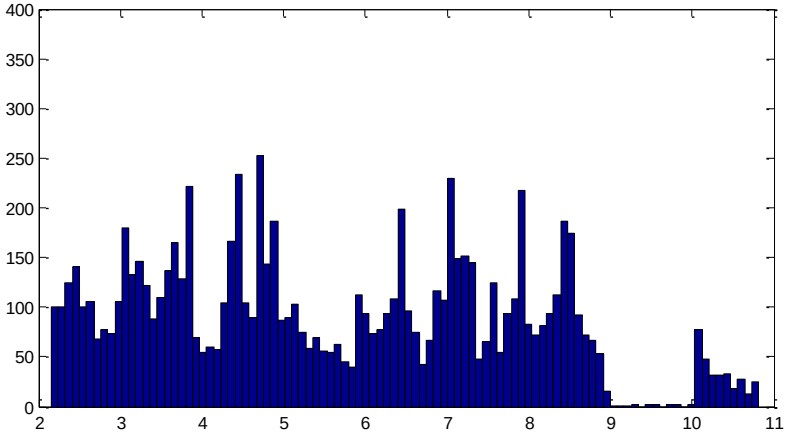

2.575 tonne + 5.4 bar + PR16

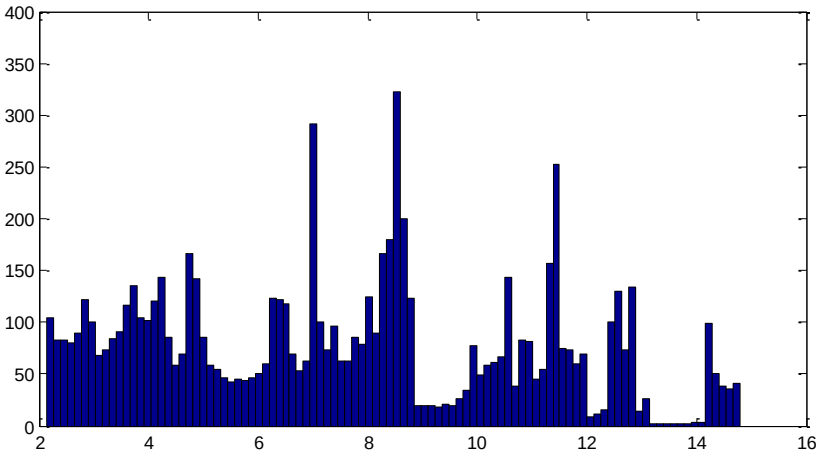

1.7 tonne + 2.7 bar PR 8

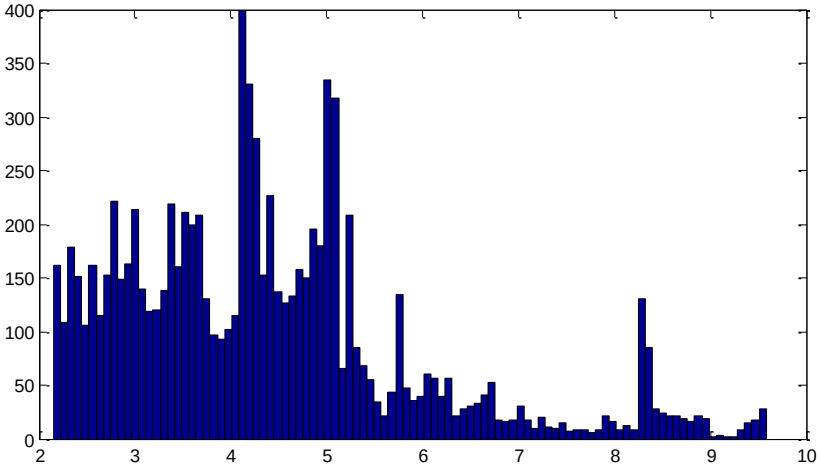

1.7 tonne + 2.7 bar PR 10

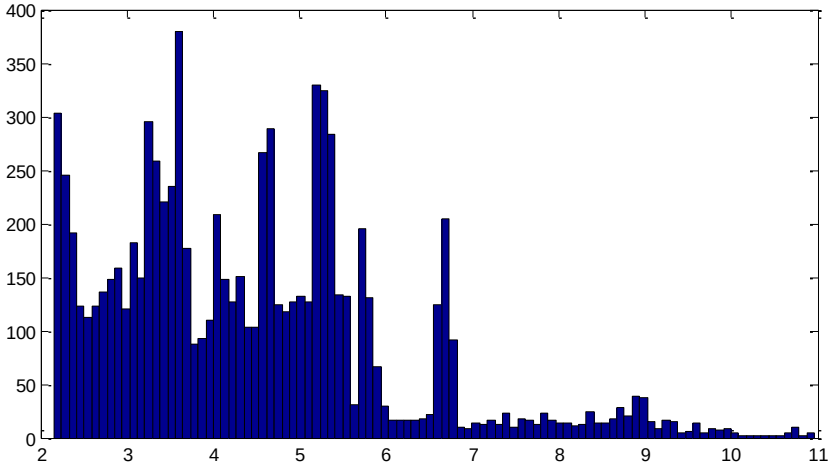

1.7 tonne + 2.7 bar PR 12

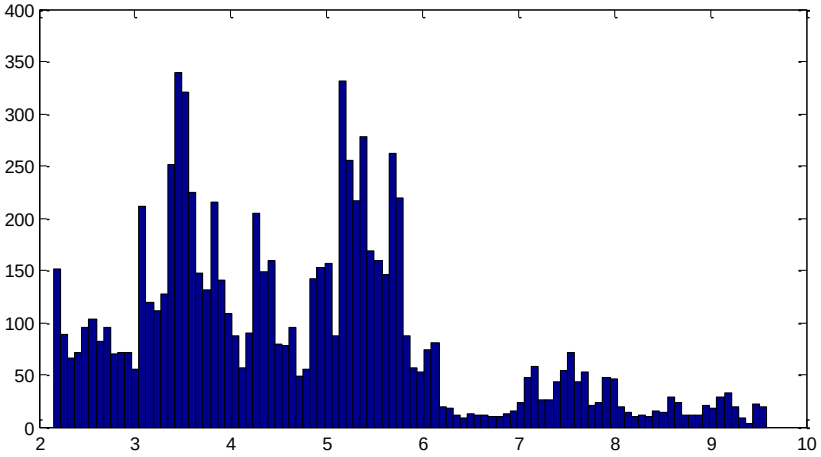

1.7 tonne + 2.7 bar PR 14

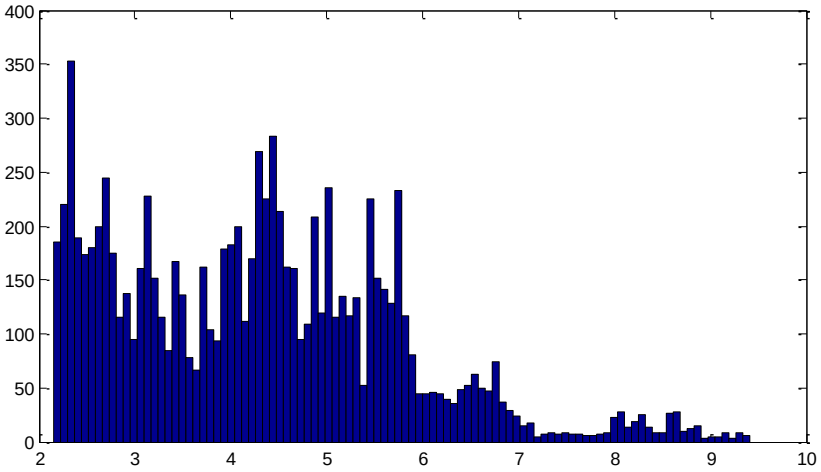

1.7 tonne + 2.7 bar PR 16

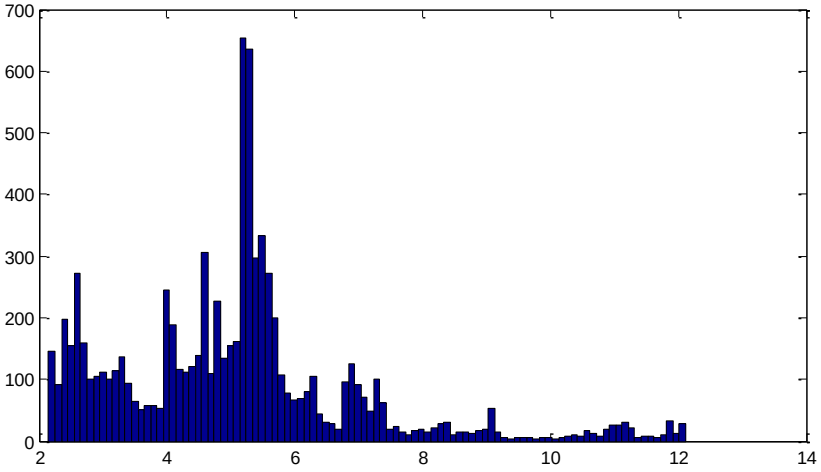

APPENDIX L

TYRE LOAD – DEFLECTION CHARACTERISTIC FOR THE IMPLEMENT TYRES

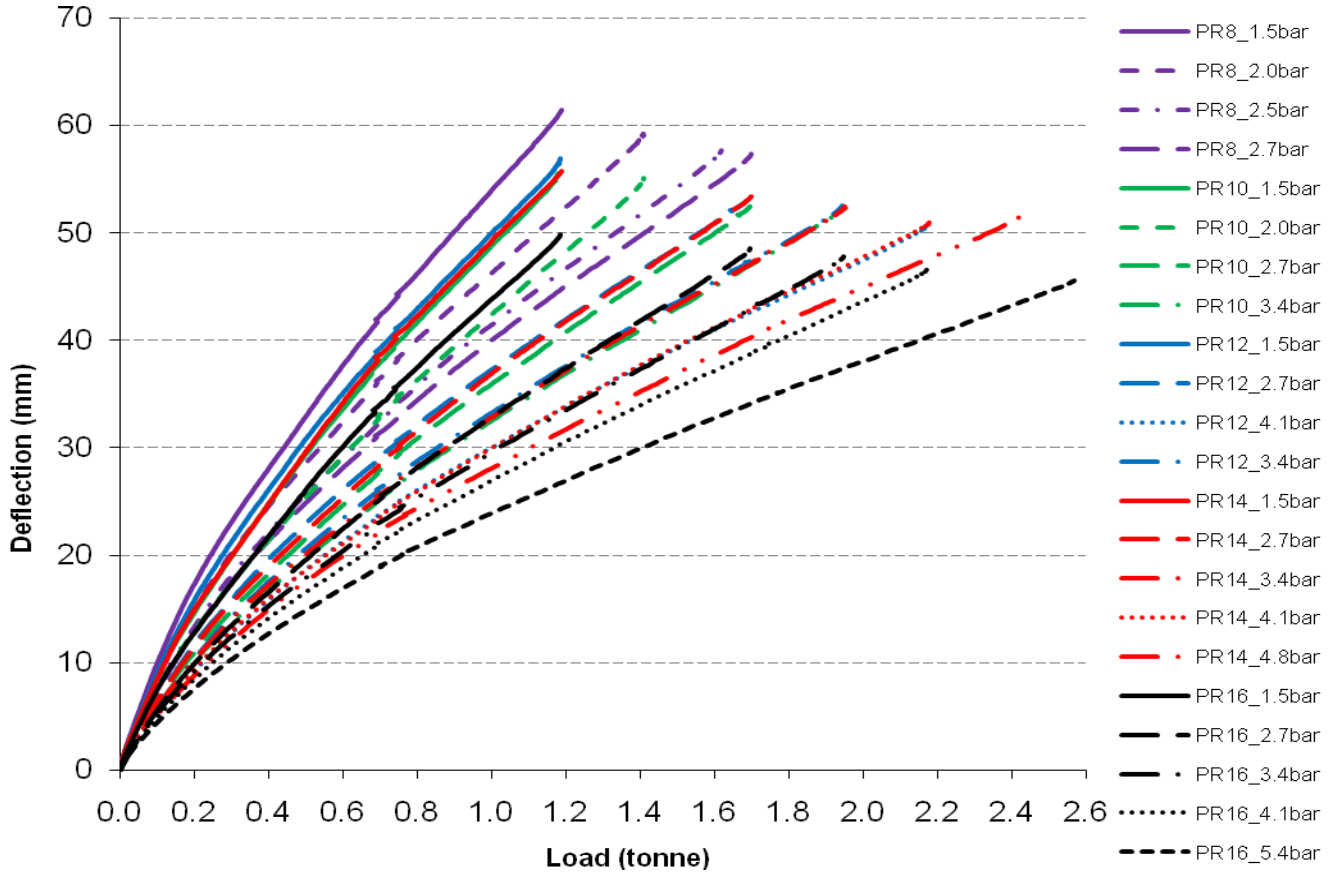

Figure L.1 Tyre load – deflection for the implement tyres varying in ply rating

APPENDIX M

STATISTICAL ANALYSIS – SOIL RESULTS

M.1 Tekscan Soil Profile Tests: Combine tyres (smooth and treaded) – Area – effect of depth and presence of tread (Factorial ANOVA)

Effect	Univariate Tests of Significance for Area (Spreadsheet1) Sigma-restricted parameterization Effective hypothesis decomposition				
	SS	Degr. Of Freedom	MS	F	p
Intercept	6.805793	1	6.805793	3038.824	0.000000
Depth	1.236612	4	0.309153	138.039	0.000000
Tyre tread	0.000682	1	0.000682	0.305	0.591983
Depth*Tyre tread	0.017862	4	0.004465	1.994	0.165066
Error	0.024636	11	0.002240		

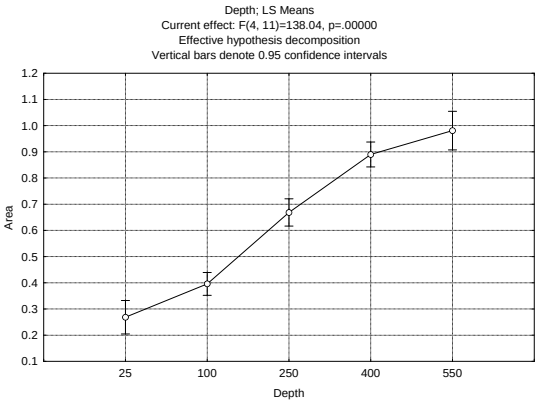

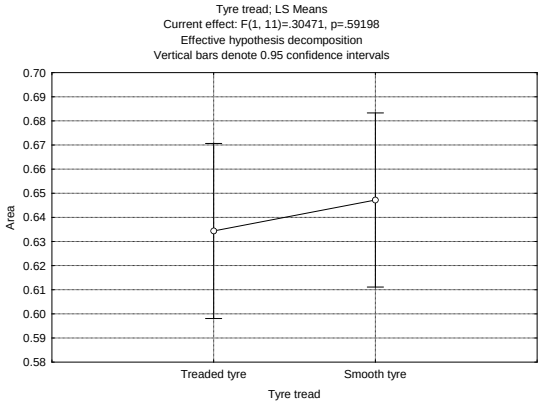

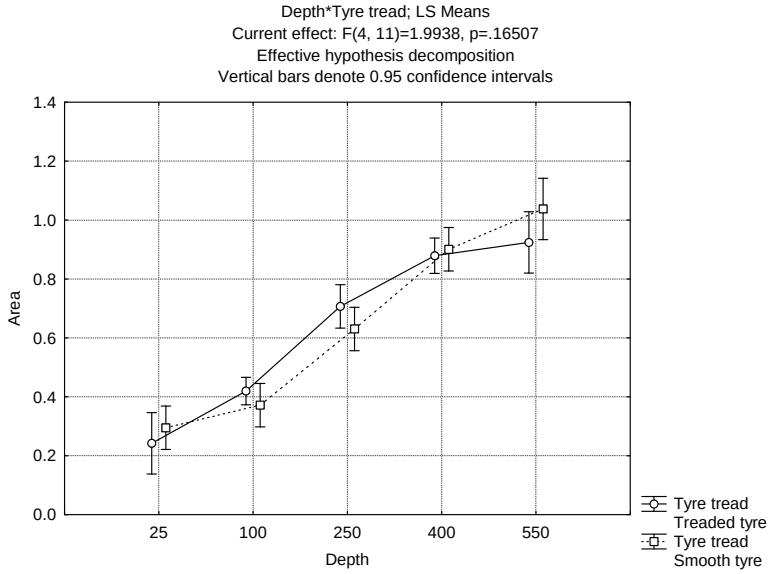

Cell No.	LSD test; variable Area (Spreadsheet1) Probabilities for Post Hoc Tests Error: Between MS = .00224, df = 11.000							
	Depth	Tyre tread	1 .24214	2 .29503	3 .41962	4 .37190	5 .70689	6 .63034
1	25	Treaded tyre		0.381140	0.005689	0.046804	0.000006	0.000034
2	25	Smooth tyre	0.381140		0.009297	0.132554	0.000003	0.000020
3	100	Treaded tyre	0.005689	0.009297		0.253480	0.000016	0.000244
4	100	Smooth tyre	0.046804	0.132554	0.253480		0.000020	0.000198
5	250	Treaded tyre	0.000006	0.000003	0.000016	0.000020		0.134039
6	250	Smooth tyre	0.000034	0.000020	0.000244	0.000198	0.134039	
7	400	Treaded tyre	0.000000	0.000000	0.000000	0.000000	0.002148	0.000127
8	400	Smooth tyre	0.000000	0.000000	0.000000	0.000000	0.001759	0.000135
9	550	Treaded tyre	0.000001	0.000000	0.000001	0.000001	0.003207	0.000360
10	550	Smooth tyre	0.000000	0.000000	0.000000	0.000000	0.000136	0.000022

Cell No.	LSD test; variable Area (Spreadsheet1) Probabilities for Post Hoc Tests Error: Between MS = .00224, df = 11.000			
	7 .87896	8 .90093	9 .92428	10 1.0379
1	0.000000	0.000000	0.000001	0.000000
2	0.000000	0.000000	0.000000	0.000000
3	0.000000	0.000000	0.000001	0.000000
4	0.000000	0.000000	0.000001	0.000000
5	0.002148	0.001759	0.003207	0.000136
6	0.000127	0.000135	0.000360	0.000022
7		0.621106	0.424581	0.014246
8	0.621106		0.694822	0.037654
9	0.424581	0.694822		0.117761
10	0.014246	0.037654	0.117761	

M.2 Tekscan Soil Profile Tests: Combine tyres (smooth and treaded) – Mean pressure – effect of depth and presence of tread (Factorial ANOVA)

Effect	Univariate Tests of Significance for Mean pressure (Spreadsheet1_EffectOfTreadNDepth.sta) Sigma-restricted parameterization Effective hypothesis decomposition				
	SS	Degr. of Freedom	MS	F	p
Intercept	28.96390	1	28.96390	632.6432	0.000000
Depth	7.57108	4	1.89277	41.3428	0.000001
Tyre tread	0.06078	1	0.06078	1.3275	0.273670
Depth*Tyre tread	0.04791	4	0.01198	0.2616	0.896486
Error	0.50361	11	0.04578		

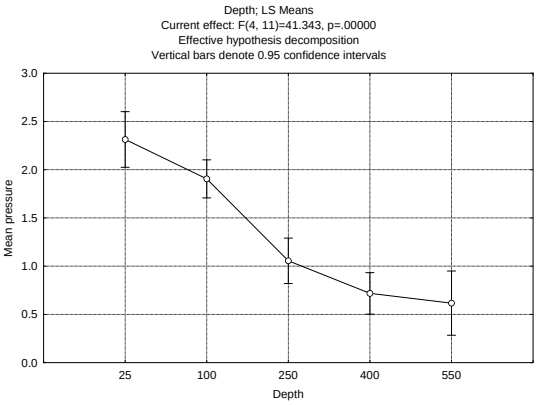

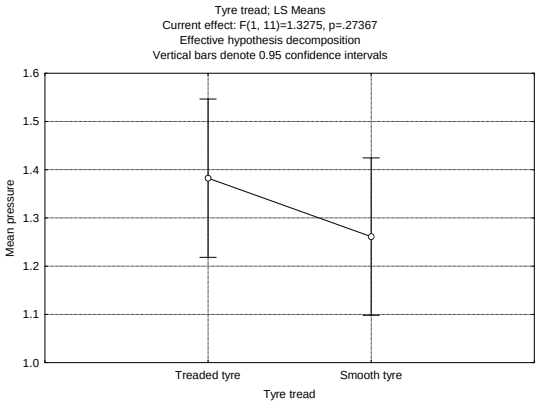

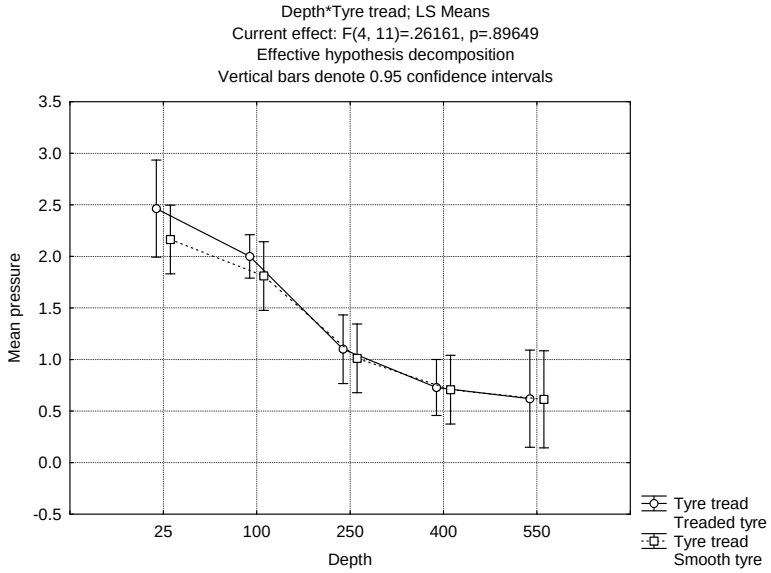

Cell No.	LSD test; variable Mean pressure (Spreadsheet1_EffectOfTreadNDepth.sta) Probabilities for Post Hoc Tests Error: Between MS = .04578, df = 11.000							
	Depth	Tyre tread	1 2.4636	2 2.1637	3 2.0000	4 1.8096	5 1.1000	6 1.0116
1	25	Treaded tyre		0.276712	0.073516	0.029722	0.000293	0.000175
2	25	Smooth tyre	0.276712		0.380072	0.126117	0.000421	0.000222
3	100	Treaded tyre	0.073516	0.380072		0.310220	0.000386	0.000180
4	100	Smooth tyre	0.029722	0.126117	0.310220		0.006877	0.003328
5	250	Treaded tyre	0.000293	0.000421	0.000386	0.006877		0.687572
6	250	Smooth tyre	0.000175	0.000222	0.000180	0.003328	0.687572	
7	400	Treaded tyre	0.000022	0.000015	0.000006	0.000177	0.083873	0.175465
8	400	Smooth tyre	0.000034	0.000029	0.000017	0.000319	0.093939	0.183235
9	550	Treaded tyre	0.000078	0.000105	0.000105	0.000845	0.094192	0.163171
10	550	Smooth tyre	0.000076	0.000101	0.000101	0.000815	0.090759	0.157567

Cell No.	LSD test; variable Mean pressure (Spreadsheet1_EffectOfTreadNDepth.sta) Probabilities for Post Hoc Tests Error: Between MS = .04578, df = 11.000			
	7 .72878	8 .70774	9 .62000	10 .61421
1	0.000022	0.000034	0.000078	0.000076
2	0.000015	0.000029	0.000105	0.000101
3	0.000006	0.000017	0.000105	0.000101
4	0.000177	0.000319	0.000845	0.000815
5	0.083873	0.093939	0.094192	0.090759
6	0.175465	0.183235	0.163171	0.157567
7		0.916172	0.668273	0.651893
8	0.916172		0.744068	0.727905
9	0.668273	0.744068		0.985065
10	0.651893	0.727905	0.985065	

M.3 Tekscan Soil Profile Tests: Combine tyres (smooth and treaded) – Maximum pressure – effect of depth and presence of tread (Factorial ANOVA)

Effect	Univariate Tests of Significance for Maximum pressure (Spreadsheet1) Sigma-restricted parameterization Effective hypothesis decomposition				
	SS	Degr. Of Freedom	MS	F	p
Intercept	320.4817	1	320.4817	6262.988	0.000000
Depth	56.6075	4	14.1519	276.562	0.000000
Tyre tread	5.4859	1	5.4859	107.208	0.000001
Depth*Tyre tread	16.3215	4	4.0804	79.740	0.000000
Error	0.5629	11	0.0512		

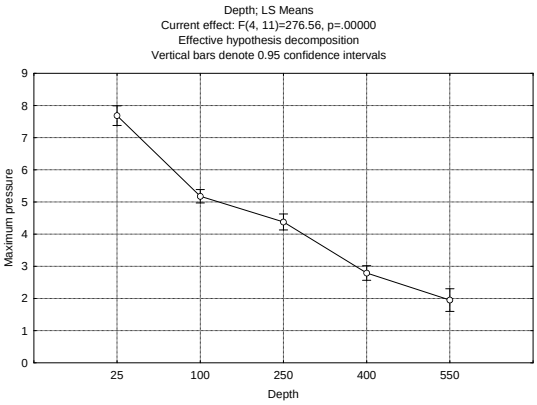

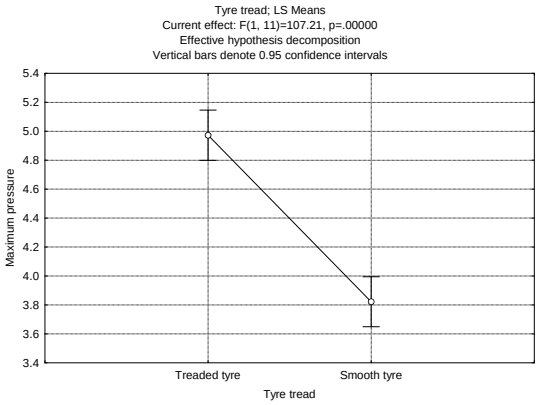

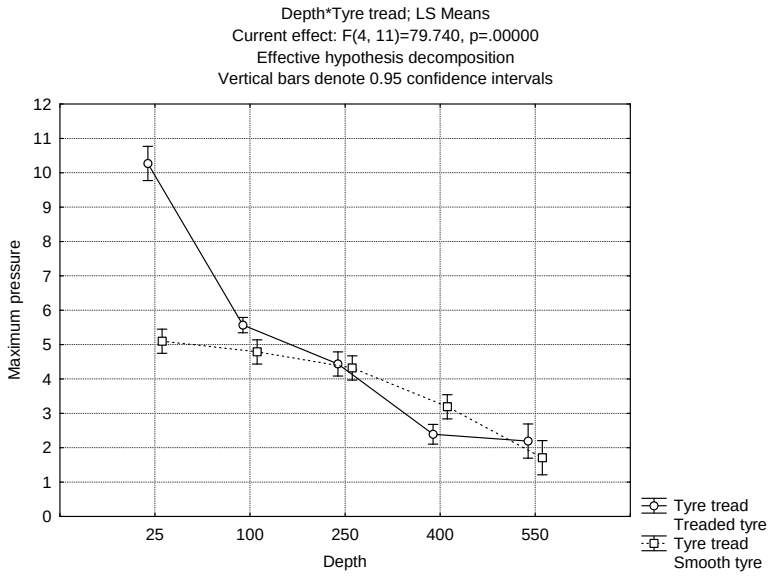

Cell No.	LSD test; variable Maximum pressure (Spreadsheet1_EffectOfTreadNDepth.sta) Probabilities for Post Hoc Tests Error: Between MS = .05117, df = 11.000							
	Depth	Tyre tread	1 10.270	2 5.0988	3 5.5688	4 4.7875	5 4.4375	6 4.3217
1	25	Treaded tyre		0.000000	0.000000	0.000000	0.000000	0.000000
2	25	Smooth tyre	0.000000		0.030397	0.196053	0.013850	0.005571
3	100	Treaded tyre	0.000000	0.030397		0.001677	0.000092	0.000039
4	100	Smooth tyre	0.000000	0.196053	0.001677		0.150115	0.063994
5	250	Treaded tyre	0.000000	0.013850	0.000092	0.150115		0.618941
6	250	Smooth tyre	0.000000	0.005571	0.000039	0.063994	0.618941	
7	400	Treaded tyre	0.000000	0.000000	0.000000	0.000000	0.000001	0.000001
8	400	Smooth tyre	0.000000	0.000004	0.000000	0.000021	0.000185	0.000406
9	550	Treaded tyre	0.000000	0.000000	0.000000	0.000001	0.000006	0.000010
10	550	Smooth tyre	0.000000	0.000000	0.000000	0.000000	0.000001	0.000001

Cell No.	LSD test; variable Maximum pressure (Spreadsheet1_EffectOfTreadNDepth.sta) Probabilities for Post Hoc Tests Error: Between MS = .05117, df = 11.000			
	7 2.3930	8 3.1920	9 2.1934	10 1.7097
1	0.000000	0.000000	0.000000	0.000000
2	0.000000	0.000004	0.000000	0.000000
3	0.000000	0.000000	0.000000	0.000000
4	0.000000	0.000021	0.000001	0.000000
5	0.000001	0.000185	0.000006	0.000001
6	0.000001	0.000406	0.000010	0.000001
7		0.002612	0.460856	0.023989
8	0.002612		0.004139	0.000234
9	0.460856	0.004139		0.158663
10	0.023989	0.000234	0.158663	

M.4 Tekscan Soil Profile Tests: Combine smooth tyre – Area – effect of depth and load (Linear regression)

Statistic	Summary Statistics; DV: Contact area (m2) (Spreadsheet1)
	Value
Multiple R	0.989807995
Multiple R^2	0.979719866
Adjusted R^2	0.977015848
F(2,15)	362.320045
p	0.00000000000020092371
Std.Err. of Estimate	0.0464863703

N=18	Regression Summary for Dependent Variable: Contact area (m2) (Spreadsheet1) R= .98980799 R^2= .97971987 Adjusted R^2= .97701585 F(2,15)=362.32 p<.00000 Std.Error of estimate: .04649					
	b*	Std.Err. of b*	b	Std.Err. of b	t(15)	p-value
Intercept			-0.017222	0.034297	-0.50215	0.622850
Load (tonne)	0.245161	0.036770	0.044737	0.006710	6.66748	0.000008
Depth (mm)	0.958966	0.036770	0.001420	0.000054	26.08035	0.000000

M.5 Tekscan Soil Profile Tests: Combine smooth tyre – Mean pressure – effect of depth and load (Factorial ANOVA)

Effect	Univariate Tests of Significance for Mean pressure (bar) (Spreadsheet1) Sigma-restricted parameterization Effective hypothesis decomposition				
	SS	Degr. Of Freedom	MS	F	p
Intercept	23.91332	1	23.91332	904.2596	0.000000
Load (kg)	0.75989	2	0.37995	14.3673	0.000405
Depth (mm)	6.21006	4	1.55251	58.7068	0.000000
Load (kg)*Depth (mm)	0.10510	8	0.01314	0.4968	0.839102
Error	0.37023	14	0.02645		

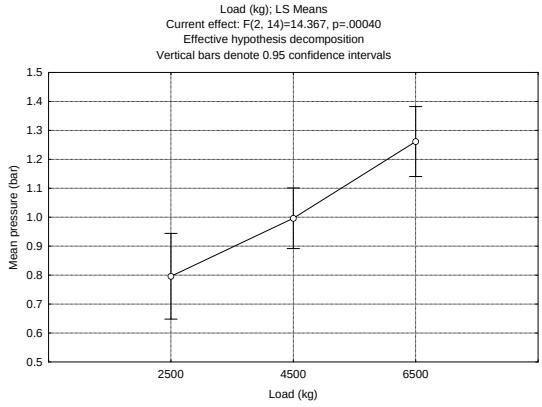

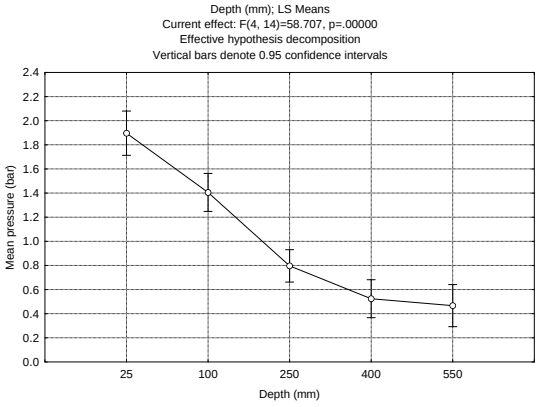

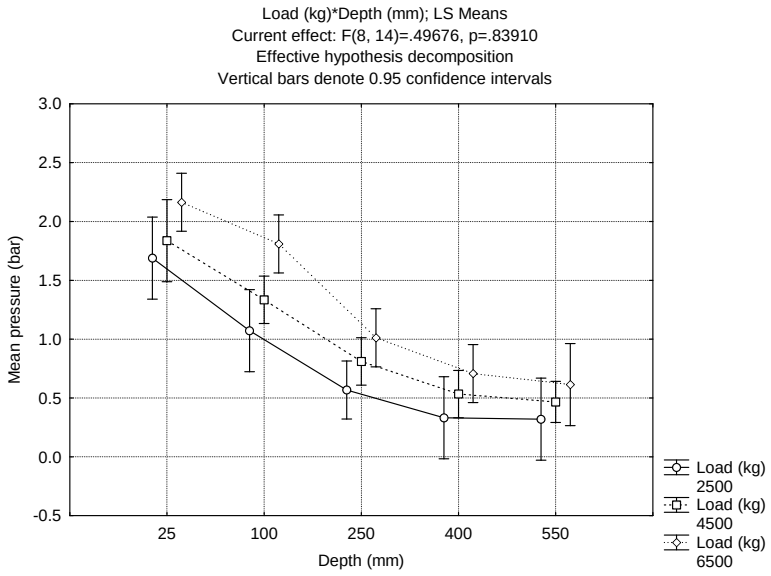

Cell No.	LSD test; variable Mean pressure (bar) (Spreadsheet1) Probabilities for Post Hoc Tests Error: Between MS = .02645, df = 14.000								
	Load (kg)	Depth (mm)	1 1.6886	2 1.0722	3 .56764	4 .33221	5 .32006	6 1.8371	7 1.3343
1	2500	25		0.017926	0.000062	0.000039	0.000035	0.529008	0.080065
2	2500	100	0.017926		0.023885	0.006201	0.005582	0.004996	0.184474
3	2500	250	0.000062	0.023885		0.256861	0.234247	0.000017	0.000144
4	2500	400	0.000039	0.006201	0.256861		0.958603	0.000013	0.000105
5	2500	550	0.000035	0.005582	0.234247	0.958603		0.000012	0.000093
6	4500	25	0.529008	0.004996	0.000017	0.000013	0.000012		0.018027
7	4500	100	0.080065	0.184474	0.000144	0.000105	0.000093	0.018027	
8	4500	250	0.000358	0.185610	0.123757	0.023185	0.020444	0.000083	0.001472
9	4500	400	0.000025	0.012341	0.819669	0.302658	0.275490	0.000007	0.000031
10	4500	550	0.000010	0.004946	0.484520	0.472301	0.433984	0.000003	0.000006
11	6500	25	0.031751	0.000081	0.000000	0.000000	0.000000	0.123302	0.000067
12	6500	100	0.553475	0.002366	0.000002	0.000003	0.000003	0.891992	0.006401
13	6500	250	0.004320	0.765672	0.016263	0.004217	0.003735	0.000992	0.047395
14	6500	400	0.000224	0.088658	0.403488	0.080289	0.071947	0.000058	0.000856
15	6500	550	0.000360	0.066329	0.818542	0.240359	0.221686	0.000109	0.001821

Cell No.	LSD test; variable Mean pressure (bar) (Spreadsheet1) Probabilities for Post Hoc Tests Error: Between MS = .02645, df = 14.000							
	8 .81076	9 .53316	10 .46652	11 2.1637	12 1.8096	13 1.0116	14 .70774	15 .61421
1	0.000358	0.000025	0.000010	0.031751	0.553475	0.004320	0.000224	0.000360
2	0.185610	0.012341	0.004946	0.000081	0.002366	0.765672	0.088658	0.066329
3	0.123757	0.819669	0.484520	0.000000	0.000002	0.016263	0.403488	0.818542
4	0.023185	0.302658	0.472301	0.000000	0.000003	0.004217	0.080289	0.240359
5	0.020444	0.275490	0.433984	0.000000	0.000003	0.003735	0.071947	0.221686
6	0.000083	0.000007	0.000003	0.123302	0.891992	0.000992	0.000058	0.000109
7	0.001472	0.000031	0.000006	0.000067	0.006401	0.047395	0.000856	0.001821
8		0.055274	0.014994	0.000000	0.000010	0.197451	0.499044	0.312950

Cell No.	LSD test; variable Mean pressure (bar) (Spreadsheet1) Probabilities for Post Hoc Tests Error: Between MS = .02645, df = 14.000							
	8 .81076	9 .53316	10 .46652	11 2.1637	12 1.8096	13 1.0116	14 .70774	15 .61421
9	0.055274		0.599982	0.000000	0.000001	0.006132	0.259205	0.672601
10	0.014994	0.599982		0.000000	0.000000	0.001697	0.108792	0.430209
11	0.000000	0.000000	0.000000		0.047017	0.000005	0.000000	0.000002
12	0.000010	0.000001	0.000000	0.047017		0.000231	0.000009	0.000032
13	0.197451	0.006132	0.001697	0.000005	0.000231		0.082719	0.065828
14	0.499044	0.259205	0.108792	0.000000	0.000009	0.082719		0.645858
15	0.312950	0.672601	0.430209	0.000002	0.000032	0.065828	0.645858	

M.6 Tekscan Soil Profile Tests: Combine smooth tyre – Maximum pressure – effect of depth and load (Factorial ANOVA)

Effect	Univariate Tests of Significance for Maximum pressure (bar) (Spreadsheet1) Sigma-restricted parameterization Effective hypothesis decomposition				
	SS	Degr. Of Freedom	MS	F	p
Intercept	248.3349	1	248.3349	3339.238	0.000000
Load (kg)	3.9368	2	1.9684	26.468	0.000018
Depth (mm)	48.9372	4	12.2343	164.509	0.000000
Load (kg)*Depth (mm)	5.1197	8	0.6400	8.605	0.000293
Error	1.0412	14	0.0744		

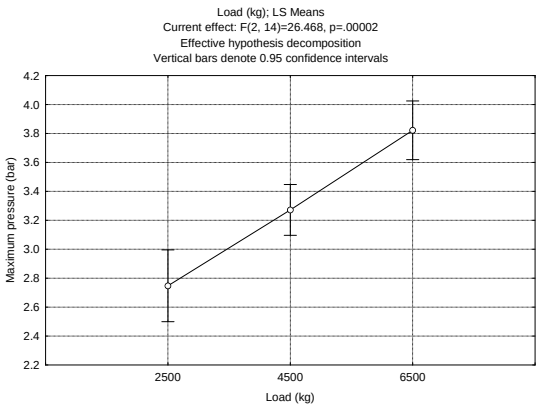

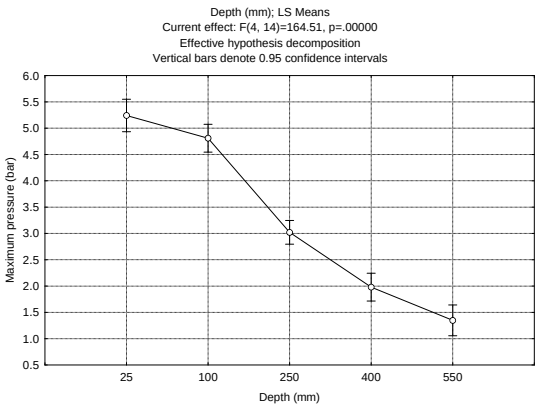

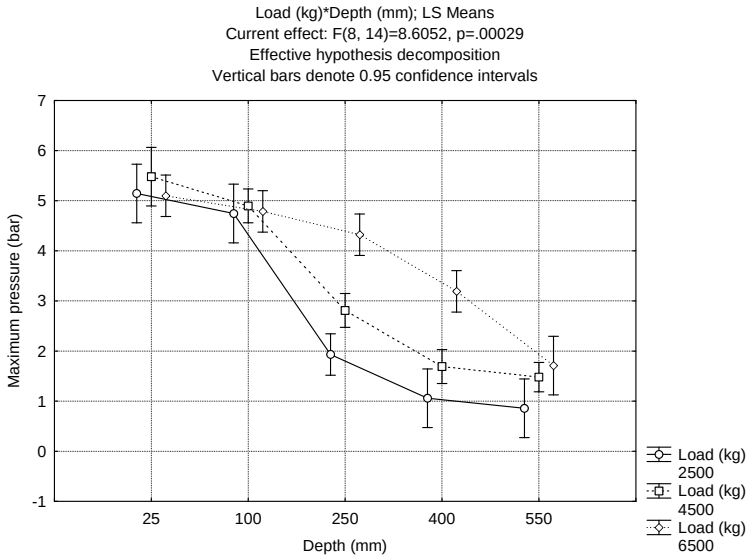

Cell No.	LSD test; variable Maximum pressure (bar) (Spreadsheet1) Probabilities for Post Hoc Tests Error: Between MS = .07437, df = 14.000								
	Load (kg)	Depth (mm)	1 5.1452	2 4.7452	3 1.9317	4 1.0584	5 .85754	6 5.4808	7 4.8970
1	2500	25		0.317297	0.000000	0.000000	0.000000	0.398749	0.443871
2	2500	100	0.317297		0.000001	0.000000	0.000000	0.077188	0.637133
3	2500	250	0.000000	0.000001		0.020383	0.006218	0.000000	0.000000
4	2500	400	0.000000	0.000000	0.020383		0.610644	0.000000	0.000000
5	2500	550	0.000000	0.000000	0.006218	0.610644		0.000000	0.000000
6	4500	25	0.398749	0.077188	0.000000	0.000000	0.000000		0.084928
7	4500	100	0.443871	0.637133	0.000000	0.000000	0.000000	0.084928	
8	4500	250	0.000003	0.000026	0.003313	0.000070	0.000023	0.000001	0.000000
9	4500	400	0.000000	0.000000	0.348859	0.064449	0.019218	0.000000	0.000000
10	4500	550	0.000000	0.000000	0.075999	0.189193	0.060808	0.000000	0.000000
11	6500	25	0.891642	0.307641	0.000000	0.000000	0.000000	0.271886	0.431188
12	6500	100	0.302298	0.901135	0.000000	0.000000	0.000000	0.056790	0.666519
13	6500	250	0.027225	0.225510	0.000000	0.000000	0.000000	0.003749	0.036579
14	6500	400	0.000042	0.000375	0.000396	0.000017	0.000006	0.000008	0.000008
15	6500	550	0.000000	0.000002	0.516949	0.113422	0.044306	0.000000	0.000000

Cell No.	LSD test; variable Maximum pressure (bar) (Spreadsheet1) Probabilities for Post Hoc Tests Error: Between MS = .07437, df = 14.000							
	8 2.8112	9 1.6904	10 1.4792	11 5.0988	12 4.7875	13 4.3217	14 3.1920	15 1.7097
1	0.000003	0.000000	0.000000	0.891642	0.302298	0.027225	0.000042	0.000000
2	0.000026	0.000000	0.000000	0.307641	0.901135	0.225510	0.000375	0.000002
3	0.003313	0.348859	0.075999	0.000000	0.000000	0.000000	0.000396	0.516949
4	0.000070	0.064449	0.189193	0.000000	0.000000	0.000000	0.000017	0.113422
5	0.000023	0.019218	0.060808	0.000000	0.000000	0.000000	0.000006	0.044306
6	0.000001	0.000000	0.000000	0.271886	0.056790	0.003749	0.000008	0.000000
7	0.000000	0.000000	0.000000	0.431188	0.666519	0.036579	0.000008	0.000000
8		0.000183	0.000017	0.000000	0.000001	0.000029	0.148366	0.003549
9	0.000183		0.327715	0.000000	0.000000	0.000000	0.000031	0.952148

Cell No.	LSD test; variable Maximum pressure (bar) (Spreadsheet1) Probabilities for Post Hoc Tests Error: Between MS = .07437, df = 14.000							
	8 2.8112	9 1.6904	10 1.4792	11 5.0988	12 4.7875	13 4.3217	14 3.1920	15 1.7097
10	0.000017	0.327715		0.000000	0.000000	0.000000	0.000004	0.462240
11	0.000000	0.000000	0.000000		0.272705	0.012861	0.000006	0.000000
12	0.000001	0.000000	0.000000	0.272705		0.109742	0.000042	0.000000
13	0.000029	0.000000	0.000000	0.012861	0.109742		0.000996	0.000002
14	0.148366	0.000031	0.000004	0.000006	0.000042	0.000996		0.000562
15	0.003549	0.952148	0.462240	0.000000	0.000000	0.000002	0.000562	

M.7 Tekscan Shallow Tests: Combine smooth tyre – Area – effect of depth and combination of load and inflation pressure (Factorial ANOVA)

Effect	Univariate Tests of Significance for Area (m2) (Spreadsheet1) Sigma-restricted parameterization Effective hypothesis decomposition				
	SS	Degr. Of freedom	MS	F	p
Intercept	1.911024	1	1.911024	1302.143	0.000000
Depth (mm)	0.053978	1	0.053978	36.780	0.000022
Combination of load and inflation pressure (tonne/bar)	0.126096	8	0.015762	10.740	0.000057
Depth (mm)*Combination of load and inflation pressure (tonne/bar)	0.002453	8	0.000307	0.209	0.984358
Error	0.022014	15	0.001468		

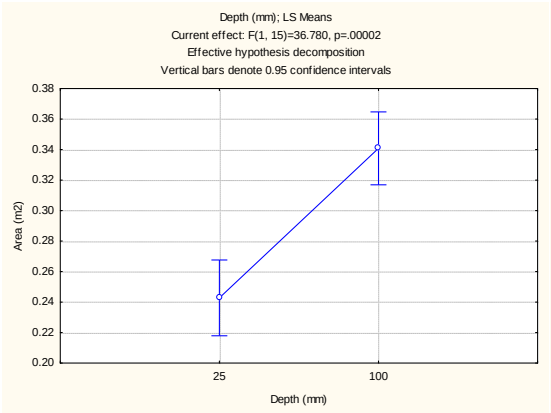

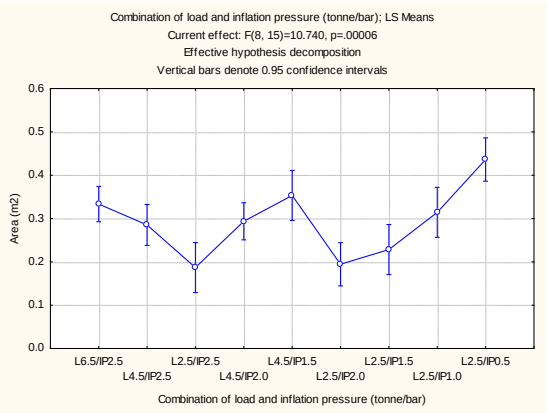

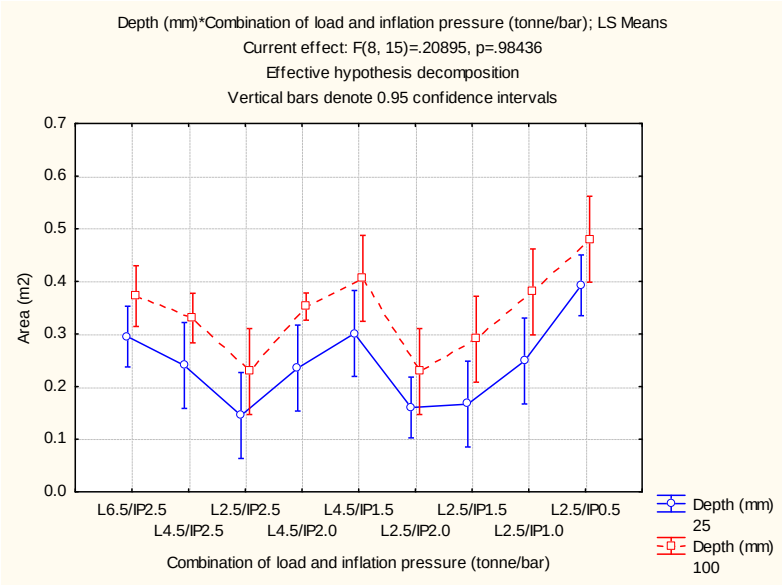

Cell No.	LSD test; variable Area (m2) (Spreadsheet1) Probabilities for Post Hoc Tests Error: Between MS = .00147, df = 15.000					
	Depth (mm)	Combination of load and inflation pressure (tonne/bar)	1 .29503	2 .24019	3 .14507	4 .23520
1	25	L6.5/IP2.5		0.260754	0.006012	0.221642
2	25	L4.5/IP2.5	0.260754		0.099529	0.927763
3	25	L2.5/IP2.5	0.006012	0.099529		0.116954
4	25	L4.5/IP2.0	0.221642	0.927763	0.116954	
5	25	L4.5/IP1.5	0.900404	0.279347	0.011494	0.243304
6	25	L2.5/IP2.0	0.003110	0.109130	0.750410	0.131143
7	25	L2.5/IP1.5	0.015398	0.195514	0.694183	0.225983
8	25	L2.5/IP1.0	0.338724	0.877857	0.075163	0.807097
9	25	L2.5/IP0.5	0.022531	0.005443	0.000094	0.004375
10	100	L6.5/IP2.5	0.063147	0.013264	0.000219	0.010693
11	100	L4.5/IP2.5	0.329884	0.059836	0.000795	0.048396
12	100	L2.5/IP2.5	0.177769	0.834616	0.143597	0.905877
13	100	L4.5/IP2.0	0.073636	0.013867	0.000118	0.010784
14	100	L4.5/IP1.5	0.032353	0.008030	0.000229	0.006652
15	100	L2.5/IP2.0	0.177769	0.834616	0.143597	0.905877
16	100	L2.5/IP1.5	0.916122	0.372443	0.017301	0.327779
17	100	L2.5/IP1.0	0.090198	0.020890	0.000587	0.017381
18	100	L2.5/IP0.5	0.001303	0.000490	0.000018	0.000408

Cell No.	LSD test; variable Area (m2) (Spreadsheet1) Probabilities for Post Hoc Tests Error: Between MS = .00147, df = 15.000							
	5 .30100	6 .16027	7 .16679	8 .24866	9 .39243	10 .37190	11 .33024	12 .22868
1	0.900404	0.003110	0.015398	0.338724	0.022531	0.063147	0.329884	0.177769
2	0.279347	0.109130	0.195514	0.877857	0.005443	0.013264	0.059836	0.834616
3	0.011494	0.750410	0.694183	0.075163	0.000094	0.000219	0.000795	0.143597
4	0.243304	0.131143	0.225983	0.807097	0.004375	0.010693	0.048396	0.905877
5		0.008985	0.025630	0.349339	0.070296	0.151506	0.518555	0.201840

Cell No.	LSD test; variable Area (m2) (Spreadsheet1) Probabilities for Post Hoc Tests Error: Between MS = .00147, df = 15.000							
	5 .30100	6 .16027	7 .16679	8 .24866	9 .39243	10 .37190	11 .33024	12 .22868
6	0.008985		0.891409	0.079119	0.000022	0.000058	0.000208	0.165456
7	0.025630	0.891409		0.151515	0.000230	0.000547	0.002161	0.271187
8	0.349339	0.079119	0.151515		0.007873	0.019056	0.084981	0.717444
9	0.070296	0.000022	0.000230	0.007873		0.600014	0.095658	0.003291
10	0.151506	0.000058	0.000547	0.019056	0.600014		0.252056	0.008061
11	0.518555	0.000208	0.002161	0.084981	0.095658	0.252056		0.036509
12	0.201840	0.165456	0.271187	0.717444	0.003291	0.008061	0.036509	
13	0.222807	0.000011	0.000339	0.021148	0.194218	0.514626	0.399803	0.007753
14	0.072461	0.000102	0.000507	0.011036	0.781537	0.482745	0.108775	0.005200
15	0.201840	0.165456	0.271187	0.717444	0.003291	0.008061	0.036509	1.000000
16	0.841869	0.014445	0.038069	0.457265	0.045338	0.101317	0.377344	0.275474
17	0.165401	0.000294	0.001322	0.028442	0.794735	0.865304	0.278347	0.013650
18	0.004819	0.000006	0.000036	0.000671	0.081646	0.035953	0.004078	0.000321

Cell No.	LSD test; variable Area (m2) (Spreadsheet1) Probabilities for Post Hoc Tests Error: Between MS = .00147, df = 15.000					
	13 .35210	14 .40567	15 .22868	16 .29000	17 .38000	18 .48000
1	0.073636	0.032353	0.177769	0.916122	0.090198	0.001303
2	0.013867	0.008030	0.834616	0.372443	0.020890	0.000490
3	0.000118	0.000229	0.143597	0.017301	0.000587	0.000018
4	0.010784	0.006652	0.905877	0.327779	0.017381	0.000408
5	0.222807	0.072461	0.201840	0.841869	0.165401	0.004819
6	0.000011	0.000102	0.165456	0.014445	0.000294	0.000006
7	0.000339	0.000507	0.271187	0.038069	0.001322	0.000036
8	0.021148	0.011036	0.717444	0.457265	0.028442	0.000671
9	0.194218	0.781537	0.003291	0.045338	0.794735	0.081646
10	0.514626	0.482745	0.008061	0.101317	0.865304	0.035953
11	0.399803	0.108775	0.036509	0.377344	0.278347	0.004078
12	0.007753	0.005200	1.000000	0.275474	0.013650	0.000321
13		0.202289	0.007753	0.143054	0.498017	0.006171
14	0.202289		0.005200	0.049657	0.642410	0.190264
15	0.007753	0.005200		0.275474	0.013650	0.000321
16	0.143054	0.049657	0.275474		0.117424	0.003178
17	0.498017	0.642410	0.013650	0.117424		0.084753
18	0.006171	0.190264	0.000321	0.003178	0.084753	

M.8 Tekscan Shallow Tests: Combine smooth tyre – Mean contact pressure – effect of depth and combination of load and inflation pressure (Factorial ANOVA)

Effect	Univariate Tests of Significance for Mean pressure (bar) (Spreadsheet1) Sigma-restricted parameterization Effective hypothesis decomposition				
	SS	Degr. Of Freedom	MS	F	p
Intercept	38.61818	1	38.61818	1253.488	0.000000
Depth (mm)	0.58609	1	0.58609	19.023	0.000558
Combination of load and inflation pressure (tonne/bar)	3.33609	8	0.41701	13.536	0.000014
Depth (mm)*Combination of load and inflation pressure (tonne/bar)	0.29264	8	0.03658	1.187	0.368104
Error	0.46213	15	0.03081		

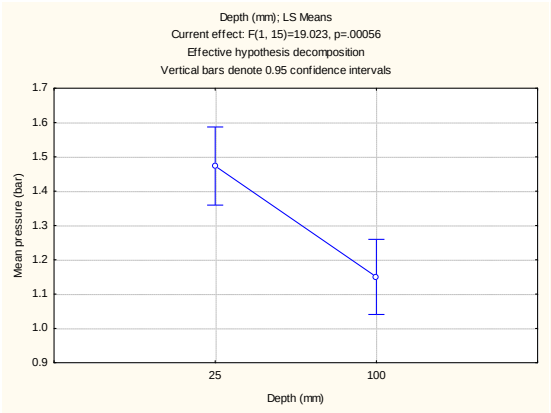

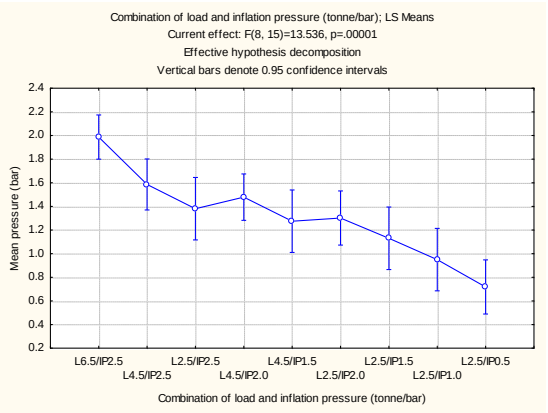

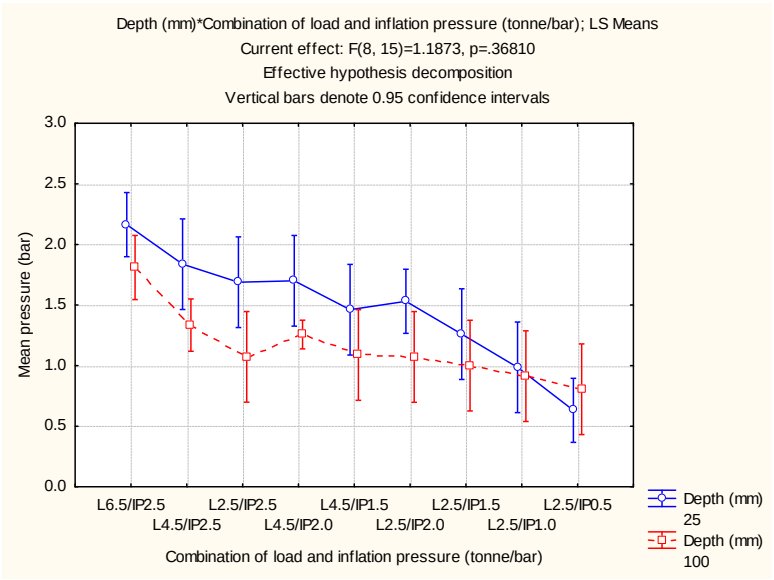

Cell No.	LSD test; variable Mean pressure (bar) (Spreadsheet1) Probabilities for Post Hoc Tests Error: Between MS = .03081, df = 15.000					
	Depth (mm)	Combination of load and inflation pressure (tonne/bar)	1 2.1637	2 1.8371	3 1.6886	4 1.7000
1	25	L6.5/IP2.5		0.149481	0.043072	0.047632
2	25	L4.5/IP2.5	0.149481		0.558701	0.588863
3	25	L2.5/IP2.5	0.043072	0.558701		0.964097
4	25	L4.5/IP2.0	0.047632	0.588863	0.964097	
5	25	L4.5/IP1.5	0.005209	0.151131	0.374855	0.352080
6	25	L2.5/IP2.0	0.002592	0.174586	0.473946	0.443316
7	25	L2.5/IP1.5	0.000767	0.034521	0.104734	0.096604
8	25	L2.5/IP1.0	0.000064	0.003733	0.012659	0.011539
9	25	L2.5/IP0.5	0.000000	0.000050	0.000185	0.000167
10	100	L6.5/IP2.5	0.061884	0.899764	0.582079	0.617707
11	100	L4.5/IP2.5	0.000113	0.025450	0.100840	0.091287
12	100	L2.5/IP2.5	0.000136	0.007598	0.025317	0.023129
13	100	L4.5/IP2.0	0.000007	0.006552	0.033034	0.029288
14	100	L4.5/IP1.5	0.000157	0.008635	0.028640	0.026178
15	100	L2.5/IP2.0	0.000136	0.007587	0.025281	0.023096
16	100	L2.5/IP1.5	0.000072	0.004189	0.014178	0.012927
17	100	L2.5/IP1.0	0.000034	0.002041	0.006956	0.006335
18	100	L2.5/IP0.5	0.000014	0.000842	0.002854	0.002598

Cell No.	LSD test; variable Mean pressure (bar) (Spreadsheet1) Probabilities for Post Hoc Tests Error: Between MS = .03081, df = 15.000							
	5 1.4616	6 1.5307	7 1.2600	8 .98606	9 .63093	10 1.8096	11 1.3343	12 1.0722
1	0.005209	0.002592	0.000767	0.000064	0.000000	0.061884	0.000113	0.000136
2	0.151131	0.174586	0.034521	0.003733	0.000050	0.899764	0.025450	0.007598
3	0.374855	0.473946	0.104734	0.012659	0.000185	0.582079	0.100840	0.025317
4	0.352080	0.443316	0.096604	0.011539	0.000167	0.617707	0.091287	0.023129
5		0.752207	0.429400	0.074659	0.001529	0.126356	0.539368	0.137532
6	0.752207		0.227136	0.022927	0.000124	0.133012	0.239109	0.049840
7	0.429400	0.227136		0.287167	0.010424	0.021916	0.719062	0.460954
8	0.074659	0.022927	0.287167		0.119313	0.001637	0.106332	0.733497
9	0.001529	0.000124	0.010424	0.119313		0.000007	0.000528	0.057994
10	0.126356	0.133012	0.021916	0.001637	0.000007		0.009613	0.003720
11	0.539368	0.239109	0.719062	0.106332	0.000528	0.009613		0.215463
12	0.137532	0.049840	0.460954	0.733497	0.057994	0.003720	0.215463	
13	0.282697	0.061937	0.984968	0.162517	0.000346	0.001010	0.510861	0.332623
14	0.152809	0.057117	0.498330	0.687858	0.050614	0.004316	0.242606	0.950787
15	0.137364	0.049762	0.460535	0.734028	0.058084	0.003714	0.215166	0.999434
16	0.082670	0.026058	0.311489	0.955961	0.106584	0.001869	0.119846	0.775238
17	0.043055	0.011599	0.182456	0.772499	0.209228	0.000820	0.055220	0.531026
18	0.018382	0.004162	0.086783	0.477202	0.430522	0.000301	0.019661	0.298960

Cell No.	LSD test; variable Mean pressure (bar) (Spreadsheet1) Probabilities for Post Hoc Tests Error: Between MS = .03081, df = 15.000					
	13 1.2565	14 1.0877	15 1.0720	16 1.0000	17 .91299	18 .80509
1	0.000007	0.000157	0.000136	0.000072	0.000034	0.000014
2	0.006552	0.008635	0.007587	0.004189	0.002041	0.000842
3	0.033034	0.028640	0.025281	0.014178	0.006956	0.002854
4	0.029288	0.026178	0.023096	0.012927	0.006335	0.002598
5	0.282697	0.152809	0.137364	0.082670	0.043055	0.018382
6	0.061937	0.057117	0.049762	0.026058	0.011599	0.004162
7	0.984968	0.498330	0.460535	0.311489	0.182456	0.086783
8	0.162517	0.687858	0.734028	0.955961	0.772499	0.477202
9	0.000346	0.050614	0.058084	0.106584	0.209228	0.430522
10	0.001010	0.004316	0.003714	0.001869	0.000820	0.000301
11	0.510861	0.242606	0.215166	0.119846	0.055220	0.019661
12	0.332623	0.950787	0.999434	0.775238	0.531026	0.298960
13		0.373883	0.332169	0.183866	0.081739	0.026938
14	0.373883		0.950222	0.728641	0.492202	0.272692
15	0.332169	0.950222		0.775780	0.531482	0.299272
16	0.183866	0.728641	0.775780		0.730810	0.444562
17	0.081739	0.492202	0.531482	0.730810		0.669995
18	0.026938	0.272692	0.299272	0.444562	0.669995	

M.9 Tekscan Shallow Tests: Combine smooth tyre – Maximum contact pressure – effect of depth and combination of load and inflation pressure (Factorial ANOVA)

Effect	Univariate Tests of Significance for Maximum pressure (bar) (Spreadsheet1_EffectOfDepthNCombinationOfLoadNPressure.sta) Sigma-restricted parameterization Effective hypothesis decomposition				
	SS	Degr. Of Freedom	MS	F	p
Intercept	350.2914	1	350.2914	1906.810	0.000000
Depth (mm)	1.4626	1	1.4626	7.962	0.012885
Combination of load and inflation pressure (tonne/bar)	18.7976	8	2.3497	12.791	0.000020
Depth (mm)*Combination of load and inflation pressure (tonne/bar)	0.2189	8	0.0274	0.149	0.994747
Error	2.7556	15	0.1837		

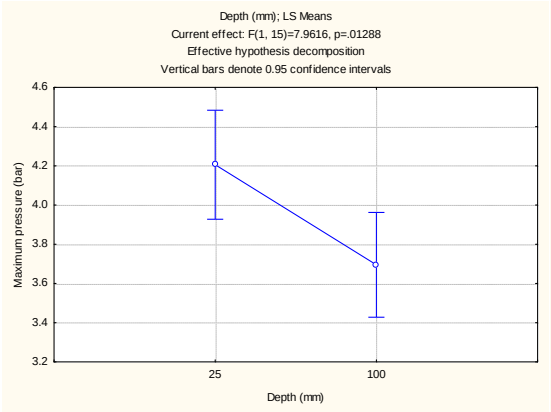

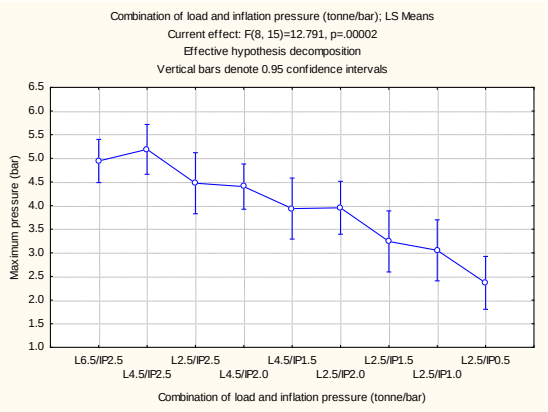

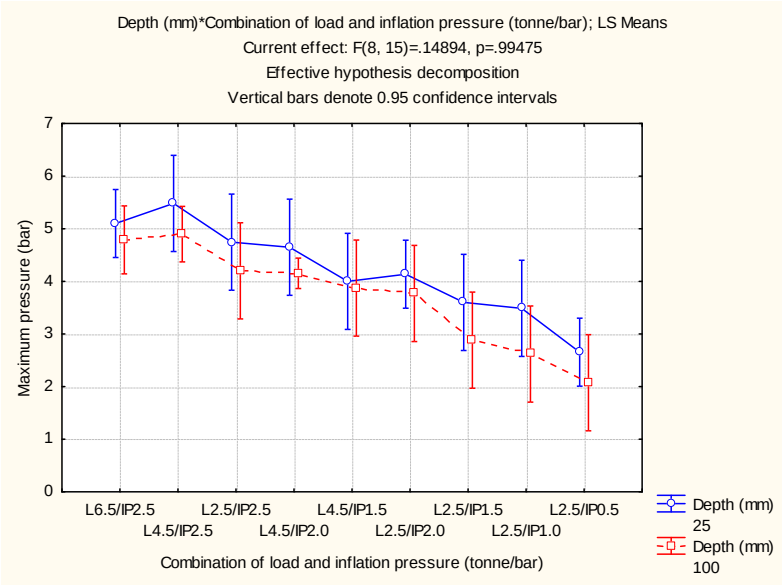

Cell No.	LSD test; variable Maximum pressure (bar) (Spreadsheet1_EffectOfDepthNCombinationOfLoadNPressure.sta) Probabilities for Post Hoc Tests Error: Between MS = .18371, df = 15.000					
	Depth (mm)	Combination of load and inflation pressure	1 5.0988	2 5.4808	3 4.7450	4 4.6479
1	25	L6.5/IP2.5		0.477970	0.510546	0.403892
2	25	L4.5/IP2.5	0.477970		0.243523	0.189591
3	25	L2.5/IP2.5	0.510546	0.243523		0.874910
4	25	L4.5/IP2.0	0.403892	0.189591	0.874910	
5	25	L4.5/IP1.5	0.053733	0.027412	0.237975	0.301996
6	25	L2.5/IP2.0	0.039986	0.021597	0.263374	0.343998
7	25	L2.5/IP1.5	0.012038	0.007273	0.078384	0.104356
8	25	L2.5/IP1.0	0.007771	0.004966	0.055562	0.074722
9	25	L2.5/IP0.5	0.000042	0.000076	0.001204	0.001756
10	100	L6.5/IP2.5	0.478742	0.206330	0.936607	0.794020
11	100	L4.5/IP2.5	0.613568	0.256525	0.762911	0.622042
12	100	L2.5/IP2.5	0.107440	0.051762	0.382793	0.471320
13	100	L4.5/IP2.0	0.012178	0.009846	0.207467	0.288044
14	100	L4.5/IP1.5	0.033700	0.018032	0.170293	0.219888
15	100	L2.5/IP2.0	0.023085	0.012888	0.128783	0.168368
16	100	L2.5/IP1.5	0.000738	0.000648	0.007726	0.010703
17	100	L2.5/IP1.0	0.000272	0.000273	0.003174	0.004409
18	100	L2.5/IP0.5	0.000038	0.000049	0.000511	0.000704

Cell No.	LSD test; variable Maximum pressure (bar) (Spreadsheet1_EffectOfDepthNCombinationOfLoadNPressure.sta) Probabilities for Post Hoc Tests Error: Between MS = .18371, df = 15.000							
	5 4.0000	6 4.1350	7 3.6000	8 3.4870	9 2.6550	10 4.7875	11 4.8970	12 4.2000
1	0.053733	0.039986	0.012038	0.007771	0.000042	0.478742	0.613568	0.107440
2	0.027412	0.021597	0.007273	0.004966	0.000076	0.206330	0.256525	0.051762
3	0.237975	0.263374	0.078384	0.055562	0.001204	0.936607	0.762911	0.382793

Cell No.	LSD test; variable Maximum pressure (bar) (Spreadsheet1_EffectOfDepthNCombinationOfLoadNPressure.sta) Probabilities for Post Hoc Tests Error: Between MS = .18371, df = 15.000							
	5 4.0000	6 4.1350	7 3.6000	8 3.4870	9 2.6550	10 4.7875	11 4.8970	12 4.2000
4	0.301996	0.343998	0.104356	0.074722	0.001756	0.794020	0.622042	0.471320
5		0.800539	0.519317	0.410666	0.021667	0.154341	0.089968	0.745997
6	0.800539		0.324279	0.236031	0.003550	0.148743	0.070426	0.903098
7	0.519317	0.324279		0.854610	0.091966	0.038971	0.019286	0.337941
8	0.410666	0.236031	0.854610		0.133829	0.025624	0.012190	0.257811
9	0.021667	0.003550	0.091966	0.133829		0.000166	0.000040	0.010071
10	0.154341	0.148743	0.038971	0.025624	0.000166		0.783245	0.280698
11	0.089968	0.070426	0.019286	0.012190	0.000040	0.783245		0.179401
12	0.745997	0.903098	0.337941	0.257811	0.010071	0.280698	0.179401	
13	0.738666	0.957992	0.237752	0.159288	0.000414	0.075214	0.018638	0.917737
14	0.835461	0.623493	0.660160	0.535005	0.034973	0.101585	0.055986	0.596248
15	0.710411	0.498198	0.782191	0.646582	0.050590	0.071803	0.037942	0.489568
16	0.084981	0.030605	0.254689	0.334126	0.671455	0.002471	0.001003	0.046103
17	0.037767	0.011265	0.126387	0.172634	0.946175	0.000889	0.000345	0.019768
18	0.006250	0.001348	0.023687	0.034128	0.285981	0.000114	0.000042	0.003177

Cell No.	LSD test; variable Maximum pressure (bar) (Spreadsheet1_EffectOfDepthNCombinationOfLoadNPressure.sta) Probabilities for Post Hoc Tests Error: Between MS = .18371, df = 15.000					
	13 4.1528	14 3.8719	15 3.7706	16 2.8821	17 2.6190	18 2.0742
1	0.012178	0.033700	0.023085	0.000738	0.000272	0.000038
2	0.009846	0.018032	0.012888	0.000648	0.000273	0.000049
3	0.207467	0.170293	0.128783	0.007726	0.003174	0.000511
4	0.288044	0.219888	0.168368	0.010703	0.004409	0.000704
5	0.738666	0.835461	0.710411	0.084981	0.037767	0.006250
6	0.957992	0.623493	0.498198	0.030605	0.011265	0.001348
7	0.237752	0.660160	0.782191	0.254689	0.126387	0.023687
8	0.159288	0.535005	0.646582	0.334126	0.172634	0.034128
9	0.000414	0.034973	0.050590	0.671455	0.946175	0.285981
10	0.075214	0.101585	0.071803	0.002471	0.000889	0.000114
11	0.018638	0.055986	0.037942	0.001003	0.000345	0.000042
12	0.917737	0.596248	0.489568	0.046103	0.019768	0.003177
13		0.541457	0.408607	0.012753	0.003861	0.000331
14	0.541457		0.869535	0.123290	0.056440	0.009620
15	0.408607	0.869535		0.163334	0.076836	0.013495
16	0.012753	0.123290	0.163334		0.670394	0.202482
17	0.003861	0.056440	0.076836	0.670394		0.383002
18	0.000331	0.009620	0.013495	0.202482	0.383002	

M.10 Tekscan Tests: Implement tyres – Area – effect of ply rating and depth (Factorial ANOVA)

Effect	Univariate Tests of Significance for Contact area (m2) (Spreadsheet1) Sigma-restricted parameterization Effective hypothesis decomposition				
	SS	Degr. Of Freedom	MS	F	p
Intercept	1.010233	1	1.010233	8305.536	0.000000
Depth	0.744747	2	0.372373	3061.433	0.000000
PR	0.001325	4	0.000331	2.723	0.072305
Depth*PR	0.002751	8	0.000344	2.827	0.042753
Error	0.001703	14	0.000122		

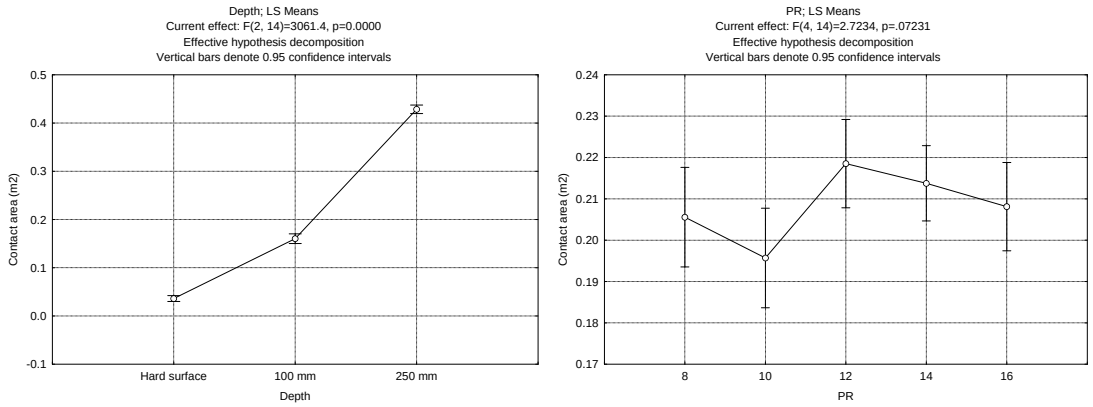

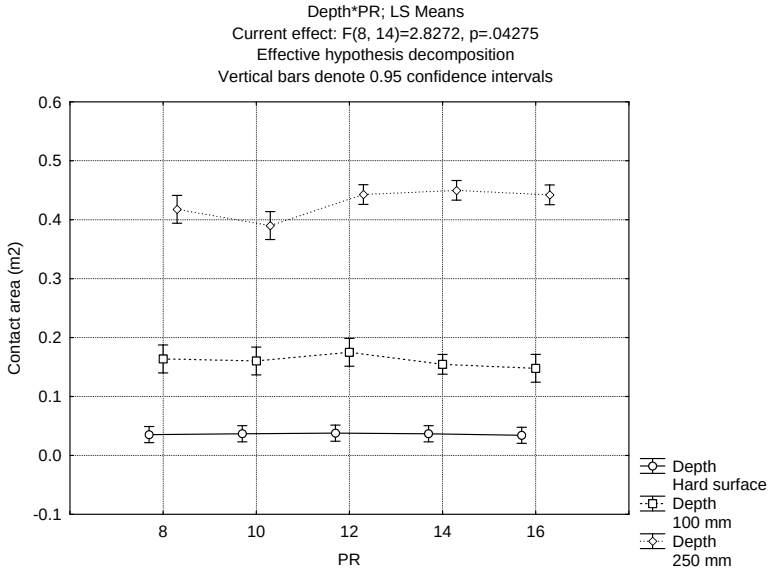

Cell No.	LSD test; variable Contact area (m2) (Spreadsheet1) Probabilities for Post Hoc Tests Error: Between MS = .00012, df = 14.000								
	Depth	PR	1 .03536	2 .03679	3 .03781	4 .03679	5 .03418	6 .16375	7 .16027
1	Hard surface	8		0.875681	0.788908	0.875915	0.898037	0.000000	0.000000
2	Hard surface	10	0.875681		0.911189	0.999763	0.776200	0.000000	0.000000
3	Hard surface	12	0.788908	0.911189		0.910954	0.692751	0.000000	0.000000
4	Hard surface	14	0.875915	0.999763	0.910954		0.776426	0.000000	0.000000
5	Hard surface	16	0.898037	0.776200	0.692751	0.776426		0.000000	0.000000

Cell No.	LSD test; variable Contact area (m2) (Spreadsheet1) Probabilities for Post Hoc Tests Error: Between MS = .00012, df = 14.000								
	Depth	PR	1 .03536	2 .03679	3 .03781	4 .03679	5 .03418	6 .16375	7 .16027
6	100 mm	8	0.000000	0.000000	0.000000	0.000000	0.000000		0.826924
7	100 mm	10	0.000000	0.000000	0.000000	0.000000	0.000000	0.826924	
8	100 mm	12	0.000000	0.000000	0.000000	0.000000	0.000000	0.480967	0.359788
9	100 mm	14	0.000000	0.000000	0.000000	0.000000	0.000000	0.510505	0.682271
10	100 mm	16	0.000000	0.000000	0.000001	0.000000	0.000000	0.326666	0.440640
11	250 mm	8	0.000000	0.000000	0.000000	0.000000	0.000000	0.000000	0.000000
12	250 mm	10	0.000000	0.000000	0.000000	0.000000	0.000000	0.000000	0.000000
13	250 mm	12	0.000000	0.000000	0.000000	0.000000	0.000000	0.000000	0.000000
14	250 mm	14	0.000000	0.000000	0.000000	0.000000	0.000000	0.000000	0.000000
15	250 mm	16	0.000000	0.000000	0.000000	0.000000	0.000000	0.000000	0.000000

Cell No.	LSD test; variable Contact area (m2) (Spreadsheet1) Probabilities for Post Hoc Tests Error: Between MS = .00012, df = 14.000							
	8 .17504	9 .15463	10 .14789	11 .41762	12 .39004	13 .44270	14 .44987	15 .44227
1	0.000000	0.000000	0.000000	0.000000	0.000000	0.000000	0.000000	0.000000
2	0.000000	0.000000	0.000000	0.000000	0.000000	0.000000	0.000000	0.000000
3	0.000000	0.000000	0.000001	0.000000	0.000000	0.000000	0.000000	0.000000
4	0.000000	0.000000	0.000000	0.000000	0.000000	0.000000	0.000000	0.000000
5	0.000000	0.000000	0.000000	0.000000	0.000000	0.000000	0.000000	0.000000
6	0.480967	0.510505	0.326666	0.000000	0.000000	0.000000	0.000000	0.000000
7	0.359788	0.682271	0.440640	0.000000	0.000000	0.000000	0.000000	0.000000
8		0.152948	0.103699	0.000000	0.000000	0.000000	0.000000	0.000000
9	0.152948		0.625932	0.000000	0.000000	0.000000	0.000000	0.000000
10	0.103699	0.625932		0.000000	0.000000	0.000000	0.000000	0.000000
11	0.000000	0.000000	0.000000		0.098782	0.084475	0.031613	0.089434
12	0.000000	0.000000	0.000000	0.098782		0.001605	0.000572	0.001710
13	0.000000	0.000000	0.000000	0.084475	0.001605		0.526334	0.969142
14	0.000000	0.000000	0.000000	0.031613	0.000572	0.526334		0.501965
15	0.000000	0.000000	0.000000	0.089434	0.001710	0.969142	0.501965	

M.11 Tekscan Tests: Implement tyres – Mean pressure – effect of ply rating and depth (Factorial ANOVA)

Effect	Univariate Tests of Significance for Mean pressure (bar) (Spreadsheet1) Sigma-restricted parameterization Effective hypothesis decomposition				
	SS	Degr. Of Freedom	MS	F	p
Intercept	91.1731	1	91.17305	1460.821	0.000000
Depth	102.0292	2	51.01462	817.382	0.000000
PR	0.2070	4	0.05175	0.829	0.528419
Depth*PR	0.3475	8	0.04344	0.696	0.690336
Error	0.8738	14	0.06241		

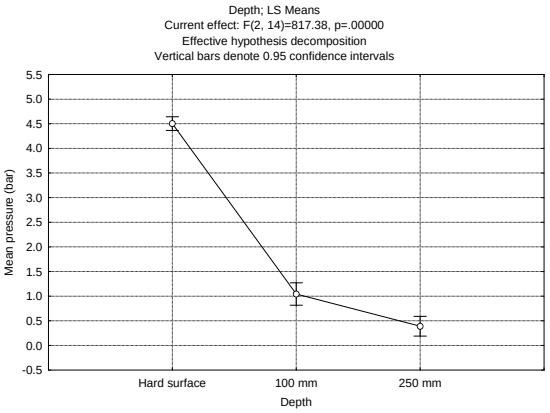

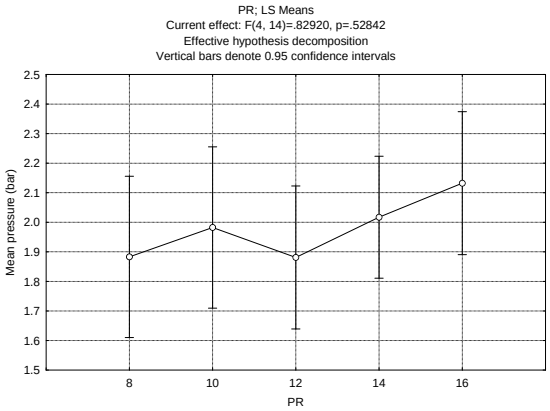

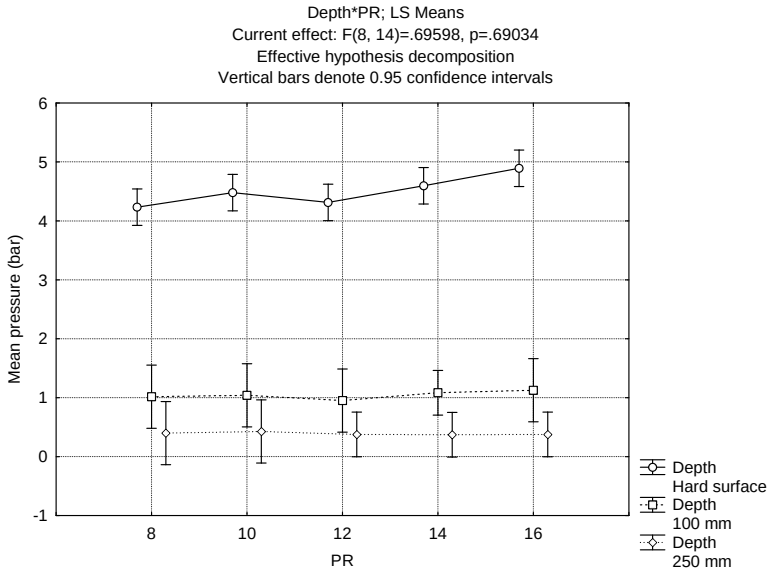

Cell No.	LSD test; variable Mean pressure (bar) (Spreadsheet1) Probabilities for Post Hoc Tests Error: Between MS = .06241, df = 14.000								
	Depth	PR	1 4.2324	2 4.4795	3 4.3140	4 4.5961	5 4.8928	6 1.0172	7 1.0401
1	Hard surface	8		0.245839	0.695287	0.096245	0.005955	0.000000	0.000000
2	Hard surface	10	0.245839		0.430710	0.576461	0.062200	0.000000	0.000000
3	Hard surface	12	0.695287	0.430710		0.188234	0.013159	0.000000	0.000000
4	Hard surface	14	0.096245	0.576461	0.188234		0.167824	0.000000	0.000000
5	Hard surface	16	0.005955	0.062200	0.013159	0.167824		0.000000	0.000000
6	100 mm	8	0.000000	0.000000	0.000000	0.000000	0.000000		0.949273
7	100 mm	10	0.000000	0.000000	0.000000	0.000000	0.000000	0.949273	
8	100 mm	12	0.000000	0.000000	0.000000	0.000000	0.000000	0.854952	0.805477
9	100 mm	14	0.000000	0.000000	0.000000	0.000000	0.000000	0.829709	0.887286
10	100 mm	16	0.000000	0.000000	0.000000	0.000000	0.000000	0.759893	0.808578
11	250 mm	8	0.000000	0.000000	0.000000	0.000000	0.000000	0.102109	0.091144
12	250 mm	10	0.000000	0.000000	0.000000	0.000000	0.000000	0.117161	0.104772
13	250 mm	12	0.000000	0.000000	0.000000	0.000000	0.000000	0.055251	0.048086
14	250 mm	14	0.000000	0.000000	0.000000	0.000000	0.000000	0.053160	0.046249
15	250 mm	16	0.000000	0.000000	0.000000	0.000000	0.000000	0.055131	0.047980

Cell No.	LSD test; variable Mean pressure (bar) (Spreadsheet1) Probabilities for Post Hoc Tests Error: Between MS = .06241, df = 14.000							
	8 .95144	9 1.0843	10 1.1273	11 .39918	12 .42729	13 .37746	14 .37109	15 .37710
1	0.000000	0.000000	0.000000	0.000000	0.000000	0.000000	0.000000	0.000000
2	0.000000	0.000000	0.000000	0.000000	0.000000	0.000000	0.000000	0.000000
3	0.000000	0.000000	0.000000	0.000000	0.000000	0.000000	0.000000	0.000000
4	0.000000	0.000000	0.000000	0.000000	0.000000	0.000000	0.000000	0.000000
5	0.000000	0.000000	0.000000	0.000000	0.000000	0.000000	0.000000	0.000000
6	0.854952	0.829709	0.759893	0.102109	0.117161	0.055251	0.053160	0.055131
7	0.805477	0.887286	0.808578	0.091144	0.104772	0.048086	0.046249	0.047980
8		0.670796	0.626307	0.140337	0.160084	0.081671	0.078683	0.081500
9	0.670796		0.890082	0.041906	0.049773	0.013386	0.012729	0.013348
10	0.626307	0.890082		0.058386	0.067532	0.028000	0.026898	0.027937
11	0.140337	0.041906	0.058386		0.937709	0.944423	0.928146	0.943505
12	0.160084	0.049773	0.067532	0.937709		0.872966	0.856891	0.872058
13	0.081671	0.013386	0.028000	0.944423	0.872966		0.979996	0.998872
14	0.078683	0.012729	0.026898	0.928146	0.856891	0.979996		0.981123
15	0.081500	0.013348	0.027937	0.943505	0.872058	0.998872	0.981123	

M.12 Tekscan Tests: Implement tyres – Maximum pressure – effect of ply rating and depth (Factorial ANOVA)

Effect	Univariate Tests of Significance for Maximum pressure (bar) (Spreadsheet1) Sigma-restricted parameterization Effective hypothesis decomposition				
	SS	Degr. Of Freedom	MS	F	p
Intercept	706.9247	1	706.9247	253.1385	0.000000
Depth	381.1565	2	190.5782	68.2430	0.000000
PR	2.8902	4	0.7225	0.2587	0.899476
Depth*PR	3.2642	8	0.4080	0.1461	0.994932
Error	39.0970	14	2.7926		

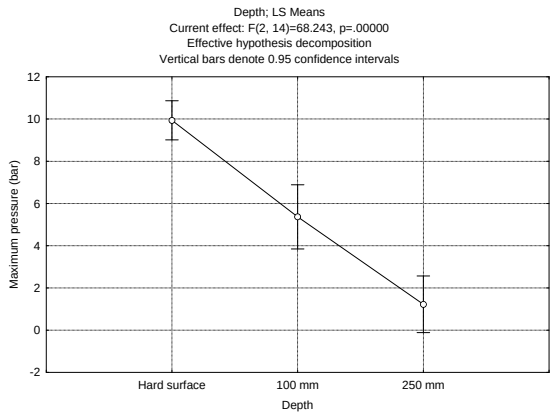

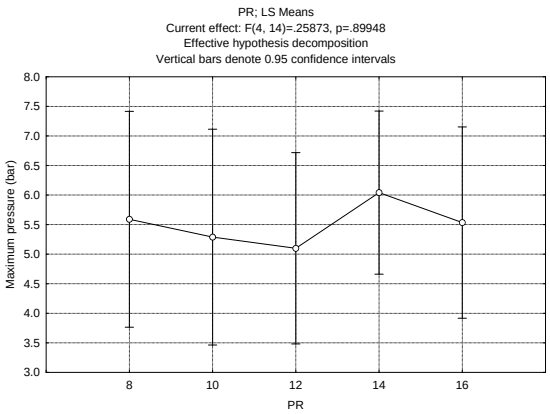

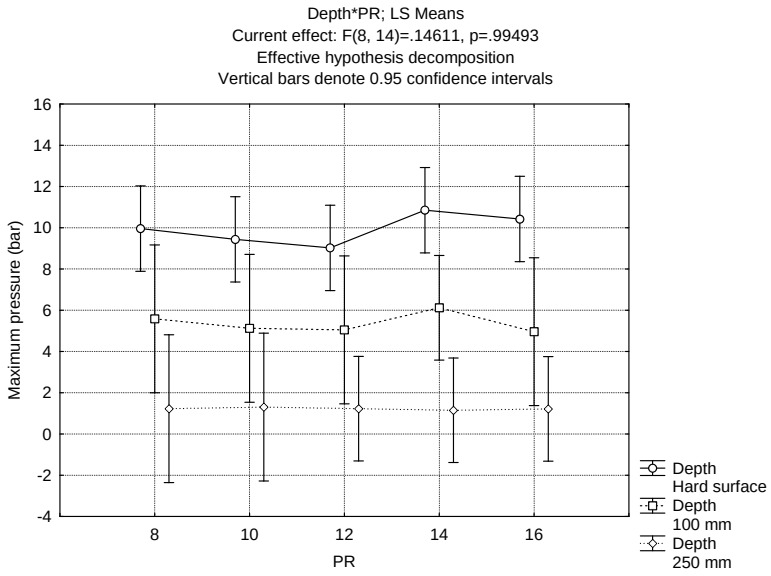

Cell No.	LSD test; variable Maximum pressure (bar) (Spreadsheet1) Probabilities for Post Hoc Tests Error: Between MS = 2.7926, df = 14.000								
	Depth	PR	1 9.9599	2 9.4380	3 9.0238	4 10.852	5 10.424	6 5.5813	7 5.1251
1	Hard surface	8		0.707794	0.503865	0.523943	0.738740	0.039596	0.025193
2	Hard surface	10	0.707794		0.765952	0.317683	0.481716	0.065449	0.042224
3	Hard surface	12	0.503865	0.765952		0.201681	0.322154	0.096102	0.062895
4	Hard surface	14	0.523943	0.317683	0.201681		0.758594	0.016229	0.010181
5	Hard surface	16	0.738740	0.481716	0.322154	0.758594		0.024992	0.015763
6	100 mm	8	0.039596	0.065449	0.096102	0.016229	0.024992		0.849697
7	100 mm	10	0.025193	0.042224	0.062895	0.010181	0.015763	0.849697	
8	100 mm	12	0.023350	0.039211	0.058527	0.009420	0.014593	0.825163	0.974889
9	100 mm	14	0.024613	0.047219	0.077670	0.007797	0.013581	0.796502	0.634660
10	100 mm	16	0.021411	0.036028	0.053897	0.008621	0.013365	0.797475	0.946350
11	250 mm	8	0.000476	0.000802	0.001219	0.000199	0.000302	0.086850	0.121534
12	250 mm	10	0.000513	0.000864	0.001314	0.000214	0.000325	0.091811	0.128194
13	250 mm	12	0.000053	0.000097	0.000159	0.000019	0.000031	0.051645	0.077604
14	250 mm	14	0.000048	0.000088	0.000145	0.000018	0.000028	0.048236	0.072645
15	250 mm	16	0.000052	0.000096	0.000157	0.000019	0.000031	0.051192	0.076946

Cell No.	LSD test; variable Maximum pressure (bar) (Spreadsheet1) Probabilities for Post Hoc Tests Error: Between MS = 2.7926, df = 14.000							
	8 5.0493	9 6.1192	10 4.9631	11 1.2295	12 1.3037	13 1.2272	14 1.1521	15 1.2175
1	0.023350	0.024613	0.021411	0.000476	0.000513	0.000053	0.000048	0.000052
2	0.039211	0.047219	0.036028	0.000802	0.000864	0.000097	0.000088	0.000096
3	0.058527	0.077670	0.053897	0.001219	0.001314	0.000159	0.000145	0.000157
4	0.009420	0.007797	0.008621	0.000199	0.000214	0.000019	0.000018	0.000019
5	0.014593	0.013581	0.013365	0.000302	0.000325	0.000031	0.000028	0.000031
6	0.825163	0.796502	0.797475	0.086850	0.091811	0.051645	0.048236	0.051192
7	0.974889	0.634660	0.946350	0.121534	0.128194	0.077604	0.072645	0.076946
8		0.609322	0.971427	0.128334	0.135312	0.082914	0.077648	0.082216

Cell No.	LSD test; variable Maximum pressure (bar) (Spreadsheet1) Probabilities for Post Hoc Tests Error: Between MS = 2.7926, df = 14.000							
	8 5.0493	9 6.1192	10 4.9631	11 1.2295	12 1.3037	13 1.2272	14 1.1521	15 1.2175
9	0.609322		0.581111	0.031521	0.033781	0.011028	0.010090	0.010902
10	0.971427	0.581111		0.136468	0.143822	0.089351	0.083718	0.088605
11	0.128334	0.031521	0.136468		0.975394	0.999115	0.970369	0.995401
12	0.135312	0.033781	0.143822	0.975394		0.970705	0.942001	0.966994
13	0.082914	0.011028	0.089351	0.999115	0.970705		0.964797	0.995451
14	0.077648	0.010090	0.083718	0.970369	0.942001	0.964797		0.969342
15	0.082216	0.010902	0.088605	0.995401	0.966994	0.995451	0.969342	

M.13 Tekscan Tests: Implement tyres – Area – effect of depth and combination of inflation pressure and load (Factorial ANOVA)

Effect	Univariate Tests of Significance for Contact area (m2) (Spreadsheet9) Sigma-restricted parameterization Effective hypothesis decomposition				
	SS	F	p	Degr. Of Freedom	MS
Intercept	0.916858	336444.1	0.000000	1	0.916858
Depth	0.660396	121167.3	0.000000	2	0.330198
Inflation pressure and load combination (bar & tonne)	0.003780	346.7	0.000000	4	0.000945
Depth*Inflation pressure and load combination	0.004871	223.4	0.000000	8	0.000609
Error	0.000030			11	0.000003

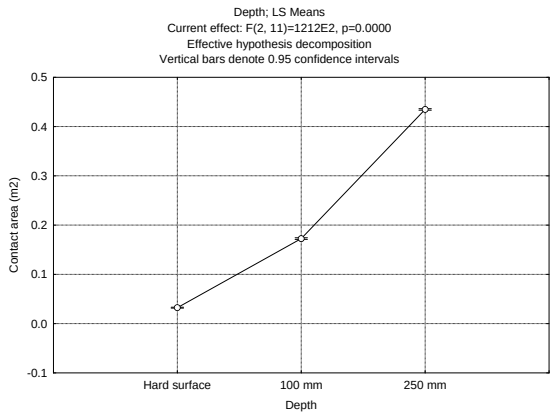

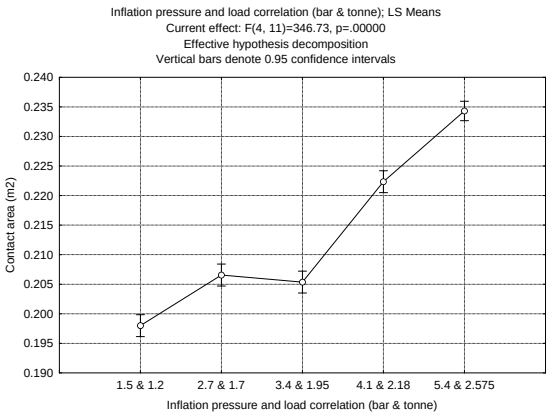

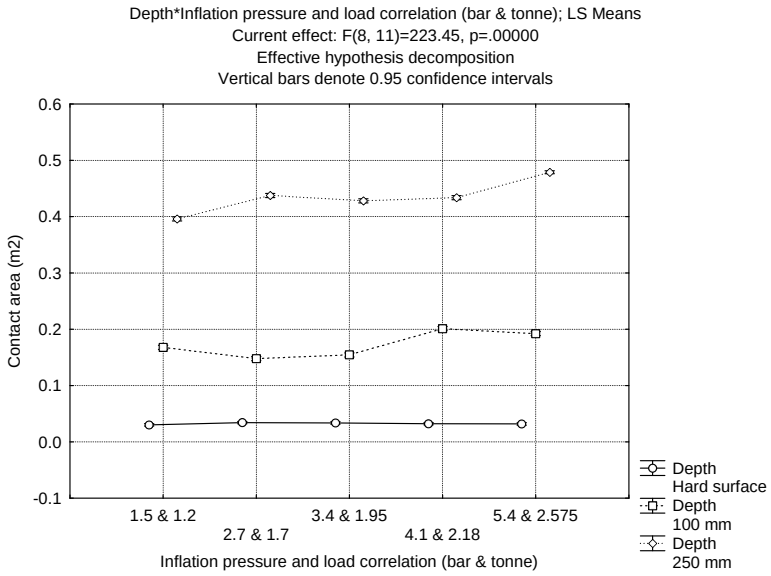

Cell No.	LSD test; variable Contact area (m2) (Spreadsheet9) Probabilities for Post Hoc Tests Error: Between MS = .00000, df = 11.000							
	Depth	Inflation pressure and load correlation (bar & tonne)	1 .03022	2 .03418	3 .03364	4 .03226	5 .03187	6 .16787
1	Hard surface	1.5 & 1.2		0.013491	0.027696	0.159104	0.245822	0.000000
2	Hard surface	2.7 & 1.7	0.013491		0.694963	0.181138	0.114857	0.000000
3	Hard surface	3.4 & 1.95	0.027696	0.694963		0.327312	0.216998	0.000000
4	Hard surface	4.1 & 2.18	0.159104	0.181138	0.327312		0.781284	0.000000
5	Hard surface	5.4 & 2.575	0.245822	0.114857	0.216998	0.781284		0.000000
6	100 mm	1.5 & 1.2	0.000000	0.000000	0.000000	0.000000	0.000000	
7	100 mm	2.7 & 1.7	0.000000	0.000000	0.000000	0.000000	0.000000	0.000003
8	100 mm	3.4 & 1.95	0.000000	0.000000	0.000000	0.000000	0.000000	0.000125
9	100 mm	4.1 & 2.18	0.000000	0.000000	0.000000	0.000000	0.000000	0.000000
10	100 mm	5.4 & 2.575	0.000000	0.000000	0.000000	0.000000	0.000000	0.000000
11	250 mm	1.5 & 1.2	0.000000	0.000000	0.000000	0.000000	0.000000	0.000000
12	250 mm	2.7 & 1.7	0.000000	0.000000	0.000000	0.000000	0.000000	0.000000
13	250 mm	3.4 & 1.95	0.000000	0.000000	0.000000	0.000000	0.000000	0.000000
14	250 mm	4.1 & 2.18	0.000000	0.000000	0.000000	0.000000	0.000000	0.000000
15	250 mm	5.4 & 2.575	0.000000	0.000000	0.000000	0.000000	0.000000	0.000000

Cell No.	LSD test; variable Contact area (m2) (Spreadsheet9) Probabilities for Post Hoc Tests Error: Between MS = .00000, df = 11.000								
	7 .14789	8 .15441	9 .20110	10 .19220	11 .39590	12 .43760	13 .42804	14 .43369	15 .47886
1	0.000000	0.000000	0.000000	0.000000	0.000000	0.000000	0.000000	0.000000	0.000000
2	0.000000	0.000000	0.000000	0.000000	0.000000	0.000000	0.000000	0.000000	0.000000
3	0.000000	0.000000	0.000000	0.000000	0.000000	0.000000	0.000000	0.000000	0.000000
4	0.000000	0.000000	0.000000	0.000000	0.000000	0.000000	0.000000	0.000000	0.000000
5	0.000000	0.000000	0.000000	0.000000	0.000000	0.000000	0.000000	0.000000	0.000000
6	0.000003	0.000125	0.000000	0.000000	0.000000	0.000000	0.000000	0.000000	0.000000

Cell No.	LSD test; variable Contact area (m2) (Spreadsheet9) Probabilities for Post Hoc Tests Error: Between MS = .00000, df = 11.000								
	7 .14789	8 .15441	9 .20110	10 .19220	11 .39590	12 .43760	13 .42804	14 .43369	15 .47886
7		0.017565	0.000000	0.000000	0.000000	0.000000	0.000000	0.000000	0.000000
8	0.017565		0.000000	0.000000	0.000000	0.000000	0.000000	0.000000	0.000000
9	0.000000	0.000000		0.002873	0.000000	0.000000	0.000000	0.000000	0.000000
10	0.000000	0.000000	0.002873		0.000000	0.000000	0.000000	0.000000	0.000000
11	0.000000	0.000000	0.000000	0.000000		0.000000	0.000000	0.000000	0.000000
12	0.000000	0.000000	0.000000	0.000000	0.000000		0.001780	0.122213	0.000000
13	0.000000	0.000000	0.000000	0.000000	0.000000	0.001780		0.034091	0.000000
14	0.000000	0.000000	0.000000	0.000000	0.000000	0.122213	0.034091		0.000000
15	0.000000	0.000000	0.000000	0.000000	0.000000	0.000000	0.000000	0.000000	

M.14 Tekscan Tests: Implement tyres – Mean pressure – effect of depth and combination if inflation pressure and load (Factorial ANOVA)

Effect	Univariate Tests of Significance for Mean pressure (bar) (Spreadsheet9) Sigma-restricted parameterization Effective hypothesis decomposition				
	SS	F	p	Degr. Of Freedom	MS
Intercept	110.8114	1883.080	0.000000	1	110.8114
Depth	142.5255	1211.007	0.000000	2	71.2628
Inflation pressure and load combination (bar & tonne)	6.9087	29.351	0.000008	4	1.7272
Depth*Inflation pressure and load combination	11.5563	24.548	0.000006	8	1.4445
Error	0.6473			11	0.0588

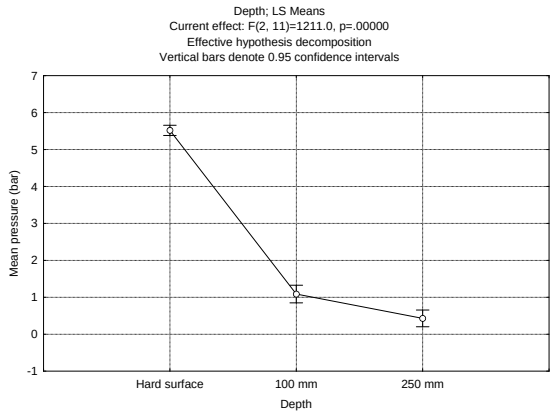

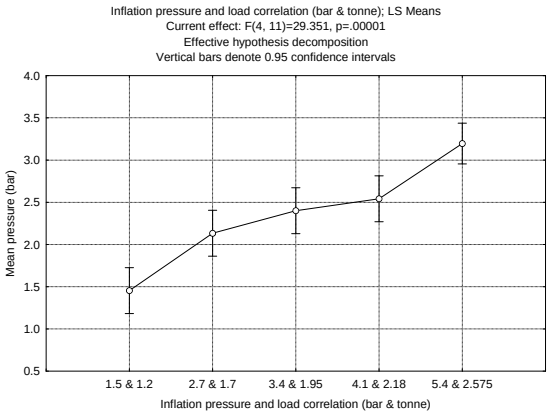

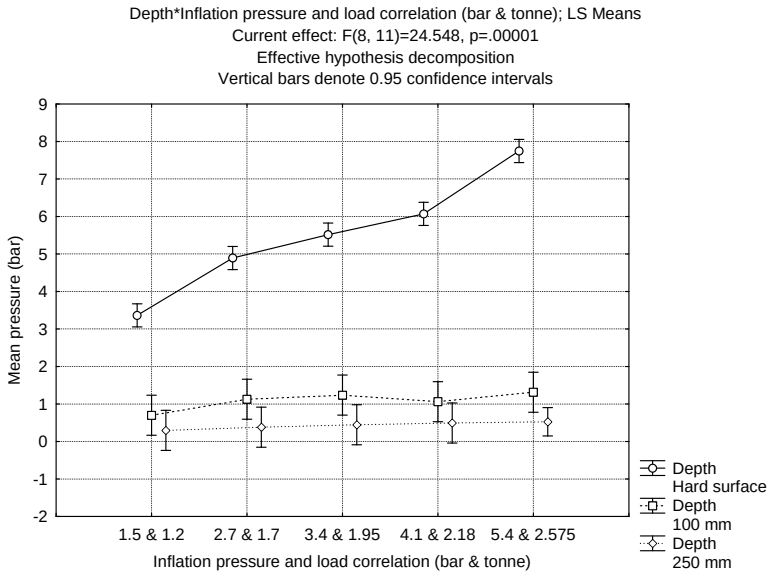

Cell No.	LSD test; variable Mean pressure (bar) (Spreadsheet9) Probabilities for Post Hoc Tests Error: Between MS = .05885, df = 11.000							
	Depth	Inflation pressure and load correlation	1 3.3643	2 4.8928	3 5.5168	4 6.0697	5 7.7472	6 .70024
1	Hard surface	1.5 & 1.2		0.000009	0.000000	0.000000	0.000000	0.000001
2	Hard surface	2.7 & 1.7	0.000009		0.009237	0.000097	0.000000	0.000000
3	Hard surface	3.4 & 1.95	0.000000	0.009237		0.017538	0.000000	0.000000
4	Hard surface	4.1 & 2.18	0.000000	0.000097	0.017538		0.000004	0.000000
5	Hard surface	5.4 & 2.575	0.000000	0.000000	0.000000	0.000004		0.000000
6	100 mm	1.5 & 1.2	0.000001	0.000000	0.000000	0.000000	0.000000	
7	100 mm	2.7 & 1.7	0.000007	0.000000	0.000000	0.000000	0.000000	0.239007
8	100 mm	3.4 & 1.95	0.000011	0.000000	0.000000	0.000000	0.000000	0.145476
9	100 mm	4.1 & 2.18	0.000005	0.000000	0.000000	0.000000	0.000000	0.313498
10	100 mm	5.4 & 2.575	0.000015	0.000000	0.000000	0.000000	0.000000	0.101321
11	250 mm	1.5 & 1.2	0.000000	0.000000	0.000000	0.000000	0.000000	0.265055
12	250 mm	2.7 & 1.7	0.000000	0.000000	0.000000	0.000000	0.000000	0.372183
13	250 mm	3.4 & 1.95	0.000000	0.000000	0.000000	0.000000	0.000000	0.475252
14	250 mm	4.1 & 2.18	0.000001	0.000000	0.000000	0.000000	0.000000	0.557841
15	250 mm	5.4 & 2.575	0.000000	0.000000	0.000000	0.000000	0.000000	0.569866

Cell No.	LSD test; variable Mean pressure (bar) (Spreadsheet9) Probabilities for Post Hoc Tests Error: Between MS = .05885, df = 11.000								
	7 1.1273	8 1.2377	9 1.0626	10 1.3136	11 .29736	12 .38108	13 .44664	14 .49289	15 .52621
1	0.000007	0.000011	0.000005	0.000015	0.000000	0.000000	0.000000	0.000001	0.000000
2	0.000000	0.000000	0.000000	0.000000	0.000000	0.000000	0.000000	0.000000	0.000000
3	0.000000	0.000000	0.000000	0.000000	0.000000	0.000000	0.000000	0.000000	0.000000
4	0.000000	0.000000	0.000000	0.000000	0.000000	0.000000	0.000000	0.000000	0.000000
5	0.000000	0.000000	0.000000	0.000000	0.000000	0.000000	0.000000	0.000000	0.000000
6	0.239007	0.145476	0.313498	0.101321	0.265055	0.372183	0.475252	0.557841	0.569866
7		0.753682	0.853741	0.597945	0.034047	0.052293	0.072744	0.091433	0.068025

Cell No.	LSD test; variable Mean pressure (bar) (Spreadsheet9) Probabilities for Post Hoc Tests Error: Between MS = .05885, df = 11.000								
	7 1.1273	8 1.2377	9 1.0626	10 1.3136	11 .29736	12 .38108	13 .44664	14 .49289	15 .52621
8	0.753682		0.619810	0.828925	0.019195	0.029663	0.041595	0.052674	0.035555
9	0.853741	0.619810		0.479618	0.047477	0.072453	0.100068	0.124990	0.098423
10	0.597945	0.828925	0.479618		0.012921	0.019992	0.028112	0.035709	0.022572
11	0.034047	0.019195	0.047477	0.012921		0.811688	0.671888	0.580167	0.457367
12	0.052293	0.029663	0.072453	0.019992	0.811688		0.851946	0.750613	0.634812
13	0.072744	0.041595	0.100068	0.028112	0.671888	0.851946		0.895185	0.793787
14	0.091433	0.052674	0.124990	0.035709	0.580167	0.750613	0.895185		0.912728
15	0.068025	0.035555	0.098423	0.022572	0.457367	0.634812	0.793787	0.912728	

M.15 Tekscan Tests: Implement tyres – Maximum pressure – effect of depth and combination of inflation pressure and load (Factorial ANOVA)

Effect	Univariate Tests of Significance for Maximum pressure (bar) (Spreadsheet9) Sigma-restricted parameterization Effective hypothesis decomposition				
	SS	F	p	Degr. Of Freedom	MS
Intercept	790.7669	301.7816	0.000000	1	790.7669
Depth	404.2122	77.1301	0.000000	2	202.1061
Inflation pressure and load combination (bar & tonne)	57.9898	5.5327	0.010866	4	14.4975
Depth*Inflation pressure and load combination (bar & tonne)	33.3058	1.5888	0.233760	8	4.1632
Error	28.8236			11	2.6203

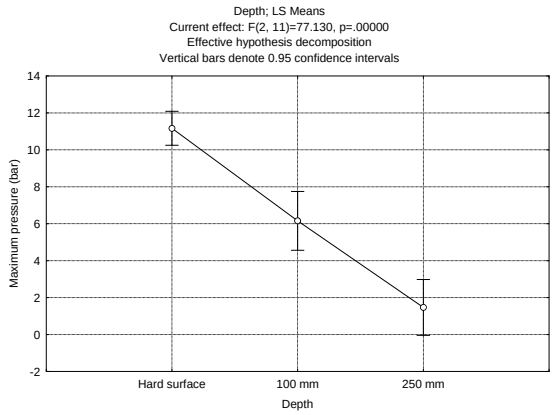

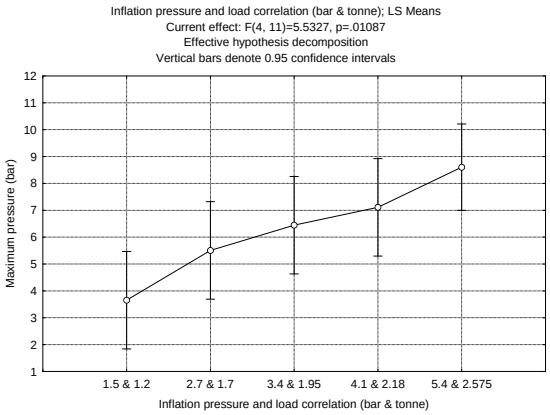

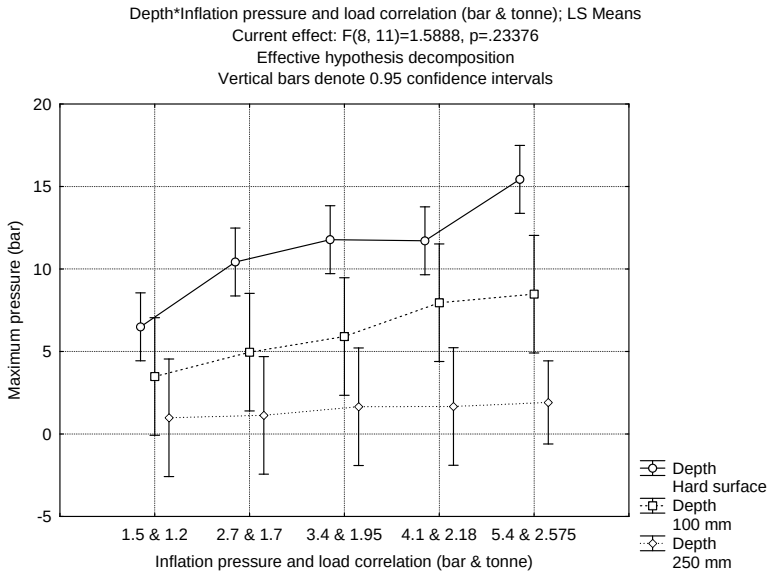

Cell No.	LSD test; variable Maximum pressure (bar) (Spreadsheet9) Probabilities for Post Hoc Tests Error: Between MS = 2.6203, df = 11.000							
	Depth	Inflation pressure and load correlation	1 6.4952	2 10.424	3 11.777	4 11.710	5 15.431	6 3.4854
1	Hard surface	1.5 & 1.2		0.012685	0.002098	0.002292	0.000031	0.135646
2	Hard surface	2.7 & 1.7	0.012685		0.327874	0.351691	0.003005	0.003428
3	Hard surface	3.4 & 1.95	0.002098	0.327874		0.959949	0.018419	0.001001
4	Hard surface	4.1 & 2.18	0.002292	0.351691	0.959949		0.016802	0.001063
5	Hard surface	5.4 & 2.575	0.000031	0.003005	0.018419	0.016802		0.000051
6	100 mm	1.5 & 1.2	0.135646	0.003428	0.001001	0.001063	0.000051	
7	100 mm	2.7 & 1.7	0.429825	0.013897	0.003850	0.004102	0.000160	0.531827
8	100 mm	3.4 & 1.95	0.758800	0.034200	0.009395	0.010024	0.000347	0.312864
9	100 mm	4.1 & 2.18	0.451457	0.213223	0.065503	0.069722	0.002087	0.076832
10	100 mm	5.4 & 2.575	0.312906	0.318715	0.104681	0.111170	0.003365	0.052021
11	250 mm	1.5 & 1.2	0.013233	0.000372	0.000124	0.000131	0.000009	0.297715
12	250 mm	2.7 & 1.7	0.015259	0.000421	0.000139	0.000147	0.000010	0.325992
13	250 mm	3.4 & 1.95	0.025103	0.000658	0.000211	0.000223	0.000014	0.440295
14	250 mm	4.1 & 2.18	0.025492	0.000667	0.000214	0.000226	0.000014	0.444223
15	250 mm	5.4 & 2.575	0.010104	0.000127	0.000035	0.000037	0.000002	0.444836

Cell No.	LSD test; variable Maximum pressure (bar) (Spreadsheet9) Probabilities for Post Hoc Tests Error: Between MS = 2.6203, df = 11.000								
	7 4.9631	8 5.9068	9 7.9544	10 8.4720	11 .98304	12 1.1319	13 1.6526	14 1.6687	15 1.9143
1	0.429825	0.758800	0.451457	0.312906	0.013233	0.015259	0.025103	0.025492	0.010104
2	0.013897	0.034200	0.213223	0.318715	0.000372	0.000421	0.000658	0.000667	0.000127
3	0.003850	0.009395	0.065503	0.104681	0.000124	0.000139	0.000211	0.000214	0.000035
4	0.004102	0.010024	0.069722	0.111170	0.000131	0.000147	0.000223	0.000226	0.000037
5	0.000160	0.000347	0.002087	0.003365	0.000009	0.000010	0.000014	0.000014	0.000002
6	0.531827	0.312864	0.076832	0.052021	0.297715	0.325992	0.440295	0.444223	0.444836
7		0.688117	0.217986	0.153575	0.109976	0.122378	0.176021	0.177966	0.152336

Cell No.	LSD test; variable Maximum pressure (bar) (Spreadsheet9) Probabilities for Post Hoc Tests Error: Between MS = 2.6203, df = 11.000								
	7 4.9631	8 5.9068	9 7.9544	10 8.4720	11 .98304	12 1.1319	13 1.6526	14 1.6687	15 1.9143
8	0.688117		0.390222	0.286338	0.054571	0.061085	0.090066	0.091140	0.069146
9	0.217986	0.390222		0.825267	0.011141	0.012514	0.018796	0.019035	0.011114
10	0.153575	0.286338	0.825267		0.007447	0.008360	0.012544	0.012703	0.006981
11	0.109976	0.054571	0.011141	0.007447		0.949327	0.775378	0.770133	0.647736
12	0.122378	0.061085	0.012514	0.008360	0.949327		0.824252	0.818909	0.700656
13	0.176021	0.090066	0.018796	0.012544	0.775378	0.824252		0.994499	0.897362
14	0.177966	0.091140	0.019035	0.012703	0.770133	0.818909	0.994499		0.903657
15	0.152336	0.069146	0.011114	0.006981	0.647736	0.700656	0.897362	0.903657	